Dissertation zur Erlangung des Doktorgrades
der Fakultät für Chemie und Pharmazie
der Ludwig-Maximilians-Universität München

Heterocyclic Borane Complexes as Hydrogen Atom Donors in Reduction Reactions

von

Florian Konrad Barth

aus Seeheim-Jugenheim, Deutschland

München 2015

Erklärung

Diese Dissertation wurde im Sinne von §7 der Promotionsordnung vom 28. November 2011 von Herrn Prof. Dr. Hendrik Zipse betreut.

Eidesstattliche Versicherung

Diese Dissertation wurde eigenständig und ohne unerlaubte Hilfe bearbeitet.

München, 12. November 2015

…….

Florian Barth

Dissertation eingereicht am: 31. August 2015
1. Gutachter: Prof. Dr. Hendrik Zipse
2. Gutachter: Prof. Dr. Konstantin Karaghiosoff
Mündliche Prüfung am: 12. Oktober 2015

Danksagung

An erster Stelle möchte ich meinem Doktorvater Prof. Dr. Hendrik Zipse meinen herzlichen Dank aussprechen. Ich danke ihm für die Möglichkeit, ein hochspannendes und in vielen Bereichen sehr forderndes Thema bearbeiten zu können. Besonders möchte ich mich für die vielen gewährten Freiheiten bei der Forschung sowie seine stets offene Tür bei jeglicher Art von Fragen bedanken. Die zahlreichen, hilfreichen Ideen und Tipps haben maßgeblich zum Gelingen dieser Arbeit beigetragen. Vielen Dank für deine Unterstützung, Hendrik!

Weiterhin möchte ich dem gesamten Prüfunkskomitee danken, insbesondere Prof. Dr. Konstantin Karaghiosoff für die Übernahme des Zweitgutachtens.

Meinen derzeitigen Laborkollegen Florian Achrainer, Harish, Julian Helberg, Dr. Sandhiya Lakshmanan, Pascal Patschinski, Ieva Teikmane und Jutta Tumpbach danke ich für die immer gute Arbeitsatmosphäre, die entgegengebrachte Hilfsbereitschaft und auch für die schöne Zeit außerhalb des Labors. Mein besonderer Dank gilt hierbei Florian Achrainer, der mir seit Beginn meiner Doktorarbeit mit Rat und Tat zur Seite stand und stets für ein nettes Laborklima sorgte. Des Weiteren möchte ich meinen ehemaligen Kollegen Carola Draxler, Dr. Johnny Hioe, Dr. Evgeny Larioniv, Dr. Christoph Lindner, Dr. Boris Maryasin, Dr. Raman Tandon und Dr. Cong Zhang danken.

Bei meinen Praktikanten Julian Helberg, Matthew Bell, Helen Funk und Stefan Woelfert bedanke ich mich für ihr Engagement und ihre wertvollen Arbeiten.

Für die Möglichkeit, spezielle NMR Messungen durchführen zu können, danke ich Dr. David Stephenson. Peter Mayer danke ich für das Ermöglichen von ^{11}B NMR Messungen in Eigenregie. Dr. Werner Spahl gilt mein Dank für die Durchführung massenspektrometrischer Messungen in speziellen Lösemitteln.

Bei Dr. Vladimir Malakhof möchte ich mich für sein geduldiges Bereitstellen zahlreicher „Leih-Chemikalien“ bedanken.

Abschließend bedanke ich mich auch bei meiner gesamten Familie und all meinen Freunden für die Unterstützung über die Jahre. Hierbei gilt meinen Eltern Gabi und „Emil“ sowie meiner Freundin Sanni ein ganz besonderer Dank. Ohne eure großartige Hilfe und euer Vertrauen in allen Lebenslagen wäre diese Arbeit nicht möglich gewesen.

TABLE OF CONTENTS

ABBREVIATIONS

AcOH	acetic acid	IR	Infra red
AIBN	Azobis(isobutyronitrile)	*J*	coupling constant (NMR)
aq.	aqueous	M	molarity
Ar	aryl	m	multiplet (NMR); medium (IR)
BDE	bond dissociation energy	Me	methyl
Bn	benzyl	min	minute
Bu	butyl	MS	mass spectrometry
br.	broad	MW	microwave
calc.	calculated	NMR	nuclear magnetic resonance
conc.	concentrated	*o*	*ortho*
d	doublet (NMR)	*p*	*para*
DBHN	dibenzyl hyponitrite	Pent	pentyl
DCM	dichloromethane	Ph	phenyl
DCPO	dicumyl peroxide	q	quartet (NMR)
DEAP	diethylaminopyridine	rt	room temperature
DHAP	dihexylaminopyridine	s	singlet (NMR); strong (IR)
DMAP	dimethylaminopyridine	t	triplet (NMR)
DMF	*N*,*N*-dimethylformamide	TBHN	*tert*-butyl hyponitrite
DMSO	dimethyl sulfoxide	TBPP	*tert*-butyl peroxypivalate
DTBP	di-*tert*-butyl peroxide	*t*Bu	*tert*-butyl
eq.	equivalent	TDT	*tert*-dodecanethiol
Et	ethyl	TFA	trifluoroacetic acid
EWG	electron withdrawing group	THF	tetrahydrofuran
GC	gas chromatography	TLC	thin layer chromatography
h	hour	TMB	1,3,5-trimetoxybenzene
Hex	hexyl	vw	very weak (IR)
HRMS	high resolution mass spectroscopy	vs	very strong (IR)
i-Pr	*iso*-propyl	w	weak (IR)

1. Introduction

More than one hundred years ago, *Gomberg* described triphenyl methyl radical, the first carbon-centered radical.[1] After this discovery it was believed that radicals are too reactive be used in synthesis. In the 1970s data of structure and reactivity of radicals was obtained, so that controlled radical reactions became possible. This was the beginning of modern radical chemistry.[2, 3, 4]

1.1. Tin hydrides

Tin hydrides like Bu_3SnH (**1a**), Ph_3SnH (**1b**) or Me_3SnH (**1c**) represent the most prominent class of hydrogen atom donors. These compounds are cheap and very effective in terms of H-transfer.[5, 6] A large number of applications in synthesis is known with tin hydrides.[7] However, all organic tin compounds have one major problem, which is their toxicity.[8] Furthermore, the separation of traces of tin-containing side products from pharmaceutically active products is also a big problem, diminishing the field of applications dramatically. Hence, there is a big ambition to solve this “tin problem” by finding alterative compounds.[9]

1.2. Silanes as radical reductants

Trialkyl silanes such as Et_3SiH (**1d**) are in comparison to tributyl tin hydride (**1a**) nontoxic. Yet, these compounds turned out to be rather ineffective reducing agents in radical chain reactions.[10] Silyl radicals have the property to generate carbon-centered radicals from a large number of precursers. However, the transfer of a hydrogen atom from a silane to a carbon-centered radical is very inefficient.[11] The reason for this is the higher bond dissociation energy (BDE). Tributyl tin hydride (**1a**) has a BDE of 329 kJ/mol, whereas the BDE for triethyl silane (**1d**) is 377 kJ/mol.[12, 13, 14] A slight improvement can be achieved by phenyl-substituted silanes, where the resulting silyl radicals are stabilized by the phenyl groups by about 42 kJ/mol.[15] However, they are still unsuitable for radical chain reactions[16, 17] and so their main application is in the *Barton-McCombie* reaction.[18] A weakening of the Si-H bond can be achieved by replacement of the alkyl (or phenyl) groups by trimethyl silyl groups.[16, 19] In 1965 *Gilman* described tris(timethylsilyl) silane (**1e**, TTMSS) for the first time.[20] Finally, it was *Chatgilialoglu*, who rediscovered the compound as a good reducing agent.[10, 21, 22] The bond dissociation energy of 352 kJ/mol is still higher than the BDE of Bu_3SnH (**1a**).[12] However, TTMSS (**1e**) has a wide scope of applications. A general scheme for reductions with **1e** and AIBN (**2a**) as initiator is shown in Figure 1.

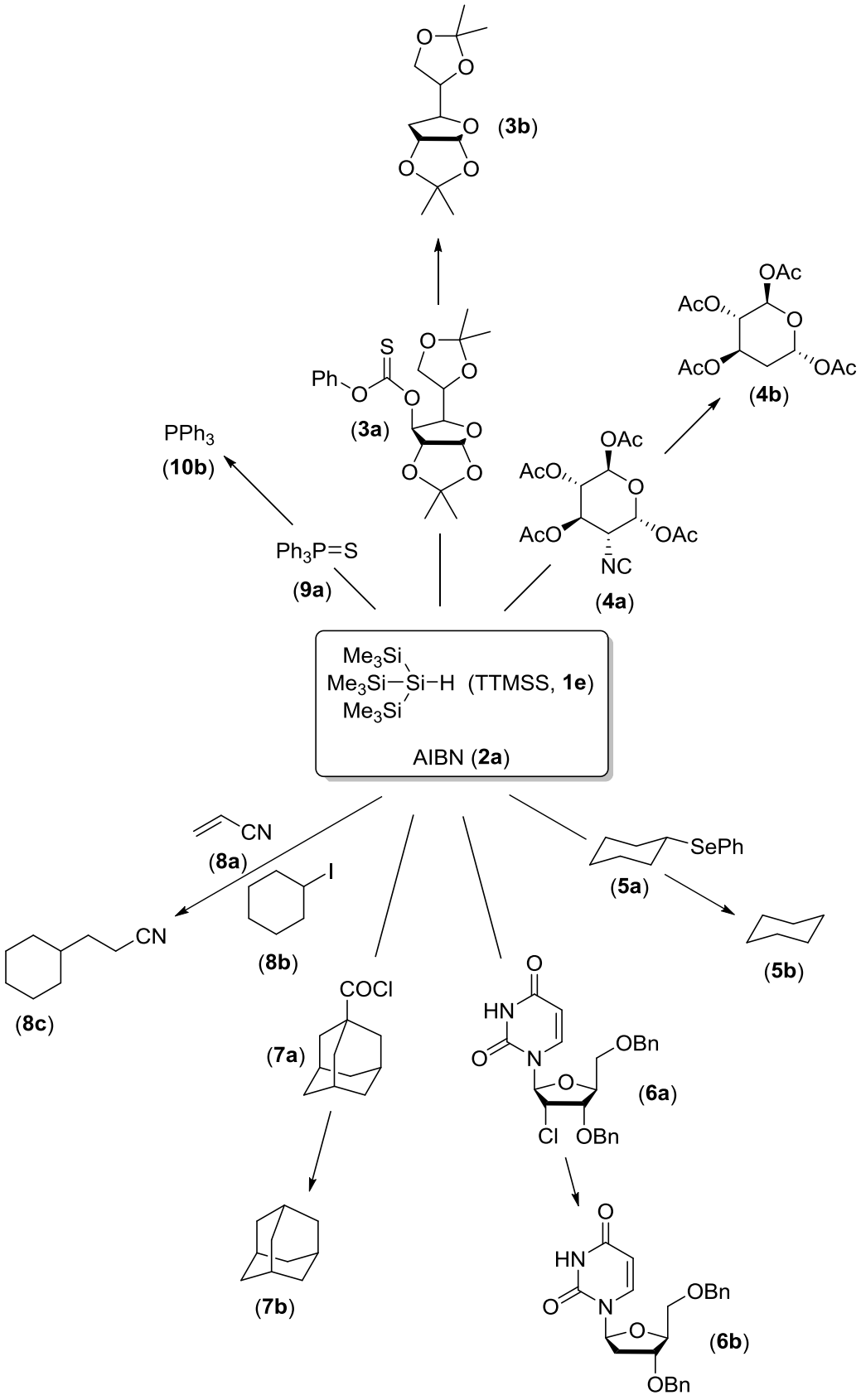

Figure 1: Versatile applications of TTMSS (**1e**) in radical chemistry.[10, 23, 24, 25, 26, 27, 28]

1.3. Further common hydrogen atom donors in radical chemistry

Germanium hydrides combine the properties of tin hydrides and silanes. The BDE of Bu_3GeH (1f, 369 kJ/mol) is between the tin and silicon analogue.[12] $(Me_3Ge)_3GeH$ (1g) was synthesized by *Chatgilialoglu* and turned out to be an even faster H-atom donor than tributyl tin hydride (**1a**). Reductions were carried out with yields of over 95 %.[29] Due to its high cost, applications for germanium hydrides are rather rare.

Reductions of reactive carbon-centered radicals with weak C-H bonds are also known in literature. One of the most prominent examples is the *Bergman* cyclisation.[30] In this reaction, radicals, which come from 3-en-1,5-diynes, are reduced with 1,4-cyclohexadiene (**11**, CHD). Thus, doubly substituted benzene derivatives can be synthesized (Figure 2a). The *Bergman* cyclisation is of special interest in the mechanism of action of some natural products, which show cytotoxic activitiy. As an example calicheamycine (**12**) is shown in Figure 2b. This enediyne antibiotic can form the diradical under physiological conditions.[31]

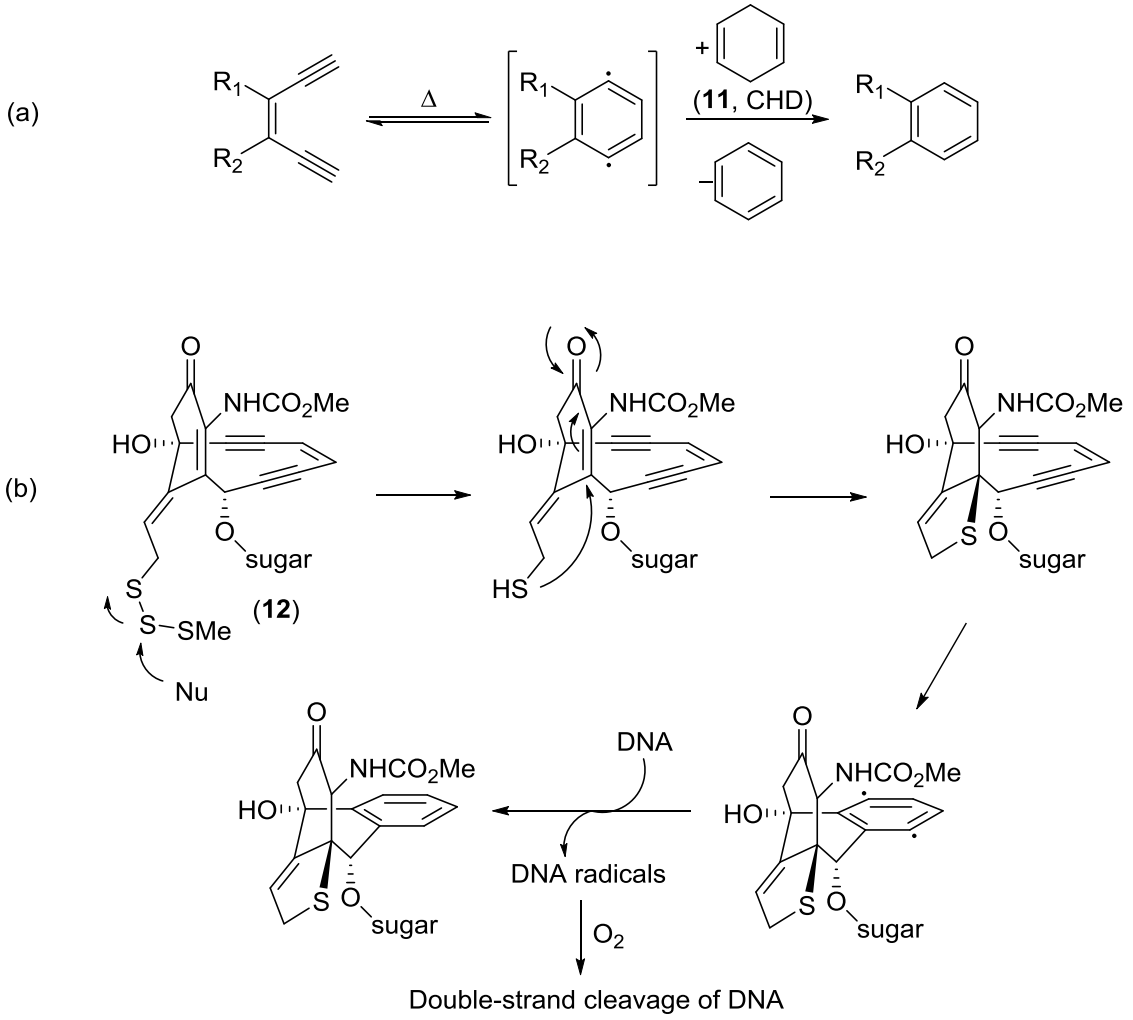

Figure 2: (a) General scheme of a *Bergman* cyclisation. (b) Example of a *Bergman* cyclisation on the basis of calicheamycine (**12**).

Furthermore, thiols are used as catalysts in radical chemistry.[32] The use of dialkyl phosphites as well as the application of hypophosphonic acids has been reported in the literature.[33, 34] From the group of pnictides diazenes are known, which can form a carbon-centered radical after N_2 elimination.[35] Yet, none of these substances has such a wide area of applications as tributyl tin hydride (**1a**). The research and development for a nontoxic, cheap and nevertheless efficient alternative still remains a big challenge for organic chemistry.

1.4. Borane complexes as hydrogen atom donors

Borane complexes with different Lewis-bases (L-BH_3) were first studied by *Roberts* (L = NR_3, PR_3 or SR_2).[36, 37] He observed that oxygen- and carbon-centered radicals could be reduced by borane complexes to the corresponding alcohols or hydrocarbons. Yet, nucleophilic C-radicals could not be effectively trapped in this way. Thus, the use of boranes seemed not very promising in the beginning, although boron-centered radicals (L-BH_2•) show a reactivity which is comparable to silyl or tin radicals.[38] Synthetic uses of borane complexes were found by *Lucarini*,[39] *Roberts*[36] and *Barton*[40]. In all cases, the boron species had to be used in an eight to ten fold excess. Much more promising results were achieved by *Curran*. In initial studies he used nitrogen-containing, heterocyclic carbene complexes (NHC boranes) for the radical reduction of xanthates with yields up to 70 %. Furthermore, *Zipse* showed, based on quantum chemical calculations, that the bond dissociation energies (BDE) of such compounds are similar to the BDE of Bu_3SnH (**1a**, 328.9 kJ/mol) (Figure 3).[41, 42]

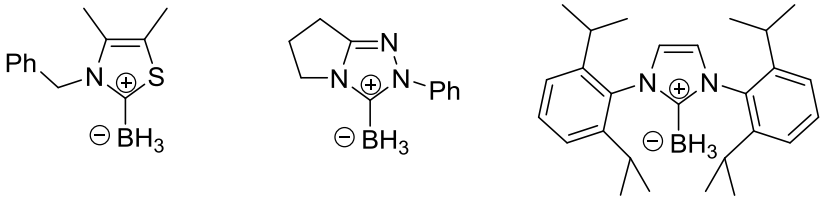

(**13a**) 309.6 kJ/mol (**13b**) 330.5 kJ/mol (**13c**) 334.7 kJ/mol

Figure 3: Examples for NHC boranes **13a**, **13b** and **13c** studied by *Curran* and *Zipse* and their calculated BDE.

Based on these calculations, several “first-generation radical reductions” were conducted with NHC boranes. For these initial studies, *Curran* used secondary xanthates and Et_3B (**2b**)/O_2 or AIBN (**2a**, 80 °C) as initiation systems. In these studies, he obtained good yields of the deoxygenated products for precursors, which would either undergo a cyclopropyl ring opening (Figure 4a) or a 5-exo-trig cyclisation (Figure 4b).[43]

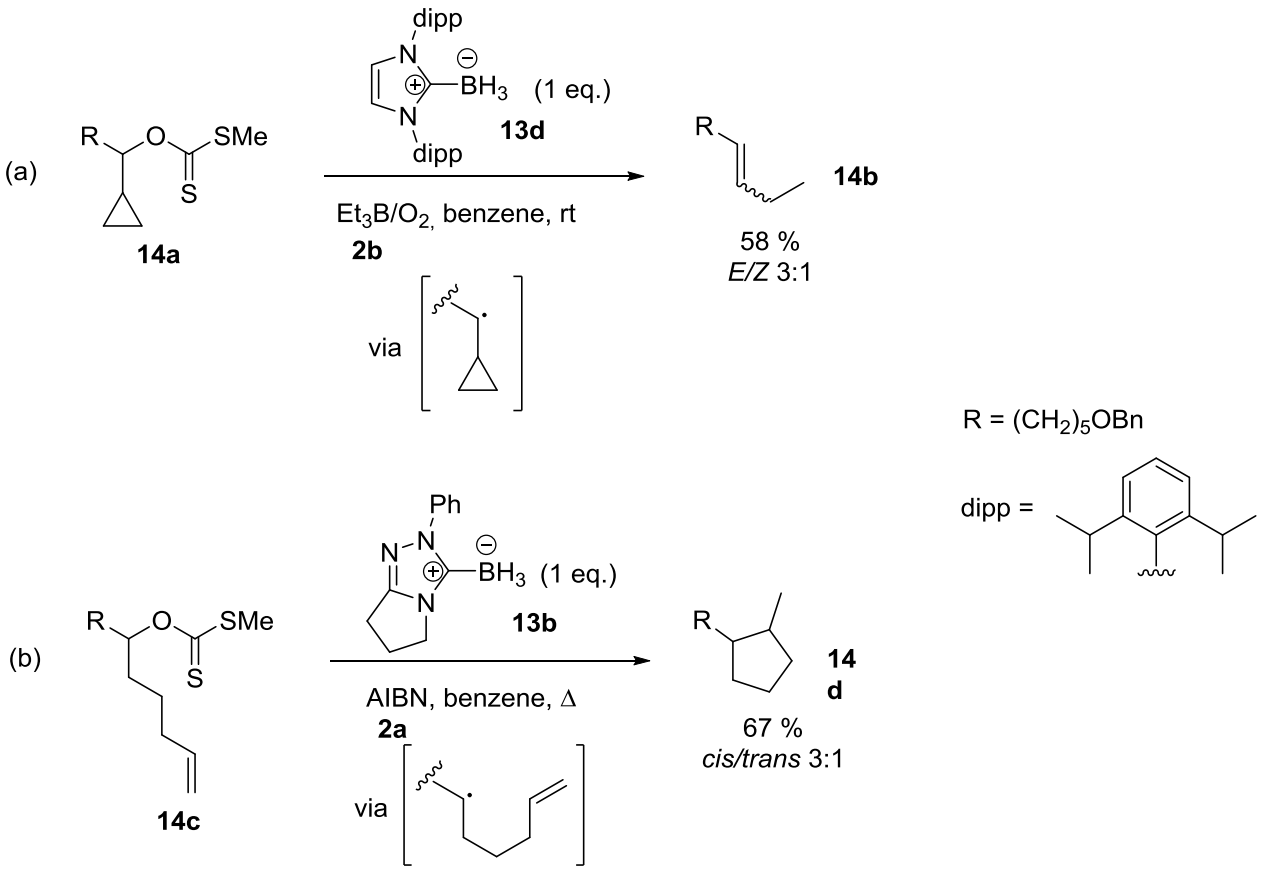

Figure 4: First generation radical reductions of xanthates (a) **14a** and (b) **14c** with NHC boranes by *Curran*.[43]

For good conversions of the xanthates, usually large amounts of the initiator were necessary (50 - 100 %).[43] An improvement was made with the development of the “second-generation-reagents”.[44] These NHC boranes are better hydrogen atom donors and their derived radicals are not persistent.[45] With this new class of hydrogen atom donors, it was possible to improve the yields of xanthate reductions, while decreasing the reaction time and lowering the amount of initiator (Figure 5 and Table 1).[43, 46]

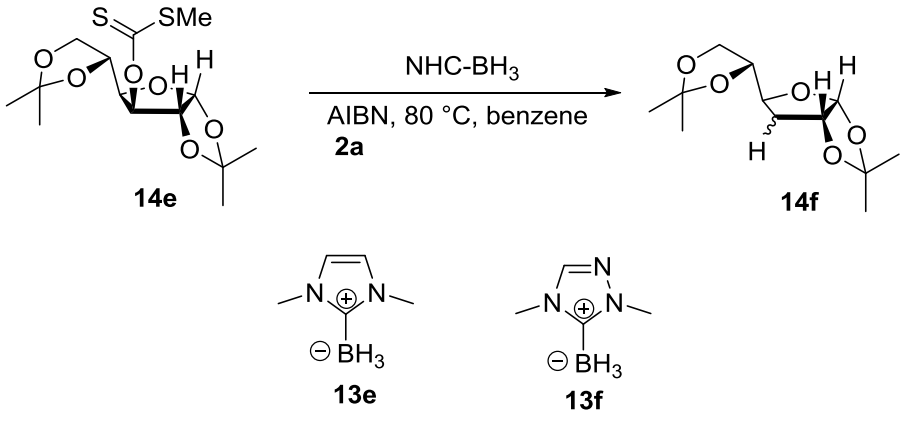

Figure 5: Reduction of xanthate **14e** with “second-generation-reagents“ **13e** and **13f** by *Curran*.[43, 46]

Table 1: Results for the reaction shown in Figure 5. [43, 46]

NHC-BH_3	eq.	AIBN (**2a**)	time [h]	yield [%]
13d	2	1.0 eq.	16	75
13e	1	10 mol%	2	89
13f	1	10 mol%	2	88

Furthermore it was possible to reduce some classes of halides which carried electron withdrawing groups close to the corresponding halide with different initiation methods (Figure 6 and Table 2).[47]

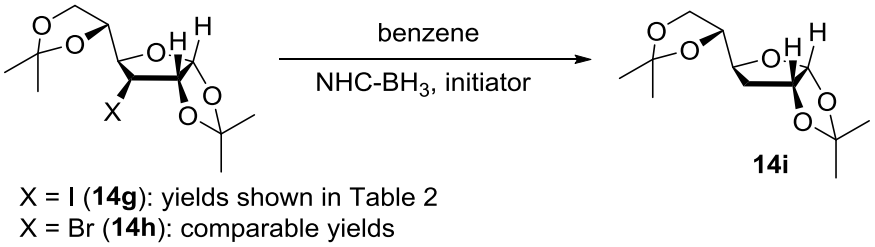

Figure 6: Reduction of halides with electron withdrawing groups.

Table 2: Results for the reactions (X = I) shown in Figure 6.

NHC-BH_3	initiator	temperature	yield [%]
13e	Et_3B (**2b**)/O_2	rt.	77 %
13e	AIBN (**2a**)	80 °C	63 %
13f	(tBuO)$_2$ (**2c**)	60 °C	75 %

Up to that, radical reductions with NHC boranes were possible for xanthates, but for halides like iodides or bromides it was always necessary to have an electron withdrawing group next to the halide.[48, 49] However, reductions of substrates like adamantyl halides or aryl halides were not possible with NHC boranes.[43] In case of slow hydrogen transfer reactions of silanes, the addition of a "polarity reversal catalyst" such as a thiol or selenide could solve this problem.[50] Recently, *Curran* showed, that the addition of a thiol as catalyst can also improve radical reactions based on NHC boranes.[51] The proposed mechanism by *Curran* is shown in Figure 7.[51] The use of a thiol as catalyst now made it possible to reduce halides, which did not undergo a reaction under the former conditions. So, adamantyl bromide (**7c**) could be reduced to adamantane (**7b**) (97 %) with thiophenol (**15a**) and *tert*-butyl hyponitrite (**2d**, TBHN) as initiator (Figure 8a), as well as aryl bromide (**14j**) with *tert*-dodecanethiol (**15b**, TDT) as catalyst (Figure 8b).

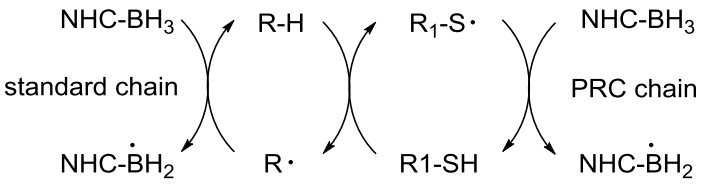

Figure 7: General mechanism of the uncatalyzed and PRC catalyzed radical chain reaction by *Curran*.[51]

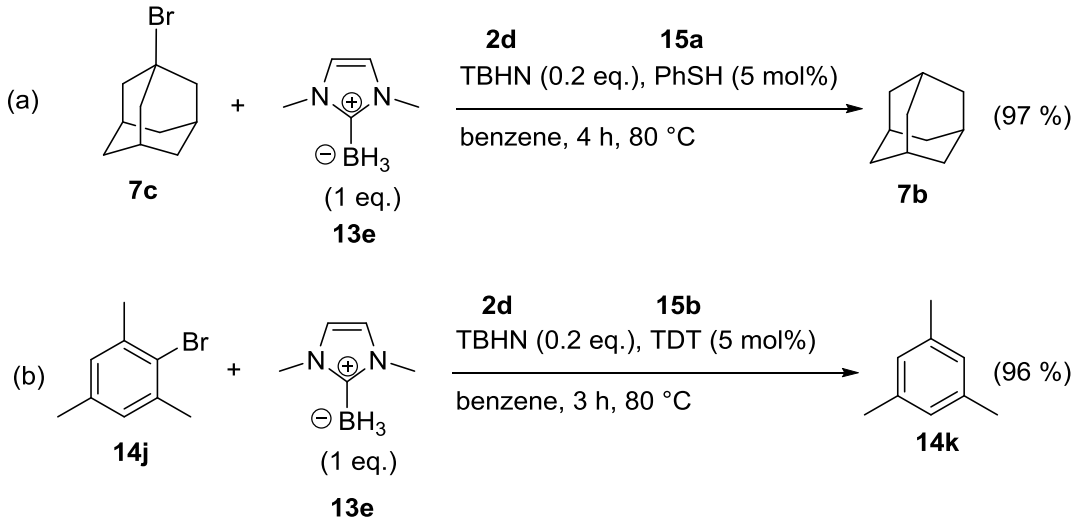

Figure 8: Examples for TDT (**15**) catalyzed radical reactions by *Curran*. (a) Reduction of adamantyl bromide (**7c**). (b) Reduction of aryl bromide **14j**.[51]

1.5. Objectives

The high toxicity of tin hydrides makes these compounds unsuitable for pharmaceutical applications. Based on the results described before and theoretical studies by *Zipse* and *Hioe*[42], the suitability of different borane complexes as hydrogen atom donors in radical reactions is the main goal. Furthermore, detailed studies on the reaction mechanisms shall help to understand the complex chemistry of heterocyclic borane complexes. The versatile structural possibilities of the borane complex itself, the initiator and the initiation conditions have to be exactly synchronized for a successful reaction outcome, which will be demonstrated and discussed in detail in this work.

2. Radical reactions

2.1. Uncatalyzed reactions

2.1.1. Substrate screening

A scheme of initially performed reactions with different substrates, reductants and initiators is shown in Figure 9. As reference reactions, three typical substrates (xanthate **18b**, iodide **18d** and bromide **18a**) were tested with tributyltin hydride (**1a**) as reducing agent. As initiation system BEt_3 (**2b**)/ O_2 was chosen and the reactions were conducted at room temperature. In all three cases quantitative conversions to the corresponding alkane **16a** were achieved (Table 3, entry 1 - 3). However, the exchange of the H-atom source by the newly synthesized borane complex **17a** led to a decrease of conversion for all three substrates under different conditions. In case of 1-bromododecane (**18a**) no conversion was observed for low temperature initiation (BEt_3 (**2b**)/ O_2 at 0 °C) and initiation at 80 °C with AIBN (**2a**, entry 4 and 5). For xanthate **18b** room temperature initiation (BEt_3 (**2b**)/ O_2) led to 8 % dodecane (**16a**) although the reaction time was increased to 14 hours (entry 6). Almost the same result was observed for xanthate **18c** when initiating at room temperature. Here 9 % conversion to the desired alkane **16a** was detected after 22.5 hours (entry 7b). For 1-iododododecane (**18d**) no reaction was observed for high temperature initiation (AIBN (**2a**), 80 °C) (entry 8). Initiation at room temperature (BEt_3 (**2b**)/ O_2) lead to 4 % dodecane (**16a**) after two hours and 16 % after 14 hours (entry 9a and 9b). However, when lowering the reaction temperature to 0 °C, 13 % of 1-iododododecane (**18d**) were reduced to dodecane (**16a**) after one hour, thus making a temperature dependence most promising (entry 10).

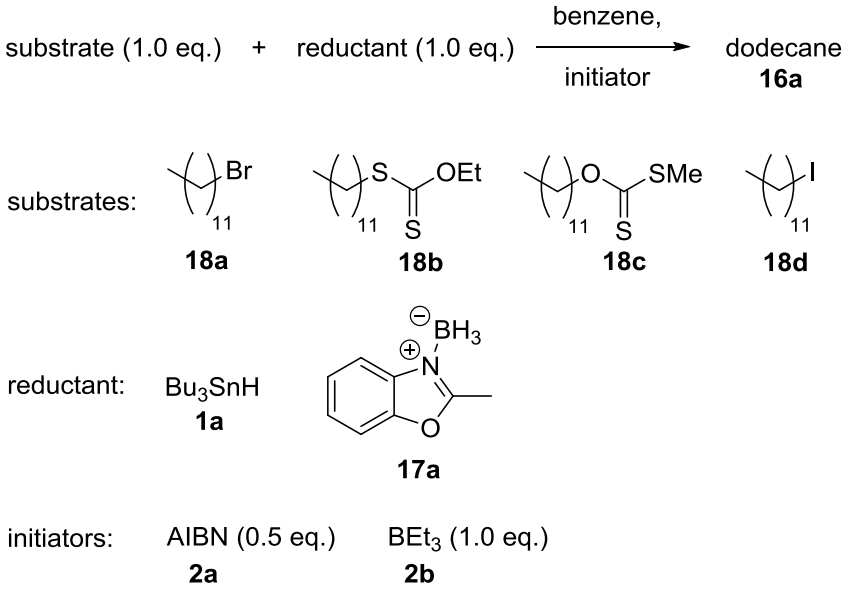

Figure 9: Reduction of dodecyl xanthates (**18b** and **18c**), bromide **18a** and iodide **18d** with Bu_3SnH (**1a**) and the synthesized borane complex **17a**.

Table 3: Conditions and results for the reactions shown in Figure 9.

entry	substrate	reductant	initiatior	temp.	time [h]	dodecane (**16a**) [%]
1	**18b**	**1a**	**2b**	rt.	2	> 99
2	**18d**	**1a**	**2b**	rt.	2	> 99
3	**18a**	**1a**	**2b**	rt.	2	98
4	**18a**	**17a**	**2b**	0 °C	2	no reaction
5	**18a**	**17a**	**2a**	80 °C	2	no reaction
6	**18b**	**17a**	**2b**	rt.	14	8
7a	**18c**	**17a**	**2b**	rt.	2	< 1
7b	**18c**	**17a**	**2b**	rt	22.5	9
8	**18d**	**17a**	**2a**	80 °C	2	no reaction
9a	**18d**	**17a**	**2b**	rt.	2	4
9b	**18d**	**17a**	**2b**	rt.	14	16
10	**18d**	**17a**	**2b**	0 °C	1	13

Subsequently the reduction of 1-iododododecane (**18d**) with complex **17a** under aerobic conditions with BEt_3 (**2b**) at 0 °C was examined in more detail. By elongation of the reaction time from one to two hours, followed by renewed addition of triethyl borane (**2b**), 26 % of dodecane (**16a**) had formed. GC/MS analysis of the final product mixture also showed the formation of small amounts of tetradecane (**16b**) and tetracosane (**16c**) (Figure 10a). The latter ones being formed due to radical recombination reactions of dodecyl radical with itself and with ethyl radicals formed during the initiation. A further recombination of two ethyl radicals could also be taken into account, however the resulting butane (**16d**) would not be detectable in the GC/MS (Figure 10b).

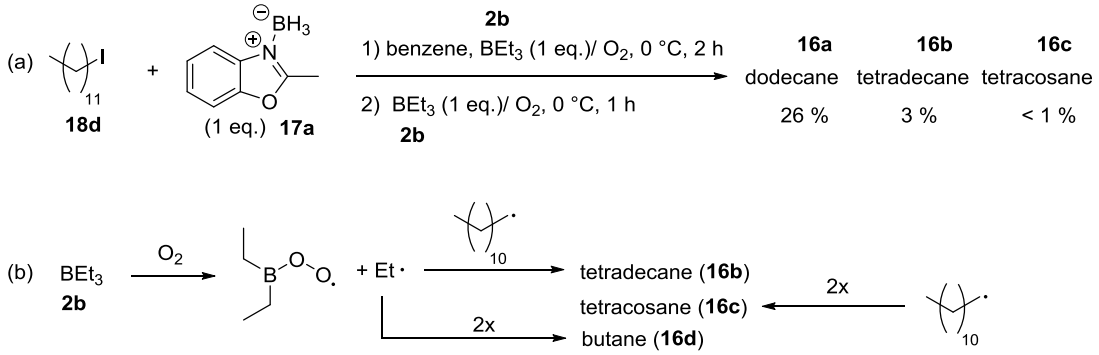

Figure 10: (a) Reduction of 1-iododododecane (**18d**) with borane complex **17a** at 0 °C. (b) Formation of recombination products.

As the increase of BEt_3 (**2b**) led to a higher yield of dodecane (**16a**), the reaction was repeated with a total amount of six equivalents of triethyl borane (**2b**). The addition of initiation agent over five hours by a syringe pump yielded 71 % dodecane (**16a**) accompanied by the formation of traces of tetradecane (**16b**) and tetracosane (**16c**) (Figure 11a). A similar result was achieved when adding six equivalents of triethyl borane (**2b**) right from the beginning and running the reaction over two hours at 0 °C. In this case the yield of dodecane (**16a**) was slightly lower than before (60 %), whereas tetradecane (**16b**) had

increased to 10 % (Figure 11b). This effect can be attributed to the higher concentration of BEt_3 (**2b**) and the resulting higher recombination process. Finally, the reaction was performed without the borane complex **17a** (Figure 11c). Here, 1-iodododecane (**18d**) was also reduced to dodecane (**16a**, 33 %), tetradecane (**16b**, 30 %) and tetracosane (**16c**, 3 %). This result shows that a reduction of primary alkyl iodides under aerobic conditions is also possible when adding triethyl borane (**2b**) in excess. The distinct higher formation of tetradecane (**16b**) indicates a higher level of a recombination process, due to the absence of borane complex **17a**. Finally borane **17a** seems to take part in the reduction process, yet the reaction requires a large excess of initiator.

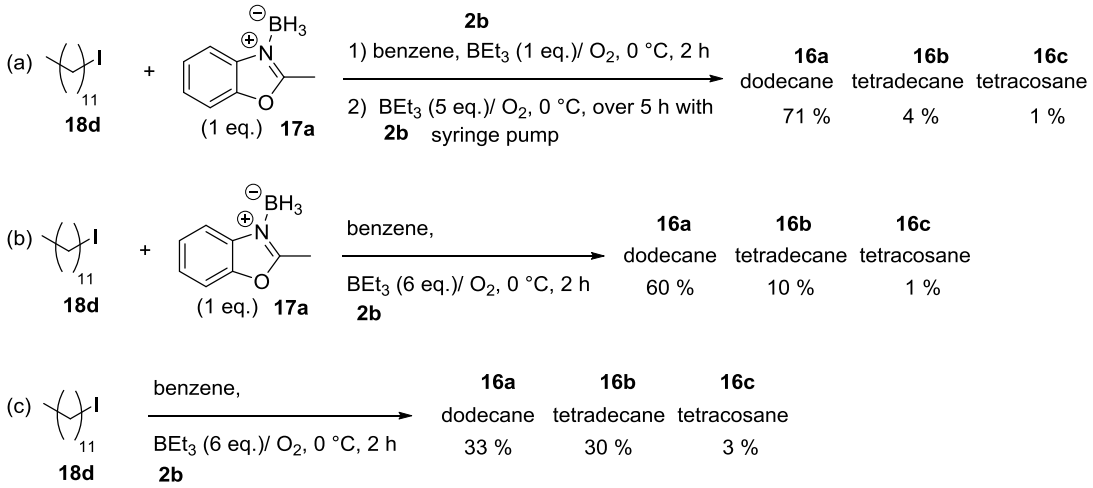

Figure 11: Reduction of 1-iodododecane (**18d**) with an excess of BEt_3 (**2b**).

2.1.2. Borane screening

In order to investigate whether a systematic improvement of the results for borane **17a** is possible, the next step was the synthesis of a variety of borane complexes. Therefore, borane complexes of different heterocyclic substance classes were synthesized, characterized and, if possible, crystallized to obtain X-ray structures. For the design of the borane complexes electronic effects were also taken into account.

2.1.2.1. Synthesis and characterization of borane complexes

Besides commercially available heterocyclic compounds, several substances were synthesized. Figure 12 shows a general synthetic route for the synthesis of precursors and borane complexes used here. In case of functionalized benzimidazoles in 2-position, a condensation of *ortho*-phenylene diamines with a carboxylic acid at high temperatures (≥160 °C) led to the desired precursors (Figure 12a). These reactions were carried out under microwave irradiation either in toluene or neat. Pure products were obtained by column chromatography on silica or by recrystallization. For *N*-methylated imidazoles, the starting compounds were first deprotonated with a strong base (usually *n*-butyllithium) and afterwards reacted with methyl iodide (Figure 12b). In most cases the *N*-methylated compounds were obtained in good quality right after an aqueous workup followed by extraction. If necessary, the crude products were recrystallized or purified by column chromatography on silica. In

order to obtain borane complexes of excellent quality, it is valuable to mention, that the precursors should be of high purity, as most of the complexes decompose on column chromatographic workup. Subsequently, the complexes were synthesized by the complexation of BH_3 to a heterocyclic nucleophile (Figure 12c). It turned out, that the most effective workup is precipitation from isohexane, whereby the borane complexes were obtained in good yields and quality.

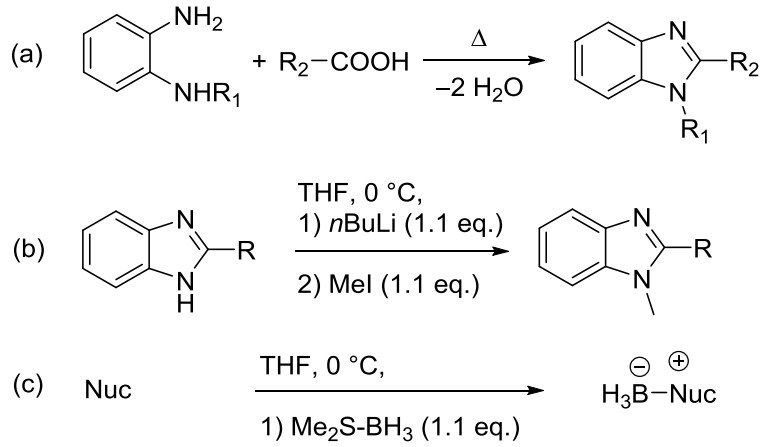

Figure 12: General routes for the synthesis of benzimidazole derivatives and borane complexes used in this work.

An overview over all heterocyclic borane complexes used for this screening is shown in Figure 13. Aside from complex **17v** and **17w**, which were commercially available, all complexes and precursors were synthesized according to the procedure outlined in Figure 12.

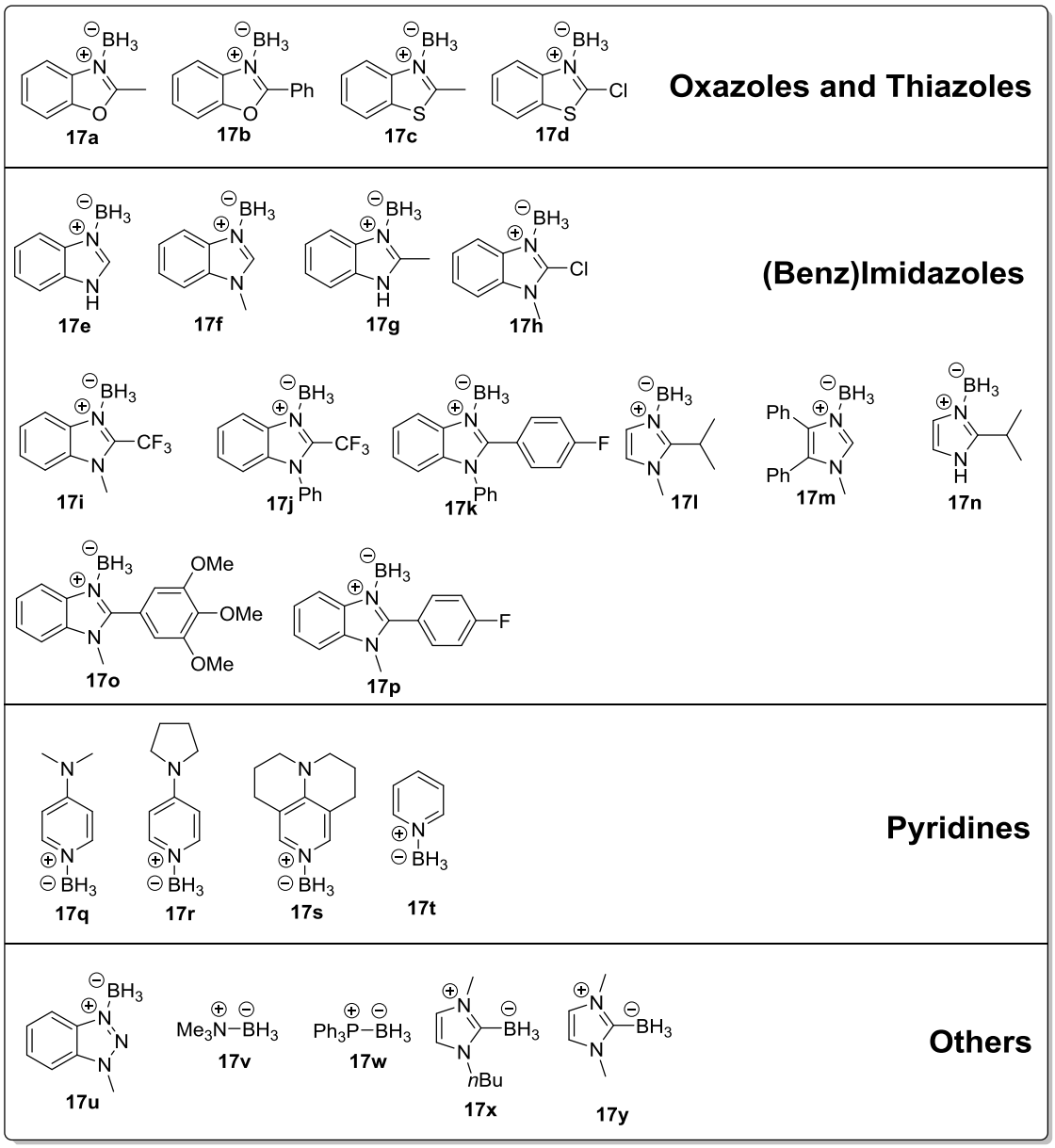

Figure 13: Borane complexes used for radical experiments.

Subsequently, all complexes were characterized by NMR (^{1}H, ^{13}C, ^{11}B and ^{19}F if necessary), IR, mass spectrometry and elemental analysis. Furthermore, decomposition points rather than melting points were determined for all non-liquid complexes. Three compounds turned out to be colorless ionic liquids (**17l**, **17t** and **17x**). For the NHC borane complex **17x** a melting point of −63 to −65 °C was determined. In some cases crystals of suitable quality for X-ray measurements could be grown by recrystallization from DCM. Table 4 shows the most characteristic analytical data for all complexes. If not differently indicated, NMR measurements were done in $CDCl_3$. For the corresponding imidazole, oxazole, thiazole and triazole borane complexes the ^{11}B NMR shifts are in a narrow region of −19.7 to −23.2 ppm. Chemical shifts for pyridine-derived borane complexes were found in the region of −12.2 to −14.2 ppm, whereas the shift region of NHC boranes is between −37.4 and −38.4 ppm. All substances show a (sometimes broad) quartet in the ^{11}B NMR, indicating the BH_3 group. The B-H vibrations can also be seen in the IR spectrum as three characteristic bands in the

region of 2400 to 2210 cm^{-1}. For complexes which could be crystallized, B-N distances were determined by X-ray crystallography. Independent of the substance class, these distances are all in a typical range of 1.571 Å to 1.596 Å.

Table 4: Characteristic analytical data for synthesized borane complexes.

complex	^{11}B NMR shift [ppm]	$\tilde{\nu}$(B-H) [cm^{-1}]	r(B-N) [Å]
17a	−23.20	2400[b]	1.584
17b	−21.80	2254[b]	n.a.
17c	−20.43	2402, 2298, 2256	n.a.
17d	−19.08	2548, 2501, 2430	n.a.
17e	−20.13[a]	2352, 2291, 2244	1.575
17f	−22.31	2340, 2289, 2254	1.571
17g	−21.80	2400, 2290, 2240	1.571
17h	−21.82	2351, 2309, 2263	n.a.
17i	−20.62	2383, 2349, 2273	n.a.
17j	−20.48	2381, 2359, 2273	n.a.
17k	−22.45	2356, 2313, 2265	n.a.
17l	−19.74	2357, 2309[c]	n.a.
17m	−19.68	2372, 2306, 2261	1.589
17n	−20.06[a]	2349, 2296, 2253	n.a.
17o	−22.06	2361, 2342, 2265	n.a.
17p	−21.79	2365, 2306, 2261	n.a.
17q	−12.75[a]	2358, 2283, 2245	1.596
17r	−14.00	2343, 2298, 2246	1.590
17s	−14.15	2349, 2291, 2249	n.a.
17t	−12.22	2360, 2310, 2281	n.a.
17u	−20.01	2356[c], 2263	1.578
17x	−38.34	2335[c], 2275	n.a.
17y	−37.49	2270[c], 2214	n.a.

[a] Measured in DMSO-d_6. [b] With two shoulders. [c] With one shoulder.

The X-ray structure of **17g** reveals a certain unexpected property which is characteristic for all investigated boranes (Figure 14a). In this case the distance between the nitrogen-bound proton and the closest boron-bound hydride is with 1.755 Å rather short. This NH-H^- hydrogen bridge was found in no other complex and is due to the cell ordering (Figure 14b). The molecules are stacked in almost perfectly parallel lying layers, which makes this short contact possible, as the BH_3 moieties point to the NH groups. In comparison the X-ray structure of benzimidazole borane (**17e**) is shown in Figure 15. Here the shortest NH-HB distance is 5.784 Å and the molecules are not stacked in parallel layers (Figure 15b). The molecules are rather sorted in two types of layers in which the NH and BH_3 groups point away from each other. Thus, a hydrogen bond as in **17g** is not formed.

(a)

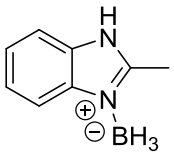

17g

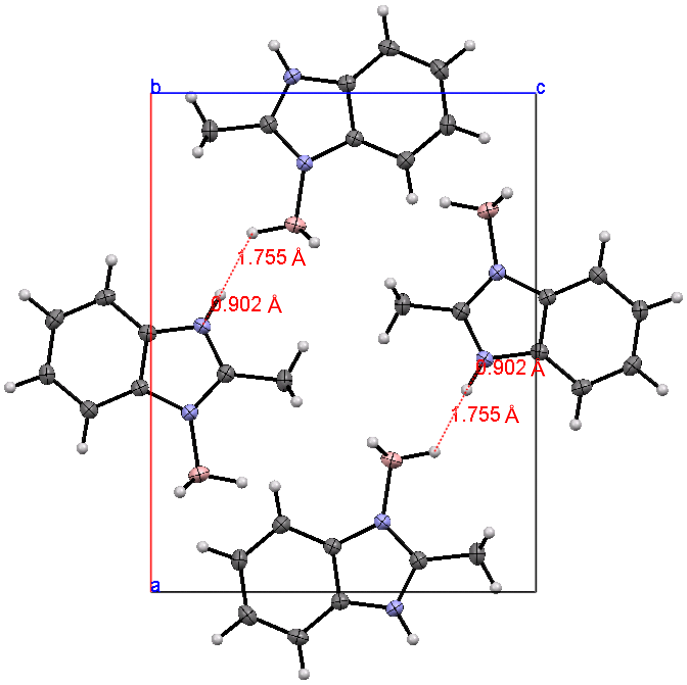

(b)

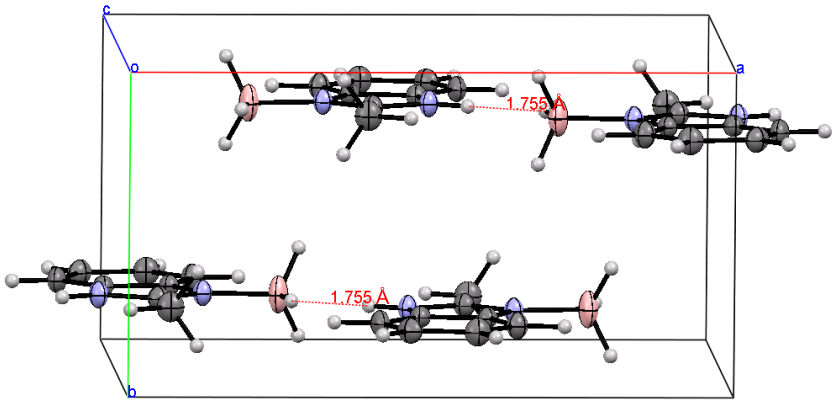

Figure 14: (a) X-ray structure of borane complex **17g** and its short N-H-H$^-$ distance of 1.755 Å. (b) Cell unit of **17g**.

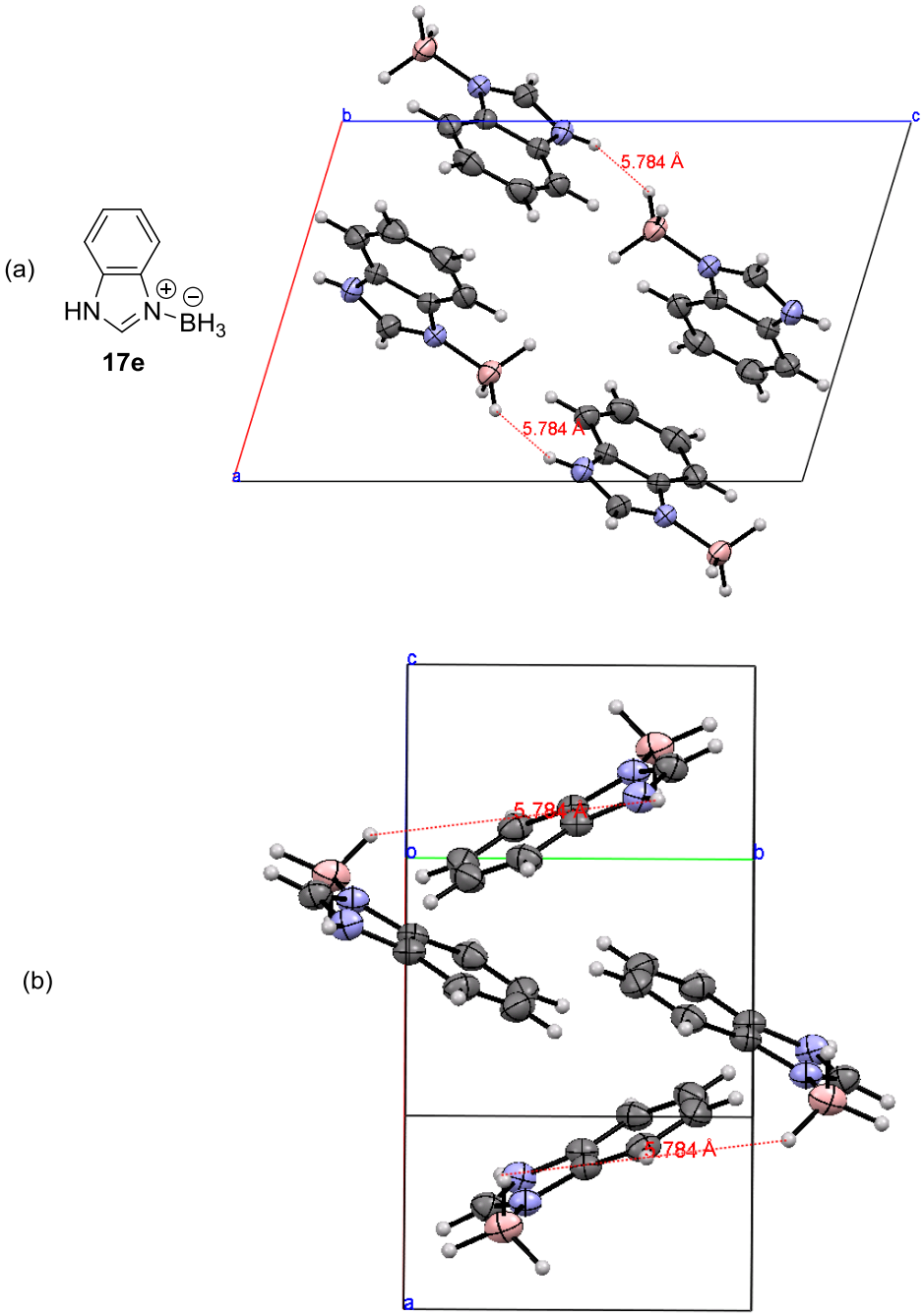

Figure 15: (a) X-ray structure of benzimidazole borane **17e** and its N-H-H$^-$ distance of 5.784 Å. (b) Cell unit of **17e**.

2.1.2.2. Low temperature initiation experiments with BEt_3 (2b)

A screening of the different substance classes was made in order to check their suitability in radical reactions. As initiation system triethyl borane (**2b**) was used under aerobic conditions and 1-iododododecane (**18d**) or 1-bromododecane (**18a**) were used as substrates (Figure 16). The reaction was carried out either at room temperature or at 0 °C for two hours. Table 5 summarizes the results of the tested borane complexes. Most of the analyzed borane complexes did not lead to any conversion at all. Only some of the tested reactions showed

traces of the desired product dodecane (**16a**), which makes triethyl borane (**2b**) an inconvenient initiator for the tested reactions.

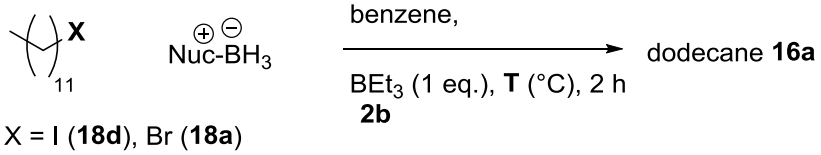

Figure 16: General reaction scheme for the reduction of 1-iodododecane (**18d**) and 1-bromododecane (**18a**) with BEt_3 (**2b**) as initiator.

Table 5: Results for the reactions shown in Figure 16.

entry	**X**	$\overset{\oplus}{Nuc}\text{-}BH_3^{\ominus}$	**T**	dodecane (**16a**) [%]
1	I	**17a**	rt	4 (16 % after 14 h)
2	I	**17a**	0 °C	13
3	Br	**17a**	0 °C	-
4	Br	**17b**	0 °C	-
5	I	**17b**	0 °C	3
6	Br	**17c**	0 °C	-
7	Br	**17d**	0 °C	-
8	Br	**17e**	0 °C	< 1
9	Br	**17f**	0 °C	-
10	I	**17f**	0 °C	3
11	Br	**17h**	0 °C	-
12	I	**17i**	rt	-
13	Br	**17i**	0 °C	-
14	I	**17j**	rt	-
15	I	**17k**	rt	3
16	Br	**17l**	0 °C	-
17	Br	**17m**	0 °C	-
18	Br	**17q**	0 °C	-
19	Br	**17r**	0 °C	-
20	Br	**17s**	0 °C	3
21	I	**17u**	rt	-
22	Br	**17v**	0 °C	-
23	Br	**17w**	0 °C	-
24	Br	**17x**	rt	3
25	Br	**17x**[a]	0 °C	-

[a] THF/benzene (1:1) was used as solvent.

2.1.2.3. Thermally initiated reactions with AIBN (2a)

The very small conversions with triethyl borane (**2b**) suggested, that a successful outcome of the reactions could be influenced by the initiation system and its initiation temperature. Therefore, some of the reactions were repeated under thermal initiation with AIBN (**2a**) at 80 °C (Figure 17). The results of the experiments are summarized in Table 6. Aside from carbene borane **17x**, all tested borane complexes showed no conversion under the described conditions (entry 8). Similar NHC boranes compounds had also been used by *Curran et al.* for radical reactions.[51] Finally, thermal initiation with AIBN (**2a**) did not lead to a successful reduction in all cases and therefore the reaction conditions had to be changed, which will be the main focus in the next section.

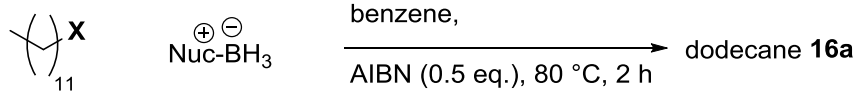

X = I (**18d**), Br (**18a**)

Figure 17: General reaction scheme for the reduction of 1-iodododecane (**18d**) and 1-bromododecane (**18a**) with AIBN (**2a**) as initiator.

Table 6: Results for the reactions shown in Figure 17.

entry	**X**	$\overset{\oplus}{\underset{}{}}\overset{\ominus}{}$ Nuc-BH_3	dodecane (**16a**) [%]
1	I	**17a**	-
2	Br	**17a**	-
3	Br	**17b**	-
4	I	**17b**	-
5	Br	**17f**	-
6	Br	**17i**	-
7	Br	**17m**	-
8	Br	**17x**[a]	14

[a] 0.1 eq. AIBN (**2a**) was used with a reaction time of 5 h.

2.2. *Tert*-dodecanethiol (TDT, 15b)-catalyzed reactions

As neither the high temperature initiation with AIBN (**2a**) nor the low temperature initiation with BEt_3 (**2b**)/ O_2 led to significant conversions, another initiation system which had been successfully used by *Curran et al*.[51] was chosen. *Curran et al.* had shown that NHC boranes become good H donors for radical reactions, when combined with a thiol as catalyst.[51]

2.2.1. *Tert*-butylhyponitrite (TBHN, 2d) as initiator

It is worth mentioning, that also the initiator seems to have a big influence on radical reactions promoted by borane complexes. Therefore, *tert*-butylhyponitrite (**2d**, TBHN), which had also been used by *Curran et al.*,[51] was synthesized as radical starter. The synthesis of

TBHN (**2d**) is shown in Figure 18. To a solution of *tert*-butylbromide (**19a**, 10 eq.) and zinc chloride (**19b**, 1 M in Et_2O, 1.1 eq.), sodium hyponitrite (**19c**) was added at 0 °C. The suspension was strirred for 90 minutes at that temperature. Inorganic salts were removed and the pure hyponitrite (**2d**) was obtained by recrystallisation from pentane in 35 % yield. As the compound already decomposes slowly at room temperature, the whole reaction and workup has to be done carefully at low temperature. The compound can be stored at −18 °C over months, but should not be exposed to room temperature over a longer period.

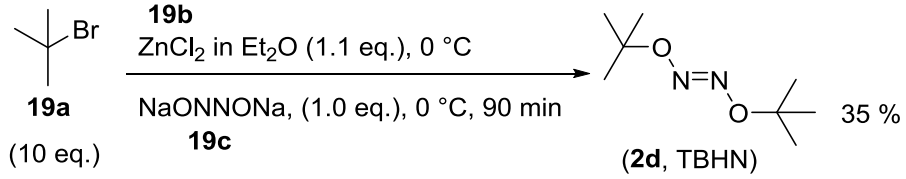

Figure 18: Synthesis of TBHN (**2d**).

2.2.2. Borane screening

Afterwards imidazole-, oxazole-, thiazole- and pyridine-based borane complexes such as a NHC borane complex, which had been used by *Curran et al.*,[51] were tested under the new conditions (Figure 19). 1-Iododododecane (**18d**) was chosen as substrate and a borane complex was added in slight excess (1.1 eq.). The reaction was conducted in benzene with 1-methylundecan-2-thiol (**15b**, *tert*-dodecylthiol, TDT) as catalyst with a loading of 5 mol%. For initiation of the reaction TBHN (**2d**) was added and the reaction mixture was heated up to 80 °C for two hours.

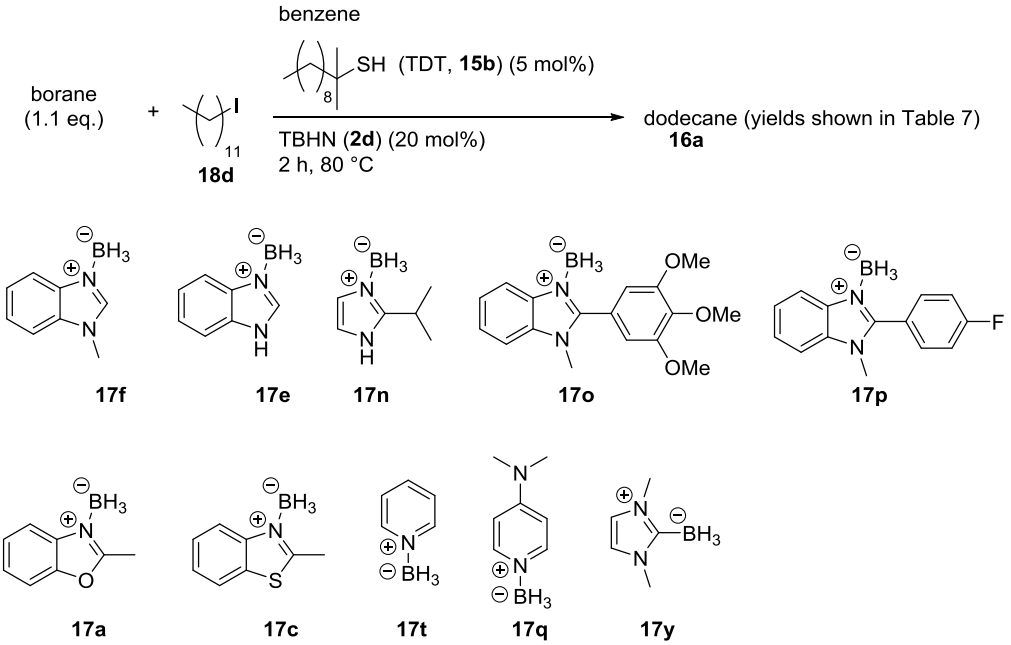

Figure 19: Reduction of 1-iododododecane (**18d**) with different borane complexes with TBHN (**2d**) and TDT (**15b**) at 80 °C.

Table 7 summarizes the results of the tested reactions for the TBHN (**2d**)/ TDT (**15b**) initiation system. NHC borane **17y** leads to a quantitative conversion of 1-iododododecane (**18d**) to dodecane (**16a**). This result is not surprising as the compound had already been successfully used under the same conditions but for different substrates by *Curran et al.*.[51] All other investigated substance classes show no or moderate yields, except 4-dimethylaminopyridine borane (**17q**) which leads to 69 % dodecane (**16a**). The fact, that pyridine borane (**17t**) leads to no conversion, shows the importance of the right design of the reducing agent. The more electron rich DMAP borane (**17q**) seems to be able to reduce the substrate under these conditions, although full conversion was not achieved.

Table 7: Results for the reactions shown in Figure 19.

borane	dodecane (**16a**) [%]
17f	27
17e	0
17n	9
17o	0
17p	0
17a	10
17c	0
17t	0
17q	69
17y	>99

2.2.3. Screening of initiation systems with DMAP borane (17q) as H atom donor

As DMAP borane (**17q**) led to the most promising result for the TBHN (**2d**)/ TDT (**15b**) method, the influence of different radical initiation was studied. Aside from some commercially available radical starters, a second representative of the hyponitrite class was also of interest, as TBHN (**2d**) already had shown the potential of these compounds. Thus, dibenzylhyponitrite (**2e**, DBHN) was chosen. The synthesis of DBHN (**2e**) is shown in Figure 20. The first step of the synthesis was carried out under light exclusion. Sodium hyponitrite (**19c**) was dissolved in water. After the addition of an aqueous silver nitrate (**20a**, 2.2 eq.) solution yellow silver hyponitrite (**20b**) precipitated, which was washed with water and ethanol. Solvents were removed and the crude silver hyponitrite (**20b**) was obtained as yellow solid (48 %), which was used without further purification for the following step. Afterwards the silver hyponitrite (**20b**) was added to a solution of benzyl bromide (**20c**, 2.0 eq.) in DCM at 0 °C. The solution was stirred for three hours at that temperature. After removal of salts the pure dibenzylhyponitrite (**2e**) was obtained by recrystallisation from pentane as white crystals (39 %). As for the synthesis of TBHN (**2d**) it is important to keep the substance cold during all steps. DBHN (**2e**) can be stored at −78 °C over a longer period.

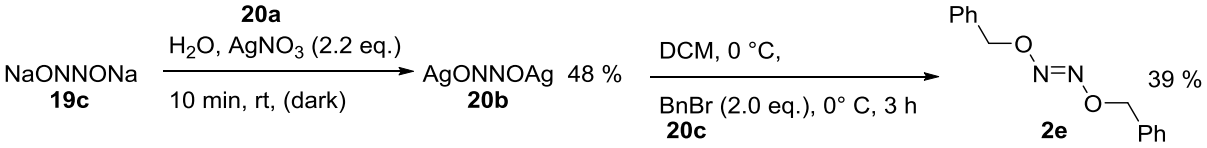

Figure 20: Synthesis of DBHN (**2e**).

Afterwards different initiators were screened by their suitability for the DMAP borane (**17q**)/ TDT (**15b**) system. The reactions were carried out in benzene for two hours and 1-iododododecane (**18d**) was used as substrate (Figure 21).

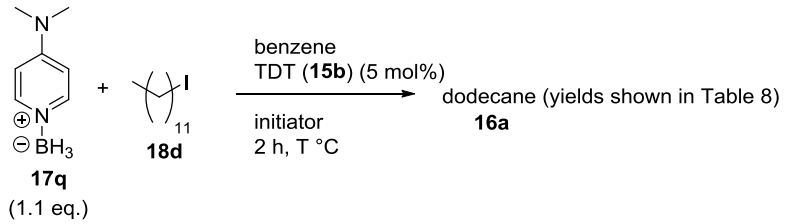

Figure 21: Reduction of 1-iododododecane (**18d**) with DMAP borane (**17q**), TDT (**15b**) in the presence of different initiators.

The results for the screening of initiators are shown in Table 8. As shown before, the initiation with BEt_3 (**2b**)/ O_2 led to low conversion (13 % dodecane (**16a**)). Di-*tert*-butyl peroxide (**2c**) as well as dicumyl peroxide (**2f**, DCPO) did not lead to the formation of **16a** at an initiation temperature of 80 °C. For AIBN (**2a**) a yield of 30 % was obtained. With respect to the class of hyponitrites, surprisingly DBHN (**2e**) turned out to be much less effective than TBHN (**2d**) under the described conditions. For DBHN (**2e**) a yield of only 17 % was obtained, whereas TBHN (**2d**) lead to 69 % of dodecane (**16a**).

Table 8: Results of the initiator screening as shown in Figure 21.

Initiator	temperature T [°C]	yield [%]
DTBP (**2c**) (20 mol%)	80	0
DCPO[a] (**2f**) (20 mol%)	80	0
BEt_3 (**2b**) (50 mol%)	rt	13
AIBN (**2a**) (20 mol%)	80	30
DBHN[b] (**2e**) (20 mol%)	80	17
TBHN (**2d**) (20 mol%)	80	69

[a] Toluene was used instead of benzene.

2.2.4. Dibenzylhyponitrite (DBHN, 2e) as initiator

In order to understand the difference in the initiation between TBHN (**2d**) and DBHN (**2e**), the decomposition of the two compounds under thermal conditions was investigated in the

absence of any other substrate. For DBHN (**2e**) a half life time of $t_{1/2}$ = 170 seconds at 60 °C was determined by ^{1}H NMR spectroscopy. In order to slow the decay of the substance down, the measurement was repeated at 40 °C and followed over 70 minutes. The mechanism of the decay of DBHN (**2e**) at 40 °C is shown in Figure 22. While releasing nitrogen, DBHN (**2e**) decomposes into two benzyloxy radicals. These may either undergo a cleavage reaction to form benzaldehyde (**21a**) or recombine to dibenzyl peroxide (**21b**). What is rather surprising is the fact that no H atom trapping by the benzyloxy radicals is observed, what would lead to benzyl alcohol (**21c**). A section of the ^{1}H NMR measurement after 30 minutes is shown in Figure 23. The upper part shows benzyl alcohol (**21c**) as reference (also measured in C_6D_6). The lower part shows remaining DBHN (**2e**) as well as the two products **21a** and **21b**, but no formation of benzyl alcohol (**21c**) is apparent.

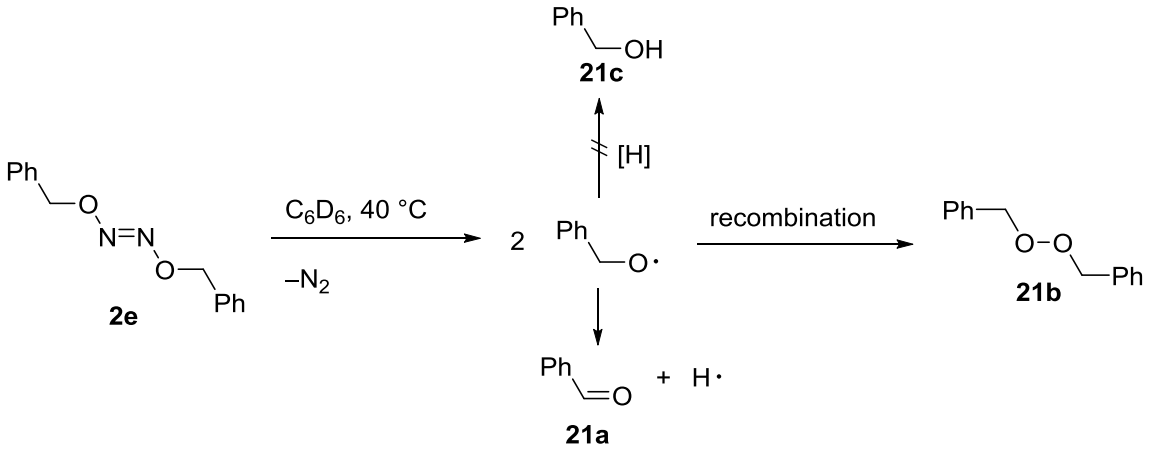

Figure 22: Mechanism of the thermal decay of DBHN (**2e**) at 40 °C.

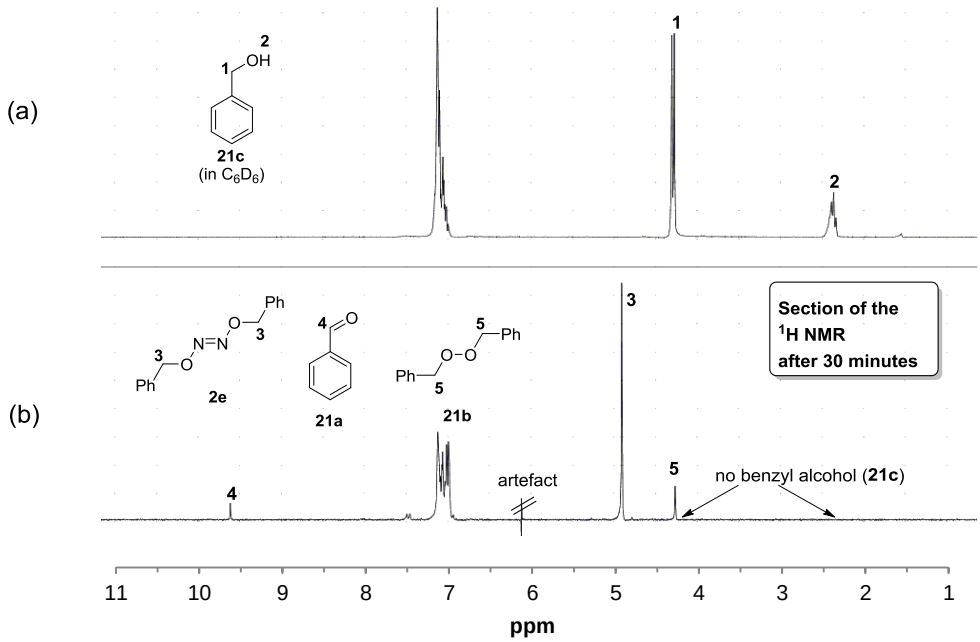

Figure 23: (a) Benzyl alcohol (**21c**). (b) Section of the ^{1}H NMR measurement of the decay of DBHN (**2e**) after 30 minutes.

The time-conversion plot of the decomposition of DBHN (**2e**) at 40 °C to benzaldehyde (**21a**) and dibenzyl peroxide (**21b**) is shown in Figure 24. The relatively high decomposition rate of DBHN (**2e**) even at low temperatures indicates that the yield of only 17 % dodecane (**16a**) in the reduction of 1-iododododecane (**18d**) may be due to the fast decay of the initiator.

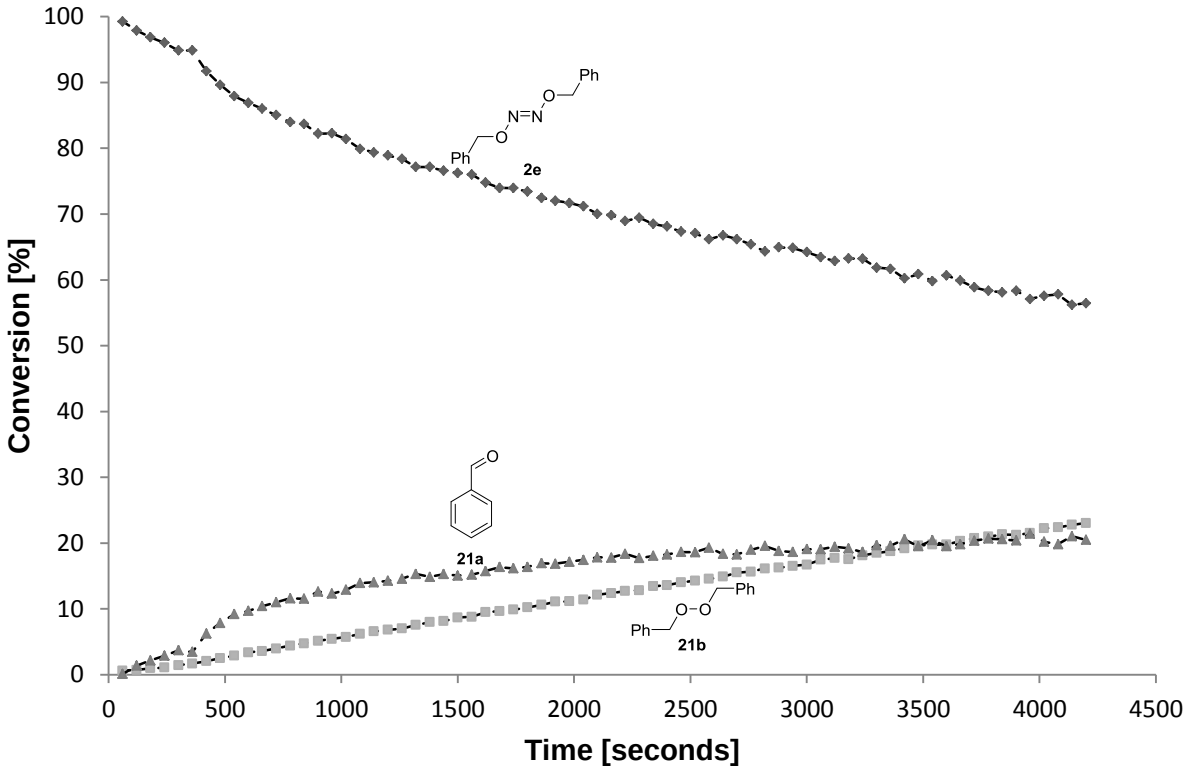

Figure 24: Decay of DBHN (**2e**) at 40 °C.

The fast decomposition of DBHN (**2e**) suggested to repeat the radical reaction at a lower temperature (Figure 25). Hence, the reaction was conducted at room temperature for two hours. 1,3,5-Trimethoxybenzene (**22**, TMB) was added as internal NMR standard. The desired reduction product **16a** was found in 2 % yield. The reaction mixture was also analyzed by GC/MS to detect possible side products. Tetracosane (**16c**) as the recombination product of two dodecyl radicals was found in traces (< 1%), the possible recombination product **23** of a benzyloxy radical with a dodecyl radical was not observed. For the low conversion two possibilities may be discussed. One obvious reason may be the bad solubility of DMAP borane (**17q**) at low temperature in nonpolar solvents such as benzene. Furthermore, it might also be possible, that higher temperatures are needed for the propagation steps of the reaction. However, as higher temperatures would again accelerate the decomposition of DBHN (**2e**), another solution was needed.

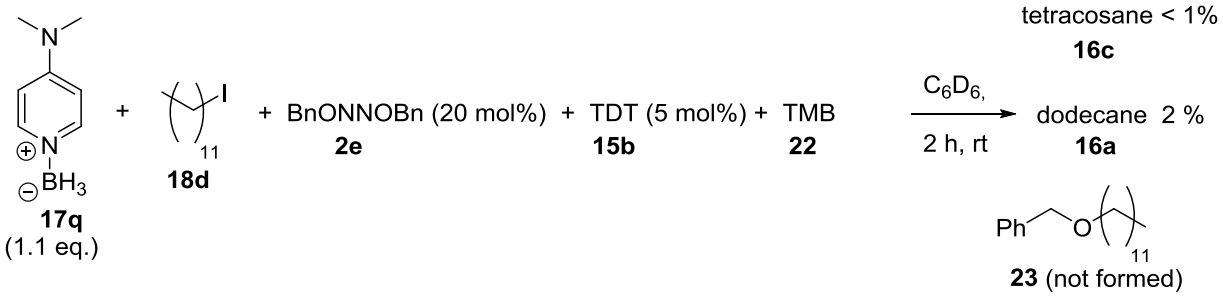

Figure 25: Reduction of 1-iodododecane (**18d**) with DMAP borane (**17q**), TDT (**15b**) and DBHN (**2e**) as initiator at room temperature.

2.2.5. Diethylaminopyridine borane (17z) as hydrogen atom donor

In order to increase the solubility of the borane complex, its structure was slightly modified. Therefore, 4-diethylaminopyridine borane (**17z**, DEAP borane) was synthesized in two steps (Figure 26). The first step was the formation of the free base **24** (DEAP). *Para*-aminopyridine (**24a**) was deprotonated stepwise with *n*BuLi (1.15 eq.) and afterwards alkylated with ethyl iodide (1.15 eq.) in THF at room temperature. This step was repeated. After quenching with water followed by extraction with chloroform, the crude product was purified by washing with isohexane and ethyl acetate. 4-diethylaminopyridine (**24**, DEAP) was obtained as slightly yellow wax (29 %). DEAP (**24**) was dissolved in THF at 0 °C and reacted with a Me_2S-BH_3 solution (1.10 eq.) for 10 minutes. Finally the pure DEAP borane (**17z**) was precipitated with isohexane as a white solid (59 %). This compound was found to be soluble in toluene as well as in benzene at room temperature, thus showing suitable properties for the low temperature radical reaction with DBHN (**2e**).

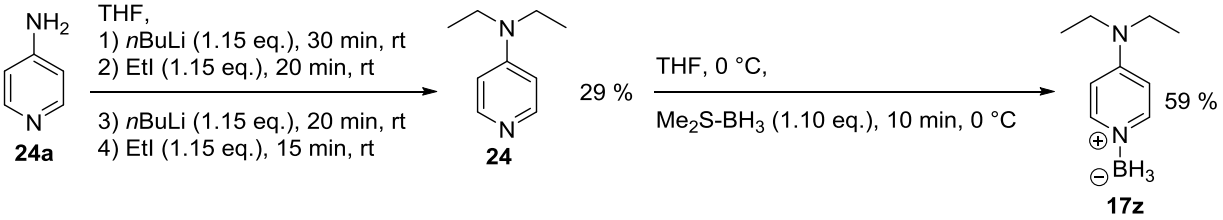

Figure 26: Synthesis of DEAP borane (**17z**).

The radical test reaction was repeated with DEAP borane (**17z**) in the same way as before with DMAP borane (**17q**) and is shown in Figure 27. However, the result turned out to be the same as before, despite the improved solubility of the reducing agent. Once again almost no conversion (2 %) to dodecane (**16a**) was observed. The solubility seems not to affect the reaction outcome very much. It is much more likely, that higher temperatures are required for a successful reduction with *N*-alkylated pyridine borane complexes, what makes DBHN (**2e**) an unsuitable initiator for this purpose.

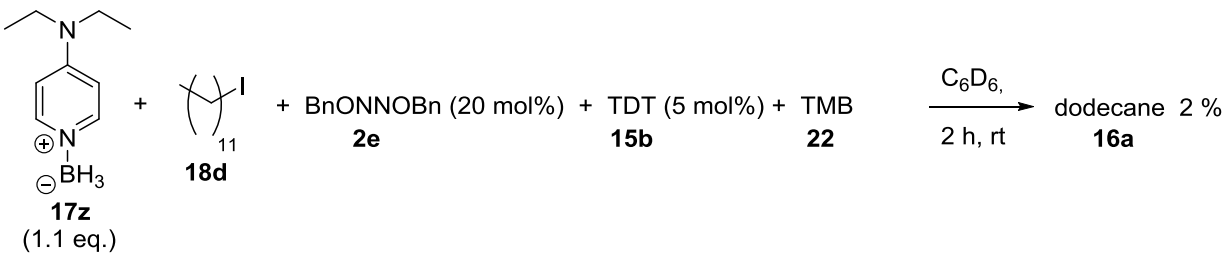

Figure 27: Reduction of 1-iodododecane (**18d**) with DEAP borane (**17z**), TDT (**15b**) and DBHN (**2e**) as initiator at room temperature.

2.3. Mechanistic aspects of the radical reduction of 1-iodododecane (18d) with dialkylaminopyridine boranes

2.3.1. Thermal decay of TBHN (2d)

The thermal decay of TBHN (**2d**) was investigated, as the compound had already shown promising results as initiator. The mechanism of the decomposition of TBHN (**2d**) at 80 °C is shown in Figure 28. Under release of nitrogen, the hyponitrite **2d** forms two *tert*-butoxy radicals. These may undergo either a recombination reaction to form di-*tert*-butylperoxide (**2c**) or a cleavage reaction which forms acetone (**25a**) and a methyl radical. As no further methylated products could be detected, these methyl radicals may now trap an H atom (e. g. from the solvent) or recombine to ethane (**16e**). A third pathway, which leads to *tert*-butanol (**25b**) by H atom trapping, was also observed. This finding is in contrast to DBHN (**2e**), where the formation of the corresponding alcohol was not detected.

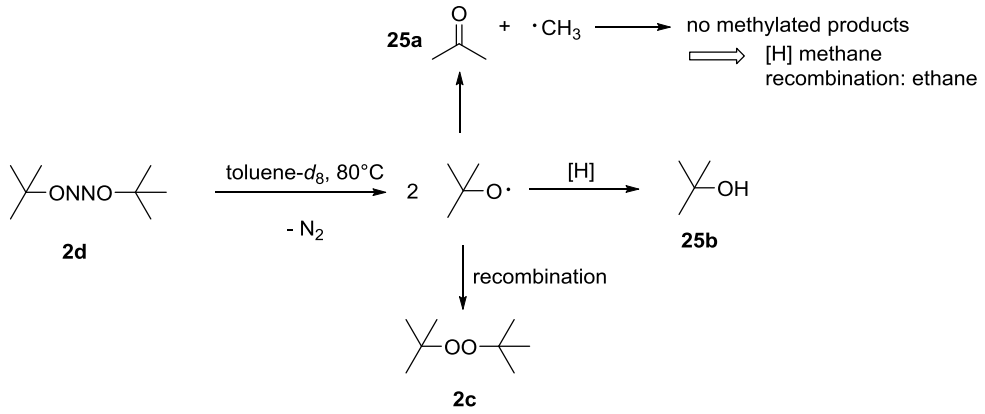

Figure 28: Mechanism of the decay of TBHN (**2d**) at 80 °C.

Figure 29 shows a section of the ^{1}H NMR spectrum taken during of the decay of TBHN (**2d**). The formation of the three products *tert*-butanol (**25b**), acetone (**25a**), and di-*tert*-butylberoxid (**2c**) such as remaining TBHN (**2d**) can be clearly seen. The chemical shifts in the mixture were compared to NMR spectra of the pure substances.

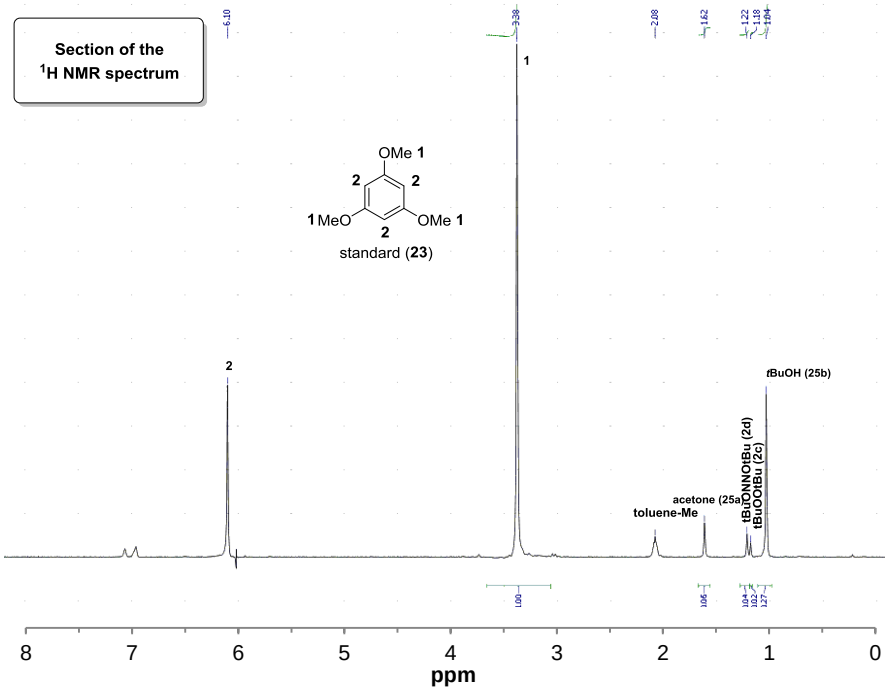

Figure 29: ^{1}H NMR spectrum of the decay of TBHN (**2d**).

The time-conversion plot of the decay of TBHN (**2d**) at 80 °C in toluene-d_8 is depicted in Figure 30 and was monitored by ^{1}H NMR spectroscopy. The half-life time of TBHN (**2d**) at 80 °C was assigned as $t_{1/2}$ = 520 seconds. After the measurement the ratio of the three products was determined as *tert*-butanol (**25b**) : acetone (**25a**) : di-*tert*-butylperoxide (**2c**) = 73 : 25 : 2. This shows, that the H trapping product is mainly formed here, whereas the recombination product plays only a minor role.

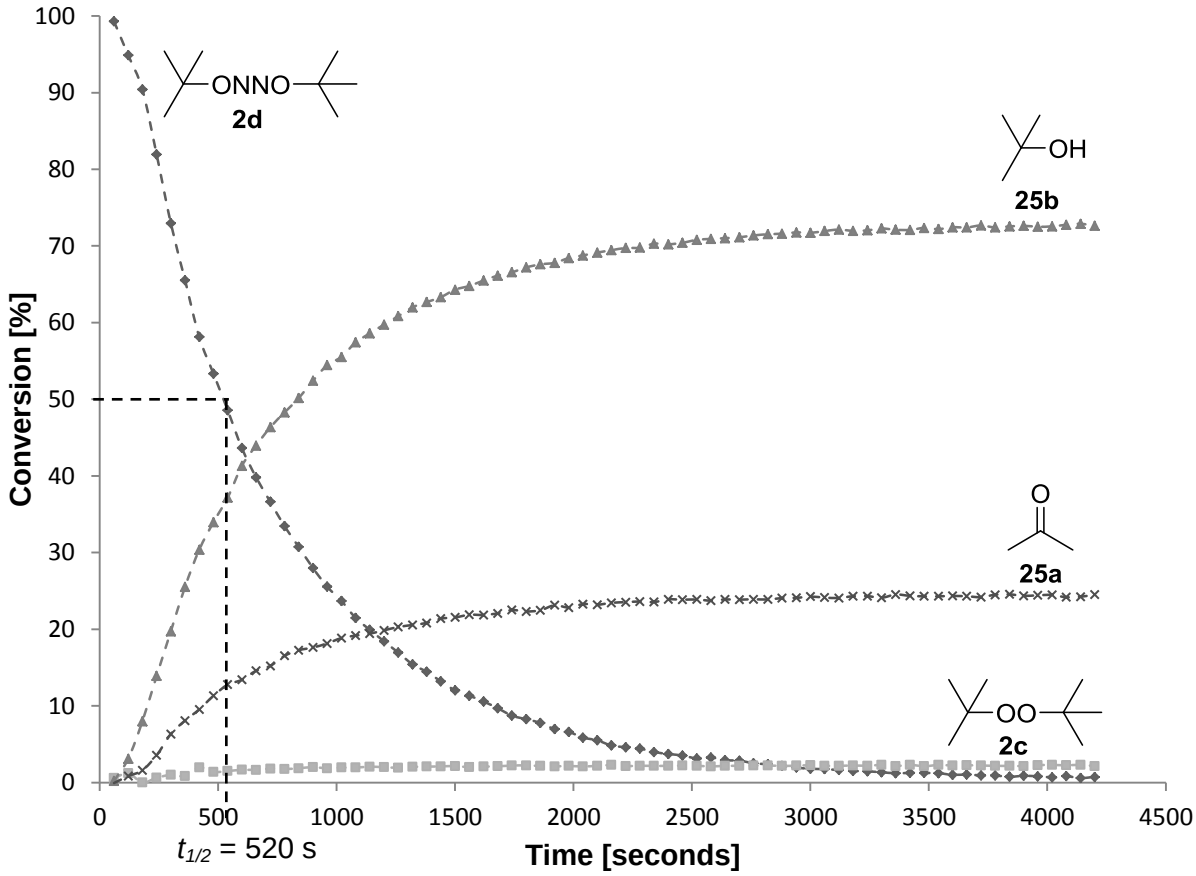

Figure 30: Time-conversion plot of the decay of TBHN (**2d**) at 80 °C in toluene-d_8.

2.3.2. Thermally induced decomposition of TBHN (2d) in the presence of DEAP borane (17z)

In order to understand the mechanism of the reduction of 1-iododododecane (**18d**), the reaction of the borane complex and the initiator was investigated. Therefore, DEAP borane (**17z**) was used, due to the better solubility in toluene, compared to DMAP borane (**17q**).

2.3.2.1. Mechanism

As in the previous radical experiments 20 mol% of TBHN (**2d**) was used and the reaction of the thermally activated initiator and the borane complex **17z** was monitored by ^{1}H and ^{11}B NMR spectroscopy in toluene-d_8 as solvent (Figure 31). The first step is again the formation of *tert*-butoxy radicals under evolution of nitrogen. These oxygen-centered radicals now can abstract an H atom from the borane complex to form boryl radical **25c** and *tert*-butanol (**25b**). A recombination of two *tert*-butoxy radicals or a cleavage reaction was not observed. Boryl radical **25c** now undergoes either a recombination with another *tert*-butoxy radical or attacks the oxygen of free TBHN (**2d**). This step forms borane complex **25d**, which could not be detected by NMR measurements. Thus, a fast decay of complex **25d** must be the following step. The reaction with *tert*-butanol (**25b**) leads to di-*tert*-butoxy borane (**25e**) and the free base DEAP (**24**). At that stage of the ongoing reaction the borane is not complexed any more to the base. Furthermore, hydrogen gas is released, which is also

detected in the ^{1}H NMR spectrum. As a final step, di-*tert*-butoxy borane (**25e**) reacts one more time with *tert*-butanol (**25b**) to form tert-butoxy borate (**25f**) as the final reaction product.

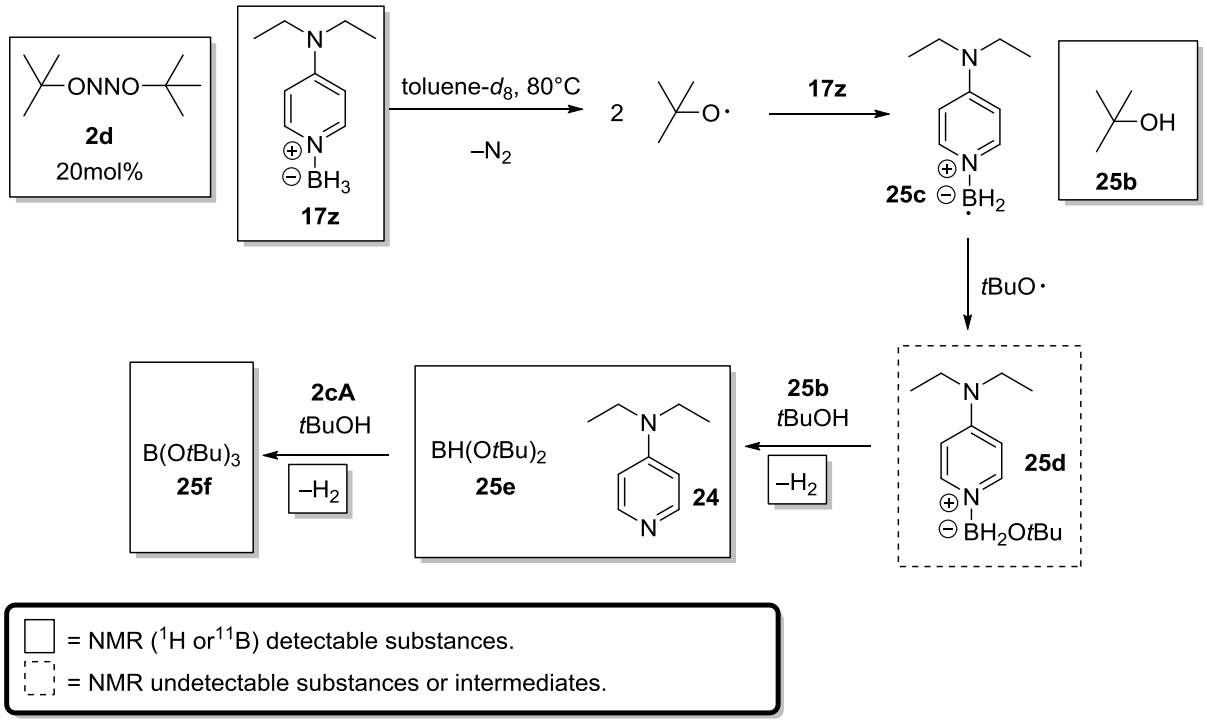

Figure 31: Mechanism of the decomposition of TBHN (**2d**) in presence of DEAP borane (**17z**) at 80 °C.

2.3.2.2. NMR studies

Figure 32a shows an example of a time dependent ^{11}B NMR study, where the formation of **25e** is detected. Figure 32b shows a section of the ^{11}B NMR measurement. Remaining DEAP borane (**17z**, quartet), which was used in excess, and di-*tert*-butoxy borane (**25e**, doublet) are detected. The final *tert*-butoxy borate (**25f**) has only formed to a small part at that stage of the reaction.

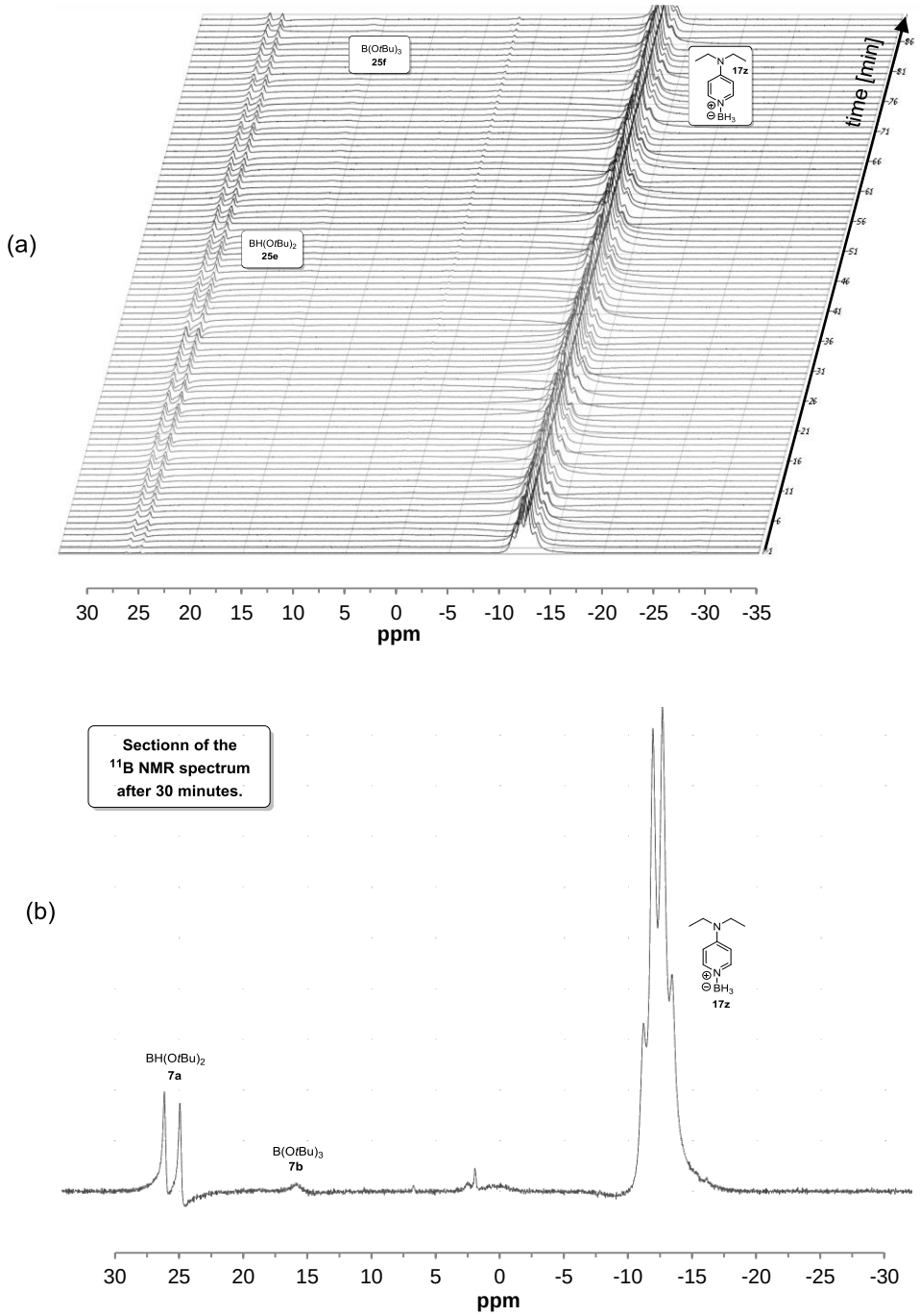

Figure 32: (a) Example of a time dependent ^{11}B NMR measurement of the decay of TBHN (**2d**) in the presence of DEAP-BH_3 (**17z**). (b) Section of the measurement after 30 minutes.

A time-conversion plot of the reaction between DEAP borane (**17z**) and the initiator could not be obtained, due to the complexity of the ^{1}H NMR spectrum, which did not allow an exact integration of the signals. A part of the ^{1}H NMR spectrum taken after ten minutes is shown in Figure 33. DEAP borane (**17z**) and the free corresponding base DEAP (**24**) are represented by the signals 1 to 8. Further substances (*tert*-butanol (**25b**, 1.06 ppm), TBHN (**2d**, 1.21 ppm), di-*tert*-butoxy borane (**25e**,1.24 ppm)) were identified by the NMR shift of their methyl groups, which was proven by independent measurements of the pure substances. The absence of the recombination product di-*tert*-butyl peroxide (**2c**, 1.18 ppm) as well as acetone (**25a**, 1.62 ppm) as the cleavage product is also obvious.

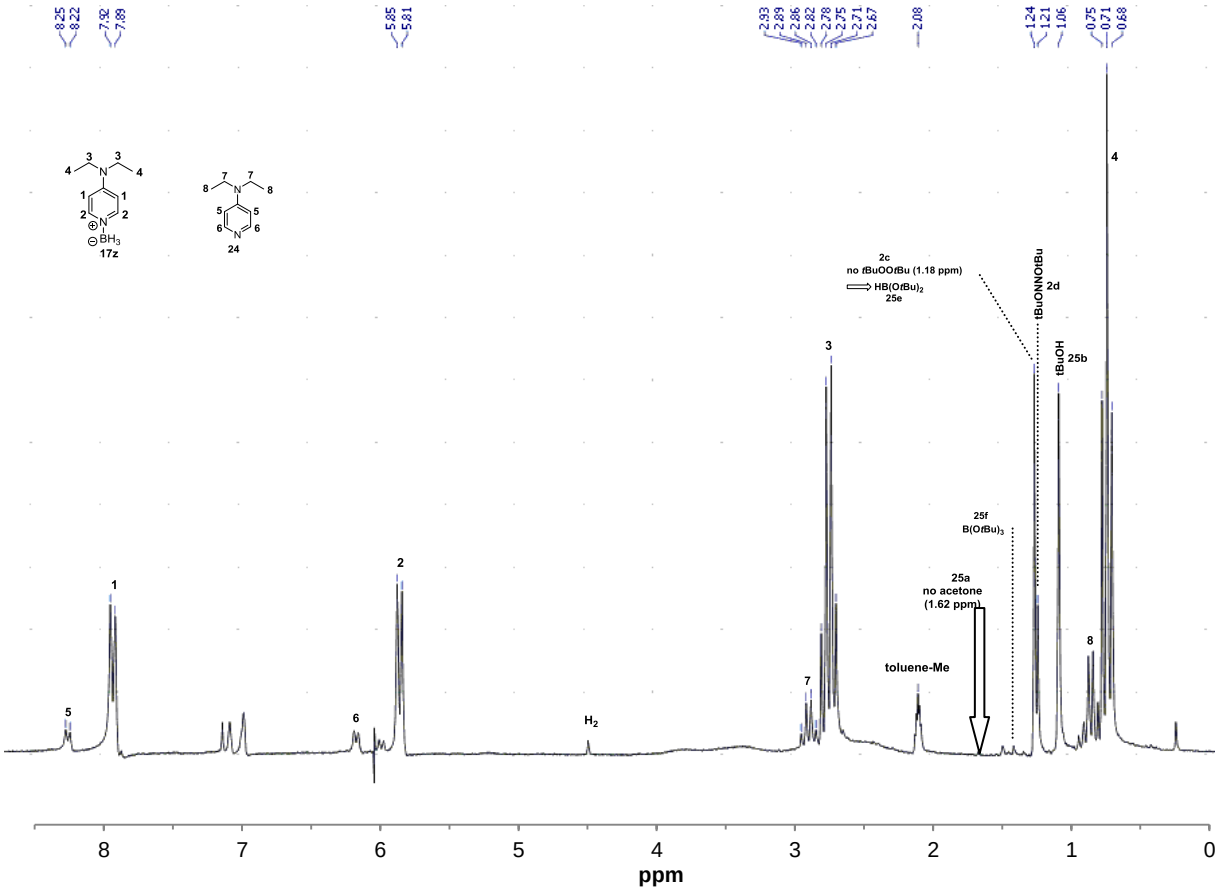

Figure 33: Products of the reaction of TBHN (**2d**) and DEAP borane (**17z**) at 80 °C in toluene-d_8. (^{1}H NMR measurement after 10 minutes.)

2.3.2.3. Independent control experiments

The versatile products of the thermal decomposition of TBHN (**2d**) and the reaction between DEAP borane (**17z**) and the initiator might also lead to side reactions. Therefore possible side reactions were checked independently (Figure 34). A reaction of DEAP borane (**17z**) with *tert*-butanol (**25b**) and acetone (**25a**) at 80 °C in toluene respectively could be excluded (Figure 34a and Figure 34b). Furthermore, di-*tert*-butoxy borane (**25e**) was synthesized by the reaction of Me_2S-BH_3 and *tert*-butanol (**25b**, 2 eq.) and immediately reacted with DEAP **24**, Figure 34c). The same was done with *tert*-butoxy borate (**25f**) and **24** (Figure 34d). In both cases no complexation was observed (determined by ^{11}B NMR). This finding indicates, that during the radical reaction a dissociation of the base and the borane occurs. A possible reaction between di-*tert*-butyl peroxide (**2c**) and the dissociated boron species **25e** and **25f** was also shown not to happen (Figure 34e and Figure 34f)

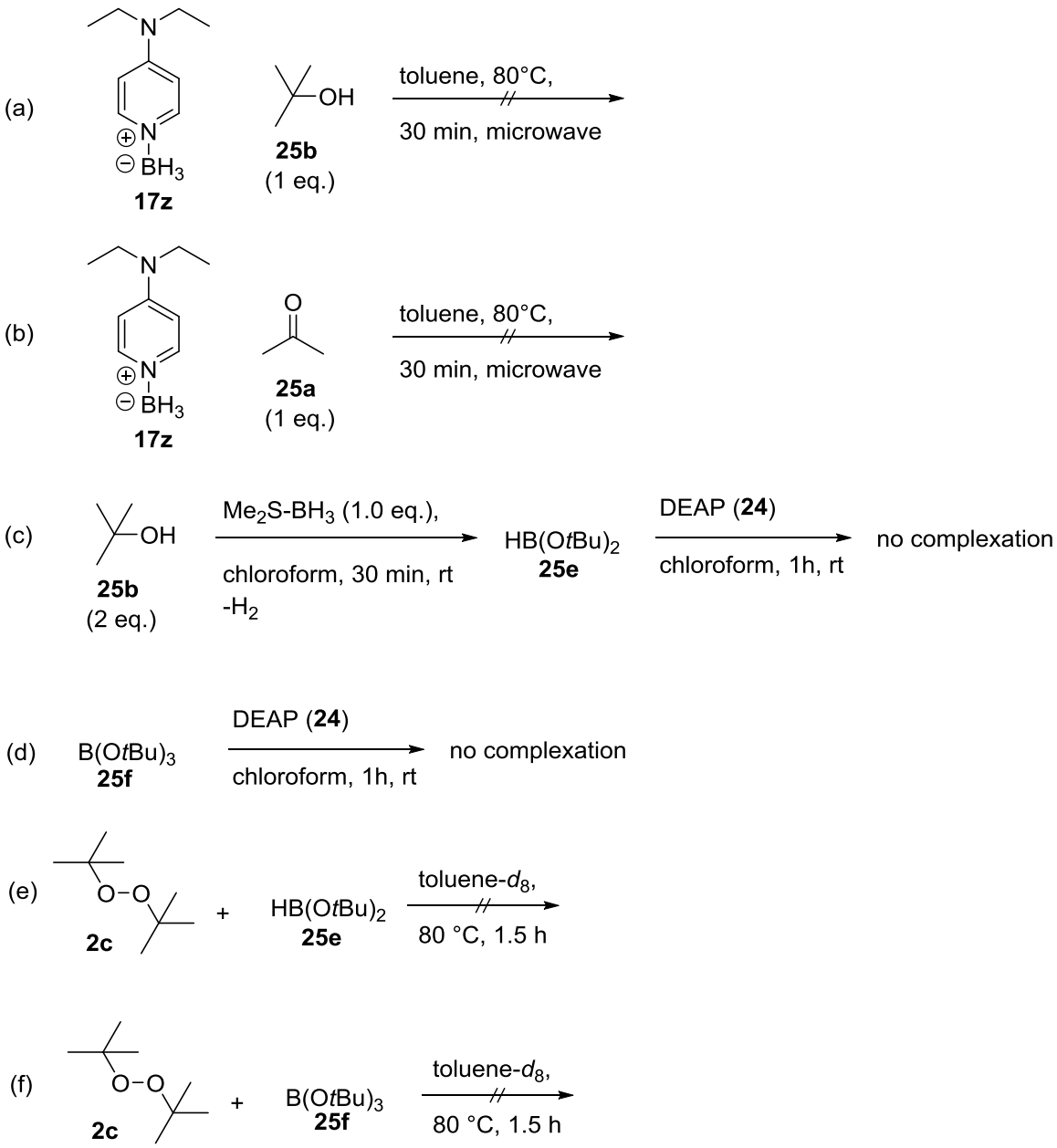

Figure 34: Independent investigation of possible side reactions, which could occur during the reaction of TBHN (**2d**) and DEAP borane (**17z**).

2.3.3. Closer analysis of the initiation with TBHN (2d) in the presence of DEAP borane (17z)

While the recombination product di-*tert*-butyl peroxide (**2c**) was formed in small amounts during the decay of TBHN (**2d**), for the reaction between initiator and borane this compound did not show up. Therefore, further studies on the initiation step were necessary, which will be discussed next.

2.3.3.1. Comparison with di-*tert*-butyl peroxide (2c)

In an independent test reaction it could be shown, that di-*tert*-butyl peroxide (**2c**, which is also a commercially available initiator) does not react with DEAP borane (**17z**) at 80 °C in toluene-d_8 over 1.5 hours (Figure 35). Subsequently this reaction can be excluded to happen during the initiation step with TBHN (**2d**). It is rather likely that an oxygen-centered radical is needed to abstract an H atom from the borane complex to generate boryl radical **25c**.

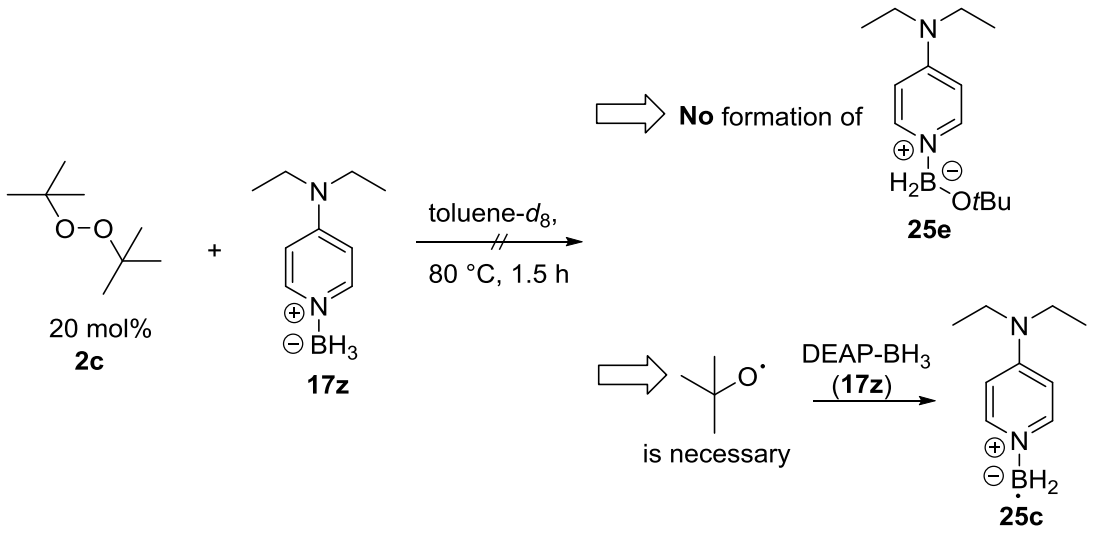

Figure 35: Investigation on the reaction of di-*tert*-butyl peroxide (**2c**) and DEAP borane (**17z**) at 80 °C in toluene-d_8.

2.3.3.2. Comparison with AIBN (2a)

The question came up, whether boryl radical **25c** is also able to attack on the oxygen of TBHN (**2d**) or eventually even on the nitrogen. Therefore the borane complex was reacted with the initiator AIBN (**2a**) at 80 °C in toluene-d_8 for 90 minutes and the reaction monitored by ^{1}H and ^{11}B NMR (Figure 36). Beside the decay of AIBN (**2a**) there was no reaction with the borane complex evident. This fact indicates, that the H abstraction from the borane complex by carbon-centered radicals is not very efficient, so that the boryl radical **25c** may not be formed unter these conditions.

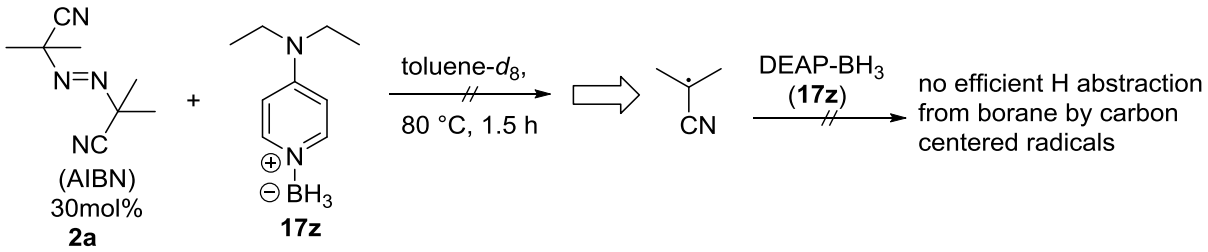

Figure 36: Reaction of AIBN (**2a**) and DEAP borane (**17z**) at 80 °C in toluene-d_8.

2.3.3.3. Competition experiment of TBHN (2d) and AIBN (2a)

In order to repeat the reaction in the presence of boryl radicals, TBHN (**2d**) was added (Figure 37). The decay of TBHN (**2d**) and the following reaction forms boryl radical **25c**. After 90 minutes, only the free base **24** as well as di-*tert*-butoxy borane (**25e**) and *tert*-butoxy borate (**25f**) was detected. No further reaction with AIBN (**2a**) or a recombination product from boryl radical **25c** and a carbon-centered radical was apparent. This finding supports the hypothesis, that boryl radical **25c** may attack the oxygen of TBHN (**2d**) but not on the nitrogen. Also a recombination of boryl radical **25c** with a non-oxygen-centered radical is very unlikely.

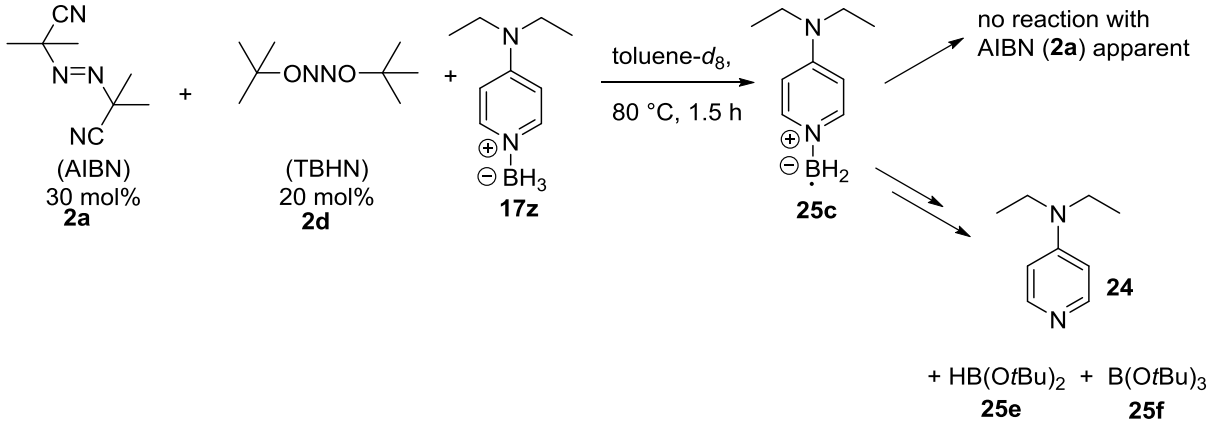

Figure 37: Investigation on the reaction of AIBN (**2a**) and DEAP borane (**17z**) in presence of TBHN (**2d**) at 80 °C in toluene-d_8.

2.3.3.4. Initiation in the presence of TBHN (2d) and di-*tert*-butyl peroxide (2c)

In order to determine if an attack of the boryl radical **25c** on the oxygen of the starter is possible, di-*tert*-butyl peroxide (**2c**, 30 mol%), TBHN (**2d**, 20 mol%) and DEAP borane (**17z**) were reacted at 80 °C in toluene-d_8 and monitored by ^{1}H NMR spectroscopy over 70 minutes (Figure 38).

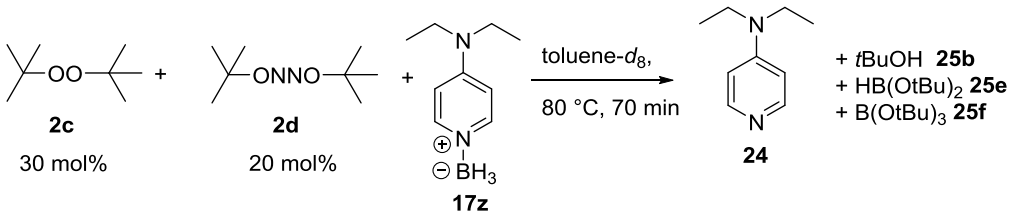

Figure 38: Reaction of di-*tert*-butyl peroxide (**2c**) and DEAP borane (**17z**) in the presence of TBHN (**2d**) at 80 °C in toluene-d_8.

The result of the experiment is shown in Figure 39 as a time-conversion plot. The most important result of this measurement is the complete decay of di-*tert*-butyl peroxide (**2c**) within ten minutes. This fact shows obviously, that once the boryl radical **25c** is formed, it reacts with the oxygen atoms of both initiators. In the absence of these radicals di-*tert*-butyl

peroxide (**2c**) had shown no reaction with DEAP borane (**17z**) under the same conditions. Thus, TBHN (**2d**) is capable for the formation of the boryl radical **25c**. Once it is formed also a peroxide, which usually would initiate at higher temperatures ($t_{1/2}$(141 °C) = 60 min)[52] can be involved in the reaction. Furthermore a fast rise of *tert*-butanol (**25b**) in the first ten minutes is detected, which than decreases as it may react with di-*tert*-butoxy borane (**25e**) or also undergo a reaction with the boryl radical **25c**.

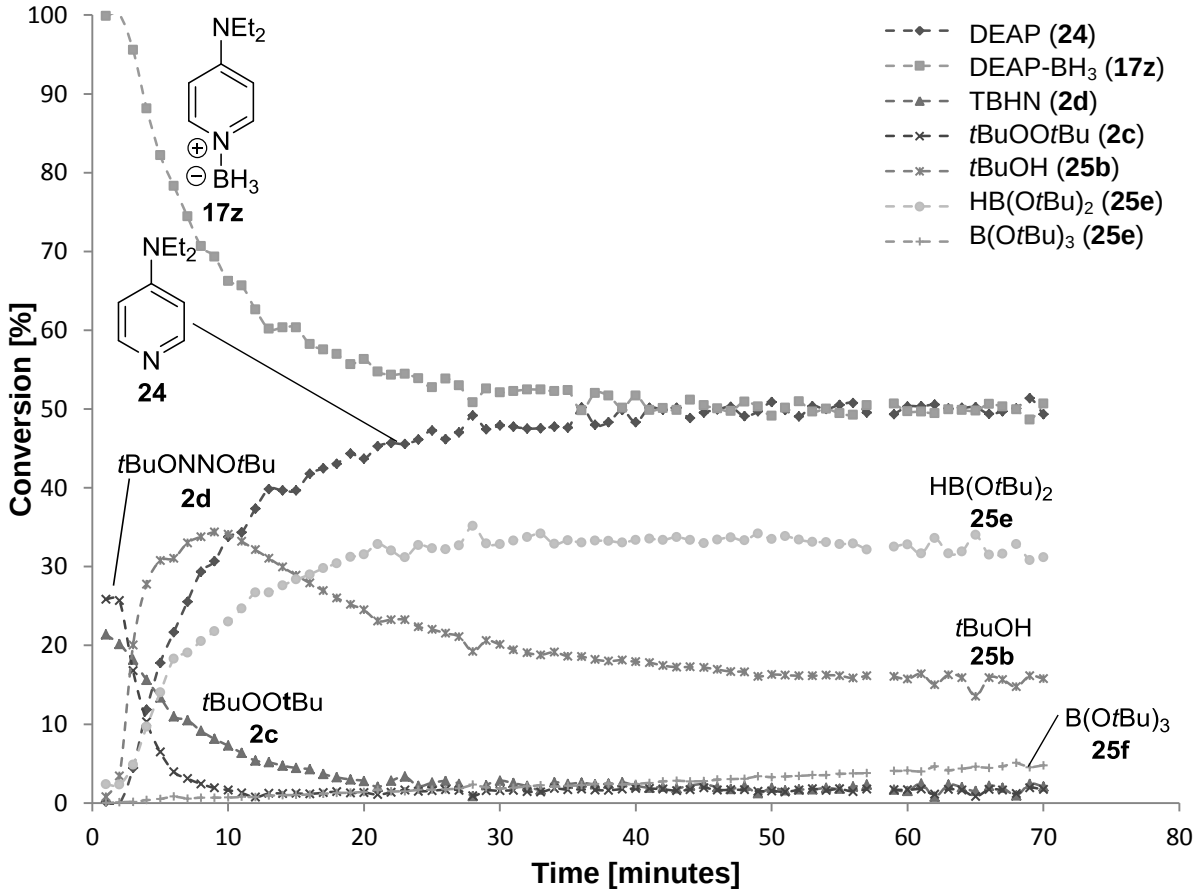

Figure 39: Time-conversion plot of the reaction of di-*tert*-butyl peroxide (**2c**) and DEAP borane (**17z**) in presence of TBHN (**2d**) at 80 °C in toluene-d_8.

The mechanism of the reaction of TBHN (**2d**) with DEAP borane (**17z**) in the presence of di-*tert*-butyl peroxide (**2c**) at 80 °C is shown in Figure 40. The decomposition of TBHN (**2d**) delivers two oxygen-centered radicals, whereas di-*tert*-butyl peroxide (**2c**) does not initiate at that temperature. The oxygen-centered radical abstracts an H atom from the borane complex **17z** to form boryl radical **25c** and *tert*-butanol (**25b**). At that stage three possible pathways can be discussed. The boryl radical may react with one of the oxygens of the hyponitrite **2d** or the peroxide **2c**. Another plausible pathway, which should be considered as a side reaction, is the recombination of a *tert*-butoxy radical with boryl radical **25c**. All steps lead to the formation of borane complex **25d**, which then leads to the free base **24** and the final boron species **25e** and **25f**.

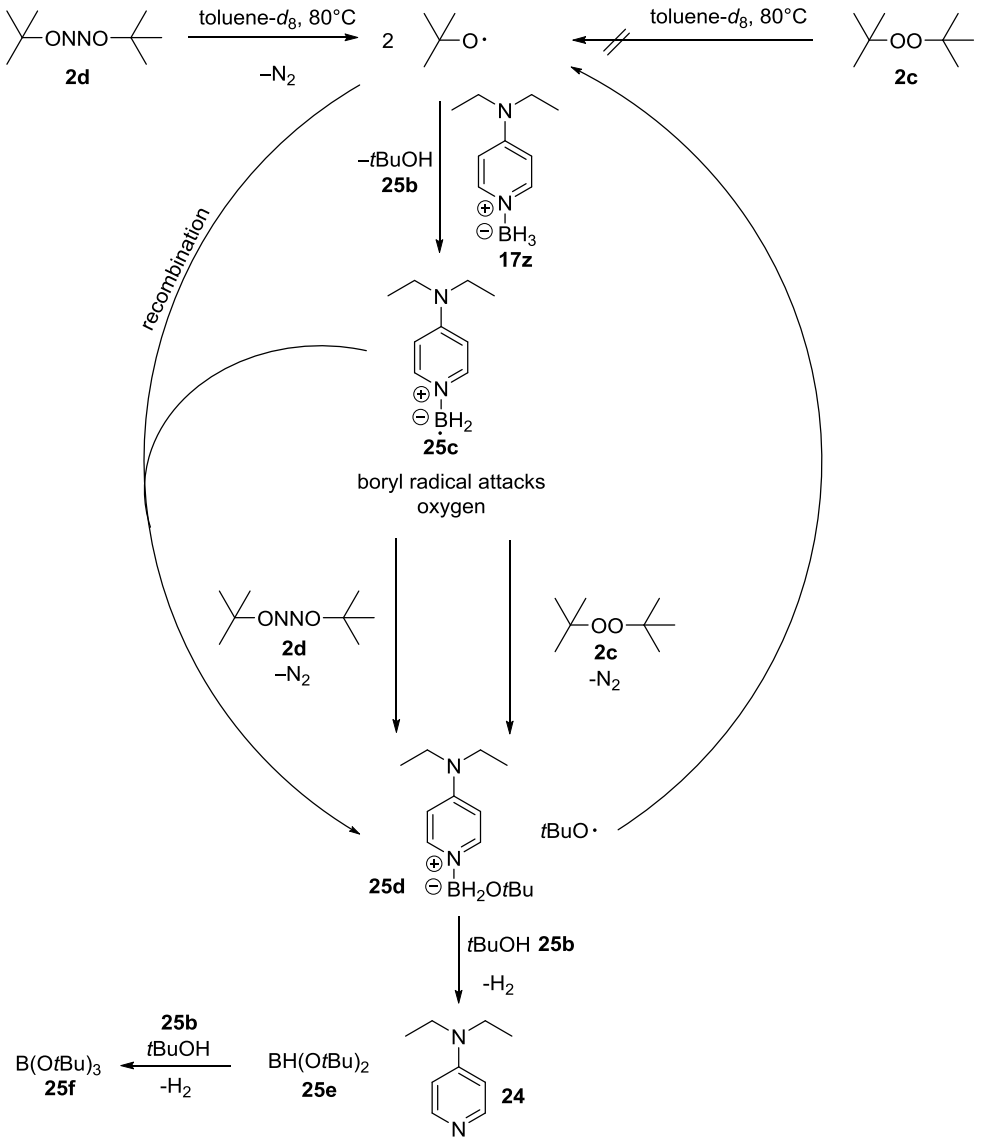

Figure 40: Mechanism of the reaction of di-*tert*-butyl peroxide (**2c**) and DEAP borane (**17z**) in presence of TBHN (**2d**) at 80 °C.

2.3.3.5. Comparison with di-*tert*-butyl peroxide (2c) and dicumyl peroxide (2f) as high temperature initiatiors

The results described above suggest that the much cheaper di-*tert*-butyl peroxide (**2c**) can also be a useful initiator, as it produces two oxygen-centered radicals during thermal initiation. Based on the previous results, it seemed obvious, that the formation of an oxygen-centered radical was the key step for a successful outcome of the radical reaction. So, the initial reduction of 1-iodododecane (**18d**) was repeated with DTBP (**2c**, 20 mol%) at 100 °C and 110 °C without success (Figure 41). The explanation for this result seems to be the too low initiation temperature for this radical starter. With half-life times of DTBP (**2c**) of $t_{1/2}$(141 °C) = 60 min and $t_{1/2}$(121 °C) = 10 h, the temperature of 110 °C is just too low for a sufficient initiation. Furthermore a thermal initiation at higher temperatures is not possible as the borane complex **17z** undergoes a fast ionic reduction of alkyl halides at temperatures above 110 °C, which will be discussed in a later section. Subsequently dicumyl peroxide (**2f**),

which initiates at slightly lower temperatures, was chosen ($t_{1/2}$(132 °C) = 60 min, $t_{1/2}$(112 °C) = 10 h). The thermal initiated reduction of 1-iodododecane (**18d**) was tried again at 110 °C with dicumyl peroxide (**2f**, 20 mol%) as initiator with the same result as before (Figure 41). Although initiation with dicumyl peroxide (**2f**) takes place at moderate lower temperatures compared to di-*tert*-butyl peroxide (**2c**), the formation of oxygen-centered radicals at 110 °C seems not to be efficient enough.

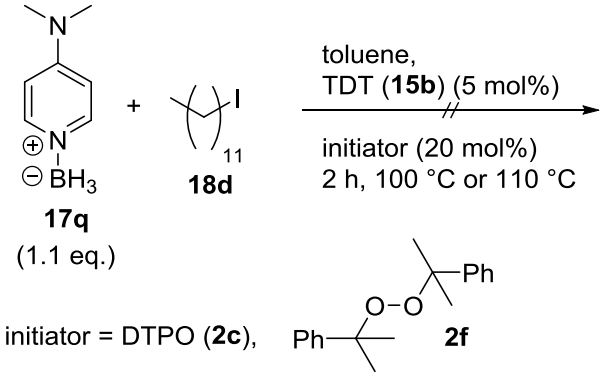

Figure 41: Reduction of 1-iodododecane (**18d**) with DMAP borane (**17q**) and TDT (**15b**) with the high temperature initiating peroxides **2c** and **2f**.

2.3.3.6. Comparison with initiation on irradiation

As DTBP (**2c**) and dicumyl peroxide (**2f**) are also known to decompose on irradiation, this kind of initiation method was tried next. Therefore the solvent was changed, as the absorption of toluene or benzene below 290 nm would compensate the UV light. Dicumyl peroxide (**2f**) was dissolved in $CDCl_3$ and put under an UV lamp (254 nm) for one hour and the decomposition checked by ^{1}H NMR (Figure 42a). After one hour acetophenone (**26a**, 19 %) as the cleavage product and 2-phenyl-2-propanol (**26b**, 11 %) as the H trapping product had formed. The ^{1}H NMR analysis of the reaction is shown in Figure 42b. The formation of the products as well as remaining dicumyl peroxide (**2f**) is obvious and can be characterized by the NMR shifts of the corresponding methyl groups.

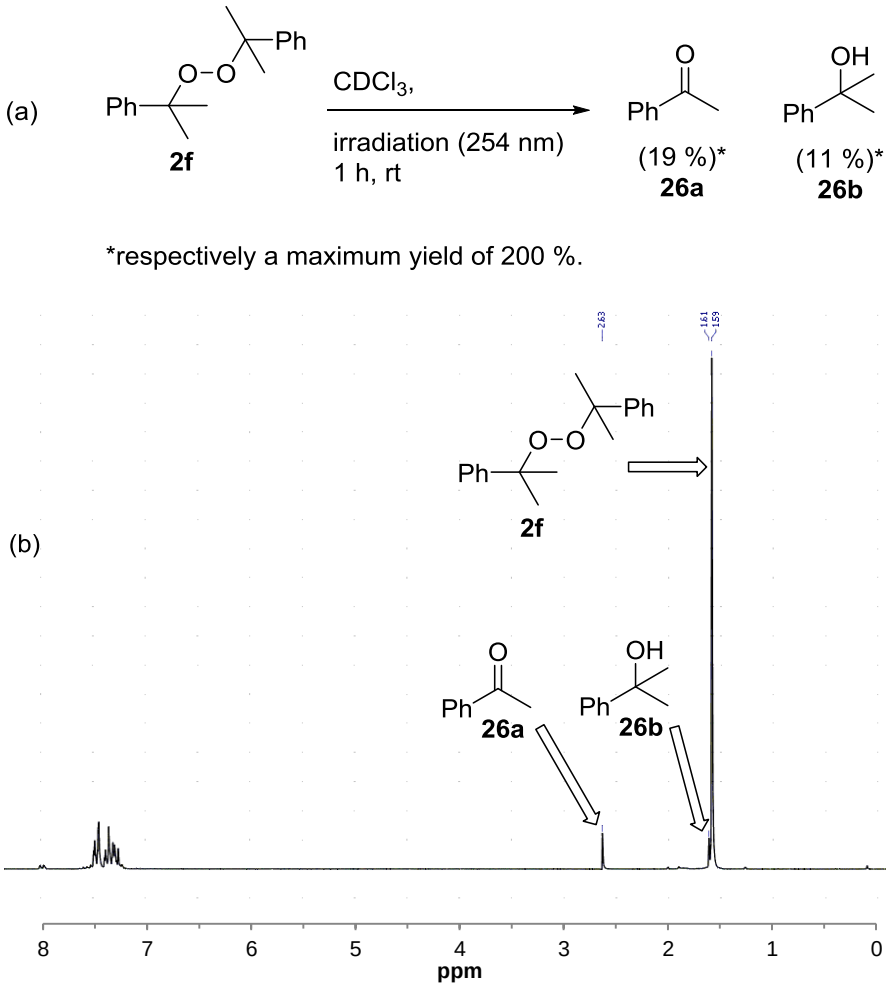

Figure 42: Decay of dicumyl peroxide (**2f**) by irradiation (254 nm) after one hour at room temperature in $CDCl_3$.

With this result in hand, the reduction of 1-iododododecane (**18d**) by irradiation of the initiator was performed again in $CDCl_3$ at room temperature (Figure 43a). As no formation of dodecane (**16a**) was detected, the reaction was repeated at a higher temperature. Previous studies with TBHN (**2d**) and DBHN (**2e**) had also shown temperature dependence for the reduction of 1-iododododecane (**18d**). As the reaction was performed in an open vessel, in order to irradiate the mixture with an UV lamp from above, chloroform (bp. 61 °C) was replaced by 1,4-dioxane (bp. 101 °C) and the reaction was repeated at 80 °C (Figure 43b). However, even at 80 °C no formation of dodecane (**16a**) was apparent. Finally, 1-iododododecane (**18d**) was replaced by xanthate **18c** (Figure 43c), which usually is also very potent for TBHN (**2d**) initiation at 80 °C (which will be discussed later). Yet, no reduction of the xanthate was observed.

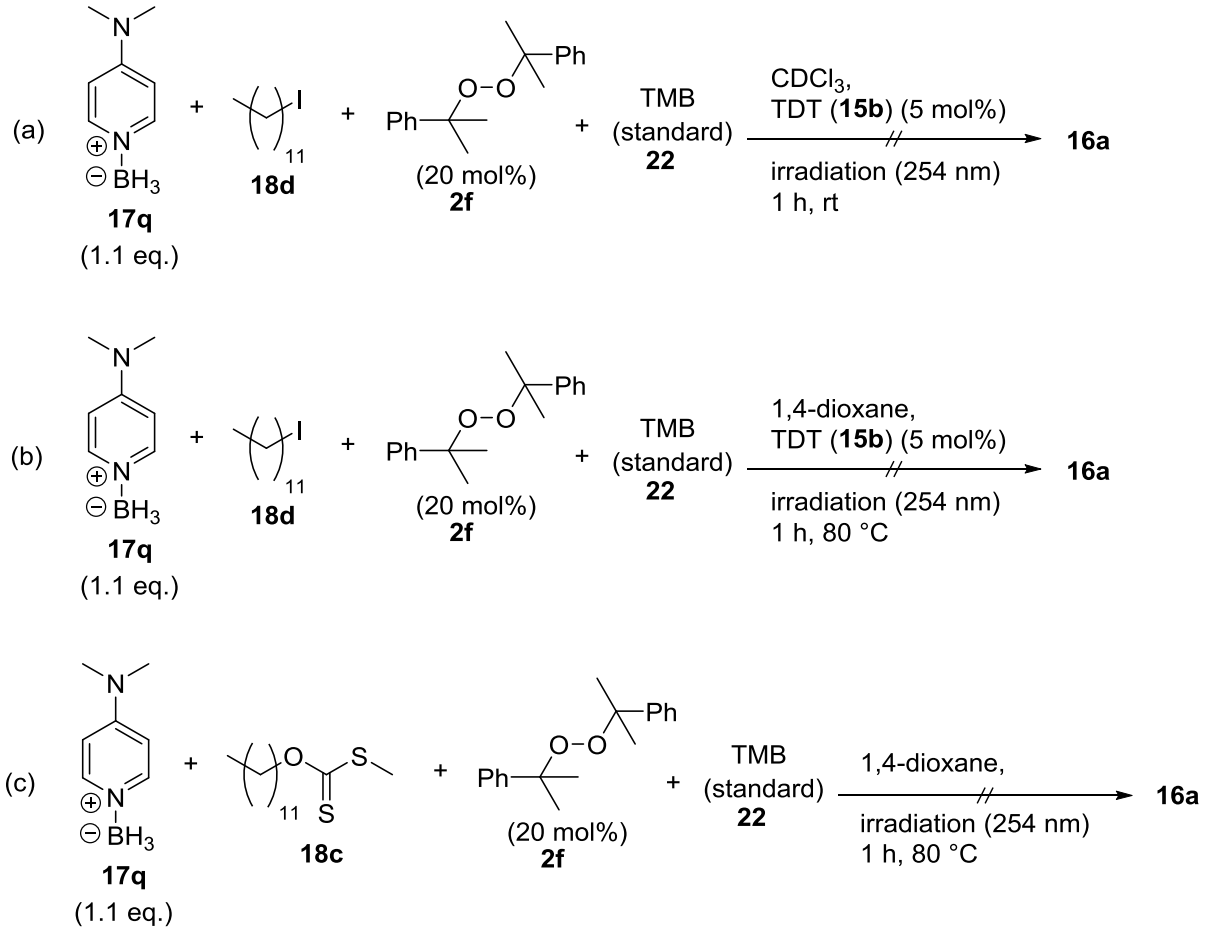

Figure 43: Reduction reactions with DMAP borane (**17q**) and dicumyl peroxide (**2f**) by UV-irradiation (254 nm). (a) In $CDCl_3$ at room temperature. (b) In 1,4-dioxane at 80 °C. (c) With xanthate **18c** in 1,4-dioxane at 80 °C.

In order to find a reason for the unsatisfactory reaction outcome, DMAP borane (**17q**) was dissolved in $CDCl_3$ and irradiated for one hour (254 nm) at room temperature. Surprisingly, 44 % of borane complex **17q** had decomposed to form DMAP (**27**) and BH_3 (**28**, Figure 44). The formation of the free base was monitored by ^1H NMR spectroscopy. Subsequently, the release of BH_3 (**28**) leads to the formation of boric acid (**28a**) by reaction with air humidity, which can be seen as a white precipitate from the former clear $CDCl_3$ solution. This indirectly proves the formation of gaseous BH_3 (**28**), which was not detected spectroscopically. The outcome of this experiment clearly indicates, why dicumyl peroxide (**2f**) is not a suitable initiator upon irradiation. The decomposition of the borane complex seems to compete with the decay of the radical starter. Thus, the rise of temperature to 80 °C does also speed up the decay of the complex, no reduction of the alkyl halide being the consequence.

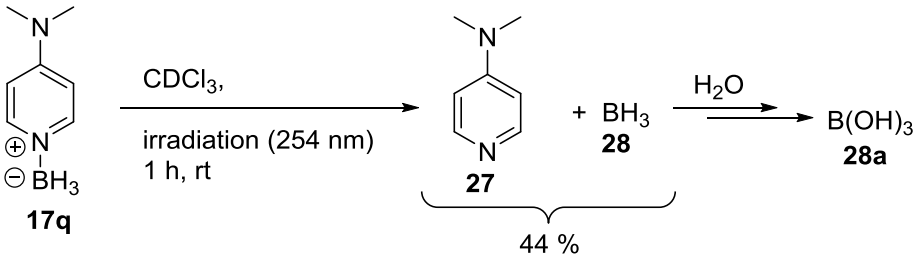

Figure 44: Decomplexation of DMAP borane (**17q**) at room temperature by irradiation (254 nm) after 1 h.

2.3.4. Reduction of 1-iododododecane (18d) with DEAP borane (17z) and TBHN (2d)

All the results up to that point indicate that the choice of the initiator, as well as the right condition is very important for a successful reduction with pyridine-derived borane complexes. The formation of an oxygen-centered radical during the initiation step seems essential and limits possible initiation systems. Beside hyponitrites, peroxides or peresters may deliver these radicals. However, only the formation of an oxygen-centered radical does not automatically grant success, what DBHN (**2e**) and dicumyl peroxide (**2f**) have shown. At too low temperature, the reduction becomes inefficient, despite the presence of oxygen-centered radicals (compare DBHN (**2e**)). The same unsatisfying result is achieved if the initiator is decomposing too fast at higher temperatures (DBHN (**2e**)). Yet, temperatures above 120 °C lead to an undesired ionic reduction of the alkyl halide (which will be discussed later), resulting in the exclusion of high temperature initiators such as dicumyl peroxide (**2f**). Furthermore, irradiation (at the wavelength of 254 nm applied here) leads to decomplexation of the borane faster than any effective initiation could occur. All these findings demonstrate, that there is only a very small region, in which the borane complex is compatible with the radical starter.

2.3.4.1. Mechanism

Subsequently, the promising system of DEAP borane (**17z**) and TBHN (**2d**, 20 mol%), together with 1-iododododecane (**18d**) as substrate, was analyzed in more detail at 80 °C. The yield of dodecane (**16a**) was 45 % under these conditions. The complex mechanism was clarified by ^{1}H and ^{11}B NMR spectroscopy and is shown in Figure 45.

The initiation step is the thermal decomposition of TBHN (**2d**), which leads to *tert*-butoxy radicals. These react with DEAP borane (**17z**) to the boryl radical **25c** and *tert*-butanol (**25b**). Two chain reactions may be considered for the mechanism. The first chain reaction is the reaction of radical **25c** with the initiator, which leads to a *tert*-butoxy radical and borane complex **25d**. The *tert*-butoxy radical is reinvolved in the chain reaction, whereas borane complex **25d** leads to versatile ionic side reactions. The second chain reaction is the halide-abstraction by boryl radical **25c**, leading to a dodecyl radical and borane complex **25h**. The desired product dodecane (**16a**) is formed by a hydrogen transfer from DEAP borane (**17z**) to the dodecyl radical, which regenerates boryl radical **25c**. As termination step, the recombination of an oxygen-centered radical with boryl radical **25c** seems most plausible. Other recombination reactions (for example the recombination of two dodecyl radicals) may

also be taken into account. However, no other recombination products could be detected by NMR spectroscopy and GC/MS analysis. Problematic for the moderate yield of only 45 % of **16a** are the versatile side reactions, especially the formation of the bispyridyl borane complex **25i**. Borane complex **25h** as well as the free base DEAP (**24**) could not be detected during the reaction, thus these species must undergo fast side reactions, one of them leading directly to the bispyridyl borane complex **25i**. The formation of free diethylaminopyridine (**24**) is attributed to the decomplexation of the borane species **25d** and **25g**. Furthermore, borane complex **25h** reacts fast with *tert*-butanol (**25b**), leading to the instable *tert*-butoxy borane (**25n**) and DEAP hydroiodide (**25j**). The hydroiodide species **25j** can now react with DEAP borane (**17z**) and build up bispyridyl borane complex **25i**. The side reactions, which lead to the bispyridyl species **25i**, will be looked at in detail in the next section.

Finally, *tert*-butoxy borane (**25n**) may either disproportionate or react with *tert*-butanol (**25b**) and/or acetone (**25a**), which comes from the cleavage reaction of the *tert*-butoxy radical. The final products are disubstituted and trisubstitutet boron species (**25e**, **25f**, **25k, 25l** and **25m**), which show small differences in their ^{11}B NMR shifts, which will be shown later. It should be mentioned, that the formation of elemental hydrogen can also be detected by ^{1}H NMR spectroscopy (singlet at 4.50 ppm in toluene-d_8). The large number of possible side reactions seems to be a plausible explanation for the yield of only 45 % of dodecane (**16a**).

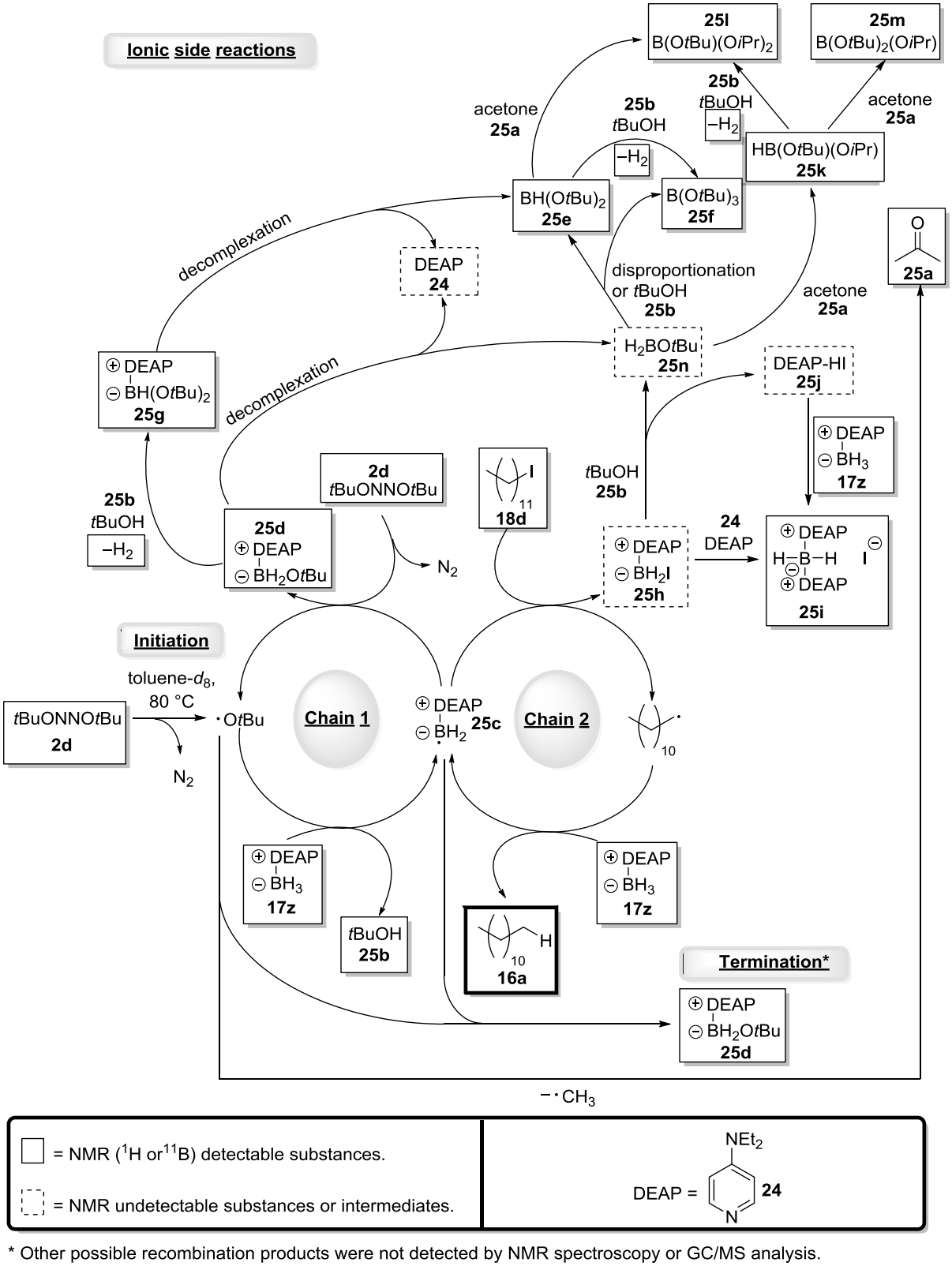

* Other possible recombination products were not detected by NMR spectroscopy or GC/MS analysis.

Figure 45: Mechanism of the reduction of 1-iodododecane (**18d**) with DEAP borane (**17z**) and TBHN (**2d**) at 80 °C in toluene-d_8.

2.3.4.2. NMR studies

In order understand the complexity of the proposed mechanism better, the time-dependent ^{11}B NMR is shown in Figure 46. The reaction was monitored over 90 minutes (Figure 46, y-axis). It is obvious, that the main part of the reaction takes place in the first 30 minutes. The decay of the borane complex **17z**, which leads to the formation of borane complex **25d** and the mixed *tert*-butoxy and *iso*-propoxy borane species, is the main reaction during these first 30 minutes. The fact, that most of the starting borane **17z** is consumed after 30 minutes is consistent with the decay of TBHN (**2d**) after that time (Figure 30, page 26). The formation of the borane species **25g** as well as the appearance of the final mixed borate species is much slower. Nevertheless, the reaction between DEAP borane (**17z**) and the initiator TBHN (**2d**) seems to compete against a successful hydrogen atom transfer to the dodecyl radical.

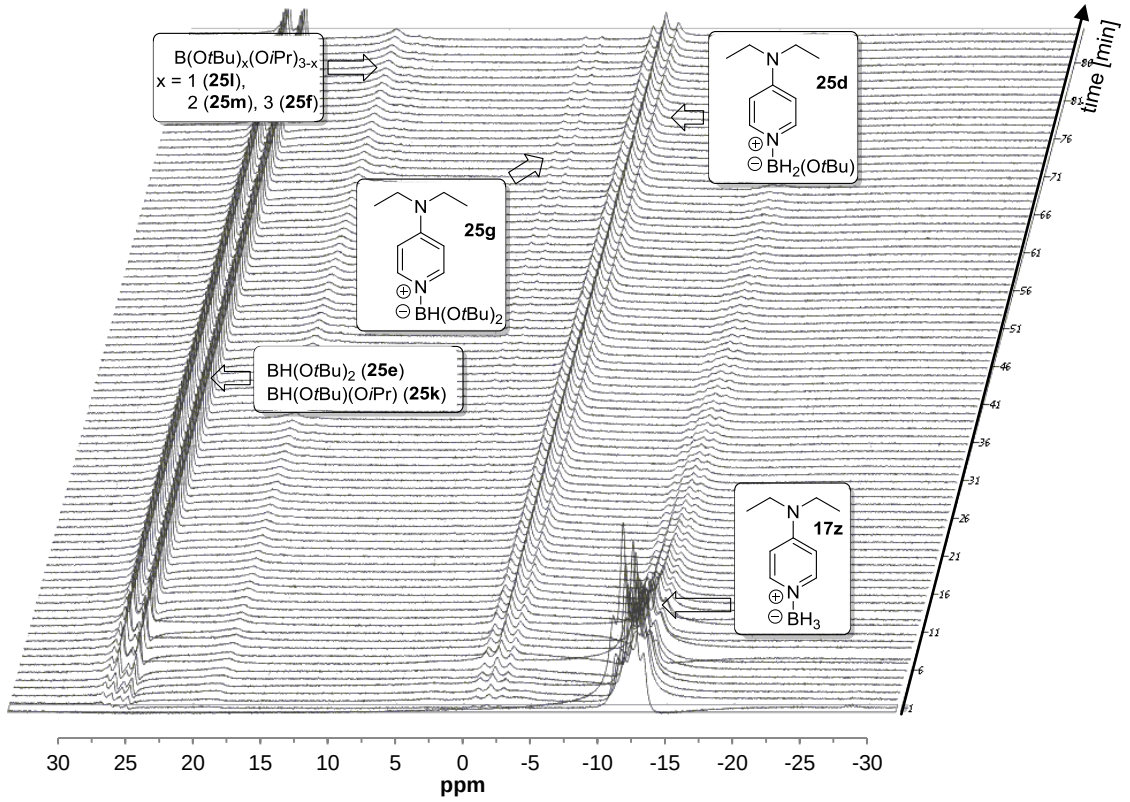

Figure 46: Time-dependent ^{11}B NMR measurement of the reduction of 1-iododododecane (**18d**) with DEAP (**17z**) borane and TBHN (**2d**) at 80 °C in toluene-d_8.

Results from the ^{11}B NMR measurements after 60 minutes reaction time are shown in Figure 47. Figure 47a shows the ^{1}H coupled measurement after 60 minutes, Figure 47b displaying the {^{1}H} ^{11}B NMR measurement. The comparison of both spectra is necessary to prove the number and kind of species with the help of their multiplets. The presence of the three borane complexes **25d**, **25g** and DEAP borane (**17z**) can be detected as a doublet, a triplet and a quartet. The two mixed borane species **25e** and **25k** show up as two doublets (two singlets in the {^{1}H} ^{11}B NMR measurement). The final mixed borate species **25f**, **25l** and **25m** are reflected by singlets in both spectra.

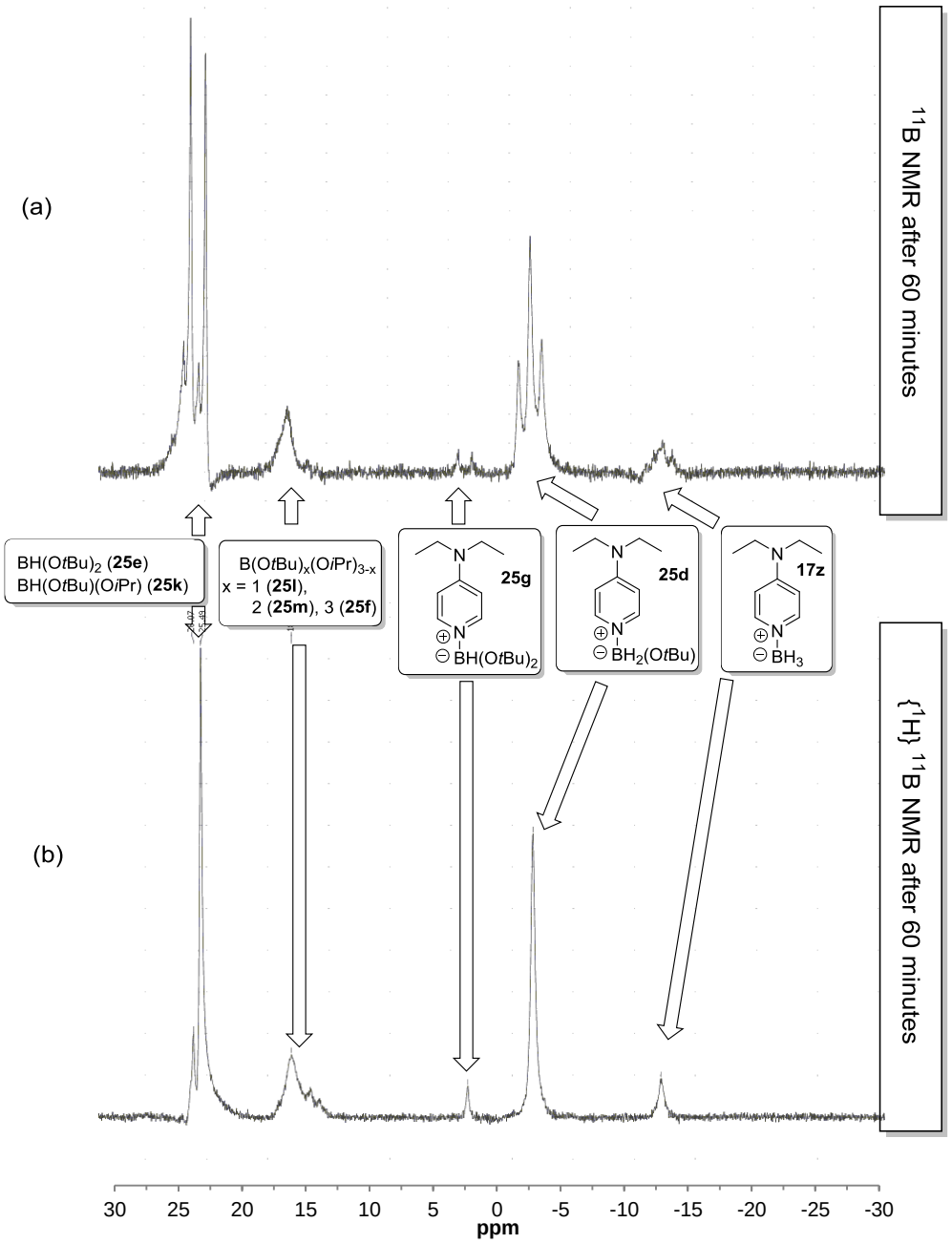

Figure 47: ^{11}B NMR product analysis of the reduction of 1-iododododecane (**18d**) with DEAP borane (**17z**) and TBHN (**2d**) at 80 °C in toluene-d_8.

2.3.4.3. Formation of a bispyridyl borane complex

Bispyridyl borane complex **25i** cannot be detected at all during ^{11}B NMR the measurements. This is due to precipitation of **25i** as a white solid during the reactions. This precipitate could be recrystallized from toluene/DCM through slow evaporation of DCM yielding crystals suitable for X-ray analysis. The X-ray structure of bispyridyl borane complex **25i** is shown in Figure 48. The BN distance of 1.576 Å of this complex is slightly shorter than the BN distance in DMAP-BH$_3$ (**17q**, 1.596 Å). This might be due to electronic effects by attaching a second pyridine ligand to the boron atom.

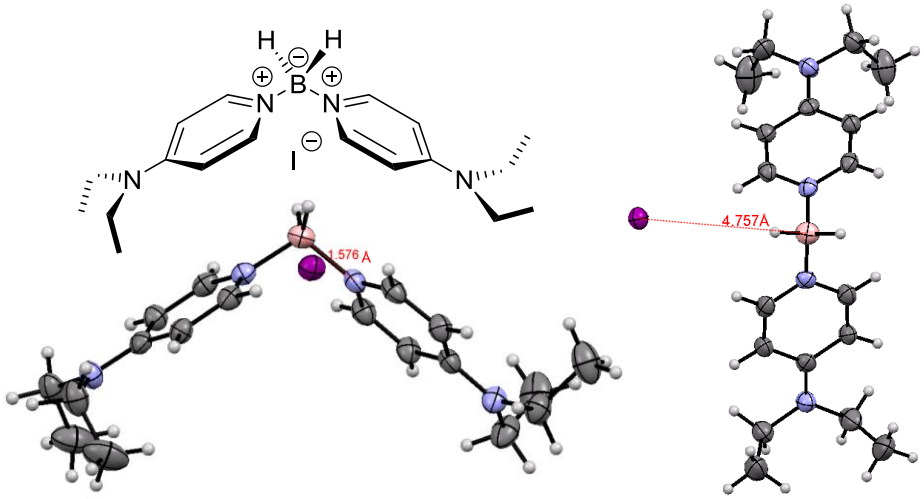

Figure 48: X-ray structure of bispyridyl borane complex **25i** (d(BN) = 1.576 Å, d(BI) = 4.757 Å).

As complex **25i** is completely unsoluble in toluene, it did never show up during NMR measurements of the radical reaction. However, by dissolving the substance in DMSO-d_6, NMR spectra of bispyridyl borane complex **25i** could be obtained. The ^{1}H and ^{11}B NMR spectra are shown in Figure 49.

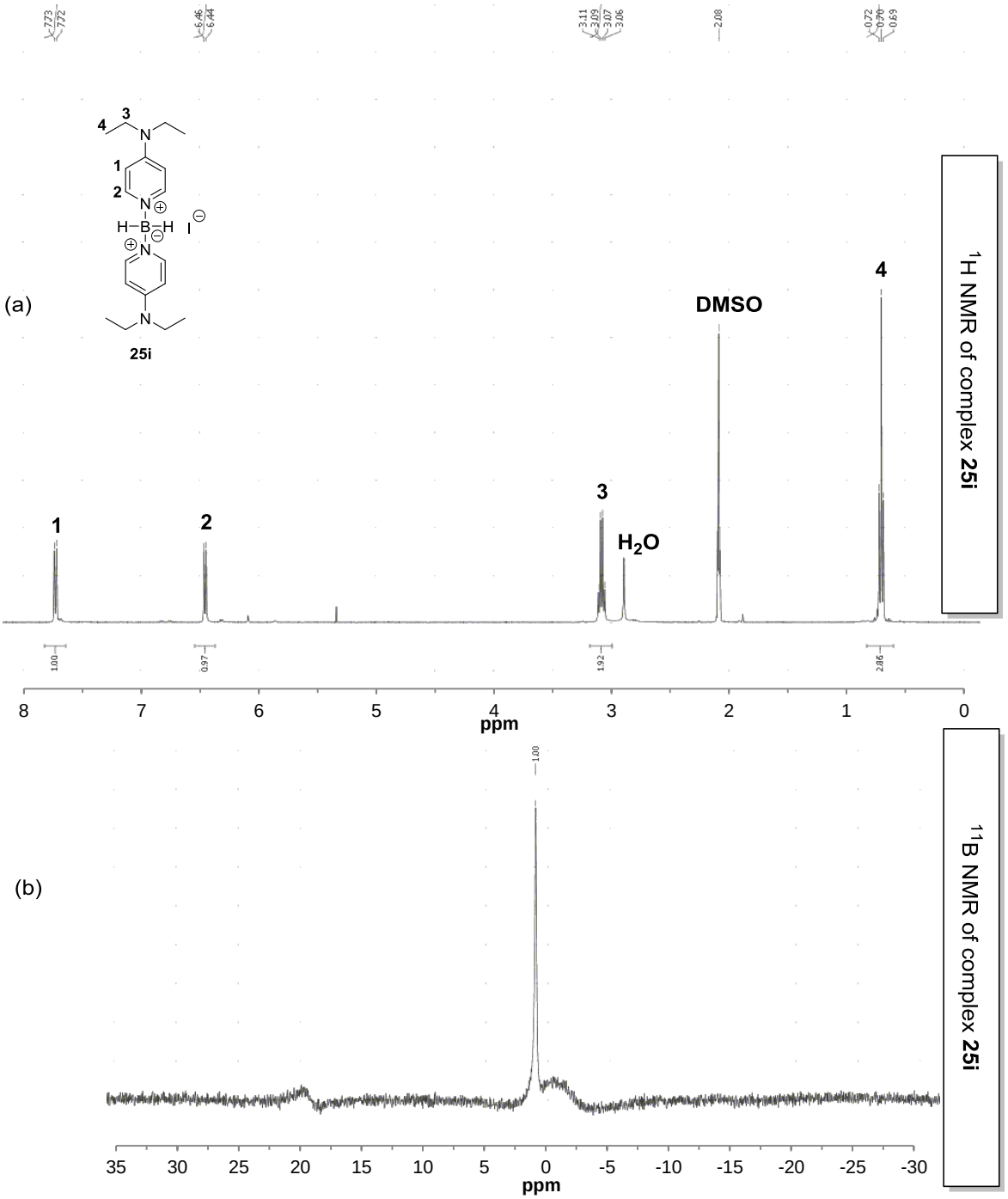

Figure 49: (a) ^{1}H NMR and (b) ^{11}B NMR measurements of bispyridyl borane complex **25i** in DMSO-d_6.

As expected, the ^{1}H NMR spectrum shows the two ethyl groups and the aromatic protons of complex **25i**. The BH_2 moiety does not show up as a sharp signal. It is very likely, that the signal is just too broad, to be integrated properly. Surprisingly, for the ^{11}B NMR, only one sharp signal in the ^{1}H coupled and {^{1}H} measurement was found at +1.00 ppm. The question why the ^{1}H coupled measurement does not show a triplet is not yet answered.

2.3.4.4. Independent control experiments

As the mechanism of the radical reduction of 1-iodododecane (**18d**) would also allow further side reactions, possible reactions were performed as an independent proof for the depicted reaction scheme (Figure 50). The reaction of DMAP (**27**) and 1-iodododecane (**18d**) at 80 °C leads to the pyridinium iodide **29a**, which can be detected by ^{1}H NMR spectroscopy in toluene-d_8 (Figure 50a). A reaction of this iodide salt with DMAP borane (**17q**), which could form the bispyridyl borane species **29b** and dodecane (**16a**) was not found at 80 °C. In terms of the radical reaction, no reaction between the free base and the substrate was detected. Subsequently, the free base reacts much faster to the bispyridyl species then with the substrate 1-iodododecane (**18d**). This reaction will be discussed in a later section. Figure 50b shows that there is also no reaction between DMAP borane (**17q**) and the substrate **18d** at 80 °C. Finally, a reaction of the initiator **2d** and the alkyl iodide **18d** could also be excluded (Figure 50c). In this case only the decay of TBHN (**2d**) was found. With these findings, undesired side reactions of 1-iodododecane (**18d**) could be ruled out.

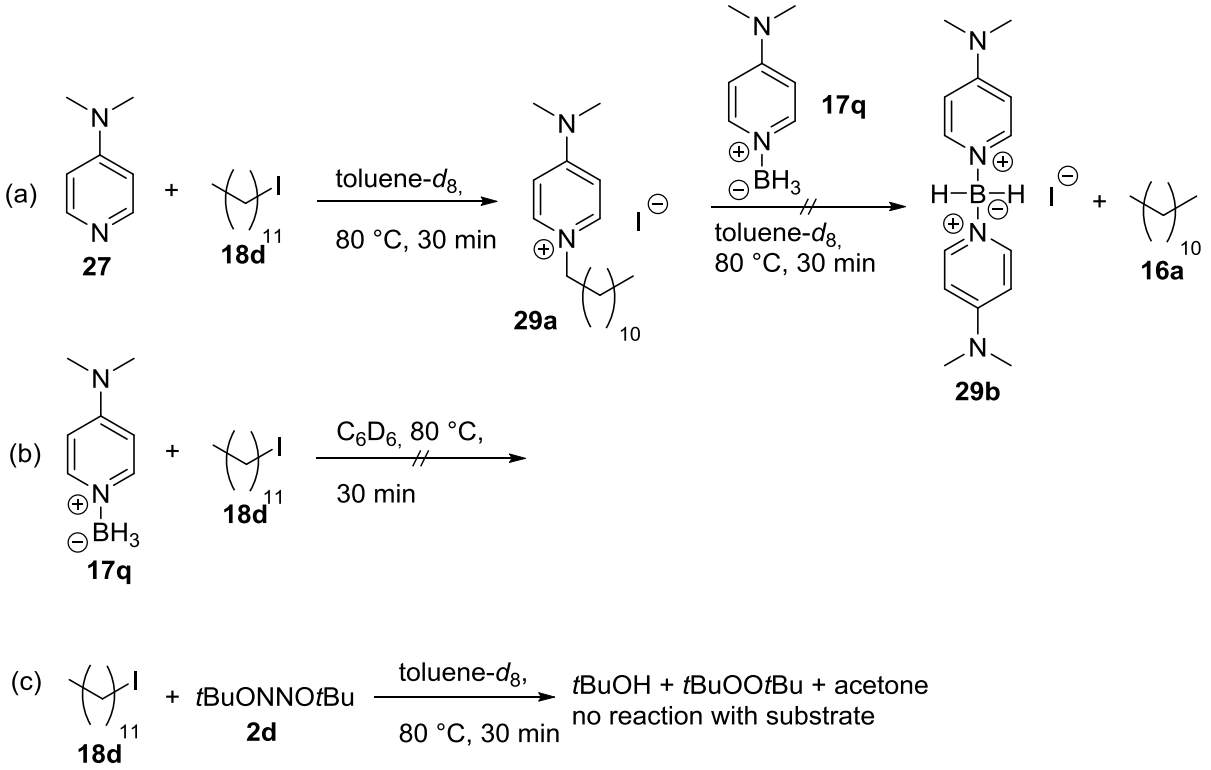

Figure 50: Independent check of possible side reactions, which could occur during the reduction of 1-iodododecane (**18d**) with DEAP borane (**17z**) and TBHN (**2d**) at 80 °C.

In order to obtain analytical data for possible iodoborane complexes, DMAP borane (**17q**) was reacted with different amounts of elemental iodine for ten minutes at room temperature in $CDCl_3$ (Figure 51). With the resulting ^{11}B NMR measurements the three iodoborane complexes (**29c**, **29d** and **29e**) could be clearly characterized. There is no doubt, that none of the complexes appears in a detectable concentration during the radical reaction.

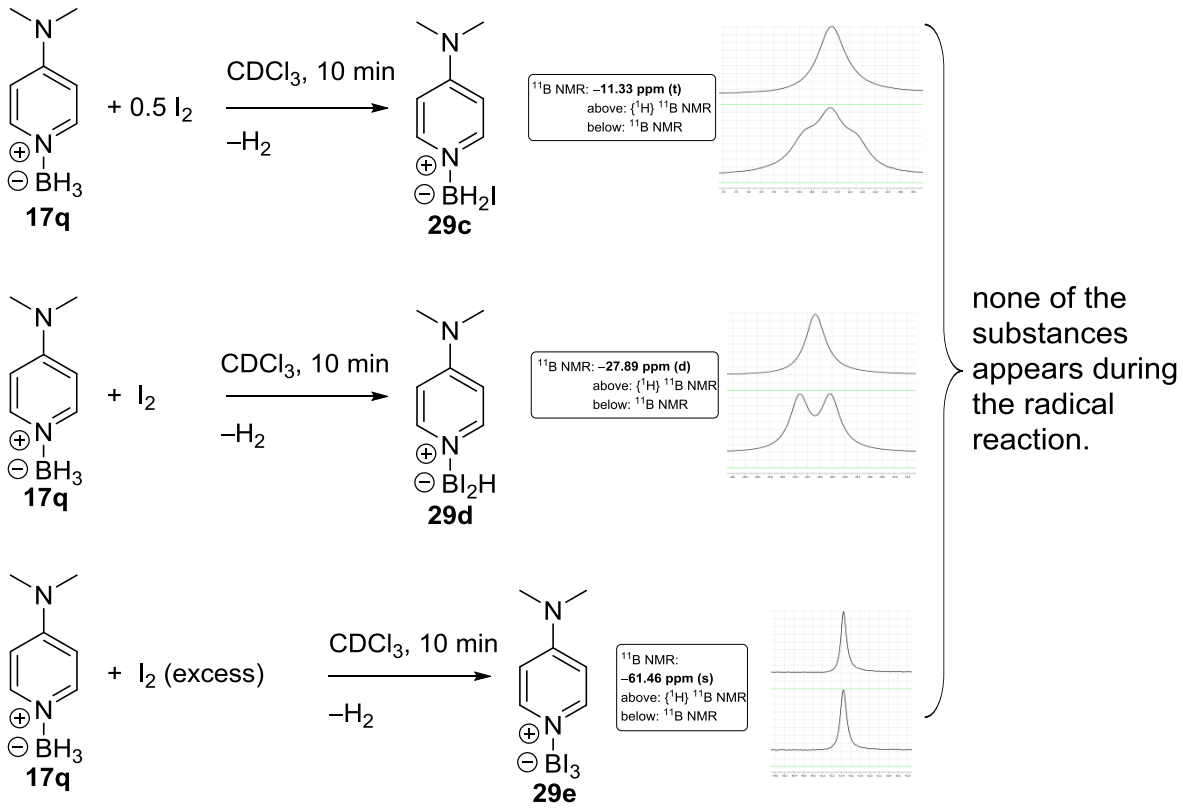

Figure 51: Synthesis of iodoborane complexes **29c**, **29d** and **29e**.

Bispyridyl borane complex **29b** can be synthesized in two different ways (Figure 52). The reaction of DMAP (**27**) with an aqueous solution of HI in excess lead to DMAP hydroiodide (**29f**). By addition of DMAP borane (**17q**), this salt could be turned over into bispyridyl borane complex **29b**. Furthermore the reaction of iodoborane **29c** and DMAP (**27**) caused the same result. Both reactions are very fast as the bispyridyl complex **29b** precipitates immediately from a THF/chloroform (1:1) solution. The reason why neiter the free base **27**, nor the iodoborane species **29c** was found during the radical experiment must subsequently lie in the fast precipitation of complex **29b**. Moreover this compound seems to be very stable, as it can be handled without inert gas atmosphere. It is even not decomposing in the presence of water, indicated by ^{1}H NMR spectroscopy.

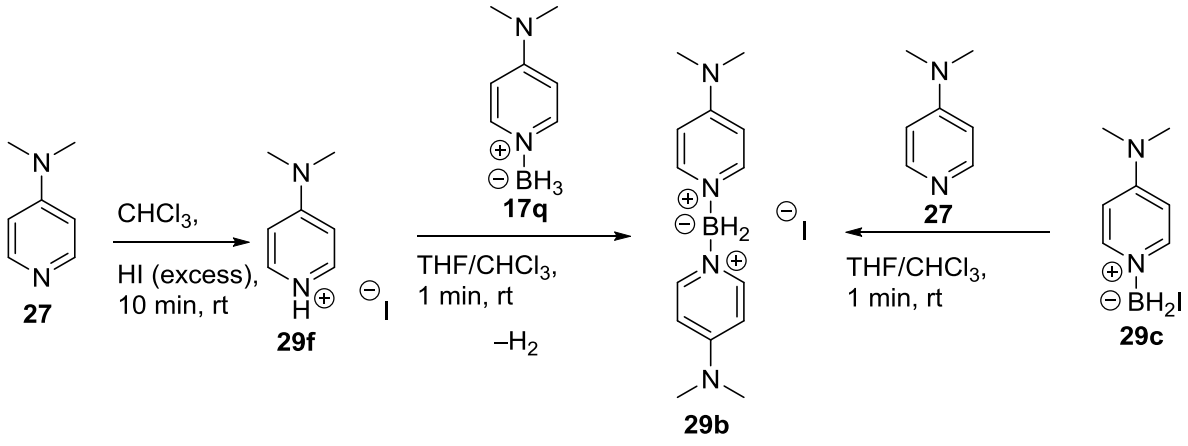

Figure 52: Different synthetic routs for the bispyridyl borane complex **29b**.

The attempt to exchange the anion with potassium *tert*-butanolate at 90 °C in THF (closed vessel, microwave) did not lead to the desired result (Figure 53). Bispyridyl borane complex **29b** was recovered unchanged after 30 minutes.

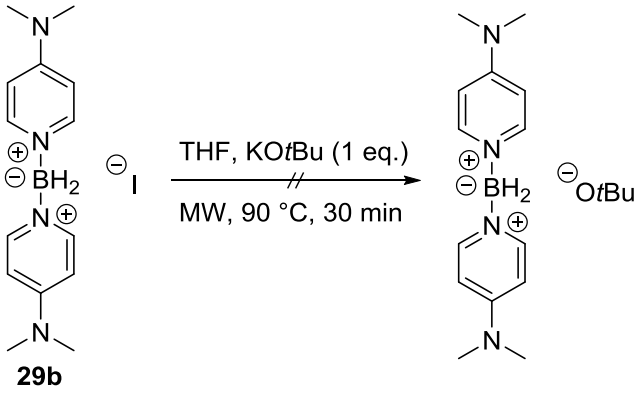

Figure 53: Attempt of an anion exchange of bispyridyl species **29b**.

The fact, that iodoborane complexes were not detected during the radical reaction can also be attributed to the reaction with *tert*-butanol (**25b**). The reaction of iodoborane **25h** with *tert*-butanol (**25b**) is shown in Figure 54. Here, the possible oxidized form **25o** of the complex was not found. The reaction with the alcohol leads to the hydroiodide **25j** and *tert*-butoxy borane (**25e**), which rapidly decomposes. It is assumed, that borane complex **25d** is formed in a first step, which decomplexes rapidly and recomplexes with HI. This is also an important information with regard to the mechanism of the radical reaction. As shown in Figure 52, the hydroiodide salt reacts very fast with DMAP borane (**17q**), which leads to the formation of the bispyridyl species **29b**. Thus, it seems very clear on which pathways the precipitating complex **25i** may be formed and why some species just do not show up in NMR measurements.

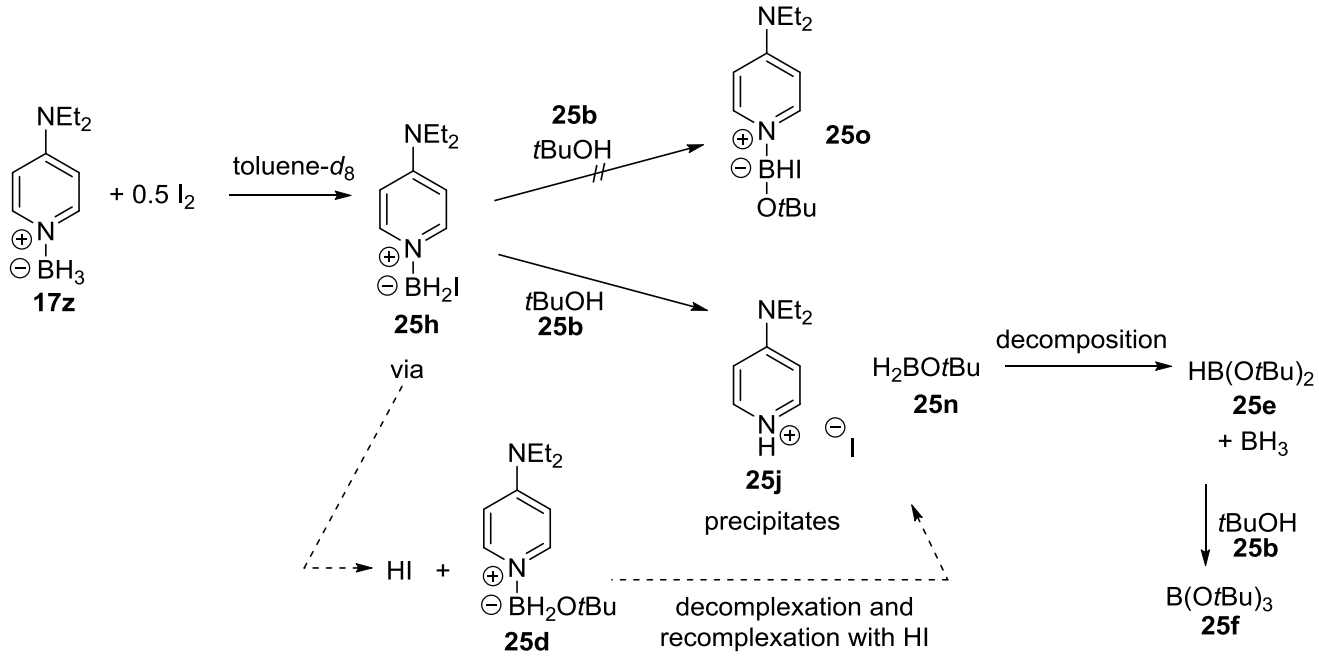

Figure 54: Reaction of iodoborane **25h** and *tert*-butanol (**25b**).

The oxidized borane complex **29g**, which appears in the radical experiment, could be generated form the reaction of iodoborane **29c** and potassium *tert*-butanolate (Figure 55a). ^{11}B NMR analysis of the compound proves the existence of the oxidized species **29g**. As a comparison, a section of the ^{11}B NMR measurement of the radical reaction is shown in Figure 55b. The corresponding signal in the 11B NMR measurement is shifted by 3.58 ppm. This may be caused by the different solvent ($CDCl_3$ vs. toluene-d_8), the temperature difference (rt vs. 80 °C) or the difference in the Lewis-base itself (DMAP vs. DEAP). Nevertheless, it seems very unlikely that the signal at −1.74 ppm can be attributed to another species than **25d**.

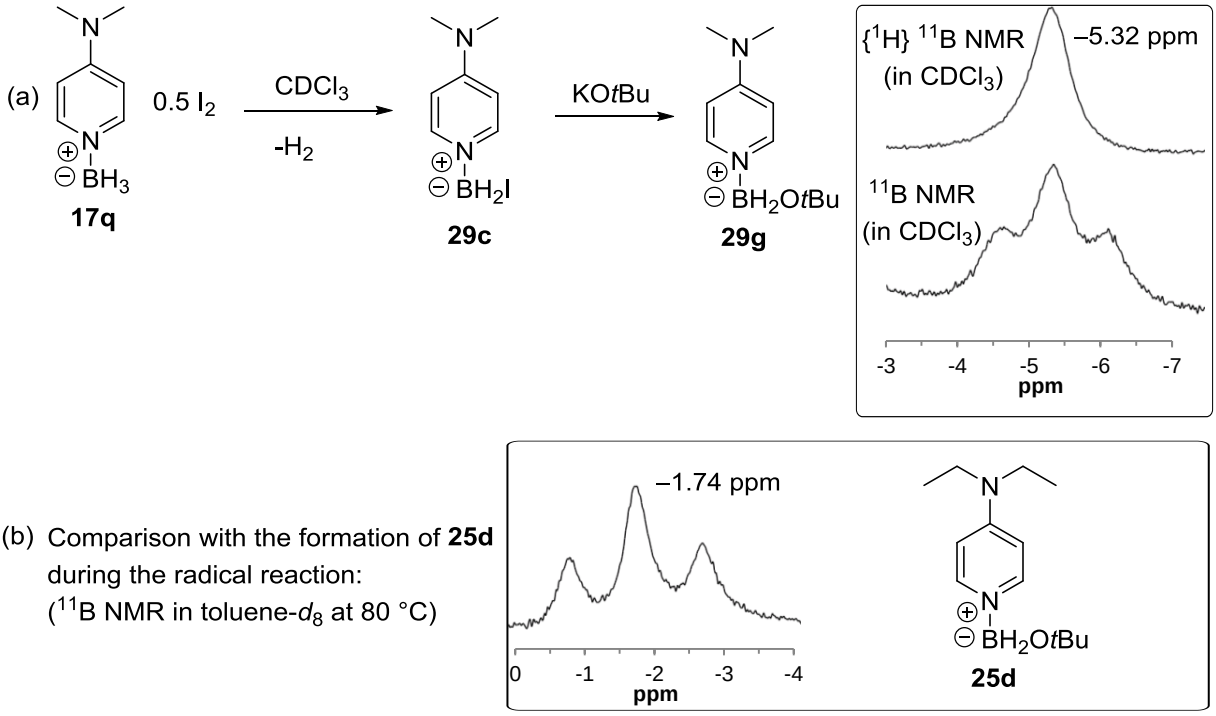

Figure 55: (a) Synthesis of the oxidized borane complex **29g** and the corresponding ^{11}B NMR measurements. (b) Comparison with complex **25d** formed during the radical reaction.

These control experiments help to confirm and understand the complex mechanism of the radical reaction. It seems reasonable, that the conversion of 1-iodododecane (**18d**) is limited to 45 %, due to numerous side reactions of the borane with the radical starter. Furthermore, the consumption of the borane complex, which leads to the bispyridyl species **25i**, also affects the reaction outcome.

2.3.5. Reduction of 1-iodododecane (18d) with DEAP borane (17z), TBHN (2d) and the catalyst TDT (15b)

In order to improve the yield of dodecane (**16a**), the reaction was repeated under the same conditions as before, with the addition of the thiol TDT (**15b**, 5 mol%) as catalyst. The yield of dodecane (**16a**) increased to 65 % in this case.

2.3.5.1. Mechanism

The mechanism of the thiol-catalyzed reaction is shown in Figure 56. The addition of TDT (**15b**) leads to a catalytic cycle, which is involved in chain 2. A hydrogen transfer from the thiol to the dodecyl radical leads to dodecane and a thiyl radical, which then abstracts a H atom from DEAP borane (**17z**). This leads to an increased formation of the desired product dodecane (**16a**). The oxidized borane **25d** is formed slower than before, which can be seen based on ^{11}B NMR studies and will be shown in the next section. This decreased formation of **25d** shows that the recombination process of boryl radical **25c** and the *tert*-butoxy radical is reduced, lowering the termination process. The addition of TDT also accelerates the formation of *tert*-butanol (**25b**) from the *tert*-butoxy radical, which is involved in chain 1. This has two effects on the reaction. On the one hand, less *tert*-butoxy radicals can undergo a recombination, avoiding to the termination step. On the other hand, more *tert*-butanol (**25b**) leads to an increased formation of borane complex **25g**, which can undergo a decomplexation, leading to di-*tert*-butoxy borane (**25e**) and free DEAP (24). A ^{11}B NMR study on these effects will be shown later.

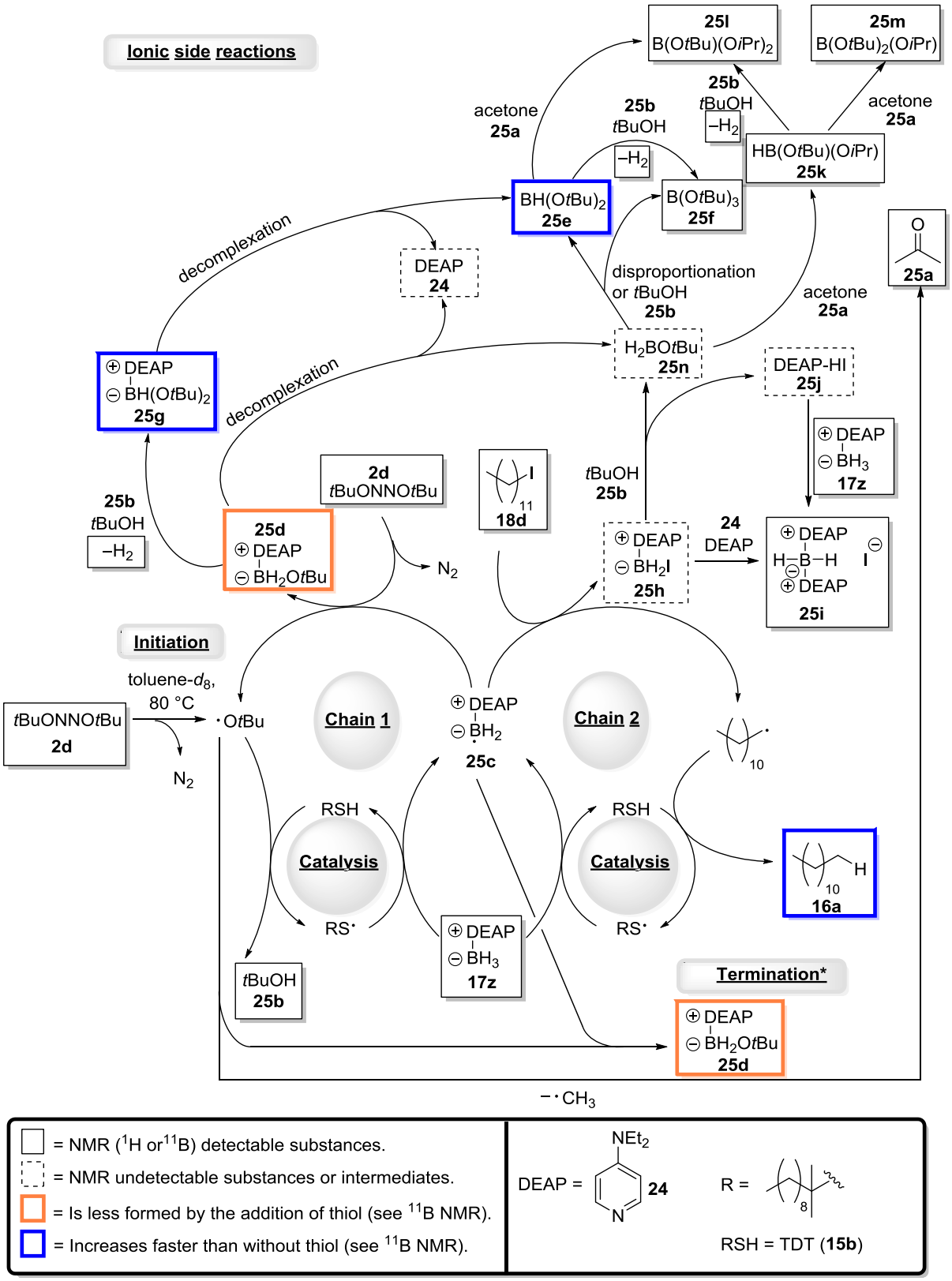

* Other possible recombination products were not detected by NMR spectroscopy or GC/MS analysis.

Figure 56: Mechanism of the reduction of 1-iodododecane (**18d**) with DEAP borane (**17z**) and TBHN (**2d**) in presence of the catalyst TDT (**15b**) at 80 °C in toluene-d_8.

2.3.5.2. NMR studies

A comparison between the ^{11}B NMR measurements of the uncatalyzed and the catalyzed reaction is shown in Figure 57. Figure 57a shows the uncatalyzed reaction after 60 minutes, Figure 57b displays the catalyzed reaction after 30 minutes, where the precipitation of bispyridyl borane **25i** occurs also faster. The increase of the borane species **25g**, **25e** and **25k** as well as the decrease of the oxidized borane **25d** is obvious. The comparison of the ^{11}B NMR measurements is absolutely in line with the mechanism shown before, as the decrease and increase of the species clearly reflect the pathways of the reaction. The addition of thiol as catalyst improves the yield of the reaction by 20 %. However, there are still versatile side reactions which prohibit a better yield.

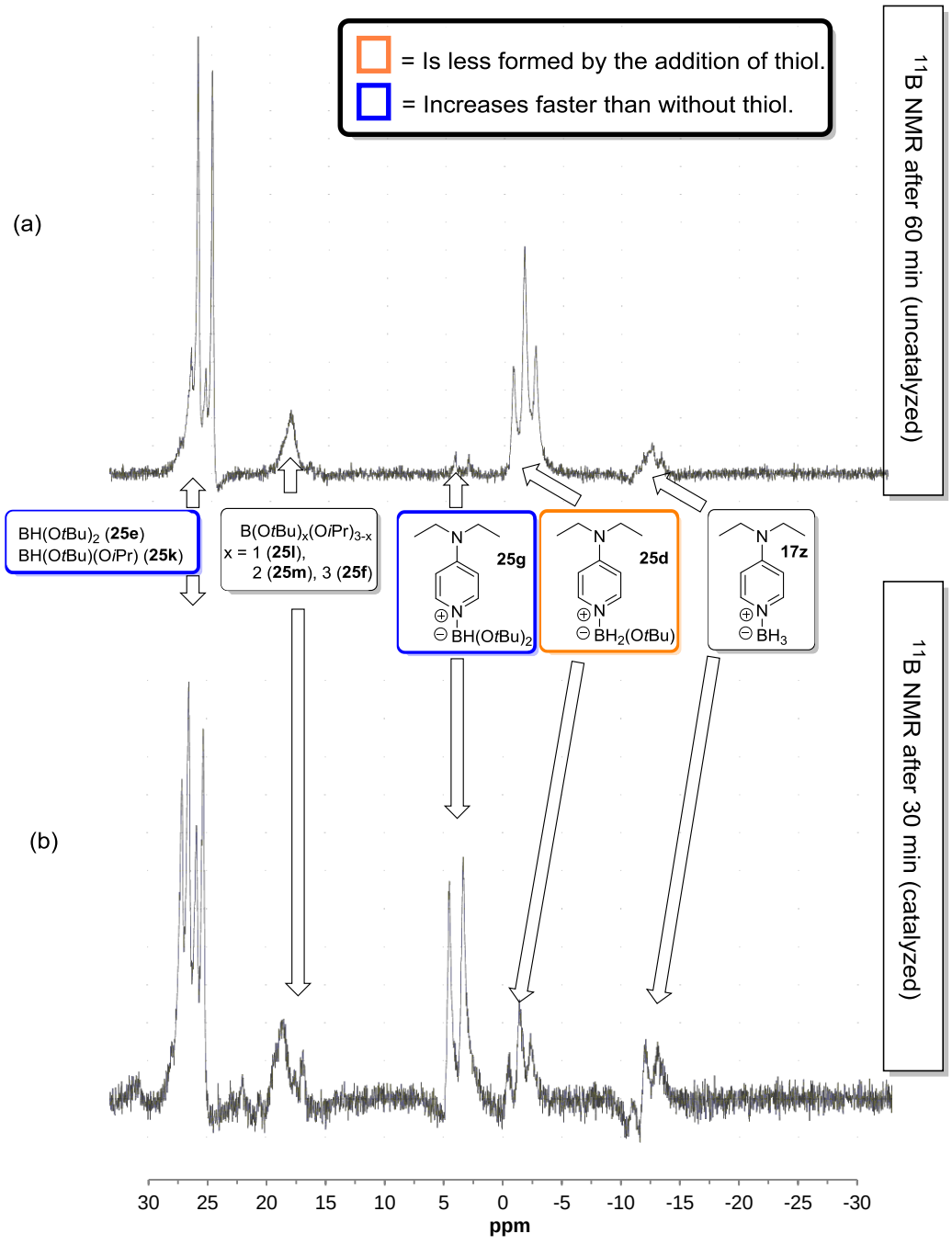

Figure 57: Comparison of ^{11}B NMR measurements. (a) Uncatalyzed reduction of 1-iodododecane (**18d**). (b) TDT (**15b**)-catalyzed reduction.

2.3.6. Solubility of dialkylaminopyridine boranes

A main problem of the moderate yield of the reduction product seems to be the solubility of the borane complex. Whereas DMAP borane (**17q**) is almost insoluble in toluene at room temperature, DEAP borane (**17z**) is soluble. However, the solubility of the precipitating bispyridyl borane species **25i** in toluene is very low, even at 80 °C. This fact, that not even traces of the complex could be detected during NMR studies proves the poor solubility. The hypothetic effect a better soluble bispyridyl borane species is shown in Figure 58. If it would be possible to abstract an H atom from the bispyridyl species, the radical reaction could in principle proceed in the same way as described before. The abstraction of the iodide would lead to an alkyl radical, which then would undergo an H atom transfer from the thiol.

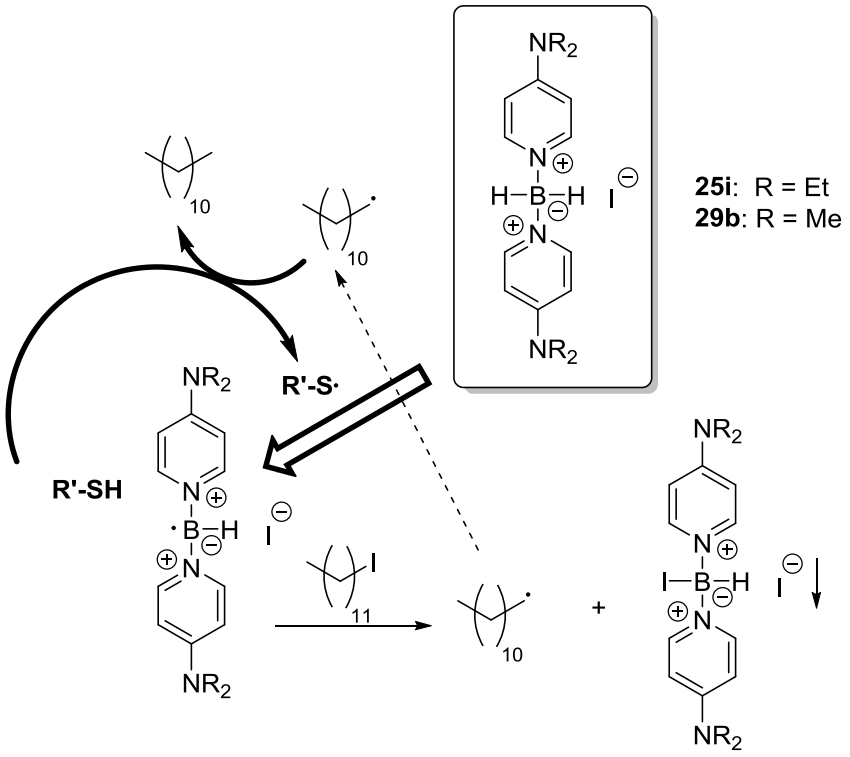

Figure 58: Hypothetic involvement of a bispyridyl borane complex into the radical reaction.

2.3.6.1. Synthesis of dihexylaminopyridine borane (DHAP borane, 30f)

For the improvement of the solubility of the bispyridyl borane species, a new borane complex was synthesized (Figure 59). The reaction was carried out under an inert gas atmosphere. Step 1 describes the synthesis of the free base **30a**. Therefore, *para*-aminopyridine (**30b**) was deprotonated with *n*-butyllithium (2.2 eq.) and subsequently alkylated with *n*-hexyl iodide. Afterwards, the side products decane (**30c**), the mono alkylated base (**30d**) and remaining starting material were removed by column chromatography. The remaining pyridinium iodide salt **30e** was precipitated with isohexane and the final product **30f** obtained as a yellow oil (24 %). In the next step the complex was generated by addition of a Me_2S-BH_3 solution (1.01 eq.), followed by removal of all volatiles. 4-Dihexylaminopyridine borane (**30f,** DHAP-BH_3) was obtained in quantitative yield as a colorless oil, soluble in isohexane, which already demonstrates the improved solubility in nonpolar solvents.

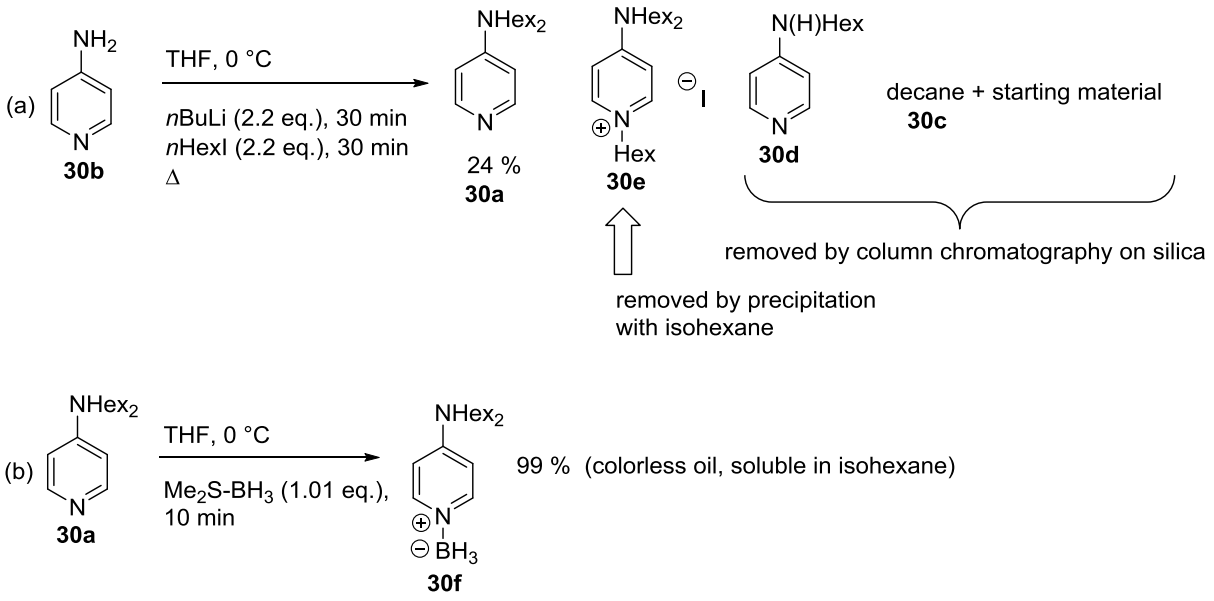

Figure 59: Synthesis of DHAP borane (**30f**).

2.3.6.2. DHAP borane (30f) as hydrogen atom donor

After this, the radical experiment was repeated under the same conditions as before with DHAP borane (**30f**) as H atom donor (Figure 60, entry 1). With a yield of 60 % of dodecane (**16a**), the result is quite similar to the reduction with DEAP borane (**17z**, 65 %). However, in this case, no precipitation of any compound was observed. Subsequently, the bispyridyl borane species does not influence the radical reaction, neither in solution nor as precipitate. In order to find out if a higher quantity of reducing agent could affect the reaction, the experiment was redone with an increased amount of DHAP borane (**30f**, 2.0 eq., Figure 60, entry 2). The slight increase of 17 % product formation shows, that even doubling the amount of the hydrogen atom donor improves the reaction outcome only slightly.

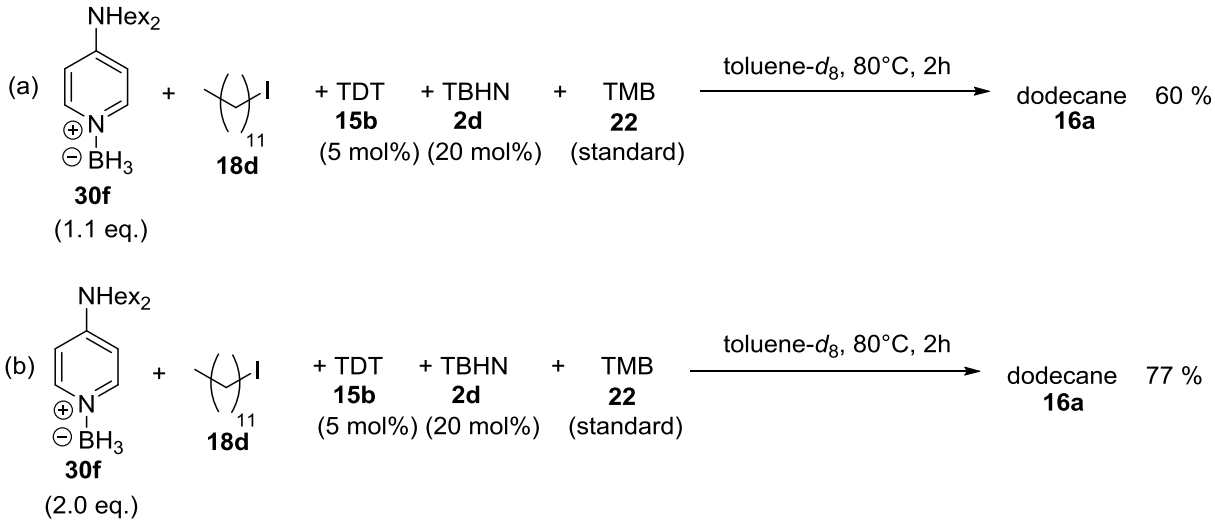

Figure 60: Reduction reactions of 1-iodododecane (**18d**) with DHAP borane (**30f**), TDT (**15b**) and TBHN (**2d**) at 80 °C in toluene-d_8.

The corresponding ^{11}B NMR measurement of the reduction with 1.1 eq. DEAP borane (**17z**) is shown in Figure 61. The formation of bispyridyl borane **30g**, which now stays in solution (+2.88 ppm) can be identified. Furthermore, the amount of the final borates is higher, as the measurement was done 24 hours after the reaction. This is due to the fact, that the borane species (**25e** and **25k**) may react with remaining *tert*-butanol (**25b**) or acetone (**25a**) over that period. A small amount of remaining DHAP borane (**30f**) is still present. All findings are consistent with the experiment with DEAP borane (**17z**) and thus demonstrate, that once the bispyridyl borane species is formed no subsequent step will occur.

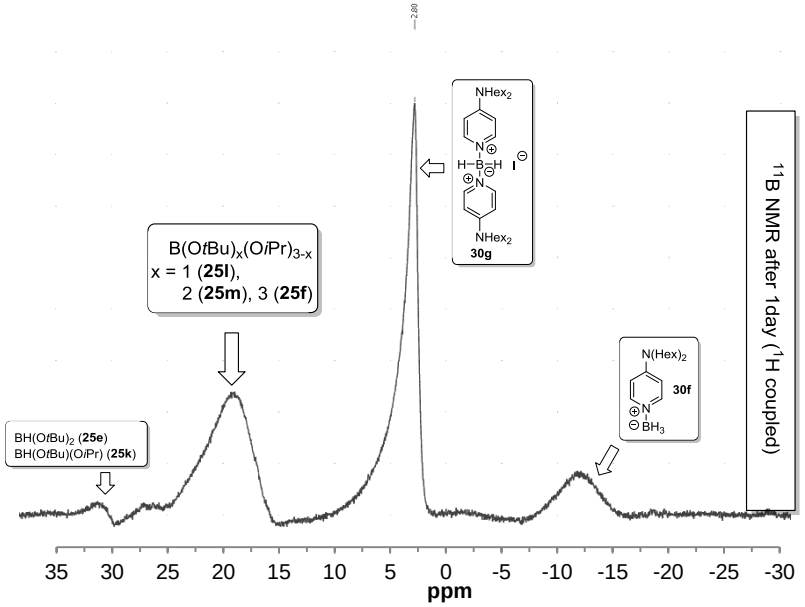

Figure 61: ^{11}B NMR product analysis of the reduction of 1-iododododecane (**18d**) with DHAP borane (**30f**).

2.3.7. Optimization of the TDT (15b) catalyzed reduction of 1-iododododecane (18d) with DEAP borane (17z) and TBHN (2d)

The only possibility to improve the yield and to minimize side reactions was to reduce the amount of the initiator. Therefore, the amount of TBHN (**2d**) was reduced by half (Figure 62). In this case a full conversion to dodecane (**16a**) was achieved. This reflects the importance of the right amount of the initiator in order to minimize undesired reactions.

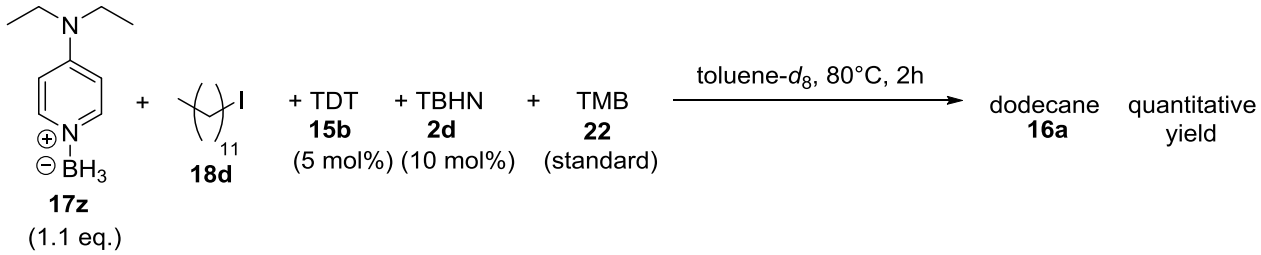

Figure 62: Quantitative reduction of 1-iododododecane (**18d**) with DEAP borane (**17z**), TDT (**15b**) and TBHN (**2d**) at 80 °C.

2.3.8. Proof of the initiation concept

Finally, there are three main factors which determine the reaction outcome. First, the starter must generate an oxygen-centered radical. Second, the initiation temperature should be in the region of 80 °C – 110 °C and the radical starter should not decompose too fast at that temperature. A half-life time of about 10 minutes at the relevant temperature seems to be a good compromise. Lastly, the amount of starter can also affect the reaction.

2.3.8.1. Synthesis of *tert*-butyl peroxypivalate (TBPP, 31a)

To proove this concept, a second initiation system, showing similar properties as TBHN (**2d**), was needed. Therefore *tert*-butyl peroxypivalate (**31a,** TBPP) was synthesized (Figure 63). The reaction was carried out under a nitrogen atmosphere. A commercially available solution of *tert*-butyl hydroperoxide (**31b**, 5.5 M in decane) was mixed with pentane and cooled to −20 °C. Afterwards, *n*-butyllithium (1.0 eq.) was slowly added. After five minutes pivaloyl chloride (**31c**, 1.0 eq.) was added and brought to room temperature. After aqueous extraction, pentane was removed under reduced pressure (over five minutes) and a colorless *tert*-butyl peroxypivalate (**31a**) solution in decane was obtained (quantitative). The amount of **31a** in the solution was determined by ^{1}H NMR spectroscopy.

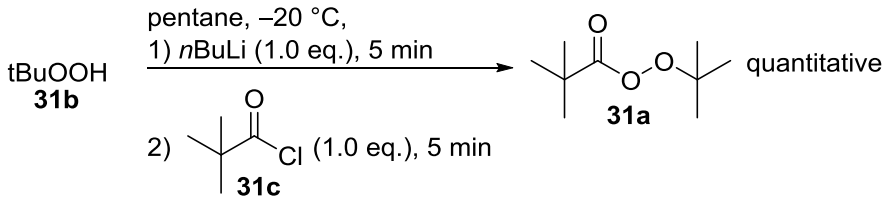

Figure 63: Synthesis of *tert*-butyl peroxypivalate (**31a**, TBPP).

2.3.8.2. TBPP (31a) as thermal initiation system

The decay of TBPP (**31a**) was monitored by ^{1}H NMR spectroscopy in toluene-d_8 at 90 °C. The mechanism for this decay is shown in Figure 64. In an initial step, TBPP (**31a**) generates two oxygen-centered radicals. The pivaloyl radical afterwards eliminates CO_2 to form a *tert*-butyl radical. This radical may now trap a hydrogen atom which leads to *iso*-butane (**31d**) or undergo a recombination reaction with another alkyl radical to form **31e** or **31f**. Furthermore, the formation of the *tert*-butoxy radical is the more important part in terms of the reduction with a borane complex. The following steps are the same as in the case of TBHN (**2d**).

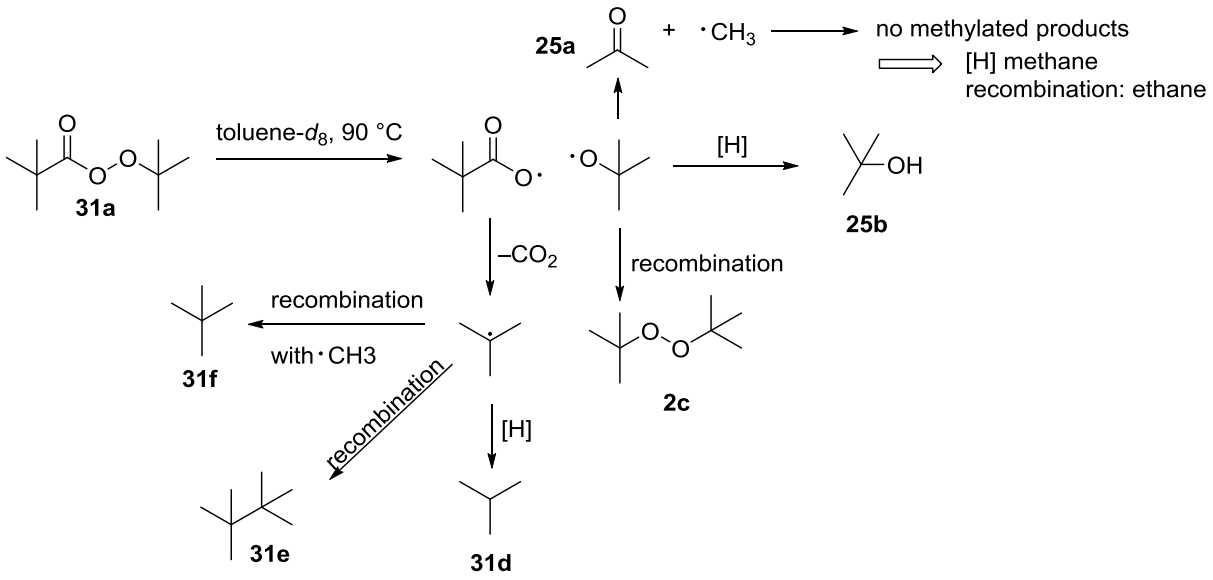

Figure 64: Mechanism of the thermal decomposition of TBPP (**31a**) at 90 °C in toluene-d_8.

The decomposition of TBPP (**31a**) at 90 °C is shown in Figure 65. The half-life time $t_{1/2}$(90 °C) = 390 s makes the compound a promising initiator (compare TBHN (**2d**): $t_{1/2}$(80 °C) = 520 s). The final decomposition products *tert*-butanol (**25b**), acetone (**25a**) and DTBP (**2c**) which result from the *tert*-butoxy radical are the same as for TBHN (**2d**). Only the amount of DTBP (**2c**) as recombination product is slightly higher.

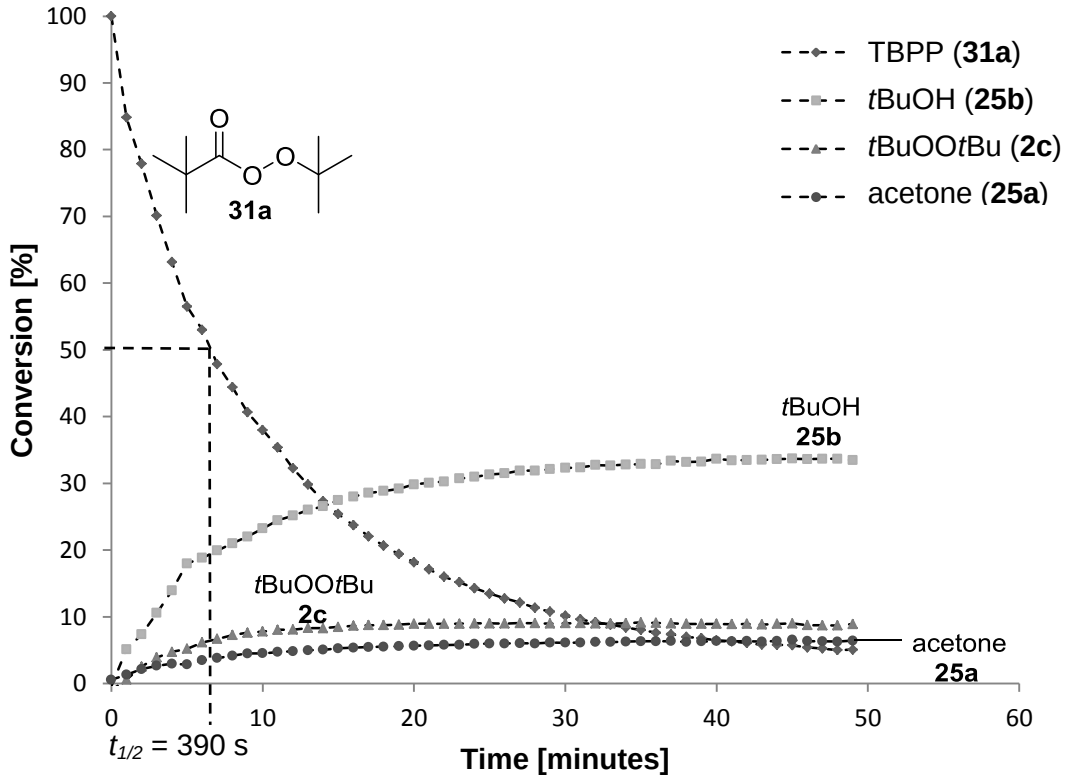

Figure 65: Time-conversion plot of the thermal decomposition of TBPP (**31a**) at 90 °C in toluene-d_8.

2.3.8.3. Thermal decay of TBPP (31a) in the presence of DMAP borane (17q)

The decay of TBPP (**31a**, 0.5 eq.) in the presence of DMAP borane (**17q**) at 90 °C is shown in Figure 66. The rate increase indicates a reaction between the borane complex and the initiator, as already shown for the system TBHN (**2d**)/ DEAP borane (**17z**). After 10 minutes the consumption of the perester is completed. In contrast to other systems like AIBN (**2a**)/ DMAP borane (**17q**), where no reaction of the complex with the starter is observed, the shown system undergoes a fast reaction, which seems promising for the reduction of an alkyl iodide.

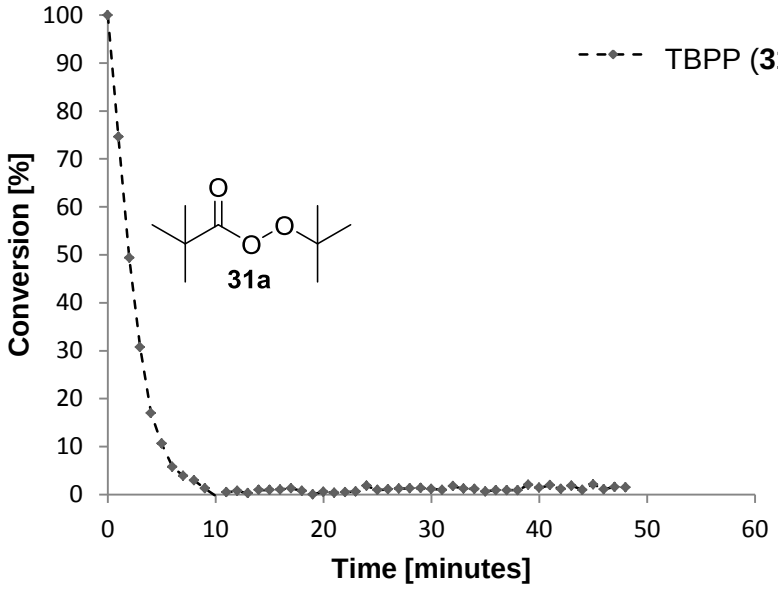

Figure 66: Time-conversion plot of the thermal decomposition of TBPP (**31a**) in the presence of DMAP borane (**17q**) at 90 °C in toluene-d_8.

2.3.8.4. Radical reduction of 1-iododododecane (18d) with TBPP (31a) as initiator

The radical reduction of 1-iododododecane (**18d**) was repeated with TBPP (**31a**, 20 mol%) as radical starter (Figure 67a). In order to generate a comparable amount of tert-butoxy radicals as with TBHN (**2d**), 20 mol% of TBPP (**31a**) were added. The reaction was monitored by ^{1}H NMR spectroscopy at 90 °C. After only two minutes no further conversion of 1-iododododecane (**18d**) into dodecane (**16a**) was detected (Figure 67b). As the reaction of DMAP borane (**17q**) and TBPP (**31a**) is also very fast, the missing 12 % of conversion have to be attributed to this side reaction. Surprisingly, no conversion was found in the absence of TDT (**15b**), which reflects the importance of the catalyst for the system. With *tert*-butyl peroxypivalate (**31a**), an initiator with similar properties as TBHN (**2d**) was found. The big advantage of TBPP (**31a**) over TBHN (**2d**) is the easy synthesis from cheap commercially available compounds.

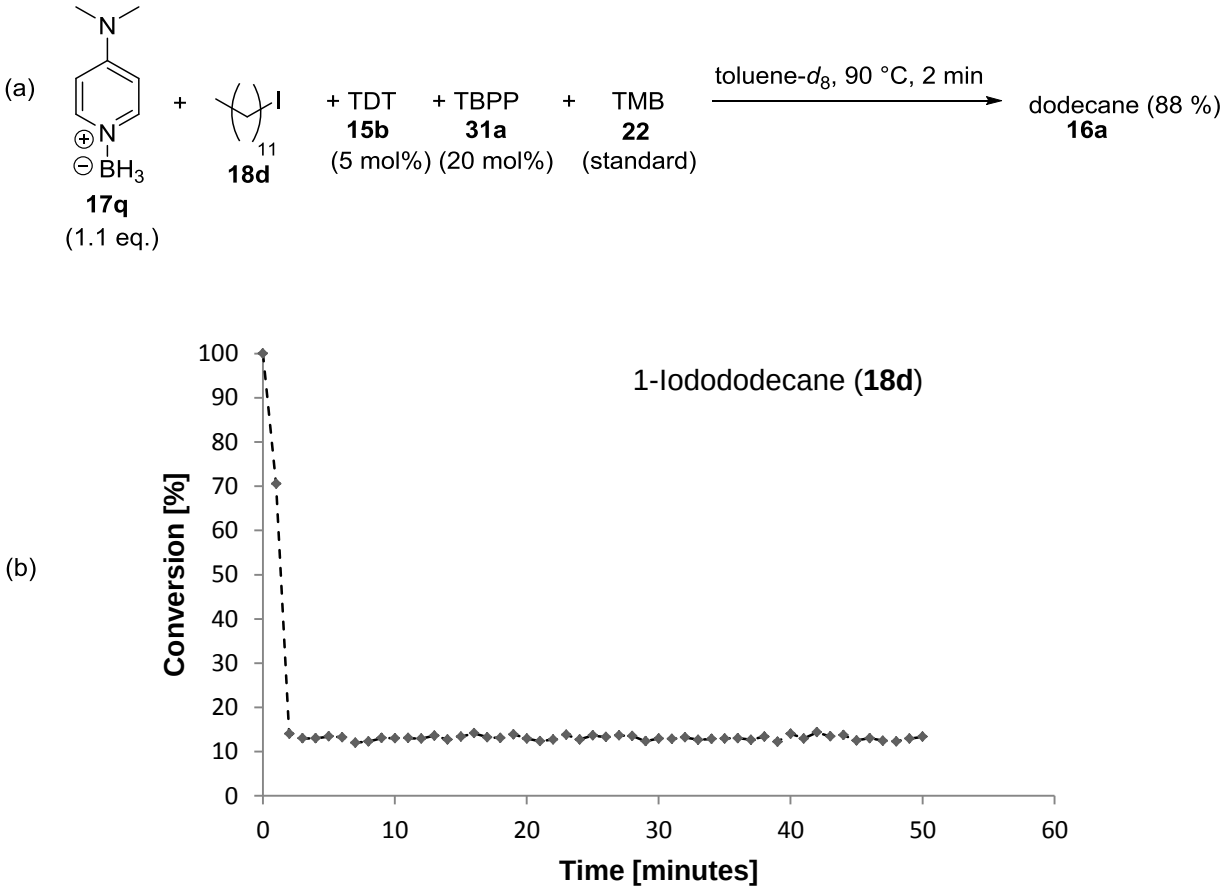

Figure 67: (a) Reduction of 1-iododododecane (**18d**) with DMAP borane (**17q**), TDT (**15b**) and TBPP (**31a**) as initiator at 90 °C in toluene-d_8. (b) Time-conversion plot of the reduction.

2.3.8.5. Reactions with TBPP (31a) as initiator - a substrate screening

In order to check how effective the TBPP (**31a**)/ DMAP borane (**17q**) system is, two other substrates were investigated (Figure 68). A reduction of 1-bromododecane (**18a**) to the corresponding alkane was not successful. However, when going to the class of xanthates, a comparably fast reaction as for 1-iododododecane (**18d**) was observed (Figure 68b). The yield of dodecane (**16a**) was 85 % after 10 minutes. The time-conversion curve of the reaction is shown in Figure 68c and displays the fast reduction of the xanthate. Furthermore, it is remarkable, that for the reduction of the xanthate no addition of a thiol as catalyst is necessary, whereas the alkyl iodide is not reduced in the absence of a thiol. Finally, alkyl iodides as well as xanthates can be reduced by DMAP borane (**17q**) and a suitable initiator, such as TBHN (**2d**) or TBPP (**31a**).

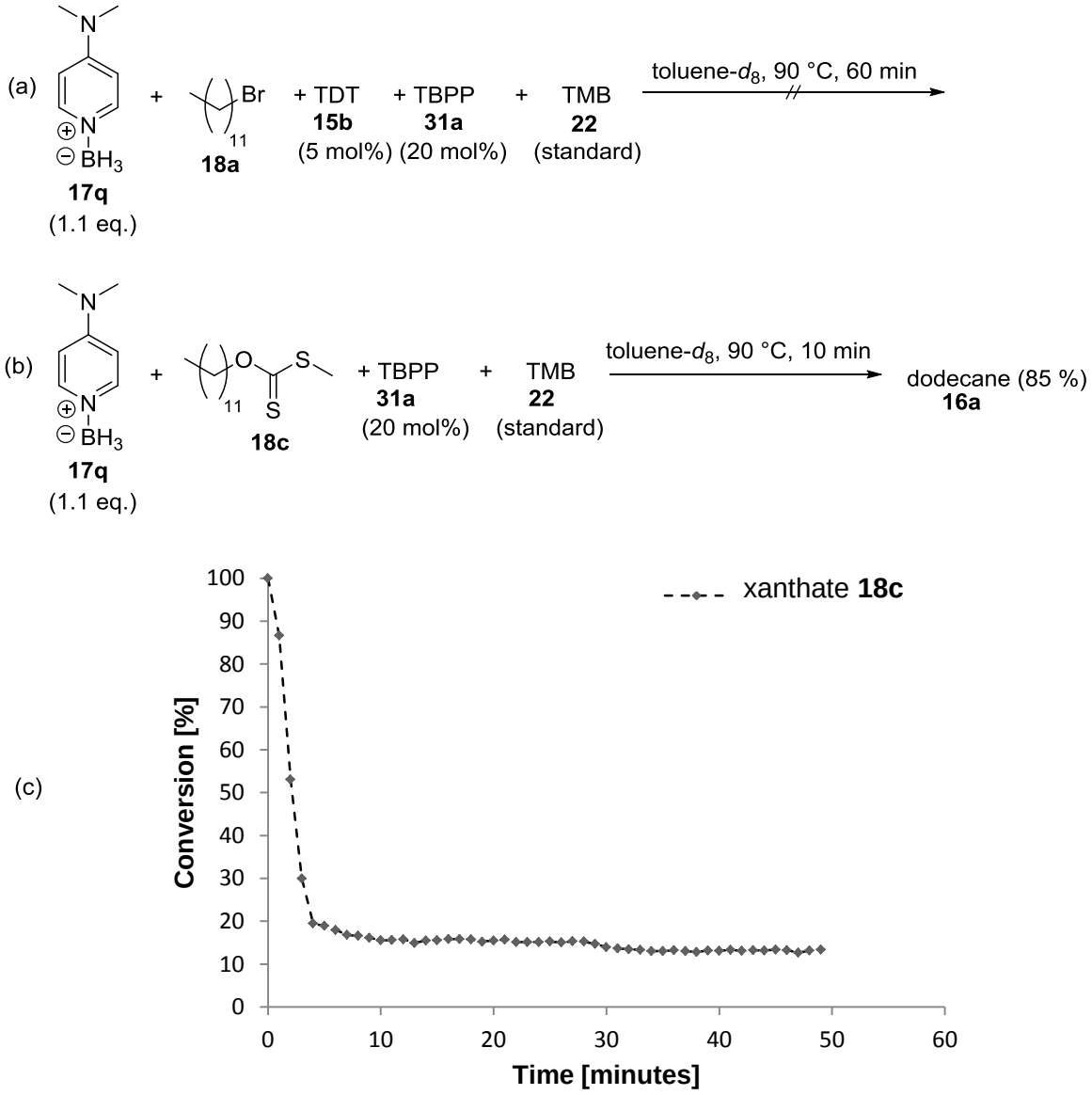

Figure 68: (a) Reduction of alkyl bromide **18a** and (b) xanthate **18c** with DMAP borane (**17q**) and TBPP (**31a**) as initiator at 90 °C in toluene-d_8. (c) Time-conversion plot of the uncatalyzed reduction of xanthate **18c**.

2.4. High temperature initiation experiments with 1-bromododecane (18a)

The final question was why alkyl iodides would undergo such a fast reaction, whereas alkyl bromides seemed to be inert under the chosen conditions. As the C-I bond strength of 218 kJ/mol is lower than the C-Br bond strength of 285 kJ/mol, a cleavage of the C-Br bond is less favored.[53] In order to see how a rise of reaction temperature could affect the C-Br cleavage, another initiator was necessary, as TBHN (**2d**) and TBPP (**31a**) would decompose too fast at temperatures over 90 °C. The requirement of the radical starter was to form an oxygen-centered radical during the initiation and to have a similar half-life time as TBHN (**2d**) at 80 °C (520 s). Thus, two commercially available high temperature initiators were chosen for this purpose. In order to cover a wide range of initiation temperatures, *tert*-butyl peroxybenzoate (**2g**, $t_{1/2}$(142 °C) = 360 s) and dicumyl peroxide (**2f**, $t_{1/2}$(154 °C) = 360 s), which are commercially available, were chosen. Initiation temperatures higher than 154 °C

were excluded, as DMAP borane (**17q**) decomposes at temperatures over 169 °C. Subsequently, the reactions were carried out in toluene-d_8 under the relevant conditions (Figure 69a and b). For both radical starters no conversion was observed. The reason for this becomes obvious, when looking at the ^{11}B NMR measurement (Figure 69c, which was taken 1 day after the reaction with dicumyl peroxide (**2f**)). The decay of the initiator and its reaction with DMAP borane (**17q**) to the final boranes becomes clear. As in the cases before, two borane species (**31j** and **31k**) are present, which arise from the decay of the initiator to the corresponding alcohol (H trapping) and the ketone (cleavage). However, the rise in temperature only seems to accelerate the reaction of the radical starter with the borane complex **17q**. Thus, a C-Br cleavage does not occur.

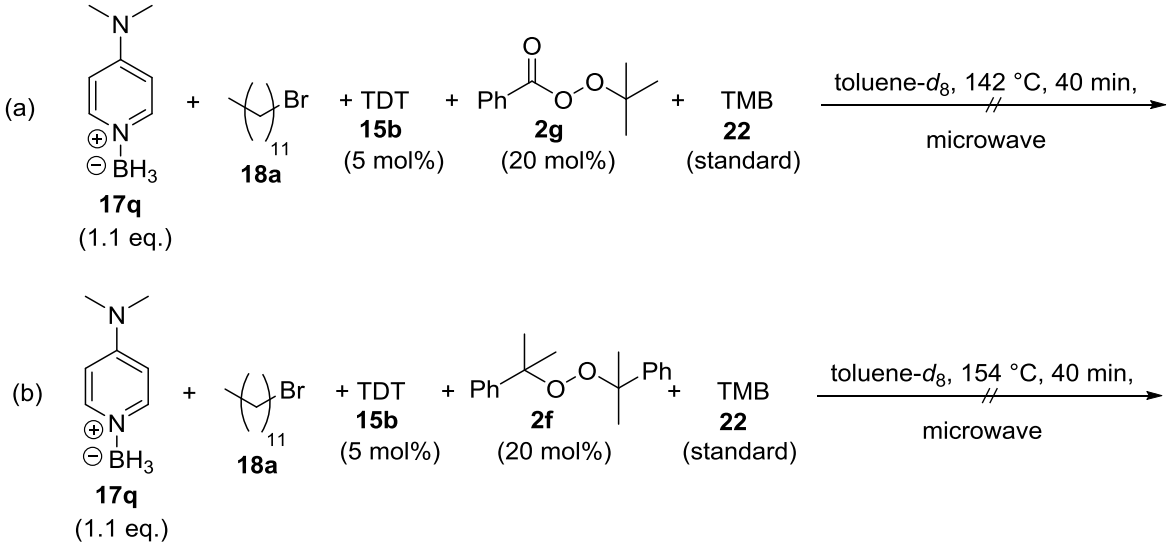

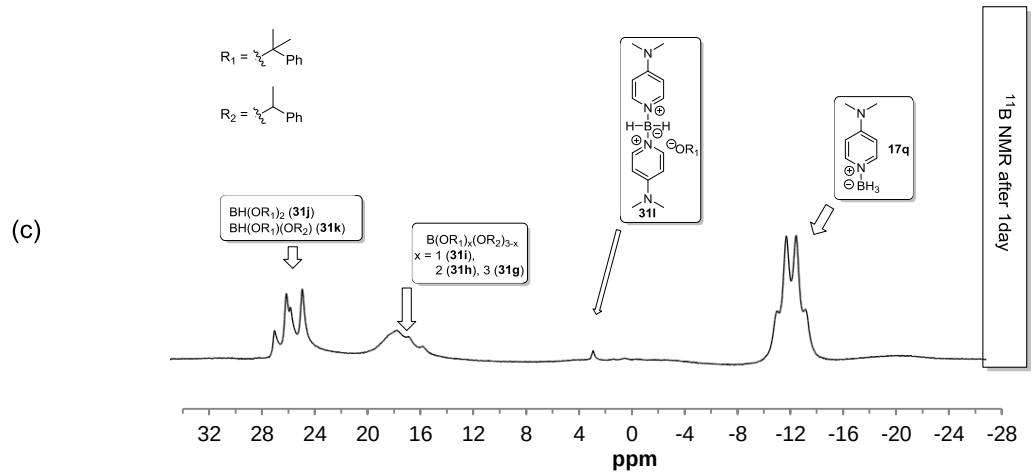

Figure 69: Reduction of 1-bromododecane (**18a**) with the high temperature initiatiors (a) *tert*-butyl peroxybenzoate (**2g**) and (b) dicumyl peroxide (**2f**). (c) ^{11}B NMR measurement of the reduction with dicumyl peroxide (**2f**) at 154 °C.

2.5. Radical reductions of xanthates

Two very effective initiation systems have been found. TBHN (**2d**)/ DMAP borane (**17q**) as well as TBPP (**31a**)/ DMAP-BH_3 (**17q**) can reduce alkyl iodides and xanthates efficiently. The importance of the formation of an oxygen-centered radical, as well as the right initiation temperature (80 °C for TBHN (**2d**), 90 °C for TBPP (**31a**)), has been documented. The strong oxophilicity of the boron atom leads to versatile side products and is also the reason why a reduction of alkyl bromides does not take place. Here, the C-Br cleavage is competing against the formation of a B-O bond and even at higher temperatures, the B-O formation is strongly favored. The addition of a thiol as catalyst is necessary in the case of iodides, whereas xanthates are reduced without catalyst. This behavior is surprising, as the reactivity of xanthates in radical reactions is usually similar to bromides, whereas iodides react much faster. As the reduction of dodecyl xanthate (**18c**) with DMAP borane (**17q**) and TBPP (**31a**) turned out to be fast and gave a good yield (85 %), the radical reduction of xanthates will be adressed in the following section. Therefore, the standard setup, used for the reductions of 1-iodododecane (**18d**) was again employed for xanthate **18c**. The reaction was followed by ^{1}H NMR spectroscopy at 80 °C. Full conversion to the corresponding alkane was observed after 4 minutes (Figure 70).

Figure 70: Reduction of xanthate **18c** with DMAP borane (**17q**), TDT (**15b**) and TBHN (**2d**) as initiator at 80 °C in toluene-d_8.

2.5.1. Variation of reaction conditions

As a consequence of the fast reduction of xanthate **18c**, the reaction conditions were varied.

2.5.1.1. Variations of the initiation system

Surprisingly, even in absence of the thiol catalyst and by lowering the amount of initiator to 2 mol%, 92 % dodecane (**16a**) were formed (Figure 71a). Hence, the use of AIBN (**2a**) instead of TBHN (**2d**) did not lead to a reduction of xanthate **18c** (Figure 71b). These two results show, that the formation of an oxygen-centered radical from the starter is also essential for the reduction of a xanthate. However, the influence of the catalyst seems to be not as strong as in the reduction of 1-iodododecane (**18d**). A time-conversion for the reduction of xanthate **18c** with TBHN (**2d**, 2 mol%) was measured by ^{1}H NMR spectroscopy at 80 °C and is shown in Figure 71a. The time-conversion plot shows the fast reduction of xanthate **18c** ($t_{1/2}$ = 445 s) with only 2 mol% initiator.

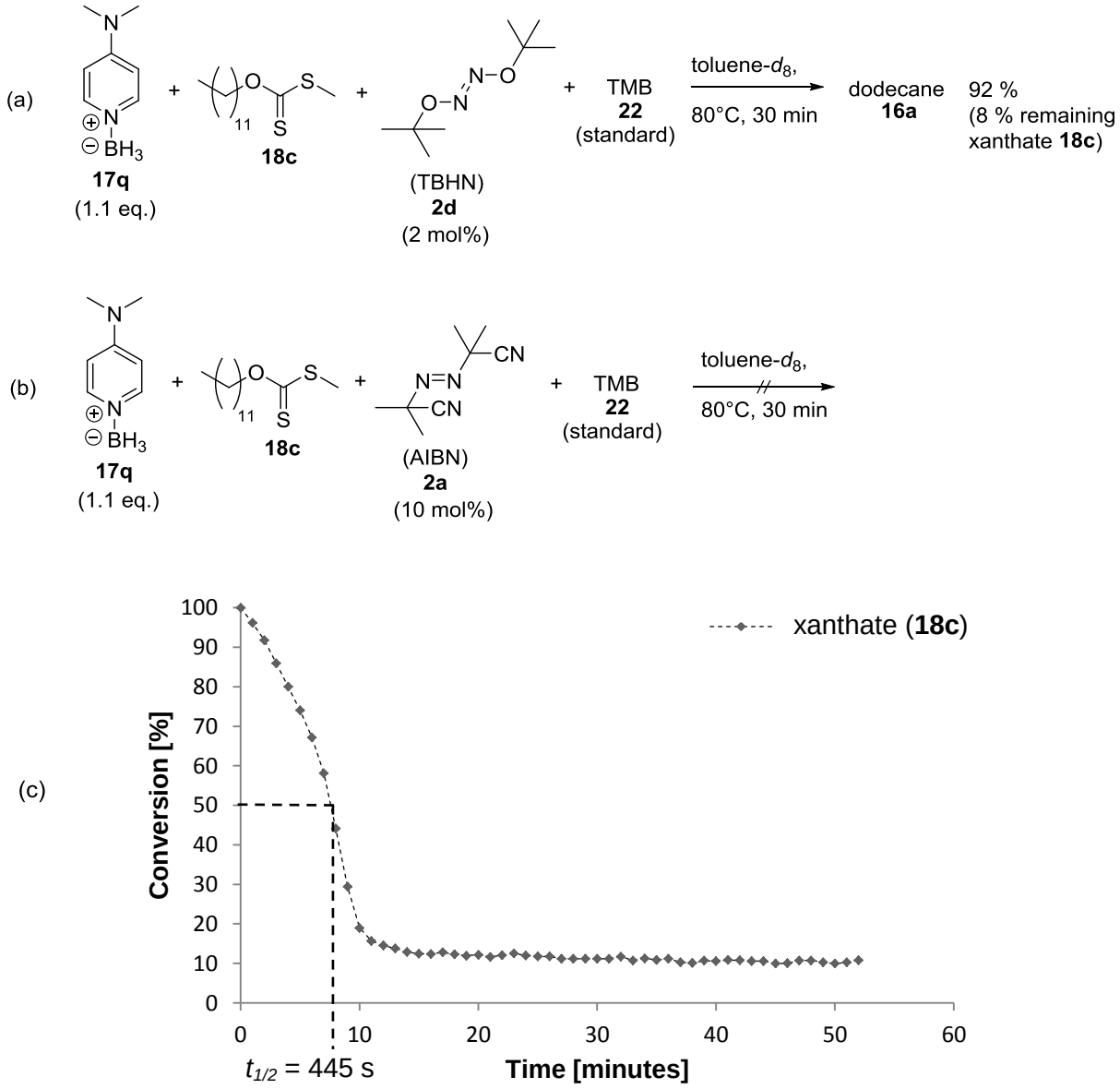

Figure 71: Radical reactions of xanthate **18c** with (a) TBHN (**2d**) and (b) AIBN (**2a**) as initiators. (c) Time-conversion plot for reaction (a).

2.5.1.2. Variations of DMAP borane (17q) as hydrogen atom donor

As the DMAP borane (**17q**) had turned out to be a good reducing agent for xanthate **18c**, the question came up, how atom efficient the borane species would be. Therefore the amount of borane **17q** was successively reduced (Figure 72a). It is obvious, that more than one hydrogen atom is transferred in this reaction. The diagram in Figure 72b shows the measured values compared with an idealized 1 : 1 reduction curve. The slope of the line reflects the number of hydrogen atoms transferred by DMAP borane (**17q**). However, the intercept of the measured line can be discussed. As only three data points are available, it is not clear how the curve progression below 0.33 equivalents would look like. For a rough estimation the origin (0 eq. = 0 % conversion) as a fourth data point was also taken into account (blue dotted line). In summary it can be stated, that DMAP borane (**17q**) delivers

between 1.29 and 1.52 hydrogen atoms in this reaction. For a more exact statement, further data points would be necessary.

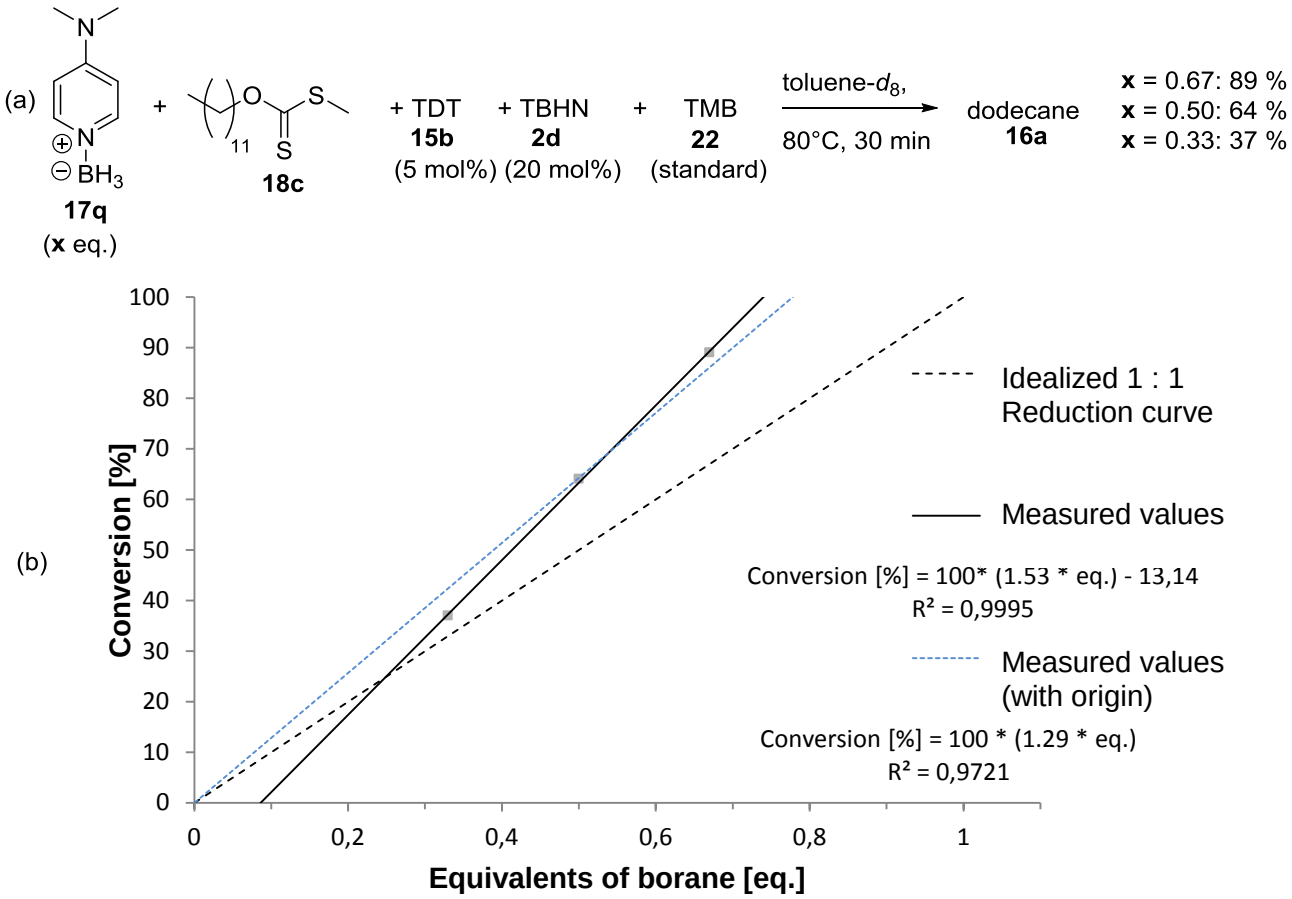

Figure 72: (a) Reduction of xanthate **18c** with different amounts of DMAP borane (**17q**). (b) Comparison of the measured values with an idealized 1 : 1 reduction curve.

2.5.2. NMR studies

The reason for this non-stoichiometric transfer of hydrogen atoms becomes more evident when looking at the reaction in more detail. Precipitation of an off-white solid during the reaction may lead to this incompleted hydrogen atom transfer. Figure 73 shows the ^{11}B NMR measurements after the reaction with 0.33 eq. DMAP borane (**17q**). The triplet (−6.97 ppm) indicates the major borane species **29i**, formed during the reduction. The minor borane species **29h** shows a doublet (−2.01 ppm) in the ^{11}B NMR measurement. The solubility of both compounds in toluene is rather low, as indicated by the noisy baseline in the ^{11}B NMR measurement. Thus, the reason why the second hydrogen atom is not completely transferred during the radical reaction can be attributed to the poor solubility of the borane species **29i**. A third hypothetic borane complex with three substituted hydrogens was not detected.

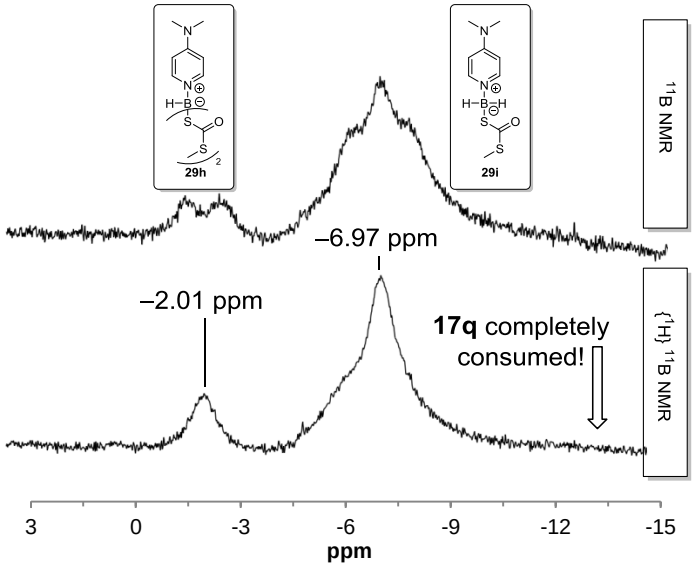

Figure 73: ^{11}B NMR measurement of the two borane species **29h** and **29i**, formed during the reduction of xanthate **18c** with DMAP borane (**17q**, 0.33 eq.) in toluene-d_8.

2.5.3. Independent control experiments

In order to exclude eventual side reactions, which could influence the radical reaction, a set of control experiments was performed (Figure 74). A reaction of DMAP borane (**17q**) in excess and xanthate **18c** at 80 °C was not observed (Figure 74a). As xanthates usually undergo pyrolysis at higher temperatures, the reaction temperature was increased to 120 °C and the xanthate exposed to this temperature in the microwave cavity (closed vessel) for 30 minutes (Figure 74b). As no reaction did take place, a pyrolysis reaction at 80 °C could also be excluded. Finally, a reaction of xanthate **18c** and the radical initiator TBHN (**2d**) was also not observed at 80 °C (Figure 74c).

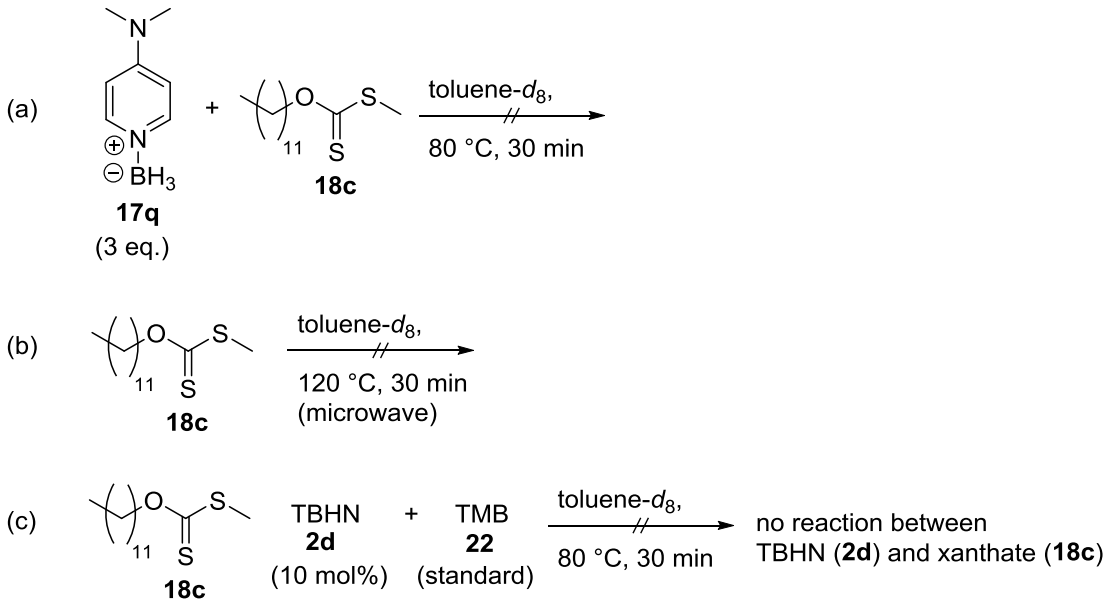

Figure 74: Control reactions for the reduction of xanthate **18c** with DMAP borane (**17q**).

Furthermore, as an independent proof for the existence of the boryl species **29h**, a closely similar compound was designed (Figure 75a). Therefore boryl iodide **29c** was generated from DMAP borane (**17q**) and iodine in $CDCl_3$ solution. Afterwards sodium ethyl xanthate (**21d**) was added in excess to the solution and stirred for 15 minutes. After removal of salts, the desired borane **29j** was precipitated with isohexane (73 %). The ^{11}B NMR measurements are shown in Figure 75b. The triplet at −6.87 ppm provides strong support for the assignment of **29i** formed during the radical reaction (with $\delta(^{11}B) = -6.97$ ppm).

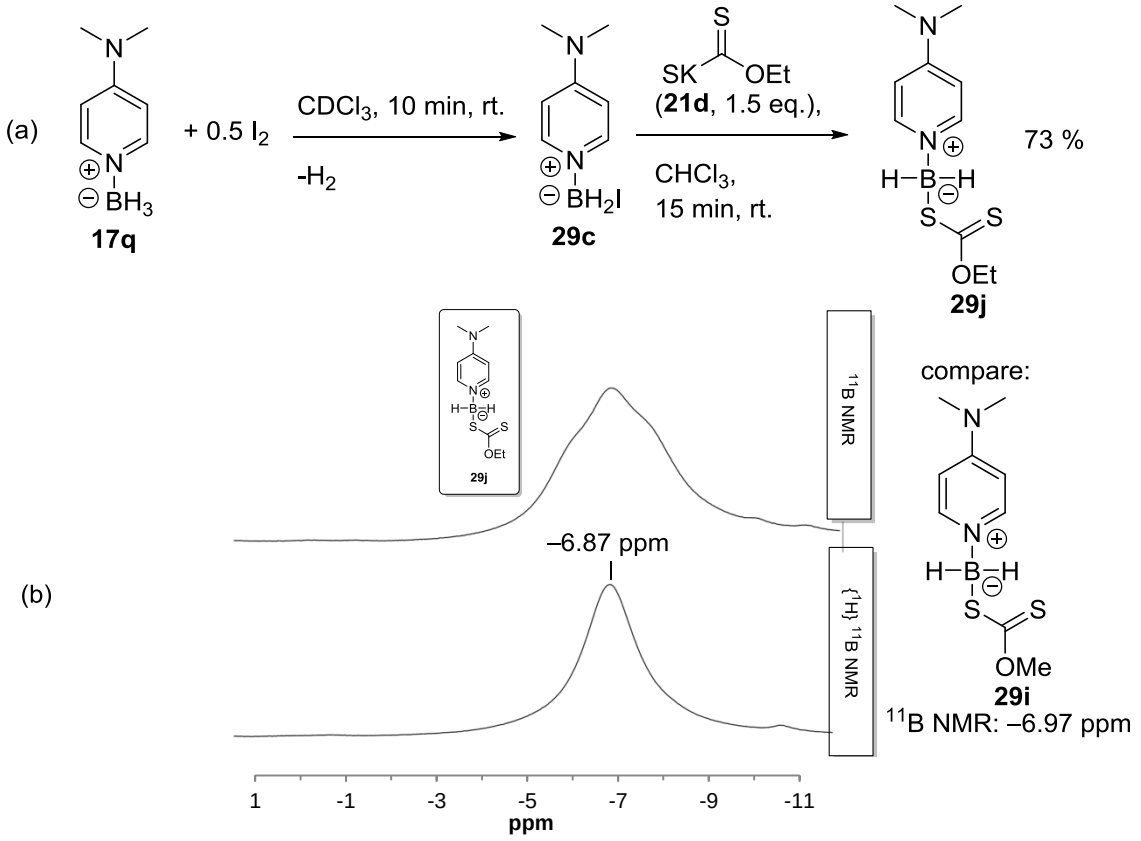

Figure 75: (a) Synthesis of borane **29j**. (b) ^{11}B NMR measurement of **29j** in $CDCl_3$.

2.5.4. Mechanism for the radical reduction of xanthate 18c with DMAP borane (17q) and TBHN (2d)

With these results in hand a mechanism for the reduction of xanthate **18c** can be proposed (Figure 76). With respect to the initiation, the formation of an oxygen-centered radical (from TBHN (**2d**)) is of major importance. This radical reacts with DMAP borane (**17q**) and leads to the boryl radical **29k**. Acetone (**25a**) and methane as minor side products from the decay of the starter could also be detected in the ^1H NMR measurements. However, there is one main difference in the reduction of xanthate **18c** compared to 1-iodododecane (**18d**). The recombination of two *tert*-butoxy radicals leads to di-*tert*-butyl peroxide (**2c**). In the case of the reduction of 1-iodododecane (**18d**) the formation of the peroxide is not observed, thus meaning, that DMAP borane (**17q**) reacts with the peroxide as shown in Figure 40 (page 34). This is not the case for the reduction of xanthate **18c**. Here, the formation of di-*tert*-butyl peroxide (**2c**) is observed. The most plausible explanation for this is that boryl radical **29k**

reacts faster with xanthate **18c** than with the peroxide species **2c**. The formation of borane **29g** is not detected by ^{11}B NMR spectroscopy in this case, whereas it was found for the reduction of 1-iododododecane (**18d**). This shows, that a reaction of boryl radical **29k** with TBHN (**2d**) as well as a recombination of **29k** and a tert-butoxy radical is very unlikely. Thus, ionic side reactions are avoided and the main processes are two radical chain reactions, which lead effectively to the desired product dodecane (**16a**). The reaction of **29k** with xanthate **18c** is the first step of chain 1. The so formed boryl radical **29l** collapses in the following step into a dodecyl radical and the borane complex **29i** (which was detected by ^{11}B NMR measurements). The same steps can now be repeated for the newly formed complex **29i** (H abstraction, followed by reaction with xanthate **18c**), which leads again to a dodecyl radical and borane complex **29h** in chain 2. Finally, a hydrogen atom is transferred to the dodecyl radical by DMAP borane (**17q**), which leads to the final product dodecane (**16a**) regenerating the boryl radical **29k**. As there are much less side reactions (as compared to 1-iododododecane (**18d**)) and two possible chain reactions which both regenerate boryl radical **29k**, the reduction of xanthate **18c** works much more efficiently than the reduction of 1-iododododecane (**18d**). For the xanthate not even a thiol as catalyst is necessary. As both borane complexes (**29h** and **29i**) are precipitating during the reaction, this is the reason, why the second H atom is not completely transferred in this reaction. This precipitation might also be the reason, why the transfer of all three hydrogen atoms was not found.

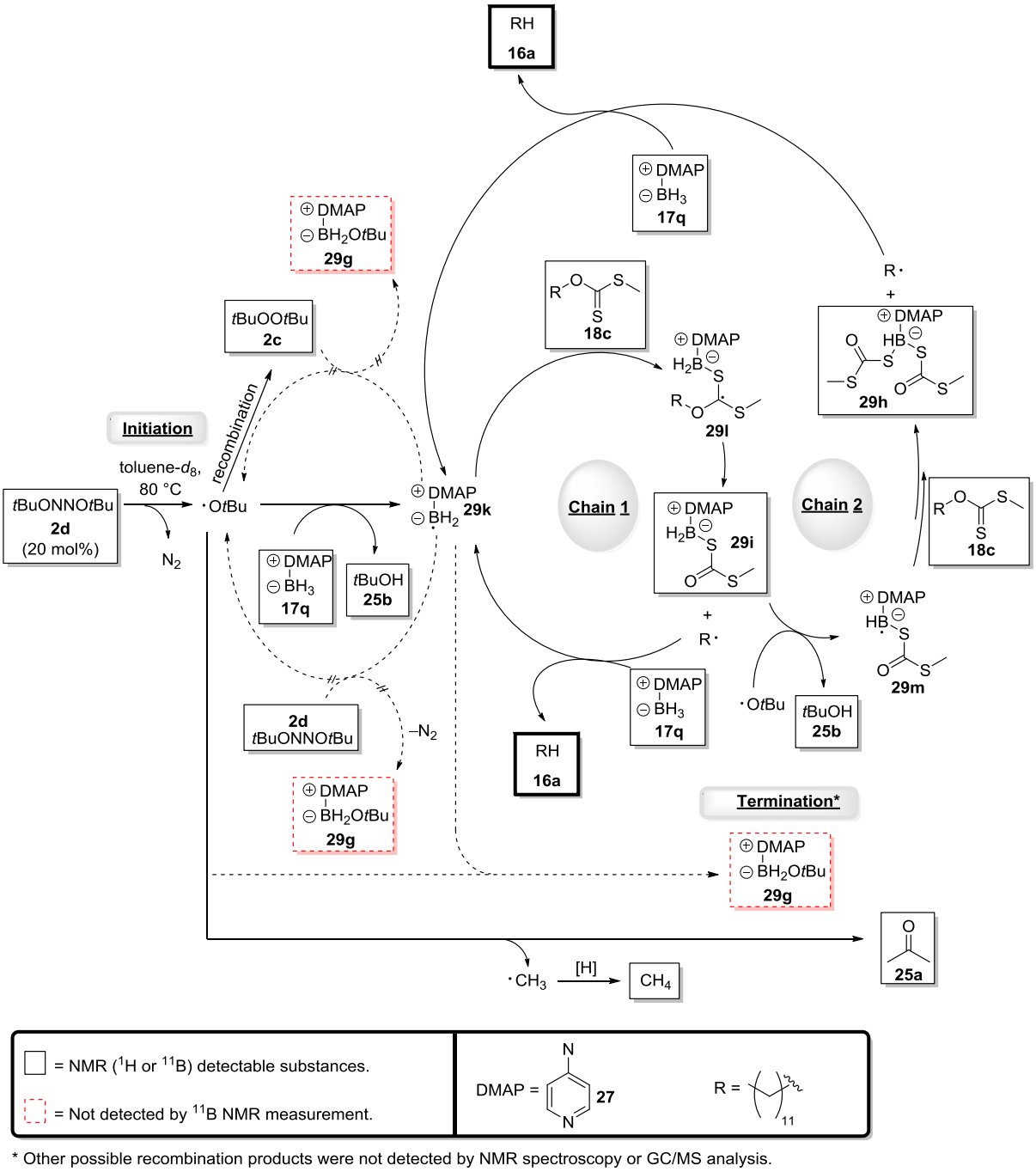

* Other possible recombination products were not detected by NMR spectroscopy or GC/MS analysis.

Figure 76: Proposed mechanism for the TBHN (**2d**)-initiated radical reduction of xanthate **18c** with DMAP borane (**17q**).

2.5.5. Reduction of xanthate 18b

As the reduction of xanthate **18c** had shown the formation of dodecane (**16a**), the expectation for the reduction of xanthate **18b** is the formation of ethane (**16e**), when systematically reducing the oxygen-attached moiety of the xanthate (Figure 77a). The formation of ethane (**16e**) was proven by ^{1}H NMR measurement (Figure 77b).

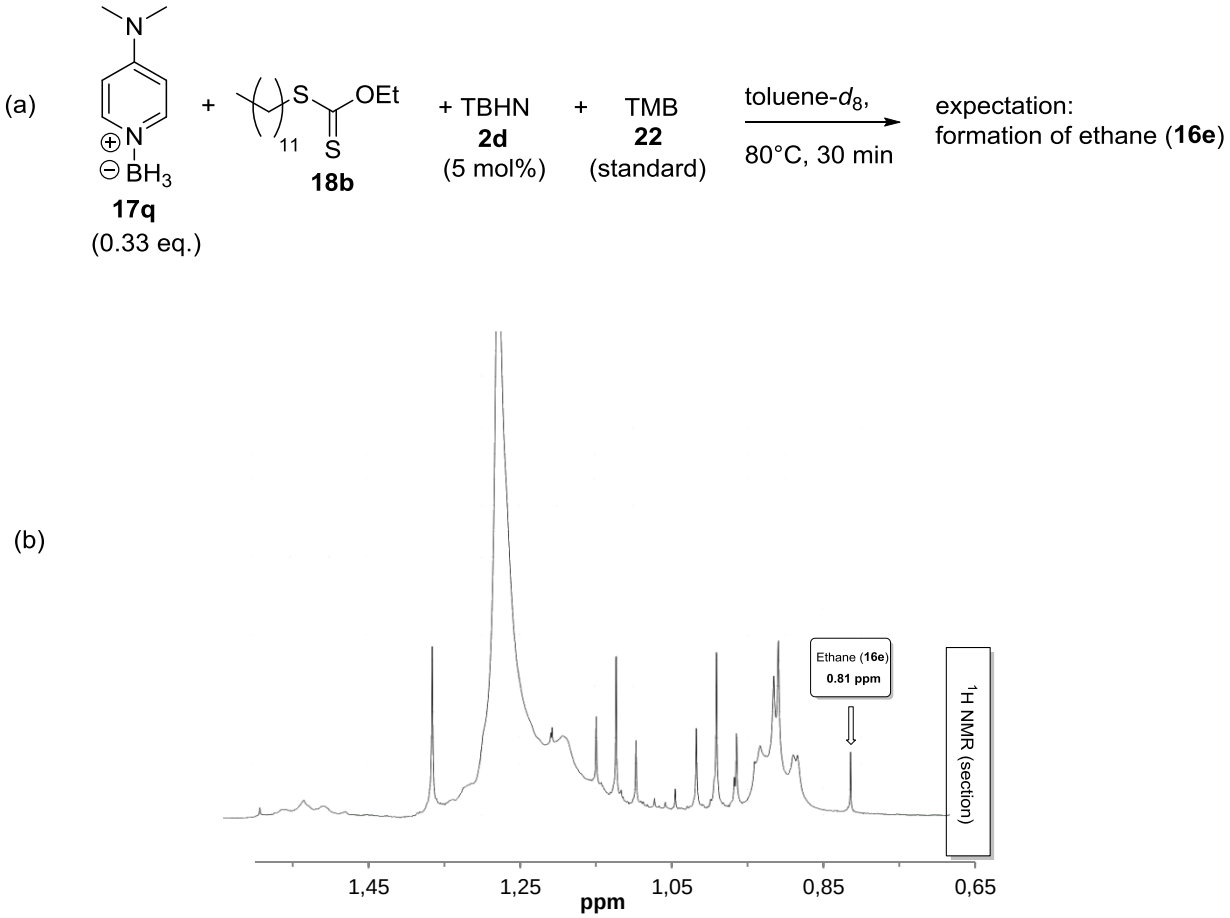

Figure 77: (a) Reduction of xanthate **18b**. (b) Section of the ^{1}H NMR spectrum taken during the reduction of **18b** in toluene-d_8.

2.5.5.1. Differences in the reduction of xanthate 18b

However, when analyzing the reaction mixture by GC/MS, also the formation of dodecane (**16a**) became apparent. This finding shows that for xanthate **18b** not only the oxygen side of the xanthate is reduced during the radical reaction, but also the sulfur attached moiety. Furthermore, the X-ray structure shown in Figure 78a was obtained from the radical reaction of xanthate **18b**. The bispyridyl species **29n** was obtained by crystallizing the compound from the crude reaction mixture in toluene. This bispyridyl borane is structurally similar to the bispyridyl borane **25i**, formed during the radical reduction of 1-iodododecane (**18d**). The formation of this compound suggests that free DMAP (**27**) must also be involved at some stage of the radical reaction. A very probable formation of bispyridyl species **29n** (similar to bispyridyl borane **25i**) is shown in Figure 78b.

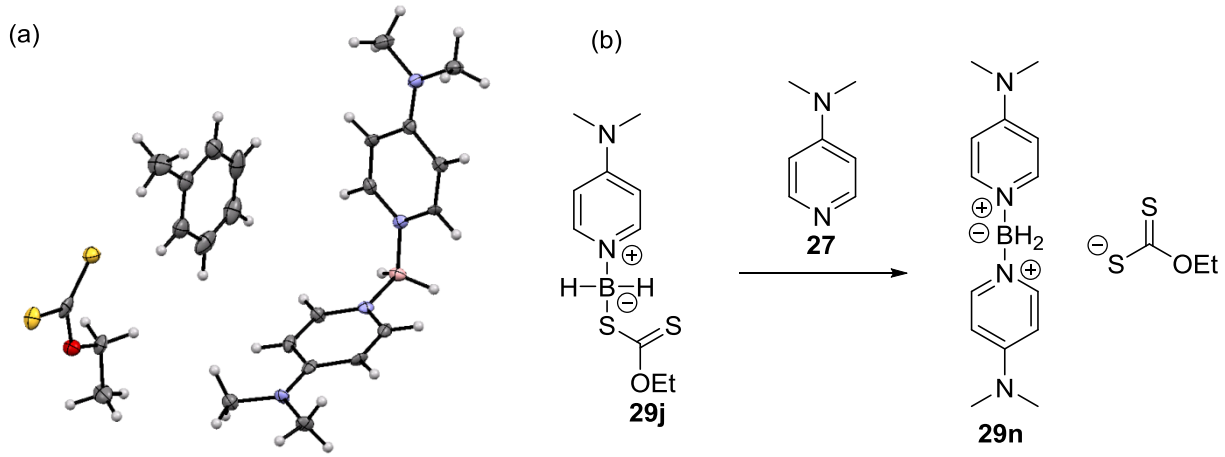

Figure 78: (a) X-ray structure of bispyridyl borane **29n**. (b) Tentative mechanism for the formation of **29n**.

As in the radical reduction of 1-iodododecane (**18d**), the decomplexation of the final borane species from the base may lead to free DMAP (**27**, Figure 79a). Hence, in the case of xanthate reduction another mechanism may be discussed (Figure 79b).

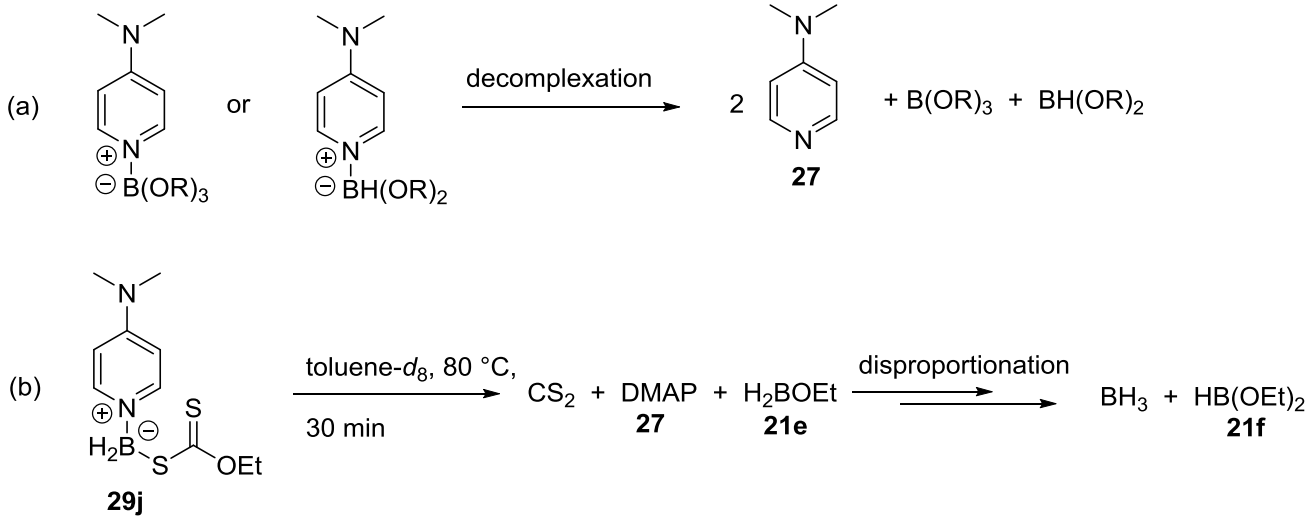

Figure 79: (a) Formation of DMAP (**27**) by decomplexation. (b) Formation of DMAP (**27**) from borane **29j** at 80 °C.

2.5.5.2. ^{13}C NMR study

The degradation of borane complex **29j** at 80 °C was monitored by ^{13}C NMR measurements. A section of the ^{13}C NMR of borane **29j** is shown in Figure 80 (spectrum 1). Due to the poor solubility of the compound in toluene, the background noise is rather significant. In the middle of Figure 80, reference NMR spectrum of CS_2 (spectrum 2) and DMAP (**27**, spectrum 3) in toluene-d_8 are shown. Spectrum 4 of Figure 80 shows the ^{13}C NMR measurement after the

exposition of borane complex **29j** to 80 °C for 30 minutes. The formation of CS_2 and DMAP (**27**) as well as the disappearance of **29j** can be observed (Figure 79b).

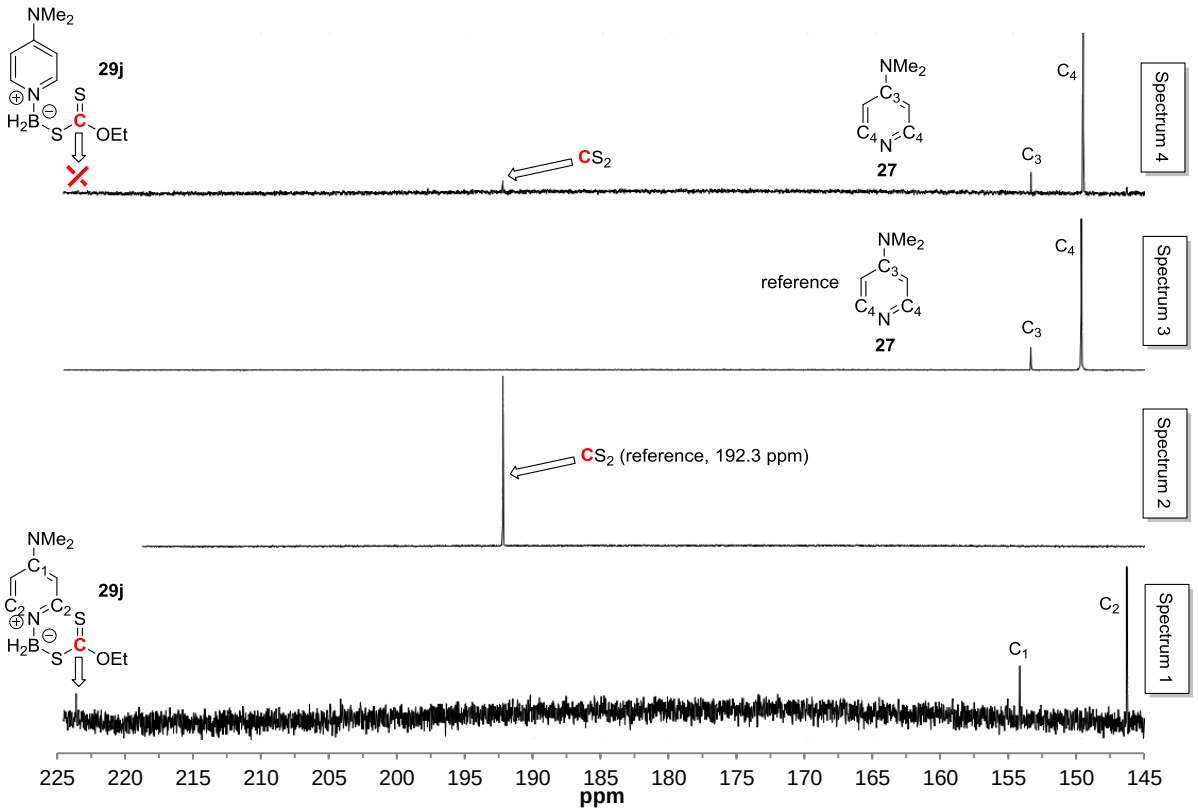

Figure 80: ^{13}C NMR measurements in toluene-d_8. Reference spectrum of borane **29j** (spectrum 1), CS_2 (spectrum 2), DMAP (**27**, spectrum 3) and borane complex **29j** after 30 minutes at 80 °C (spectrum 4).

2.5.5.3. Reaction of DMAP borane (17q) with carbon disulfide

However, during the radical reduction of xanthate **18b** with DMAP borane (**17q**), CS_2 was not observed spectroscopically. Subsequently there must be a process which consumes the carbon disulfide. Therefore, the reaction of DMAP borane (**17q**) with CS_2 in toluene-d_8 at 80 °C was monitored by ^{11}B and ^{1}H NMR (Figure 81). The ^{11}B NMR measurement shows a triplet (−6.82 ppm, J = 116.4 Hz) which can be assigned to the borane species **29o** (Figure 81b). To prove the formation of this compound ^{1}H MNR measurements were also taken into account as shown in Figure 81c. Thus, the formation of borane species **29o** can be proven by the appearance of a sharp singlet at 12.12 ppm, in accordance with a sulfur analogue of formate.

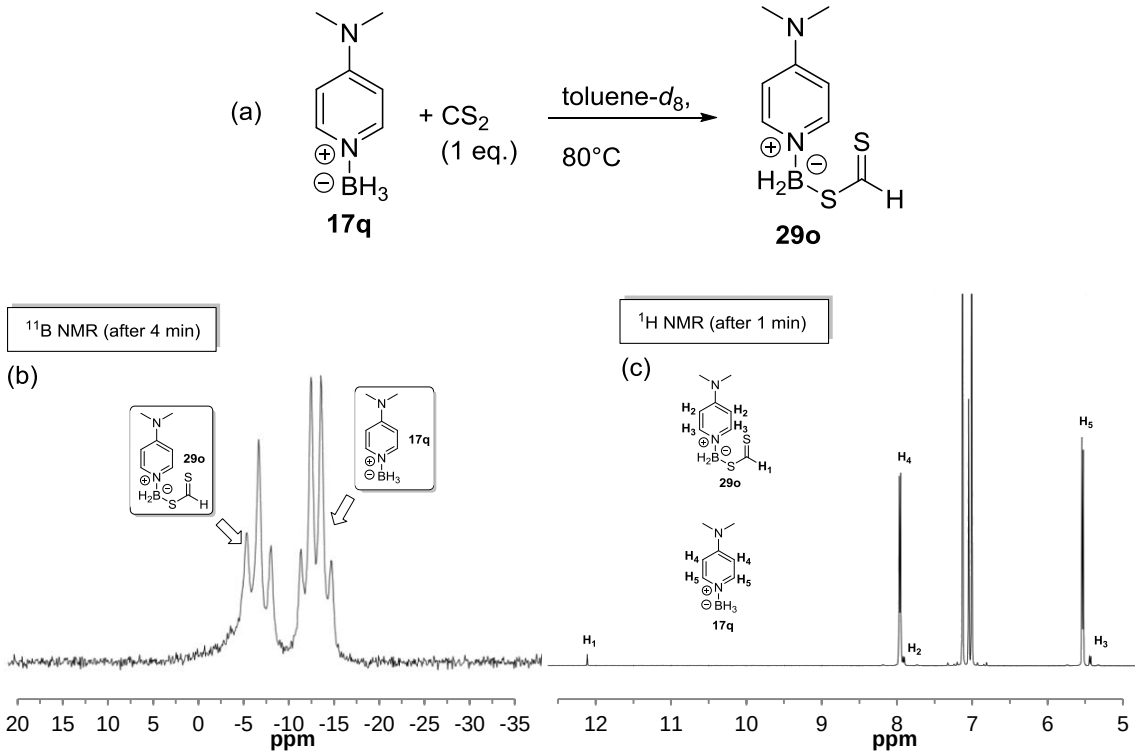

Figure 81: (a) Reaction of DMAP borane (**17q**) with CS_2 at 80 °C. (b) ^{11}B NMR measurement of the reaction in toluene-d_8 at 80 °C after 4 minutes. (c) ^{1}H NMR measurement of the reaction in toluene-d_8 at 80 °C after 1 minute.

2.5.5.4. GC/MS analysis

For further investigations of the reduction of xanthate **18b**, the radical reaction was repeated. After the reaction had cooled down to room temperature, pentane was added in order to precipitate all borane species as well as free DMAP (**27**). The absence of borane species was proven by ^{11}B NMR. This clear pentane solution was used for GC/MS analysis (Figure 82). (To make sure, that xanthate **18b** would not decompose during the GC/MS analysis, the pure starting material was also checked and no traces of decomposition were found.) The main product of the reaction is dodecane (**16a**). Ethane (**16e**), which is also formed, is not detectable by GC/MS. Besides a large signal from the starting material **18b**, there are minor side products. How these side products are formed will be discussed in the following paragraph.

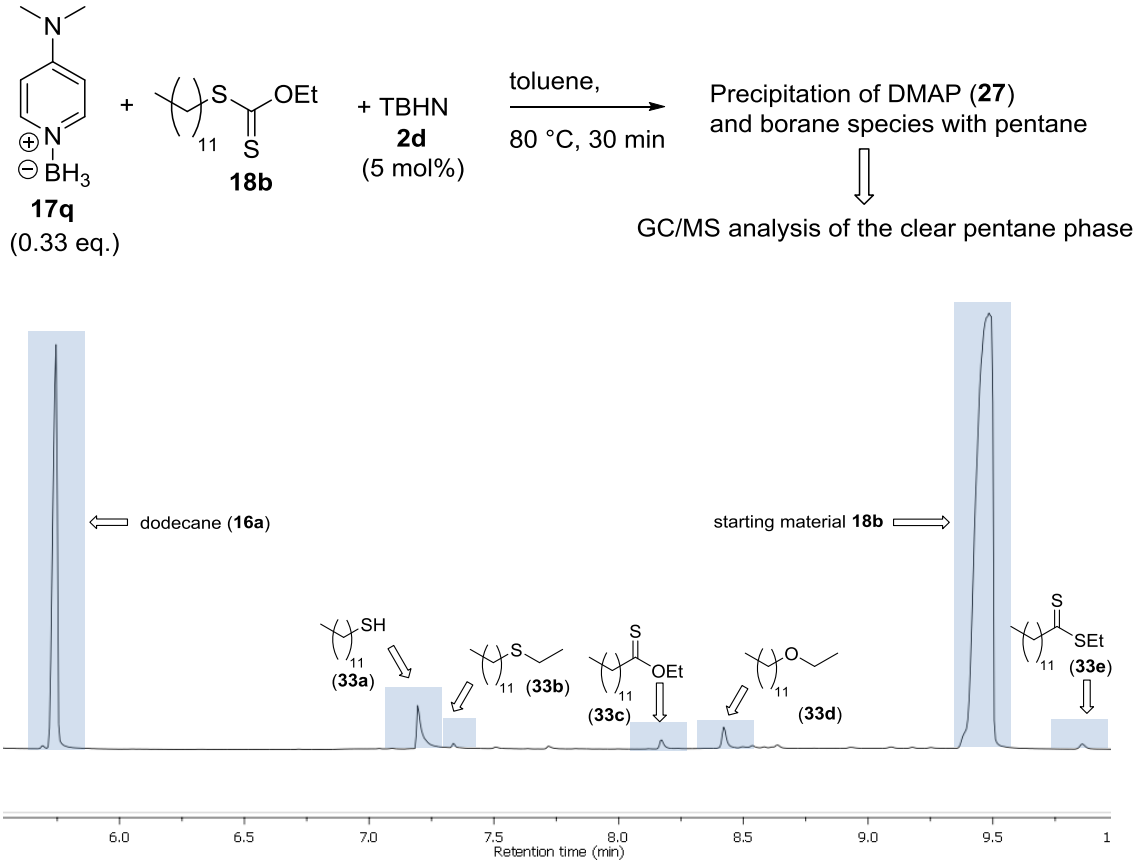

Figure 82: GC/MS analysis of the radical reduction of xanthate **18b**.

Xanthate **18b** generates a comparatively broad signal in the GC/MS spectrum. Therefore the sample was successively diluted with pentane and reanalyzed by GC/MS analysis. At approximately 50-fold dilution, the broad signal of the starting material splits up into two separate signals with a difference in the retention time of only 5 seconds (Figure 83a). When looking at the fragmentation patterns of the two compounds, it becomes clear that both are very similar (Figure 83b and c). The MS fragmentation pattern of xanthate **18b** (Figure 83b) was compared with the pure starting material before the reaction and is identical. The only meaningful explanation for the second structure is the exchange of an oxygen atom and a sulfur atom, leading to the carbodithioate **33f**.

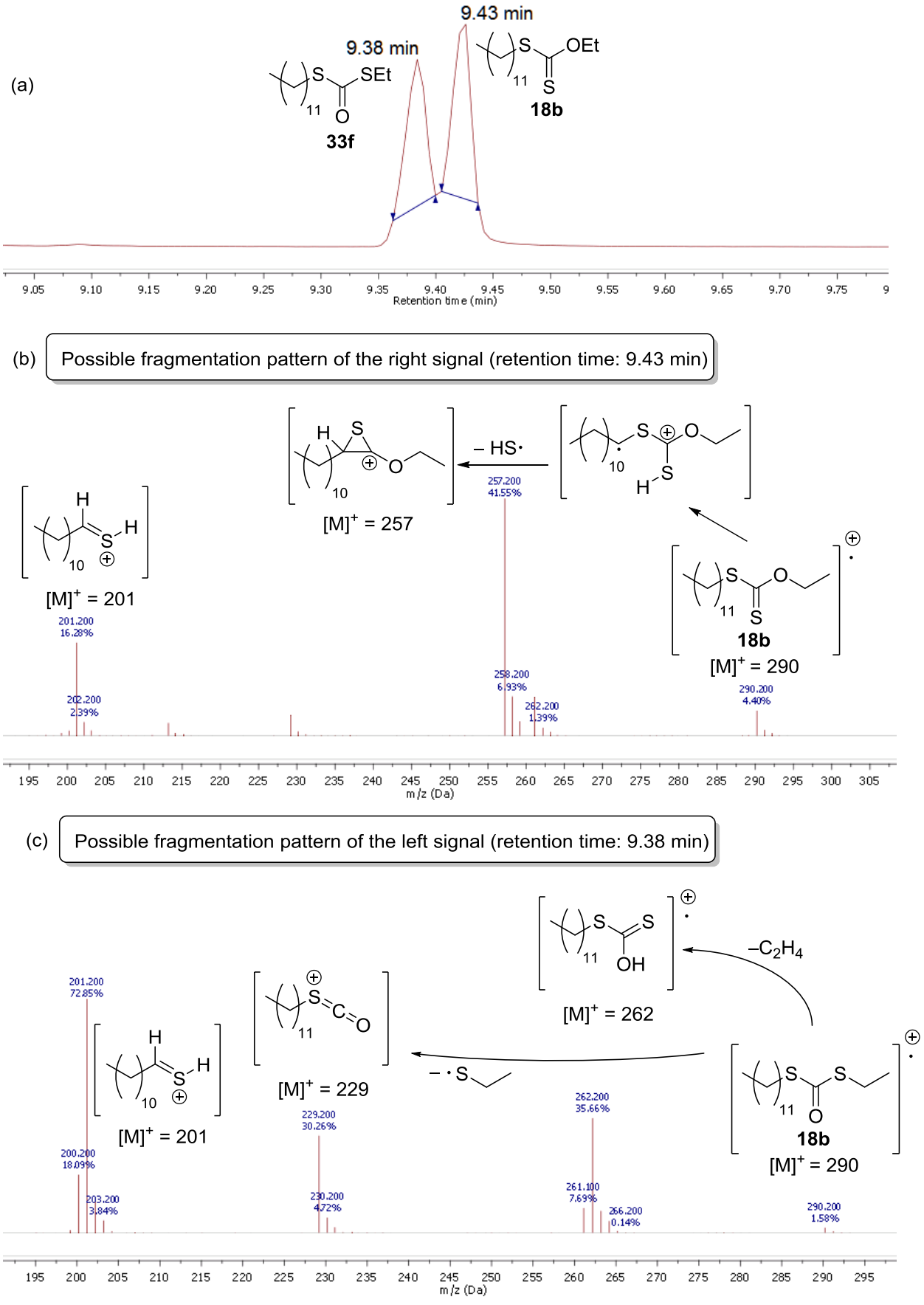

Figure 83: (a) Section of a GC after the radical reaction with xanthate **18b**. Possible MS fragmentation pattern of the signal at (b) 9.34 min and (c) 9.38 min.

2.5.5.5. Mechanism for the formation of carbodithioate 33f

The formation of carbodithioate **33f** during the radical reaction is explained in Figure 87. The attack of an ethyl radical at the sulfur of xanthate **18b** leads to a new radical (**33g**). This may now collapse to release an ethyl radical as well as the carbodithioate **33f**. Further side products can be explained by the reaction of xanthate **18b** with a dodecyl or an ethyl radical, which leads to the radicals **33ha** and **33hb**. Subsequently both compounds can form either a thiyl radical or an oxygen-centered radical under the release of **33hc**, **33hd**, **33c** and **33e**. Due to recombination reactions thioether **33b** and the ether **33d** are formed, whereas a thiyl radical can trap a hydrogen atom to form 1-dodecanethiol (**33a**). This result explains impressively, why no external catalyst (like TDT (**15b**)) is necessary for the xanthate reduction. Here the system creates its own catalyst.

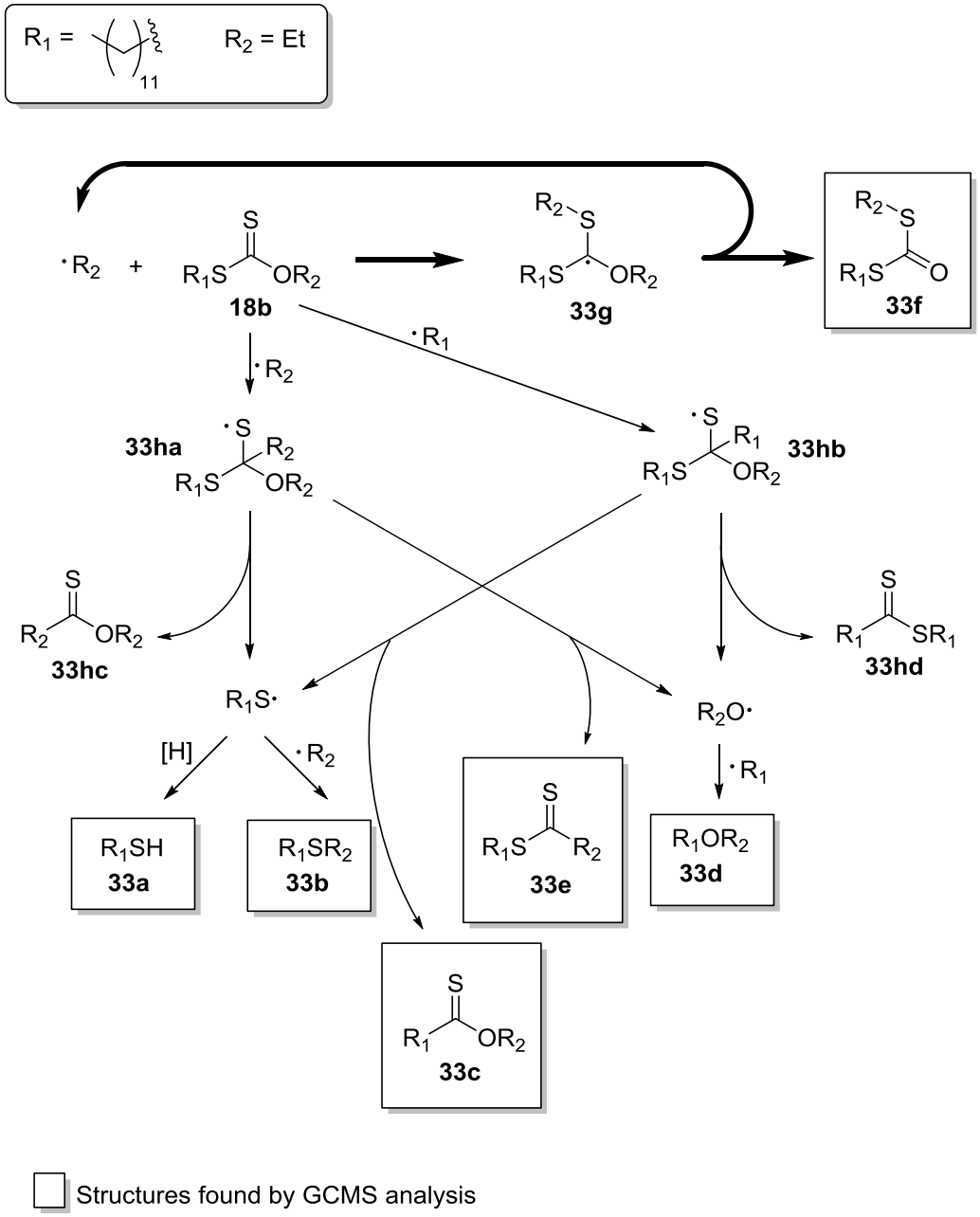

Figure 84: Formation of carbodithioate **33f** and side reactions.

2.5.5.6. Reduction of xanthate 18e - A comparison

In order to make a more quantitative statement of the reaction, a new xanthate was synthesized, as ethane (**16e**) is too volatile to be detected (Figure 85). Therefore, 1-decanol (**21g**) was first deprotonated with *n*BuLi. After addition of CS_2 and 1-iodododecane (**18d**), xanthate **18e** was purified by column chromatography and yielded 55 % of a yellow oil.

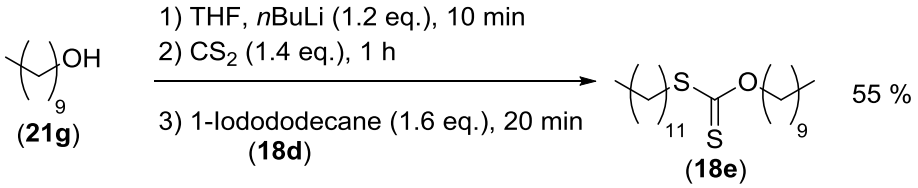

Figure 85: Synthesis of xanthate **18e**.

Subsequently, the radical reduction was repeated with xanthate **18e** and the reaction outcome was analyzed by GC/MS. To get a better overview of how side reactions would take place, the reaction was done with 0.75 and 0.50 eq. of DMAP borane (**17q**). The reactions with possible products are shown in Figure 86. The results for the reactions are summarized in Table 9. As each xanthate (**18e**) molecule can be reduced either at the oxygen side or at the sulfur side, the yields correspond to a full equivalent on each side. When looking at reaction 1 (0.75 eq. DMAP borane (**17q**)), a full conversion of xanthate **18e** is observed. Dodecane (**16a**) is with 75 % the main product, whereas decane (**30c**) is only formed in 15 % yield. However, as shown before, there is a side reaction leading to 25 % of 1-dodecanethiol (**33a**), which can catalyze the reaction. All other products are only formed in traces. In reaction 2 (0.5 eq. DMAP borane (**17q**)) no full conversion is achieved. The exact amount of remaining xanthate **18e** and the carbodithioate **34a** cannot be determined as there is no signal separation due to their structural similarity. The yield of dodecane (**16a**) drops down to 54 %, decane (**30c**) to 11 %. Hence, the yield of 1-dodecanethiol (**33a**, 27 %) is even slightly higher as before, which is also the case for thioether **34c** (2 %). This result indicates that the radical reaction is still running once the H atom donor (DMAP borane (**17q**)) is consumed, leading to different side products. Furthermore, the product distribution of **16a** : **30c** (reaction 1 = 5.00; reaction 2 = 4.91) shows, that the formation of dodecane (**16a**), which is the sulfur side product, is roughly 5 times larger in both cases.

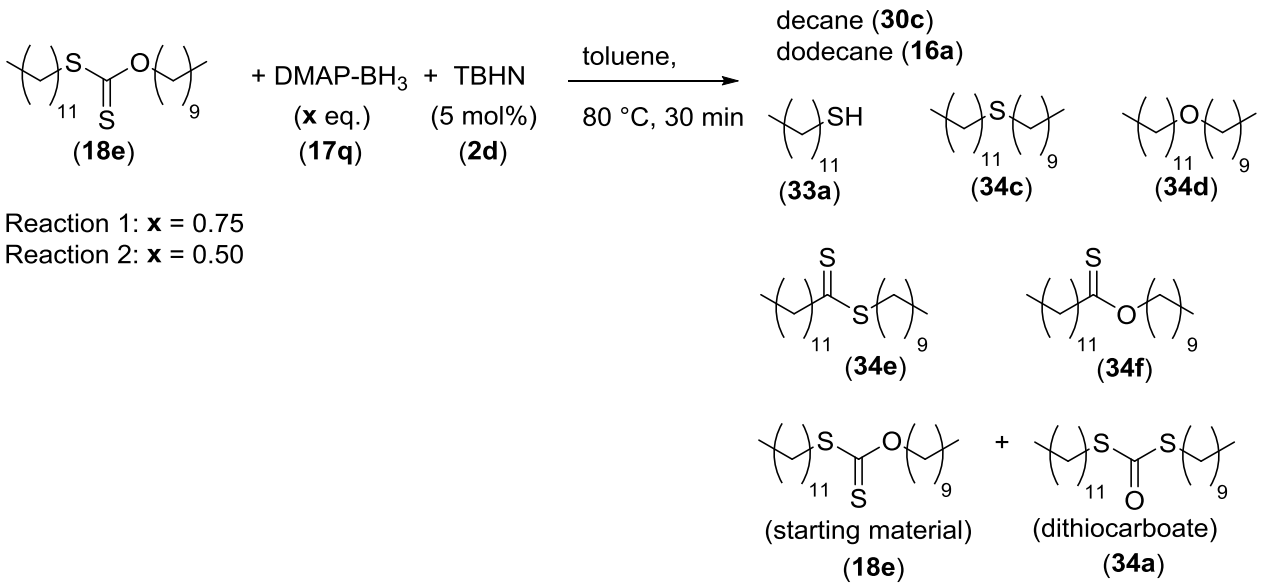

Figure 86: Radical reduction of xanthate **18e** and possible products.

Table 9: Results for the reactions shown in Figure 86.

	decane (**30c**)	dodecane (**16a**)	Ratio **16a** : **30c**	**33a**	**34c**	**34d**, **34e** **34f**	**18e**+**34a**
Reaction 1	15 %	75 %	5.00	25 %	traces	traces	none
Reaction 2	11 %	54 %	4.91	27 %	2 %	traces	17 %

2.5.5.7. Mechanism for the reduction of xanthate 18b

Finally, a plausible reaction mechanism is shown in Figure 87. Similar to the reduction of 1-iododododecane (**18d**), the formation of the boryl radical **29k** from an oxygen-centered radical is essential. This can now react with the xanthate **18b** to form the new radical **29p**. There are two main steps, which lead either to a cleavage on the oxygen side or a cleavage on the sulfur side of the xanthate. Thus (in the shown case) an ethyl radical and a dodecyl radical are formed. Considering main step 2, the ethyl radical can now trap a hydrogen atom to form ethane (**16e**). (This is shown simplified in Figure 87.) However, the ethyl radical may also attack at the sulfur of the xanthate, leading to radical **33g**. This reaction seems to happen mainly when an insufficient amount of the H atom donor (DMAP borane (**17q**)) is present. The reaction of xanthate **18b** with either an ethyl radical or a dodecyl radical can also lead to **33ha** and **33hb**, which subsequently leads to **33a**, **33b**, **33c**, **33d** and **33e**. This process is also shown simplified here. (For more detailed information compare Figure 84.) The so formed thiol **33a** is involved in the H atom transfer from DMAP borane (**17q**) as catalyst. When looking at main step 1, the dodecyl radical can also catch a H atom (either catalyzed by a thiol or by direct transfer), which leads to dodecane (**16a**). Borane complex **29j** decomposes at 80 °C to CS_2 and in following steps to DMAP (**27**) and the final borates. The formed carbon disulfide however can react with DMAP borane (**17q**) to form the borane species **29o**. The free base DMAP (**27**) will also react with the borane species **29j**, which leads to the bispyridyl borane **29n**. Yet, borane **29j** can also act as a hydrogen atom donor.

By reaction of the resulting boryl radical **29q** with the xanthate, borane species **29r** is formed. The transfer of a third hydrogen atom was not observed.

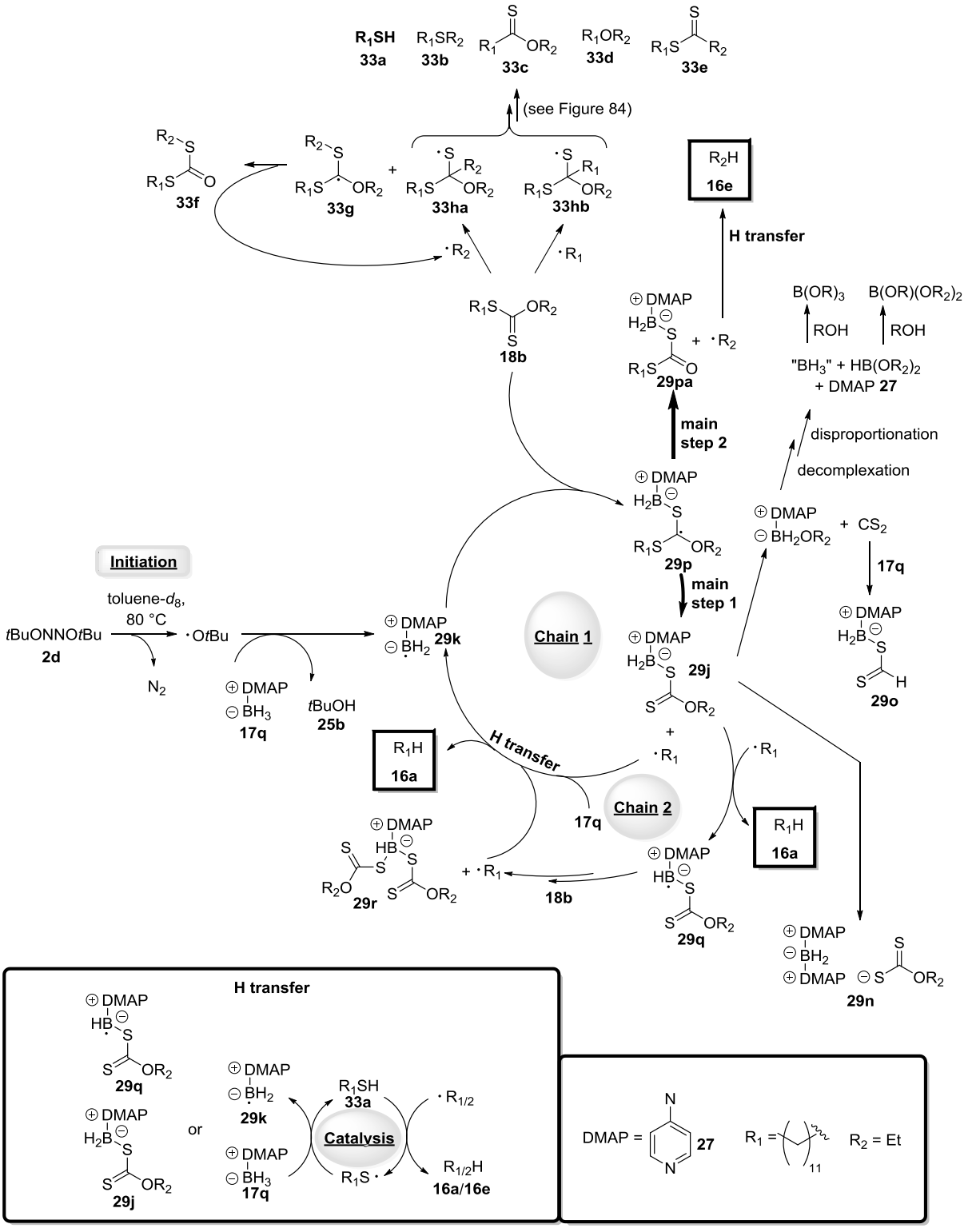

Figure 87: Reaction mechanism for the TBHN (**2d**)-initiated radical reduction of xanthate **18b** with DMAP borane (**17q**).

It seems obvious, that the structure of the xanthate has a big influence on the product distribution of the reduction. Xanthates, which have methyl groups attached to the sulfur, seem to form exclusively the “oxygen side” product, which was shown for xanthate **18c** which leads to a full conversion into dodecane (**16a**). The formation of methane could also be discussed in this case, as traces of methane were found in the ^{1}H NMR spectra. However, it seems more likely that these traces of methane are formed by the cleavage reaction of *tert*-butoxy radicals (which come from TBHN (**2d**)), as acetone could also be detected. Yet, the full conversion into dodecane (**16a**) could be proven by the use of an internal NMR standard (TMB (**22**)). For xanthates bearing a longer alkyl chain at the sulfur, the reactivity changes. In the previous studies two xanthates with a dodecyl moiety attached to the sulfur were used. For both xanthates a large amount of dodecane (**16a**) was found and so favoring the “sulfur side” product. This behavior seems not to be influenced by the length of the alkyl group attached to the oxygen (here: an ethyl or a dodecyl group), as the formation of dodecane (**16a**) is the main product in both cases. An interesting question for future studies could be the correlation of chain length and reactivity of xanthates in radical reductions with DMAP borane (**17q**).

2.5.6. Reduction of a secondary xanthate

In order to prove the behavior of *S*-methylated xanthates, compound **18f** was synthesized from 2-decanol (**35a**) under standard conditions for *Barton-McCombie* xanthates (Figure 88a). After column chromatography xanthate **18f** was obtained as a yellow oil (78 %). This compound was used for the radical reduction with DMAP borane (**17q**) and led to a quantitative yield of decane (**30c**) (Figure 88b). This result confirms the formation of the “oxygen side” product of *S*-methylated xanthates. Furthermore it shows, that the reduction of secondary xanthates is also possible under the used conditions.

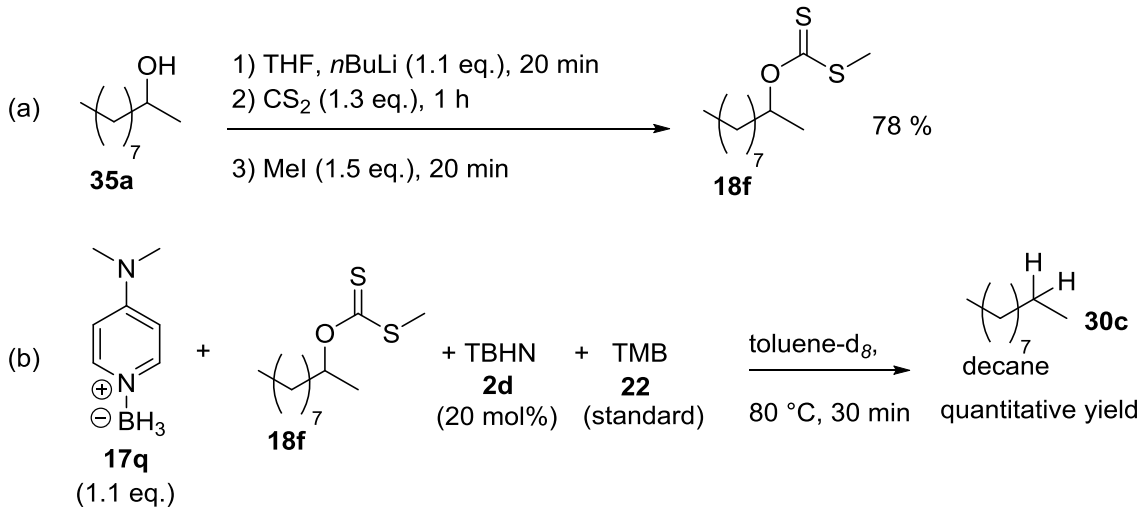

Figure 88: (a) Synthesis of xanthate **18f**. (b) Radical reduction of xanthate **18f** with DMAP borane (**17q**).

2.5.7. Reduction of a tertiary xanthate

For a systematic completion, a tertiary xanthate was also taken into account. Therefore, adamantyl xanthate **18g** was synthesized (Figure 89a) from 1-adamantanol (**35b**). However, when trying to convert the tertiary xanthate **18g** to adamantane (**7b**) in a radical reaction with DMAP borane (**17q**), only traces of the desired product were found (Figure 89b). Hence, a radical reduction with DMAP borane (**17q**) seems to be limited to primary and secondary xanthates.

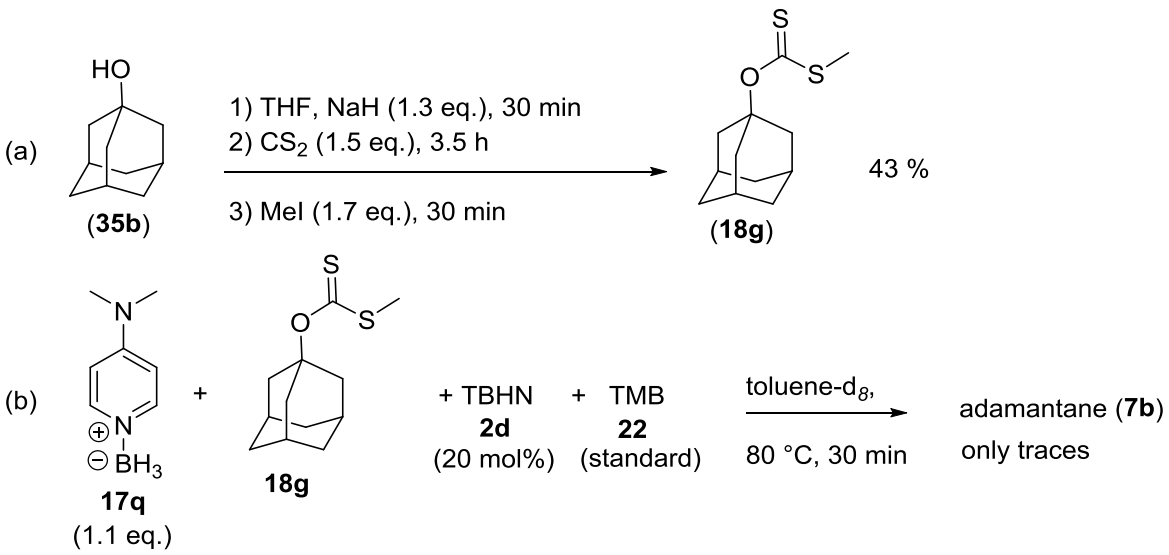

Figure 89: (a) Synthesis of xanthate **18g**. (b) Attempt of a radical reduction of xanthate **18g** with DMAP borane (**17q**).

2.5.8. Reduction of a benzylic xanthate

As the reaction with primary xanthates has shown quite fast reactions and good yields, the question came up, how reactive a benzylic xanthate would be under the tested conditions. Thus, xanthate **18h** was synthesized from naphthylmethanol (Figure 90) and isolated as viscous yellow oil (26 %) after column chromatography.

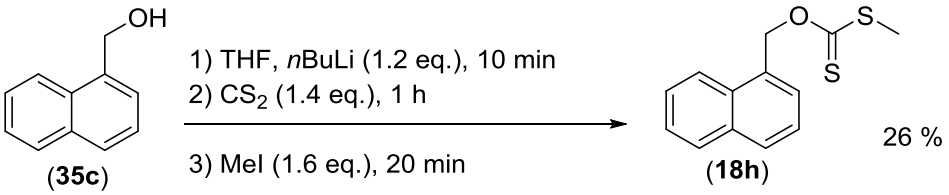

Figure 90: Synthesis of xanthate **18h**.

The reduction of xanthate **18h** was conducted under the same conditions as before and yielded 10 % 1-methylnaphthalene (**35d**, Figure 91a). Further side products were not present. The ^{11}B NMR measurements after the reaction (Figure 91b) show that only one hydrogen atom was transferred from DMAP borane (**17q**).

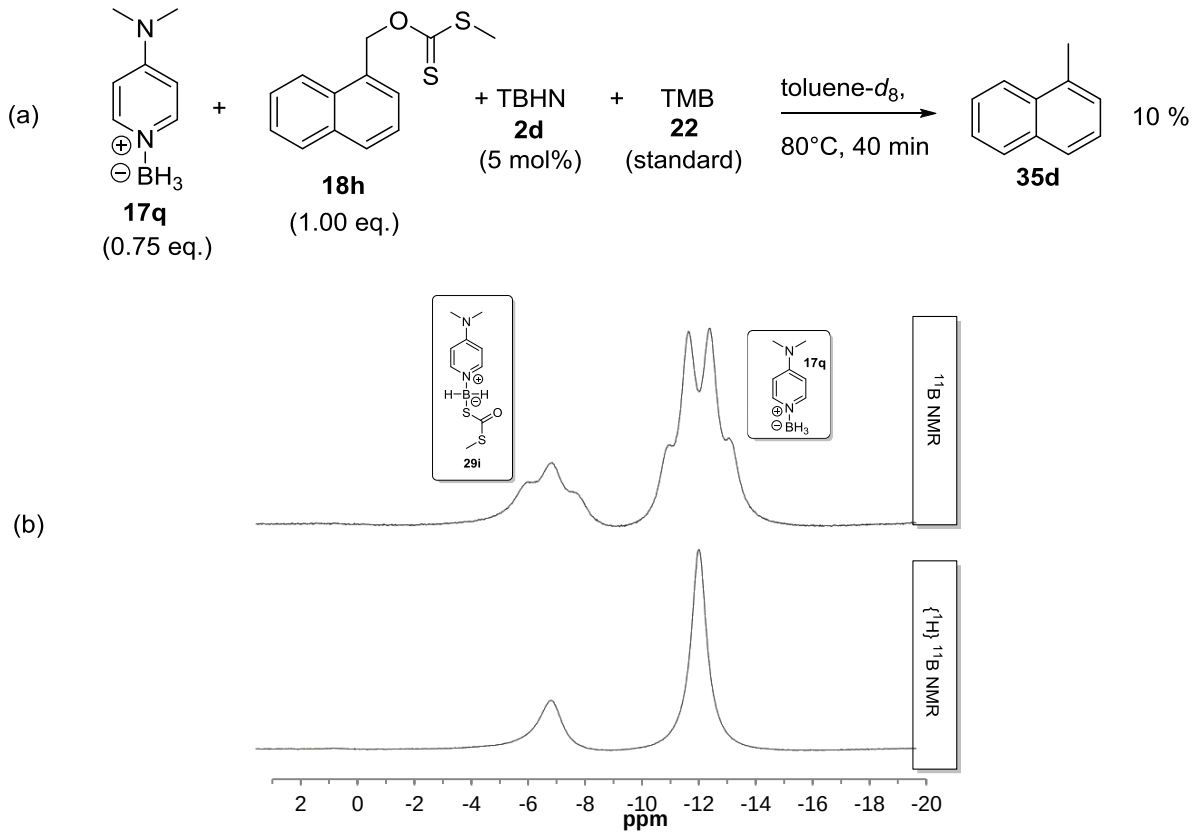

Figure 91: (a) Reduction of xanthate **18h** with DMAP borane (**17q**) and TBHN (**2d**) as initiator. (b) ^{11}B NMR measurements after the reaction.

The result of this reaction is easily understood, when looking at the mechanism (Figure 92). After boryl radical **29k** is formed, it reacts with xanthate **18h**. The so formed boryl radical **29s** collapses into 1-methylnaphthyl radical and the final borane species **29i**. However, there is no radical chain, as the benzylic radical is just too stable. After trapping a hydrogen atom, the reaction is over. In this way, the yield of 10 % can also be understood, as 5 mol% TBHN (**2d**) were used. These 5 mol% can deliver 10 mol% of *tert*-butoxy radicals, which act more like a reagent than a starter in this case. A possible recombination product is not detected in this case.

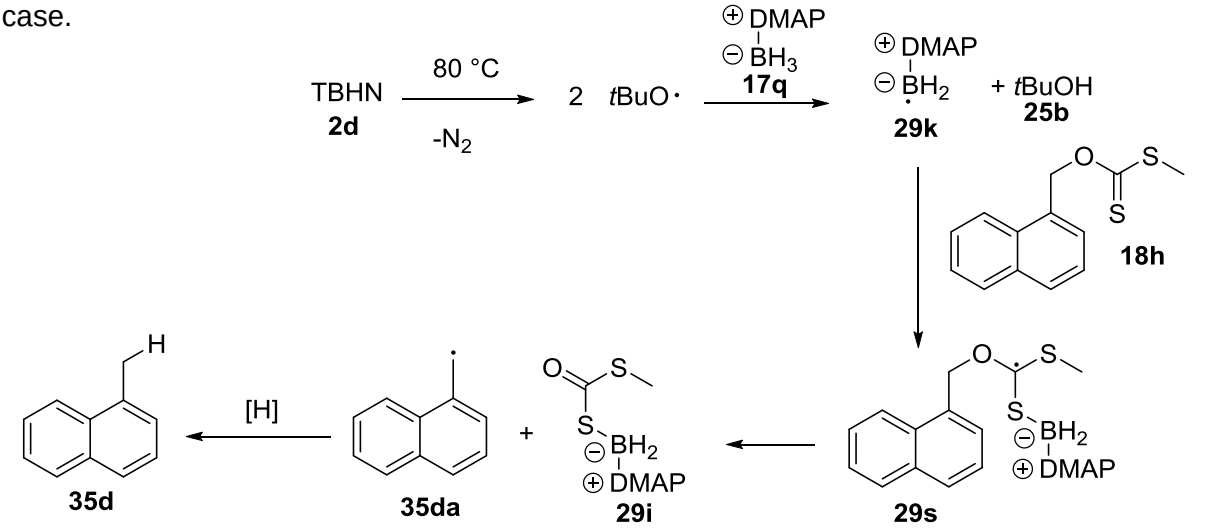

Figure 92: Reaction mechanism of the reduction of xanthate **18h**.

2.6. Xanthate vs. alkyl iodide – A selectivity study with different hydrogen atom donors

As a final study, the selectivity of radical reductions with different hydrogen atom donors was investigated. Therefore 1-iodododecane (**18d**) and xanthate **18c** were used in a 1:1 ratio (one equivalent each), and reacted with 0.75 eq. borane complex. The decay of the substrates as well as the decay of the complex was then monitored by ^{1}H NMR spectroscopy in toluene-d_8 at 80 °C.

2.6.1. DEAP borane (17z)

In order to follow the decay of the borane complex, DEAP borane (**17z**) was chosen for initial measurements due to its better solubility in toluene (Figure 93a). As in previous ^{1}H NMR measurements the CH_2-I signal of 1-iodododecane (**18d**) can be used to determine the decay of the alkyl iodide. However as the ^{1}H NMR signals of the alkyl groups of DEAP borane (**17z**) overlap with the CH_2-I signal of 1-iodododecane (**18d**), the decay of the alkyl halide could not be determined in this way (Figure 93b). After 8 minutes the consumption of DEAP borane (**17z**) is complete and the overall conversion of xanthate **18c** is 78 %.

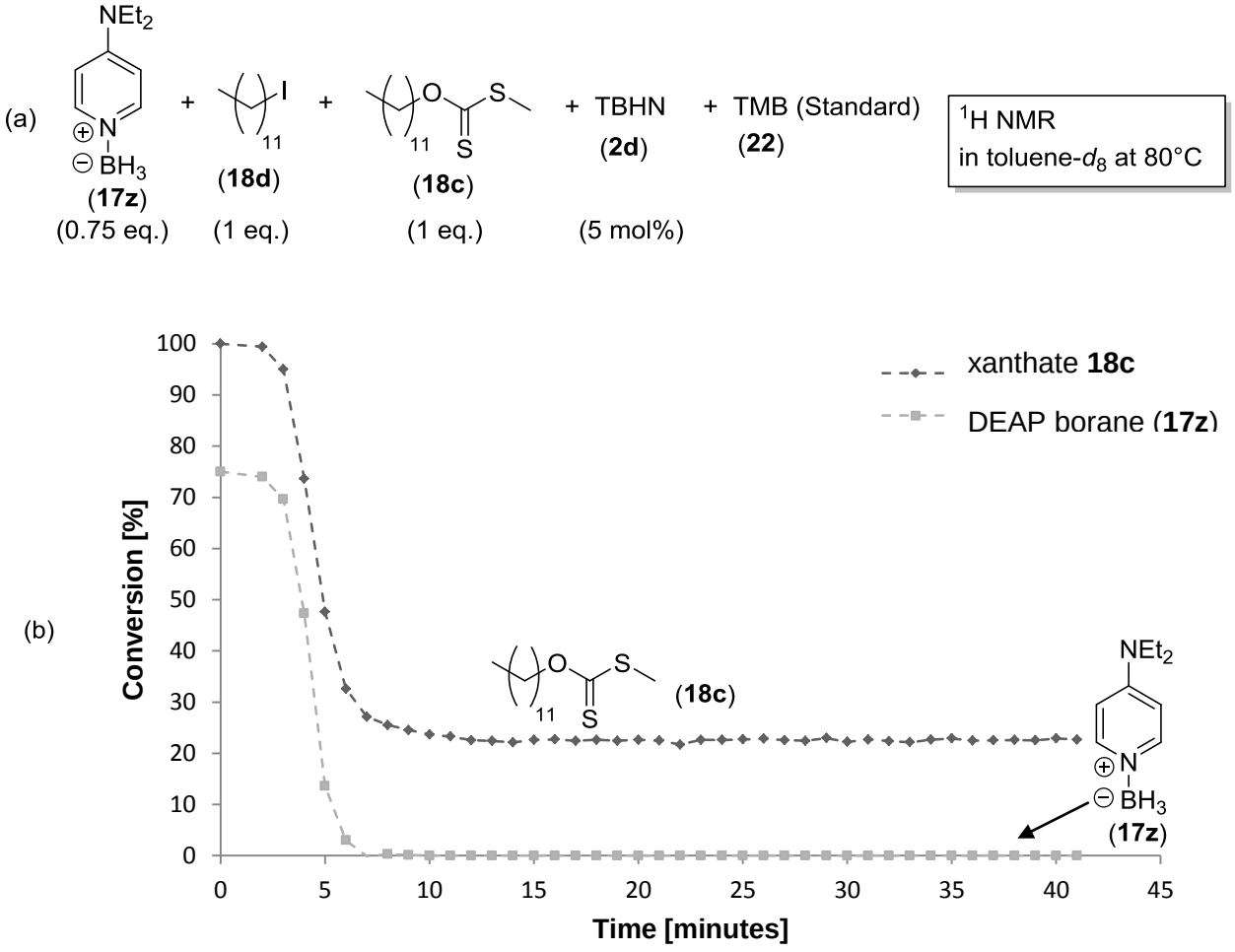

Figure 93: (a) Competition reaction of 1-iodododecane (**18d**) and xanthate **18c** in a radical reduction with DEAP borane (**17z**). (b) Time-conversion plot of the reaction.

2.6.2. DMAP borane (17q)

Yet, to make a statement on the conversion ratio of 1-iodododecane (**18d**) against xanthate **18c**, the reaction was repeated by replacing DEAP borane (**17z**) by DMAP borane (**17q**) (Figure 94a). The CH_2-I signal of 1-iodododecane (**18d**) does now not overlap with other signals. Due to the poor solubility of DMAP borane (**17q**) in toluene, the decay of the borane complex could not be followed in this case. As shown in previous studies it is assumed, that the reactivity of DEAP borane (**17z**) and DMAP borane (**17q**) is very similar. This is supported by the time-conversion plot of the reaction with DMAP borane (**17q**) (Figure 94b). The decay of xanthate **18c** is the same as in the previous case with DEAP borane (**17z**) and its conversion ends at 78 %. The overall conversion of 1-iodododecane (**18d**) stops at 18 %. Hence, the conversion ratio of 1-iodododecane (**18d**) : xanthate **18c** is 1 : 4.33. This finding is very surprising, as usually primary iodides react much faster than xanthates in radical reactions. In case of the reduction with DMAP borane (**17q**) the reaction with the xanthate is favored.

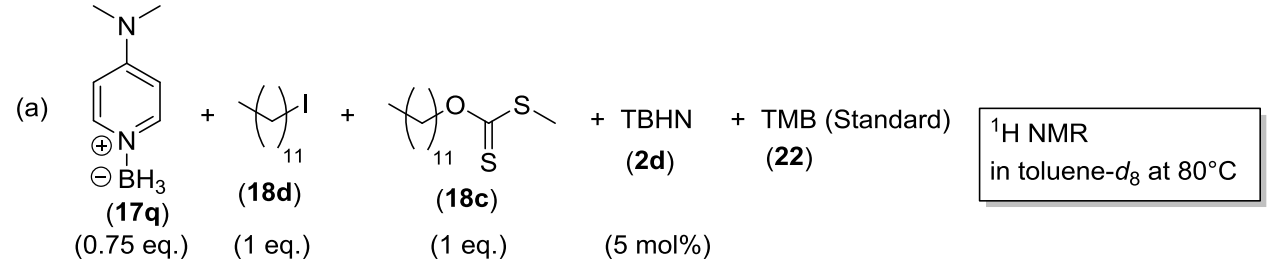

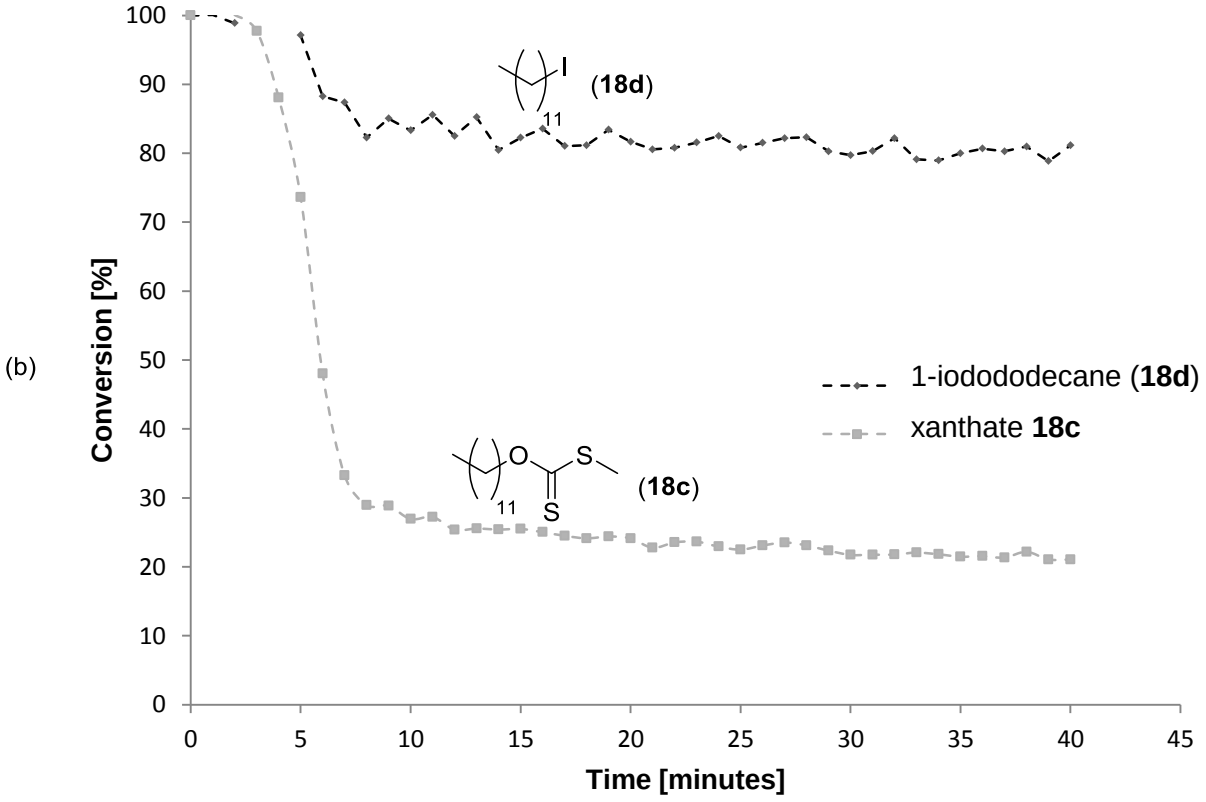

Figure 94: (a) Competition reaction of 1-iodododecane (**18d**) and xanthate (**18c**) in a radical reduction with DMAP borane (**17q**). (b) Time-conversion plot of the reaction.

2.6.3. NHC borane 17y

To compare this behavior of DMAP borane (**17q**) towards xanthates with other options, the competition experiment was repeated under the same conditions with NHC borane **17y** (Figure 95a). When omitting TDT (**15b**) as catalyst, the reaction is slightly slower than with DMAP borane (**17q**). In this case no change in the conversion is observed after 15 minutes (Figure 95b). However, only 1-iododododecane (**18d**) is reacting with a final conversion of 25 %. No reaction with xanthate **18c** was observed at all. The formation of iodoborane **36a** as the only product from NHC borane **17y** is shown in terms of the ^{11}B NMR after the reaction (Figure 95b). The reaction was repeated with the addition of thiol **15b** (5 mol%) as catalyst. As in the case of DMAP borane (**17q**), the reaction is finished after 8 minutes (Figure 95c). Another effect achieved by TDT (**15b**) is a slight rise in the conversion of 1-iododododecane (**18d**) to 45 %. Yet, there is no reaction with xanthate **18c**. This result shows impressively the special behavior of DMAP borane (**17q**) with respect to the reduction of xanthates.

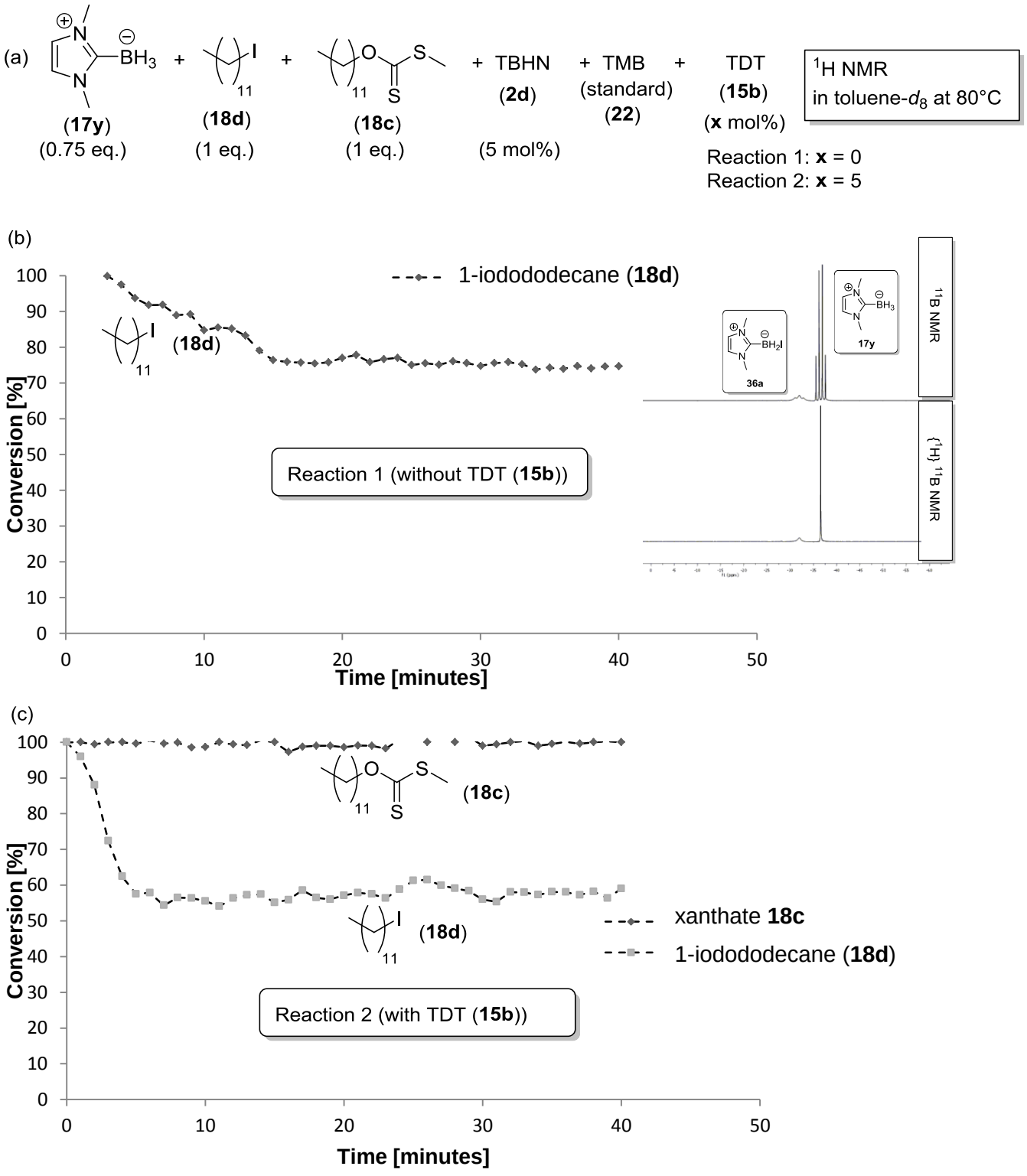

Figure 95: (a) Competition reactions of 1-iododododecane (**18d**) and xanthate (**18c**) in a radical reductions with NHC borane **17y**. Time-conversion plots of the reaction (b) in the absence and (c) in the presence of TDT (**15b**).

2.6.4. Bu_3SnH (1a)

As a reference reaction, Bu_3SnH (**1a**) was used as hydrogen atom donor in the competition experiment (Figure 96). The reaction was finished after 20 minutes. As expected, the reduction of 1-iododododecane (**18d**) was favored over the xanthate **18c** in a ratio of 2.75. Furthermore, 0.75 eq. of Bu_3SnH (**1a**) are completely consumed under these conditions, leading to 20 % dodecane (**16a**, from the xanthate) and 55 % dodecane (**16a**, from the alkyl iodide).

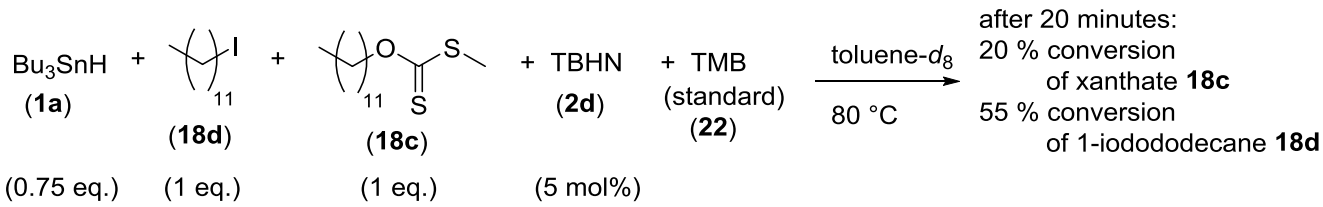

Figure 96: Competition reaction of 1-iododododecane (**18d**) and xanthate (**18c**) in a radical reductions with Bu_3SnH (**1a**).

2.6.5. Summary

Table 10 summarizes the results of the competition experiments. Whereas NHC borane **17y** leads to a moderate conversion of 45 % (when using TDT (**15b**) as catalyst) of 1-iododododecane (**18d**), its selectivity seems to be completely on the side of the iodide. In case of Bu_3SnH (**1a**), the reduction of 1-iododododecane (**18d**) is also favored, but not the only product. For synthetic purposes DMAP borane (**17q**) could be of a big interest. Here, the selectivity for the reduction of the xanthate is about 12 times larger than with Bu_3SnH (**1a**). For synthetic purposes, where selectively one substrate should be reduced, the combination of NHC borane **17y** (for iodides) and DMAP borane (**17q**) for xanthates are a much better (and less toxic) alternative than Bu_3SnH (**1a**).

Table 10: Summary of the results for the competition experiments of xanthate **18c** (1 eq.) and 1-iododododecane (**18d**, 1eq.) with different H atom donors (0.75 eq.).

H atom donor (0.75 eq.)	reaction time [min]	TDT (**15b**)	Conversion ratio Iodide : xanthate	Overall conversion (iodide+xanthate)
DMAP borane (**17q**)	8	---	1 : 4.33	96 %
NHC borane **17y**	15	---	1 : 0	25 %
NHC borane **17y**	8	5 mol%	1 : 0	45 %
Bu_3SnH (**1a**)	20	---	1 : 0.36	75 %

3. Ionic Reactions

3.1. Introduction

Reduction reactions with inorganic reductants are well known and widely used in organic chemistry. One of the most prominent compounds, which can reduce a large number of functional groups, is lithium aluminumhydride. A general overview of reductions with $LiAlH_4$ is shown in Figure 97. Thus, lithium aluminumhydride can reduce aldehydes, acid chlorides, anhydrides, acids and esters to the corresponding primary alcohols, whereas ketones are reduced to the secondary alcohols.[55, 56, 57, 58] Amides, oximes, nitro compounds, nitriles and azides are reduced to amines by lithium aluminumhydride, alkyl halides to the corresponding alkanes.[59, 60, 61]

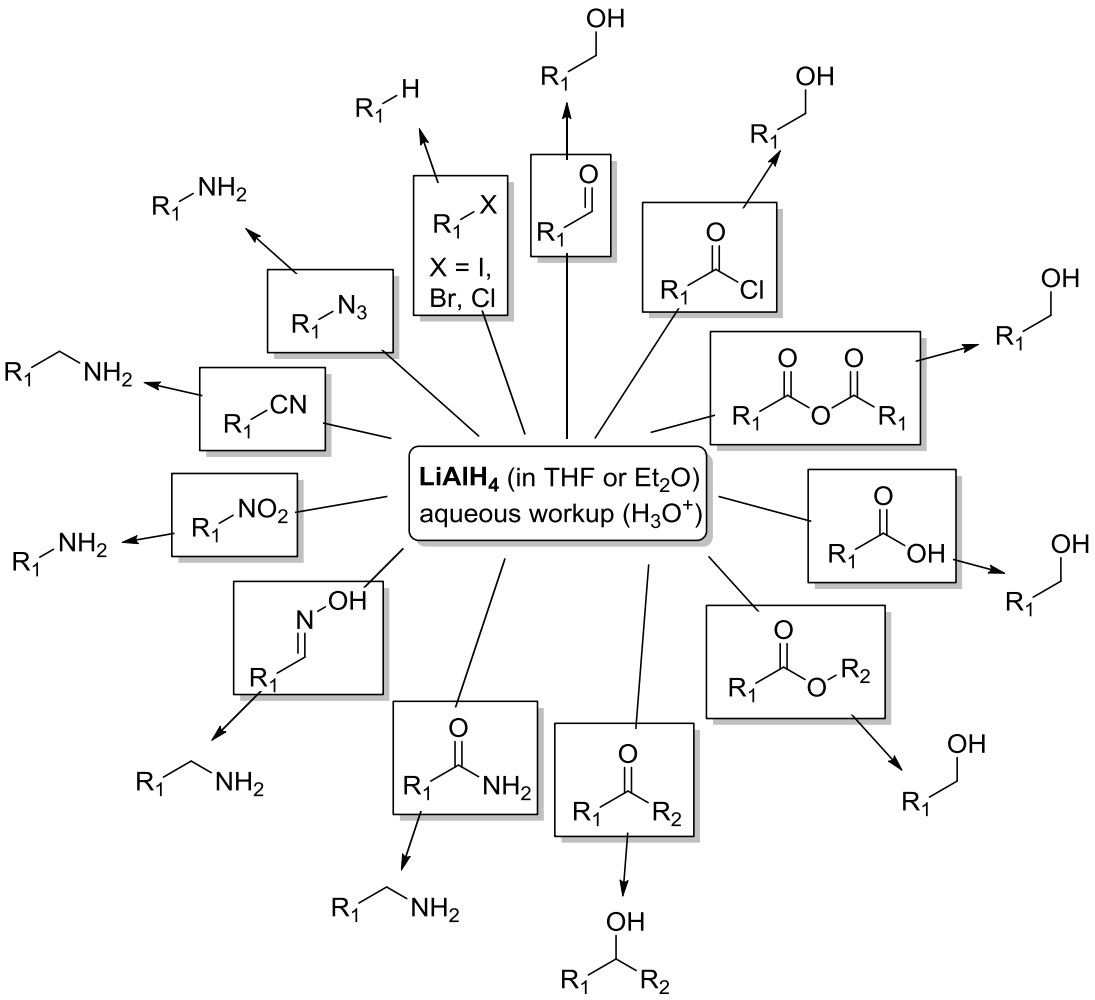

Figure 97: General scheme for reductions with $LiAlH_4$.

3.1.1. Sodium borohydride as reductant

Although $LiAlH_4$ is a powerful reductant, its use is limited. On the one hand it can only be used with ethers as solvents, as it is insoluble in nonpolar solvents. On the other hand the

reductive potential towards such a large number of functional groups can also be a hindrance, when it comes to selective reductions. Sodium borohydride is, compared to $LiAlH_4$, a relatively mild reductant. It is widely used for reductions of aldehydes or ketones to alcohols. The addition of metal salts like $CeCl_3$ can make the reduction selective for ketones (*Luche* reduction, Figure 98a and b).[62, 63, 64, 65, 66] Even a selective reduction of esters can be achieved when employing cobalt(II) chloride as catalyst in combination with $NaBH_4$.[67] Furthermore, several reductions of imines are known with sodium borohydride, an example is shown in Figure 98c.[68, 69, 70]

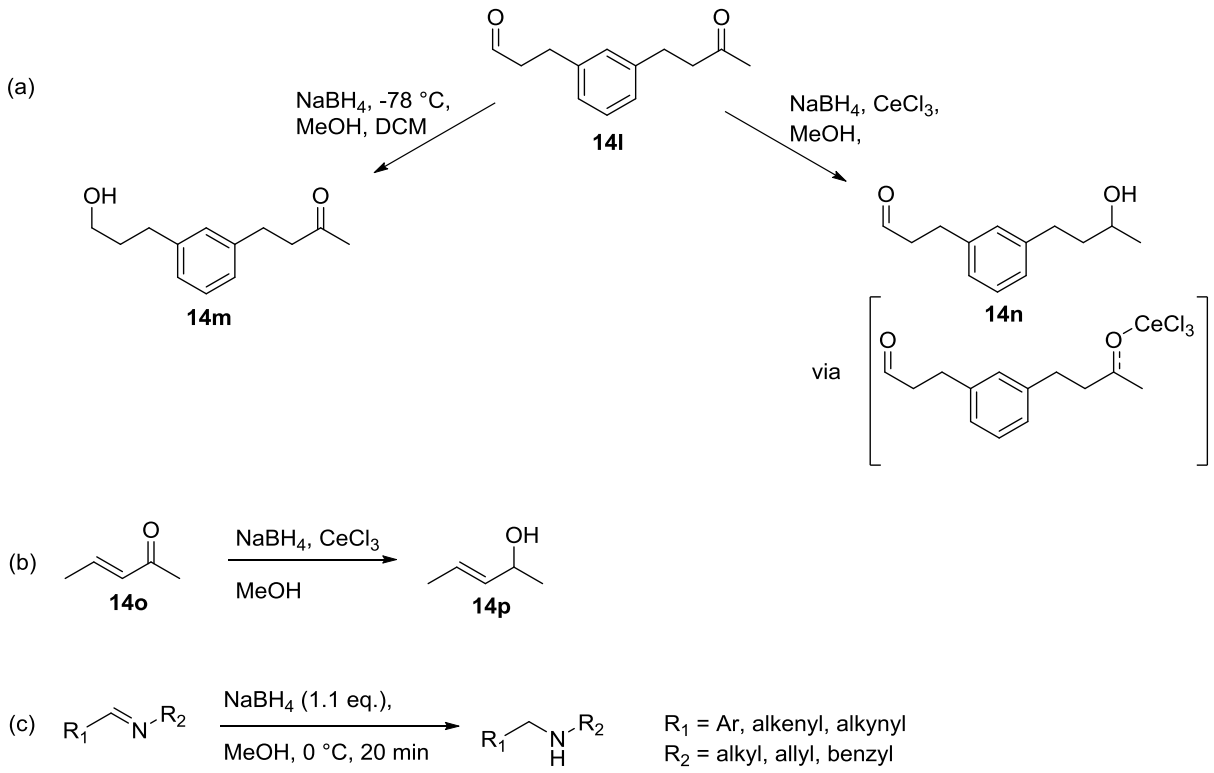

Figure 98: Examples for reductions with sodium borohydride.

3.1.2. The *Corey-Bakshi-Shibata* reduction

Beside these inorganic salts, "BH_3" (in form of THF-BH_3 or Me_2S-BH_3 solutions) can also be applied for reductions of carbonyl compounds. However, reductions of ketones with "BH_3" are rather slow. A good example for a fast and enantioselective reduction of ketones with "BH_3" is the CBS reduction (Figure 99).[71] The mechanism shows that an attack of the hydride is only possible from one side of the ketone, as long as the two groups (R_1 and R_2) differ in size. The regeneration of the CBS catalyst and the complexation of "BH_3" grant a fast and effective reduction.

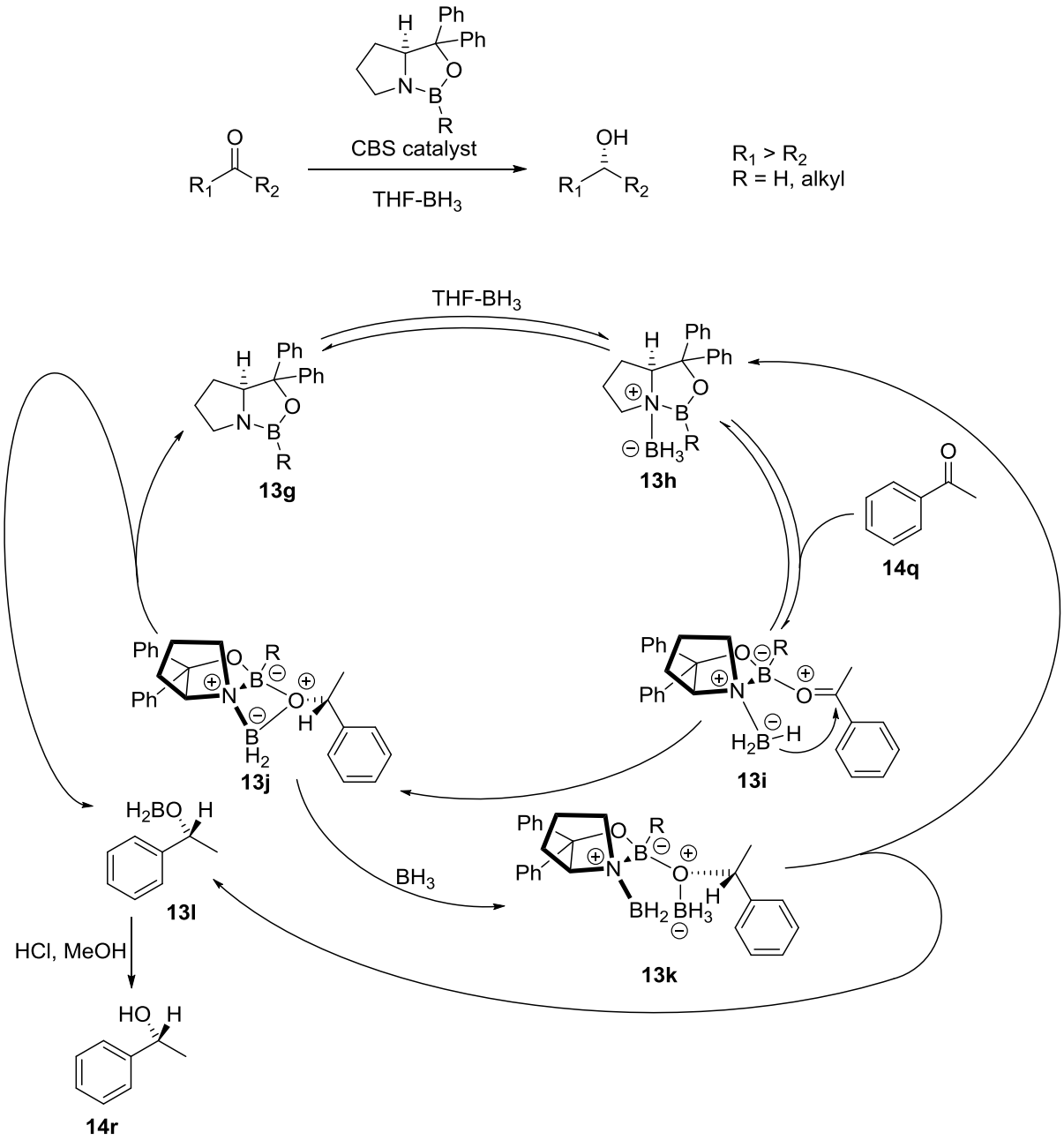

Figure 99: Enantioselective CBS reduction of ketones.

3.1.3. NHC boranes in hydroborations

Another example for the synthetic use of "BH_3" is the hydroboration, developed by *H. C. Brown.*[72] In the last years, the use of NHC boranes in radical chemistry as well as in ionic reactions documented a versatile field of applications. Although these NHC boranes do not react with alkenes or alkynes[73, 74, 75], a recent study by *D. P. Curran* showed that hydroborations of *in situ* generated arynes are possible with NHC boranes (Figure 100).[76]

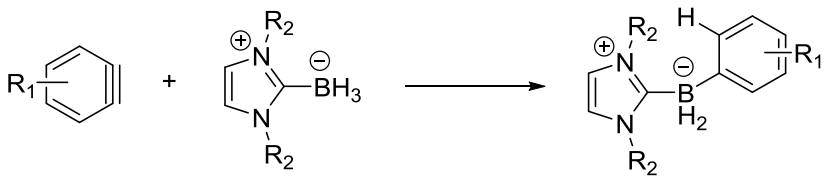

Figure 100: General scheme for the hydroboration of arynes with NHC boranes.

3.1.4. Versatile applications of NHC boranes

Further examples for the versatile use of NHC boranes are shown in Figure 101. A thermal conversion of alkyl halides to the corresponding alkanes is possible (Figure 101a).[77] Furthermore, imines can be reduced in the presence of acetic acid by NHC boranes (Figure 101b).[78] A direct one pot reductive amination from an aldehyde and aniline in presence of acetic acid is also possible.[78] A silica gel promoted reduction of ketons and aldehydes was also reported by *Curran* (Figure 101c).[79] Those versatile applications of borane complexes show their potential for future studies. In the following section, the focus is on heterocyclic borane complexes in ionic reactions.

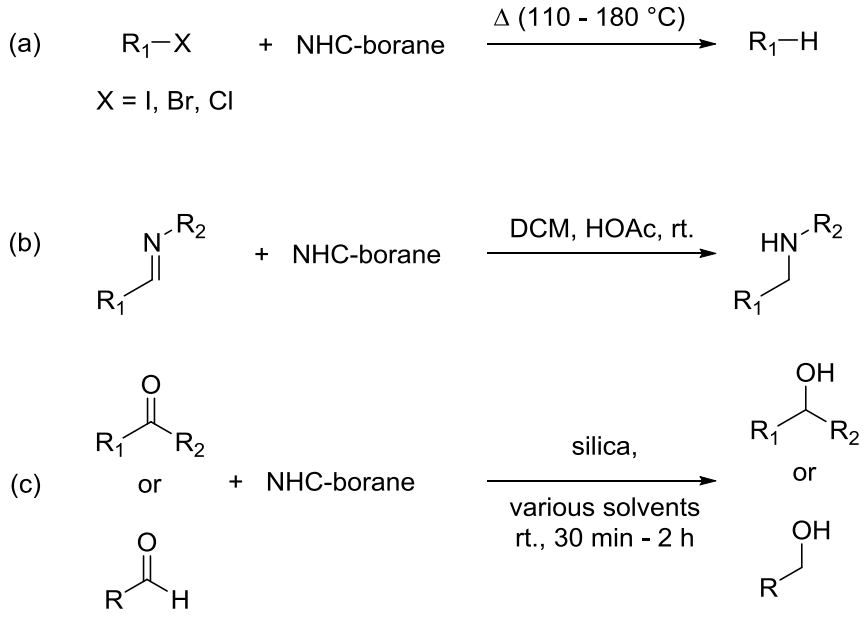

Figure 101: Versatile applications of NHC boranes in ionic reductions.

3.2. Ionic reductions of carbonyl compounds

The class of imidazole and benzimidazole borane complexes shows very unique properties compared to all other borane complexes used in this work. This special behavior was discovered, when trying to recrystallize benzimidazole borane (**17e**) from acetone, where an immediate strongly exothermic reduction occurred, while most of the used borane complexes could be stored in acetone over hours.

3.2.1. Borane screening

Borane complexes of N-heterocycles have been synthesized through BH_3 exchange reaction between the respective heterocycle (in the following abbreviated as "Nuc") and $H_3B{\bullet}SMe_2$ in THF at 0 °C (Figure 102). After precipitation with isohexane and recrystallization from DCM the complexes were obtained analytically pure as crystalline material. X-ray crystal structure analysis could be performed successfully on most of these compounds, showing monomeric borane complexes in all cases. This is also in agreement with all other analytical data shown in Table 4 (page 13). Furthermore, the complexes used for the following studies are shown in Figure 102.

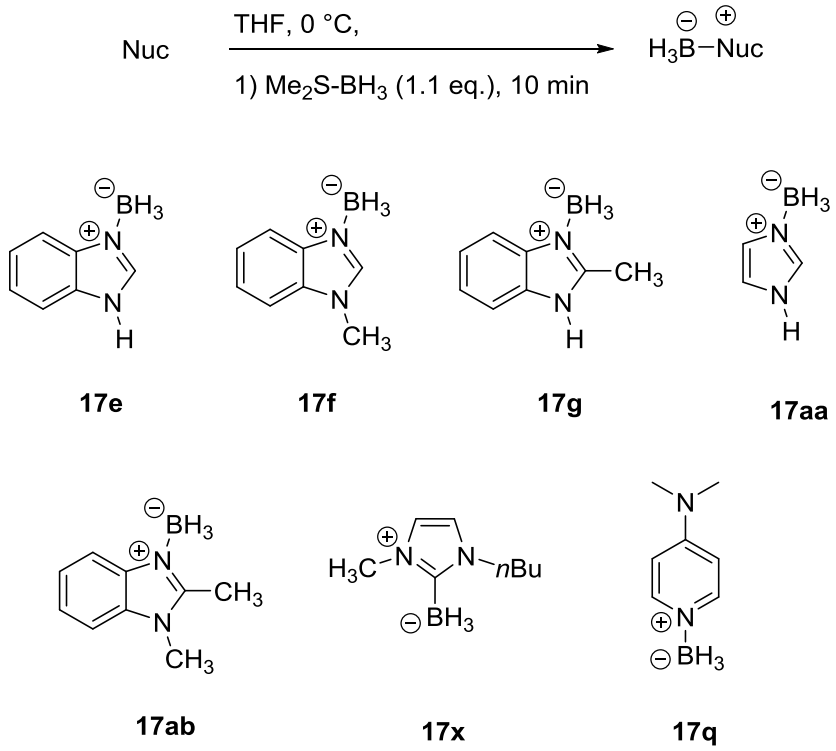

Figure 102: Synthesis and structures of borane complexes. Complex **17x** was synthesized according to the literature.[54]

3.2.1.1. Comparison of X-ray structures

Although the reactivity of **17e** and **17f** towards carbonyl compounds differs greatly, the structural differences are quite small (Figure 103). The B-N bond length, which shows a difference of only 0.003 Å, has thus apparently little influence on the hydride donor ability towards electrophiles.

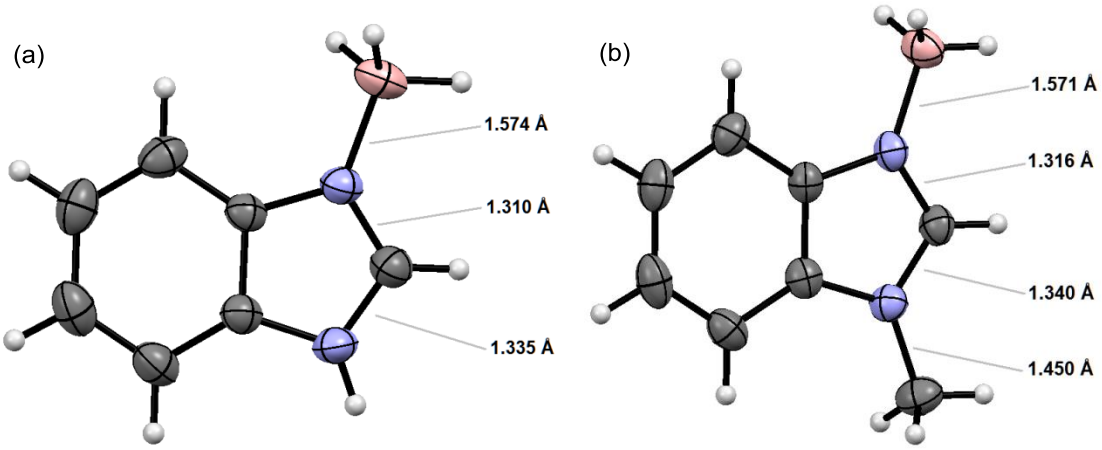

Figure 103: X-ray structures of borane complexes (a) **17e** and (b) **17f**.

3.2.1.2. Reduction of dibenzylketone (37a)

For an initial screening of the reactivity of different borane complexes dibenzylketone (**37a**) was chosen as a substrate (Figure 104). In all cases the reaction was performed with and without addition of an external acid. Due to the solubility of the borane complexes, THF was chosen as solvent. After 5 minutes THF was removed and the crude product was checked by GC/MS, thus leading directly to the alcohol **38a** via a transesterification of initially formed borates (Table 11).

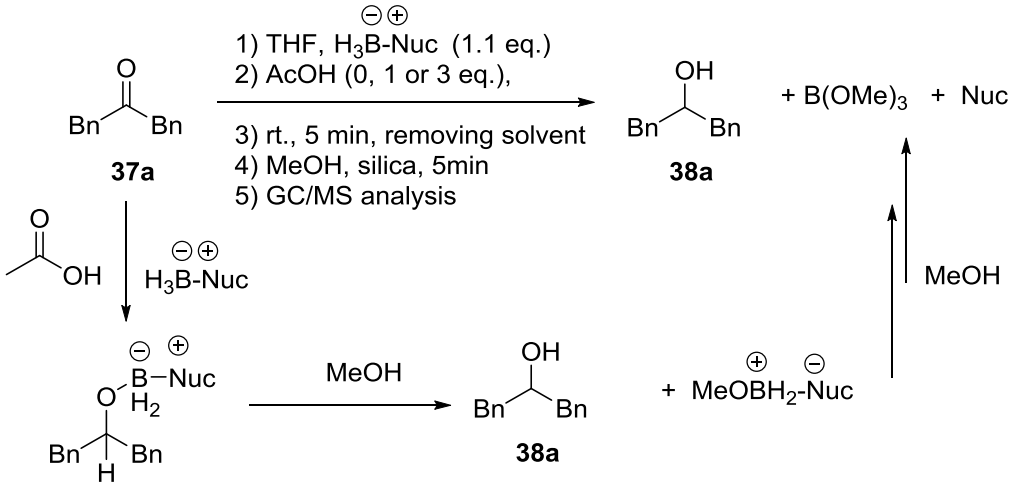

Figure 104: Initial reactivity screening with various borane complexes.

Table 11: Substrate screening for the reaction of dibenzylketone (**37a**) with various borane complexes.

entry	borane	addition of AcOH [eq.]	conversion
1	**17e**	–	full
2	**17e**	1	full
3	**17e**	3	full
4	**17g**	–	full
5	**17g**	1	full
6	**17g**	3	full
7	**17aa**	–	full
8	**17aa**	1	full
9	**17aa**	3	full
10	**17f**	–	no reaction
11	**17f**	1	14 %
12	**17f**	3	no reaction
13	**17ab**	–	no reaction
14	**17ab**	1	no reaction
15	**17x**	–	no reaction
16	**17x**	1	no reaction
17	**17q**	–	no reaction
18	**17q**	1	17 %
19	**17q**	3	no reaction

Table 11 shows that full conversion of ketone **37a** is achieved by using the borane complexes **17e**, **17g** and **17aa** which have a free NH moiety (entries 1-9). Also the addition of acetic acid does not affect the reaction in all three cases. However, the *N*-methylated complex **17f** shows no conversion after the indicated time (entry 10). The addition of one equivalent of external acid leads only to a conversion of 14 % (entry 11). Addition of acid in excess again leads to no conversion (entry 12). In case of the *N*-methylated complex **17ab**, no reaction was observed with and without addition of acetic acid (entry 13 and 14). Thus, the free NH moiety seems to be significant for a successful reduction rather than the proton on the C2 position. This fact is proven by the complexes **17x** and **17q**. In both compounds the NH moiety is absent, subsequently no reaction could be observed (entry 15 and 17). Addition of acid to NHC-borane (**17x**) does not result in any reduction (entry 16), while in the case of complex **17q** a conversion of 17 % can be achieved with one equivalent of external acid (entry 18). When adding acid in excess, no conversion was observed for compound **17q** (entry 19). In conclusion, the addition of an external acid does not influence the reduction of ketone **37a** with boranes containing a NH moiety. For all other boranes, the addition of one equivalent of acid can lead to low conversions of ketone **37a**.

3.2.2. Substrate screening with benzimidazole borane (17e) as reductant

After an initial borane screening which reavealed the importance of the NH moiety, a substrate screening was conducted (Figure 105).

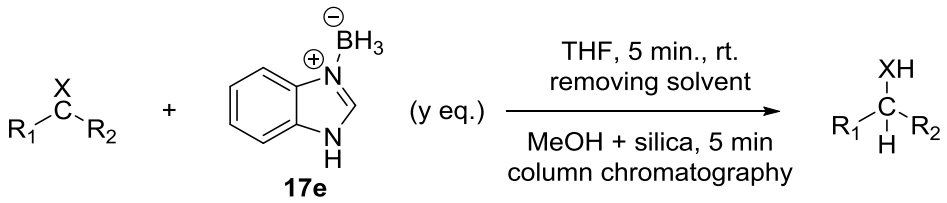

Figure 105: General procedure for a substrate screening with benzimidazole borane (**17e**).

In a typical setup the borane complex was added to a 0.5 M solution of the substrate in THF and stirred for 5 minutes. Afterwards the solvent was removed, and the crude product was further stirred for 5 minutes with methanol and silica. After column chromatography the isolated product was analyzed by NMR spectroscopy. The results are shown in Table 12.

Table 12: Reduction reactions with benzimidazole borane (**17e**) with a reaction time of 5 minutes.

entry	reactant	product	R_1	R_2	CX	y eq.	isolated yield
1	**37b**	**38b**	*p*Cl-Ph	Me	C=O	1.0	99 %
2	**37b**	**38b**	*p*Cl-Ph	Me	C=O	0.67	88 %
3	**37b**	**38b**	*p*Cl-Ph	Me	C=O	0.33	50 %
4	**37c**	**38c**	*p*Me-Ph	Me	C=O	1.0	88 %
5	**26a**	**26c**	Ph	Me	C=O	1.0	75 %
6	**37a**	**38a**	Bn	Bn	C=O	1.0	99 %
7	**37e**	-	*t*Bu	*t*Bu	C=O	1.0	no reaction
8	**37f**	**38f**	*p*Cl-Ph	H	C=O	1.0	88 %
9	**37g**	**38g**	*p*Me-Ph	H	C=O	1.0	93 %
10	**37h**	**38h**	Ph	H	C=O	1.0	86 %
11	**37i**	-	*p*Cl-Ph	OEt	C=O	1.0	no reaction
12	**37j**	-	*p*Me-Ph	OEt	C=O	1.0	no reaction
13	**37k**	-	Ph	OEt	C=O	1.0	no reaction
14	**37l**	-	*p*Cl-Ph	-	CN	1.0	no reaction
15	**37m**	-	*p*Me-Ph	-	CN	1.0	no reaction
16	**37n**	-	Ph	-	CN	1.0	no reaction
17	**37o**	-	Ph	OH	C=O	1.0	no reaction
18	**37p**	-	Ph	NH_2	C=O	1.0	no reaction
19	xanthate **18c**	-				1.0	no reaction
20	 **18a**	-				1.0	no reaction
21	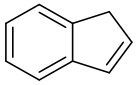 **37q**	-				1.0	no reaction
22	styrene (**37r)**	-				1.0	no reaction

Entries 1 to 6 show the reductions of differently substituted ketones to the corresponding alcohols. Consequently lowering the amount of reducing agent by 1/3 (entry 1-3) leads from full conversion to only 50 %. This fact is reasonable considering the fact of hydrogen elimination (see mechanism, Figure 108, page 96). Entries 4 to 6 show that good to excellent yields can be achieved with various substituted ketones. In the case of the sterically hindered ketone **37e** (entry 7), no reduction to the corresponding alcohol was observed after 5 minutes. For the reduction of aldehydes (entries 8-10) also good yields were achieved for differently substituted substrates. All other functional groups like esters (entries 11-13), nitriles (entries 14-16), acids (entry 17), amides (entry 18), xanthates (entry 19), bromides (entry 20) or alkenes (entries 21 and 22) did not react with benzimidazole borane (**17e**).

In order to study the influence of the reaction time for the unreactive substrates, three substrate classes were chosen and the same reactions were repeated over a period of three weeks (Table 13). Ester **37j** and nitrile **37m** showed no reaction again (entry 1 and 2). Surprisingly, a reduction of ketone **37e** to the alcohol **38e** had taken place with a yield of 79 %. Finally it can be stated that benzimidazole borane (**17e**) is an effective reducing reagent for ketones and aldehydes.

Table 13: Reduction reactions with benzimidazole borane (**17e**) with a reaction time of 3 weeks.

entry	educt	product	R_1	R_2	CX	y eq.	yield
1	**37j**	-	*p*Me-Ph	OEt	C=O	1.0	no reaction
2	**37m**	-	*p*Me-Ph	-	CN	1.0	no reaction
3	**37e**	**38e**	*t*Bu	*t*Bu	C=O	1.0	79 % [(a)]

[(a)] Yield was determined by ^{1}H NMR.

3.2.3. Workup optimization

With regard to the reaction of acetophenone (**26a**) with benzimidazole borane (**17e**), which yielded only 75 % of **26c** after the workup (Table 12, entry 5, page 93), it was tried to improve and simplify the workup procedure. The reaction was repeated under the same conditions as before and THF was removed after 5 minutes. Afterwards the crude product was stirred for 5 minutes with 2 equivalents of 2 M aq. HCl and the same volume of chloroform. This step separates the alcohol (organic layer) and benzimidazolium hydrochloride (**39a**) as well as water-soluble boron salts (aqueous layer). After extraction with chloroform, drying with anhydrous $MgSO_4$ and removal of the solvent, pure alcohol **26c** was obtained in quantitative yield (Figure 106). As benzimidazole borane (**17e**) is stable in methanol for at least 24 hours, the same reaction was repeated in methanol as solvent with a yield of 97 %. The importance of the removal of the solvent was proven by a control experiment. Here, THF was used as solvent and the reaction was performed as before. After 5 minutes, aqueous HCl was directly added to the reaction mixture. In this case only 48 % of alcohol **26c** was obtained, the rest being starting material **26a**. This implies that a significant part of the reaction process takes place while removing the solvent through rotatory evaporation.

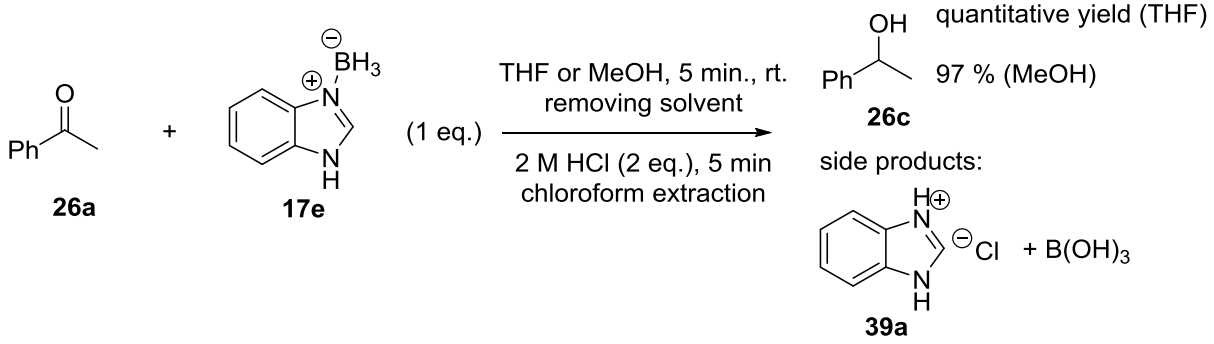

Figure 106: Reduction of **26a** in THF or MeOH with improved workup.

3.2.4. Solvent effects

It should be mentioned that the solubility of the complexes **17e**, **17g** and **17aa** is poor in apolar solvents like toluene or benzene. However, the use of more polar, oxygen-containing solvents increases the solubility strongly, but also lowers the reactivity of the borane complexes significantly. In these cases ^{1}H NMR studies showed a distinctive broadening of the NH-signal due to the formation of hydrogen bonds with the solvent (R'_2N---H---OR_2), thus demonstrating the acidic character of the NH moiety. Nevertheless, oxygen-containing solvents may be used for synthetic applications as long as the solvent is removed before the final workup, thus increasing the concentration of the borane-substrate mixture. In terms of mechanistic NMR studies, toluene-d_8 or $CDCl_3$ were chosen as solvents to avoid interactions between the complexes and the solvent. In both cases the initial borane complex suspensions became clear solutions during the reaction. Furthermore, the use of toluene-d_8 as solvent offered the possibility of high-temperature NMR studies. Results from ^{11}B NMR measurements will be shown in a later section as important experiments for the elucidation of the mechanism. It should be mentioned, that the solubility in apolar solvents can be improved by attaching a long aliphatic chain at the C2 position of the imidazole ring. Complex **17ac**, which is soluble in benzene and toluene, was produced by a two-step synthesis and thus offered the possibility to conduct reductions in apolar solvents (Figure 107).

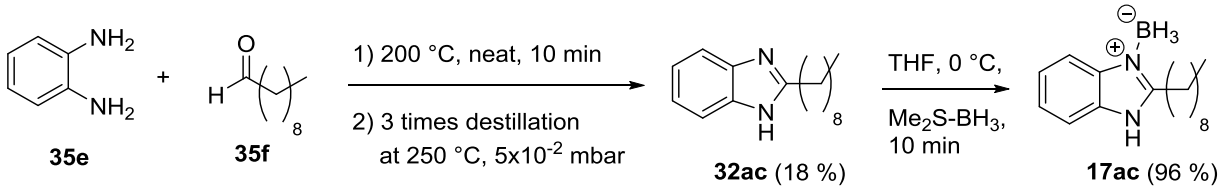

Figure 107: Synthesis of complex **17ac**, which is soluble in benzene and toluene.

3.2.5. Mechanistic aspects of ketone reductions with imidazole borane (17aa)

In order to clarify the mechanism of ketone reductions, imidazole borane (**17aa**) was chosen as reductant and acetone as the ketone. The mechanism, which will be discussed afterwards in detail, is depicted in Figure 108. The elucidation of the mechanism was performed by several independent NMR measurements and ESI-MS spectrometry which will be described in the following sections.

3.2.5.1. Mechanism

The mechanism for the reduction of acetone with imidazole borane (**17aa**) is shown in Figure 108.

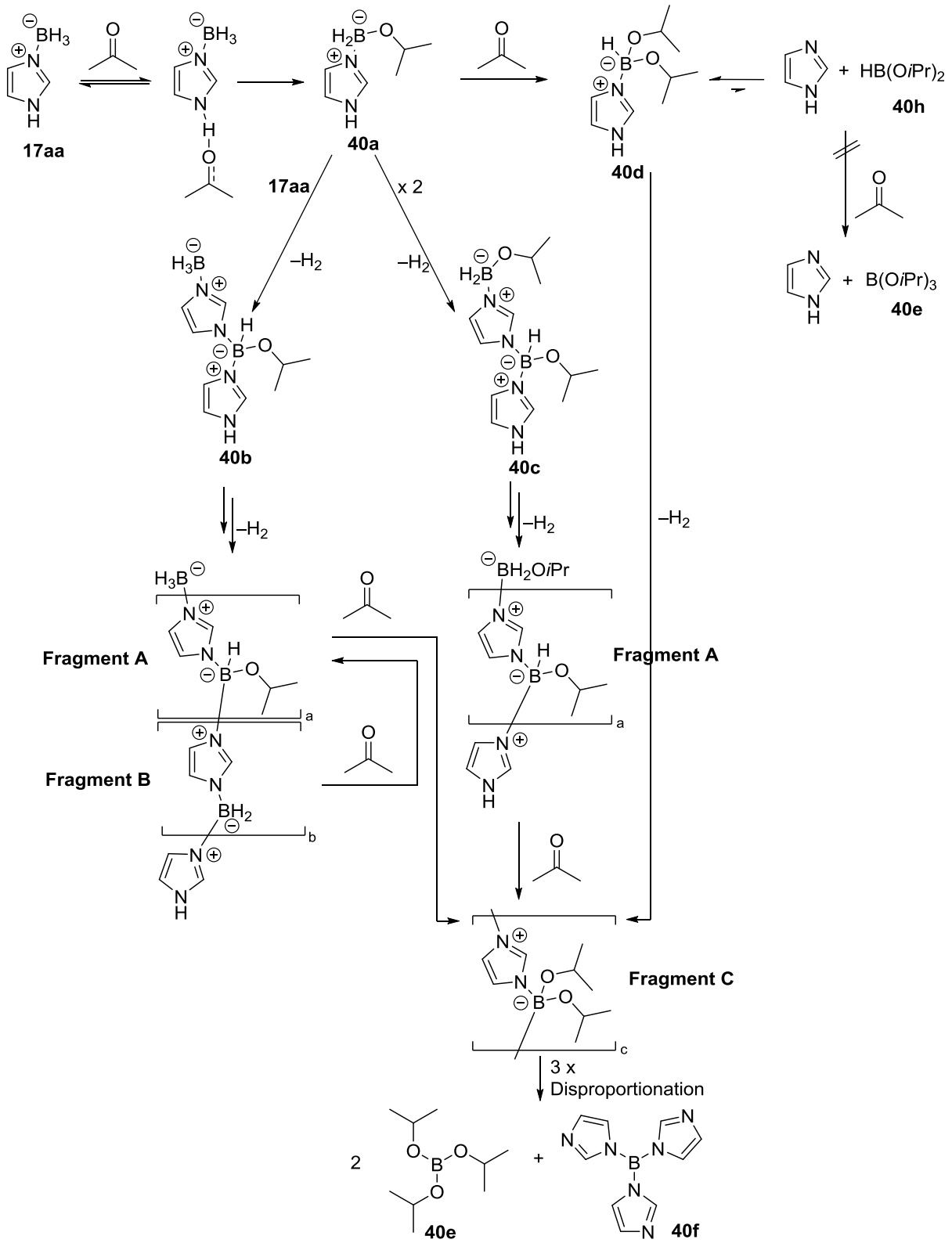

Figure 108: General mechanism of the ketone reduction with imidazole borane (**17aa**).

The formation of the monomeric alkoxyborinate-complex **40a** is the key step for the reaction. It is assumed that this species can only be formed when the carbonyl group is activated by the NH moiety of the initial borane-complex (**17aa**). Thus, a reduction with *N*-methylated complexes, e. g. 1-methyl-benzimidazole borane (**17f**), was never observed. Also the formation of an alkoxyborinate-species was never observed when using *N*-methylated compounds.Three potentional pathways may be discussed. The borinate-complex **40a** now can either react with **17aa** or react with itself, leading to the dimeric structures **40b** and **40c**, which undergo polymerization. Finally polymers containing fragments A and B are formed. Both pathways lead to the evolution of hydrogen gas, which is observed during the reaction and is also detected when following the reaction by ^{1}H NMR spectroscopy. Fragment B can be converted to fragment A by the reaction with acetone. Fragment A, bearing only one hydride, may subsequently react with the ketone, forming fragment C. A third pathway leading to fragment C is also possible, in which a dialkoxyborane-complex **40d** is generated from the reaction of acetone and borinate-complex **40a**. Polymerization of this dialkoxyborane-complex **40d** with any other chain or monomer also leads to fragment C. A final disproportionation of fragment C to borate **40e** and **40f** is also possible.

3.2.5.2. Control experiments

As independent reference experiments, borate **40g** was exposed to imidazole, imidazole-borane (**17aa**), alcohol **26c** and acetophenone (**26a**) and monitored by ^{1}H and ^{11}B NMR (Figure 109a). In all cases no reaction could be observed, thus confirming that no further reaction takes place, once a trialkoxyborate is formed. The same set of control experiments was performed with dialkoxyborane **40h** (Figure 109b). No reaction was detected in the cases of acetophenone (**26a**) and imidazole borane (**17aa**). The reaction of alcohol **26c** leads to trialkoxyborate **40g**. The addition of free imidazole to borane **40h** causes polymerization, leading to polymer **40i** which shows a broad singlet in the ^{11}B NMR spectra at ca. +1.5 ppm. The same fact was found when adding imidazole and acetophenone (**26a**) at the same time to borane **40h**.

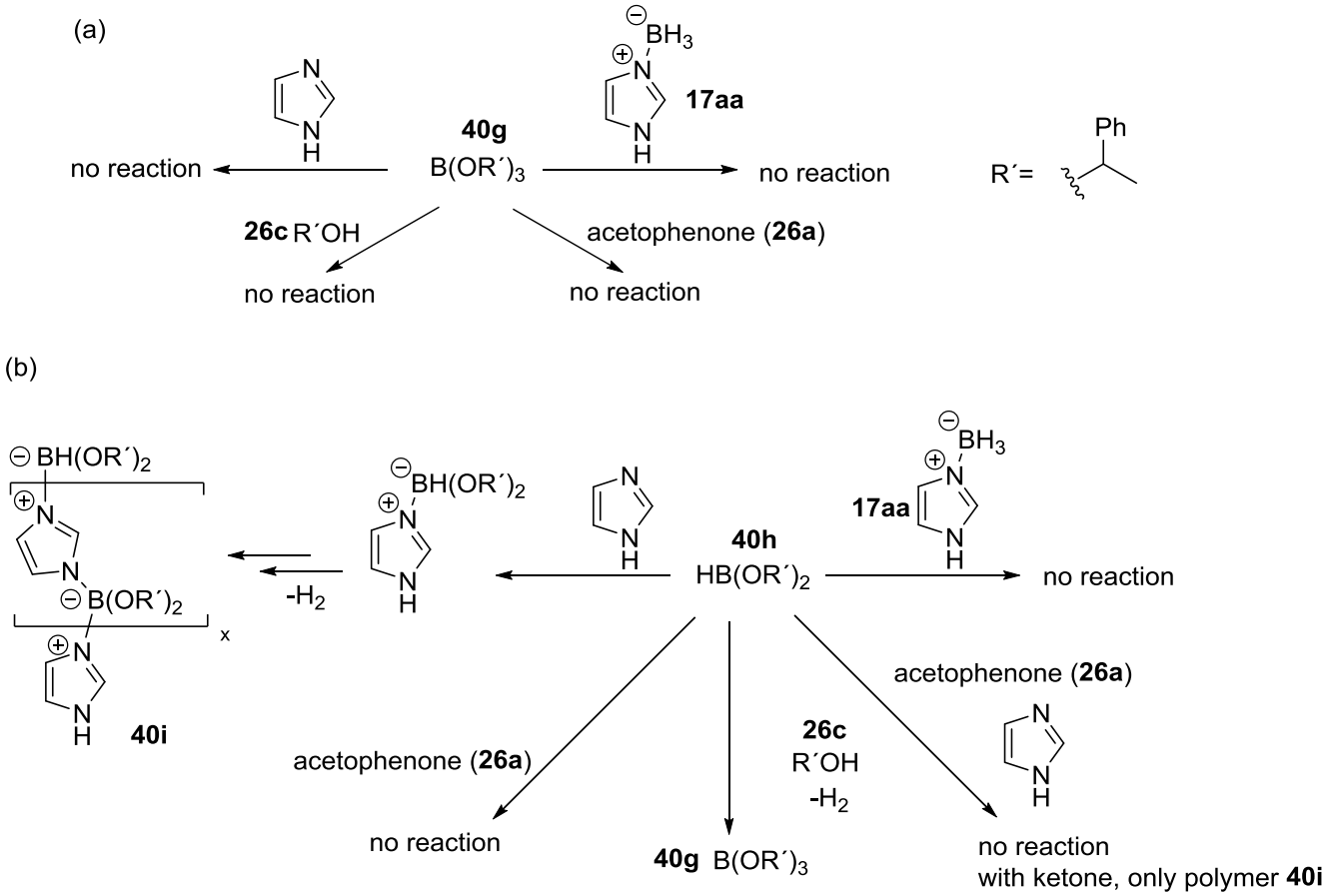

Figure 109: Control experiments of various borane species analyzed by ^{1}H and ^{11}B NMR spectroscopy in toluene-d_8.

3.2.5.3. ESI-MS spectrometry

The strong tendency to form oligomers could be determined by ESI-MS spectrometry and will be described next. Therefore a 1: 1 mixture of imidazole borane (**17aa**) and acetone was prepared in $CDCl_3$ under inert gas atmosphere and stirred for 15 minutes. All volatiles were then removed under reduced pressure and the crude reaction mixture was taken up in dry THF under nitrogen. Afterwards the clear solution was immediately used for ESI spectrometry. The negative and the positive ESI spectra are shown in Figure 110.

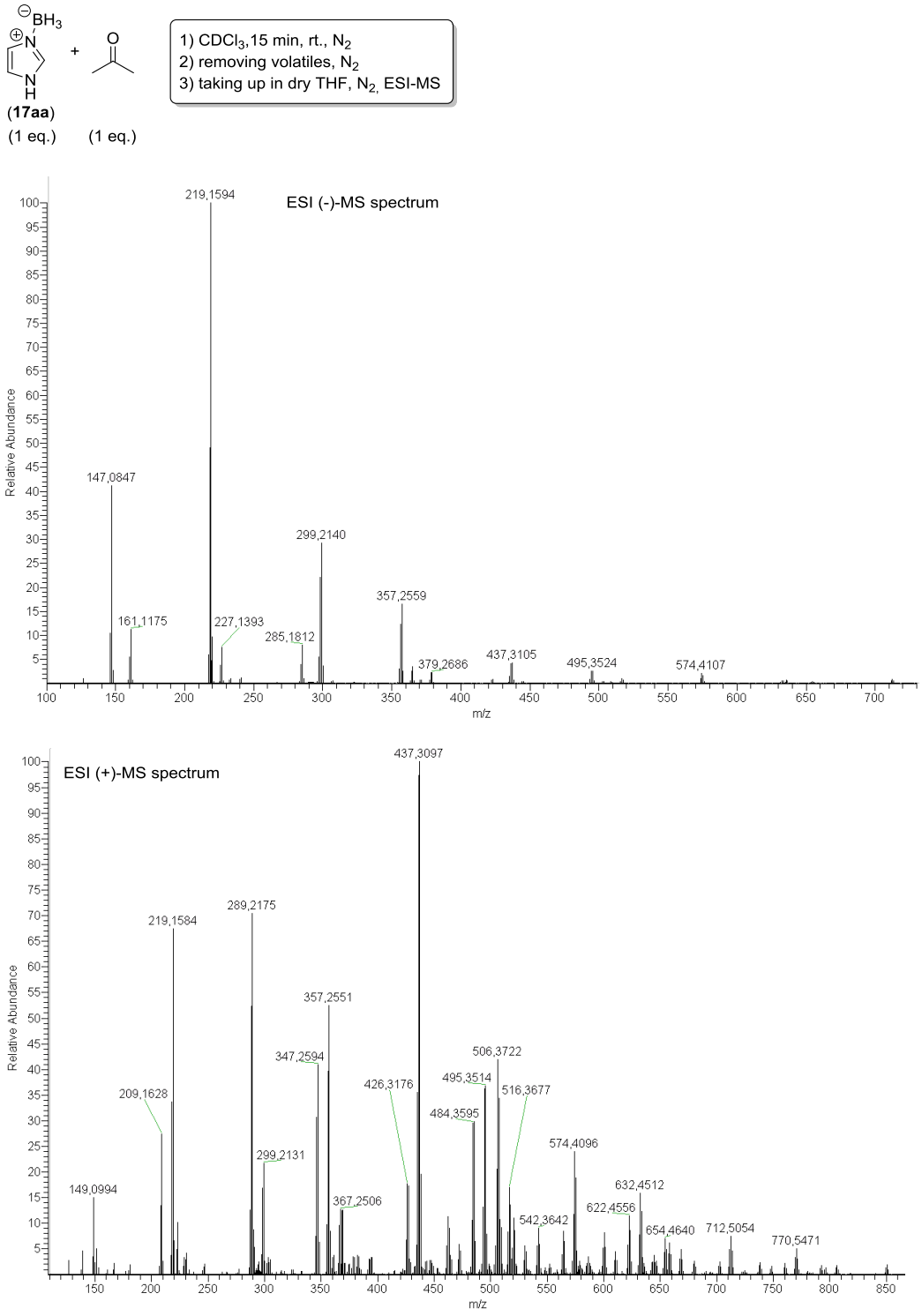

Figure 110: ESI-MS spectra of the reduction of acetone with imidazole borane (**17aa**).

It is obvious that the fragmentation patterns are rather complex. In order to assign all signals from both spectra, a spectrum for each signal was first simulated and then compared to the measurements. The isotope ratio of boron (^{10}B : ^{11}B = 19.9 : 80.1) was taken into account in order to determine the number of boron atoms in each species. An example for the analysis of the ESI-MS spectra is shown in Figure 111. Figure 111a shows an example for a negatively charged fragment containing one boron atom. An example for a positively charged

fragment which contains three boron atoms is shown in Figure 111b. The whole assignment of all signals can be found in the experimental section of this work.

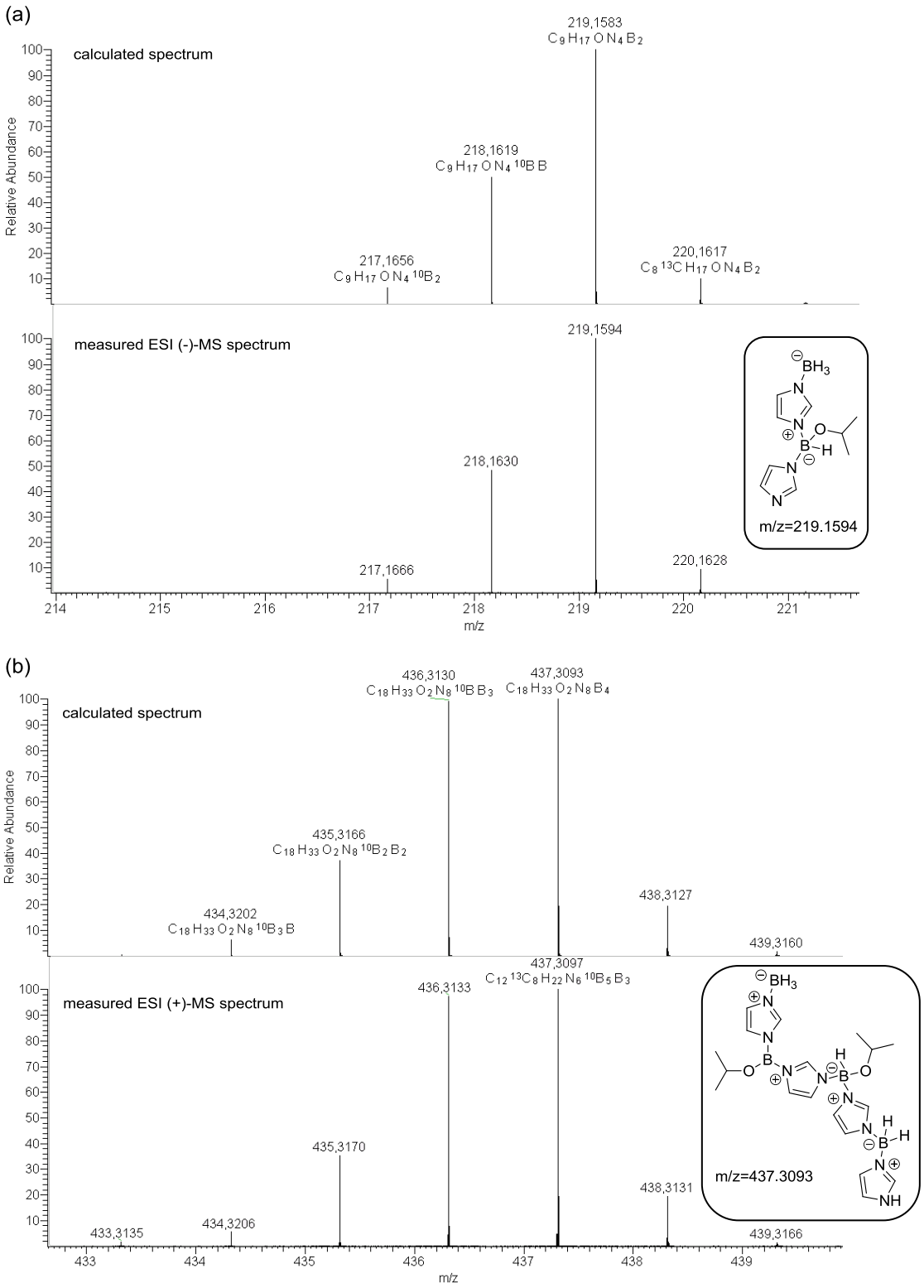

Figure 111: Examples for the analysis of the ESI-MS spectra of (a) negatively and (b) positively charged species.

By assigning the signals of the ESI-MS measurement, two complex fragmentation pathways of polymer species are obtained. The fragmentation pathway of a polymeric species in the ESI (-)-MS spectra is shown in Figure 112, the pathway for the ESI (+)-MS spectra is shown in Figure 113. Both polymers are generated in a systematic way. With respect to the reaction mechanism (Figure 108, page 96), the formation of the three fragments (A, B and C), as well as the corresponding terminal groups, is visible in the ESI-MS measurements.

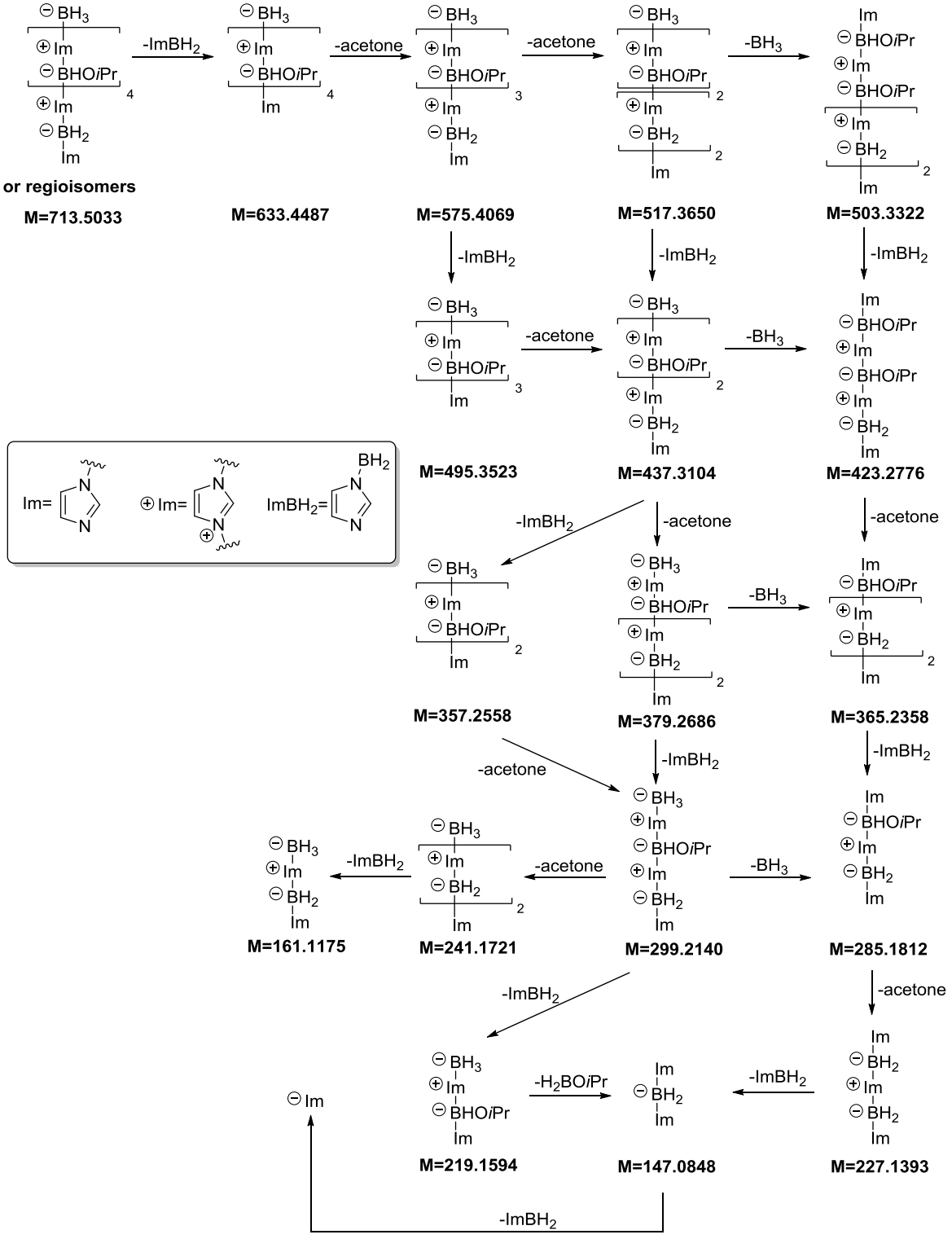

Figure 112: Fragmentation pathway of oligomeric imidazolyl boranes in the negative ion ESI (-)-MS spectra.

Figure 113: Fragmentation pathway of oligomeric imidazolyl boranes in the positive ion ESI (+)-MS spectra.

However, some signals in the ESI (+)-MS spectra could not be assigned assuring the linear imidazolyl borane polymers shown in Figure 113. In order to finally asign the remaining signals, the presence of traces of water during the measurement must be taken into account.

The resulting cyclic, polymeric structures subsequently explain all missing signals in the measurement. The formation of these cyclic structures is shown in Figure 114.

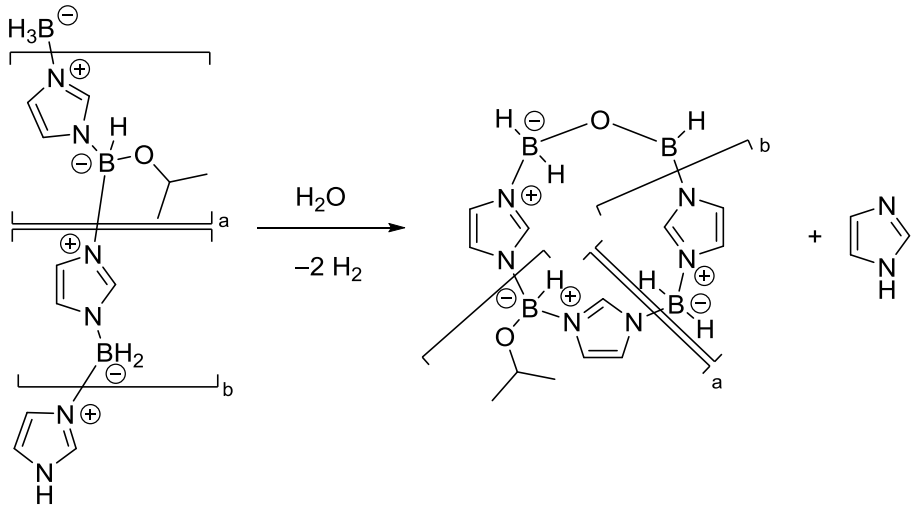

Figure 114: Formation of cyclic oligomeric species in the presence of water.

The fragmentation pathway of these cyclic oligomeric species in the ESI (+)-MS spectra is shown in Figure 115. The ring structures differ in size, but show the same systematic composition as the “linear” structures that were discussed before.

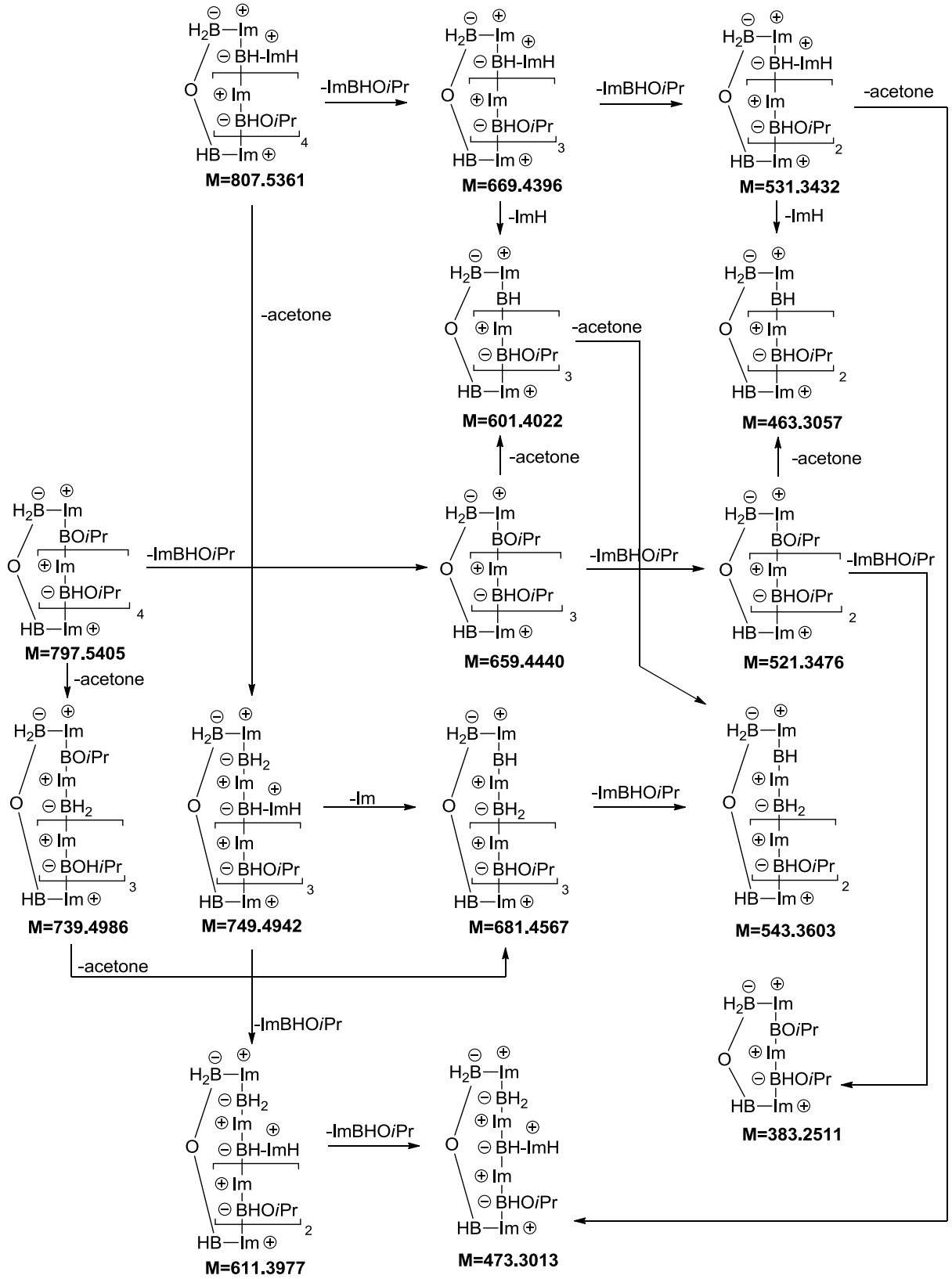

Figure 115: Fragmentation pathway of cyclic oligomeric species in the ESI (+)-MS spectra.

An example of two cyclic species with different ring sizes is shown in Figure 116. The whole assignment of all cyclic, polymeric species can be found in the experimental section.

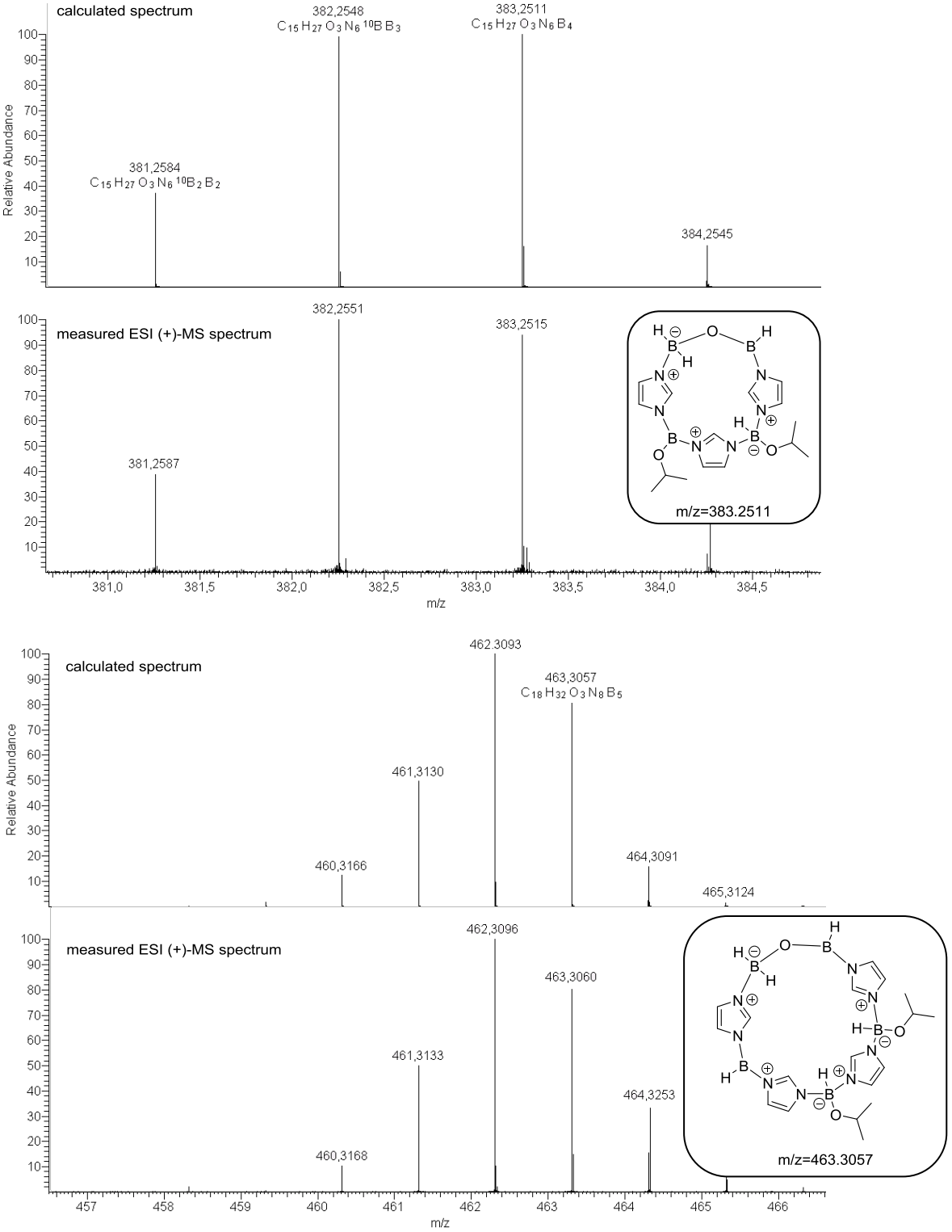

Figure 116: Examples for two cyclic oligomeric species.

3.2.5.4. ^{11}B NMR analysis

In order to confirm the results obtained by ESI-MS spectrometry, the reduction of acetone with imidazole borane (**17aa**) was repeated and monitored by ^{11}B NMR spectroscopy in DCM-d_2 as solvent at room temperature (Figure 117). The ^{11}B NMR measurement reveals a fast consumption of the initial borane **17aa**. Yet, the resulting signals during the measurement were rather broad, so that an exact assignment of multiplets was not possible (Figure 117, section after 2 minutes).

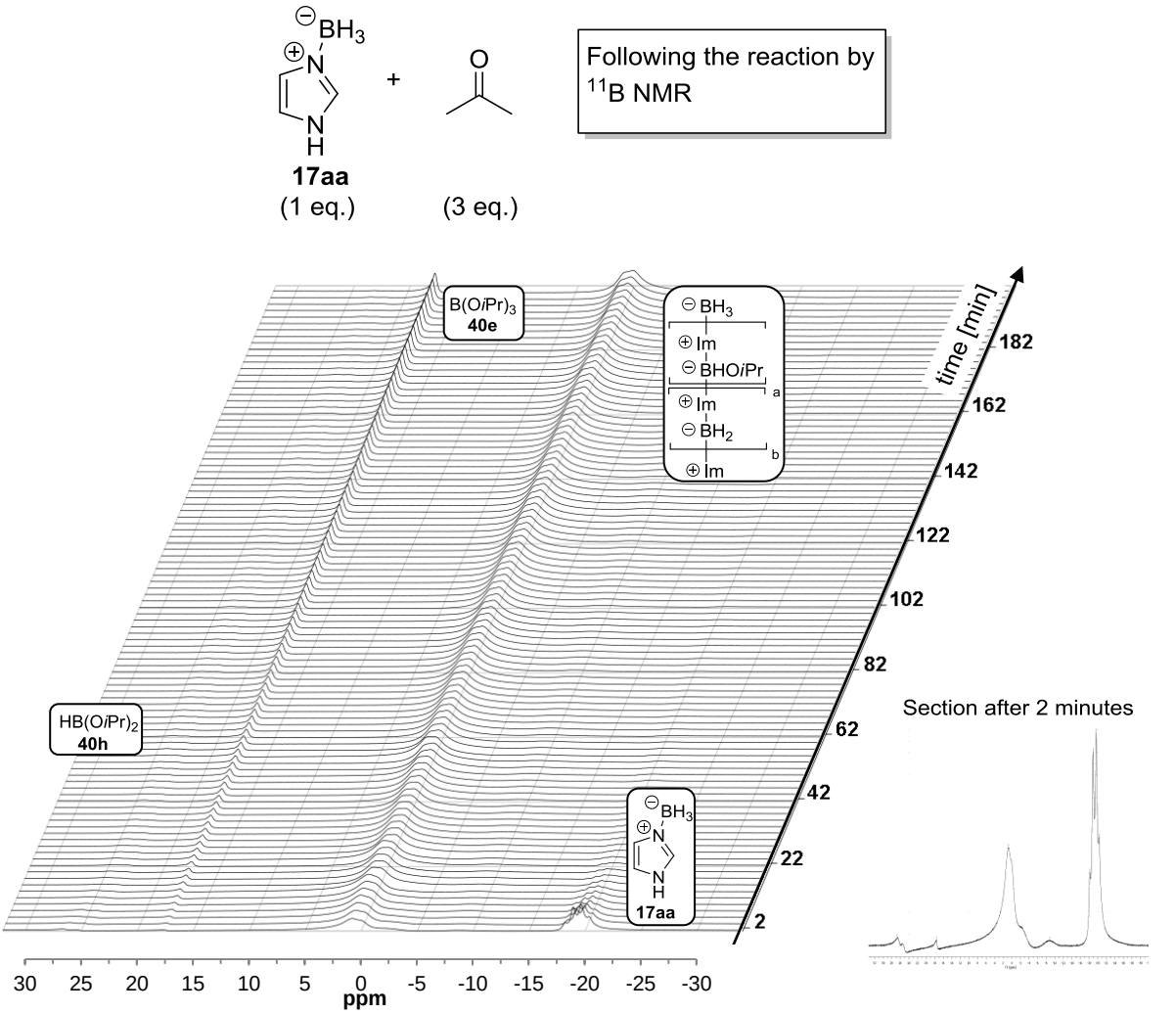

Figure 117: ^{11}B NMR monitoring of the reduction of acetone with imidazole borane (**17aa**).

Due to the poor resolution of the ^{11}B NMR measurements, the solvent was removed after the reaction and the crude reaction mixture was taken up in toluene-d_8, to yield a suspension of various products. This suspension was used for a new series of ^{11}B NMR measurements in which the temperature was successively increased (Figure 118). While raising the temperature up to 100 °C, the resolution of the signals improved significantly. In order to assign the resulting multiplets, {^{1}H} ^{11}B NMR measurements at 100 °C were taken additionally.

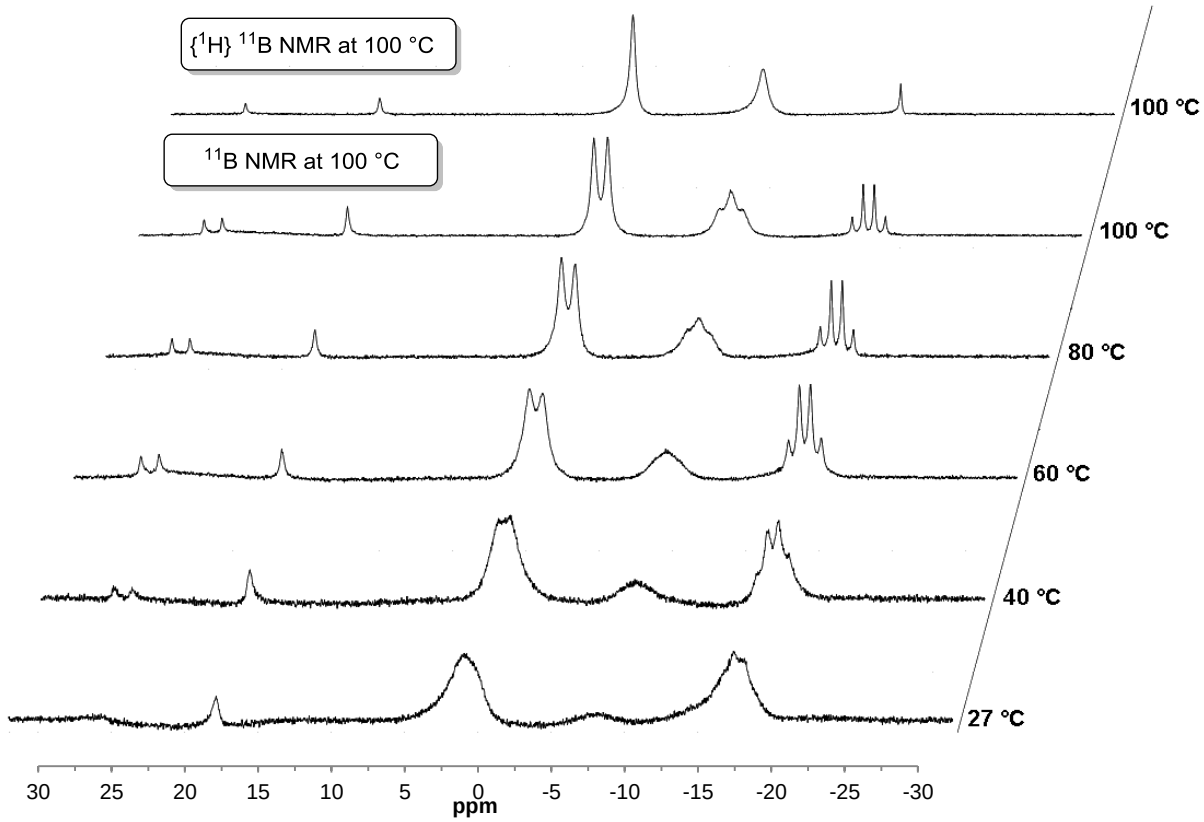

Figure 118: High-temperature ^{11}B NMR experiment.

The high-temperature ^{11}B NMR measurement taken at 100 °C is shown separately in Figure 119. The formation of different fragments becomes clear by assigning the multiplets, thus supporting the analysis from the ESI-MS spectrometry. In order to exclude a thermal decomposition to monomers at 100 °C, the sample was again cooled to 27 °C. The same signal broadening as before was observed in the final ^{11}B NMR. Therefore it is strongly assumed that the polymer stays intact during the heat up procedure.

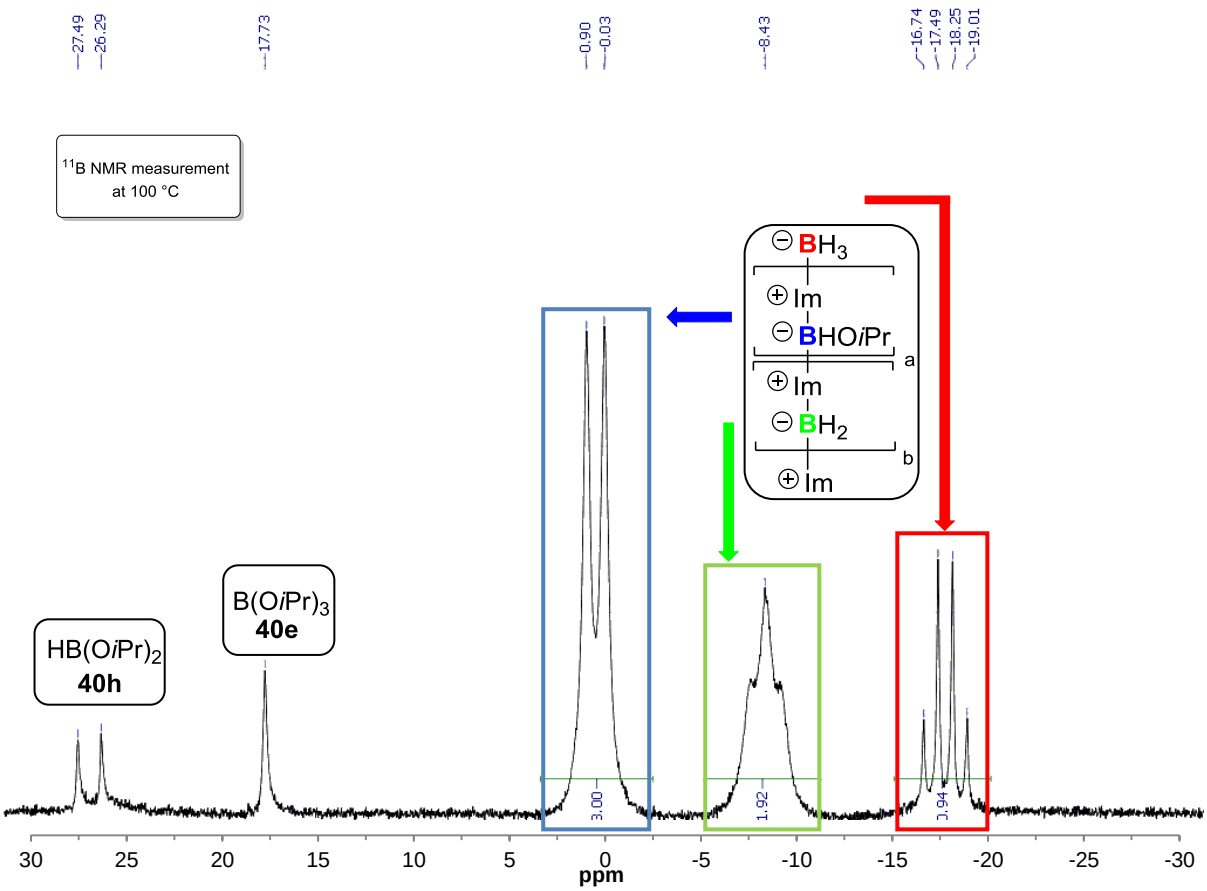

Figure 119: High-temperature ^{11}B NMR measurement at 100 °C in toluene-d_8.

Imidazole borane (**17aa**) can be stored in solution over a period of several days without oligomerisation. However, when heating a suspension of imidazole borane (**17aa**) in toluene-d_8 to 100 °C, a second species appears in the ^{11}B NMR spectrum (Figure 120). This species is the oligomerisation product of the initial borane complex, showing the "BH_2" moiety as a triplet in the ^{11}B NMR measurement. The signals of the "BH_3" end group (of the oligomer) and the "BH_3" moiety of **17aa** overlap in the ^{11}B NMR. Yet, in the {^{1}H} ^{11}B NMR measurement, a small shoulder may indicate the presence of two different "BH_3" groups. This experiment again shows the tendency of imidazole borane complexes to form oligomers. Furthermore, the structural similarity of the "BH_3" groups of monomeric and oligomeric species can be detected by ^{11}B NMR.

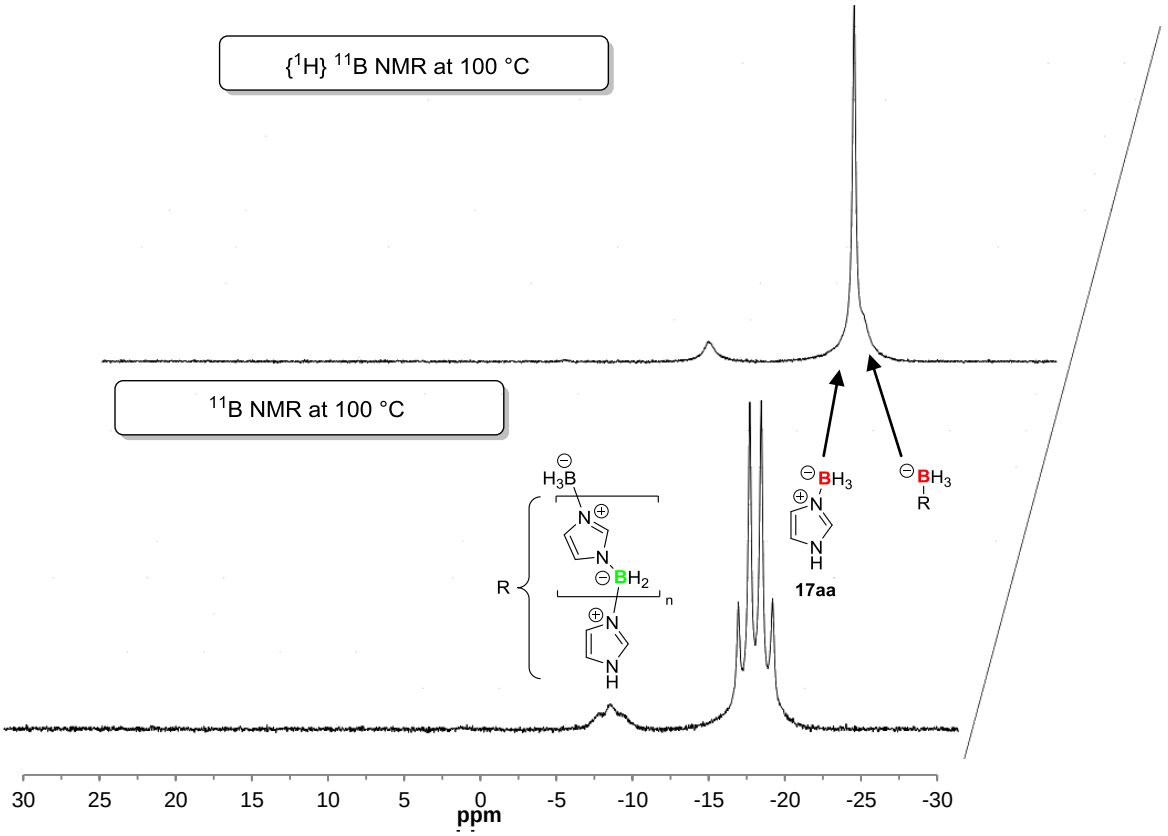

Figure 120: High-temperature ^{11}B NMR measurement of imidazole borane (**17aa**) at 100 °C in toluene-d_8 after 10 minutes.

3.2.6. Mechanistic aspects of ketone reductions with benzimidazole borane (17e)

As benzimidazole borane (**17e**) has been used for a large number of reductions, the question arose, whether this complex would undergo the same oligomerisation as imidazole borane (**17aa**). Therefore, the same reaction setup for an ESI-MS measurement was chosen. A 1: 1 mixture of benzimidazole borane (**17e**) and acetone was prepared in $CDCl_3$ under inert gas atmosphere and stirred for 15 minutes. All volatiles were removed under reduced pressure and the crude reaction mixture was taken up in dry THF under nitrogen. Afterwards the clear solution was immediately used for ESI spectrometry. The ESI (-)-MS spectrum is shown in Figure 121. The decreased number of signals in the measurement already indicates that the aggregation is less dominant in the case of benzimidazole borane (**17e**) as compared to imidazole borane (**17aa**).

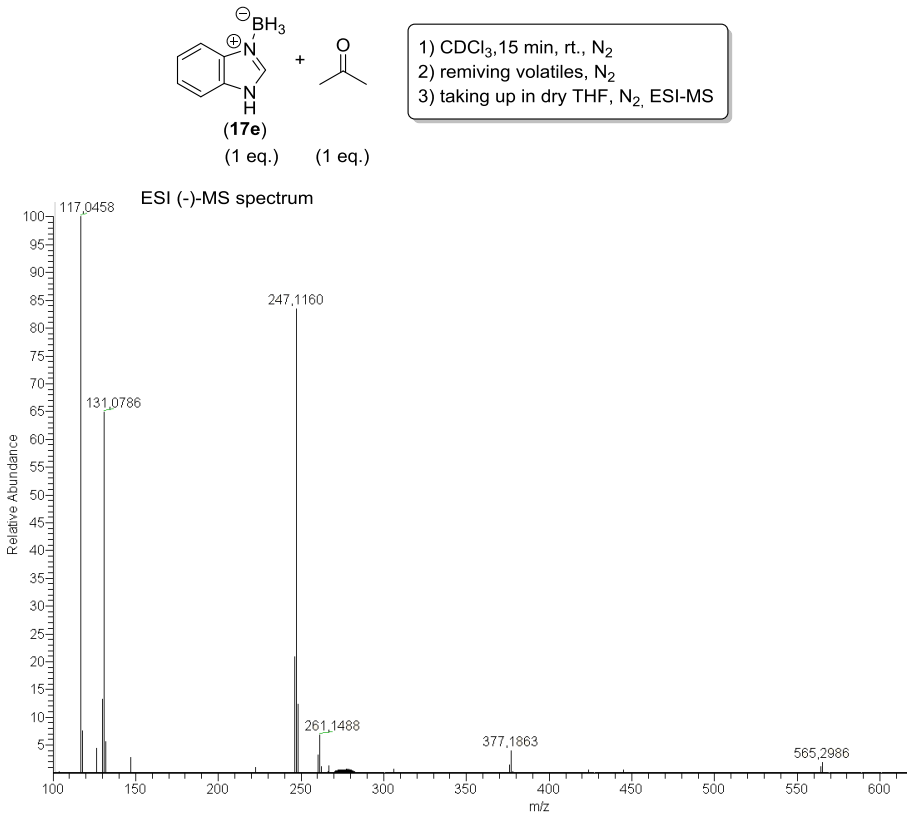

Figure 121: ESI (-)-MS spectrum of the reduction of acetone with benzimidazole borane (**17e**).

The analysis of the ESI-MS spectrometry was performed in the same way as before and can be found in the experimental section. As an example, the smallest detected anion is shown in Figure 122.

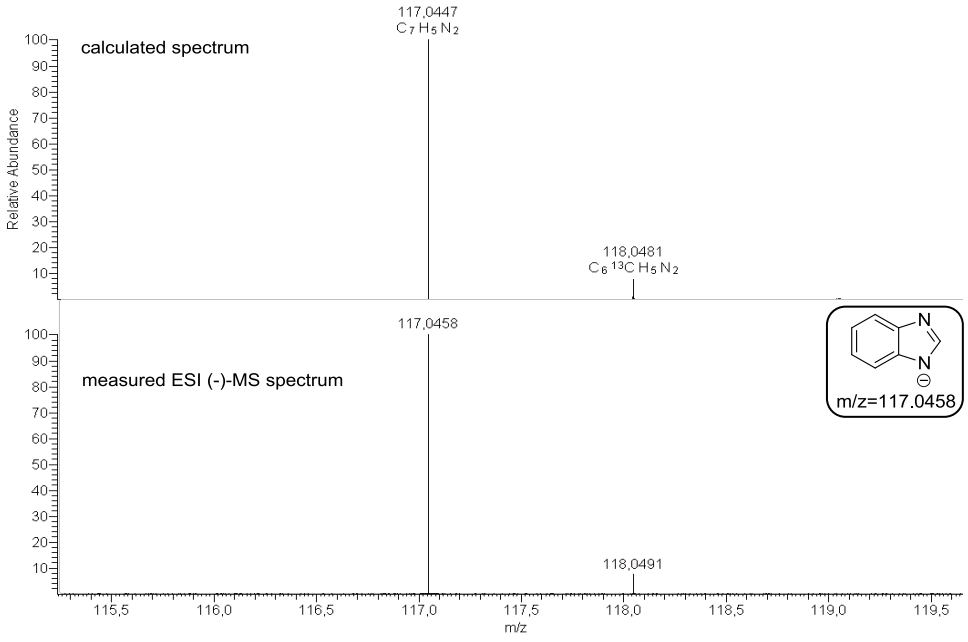

Figure 122: Example for the analysis of the ESI-MS spectrometry.

Figure 123 shows the fragmentation pathway of a polymer species in the ESI (-)-MS spectra. In comparison to the scheme shown for imidazole (Figure 112, page 101), the longest chain found consists only of two fragments. The reactivity of benzimidazole borane (**17e**) towards acetone is very similar to that of imidazole borane (**17aa**). The main difference is the size of oligomers and the absence of cyclic structures for benzimidazole borane (**17e**).

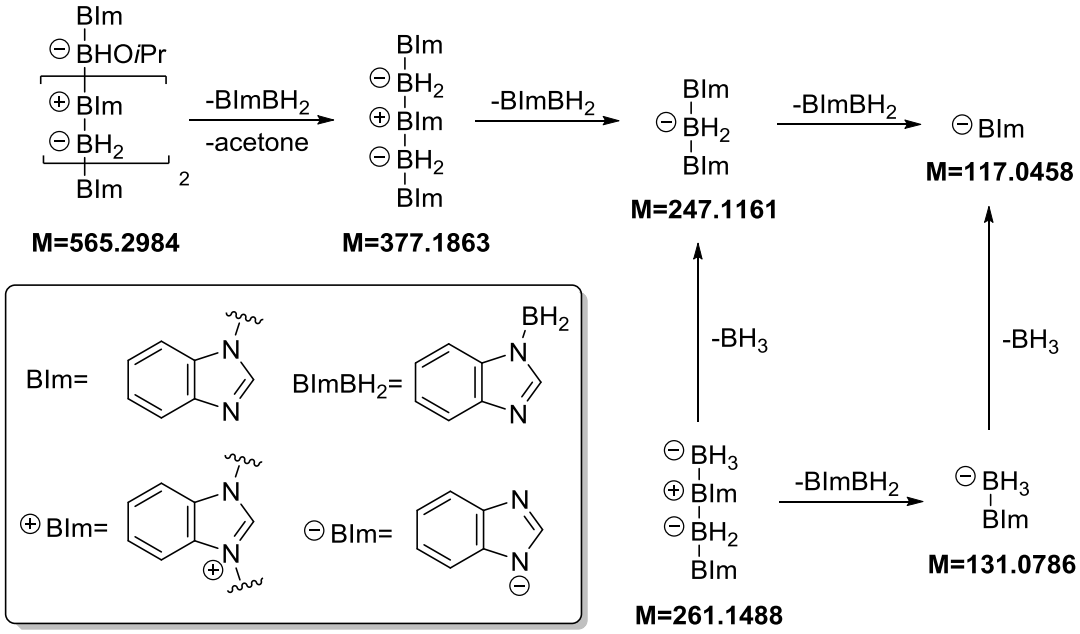

Figure 123: Fragmentation pathway of oligomeric benzimidazolyl boranes in the ESI (-)-MS spectra.

3.2.7. Mechanistic aspects of ketone reductions with *N*-methylimidazole borane (17aj)

As a further proof of the depicted mechanism, the use of *N*-methylimidazole borane (**17aj**) leads to no apparent reaction with one equivalent of acetone after 15 minutes. This changes when using acetone in large excess and monitoring the reaction over a period of several days.

3.2.7.1. ESI-MS spectrometry

N-methylimidazole borane (**17aj**) was stirred in acetone-d_6 for five days and the ongoing reaction was monitored by ESI-MS spectrometry as well as by NMR measurements. Figure 124 shows the ESI-MS spectrometry after five days.

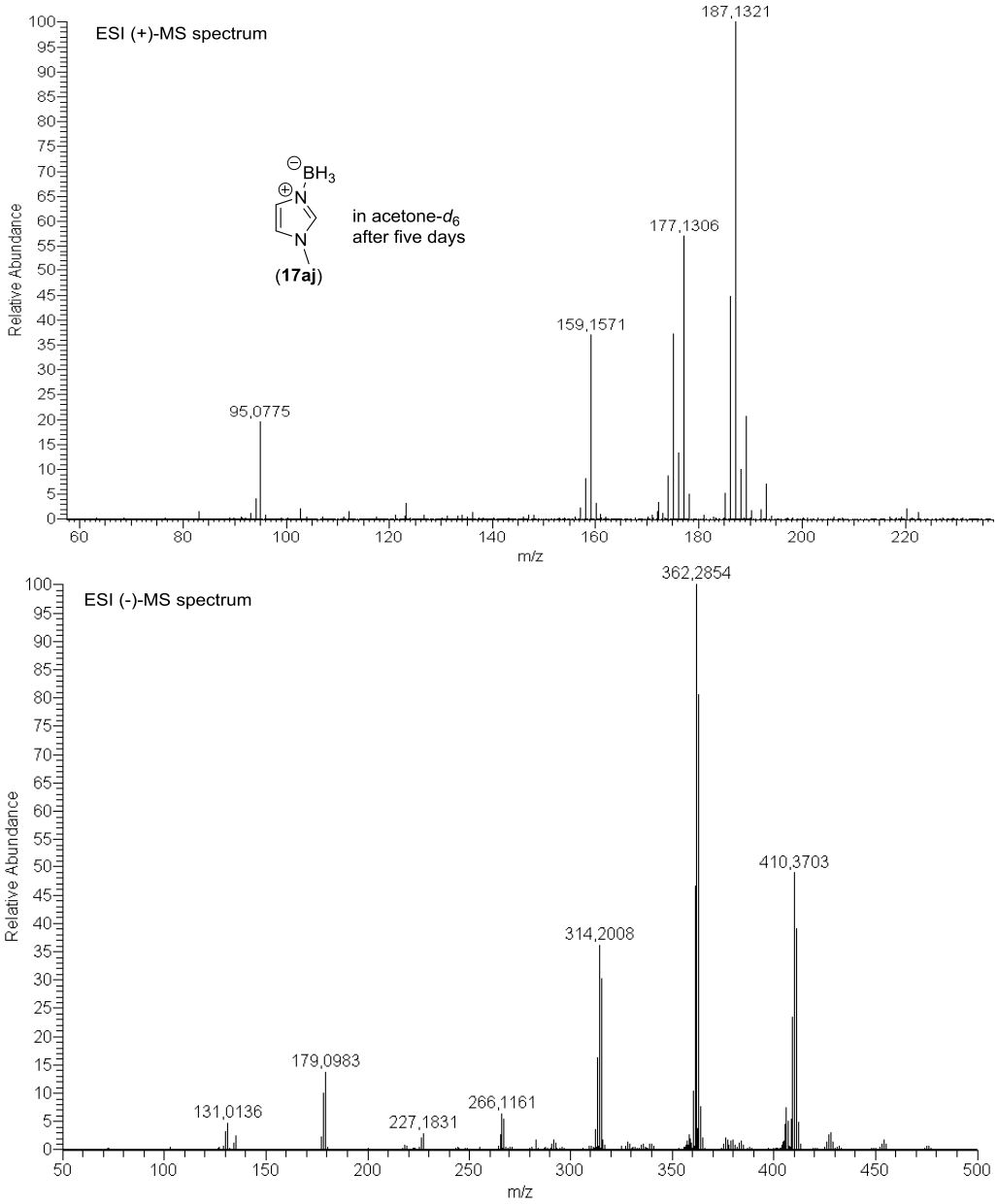

Figure 124: ESI-MS spectra of the reduction of acetone-d_6 with *N*-methylimidazole borane (**17aj**).

The assignment of the signals is shown in Figure 125 (for further information and predicted spectra see experimental part). The excessive formation of boroxines in this case can be explained by the presence of water in the experimental setup.

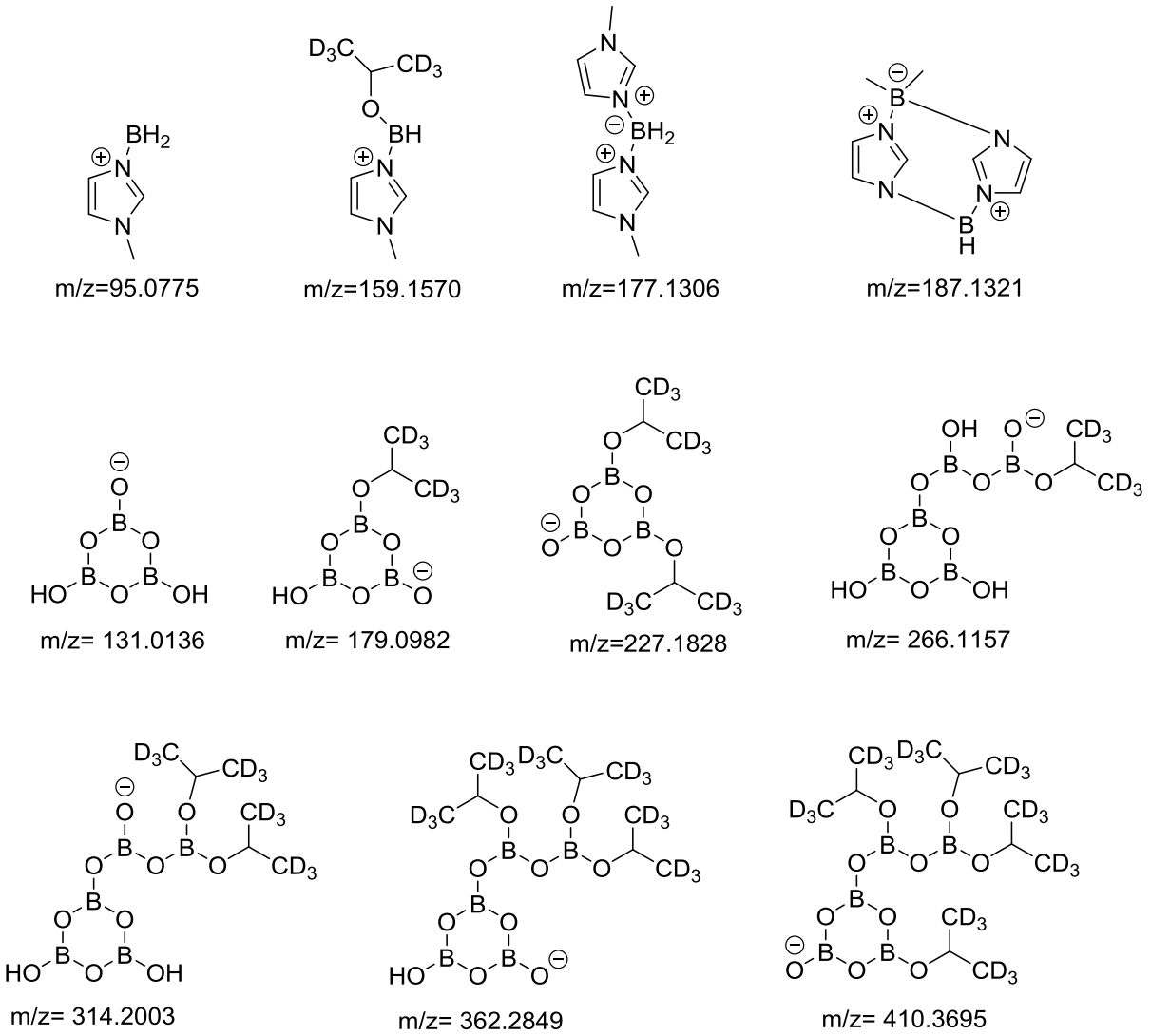

Figure 125: Most probable structure assignments for the ESI-MS measurement shown in Figure 124.

3.2.7.2. ^{1}H NMR analysis

For further investigations, the reaction outcome after 24 hours and after 5 days was compared via ^{1}H NMR spectroscopy (Figure 126). In comparison to the reaction after 24 hours, a strong decay of *N*-methylimidazole borane (**17aj**) was observed after 5 days (signals a, b, c and d), accompanied by the formation of free *N*-methylimidazole (signals 1, 2, 3 and 4). Furthermore the evolution of hydrogen was detected. A set of 4 new signals (A, B, C and D) was also observed, thus indicating the formation of a new *N*-methylimidazole species. The downfield shift of signal A led to the assumption that a protonation of the imidazole had taken place (compare signal I of *N*-methylimidazolium hydrochloride (**42**)). This downfield shift is typical for protonated imidazoles. By taking the results of the ESI-spectrometry into account, the protonation of the free imidazole by some boroxine species seems plausible, hence forming *N*-methylimidazolium boroxinates. This finding is also in accordance with signal E, which shows the isopropoxy-groups of the boroxinate species.

Signal F was assigned to be triisopropylborate, which was proved by an independent measurement and also can be seen in the ^{11}B NMR spectra.

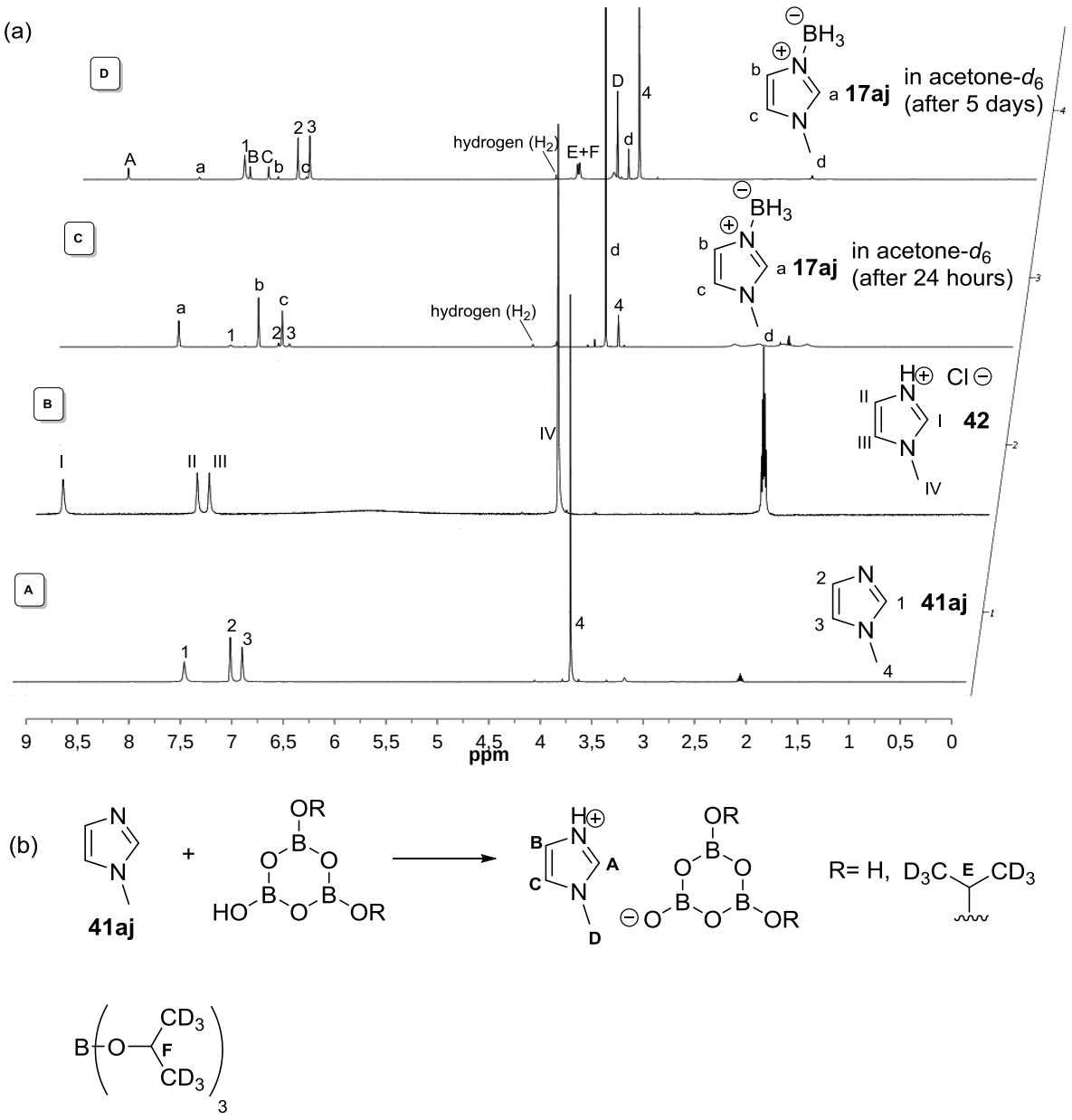

Figure 126: (a) ^{1}H NMR study in acetone-d_6. Spectrum A: *N*-methylimidazole (**41aj**). Spectrum B: *N*-methylimidazolium hydrochloride (**42**). Spectrum C: **17aj** after 24 h in acetone-d_6. Spectrum D: **17aj** after 24 h in acetone-d_6. (b) Formation of *N*-methylimidazolium boroxinates.

3.2.7.3. ^{11}B NMR analysis

Further support for these assignments was obtained from ^{11}B NMR studies (Figure 127). Therefore a {^{1}H} ^{11}B NMR (spectrum A) and ^{11}B NMR (spectrum B) was measured after 24 hours and compared with corresponding NMR measurements after 5 days (spectrum C and D). The results are in accordance with the initial findings, showing the formation of triisopropylborate (**40e**) and diisopropylborane (**40h**) after 24 hours. After 5 days no

diisopropylborane (**40h**) could be detected and the formation of several boroxine species was found.

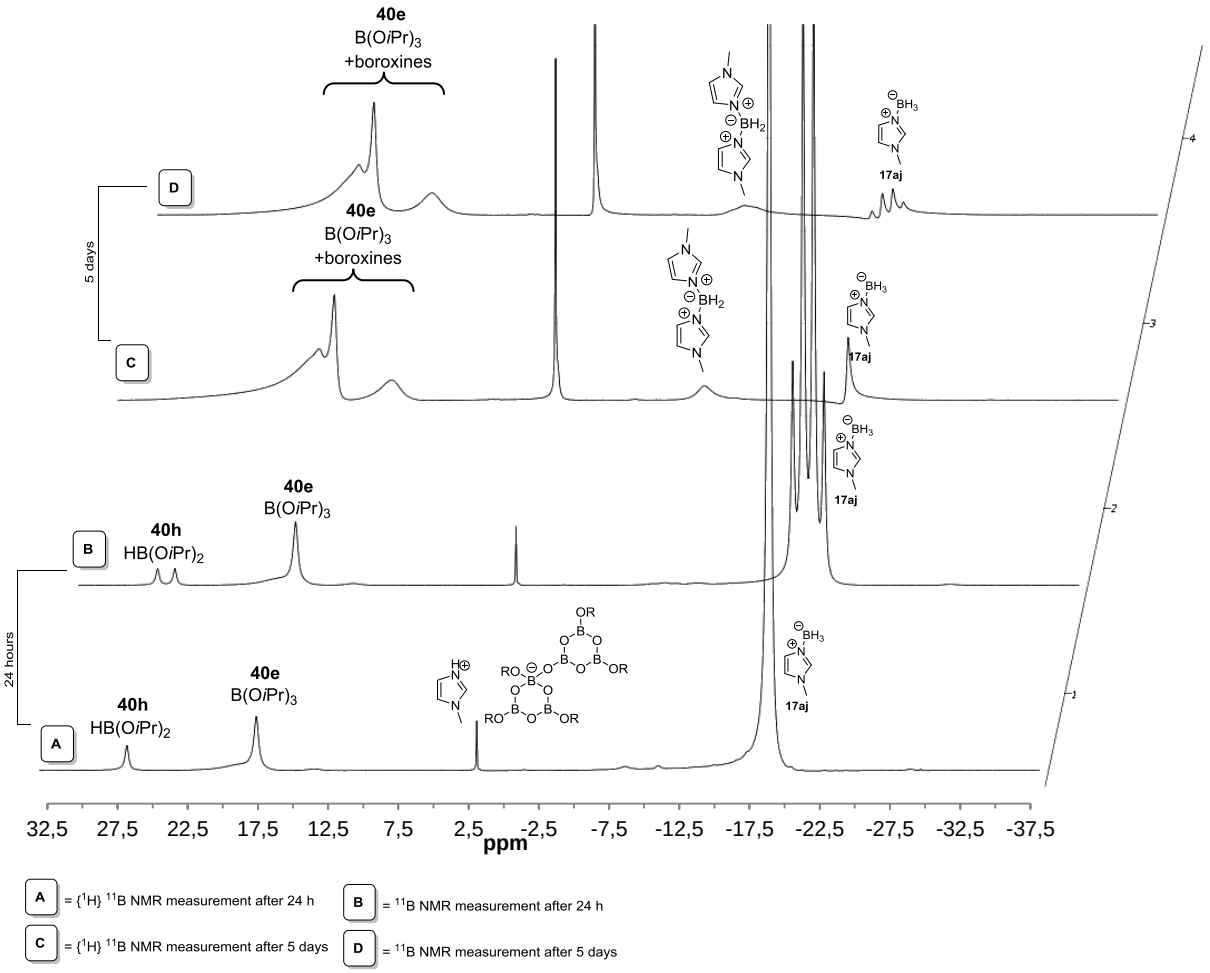

Figure 127: ^{11}B NMR measurements of **17aj** in acetone-d_6 after 24 h and after 5 days.

Finally, ketone reductions with borane complexes of imidazole derivatives bearing a free NH moiety proceed quite fast and effective. Reductions with the corresponding *N*-methylated complexes are very slow and may only work when using the substrate in large excess.

3.2.8. Reductions with imidazole-derived boranes in DMSO as solvent

When trying to conduct reductions with benzimidazole borane (**17e**) in DMSO, colorless needles began to precipitate after a few seconds. A X-ray structure of this compound could be obtained after recrystallization from chloroform/ isohexane and is shown in Figure 128. This DMSO benzimidazole borane adduct (**17ad**) has a B-N bond length of 1.580 Å, which is only slightly longer than that of benzimidazole borane (**17e**, 1.575 Å).

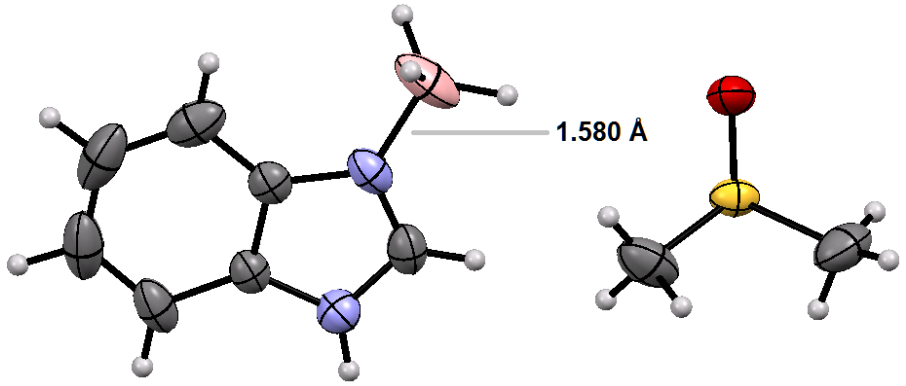

Figure 128: X-ray structure of DMSO benzimidazole borane adduct (**17ad**).

3.2.8.1. Differences of ketone reductions in DMSO

Despite of some minor structural differences between the borane and its DMSO adduct, the reactivity of benzimidazole borane (**17e**) in DMSO seems to be completely different than in other solvents. Usually ketons can be reduced fast and effective with benzimidazole borane (**17e**). However, when conducting the reaction in DMSO, no ketone reduction was observed after 30 minutes, but a fast formation of the DMSO borane adduct (**17ad**) occurred (Figure 129).

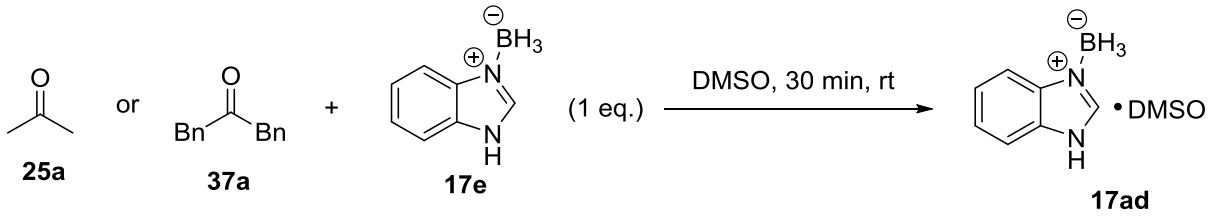

Figure 129: Formation of the DMSO benzimidazole borane adduct (**17ad**) in the presence of ketones.

3.2.8.2. Imine reductions

At first glance the DMSO benzimidazole borane adduct (**17ad**) seems not to be of any synthetic purpose. Yet, when trying to reduce imines, this complex proved to be a powerful reducing agent. The reduction of *N*-benzylideneaniline (**37s**) in DMSO with benzimidazole borane (**17e**) led to full conversion to the corresponding amine after 15 minutes. Therefore, the reaction was repeated in DMSO-d_6 with addition of an internal standard (1,4-dioxane) and monitored by ^{1}H NMR spectroscopy (Figure 130). The half-life time $t_{1/2}$ = 106 seconds shows that the DMSO benzimidalole borane adduct (**17ad**) is able to quickly reduce imines, while the reduction of ketones does not take place.

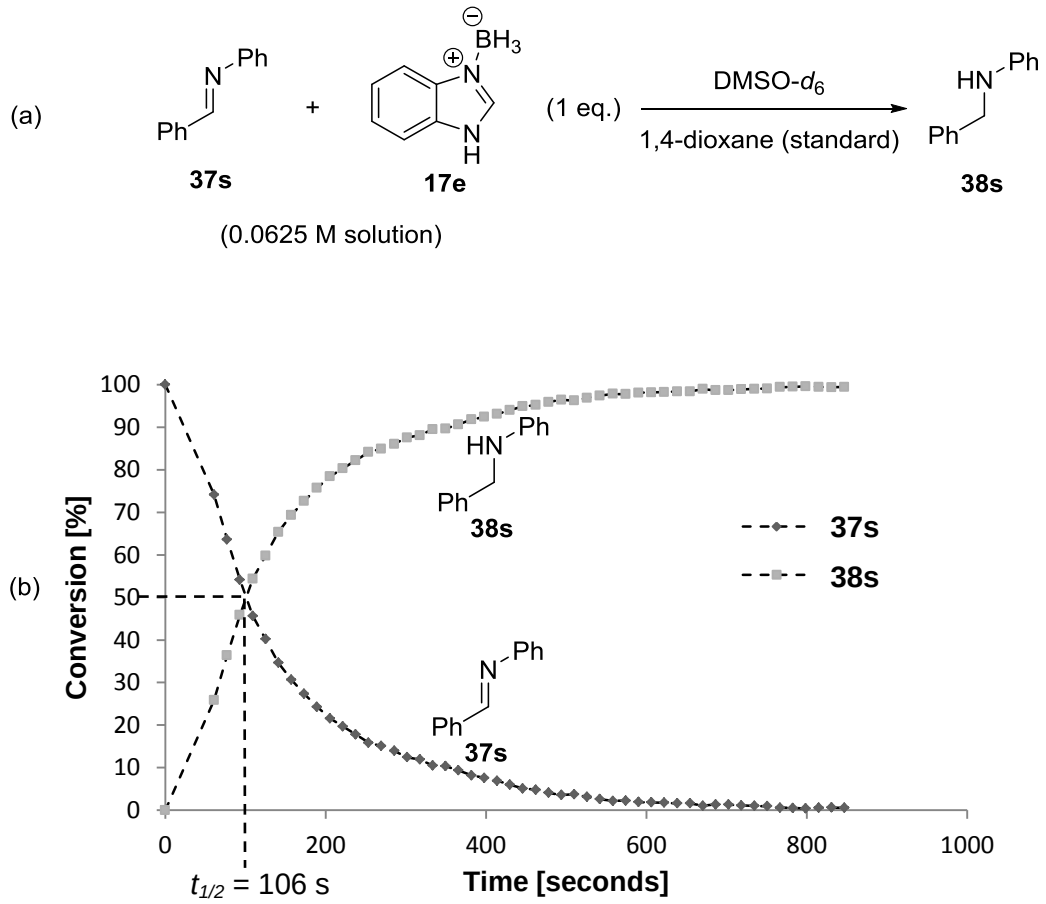

Figure 130: (a) Reduction of *N*-benzylideneaniline (**37s**) with benzimidazole borane (**17e**) in DMSO-d_6. (b) Time-conversion plot of the reaction.

In order to understand how different substituents will influence the reactivity of the borane complex in the imine reduction, the half-life times were determined for several complexes by ^{1}H NMR spectroscopy in DMSO-d_6 with *N*-benzylideneaniline (**37s**) as substrate (Figure 131 and Table 14). As benzimidazole borane (**17e**, entry 9) reacts ca. 9 times faster than imidazole borane (**17aa**, entry 7), benzimidazole borane derivatives were checked at a concentration of 0.0625 mmol/ ml, whereas imidazole derivatives were reacted at 0.25 mmol/ml. Compared to benzimidazole borane (**17e**, entry 2), the addition of a methyl group in C2-position leads to a slight slowdown (entry 1), yet a phenyl group accelerates the reaction slightly (entry 4). Addition of three methoxy groups to the phenyl ring has almost no effect (entry 3). The fastest reaction was observed for the fluorinated complex **17af** (entry 5). As mentioned above, the reaction with imidazole borane (**17aa**, entry 7) is 9 times slower than with benzimidazole borane (**17e**, entry 9). The addition of a methyl group shows the same effect as before and slows the reaction down (entry 6), whereas two phenyl groups in C4 and C5-position accelerate the reduction (entry 8). In summary, the reduction of imine **37s** with (benz)imidazole borane derivatives is fast for all tested complexes. However, benzimidazoles react distinctly faster than their imidazole analogues.

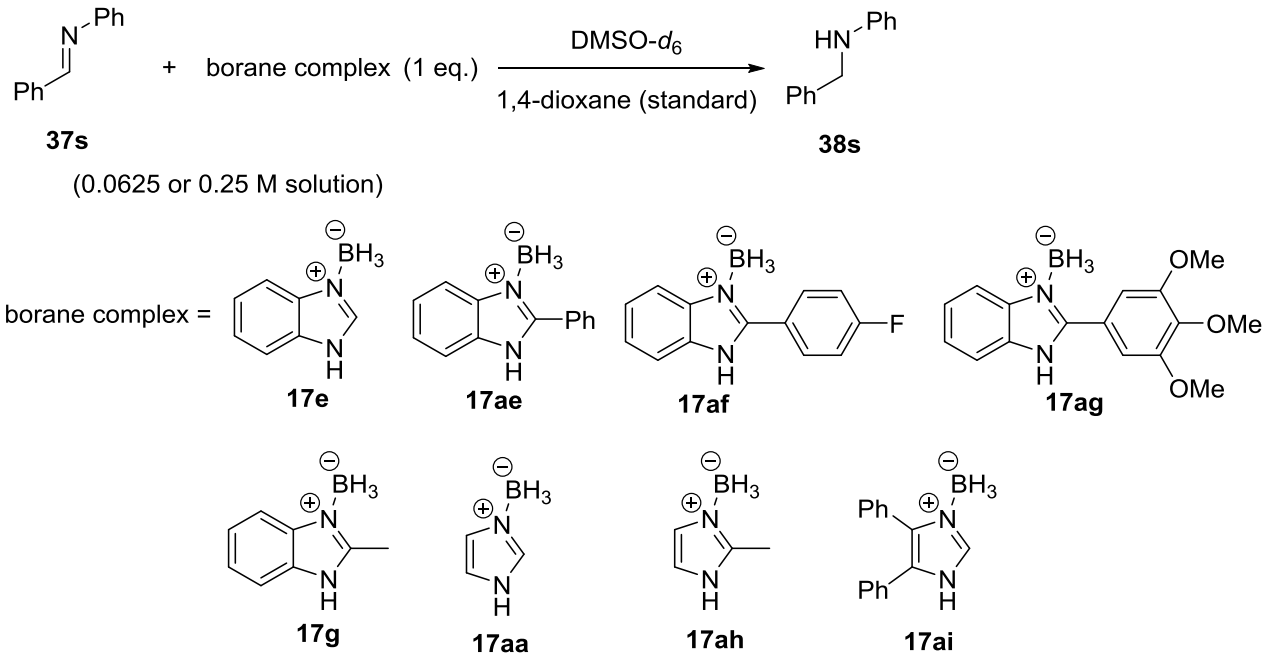

Figure 131: Borane screening for the reduction of *N*-benzylideneaniline (**37s**) as substrate.

Table 14: Results (half-life times) for the reduction of imine **37s** shown in Figure 131.

entry	borane complex	c [mmol/ ml]	$t_{1/2}$ [sec.]
1	**17g**	0.0625	171
2	**17e**	0.0625	106
3	**17ag**	0.0625	90
4	**17ae**	0.0625	85
5	**17af**	0.0625	66
6	**17ah**	0.25	517
7	**17aa**	0.25	223
8	**17ai**	0.25	53
9	**17e**	0.25	25

3.2.8.3. Selectivity of imine reductions

The formation of DMSO (benz)imidazole borane adducts, which can reduce imines but not ketones, can potetially be of big synthetic relevance. An example of a selective reduction of an imine in presence of a ketone is shown in Figure 132. A one pot mixture of imine **37s**, ketone **37a** and benzimidazole borane (**17e**) in DMSO-d_6 leads to the amine **38s** as the single reduction product after 15 minutes. Another big advantage of this chemoselective reduction is that the borane complex can even be used in excess without reducing the ketone, as the formation of the DMSO adduct seems to occur much faster than the ketone reduction.

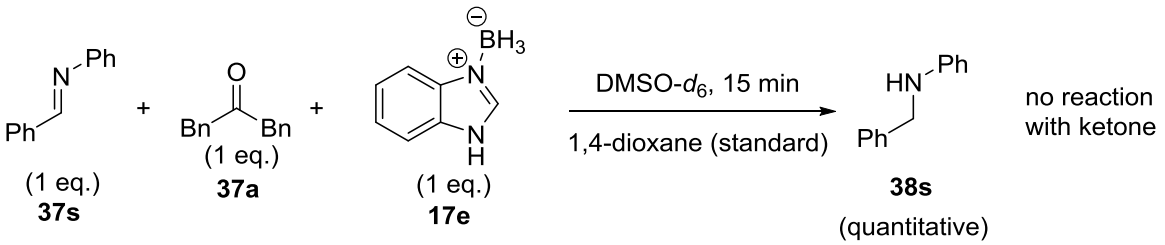

Figure 132: Selective reduction of imine **37s** in the presence of ketone **37a** with benzimidazole borane (**17e**) in DMSO-d_6.

3.2.9. Influencing factors for effective reductions

In order to measure the decay of acetophenone (**26a**) during the reduction with benzimidazole borane derivatives, toluene-d_8 was chosen as solvent. Due to the low solubility of benzimidazole borane (**17e**) in toluene, 2-nonylbenzimidazole borane (**17ac**) was also taken into account. This compound is soluble in toluene at room temperature.

3.2.9.1. Influence of the solubility of borane complexes

The reactants were used in 0.25 M solutions with an internal standard for the NMR measurements (Figure 133). The reduction with benzimidazole borane (**17e**) shows an induction phase for about 100 minutes. It is strongly assumed that this due to the low solubility of the complex, as this induction is not found for the better soluble complex **17ac**. After this period (presumeably when enough dimer is formed), polymerization occurs and the complete consumption of the ketone is observed after ca. 300 minutes. Surprisingly, the reduction with the much better soluble borane complex **17ac** does not occur faster. This fact suggests that the influence of the solubility of the complex is not as big as assumed. It rather seems that borane complexes with a low solubility show a more distinct induction phase, before the polymerization takes place. However, the consumption of acetophenone is complete after ca. 700 minutes. One explanation, why the reduction with 2-nonylbenzimidazole borane (**17ac**) is slower, may be steric hindrance due to the aliphatic chain in C2 position. Furthermore, the fact that C2-alkylated benzimidazole boranes react slower has also been shown for the reduction of imines (compare Table 14, entry 1 and 2, page 118). Hence, the use of the better soluble borane complex allows tracing the decay of the complex during the reaction. The consumption of the complex stops at ca. 30 % and thus indicates that more than one hydride is transferred, although a distinct stoichiometry could not be found.

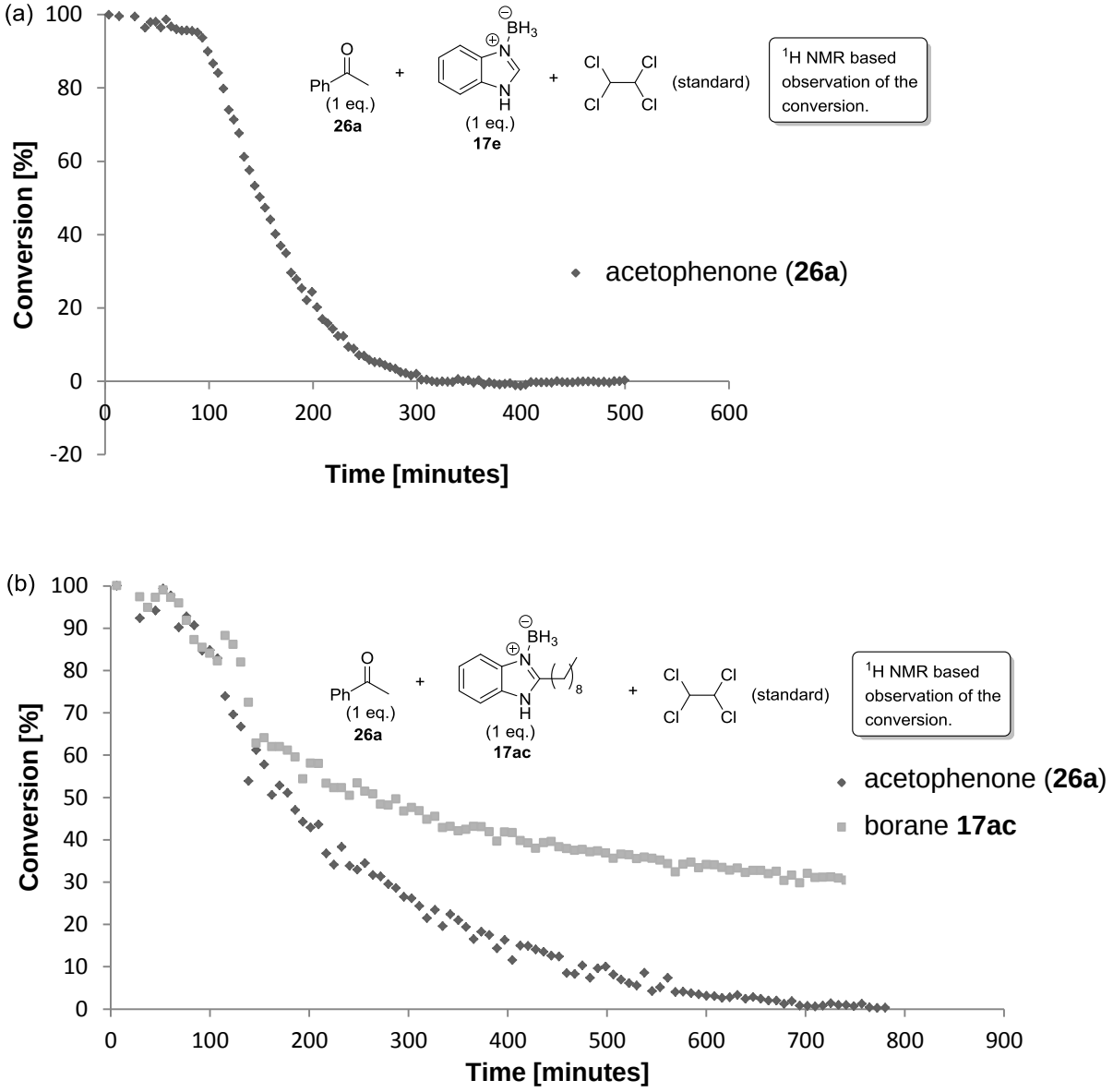

Figure 133: Time-conversion plot of the reduction of acetophenone (**26a**) in toluene-d_8 at room temperature with (a) benzimidazole borane (**17e**) and (b) with 2-nonylbenzimidazole borane (**17ac**).

3.2.9.2. Influence of the temperature

With respect to the relatively slow reaction in toluene at room temperature, the same setup (0.25 M solution in C_6D_6) was used and the decay of acetophenone (**26a**) was monitored at 60 °C by ^{1}H NMR spectroscopy (Figure 134). As in previous investigations, an induction period at the beginning of the reaction shows up. This may be caused due to the formation of the dimer species. As the reaction is carried out in a NMR tube, a heatup delay, in which the temperature of the reaction tube is risen to 60 °C, can also be taken into account. However, the complete consumption of acetophenone (**26a**) takes ca. 700 seconds. This finding may offer an attractive method for fast ketone reductions in apolar solvents at ambient temperature using a cheap reductant.

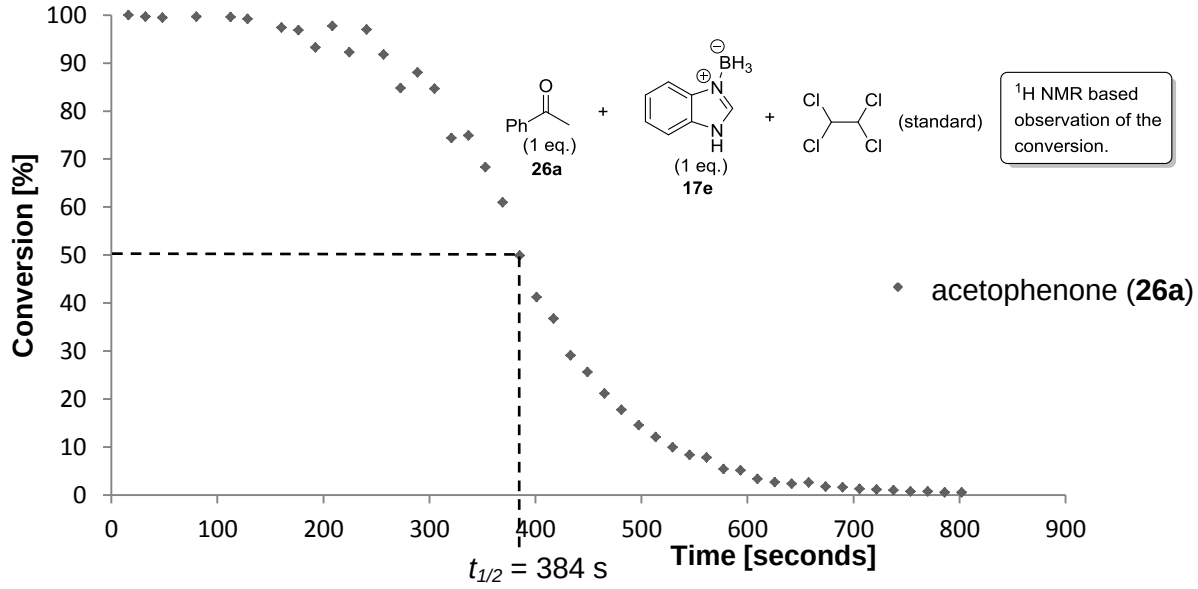

Figure 134: Time-conversion plot of the reduction of acetophenone (**26a**) with benzimidazole borane (**17e**) in C_6D_6 at 60 °C.

3.3. Ionic reductions of alkyl halides

Up to that point, dialkylaminopyridine boranes had shown good properties as H atom donors in radical reactions, whereas (benz)imidazole boranes turned out to be effective reductants for ketones, imines and aldehydes. However, an ionic reduction of alkyl halides had not been observed with any of the tested borane complexes.

3.3.1. Reductions of dodecyl halides

For exclusion of an ionic side reaction during the radical reaction, DHAP borane (**30f**) had been reacted with 1-iododododecane (**18d**) at 80 °C, where no formation of dodecane (**16a**) was observed (Figure 135).

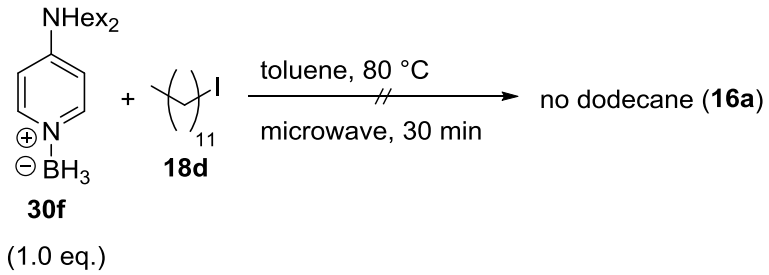

Figure 135: Attempt to react DHAP borane (**30f**) with 1-iododododecane (**18d**) at 80 °C.

3.3.1.1. Reaction optimization with 1-iododododecane (18d)

When increasing the temperature to 120 °C, formation of dodecane (**16a**) is observed. Based on this finding, an initial screening (Figure 136) of the presumed ionic reduction of

1-iododododecane (**18d**) was carried out under microwave conditions (closed vessel). Preliminary experiments had shown that the use of an inert gas atmosphere is not necessary, so the reaction vials were prepared under ambient atmosphere. The results for the reductions of 1-iododododecane (**18d**) are shown in Table 15. At 80 °C and 100 °C, no reaction with DHAP borane (**30f**) is observed, even when using the borane in excess (entry 1 and 2). The reduction of 1-iododododecane (**18d**) obviously requires higher temperatures. At 120 °C the amount of borane complex was successively increased (entry 3, 4 and 5), which leads to 92 % dodecane (**16a**) with 3 equivalents of the reductant. The use of DMAP borane (**17q**) at 120 °C leads to similar results (entry 6, 8 and 9), although the yields are slightly lower than with DHAP borane (**30f**). In order to see if solvent effects might influence the reaction, the reduction with DMAP borane (**17q**) was compared in toluene, chloroform and THF (compare entry 6 and 7 and compare entries 9, 10 and 11). The results for different solvents are very similar, therefore solvent effects seem not to influence the reduction. A further increase of the complex to 4 equivalents does not improve the yield (entry 12). Also the extension of the reaction time to 120 minutes increases the yield only slightly (entry 14), whereas already after 1 minute 9 % dodecane (**16a**) were detected (entry 13). Elevating the reaction temperature to 160 °C does not provide a higher yield (entry 15) as well as the use of DEAP borane (**17z**, entry 16). In summary, the use of 3 equivalents of cheap DMAP borane (**17q**) in toluene at 120 °C seems to be a good base for further investigations.

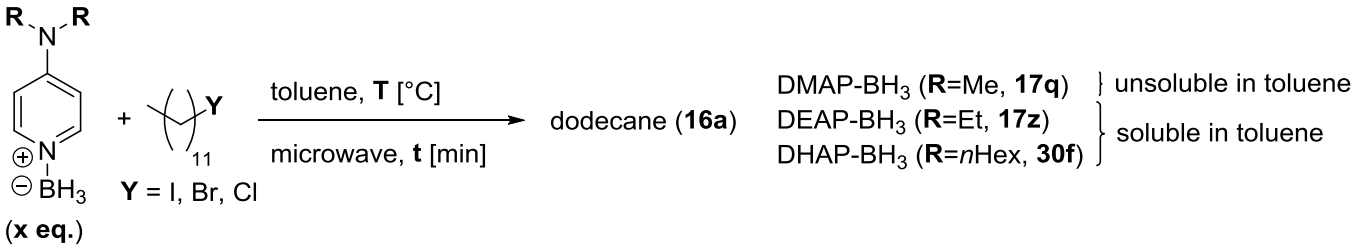

Figure 136: General scheme for the reduction of alkyl halides with dialkylaminopyridines.

Table 15: Results for the reductions of 1-iododododecane (**18d**) according to Figure 136.

entry	borane	**x eq.**	**T** [°C]	**t** [min]	yield [%]
1	DHAP-BH_3 (**30f**)	1	80	30	-
2	DHAP-BH_3 (**30f**)	3	100	60	-
3	DHAP-BH_3(**30f**)	1	120	30	43
4	DHAP-BH_3 (**30f**)	2	120	30	67
5	DHAP-BH_3 (**30f**)	3	120	30	92
6	DMAP-BH_3 (**17q**)	1	120	30	32
7	[(1)]DMAP-BH_3 (**17q**)	1	120	30	32
8	DMAP-BH_3 (**17q**)	2	120	30	57
9	DMAP-BH_3 (**17q**)	3	120	30	75
10	[(1)]DMAP-BH_3 (**17q**)	3	120	30	82
11	[(2)]DMAP-BH_3 (**17q**)	3	120	30	71
12	DMAP-BH_3 (**17q**)	4	120	30	76
13	DMAP-BH_3 (**17q**)	3	120	1	9
14	DMAP-BH_3 (**17q**)	3	120	120	83
15	DMAP-BH_3 (**17q**)	3	160	30	76
16	DEAP-BH_3 (**17z**)	3	120	30	46

[(1)] Chloroform was used instead of toluene. [(2)] THF was used instead of toluene.

3.3.1.2. Reaction optimization with 1-bromododecane (18a) and 1-chlorododecane (18i)

Based on the results for the reduction of 1-iodododecane (**18d**), the substrate was exchanged and the conditions optimized (Table 16). The reaction of 1-bromododecane (**18a**) with DMAP borane (**17q**, 3 eq.) yields only 12 % dodecane (**16a**) after 30 minutes. Therefore, the temperature was elevated (entry 2 and 3), which leads to 88 % dodecane (**16a**). Finally, when conducting the reaction for 120 minutes at 200 °C, full conversion is achieved.

Table 16: Results for the reductions of 1-bromododecane (**18a**) with DMAP borane (**17q**) according to Figure 136.

entry	**x eq.**	**T** [°C]	**t** [min]	yield [%]
1	3	120	30	12
2	3	160	30	69
3	3	200	30	88
4	3	200	120	99

In order to complete the alkyl halide reductions, 1-chlorododecane was reacted (Table 17). In this case 33 % dodecane (**16a**) is formed after 120 minutes at 200 °C (entry 1). The yield can be moderately improved to 54 % by elongation of the reaction time to 18 hours (entry 2). For exclusion of a thermal decomposition of the alkyl halides, the pure substances in toluene were exposed to 200 °C in the microwave and no formation of dodecane (**16a**) was detected. As a preliminary result it can be stated that 1-iodododecane (**18d**) can be reduced at 120 °C with DMAP borane (**17q**), whereas 200 °C and longer reaction times are needed for the bromo and chloro analogues.

Table 17: Results for the reductions of 1-chlorododecane (**18i**) with DMAP borane (**17q**) according to Figure 136.

entry	**x eq.**	**T** [°C]	**t** [min]	yield [%]
1	3	200	120	33
2	3	200	1080 (18 h)	54

3.3.1.3. Independent control experiments

In order to exclude a radical mechanism for the reaction, the reduction was repeated with addition of 30 mol% TEMPO as radical scavenger (Figure 137). After 30 minutes 75 % dodecane (**16a**) are detected. The same yield is achieved when omitting TEMPO (Table 15, entry 9, page 122), thus proving an ionic mechanism.

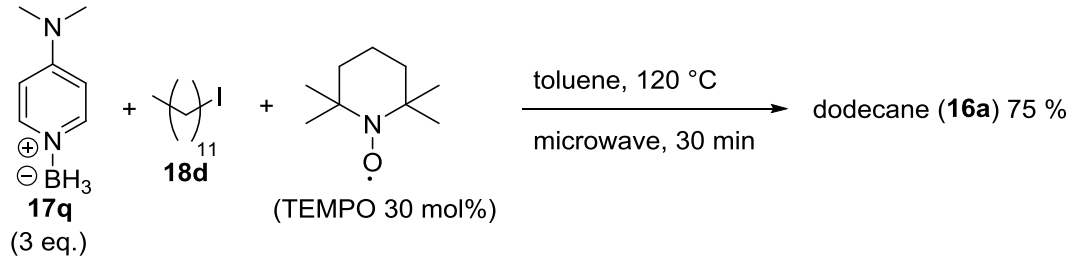

Figure 137: Reduction of 1-iodododecane (**18d**) with DMAP borane (**17q**) in the presence of TEMPO.

As benzimidazole borane (**17e**) had been used successfully in different ionic reductions, the compound was also taken into account for the alkyl halide reductions (Figure 138). However, no reduction of 1-iodododecane (**18d**) was observed for benzimidazole borane (**17e**). Other complexes were not tested in this study.

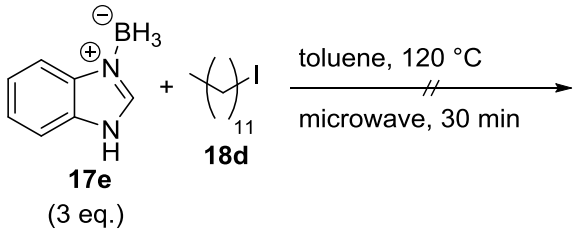

Figure 138: Attempt to reduce 1-iodododecane (**18d**) with benzimidazole borane (**17e**).

3.3.1.4. Mechanistic aspects

All reductions with DMAP borane (**17q**) in toluene led to suspensions after the reactions were finished. When analyzing these mixtures by ^{11}B NMR, only traces of the unreacted starting complex were found. Hence, it seemed obvious that some boron-containing compound had precipitated during the reaction, and that this substance was completely insoluble in toluene.

3.3.1.4.1. X-ray structures

After several attempts to crystallize some boron containing compound from the crude reaction mixtures, crystals of suitable quality were obtained for the reduction of 1-iodododecane (**18d**) and 1-bromododecane (**18a**). These crystals were grown by addition of DCM to the crude toluene suspension until a clear, saturated solution had formed. DCM was afterwards slowly removed, which led to colorless needles. The X-ray structures of the two compounds are shown in Figure 139. These kinds of bispyridyl borane species had already been found as products for the radical reduction of 1-iodododecane (**18d**, Figure 48, page 43) and for the radical reduction of xanthates (Figure 78, page 77). Further attempts to crystallize the chloro analogue from the reduction of 1-chlorododecane (**18i**) failed, but it is strongly assumed that also in this case a bispyridyl species is formed.

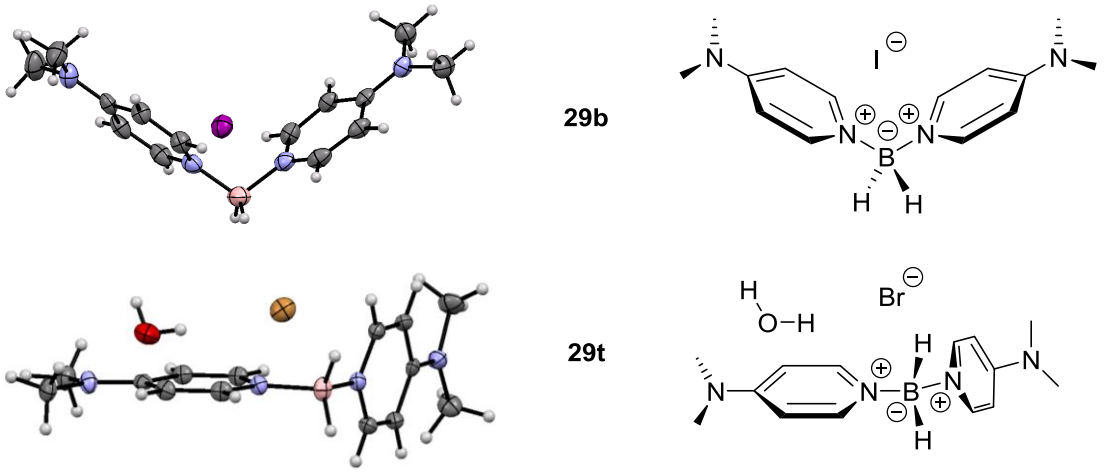

Figure 139: X-ray structures of the bispyridyl borane species **29b** and **29t**.

3.3.1.4.2. ^{11}B NMR analysis

To ensure, that the bispyridyl borane complex is the only boron-containing product, the reduction was repeated with the better soluble DHAP borane (**30f**) and 1-iodobutane (**18j**) as substrate (Figure 140a). A clear solution was obtained after 30 minutes thus ensuring to detect all non-volatile boron species in the following ^{11}B NMR measurement (Figure 140b). Beside DHAP borane (**30f**), the bispyridyl borane complex **30g** was found as the only boron containing compound.

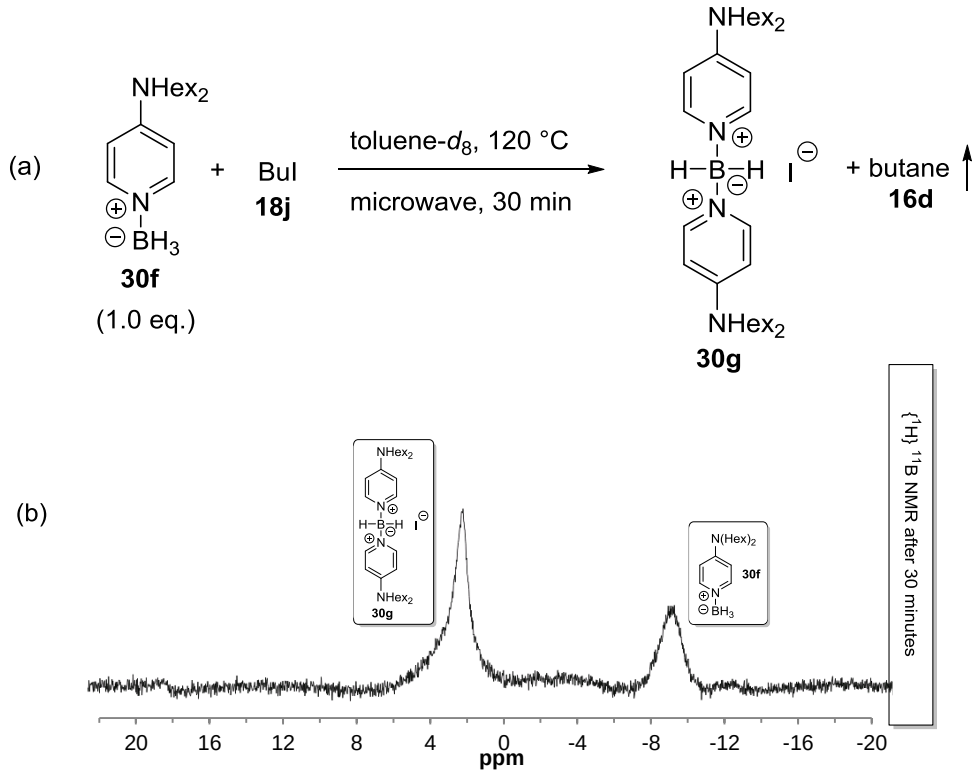

Figure 140: (a) Reduction of 1-iodobutane (**18j**) with DHAP borane (**30f**). (b) ^{11}B NMR measurement after the reaction.

3.3.1.4.3. Mechanism

The suggested mechanism for the reduction of alkyl halides with dialkylaminopyridine boranes is depicted in Figure 141. As the reaction is conducted at higher temperatures, the initial borane complex may be in equilibrium with the free base and "BH_3". The reaction of the borane complex with an alkyl halide leads to the iodoborane complex and an alkane. This iodoborane now removes the free base from the quilibrium to form the bispyridyl borane complex. The liberated "BH_3" finally may form the volatile diborane (boiling point: −93 °C).

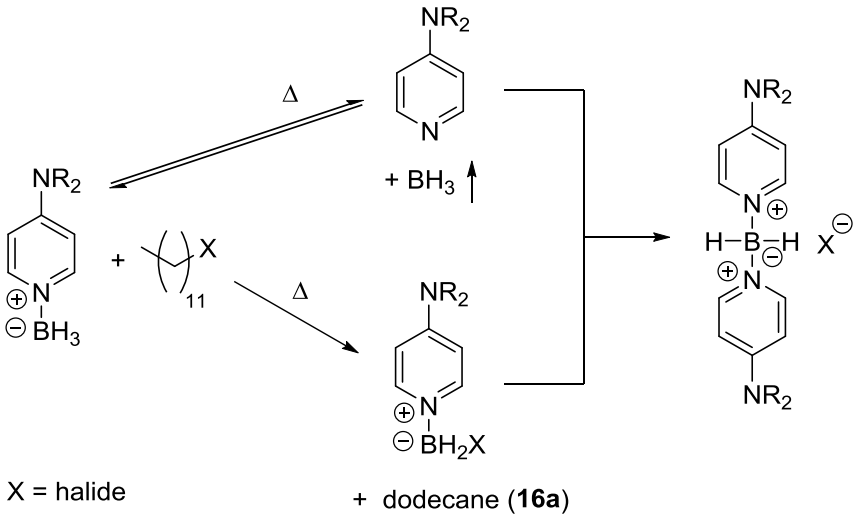

Figure 141: Suggested mechanism for the reduction of alkyl halides with dialkylaminopyridine boranes.

3.3.1.4.4. ^{1}H NMR studies

The ^{1}H NMR spectrum of pure iodoborane **29c** in $CDCl_3$ is shown in Figure 142b (below). When successively adding DMAP borane (**17q**) to the solution, the signals in the ^{1}H NMR stay unaltered and do not show a second distinguished species. This study shows on the one hand, that the bispyridyl borane species **29b** is not formed by the reaction of DMAP borane (**17q**) with iodoborane **29c**. On the other hand, a very fast exchange of the "BH_3" and the "BH_2I" group seems plausible, as only one set of signals is found, when both compounds are present.

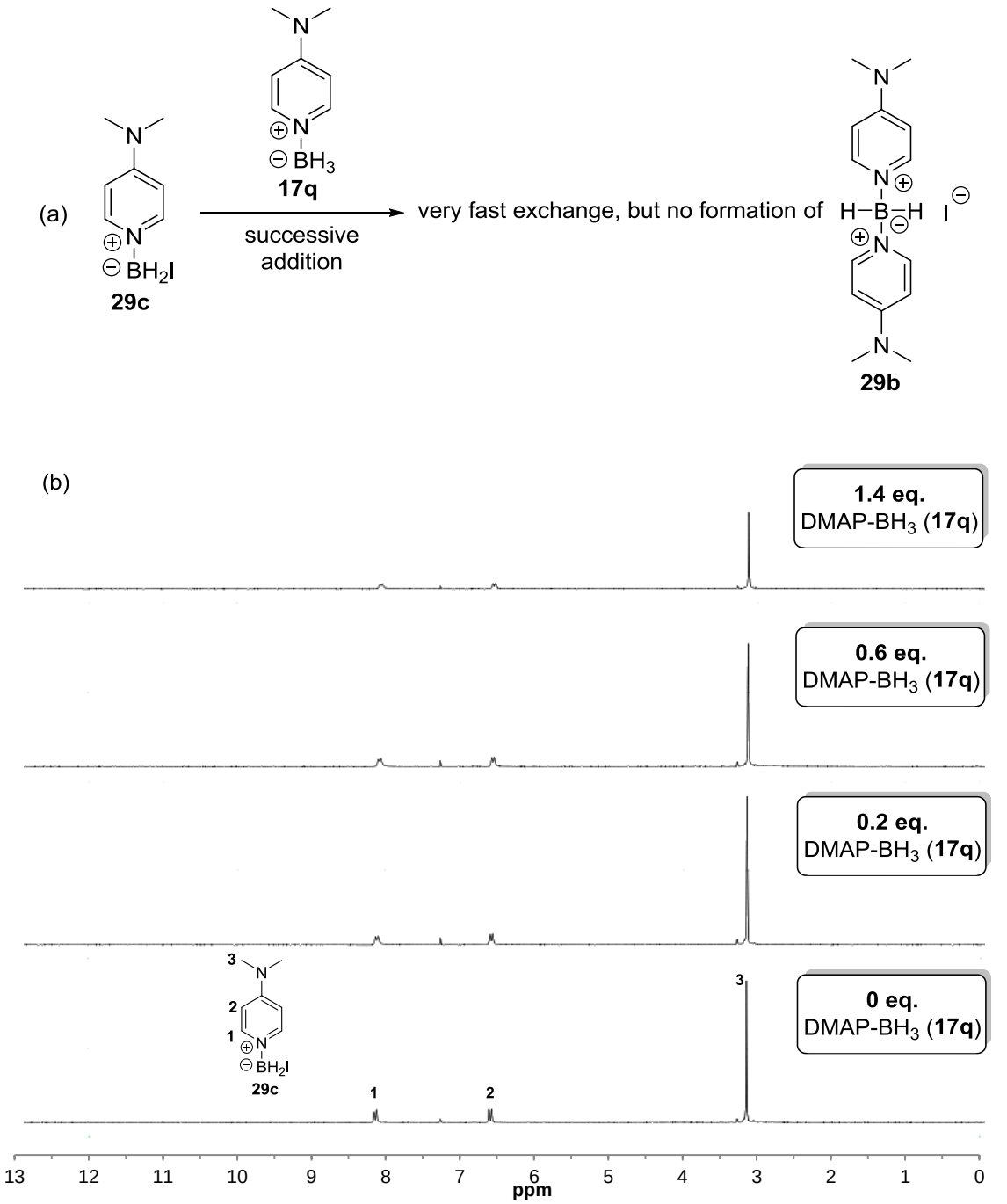

Figure 142: ^{1}H NMR study in $CDCl_3$: Successive addition of DMAP borane (**17q**) to iodoborane **29c**.

A ^{1}H NMR study on the successive addition of DMAP (**27**) to iodoborane **29c** is shown in Figure 143. The bispyridyl borane complex **29b** is formed instantly by the addition of DMAP (**27**). Subsequently, a 1:1 mixture of iodoborane **29c** and DMAP (**27**) leads to full conversion to the bispyridyl borane species **29b**. By addition of DMAP (**27**) in excess, the free base can also be seen in the ^{1}H NMR measurement. Finally, the shown ^{1}H NMR studies strongly support the suggested mechanism (Figure 141, page 126). The formation of the bispyridyl borane complex occurs by the reaction of free DMAP (**27**) and a halogenated borane complex.

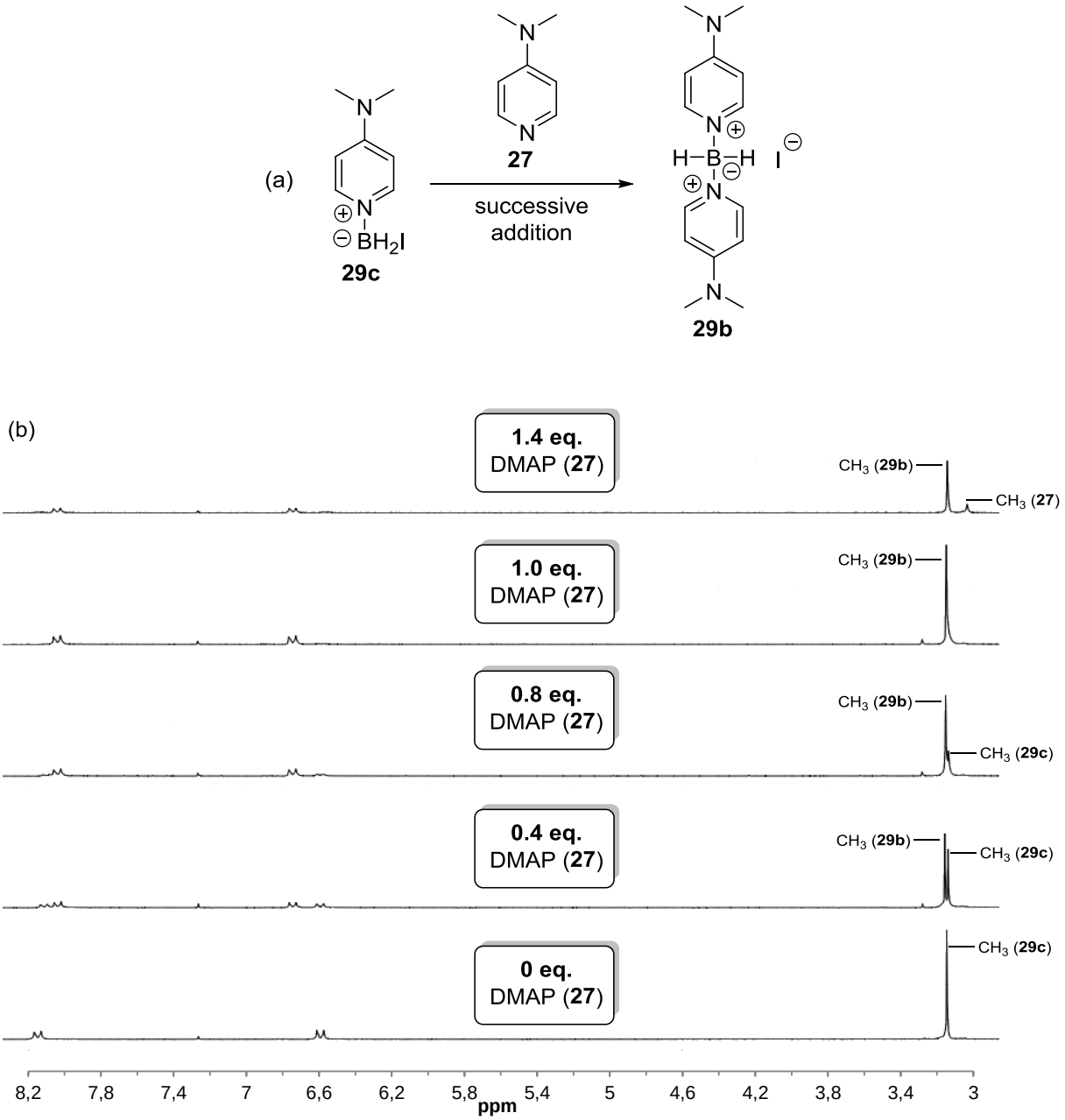

Figure 143: ^{1}H NMR study in $CDCl_3$: Successive addition of DMAP (**27**) to iodoborane **29c**.

3.3.1.5. Time-conversion measurement

A time-conversion plot for the reduction of 1-iodododecane (**18d**) with DMAP borane (**17q**) at 120 °C could not be directly followed by ^{1}H NMR due to the boiling point of toluene (111 °C) and at 100 °C no reaction was apparent. Further attempts to run the reaction at 120 °C in DMSO (boiling point: 189 °C) also failed due to a reaction of the substrate with the solvent (Figure 144).

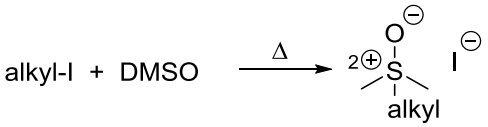

Figure 144: Reaction of alkyl halides with DMSO.

Therefore, a separate experiment was set up for each point of the time-conversion study. The borane comlex (3 eq.), 1-iododododecane (**18d**) and 0.5 ml toluene were added into a microwave vial with a magnetic stirring bar and closed with a cap. Afterwards the suspension was heated to 120 °C. The delay for the heat up from room temperature to the desired temperature was about 20 to 30 seconds and was neglected in this study. The reaction was run for a defined time and then quickly cooled down by a nitrogen flow induced by the microwave. The cooldown from 120 °C to 100 °C (where no further reaction should occur) was about 5 seconds and was also neglected. After cooling to room temperature, the solvent was removed under reduced pressure and the residue dissolved in $CDCl_3$. The resulting clear solution was used for ^1H NMR measurements. Figure 145 shows the so obtained time-conversion plot, in which each set of three points displays a separate experiment. Full conversion was obtained after a reaction time of 10 hours. Furthermore only two equivalents of DMAP borane (**17q**) are consumed, leading to one equivalent of the bispyridyl borane **29b**. These findings fit perfectly to the mechanism (Figure 141, page 126).

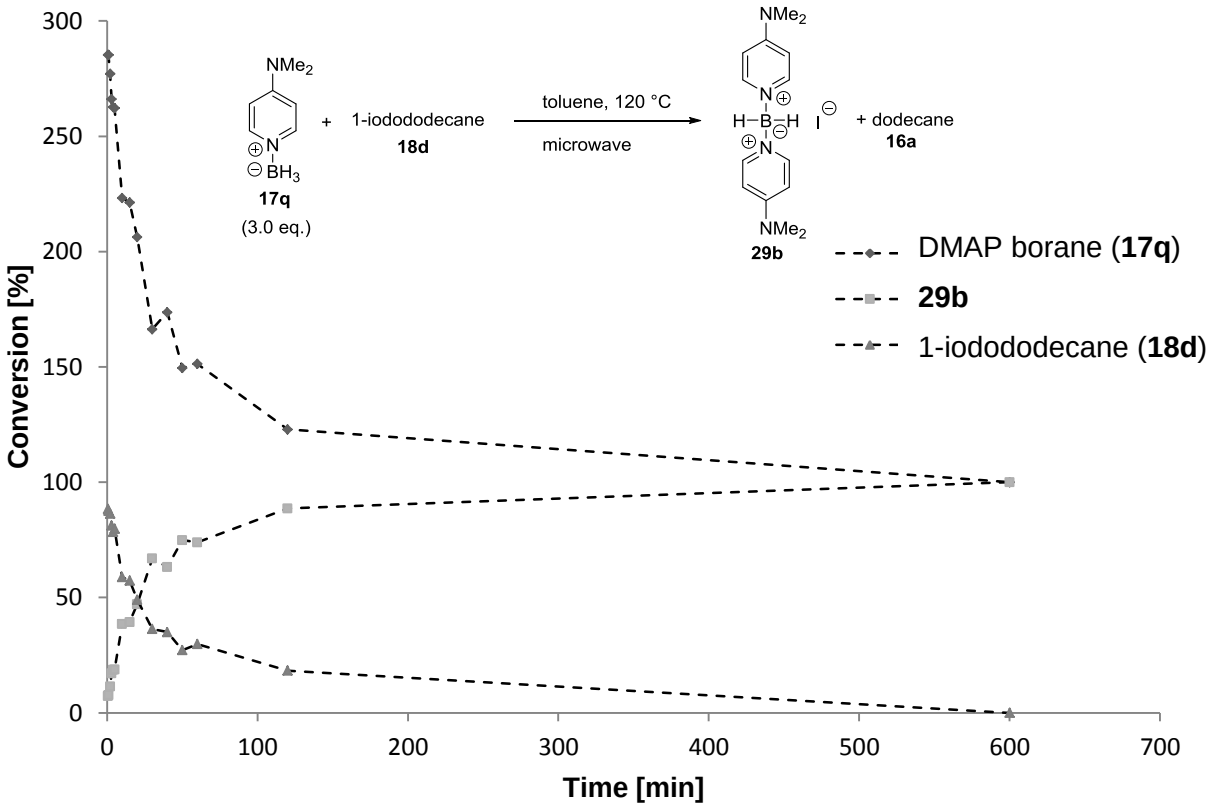

Figure 145: Time-conversion plot for the reduction of 1-iododododecane (**18d**) with DMAP borane (**17q**) at 120 °C in toluene.

3.3.2. Reduction of chloroform

When trying to repeat the time-conversion study with 1-iododododecane (**18d**) from an initially prepared stock solution in $CDCl_3$, a reaction between the solvent and the borane complex was noticed (at 120 °C).

3.3.2.1. NMR studies

The reaction of DMAP borane (**17q**) with $CDCl_3$ at 120 °C was investigated. When exposing DMAP borane (**17q**) for 16 hours to 120 °C in $CDCl_3$, the borane complex is completely consumed. The ^1H and ^{11}B NMR measurements after 16 hours are shown in Figure 146. The formation of three new dimethylaminopyridine borane species (**29u**, **29v** and **29w**) can be nicely seen in the measurements. Furthermore a triplet (^2J = 1.10 Hz) shows up in the ^1H NMR measurement at 5.23 ppm (see inlet). This signal could be assigned to DCM-d_1.

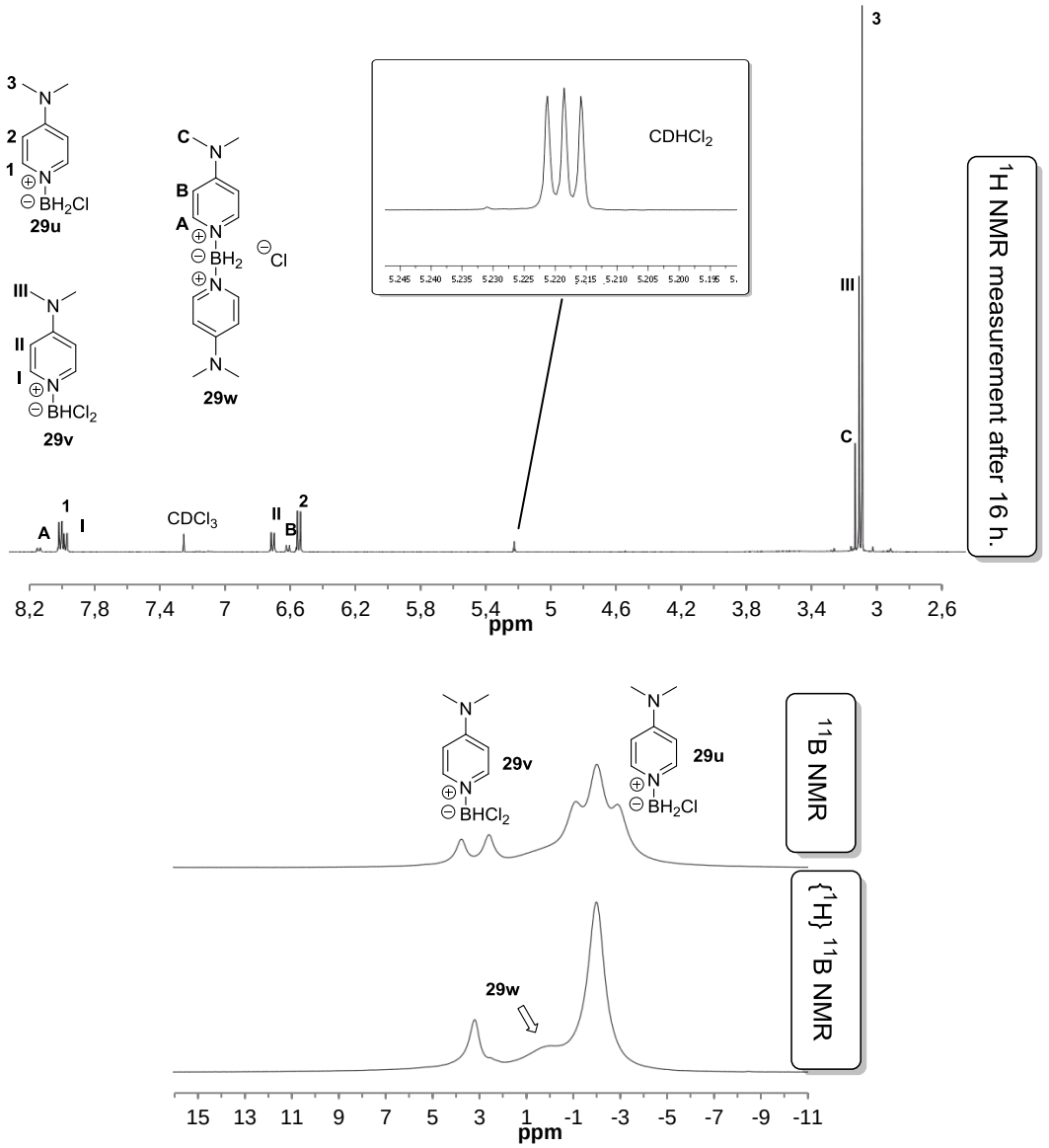

Figure 146: NMR study of the reaction of DMAP borane (**17q**) in $CDCl_3$ at 120 °C after 16 hours.

3.3.2.2. Mechanism

The depicted NMR measurements lead to a supposed mechanism (Figure 147), which is slightly different as the mechanism shown before (Figure 141, page 126). DMAP borane (**17q**) reacts with $CDCl_3$ to form cloroborane **29u** and $CDHCl_2$. This monochlorinated borane can then either react with $CDCl_3$, leading to the dichlorinated borane **29v** and $CDHCl_2$, or react with free DMAP (**27**), which leads to the bispyridyl borane **29w**. The main difference to other reactions is that $CDCl_3$ is reactant and solvent at the same time. Therefore, the formation of the bispyridyl borane species seems only to occur in traces, as $CDCl_3$ is present in large excess.

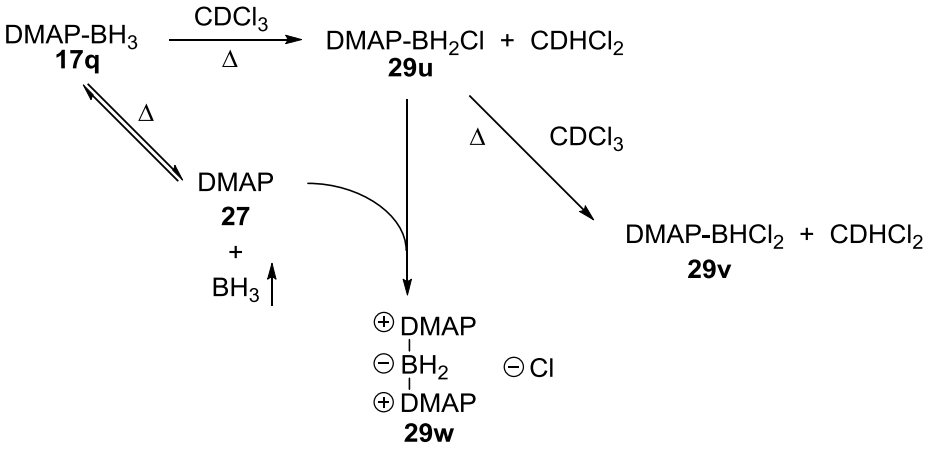

Figure 147: Suggested mechanism for the reaction of DMAP borane (**17q**) with $CDCl_3$ at 120 °C.

3.3.2.3. Time-conversion measurement

Finally, also for this reaction a time-conversion plot was measured by ^1H NMR spectroscopy. As in the study of the reduction of 1-iodododecane (**18d**) a separate experiment was applied for each point of the measurement. Therefore, a stock solution of DMAP borane (**17q**) in $CDCl_3$ was used and 0.6 mL of this solution were exposed to 120 °C under microwave irradiation (closed vessel) for a defined time. The delays for heating up (ca. 20 seconds) as well as for the cool down (ca. 5 seconds) were neglected. The resulting time-conversion plot is shown in Figure 148. The formation of DCM-d_1 was not included in the plot, due to its low boiling point. The decay of DMAP borane (**17q**) is completed after 16 hours. The formation of the monochlorinated borane complex **29u** represents the main process. The consumption of this species can be nicely seen, leading to the dichlorinated borane complex **29v** and the bispyridyl borane **29w** as a side product.

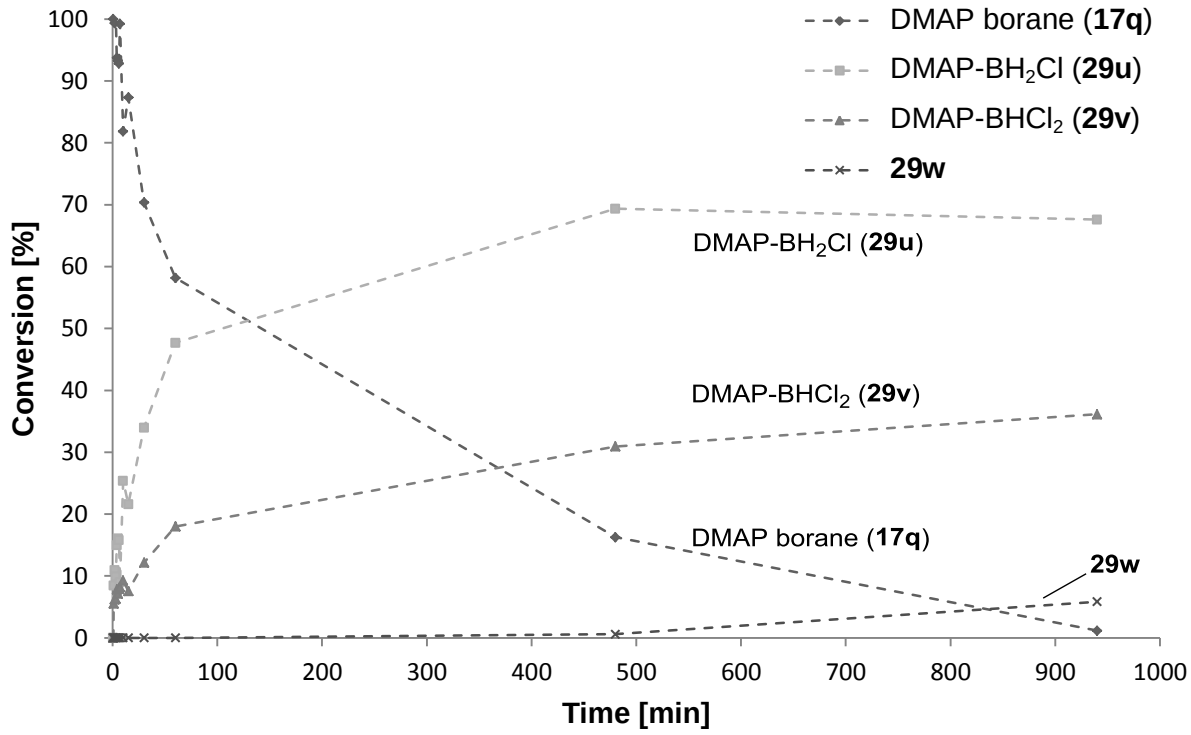

Figure 148: Time-conversion plot for the reaction of DMAP borane (**17q**) in $CDCl_3$ at 120 °C.

4. Conclusion and outlook

A general scheme of applications for borane complexes used in this work is shown in Figure 149.

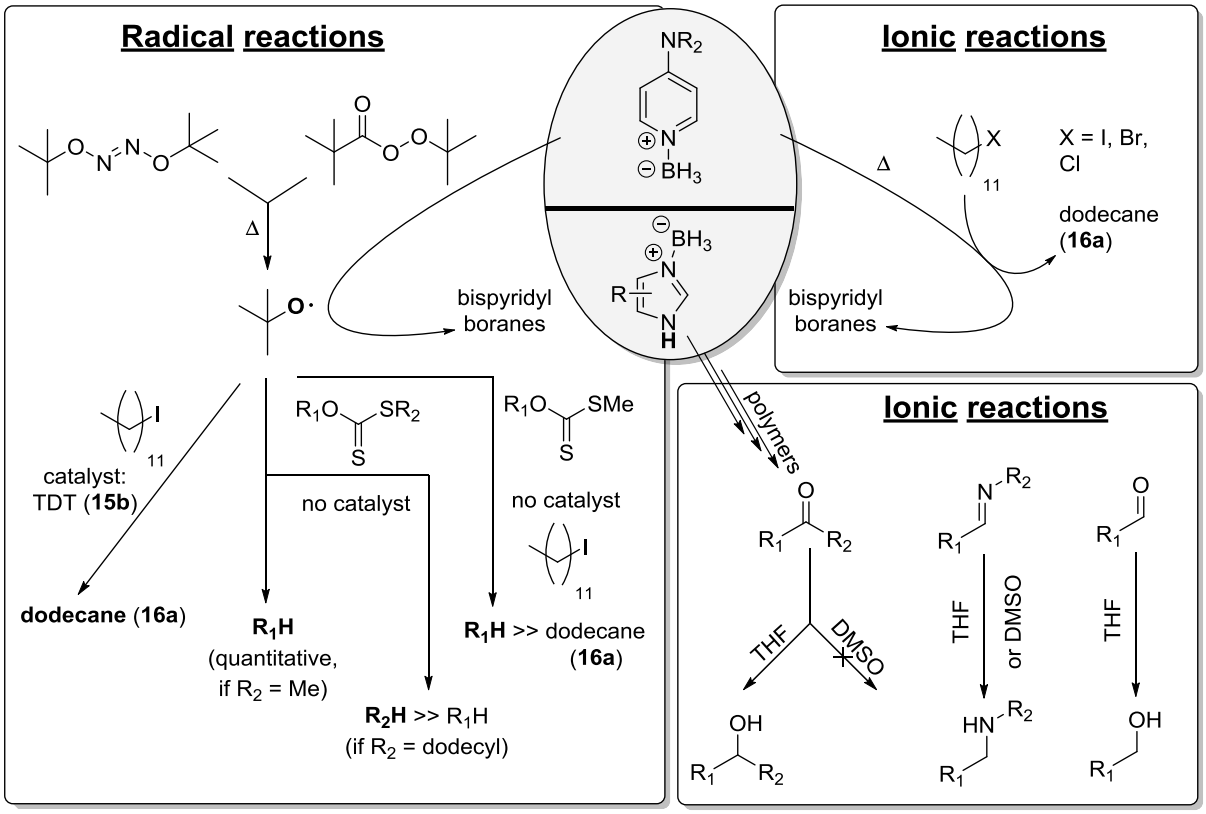

Figure 149: Applications of borane complexes used in this work: General scheme for radical and ionic reactions.

An initial screening of different classes of heterocyclic borane complexes had shown that dialkylaminopyridine boranes are suitable as hydrogen atom donors in radical chemistry, when used under the right conditions. The importance of the radical starter has been studied in detail. All tested standard initiators like AIBN (**2a**) or BEt_3 (**2b**)/O_2 turned out not to work in combination with dialkylaminopyridine boranes. The reason for this is that the formation of an oxygen-centered radical is indispensable. However commercial sources like di-*tert*-butylperoxide (**2c**) or dicumylperoxide (**2f**) could not be used for this purpose. Thermal initiation with these high temperature initiators was impossible, as the borane complexes did undergo an ionic reaction with the substrate (alkyl halides) at temperatures over 120 °C. Initiation on irradiation also failed due to decomplexation of the borane. TBHN (**2d**) which showed a half-life time of $t_{1/2}$ = 520 seconds at 80 °C led to a successful initiation, generating two tert-butoxy radicals by release of nitrogen. DBHN (**2e**) as low temperature initiating hyponitrite was also taken into account. However these experiments failed, showing the temperature dependence beside the formation of an oxygen-centered radical. As a proof of concept, TBPP (**31a**, half-life time $t_{1/2}$ = 390 seconds at 90 °C) was synthesized and also successful applied as initiator. The choice of the right starter, the right borane and a convenient temperature led to a moderate yield of dodecane (**16a**, 45 %) with respect to the

radical reduction of 1-iodododecane (**18d**). By addition of a thiol as catalyst (TDT (**15b**)) a quantitative conversion could be achieved.

Radical reductions of xanthates showed quite fast and very effective reactions with dialkylaminopyridine boranes. A full conversion of xanthate **18c** to dodecane (**16a**) could be achieved within 4 minutes. Even the use of TDT (**15b**) as catalyst is not necessary in terms of xanthate reductions, which was shown on the basis of several examples and a detailed mechanistic study. Also for the secondary xanthate **18f** an effective reduction to decane (**30c**, quantitave yield after 30 minutes) was observed. However, the structure of the xanthate seems to influence the reaction outcome. Reactions with xanthate **18c**, which bears a methyl group on the sulfur, led exclusively to dodecane (**16a**) as the product. Various experiments with xanthates having a longer chain attached to the S-atom (here a dodecyl group) showed a different product distribution. In these cases, the sulfur side of the xanthate was mainly reduced. Furthermore, studies on the selectivity between the reduction of xanthate **18c** and 1-iodododecane (**18d**) in one pot reactions have been conducted with different hydrogen atom donors. The results of these preliminary studies may be of high synthetic interest. Bu_3SnH (**1a**) showed a reduction ratio of 1 : 0.36 (iodide : xanthate), whereas NHC borane **17y** exclusively reduced the iodide. Hence, for the reduction with DMAP borane (**17q**) a high selectivity for the xanthate **18c** was observed (iodide : xanthate = 1 : 4.33).

With respect to ionic reductions the use of dialkylaminopyridine boranes as well as imidazole-derived borane complexes were studied. Primary alkyl halides could be reduced with DMAP borane (**17q**) to the corresponding alkane when exposing them to higher temperatures in toluene. The reductions were conducted in a microwave (closed vessel) and led to full conversions for 1-iodododecane (**18d**, after ten hours at 120 °C) and 1-bromododecane (**18a**, after two hours at 200 °C). 1-Chlorododecane (**18i**) yielded 54 % dodecane (**16a**) after 18 hours at 200 °C. It should be mentioned that in all cases the formation of bispyridyl borane species was observed.

Reductions of ketones and aldehydes were performed with imidazole-derived borane complexes in THF, methanol, toluene or benzene and led to the corresponding alcohols in high yields after workup. A borane screening had shown the importance of the free NH-moiety of the imidazole-derived borane complex, which is strongly assumed to activate the carbonyl group of the substrate. The complex formation of borane polymers during the reduction was studied in detail, based on ESI-MS and NMR experiments. As benzimidazole borane (**17e**) is a cheap compound that is easy to handle and can be stored under air over month, synthetic advantages of this compound are obvieous. Reductions of ketons, imines or aldehydes can be conducted at room temperature within five minutes in THF or methanol. An improved aqueous workup, followed by extraction offers a very easy and highly effective route of pure reduction products in almost quantitative yields. Another advantage is the reduction in apolar solvents like toluene or benzene and may be of high interest for synthetic purposes. As an example, the reduction of acetophenone (**26a**) with benzimidazole borane (**17e**) was shown, which led to a full conversion after 700 seconds at a moderate temperature of 60 °C in benzene.

When conducting reductions with benzimidazole borane (**17e**) in DMSO, the formation of the DMSO borane adduct (**17ad**) was observed. It is strongly assumed that due to the formation of this adduct a reduction of ketones in DMSO does not take place, whereas fast reductions of imines are possible.

Outlook:

The various studies presented in this work offer the fundament for further studies on heterocyclic borane complexes in radical and ionic reactions. Good results for the radical reduction of 1-iodododecane (**18d**) with dialkylaminopyridine boranes have been reported in this work, however attempts to reduce 1-bromododecane (**18a**) failed. Attempts to reduce 1-iodododecane (**18d**) with pyridine borane (**17t**), which also failed, strongly suggest the importance of electronic effects for an effective hydrogen atom donor. A hypothetical example for an “ultra-electron-rich” pyridine derived borane complex is shown in Figure 150, which could be a future project for an effective hydrogen atom donor.

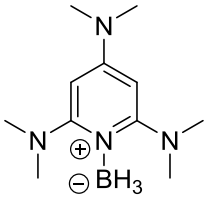

Figure 150: Hypothetic “ultra-electron-rich” borane complex.

Furthermore, the scope of substrates could be extended to secondary or tertiary alkyl halides. As the reduction of xanthates had shown very promising and effective results, a wide field of applications in this direction is also possible. One promising project could be the optimization of reaction conditions towards the selectivity in the reduction of xanthates in the presence of alkyl iodides. As the reactivity of xanthates with dialkylaminopyridine boranes seems relatively high, a lower initiation temperature (eventually by use of another radical starter) may improve the selectivity for the xanthate over the iodide (Figure 151).

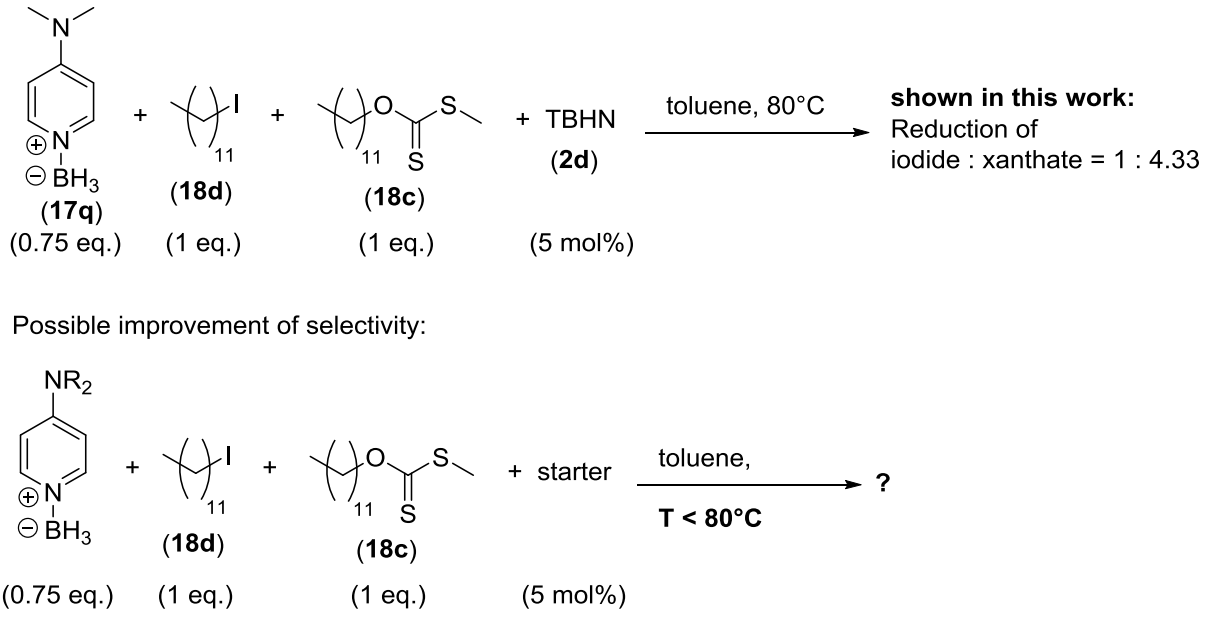

Figure 151: Improvement of the selectivity: A possible future project.

Radical reductions of xanthate **18c** led to dodecane (**16a**) and thus imply that the oxygen-bound alkyl group was reduced. Yet, xanthates with a dodecyl group on the sulfur were mainly reduced on the “sulfur-side”. Further studies on this finding may also give a more detailed insight in the reduction of xanthates. One possible idea could be the systematic elongation of the “sulfur-side” alkyl chain, followed by a product analysis after the reduction (Figure 152).

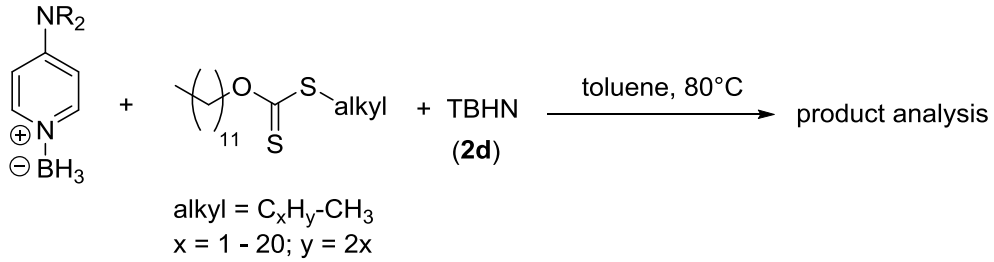

Figure 152: Systematic elongation of the “sulfur-side” alkyl chain of xanthates.

The combination of radical and ionic chemistry of a dialkylaminopyridine boranes could also offer interesting synthetic options. In a one pot reaction a xanthate could first be reduced under radical conditions at 80 °C (or eventually lower) and afterwards the iodide by just increasing the temperature to 120 °C (Figure 153, path a). This concept could also be applied the other way around on a radical pathway. With the use of an NHC borane the iodide could be reduced first and after addition of a dialkylaminopyridine borane, the xanthate could be reduced afterwards (Figure 153, path b).

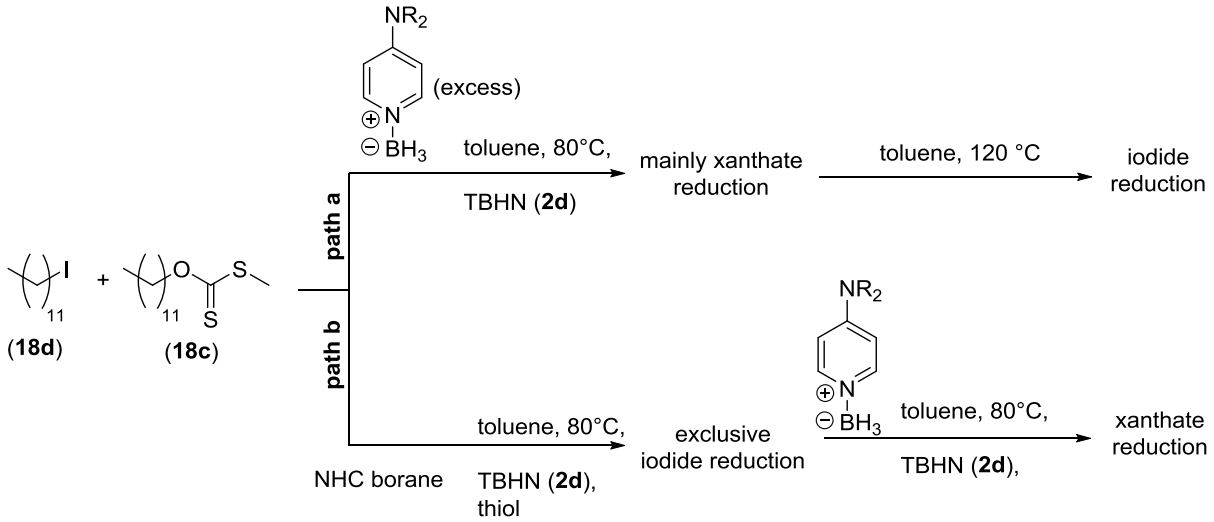

Figure 153: Selective reductions of a xanthate and an iodide.

One could also think about chiral borane complexes for enantioselective reductions. With the help of this work, very important basic investigations on reaction mechanisms were made. The high potential of the shown borane complexes in versatile reactions opens new ways and strategies for future studies.

5. Experimental details

5.1. General working techiques

All reactions were carried out according to the standard procedure in organic chemistry and, if air or moistire sensitive, under nitrogen atmosphere. Glassware was dried with a heat gun prior to use. Syringes, which were used to transfer anhydrous solvents or reagents, were purged three times with nitrogen.

5.1.1. Reagents and solvents

All chemicals were purchased at Sigma-Aldrich, Fluka, Acros, Merck KGaA or ABCR and, if not indicated, used without further purification. Tributyl tinhydride (**1a**), CS_2 and benzyl bromide (**20c**) were distilled prior to use. *Ortho*-phenylenediamine (**35e**) was recrystallized from chloroform/ isohexane prior to use. Solvents for column chromatography were of technical grade and obtained by the chemical supply of the faculty. These solvents were distilled (rotary evaporator). Solvents for reactions were either used in HPLC grade (sealed with a septum) or were dried according to standard procedures by distillation or drying agents.

CH_2Cl_2, $CHCl_3$ and $CDCl_3$ were predried over $CaCl_2$ and distilled from CaH_2 under nitrogen.

THF, benzene and toluene were continuously refluxed and freshly distilled from sodium/ benzophenone under nitrogen.

5.1.2. Chromatography

Thin layer chromatography (TLC) was performed using SiO_2 pre-coated aluminium plates (Merck TLC Silica gel 60 F_{254}). Analysis of TLCs was performed by 254 nm UV irradiation, by incubating the plates in an iodine chamber and/or by staining of the TLC plate with one of the reagents given below followed by heating with a heat gun:

$KMnO_4$ (3.0 g), conc. H_2SO_4 (5 drops) in water (300 mL).

Hanessian stain: $(NH_4)_6Mo_7O_{24}x4H_2O$ (5.0 g), 1 g $Ce(SO_4)_2$, conc. H_2SO_4 (10 mL) in water (90 mL)

Flash column chromatography was performed with SiO_2 (0.040 – 0.063 mm) from Merck.

5.2. Analytical methods

5.2.1. NMR spectroscopy

^{1}H NMR and ^{13}C NMR spectra were recorded on VARIAN Mercury 200, BRUKER ARX 300, VARIAN VXR 400 S and BRUKER AMX 600 instruments. ^{11}B NMR spectra were recorded on a Jeol GSX-270 machine. All measurements were done in standard NMR glass tubes (diameter: 5 mm). Chemical shifts are reported as δ-values in ppm relative to tetramethylsilane.[80]

$CDCl_3$ (δ 3 H = 7.26 ppm; δ C = 77.16 ppm).
DMSO-d_6 (δ 6 H = 2.50 ppm; δ C = 39.52 ppm).
C_6D_6 (δ 6 H = 7.16 ppm; δ 6 C = 128.06).
Toluene-d_8 (δ 8 H = 2.08, 6.97, 7.01 and 7.09 ppm; δ 7 C = 137.48, 128.87, 127.96, 125.13 and 20.43 ppm).

The following abbreviations were used to characterize signal multiplicities: s (singlet), d (doublet), t (triplet), q (quartet), m (multiplet) as well as br (broadened).

5.2.2. Mass spectrometry

High resolution (HRMS) and low resolution (MS) spectra were recorded on a FINNIGAN MAT 95Q mass spectrometer. Electron impact ionization (EI) was conducted with an ionization energy of 70 eV. Gas chromatograms were recorded with a Varian 3400 GC instrument with a CS-Supreme-5 capillary column. Mass numbers m/z are reported in atomic units (u). Furthermore, the relative intensities of molecular fragments (> 10 %) and, if possible, the fragmentations are reported. For high resolution spectra, the formula and the exact mass is also shown.

GC/MS
For coupled gas chromatography/mass spectrometry, a HEWLETT-PACKARD HP 6890/MSD 5973 GC/MS system was used.

ESI-MS spectrometry
Electrospray ionization measurements were recorded on a “Thermo Finnigan LTQ Ultra” FT-ICR mass spectrometer. Spectra were recorded from 100 to 800 u. The spray capillary tension was 4 kV, with a temperature of the heater capillary of 250 °C. For injections a Suveyor MS pump was used at a rate of 100 µl/min. Standard samples were measured in water/ acetonitrile (20:80). For water-sensitive substances dry solvents (eg. THF) were used and the injection was done manually by a standard Hamilton syringe. The injection volume was 1 – 10 µl.

5.2.3. IR spectroscopy

Infrared spectra (IR) were recorded from 4500 cm^{-1} to 650 cm^{-1} on a PERKIN ELMER Spectrum BX-59343 instrument. For detection a SMITHS DETECTION DuraSampl*IR* II Diamond ATR sensor was used. Wavenumbers are reported in cm^{-1}. The intensities of the transmissions is indicated by the abbreviations vs (very strong), s (strong), m (medium), w (weak), vw (very weak) as well as br (broadened).

5.2.4. Elemental analysis

Elemental analyses were conducted with a Heraeus Elementar Vario EI instrument in the micro analytical lab of the department. The content of C, H, N and S was determined.

5.2.5. Melting points

Melting points (mp) were determined on a BÜCHI B-540 melting point machine and are uncorrected. Compounds decomposing upon melting are indicated.

5.2.6. X-ray analysis

X-ray analyses were recorded in the structure analytical lab of the department on a KappaCCD or a XCalibur instrument. Measurements were conducted with a Stoe-IPDS area detector (MoK_α-radiation, λ = 0.71073 Å, graphite monochromator). Temperature control was granted by constant nitrogen flow. Final structures were obtained by the programs SHELXS-97 and SIR97.

5.3. Procedures and analytical data

5.3.1. Synthesis of hyponitrites

Di-*tert*-butyl-hyponitrite (TBHN, 2d)[81, 82, 83]

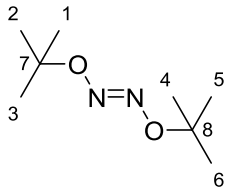

In a Schlenk flask under N_2 atmosphere, *tert*-butylbromide (5.30 mL, 47.17 mmol, 10.00 eq.) and zinc chloride (**19b**, 1 M in Et_2O, 5.20 mL, 5.19 mmol, 1.10 eq.) were added. This suspension was stirred for 5 minutes at 0 °C. Afterwards, sodium hyponitrite (**19c**, 0.50 g, 4.72 mmol, 1.00 eq.) was added in portions over 5 minutes to the mixture and stirred for 90 minutes at 0 °C. After that, the solvent was removed under reduced pressure. Therefore it is worth mentioning that the temperature of the reaction flask should not exceed 20 °C. The

residue was suspended in DCM whereat a precipitate was formed. The solid was filtered off, the solvent of the remaining solution removed while not exceeding 20 °C and the crude product was vigorously stirred with pentane (50 mL) for 3 minutes. At that point a brownish tar began to deposit at the bottom of the flask. The clear and colorless pentane phase was removed from this deposit and the solvent was removed at below 20 °C. Finally **2d** was obtained as a white solid (0.29 g, 1.64 mmol, 35 %). The compound can be stored at −18 °C over months, but should not be kept at room temperature over a longer period.

^{1}H NMR (300 MHz, $CDCl_3$) δ = 1.38 (s, 18H, H_3-C1, H_3-C2, H_3-C3, H_3-C4, H_3-C5 and H_3-C6) ppm.

^{13}C NMR (75 MHz, $CDCl_3$) δ = 81.09 (C7 and C8), 27.71 (C1, C2, C3, C4, C5 and C6) ppm.

IR (ATR) $\tilde{\nu}$ (cm^{-1}): 2975 (m), 2935 (w), 2871 (w), 1476 (w), 1457 (w), 1391 (w), 1364 (s), 1267 (m), 1246 (m), 1186 (m), 1035 (w), 985 (vs), 926 (m), 859 (m), 761 (m), 720 (vw), 594 (s), 561 (vw), 555 (vw).

Elemental analysis [$C_8H_{18}N_2O_2$]

Calc. (%): C 55.15, H 10.41, N 16.08.

Found (%): C 54.98, H 10.24, N 16.07.

Di-benzyl-hyponitrite (DBHN, 2e)[84]

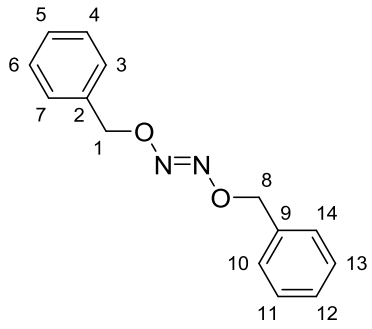

In order to protect the reaction from light, all flasks were wrapped in aluminum foil. All steps were carried out in the dark. Sodium hyponitrite (**19c**, 2.11 g, 19.91 mmol, 1.00 eq.) was dissolved in distilled water (15 mL). In a second flask a silver nitrate solution (**20a**, 7.44 g, 43.80 mmol, 2.20 eq. in 50 mL distilled water) was prepared. Afterwards the silver nitrate solution was added over ten minutes to the hyponitrite solution and a yellow solid precipitated immediately. After the addition, the yellow solid was filtered off, washed two times with distilled water (50 mL) and twice with ethanol (30 mL). Residues of solvent were removed under reduced pressure and silver hyponitrite (**20b**) was obtained as a yellow solid (2.60 g, 9.50 mmol, 48 %). The substance was used for the following steps without further purification.

The reaction mixture of **2e** should be kept cold at any time, as **2e** already decomposes slowly at room temperature. A solution of freshly distilled benzyl bromide (**20c**, 1.32 mL, 11.14 mmol, 2.00 eq. in 8 mL DCM) was cooled to 0 °C under a nitrogen atmosphere. Afterwards silver hyponitrite (**20b**, 1.53 g, 5.57 mmol, 1.00 eq.) was added in portions over five minutes. In order to optimize the reaction time, the reaction progress was checked by GC/MS until no decrease of benzyl bromide was detectable. After three hours the reaction mixture was filtered off and the solvent was removed under reduced pressure (without heating). The crude product was dissolved in pentane (20 mL). The flask was sealed with a rubber cap and slightly cooled with liquid nitrogen (external cooling) until white crystals began to precipitate. The crystals were filtered off (this should be done fast to avoid condensation from air humidity). Finally, residual solvent was removed under reduced pressure (without heating) and **2e** was obtained as white crystals (0.53 g, 2.19 mmol, 39 %). The substance can be stored at −78 °C over a longer period.

^{1}H NMR (300 MHz, $CDCl_3$) δ = 7.43 – 7.31 (m, 10H, $H_{aromatic}$), 5.27 (s, 4H, H_2-C1 and H_2-C8) ppm.

***Tert*-butyl peroxypivalate (TBPP, 31a)**

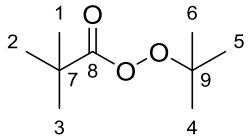

The reaction was carried out under a nitrogen atmosphere. A commercially available solution of *tert*-butyl hydroperoxide (**31b**, 5.5 M in decane, 1.00 mL, 5.50 mmol, 1.00 eq.) was mixed with pentane (10 mL) and cooled to −20 °C. Afterwards, *n*-butyllithium (2.5 M in hexane, 2.20 mL, 5.50 mmol, 1.00 eq.) was slowly added. After five minutes pivaloyl chloride (**31c**, 0.68 mL, 5.50 mmol, 1.00 eq.) was added and brought to room temperature. Distilled water (10 mL) was added, the organic layer removed and dried over $MgSO_4$. Pentane was removed under reduced pressure (300 mbar, 40 °C) by rotary evaporation for five minutes. Remaining decane was not removed and a *tert*-butyl peroxypivalate (**31a**) solution in decane was obtained (quantitative). For determination of the content of **31a** in solution, 10.00 mg of the solution were weighed into an NMR tube and 20.00 mg of TMB (**22**) were added as internal standard. The amount of **31a** (0.003 mmol/mg) in the solution was determined by ^{1}H NMR spectroscopy.

^{1}H NMR (300 MHz, $CDCl_3$) δ = 1.31 (s, 9H, H_3-C4, H_3-C5 and H_3-C6), 1.24 (s, 9H, H_3-C1, H_3-C2 and H_3-C3) ppm.

^{13}C NMR (75 MHz, $CDCl_3$) δ = 174.99 (C8), 83.31 (C9), 38.82 (C7), 27.21 (C4, C5 and C6), 26.07 (C1, C2 and C3) ppm.

5.3.2. Synthesis of borane complexes and corresponding precursors

General procedure A: Synthesis of Lewis base (LB) borane complexes (LB-BH_3):

All reactions were done under a nitrogen atmosphere. A saturated solution of a Lewis base in dry THF was cooled to 0 °C with an ice bath. Afterwards 1.10 eq. of BH_3 (5 M solution of $H_3B{\bullet}SMe_2$ in Et_2O) were added slowly at 0 °C and stirred for 10 min. At that point isohexane was added (usually 5-10 fold excess) until no further precipitation of solids was visible anymore. Stirring vigorously during the precipitation leads to the best results. The solid was then filtered off (frit N4) and washed three times with isohexane. This step does not require any cooling and inert gas atmosphere. The remaining solvent was removed under reduced pressure to give the pure LB-BH_3 complexes in good to excellent yields.

For recrystallization a saturated solution of the borane-complex in chloroform at 60 °C was prepared. Afterwards 5-10 mL of this solution were filtered into a small flask, which was allowed to stand open until the solvent had evaporated. Thus, crystals of suitable quality for X-ray measurements were grown.

2-Methylbenzoxazole borane (17a)

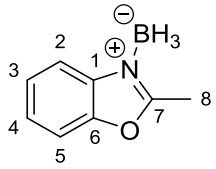

17a was prepared according to general procedure A. 2-Methylbenzoxazole (**41a**, 1.00 g, 7.51 mmol, 1.00 eq.) was dissolved in 10 mL THF under N_2 atmosphere. The solution was cooled to 0 °C and a $H_3B{\bullet}SMe_2$ solution (5 M in Et_2O, 1.65 mL, 1.10 eq.) was added. After 10 minutes the external cooling was removed and 100 mL isohexane were added while stirring vigorously. Within 5 minutes a white precititate had formed. The precipitate was filtered off and washed three times with isohexane. After removing all residues of solvent under reduced pressure, **17a** was obtained as a white solid (1.08 g, 7.36 mmol, 98 %).

Decomposition point: 115.2 – 115.7 °C.

^{1}H NMR (300 MHz, $CDCl_3$) δ = 7.93 -7.89 (m, 1H, H-C2), 7.56 – 7.53 (m, 1H, H-C5), 7.49 – 7.44 (m, 2H, H-C3 and H-C4), 2.87 (s, 3H, H_3-C8), 2.65 – 1.79 (broad, q, 3H, H_3-B) ppm.

^{13}C NMR (75 MHz, $CDCl_3$) δ = 165.2 (C7), 148.7 (C6), 135.5 (C1), 126.8 (C3), 126.2 (C4), 118.0 (C2), 110.9 (C5), 13.3 (C8) ppm.

{^{1}H} ^{11}B NMR (270 MHz, $CDCl_3$) δ = −23.2 (s) ppm.

^{11}B NMR (270 MHz, $CDCl_3$) δ = −23.2 (broad, q) ppm.

IR (ATR) $\tilde{\nu}$ (cm^{-1}): 3019 (s), 2400 (m), 1591 (w), 1522 (w), 1477 (w), 1461 (m), 1424 (w), 1346 (vw), 1329 (vw), 1216 (s), 1003 (vw), 929 (w), 791 (s), 671 (vs), 627 (w).

MS (70 eV, EI) m/z (%): 147 ($[M]^+$, 11), 146 ($[M-H]^+$, 100), 145 ($[M-2H]^+$, 35), 144 ($[M-3H]^+$, 12), 133 ($[M-BH_3]^+$, 66), 104 (17), 77 (14), 76 (12), 64 (12), 63 (16).

HRMS (70 eV, EI): $C_8H_{10}BNO$ calc. 147.0861 g/mol $[M]^+$, found 147.0778 g/mol.

Elemental analysis [$C_8H_{10}BNO$]

Calc. (%): C 65.37, H 6.86, N 9.53.

Found (%): C 63.95, H 6.71, N 9.29.

2-Phenylbenzoxazole borane (17b)

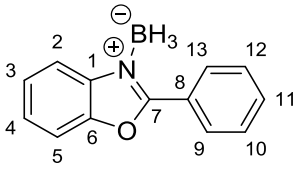

17b was prepared according to general procedure A. 2-Phenylbenzoxazole (**41b**, 1.00 g, 5.12 mmol, 1.00 eq.) was dissolved in 10 mL THF under N_2 atmosphere. The solution was cooled to 0 °C and a $H_3B{\bullet}SMe_2$ solution (5 M in Et_2O, 1.13 mL, 1.10 eq.) was added. After 10 minutes the external cooling was removed and 100 mL isohexane were added while stirring vigorously. Within 5 minutes a white precititate had formed. The precipitate was filtered off and washed three times with isohexane. After removing all residues of solvent under reduced pressure, **17b** was obtained as a white solid (0.58 g, 2.77 mmol, 54 %).

Decomposition point: 104.5 – 104.9 °C.

^{1}H NMR (300 MHz, $CDCl_3$) δ = 8.54 – 8.47 (m, 2H, H-C2 and H-C5), 8.25 (dd, *J* = 6.90 Hz, 2.89 Hz, 1H, H-C3), 8.13 (dd, *J* = 5.99 Hz, 3.41 Hz, 1H, H-C4), 7.71 -7.30 (m, 5H, H-C9, H-C10, H-C11, H-C12 and H-C13) 3.19 – 1.77 (broad, q, 3H, H_3-B) ppm.

^{13}C NMR (75 MHz, $CDCl_3$) δ = 162.3 (C7), 148.5 (C6), 137.2 (C1), 133.4 (C8), 131.2 (C10 and C12), 128.9 (C11), 128.7 (C9 and C13), 127.3 (C3), 126.4 (C4), 119.1 (C2), 111.0 (C5) ppm.

{^{1}H} ^{11}B NMR (270 MHz, $CDCl_3$) δ = −21.8 (s) ppm.

^{11}B NMR (270 MHz, $CDCl_3$) δ = −21.8 (broad, q) ppm.

IR (ATR) $\tilde{\nu}$ (cm^{-1}): 3155 (w), 2985 (w), 2254 (s), 1794 (w), 1642 (w), 1470 (m), 1382 (m), 1216 (vw), 1167 (vw), 1096 (w), 924 (s), 902 (s), 891 (s), 763 (s), 704 (s), 647 (s), 625 (w), 543 (vw), 462 (w).

MS (70 eV, EI) m/z (%): 209 ([M]$^+$, 2), 206 ([M-3H]$^+$, 19), 196 ([M-BH_2]$^+$, 13), 195 ([M-BH_3]$^+$, 100), 167 (10), 63 (11).

HRMS (70 eV, EI): $C_{13}H_{12}BNO$ calc. 209.1012 g/mol [M]$^+$, found 209.0994 g/mol.

Elemental analysis [$C_{13}H_{12}BNO$]

Calc. (%): C 74.69, H 5.79, N 6.70.

Found (%): C 74.13, H 5.74, N 6.43.

2-Methylbenzothiazole borane (17c)

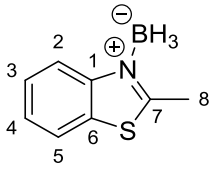

17c was prepared according to general procedure A. 2-Methylbenzothiazole (**41c**, 1.07 g, 7.17 mmol, 1.00 eq.) was dissolved in 10 mL THF under N_2 atmosphere. The solution was cooled to 0 °C and a $H_3B{\bullet}SMe_2$ solution (5 M in Et_2O, 1.58 mL, 1.10 eq.) was added. After 10 minutes the external cooling was removed and 100 mL isohexane were added while stirring vigorously. Within 5 minutes a white precititate had formed. The precipitate was filtered off and washed three times with isohexane. After removing all residues of solvent under reduced pressure, **17c** was obtained as a white solid (0.90 g, 6.61 mmol, 92 %).

Decomposition point: 123.2 – 123.8 °C.

^{1}H NMR (300 MHz, $CDCl_3$) δ = 8.41 (d, *J* = 8.5 Hz, 1H, H-C2), 7.80 (ddd, *J* = 8.0 Hz, 1.3 Hz, 0.6 Hz, 1H, H-C5), 7.60 (ddd, *J* = 8.5 Hz, 7.3 Hz, 1.3 Hz, 1H, H-C3), 7.50 (ddd, *J* = 8.0 Hz, 7.3 Hz, 1.3 Hz, 1H, H-C4), 3.01 (s, 3H, H_3-C8), 2.84 – 1.92 (broad, q, 3H, H_3-B). ppm.

^{13}C NMR (75 MHz, $CDCl_3$) δ = 170.91 (C7), 147.57 (C6), 129.99 (C1), 127.67 (C3 or C4), 126.84 (C3 or C4), 121.75 (C2 or C5), 121.53 (C2 or C5), 19.05 (C8) ppm.

{^{1}H} ^{11}B NMR (270 MHz, $CDCl_3$) δ = −20.43 (s) ppm.

^{11}B NMR (270 MHz, $CDCl_3$) δ = −20.45 (q, *J* = 97.4 Hz) ppm.

IR (ATR) $\tilde{\nu}$ (cm^{-1}): 3068 (vw), 2402 (m), 2298 (s), 2256 (m), 1955 (w), 1920 (w), 1794 (w), 1699 (w), 1610(w), 1572 (w), 1504 (w), 1457 (m), 1436 (s), 1372 (m), 1323 (m), 1287 (w), 1268 (m), 1203 (s), 1147 (s), 1130 (s), 1040 (m), 1012 (m), 957 (m), 943 (m), 925 (m), 884 (w), 852 (w), 755 (s), 726 (s), 710 (m), 660 (m).

MS (70 eV, EI) m/z (%): 163 ([M]$^+$, 9), 162 ([M-H]$^+$, 74), 161 ([M-2H]$^+$, 33), 160 ([M-3H]$^+$, 20), 150 (13), 149 ([M-BH_3]$^+$, 100), 148 ([M-Me]$^+$, 23), 120 (16), 108 (27), 69 (16).

HRMS (70 eV, EI): $C_8H_{10}BNS$ calc. 163,0627 g/mol $[M]^+$, found 163.0567 g/mol.

Elemental analysis $[C_8H_{10}BNS]$

Calc. (%): C 58.93, H 6.18, N 8.59.

Found (%): C 58.93, H 6.10, N 8.61.

2-Chlorobenzothiazole borane(17d)

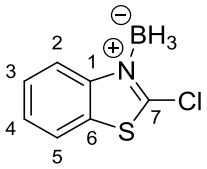

17d was prepared according to general procedure A. 2-Chlorobenzothiazole (**41d**, 1.07 g, 6.31 mmol, 1.00 eq.) was dissolved in 10 mL THF under N_2 atmosphere. The solution was cooled to 0 °C and a $H_3B{\bullet}SMe_2$ solution (5 M in Et_2O, 1.39 mL, 1.10 eq.) was added. After 10 minutes the external cooling was removed and 100 mL isohexane were added while stirring vigorously. Within 5 minutes a white precititate had formed. The precipitate was filtered off and washed three times with isohexane. After removing all residues of solvent under reduced pressure, **17d** was obtained as a slightly yellow solid (0.85 g, 4.63 mmol, 73 %).

Decomposition point: 93.0 – 93.8 °C.

^{1}H NMR (300 MHz, $CDCl_3$) δ = 8.43 (d, *J* = 8.2 Hz, 1H, H-C2), 7.82 (d, *J* = 7.9, 1H, H-C5), 7.69 – 7.64 (m, 1H, H-C3), 7.62 – 7.57 (m, 1H, H-C4), 2.99 – 1.98 (broad, q, 3H, H_3-B) ppm.

^{13}C NMR (75 MHz, $CDCl_3$) δ = 158.74 (C7), 145.75 (C6), 130.39 (C1), 128.45 (C3 or C4), 127.98 (C3 or C4), 122.53 (C2 or C5), 121.41 (C2 or C5) ppm.

{^{1}H} ^{11}B NMR (270 MHz, $CDCl_3$) δ = −19.08 (s) ppm.

^{11}B NMR (270 MHz, $CDCl_3$) δ = −19.08 (q, *J* = 98.8 Hz) ppm.

IR (ATR) $\tilde{\nu}$ (cm^{-1}): 3113 (w), 2548 (m), 2501 (m), 2430 (m), 1588 (w), 1574 (w), 1478 (m), 1466 (m), 1416 (m), 1405 (m), 1380 (m), 1355 (m), 1344 (m), 1327 (m), 1299 (s), 1272 (m), 1255 (m), 1209 (m), 1198 (m), 1161 (m), 1126 (m), 1088 (s), 1052 (m), 1020 (s), 994 (m), 978 (s), 947 (m), 923 (m), 894 (m), 855 (w), 846 (w), 832 (m), 774 (m), 756 (s), 722 (s), 706 (m), 687 (m), 668 (s), 650 (s), 600 (s), 614 (m), 572 (s).

MS (70 eV, EI) m/z (%): 182 ($[M-H]^+$, 64), 181 ($[M-2H]^+$, 20), 172 ($[M-B]^+$, 10), 171 ($[M-BH]^+$, 100), 154 (14), 134 (43), 108 (72), 77 (11), 63 (21), 58 (10), 54 (10), 50 (12).

HRMS (70 eV, EI): C_7H_7BClNS calc. 181.9997 g/mol $[M-H]^+$, found 181.9919 g/mol.

Elemental analysis [C_7H_7BClNS]

Calc. (%): C 45.83, H 3.85, N 7.63.

Found (%): C 44.95, H 3.76, N 7.51.

Benzimidazole borane (17e)

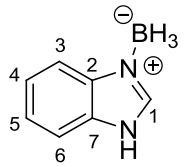

17e was prepared according to general procedure A. Benzimidazole (**41e**, 1.00 g, 8.46 mmol, 1.00 eq.) was dissolved in 10 mL THF under N_2 atmosphere. The solution was cooled to 0 °C and a $H_3B{\bullet}SMe_2$ solution (5 M in Et_2O, 1.86 mL, 1.10 eq.) was added. After 10 minutes the external cooling was removed and 100 mL isohexane were added while stirring vigorously. Within 5 minutes a white precititate had formed. The precipitate was filtered off and washed three times with isohexane. After removing all residues of solvent under reduced pressure, **17e** was obtained as a white solid (0.82 g, 6.18 mmol, 73 %).

Decomposition point: 127.1 – 128.7 °C.

^{1}H NMR (300 MHz, DMSO-*d*$_6$) δ = 13.77-13.49 (broad, s, 1H, H-N), 8.83 (s, 1H, H-C1), 7.76-7.71 (m, 1H, H-C3), 7.66-7.62 (m, 1H, H-C6), 7.43-7.38 (m, 2H, H-C4 and H-C5), 2.82-1.75 (broad, q, 3H, H_3-B) ppm.

^{13}C NMR (75 MHz, DMSO-*d*$_6$) δ = 142.54 (C1), 136.64 (C2), 132.18 (C7), 124.95 (C4 or C5), 124.30 (C4 or C5), 116.24 (C3), 113.50 (C6) ppm.

{^{1}H} ^{11}B NMR (270 MHz, DMSO-*d*$_6$) δ = −20.40 (s) ppm.

^{11}B NMR (270 MHz, DMSO-*d*$_6$) δ = −20.13 (broad, q) ppm.

IR (ATR) $\tilde{\nu}$ (cm^{-1}): 3276 (vs), 3129 (m), 3045 (w), 2913 (w), 2837 (w), 2352 (s), 2291 (s), 2244 (s), 1915 (w), 1789 (w), 1762 (m), 1626 (m), 1603 (m), 1532 (s), 1497 (w), 1466 (m), 1420 (s), 1368 (w), 1321 (s), 1254 (m), 1186 (vs), 1157 (s), 1140 (m), 1115 (m), 1039 (m), 1001 (m), 966 (m), 944 (m,), 884 (s), 850 (w), 760 (vs), 753 (vs), 677 (vs), 665 (vs).

MS (70 eV, EI) m/z (%): . 132 ($[M]^+$, 37), 131 (($[M-H]^+$, 100), 130 (($[M-2H]^+$, 37), 129 (($[M-3H]^+$, 18), 119 (($[M-BH_2]^+$, 10), 118 (($[M-BH_3]^+$, 97), 103 (21), 102 (13), 91 (24), 72 (19), 71 (17), 63 (10), 44 (12), 43 (10), 42 (44), 41 (21), 39 (10).

HRMS (70 eV, EI): $C_7H_9BN_2$ calc. 132.0859 g/mol $[M]^+$, found 132.0860 g/mol.

Elemental analysis [$C_7H_9BN_2$]

Calc. (%): C 63.71, H 6.87, N 21.23.

Found (%): C 63.67, H 6.89, N 21.17.

1-Methylbenzimidazole borane (17f)

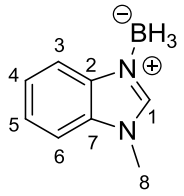

17f was prepared according to general procedure A. 1-Methylbenzimidazole (**41f**, 1.00 g, 7.57 mmol, 1.00 eq.) was dissolved in 10 mL THF under N_2 atmosphere. The solution was cooled to 0 °C and a $H_3B{\bullet}SMe_2$ solution (5 M in Et_2O, 1.67 mL, 1.10 eq.) was added. After 10 minutes the external cooling was removed and 100 mL isohexane were added while stirring vigorously. Within 5 minutes a white precititate had formed. The precipitate was filtered off and washed three times with isohexane. After removing all residues of solvent under reduced pressure, **17f** was obtained as a white solid (1.02 g, 6.96 mmol, 92 %).

Decomposition point: 118.5 – 118.9 °C.

^{1}H NMR (300 MHz, $CDCl_3$) δ = 8.15 (s, 1H, H-C1), 7.96 – 7.92 (m, 1H, H-C3), 7.47 – 7.43 (m, 3H, H-C4, H-C5, H-C6), 3.90 (s, 3H, H_3-C8), 3.06 – 1.69 (broad, q, 3H, H_3-B) ppm.

^{13}C NMR (75 MHz, $CDCl_3$) δ = 142.12 (C1), 137.08 (C2), 132.91 (C7), 125.09 (C4 or C5), 124.69 (C4 or C5), 117.30 (C3), 110.38 (C6), 32.16 (C8) ppm.

{^{1}H} ^{11}B NMR (270 MHz, $CDCl_3$) δ = −22.39 (s) ppm.

^{11}B NMR (270 MHz, $CDCl_3$) δ = −22.31 (broad, q) ppm.

IR (ATR) $\tilde{\nu}$ (cm^{-1}): 3121 (w), 3062 (w), 2945 (w), 2340 (m), 2289 (s), 2254 (s), 1760 (w), 1621 (w), 1600 (w), 1576 (w), 1543 (s), 1477 (w), 1464 (m), 1416 (w), 1385 (m), 1344 (m), 1314 (m), 1259 (m), 1209 (w), 1159 (vs), 1127 (s), 1117 (m), 1078 (m), 1004 (m), 979 (m), 939 (m), 882 (w), 872 (m), 850 (w), 771 (m), 752 (vs), 734 (vs).

MS (70 eV, EI) m/z (%): 146 ($[M]^+$, 9), 145 ($[M-H]^+$, 100), 144 ($[M-2H]^+$, 34), 132 ($[M-BH_3]^+$, 98), 131 ($[M-BH_3-H]^+$, 40), 117 ($[M-BH_3-CH_3]^+$, 20), 116 ($[M-BH_3-CH_3-H]^+$, 22), 104 (20), 77 (21), 63 (14).

HRMS (70 eV, EI): $C_8H_{11}BN_2$ calc. 146.1015 g/mol $[M]^+$, found 146.0985 g/mol.

Elemental analysis [$C_8H_{11}BN_2$]

Calc. (%): C 65.81, H 7.59, N 19.19.

Found (%): C 65.32, H 7.57, N 18.94.

2-Methylbenzimidazole borane (17g)

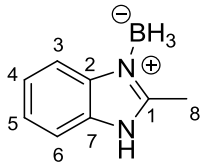

17g was prepared according to general procedure A. 2-Methylbenzimidazole (1.00 g, 7.57 mmol, 1.00 eq.) was dissolved in 10 mL THF under N_2 atmosphere. The solution was cooled to 0 °C and a $H_3B{\bullet}SMe_2$ solution (5 M in Et_2O, 1.67 mL, 1.10 eq.) was added. After 10 minutes the external cooling was removed and 100 mL isohexane were added while stirring vigorously. Within 5 minutes a white precititate had formed. The precipitate was filtered off and washed three times with isohexane. After removing all residues of solvent under reduced pressure, **17g** was obtained as a white solid (0.86 g, 5.90 mmol, 78 %).

Decomposition point: 180.0 – 182.0 °C.

^{1}H NMR (300 MHz, DMSO-*d*$_6$) δ = 13.50-13.24 (broad, 1H, H-N), 7.70-7.66 (m, 1H, H-C3), 7.56-7.51 (m, 1H, H-C6), 7.34-7.29 (m, 2H, H-C4, H-C5), 2.61 (s, 3H, H_3-C8), 2.43-1.72 (broad, q, 3H, H_3-B) ppm.

^{13}C NMR (75 MHz, DMSO-*d*$_6$) δ = 151.79 (C1), 137.47 (C2), 131.47 (C7), 124.26 (C4 or C5), 123.62 (C4 or C5), 116.06 (C3), 112.44 (C6), 13.00 (C8) ppm.

{^{1}H} ^{11}B NMR (270 MHz, DMSO-*d*$_6$) δ = −21.81 ppm.

^{11}B NMR (270 MHz, DMSO-*d*$_6$) δ = −21.80 (broad, q) ppm.

IR (ATR) $\tilde{\nu}$ (cm^{-1}): 3275 (s), 3095 (w), 2400 (s), 2290 (s), 2240 (s), 1937 (w), 1756 (w), 1628 (m), 1605 (w), 1580 (w), 1549 (s), 1507 (m), 1475 (m), 1458 (s), 1419 (m), 1395 (w), 1318 (w), 1291 (w), 1256 (w), 1244 (w), 1225 (w), 1197 (m), 1163 (s), 1152 (s), 1142 (s), 1120 (m), 1102 (m), 1069 (w), 1041 (w), 1019 (w), 1006 (m), 962 (w), 949 (m), 923 (w), 891 (w), 831 (w), 753 (m), 737 (vs), 693 (w), 659 (s).

MS (70 eV, EI) m/z (%): 146 ($[M]^+$, 9), 145 ($[M-H]^+$, 100), 144 ($[M-2H]^+$, 49), 143 ($[M-3H]^+$, 22), 132 ($[M-BH3]^+$, 32), 131 (17), 103 (18), 102 (10).

HRMS (70 eV, EI): $C_8H_{11}BN_2$ calc. 146.1015 g/mol $[M]^+$, found 146.1017 g/mol.

Elemental analysis [$C_8H_{11}BN_2$]

Calc. (%): C 65.81, H 7.59, N 19.19.

Found (%): C 65.51, H 7.53, N 19.05.

2-Chloro-1-methylbenzimidazole (41h)

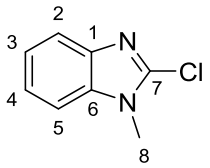

In a Schlenk flask under N_2 atmosphere 2-chlorobenzimidazole (**41ha**, 2.29 g, 15.04 mmol, 1.00 eq.) was dissolved in THF (40 mL) and cooled to 0 °C. Afterwards *n*-butyllithium (2.5 M solution in hexane, 6.60 mL, 16.54 mmol, 1.10 eq.) was added, the external cooling removed and the solution stirred for 10 minutes. Thereafter methyl iodide (1.03 mL, 16.54 mmol, 1.10 eq.) was added and the solution was stirred for 20 minutes. Distilled water (30 mL) was added, the aqueous phase was three times extracted with DCM, the combined extracts dried over $MgSO_4$ and the solvent was removed under reduced pressure. The resulting solid was washed two times with isohexane (20 mL). **41h** was obtained as white solid (1.50 g, 9.00 mmol, 60 %).

Melting point: 103.4 – 103.6 °C.

^{1}H NMR (300 MHz, $CDCl_3$) δ = 7.68 (ddd, *J* = 6.6 Hz, 3.1 Hz , 1.4 Hz, 1H, H-C2), 7.29 – 7.23 (m, 3H, H-C3, H-C4 and H-C5), 3.74 (s, 3H, H_3-C8) ppm.

^{13}C NMR (75 MHz, $CDCl_3$) δ = 141.55 (C1), 140.91 (C7), 135.57 (C6), 123.12 (C3 or C4), 122.68 (C3 or C4), 119.28 (C2), 109.24 (C5), 30.46 (C8) ppm.

IR (ATR) $\tilde{\nu}$ (cm^{-1}): 3057 (vw), 1617 (w), 1476 (s), 1466 (m), 1427 (m), 1372 (m), 1349 (m), 1329 (m), 1286 (m), 1157 (m), 1114 (w), 1006 (m), 931 (w), 896 (w), 824 (w), 762 (m), 733 (vs),656 (w).

MS (70 eV, EI) m/z (%): 166 ($[M]^+$, 44), 165 ($[M-H]^+$, 11), 154 (33), 152 (100), 117 (10), 90 (25), 63 (10).

HRMS (70 eV, EI): $C_8H_7ClN_2$ calc. 166.0298 g/mol $[M]^+$, found 166.0288 g/mol.

Elemental analysis [$C_8H_7ClN_2$]

Calc. (%): C 57.67, H 4.24, N 16.81.

Found (%): C 57.60, H 4.53, N 16.68.

2-Chloro-1-methylbenzimidazole borane (17h)

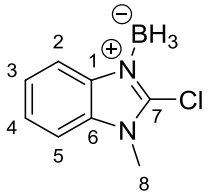

1e was prepared according to general procedure A. 2-Chloro-1-methylbenzimidazole (**41h**, 0.77 g, 4.59 mmol, 1.00 eq.) was dissolved in 10 mL THF under N_2 atmosphere. The solution was cooled to 0 °C and a $H_3B{\bullet}SMe_2$ solution (5 M in Et_2O, 1.01 mL, 1.10 eq.) was added. After 10 minutes the external cooling was removed and 100 mL isohexane were added while stirring vigorously. Within 5 minutes a white precititate had formed. The precipitate was filtered off and washed three times with isohexane. After removing all residues of solvent under reduced pressure, **17h** was obtained as a white solid (0.71 g, 3.94 mmol, 83 %).

Decomposition point: 128.8 – 129.0 °C.

^{1}H NMR (300 MHz, $CDCl_3$) δ = 8.05 – 7.90 (m, 1H, H-C2), 7.49 – 7.32 (m, 3H, H-C3, H-C4 and H-C5), 3.88 (s, 3H, H_3-C8), 2.77 – 1.87 (broad, q, 3H, H_3-B) ppm.

^{13}C NMR (75 MHz, $CDCl_3$) δ = 140.57 (C7), 136.36 (C1), 132.55 (C6), 125.44 (C3 or C4), 125.05 (C3 or C4), 117.62 (C2), 109.96 (C5), 31.39 (C8) ppm.

{^{1}H} ^{11}B NMR (270 MHz, $CDCl_3$) δ = −21.82 (s) ppm.

^{11}B NMR (270 MHz, $CDCl_3$) δ = −21.83 (broad, q) ppm.

IR (ATR) $\tilde{\nu}$ (cm^{-1}): 2351 (m), 2309 (m), 2263 (m), 1735 (w), 1509 (m), 1482 (m), 1432 (m), 1394 (m), 1343 (w), 1300 (w), 1248 (w), 1161 (s), 1143 (m), 1125 (m), 1008 (w), 940 (m), 772 (m), 750 (vs).

MS (70 eV, EI) m/z (%): 180 ($[M]^+$, 6), 179 ($[M\text{-}H]^+$, 39), 168 ($[M\text{-}BH]^+$, 32), 167 ($[M\text{-}BH_2]^+$, 17), 166 ($[M\text{-}BH_3]^+$, 100), 165 ($[M\text{-}Me]^+$, 32), 145 ($[M\text{-}Cl]^+$, 19), 132 (99), 131 (57), 129 (16), 104 (30), 90 (16), 77 (21), 63 (10).

HRMS (70 eV, EI): $C_8H_{10}BClN_2$ calc. 180.0626 g/mol $[M]^+$, found 180.0505 g/mol.

Elemental analysis [$C_8H_{10}BClN_2$]

Calc. (%): C 53.25, H 5.59, N 15.53.

Found (%): C 53.03, H 5.47, N 15.49.

2-(Trifluoromethyl)-benzimidazole (41ia)

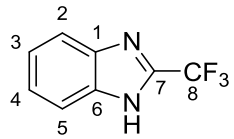

Ortho-phenylenediamine (**35e**, 2.00 g, 18.50 mmol, 1.00 eq.), trifluoroacetic acid (1.71 mL, 22.19 mmol, 1.20 eq.), toluene (30 mL) and distilled water (6 mL) were poured into a 80 mL microwave vessel under ambient atmosphere. The reaction was conducted in a microwave (closed vessel) at 160 °C for 60 minutes. After cooling down, light blue needles had grown in the toluene layer. The solid was filtered off and washed twice with toluene. After removal of all volatiles under reduced pressure, **41ia** was obtained in form of pale blue needles (2.75 g, 14.79 mmol, 80 %).

Melting point: 207.9 – 208.2 °C.

^{1}H NMR (300 MHz, DMSO-d_6) δ = 14.00 – 13.64 (broad, s, 1H, H-N), 7.83 – 7.55 (m, 1H, H-C2), 7.44 – 7.25 (m, 3H, H-C3, H-C4 and H-C5) ppm.

^{13}C NMR (75 MHz, DMSO-d_6) δ = 142.23 (C1), 140.45 (q, ^{2}J(C,F) = 39.4 Hz, C7), 134.22 (C6), 125.42 (C3 or C4), 123.60 (C3 or C4), 120.84 (C2), 119.50 (q, ^{1}J(C,F) = 270.4 Hz, C8), 113.18 (C5) ppm.

^{19}F NMR (376 MHz, DMSO-d_6) δ = −62.83 ppm.

IR (ATR) $\tilde{\nu}$ (cm^{-1}): 2969 (w), 2911 (w), 2873 (w), 2758 (w, br), 2655 (w), 1625 (w), 1594 (w), 1551(m), 1500 (m), 1462 (m), 1444 (w), 1400 (m), 1317 (m), 1287 (s), 1266 (w), 1232 (m), 1191 (s), 1168 (vs), 1141 (vs), 1129 (vs), 1117 (s), 1007 (w), 980 (s), 958 (m), 938 (w), 907 (w), 875 (w), 814 (w), 768 (w), 750 (s), 740 (vs).

MS (70 eV, EI) m/z (%): 186 ([M]$^{+}$, 100), 178 (53), 166 ([M-F-H]$^{+}$, 43), 161 (22), 128 ([M-3F-H]$^{+}$, 33), 109 (23), 69 (16), 57 (15), 44 (38), 43 (14), 42 (28), 41 (19).

HRMS (70 eV, EI): $C_8H_5F_3N_2$ calc. 186.0405 g/mol [M]$^{+}$, found 186.0406 g/mol.

Elemental analysis [$C_8H_5F_3N_2$]

Calc. (%): C 51.62, H 2.71, N 15.05.

Found (%): C 51.63, H 2.71, N 14.96.

1-Methyl-2-(trifluoromethyl)-benzimidazole (41ib)

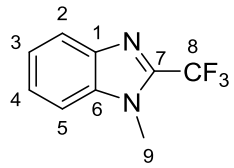

In a Schlenk flask under N_2 atmosphere 2-(trifluoromethyl)-benzimidazole (**41ia**, 2.68 g, 14.42 mmol, 1.00 eq.) was dissolved in THF (40 mL) and cooled to 0 °C. Afterwards *n*-butyllithium (2.45 M solution in hexane, 7.06 mL, 17.30 mmol, 1.20 eq.) was added, the external cooling removed and the solution stirred for 10 minutes. Thereafter methyl iodide (1.35 mL, 21.62 mmol, 1.50 eq.) was added and the solution was stirred for 20 minutes. Distilled water (30 mL) was added, the aqueous phase was three times extracted with DCM, the combined extracts dried over $MgSO_4$ and the solvent was removed under reduced pressure. The resulting solid was washed two times with isohexane (20 mL). **41ib** was obtained as pale yellow plates (2.20 g, 11.00 mmol, 76 %).

Melting point: 92.2 – 93.0 °C.

^{1}H NMR (300 MHz, $CDCl_3$) δ = 7.88 – 7.83 (m, 1H, H-C2), 7.44 – 7.30 (m, 3H, H-C3, H-C4 and H-C5), 3.93 – 3.91 (broad, q, 3H, H_3-C7) ppm.

^{13}C NMR (75 MHz, $CDCl_3$) δ = 140.96 (C1), 140.80 (q, ^2J(C,F) = 38.5 Hz, C7), 135.99 (C6), 125.27 (C3 or C4), 123.55 (C3 or C4), 121.51 (C2), 119.10 (q, ^1J(C,F) = 271.2 Hz, C8), 110.02 (C5), 30.70 (q, ^4J(C,F) = 2.2 Hz, C9) ppm.

^{19}F NMR (376 MHz, $CDCl_3$) δ = −62.63 ppm.

IR (ATR) $\tilde{\nu}$ (cm^{-1}): 3055 (vw), 1944 (vw), 1906 (vw), 1818 (vw), 1780 (vw), 1682 (vw), 1617 (vw), 1588 (w), 1553 (vw), 1517 (m), 1485 (m), 1405 (m), 1341 (w), 1335 (w), 1320 (vw), 1291 (w), 1263 (s), 1231 (s), 1179 (s), 1151 (m), 1138 (s), 1120 (s), 1088 (s), 1005 (m), 973 (w), 951 (w), 934 (w), 902 (m), 846 (w), 827 (w), 764 (m), 745 (s), 726 (s), 616 (m), 592 (m), 581 (m), 570 (w), 560 (w).

MS (70 eV, EI) m/z (%): 200 ($[M]^+$, 100), 199 ($[M-H]^+$, 28).

HRMS (70 eV, EI): $C_9H_7F_3N_2$ calc. 200.0561 g/mol $[M]^+$, found 200.0546 g/mol.

Elemental analysis [$C_9H_7F_3N_2$]

Calc. (%): C 54.01, H 3.53, N 14.00.

Found (%): C 53.09, H 3.53, N 13.75.

1-Methyl-2-(trifluoromethyl)-benzimidazole borane (17i)

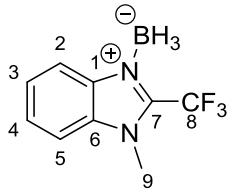

17i was prepared according to general procedure A. 1-Methyl-2-(trifluoromethyl)-benzimidazole (**41ib**, 0.18 g, 0.90 mmol, 1.00 eq.) was dissolved in 5 mL THF under N_2 atmosphere. The solution was cooled to 0 °C and a $H_3B{\bullet}SMe_2$ solution (5 M in Et_2O, 0.20 mL, 1.10 eq.) was added. After 10 minutes the external cooling was removed and 50 mL isohexane were added while stirring vigorously. Within 5 minutes a white precititate had formed. The precipitate was filtered off and washed three times with isohexane. After removing all residues of solvent under reduced pressure, **17i** was obtained as a white solid (0.17 g, 0.79 mmol, 88 %).

Decomposition point: 99.0 – 100.0 °C.

^{1}H NMR (300 MHz, $CDCl_3$) δ = 8.27 – 8.22 (m, 1H, H-C2), 7.64 – 7.52 (m, 3H, H-C3, H-C4 and H-C5), 4.09 (q, *J* = 1.7 Hz, 3H, H_3-C9), 3.01 – 1.94 (broad, q, 3H, H_3-B) ppm.

^{13}C NMR (75 MHz, $CDCl_3$) δ = 137.00 (C1), 133.08 (C7), 127.52 (C6), 126.42 (C3 and C4), 119.47 (C2), 118.03 (q, ^1J(C,F) = 274.8 Hz, C8), 110.78 (C5), 32.86 (q, ^4J(C,F) = 4.0 Hz, C9) ppm.

{^{1}H} ^{11}B NMR (270 MHz, $CDCl_3$) δ = −20.62 (s) ppm.

^{11}B NMR (270 MHz, $CDCl_3$) δ = −20.62 (broad, q) ppm.

^{19}F NMR (376 MHz, $CDCl_3$) δ = −56.96 ppm.

IR (ATR) $\tilde{\nu}$ (cm^{-1}): 3059 (vw), 2383 (w), 2349 (w), 2273 (w), 1604 (w), 1502 (m), 1488 (m), 1469 (m), 1409 (m), 1302 (m), 1286 (m), 1261 (m), 1239 (m), 1142 (s), 1126 (s), 1102 (s), 1017 (m), 982 (w), 942 (m), 847 (w), 822 (w), 777 (m), 746 (s).

MS (70 eV, EI) m/z (%): 213 ($[M\text{-}H]^+$, 5), 201 ($[M\text{-}BH_2]^+$, 11), 200 ($[M\text{-}BH_3]^+$, 100), 199 ($[M\text{-}Me]^+$, 27), 181 (15).

HRMS (70 eV, EI): $C_9H_{10}BF_3N_2$ calc. 213.0805 g/mol $[M\text{-}H]^+$, found 213.0818 g/mol.

Elemental analysis $[C_9H_{10}BF_3N_2]$

Calc. (%): C 50.51, H 4.71, N 13.09.

Found (%): C 48.05, H 4.34, N 12.37.

1-Phenyl-2-(trifluoromethyl)-benzimidazole (41j)

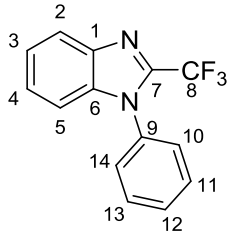

N-phenyl-*o*-phenylenediamine (0.71 g, 3.87 mmol, 1.00 eq.), trifluoroacetic acid (0.30 mL, 3.87 mmol, 1.10 eq.) and toluene (4 mL) were poured into a 10 mL microwave vessel under ambient atmosphere. The reaction was conducted in a microwave (closed vessel) at 160 °C for 30 minutes. After cooling down, the solvent was removed under reduced pressure. The crude product was purified on a column chromatography on silica (0.035-0.070 mm, 60 Å/ ethyl acetate : isohexane = 1 : 2; R_f=0.85). This gave the pure product **41j** as a pale yellow oil (0.52 g, 1.98 mmol, 51 %).

^{1}H NMR (300 MHz, $CDCl_3$) δ = 7.98 – 7.89 (m, 1H, H-C2), 7.62 – 7.52 (m, 3H, aromatic), 7.46 – 7.32 (m, 4H, aromatic), 7.19 – 7.09 (m, 1H, aromatic) ppm.

^{13}C NMR (75 MHz, $CDCl_3$) δ = 140.84 (q, ^{2}J(C,F) = 38.5 Hz, C7), 140.69 (C1), 137.23 (C9), 134.44 (C6), 129.89 (C10 or C14), 129.75 (C10 or C14), 127.41 and 127.40 (C11 and C13), 125.79 (C12), 124.01 (C3 and C4), 121.39 (C2), 118.87 (q, ^{1}J(C,F) = 271.9 Hz, C8), 111.18 (C5) ppm.

^{19}F NMR (376 MHz, $CDCl_3$) δ = −60.55 ppm.

IR (ATR) $\tilde{\nu}$ **(cm^{-1})**: 3059 (vw), 1616 (w), 1596 (m), 1525 (m), 1499 (s), 1451 (m), 1417 (m), 1334 (w), 1312 (vw), 1290 (m), 1264 (s), 1205 (s), 1160 (s), 1127 (vs), 1075 (m), 1030 (m), 1004 (m), 982 (m), 928 (w), 906 (m), 839 (w), 763 (m), 744 (s), 739 (s), 712 (m), 694 (s), 665 (w).

MS (70 eV, EI) m/z (%): 262 ([M]$^+$, 100), 193 ([M-CF_3]$^+$, 20), 192 (11), 166 (10), 77 (10).

HRMS (70 eV, EI): $C_{14}H_9F_3N_2$ calc. 262.0718 g/mol [M]$^+$, found 262.0704 g/mol.

Elemental analysis [$C_{14}H_9F_3N_2$]

Calc. (%): C 64.12, H 3.46, N 10.68.

Found (%): C 63.95, H 3.53, N 11.15.

1-phenyl-2-(trifluoromethyl)-benzimidazole borane (17j)

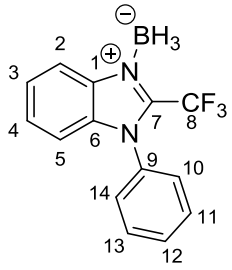

17j was prepared according to general procedure A. 1-Phenyl-2-(trifluoromethyl)-benzimidazole (**41j**, 0.25 g, 0.97 mmol, 1.00 eq.) was dissolved in 5 mL THF under N_2 atmosphere. The solution was cooled to 0 °C and a $H_3B{\bullet}SMe_2$ solution (5 M in Et_2O, 0.21 mL, 1.10 eq.) was added. After 10 minutes the external cooling was removed and 50 mL isohexane were added while stirring vigorously. Within 5 minutes a white precititate had formed. The precipitate was filtered off and washed three times with isohexane. After removing all residues of solvent under reduced pressure, **17j** was obtained as a white solid (0.14 g, 0.51 mmol, 53 %).

Decomposition point: 127.0 – 128.0 °C.

^{1}H NMR (300 MHz, $CDCl_3$) δ = 8.32 (d, *J* = 8.4 Hz, 1H, H-C2), 7.70 – 7.70 (m, 4H, aromatic), 7.56 – 7.48 (m, 1H, aromatic), 7.44 – 7.38 (m, 2H, aromatic), 7.14 (d, *J* = 8.3 Hz, 1H, aromatic), 3.05 – 2.00 (broad, q, 3H, H_3-B) ppm.

^{13}C NMR (75 MHz, $CDCl_3$) δ = 136.76 (C9), 134.40 (C7), 133.56 (C1), 131.05 (C6), 130.28 (C10 and C14), 127.93 (C12), 126.97 (C11 and C13), 126.74 (C3 and C4), 119.25 (C2), 117.59 (q, ^1J(C,F) = 275.6 Hz, C8), 112.00 (C5) ppm.

{^{1}H} ^{11}B NMR (270 MHz, $CDCl_3$) δ = −20.48 (s) ppm.

^{11}B NMR (270 MHz, $CDCl_3$) δ = −20.48 (broad, q) ppm.

^{19}F NMR (376 MHz, $CDCl_3$) δ = −55.99 ppm.

IR (ATR) $\tilde{\nu}$ (cm^{-1}): 3062 (vw), 2381 (w), 2359 (w), 2273 (w), 1595 (w), 1519 (m), 1500 (m), 1470 (m), 1456 (m), 1417 (m), 1300 (m), 1289 (m), 1267 (m), 1232 (m), 1202 (s), 1180 (s), 1148 (s), 1130 (s), 1118 (s), 1074 (m), 1040 (m), 1019 (m), 1004 (m), 983 (m), 946 (w), 928 (m), 854 (w), 840 (m), 762 (s), 747 (s), 715 (m), 692 (s), 665 (m), 653 (m).

MS (70 eV, EI) m/z (%): 275 ($[M\text{-}H]^+$, 1), 262 ($[M\text{-}BH_3]^+$, 100), 193 (16), 84 (13), 83 (20).

HRMS (70 eV, EI): $C_{14}H_{12}BF_3N_2$ calc. 275.0962 g/mol $[M\text{-}H]^+$, found 275.0949 g/mol.

Elemental analysis [$C_{14}H_{12}BF_3N_2$]

Calc. (%): C 60.91, H 4.38, N 10.15.

Found (%): C 60.08, H 4.22, N 10.00.

2-(4-Fluorophenyl)-1-phenylbenzimidazole (41k)

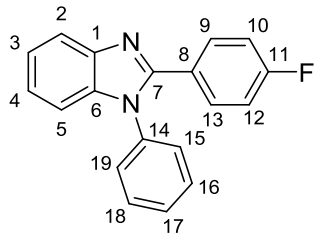

N-phenyl-*o*-phenylenediamine (1.47 g, 7.95 mmol, 1.00 eq.), *para*-fluorobenzaldehyde (1.11 g, 7.95 mmol, 1.00 eq.), triphenyl phosphite (2.50 mL, 9.54 mmol, 1.20 eq.) and pyridine (10 mL) were poured into a 80 mL microwave vessel under ambient atmosphere. The reaction was conducted in a microwave (closed vessel) at 200 °C for 40 minutes. After cooling down, the solvent was removed under reduced pressure. Afterwards distilled water (10 mL) were added, the reaction mixture was three times extracted with ethyl acetate, the combined organic phases dried over $MgSO_4$ and the solvent removed under reduced pressure. The crude product was purified by column chromatography on silica (0.035-0.070 mm, 60 Å/ ethyl acetate : isohexane = 1 : 2; R_f=0.85). As the product still showed traces of impurities, the column chromatography was repeated. This lead to the pure product **41k** as a white solid (0.53 g, 1.84 mmol, 23 %).

Decomposition point: 100.5 – 101.0 °C.

^{1}H NMR (300 MHz, $CDCl_3$) δ = 7.91 – 7.83 (m, 1H, H-C2), 7.61 – 7.43 (m, 5H, aromatic), 7.38 – 7.18 (m, 5H, aromatic), 7.02 – 6.93 (m, 2H, aromatic) ppm.

^{13}C NMR (75 MHz, $CDCl_3$) δ = 163.35 (d, ^1J(C,F) = 250.5 Hz, C11), 151.40 (C7), 142.91 (C1), 137.18 (C14), 136.82 (C6), 131.39 (d, ^3J(C,F) = 8.5 Hz, C9 and C13), 129.94 (C15 and C19), 128.68 (C17), 127.38 (C16 and C18), 126.17 (d, ^4J(C,F) = 3.3 Hz, C8), 123.40 (C3 or C4), 123.05 (C3 or C4), 119.80 (C2), 115.46 (d, ^2J(C,F) = 21.8 Hz, C10 and C12), 110.43 (C5) ppm.

^{19}F NMR (376 MHz, $CDCl_3$) δ = −110.82 ppm.

IR (ATR) $\tilde{\nu}$ (cm^{-1}): 3051 (w), 1894 (vw), 1600 (m), 1536 (w), 1498 (m), 1480 (m), 1456 (m), 1413 (m), 1383 (m), 1324 (m), 1311 (w), 1292 (w), 1280 (m), 1260 (m), 1237 (w), 1214 (s), 1194 (m), 1172 (w), 1160 (m), 1117 (w), 1098 (w), 1075 (w), 1018 (w), 1010 (w), 978 (w), 966 (w), 924 (w), 907 (w), 856 (m), 847 (s), 822 (m), 800 (m), 763 (s), 744 (s), 733 (m), 722 (m), 696 (s).

MS (70 eV, EI) m/z (%): 288 ($[M]^+$, 77), 287 ($[M-H]^+$, 100), 144 (10), 77 (20), 51 (18).

HRMS (70 eV, EI): $C_{19}H_{13}FN_2$ calc. 288.1063 g/mol $[M]^+$, found 288.1052 g/mol.

Elemental analysis [$C_{19}H_{13}FN_2$]

Calc. (%): C 79.15, H 4.54, N 9.72.

Found (%): C 78.87, H 4.56, N 9.58.

2-(4-Fluorophenyl)-1-phenyl-benzimidazole borane (17k)

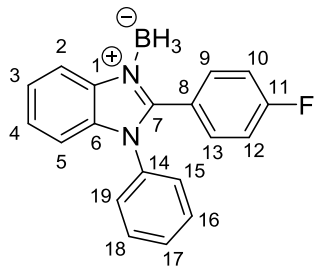

17k was prepared according to general procedure A. 2-(4-Fluorophenyl)-1-phenylbenzimidazole (**41k**, 0.41 g, 1.43 mmol, 1.00 eq.) was dissolved in 5 mL THF under N_2 atmosphere. The solution was cooled to 0 °C and a $H_3B{\bullet}SMe_2$ solution (5 M in Et_2O, 0.31 mL, 1.10 eq.) was added. After 10 minutes the external cooling was removed and 50 mL isohexane were added while stirring vigorously. Within 5 minutes a white precititate had formed. The precipitate was filtered off and washed three times with isohexane. After removing all residues of solvent under reduced pressure, **17k** was obtained as a white solid (0.36 g, 1.20 mmol, 84 %).

Decomposition point: 186.2 – 187.3 °C.

^{1}H NMR (300 MHz, $CDCl_3$) δ = 8.21 (d, *J* = 8.2 Hz, 1H, H-C2), 7.62 – 7.35 (m, 7H, aromatic), 7.31 – 7.15 (m, 3H, aromatic), 7.09 – 6.97 (m, 2H, aromatic), 3.07 – 2.00 (broad, q, 3H, H_3-B) ppm.

^{13}C NMR (75 MHz, $CDCl_3$) δ = 163.87 (d, ^1J(C,F) = 252.9 Hz, C11), 150.12 (C7), 137.33 (C14), 134.38 (C1), 133.75 (C6), 133.71 (d, ^3J(C,F) = 8.9 Hz, C9 and C13), 130.12 (C15 and C19), 129.68 (C17), 127.36 (C16 and C18), 125.63 (C3 or C4), 125.18 (C3 or C4), 121.23 (d, ^4J(C,F) = 3.5 Hz, C8), 118.25 (C2), 115.39 (d, ^2J(C,F) = 22.2 Hz, C10 and C12), 111.04 (C5) ppm.

{^{1}H} ^{11}B NMR (270 MHz, $CDCl_3$) δ = −22.45 (s) ppm.

^{11}B NMR (270 MHz, $CDCl_3$) δ = −22.46 (broad, q) ppm.

^{19}F NMR (376 MHz, $CDCl_3$) δ = −107.89 ppm.

IR (ATR) $\tilde{\nu}$ (cm^{-1}): 3058 (vw), 2356 (m), 2313 (m), 2265 (m), 1894 (vw), 1610 (m), 1596 (w), 1549 (w), 1499 (m), 1480 (m), 1458 (s), 1435 (s), 1346 (m), 1300 (w), 1288 (w), 1260 (w), 1232 (s), 1173 (s), 1160 (s), 1128 (m), 1116 (m), 1096 (m), 1075 (w), 1017 (m), 1004 (w), 973 (w), 950 (w), 849 (m), 836 (s), 803 (s), 766 (s), 758 (s), 750 (s), 698 (s), 662 (w).

MS (70 eV, EI) m/z (%): 302 ($[M]^+$, 5), 289 ($[M\text{-}BH_2]^+$, 16), 288 ($[M\text{-}BH_3]^+$, 75) 287 ($[M\text{-}H\text{-}BH_3]^+$, 100), 286 ($[M\text{-}2H\text{-}BH_3]^+$, 11), 83 (10).

HRMS (70 eV, EI): $C_{19}H_{16}BFN_2$ calc. 302.1391 g/mol $[M]^+$, found 302.1374 g/mol.

Elemental analysis [$C_{19}H_{16}BFN_2$]

Calc. (%): C 75.53, H 5.34, N 9.27.

Found (%): C 73.57, H 5.30, N 8.86.

2-Isopropyl-1-methylimidazole (41l)

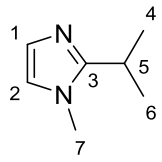

In a Schlenk flask under N_2 atmosphere 2-isopropylimidazole (**41la**, 2.13 g, 19.31 mmol, 1.00 eq.) was dissolved in THF (50 mL) and cooled to 0 °C. *n*-Butyllithium (2.5 M solution in hexane, 8.50 mL, 21.24 mmol, 1.10 eq.) was then added, the external cooling removed and the solution stirred for 10 minutes. Thereafter methyl iodide (1.32 mL, 21.24 mmol, 1.10 eq.) was added and the solution was stirred for 20 minutes. Distilled water (30 mL) was added, the aqueous phase was three times extracted with DCM, the combined extracts dried over $MgSO_4$ and the solvent was removed under reduced pressure. **41l** was obtained as colorless oil (1.43 g, 11.52 mmol, 60 %).

^{1}H NMR (300 MHz, $CDCl_3$) δ = 6.78 (d, *J* = 1.3 Hz, 1H, H-C2), 6.64 (d, *J* = 1.3 Hz, 1H, H-C1), 3.46 (s, 3H, H_3-C7), 2.90 (septett, *J* = 6.8 Hz, 1H, H-C5), 1.18 (d, *J* = 6.9 Hz, 6H, H_3-C4 and H_3-C6) ppm.

^{13}C NMR (75 MHz, $CDCl_3$) δ = 152.83 (C3), 126.49 (C1), 120.18 (C2), 32.29 (C7), 25.75 (C5), 21.21 (C4 and C6) ppm.

IR (ATR) $\tilde{\nu}$ (cm^{-1}): 3103 (vw), 2968 (m), 2930 (m), 2870 (w), 1522 (w), 1494 (s), 1472 (m), 1458 (m), 1380 (m), 1363 (m), 1318 (w), 1153 (m), 1134 (m), 1103 (m), 1070 (s), 922 (m), 836 (w), 746 (m), 717 (s), 665 (w).

MS (70 eV, EI) m/z (%): 124 ($[M]^+$, 34), 123 ($[M-H]^+$, 29), 110 ($[M-CH_2]^+$, 14), 109 ($[M-Me]^+$, 100), 96 (22), 95 (19), 81 (11), 68 (12),43 (15), 42 (20).

HRMS (70 eV, EI): $C_7H_{12}N_2$ calc. 124.1000 g/mol $[M]^+$, found 124.0995 g/mol.

Elemental analysis [$C_7H_{12}N_2$]

Calc. (%): C 67.70, H 9.74, N 22.56.

Found (%): C 67.69, H 9.23, N 22.26.

2-Isopropyl-1-methylimidazole borane (17l)

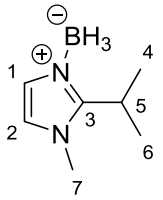

17l was prepared according to general procedure A. 2-Isopropyl-1-methylimidazole (**41l**, 0.83 g, 6.65 mmol, 1.00 eq.) was dissolved in 5 mL THF under N_2 atmosphere. The solution was cooled to 0 °C and a $H_3B{\bullet}SMe_2$ solution (5 M in Et_2O, 1.46 mL, 1.10 eq.) was added. After 10 minutes the external cooling was removed and 50 mL isohexane were added while stirring vigorously. Within 5 minutes a white precititate had formed. The precipitate was filtered off and washed three times with isohexane. After removing all residues of solvent under reduced pressure, **17l** was obtained as a white solid (0.69 g, 5.00 mmol, 75 %).

Decomposition point: 82.0 – 83.0 °C.

^{1}H NMR (300 MHz, $CDCl_3$) δ = 6.89 (d, *J* = 1.7 Hz, 1H, H-C2), 6.68 (d, *J* = 1.7 Hz, 1H, H-C1), 3.97 (s, 3H, H_3-C7), 3.84 (sept, *J* = 7.4 Hz, 1H, H-C5), 1.34 (d, *J* = 7.3 Hz, 6H, H_3-C4 and H_3-C6), 2.79-1.44 (broad, q, 3H, H_3-B) ppm.

^{13}C NMR (75 MHz, $CDCl_3$) δ = 150.38 (C3), 126.74 (C1), 120.08 (C2), 35.04 (C7), 25.36 (C5), 18.66 (C4 and C6) ppm.

{^{1}H} ^{11}B NMR (270 MHz, $CDCl_3$) δ = −19.74 (s) ppm.

^{11}B NMR (270 MHz, $CDCl_3$) δ = −19.76 (broad, q) ppm.

IR (ATR) $\tilde{\nu}$ (cm^{-1}): 3128 (w), 3054 (m), 2974 (w), 2357 (m), 2309 (m), 1691 (vw), 1626 (vw), 1583 (w), 1564 (vw), 1552 (vw), 1527 (w), 1504 (m), 1452 (m), 1432 (m), 1384 (m), 1366 (m), 1300 (m), 1252 (w), 1166 (s), 1120 (m), 1096 (s), 938 (m), 859 (w), 799 (m), 768 (vs), 730 (s).

MS (70 eV, EI) m/z (%): 138 ($[M]^+$, 3), 137 ($[M-H]^+$, 42), 136 ($[M-2H]^+$, 20), 135 ($[M-3H]^+$, 100), 134 ($[M-4H]^+$, 27), 133 ($[M-5H]^+$, 34), 124 ($[M-BH_3]^+$, 15), 120 (11), 119 (16), 109 (64), 96 (12).

HRMS (70 eV, EI): $C_7H_{15}BN_2$ calc. 138.1328 g/mol $[M]^+$, found 138.1266 g/mol.

Elemental analysis [$C_7H_{15}BN_2$]

Calc. (%): C 60.92, H 10.95, N 20.30.

Found (%):C 58.14, H 10.33, N 19.13.

1-Methyl-4,5-diphenylimidazole borane (17m)

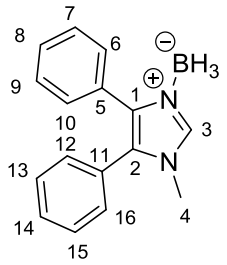

17m was prepared according to general procedure A. 1-Methyl-4,5-diphenylimidazole (**41m**, 1.00 g, 4.27 mmol, 1.00 eq.) was dissolved in 10 mL THF under N_2 atmosphere. The solution was cooled to 0 °C and a $H_3B{\bullet}SMe_2$ solution (5 M in Et_2O, 0.94 mL, 1.10 eq.) was added. After 10 minutes the external cooling was removed and 50 mL isohexane were added while stirring vigorously. Within 5 minutes a white precititate had formed. The precipitate was filtered off and washed three times with isohexane. After removing all residues of solvent under reduced pressure, **17m** was obtained as a white solid (0.86 g, 3.46 mmol, 81 %).

Decomposition point: 187.2 – 187.9 °C.

^{1}H NMR (300 MHz, $CDCl_3$) δ = 7.98 (s, 1H, H-C3), 7.54 – 7.30 (m, 5H, aromatic), 7.29 - 7.22 (m, 3H, aromatic), 7.21 – 7.13 (m, 2H, aromatic), 3.55 (s, *J*=4.6, 3H, H_3-C4), 2.89-1.54 (broad, q, 3H, H_3-B) ppm.

^{13}C NMR (75 MHz, $CDCl_3$) δ = 137.41 (C3), 136.11 (C2), 130.93 (C5), 130.57 (C7 and C9), 130.54 (C13 and C15), 129.37 (C11), 129.26 (C8), 128.93 (C6 and C10), 128.15 (C14), 127.73 (C12 and C16), 127.48 (C1), 33.49 (C4) ppm.

{^{1}H} ^{11}B NMR (270 MHz, $CDCl_3$) δ = −19.67 (s) ppm.

^{11}B NMR (270 MHz, $CDCl_3$) δ = −19.68 (broad, q) ppm.

IR (ATR) $\tilde{\nu}$ (cm^{-1}): 3132 (w), 3059 (w), 2372 (m), 2306 (m), 2261 (m), 1711 (vw), 1602 (w), 1539 (m) 1492 (w), 1444 (m), 1390 (w), 1334 (w), 1273 (w), 1184 (s), 1166 (s), 1151 (s), 1090 (w), 1072 (m), 1046 (w), 1020 (w), 1009 (w), 953 (w), 918 (w), 848 (m), 805 (m), 772 (m), 748 (s), 719 (w), 695 (vs).

MS (70 eV, EI) m/z (%): 248 ($[M]^+$, 2), 245 ($[M\text{-}3H]^+$, 29), 235 ($[M\text{-}BH_2]^+$, 18), 234 ($[M\text{-}BH_3]^+$, 100), 233 ($[M\text{-}Me]^+$, 61), 218 (16), 165 (39).

HRMS (70 eV, EI): $C_{16}H_{17}BN_2$ calc. 248.1485 g/mol $[M]^+$, found 248.1484 g/mol.

Elemental analysis [$C_{16}H_{17}BN_2$]

Calc. (%): C 77.45, H 6.91, N 11.29.

Found (%): C 76.23, H 6.80, N 11.04.

2-Isopropylimidazole borane (17n)

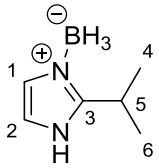

17n was prepared according to general procedure A. 2-Isopropylimidazole (**41n**, 1.25 g, 11.36 mmol, 1.00 eq.) was dissolved in 15 mL THF under N_2 atmosphere. The solution was cooled to 0 °C and a $H_3B{\bullet}SMe_2$ solution (5 M in Et_2O, 2.50 mL, 1.10 eq.) was added. After 10 minutes the external cooling was removed and 100 mL isohexane were added while stirring vigorously. Within 5 minutes a white precititate had formed. The precipitate was filtered off and washed three times with isohexane. After removing all residues of solvent under reduced pressure, **17n** was obtained as a white solid (0.85 g, 6.86 mmol, 60 %).

Decomposition point: 50.2 – 50.9 °C.

^{1}H NMR (300 MHz, DMSO-d_6) δ = 10.32 – 9.83 (broad, s, 1H, H-N), 6.86 (s, 1H, H-C2), 6.81 (s, 1H, H-C1), 3.59 – 3.44 (m, 1H, H-C5), 2.77 – 1.75 (broad, q, 3H, H_3-B), 1.24 (d, J = 6.1, 6H, H_3-C4 and H_3-C6) ppm.

^{13}C NMR (75 MHz, DMSO-d_6) δ = 152.29 (C3), 126.88 (C1), 115.01 (C2), 25.83 (C5), 20.20 (C4 and C6) ppm.

{^{1}H} ^{11}B NMR (270 MHz, DMSO-d_6) δ = −20.06 (s) ppm.

^{11}B NMR (270 MHz, DMSO-d_6) δ = −20.07 (broad, q) ppm.

IR (ATR) $\tilde{\nu}$ (cm^{-1}): 3286 (m), 3176 (w), 3165 (w), 3154 (w), 3141 (w), 2939 (m), 2975 (w), 2877 (w), 2349 (m), 2296 (s), 2253 (s), 1619 (w), 1604 (w), 1576 (m), 1491 (s), 1465 (m), 1393 (m), 1367 (m), 1316 (w), 1285 (m), 1196 (s), 1174 (s), 1163 (s), 1136 (m), 1097 (s), 1069 (s), 957 (m), 942 (m), 929 (m), 883 (w), 855 (w), 850 (m), 765 (s), 755 (s), 707 (s).

MS (70 eV, EI) m/z (%): 124 ($[M]^+$, 3), 123 ($[M-H]^+$, 53), 122 ($[M-2H]^+$, 19), 121 ($[M-3H]^+$, 100), 120 ($[M-4H]^+$, 27), 118 ($[M-6H]^+$, 11), 110 ($[M-BH_3]^+$, 8), 105 (19), 95 (39), 55 (10).

HRMS (70 eV, EI): $C_6H_{13}BN_2$ calc. 124.1172 g/mol $[M]^+$, found 124,1100 g/mol.

Elemental analysis [$C_6H_{13}BN_2$]

Calc. (%): C 58.12, H 10.57, N 22.59.

Found (%): C 56.32, H 10.13, N 22.26.

2-(3,4,5-Trimethoxyphenyl)-benzimidazole (41oa)

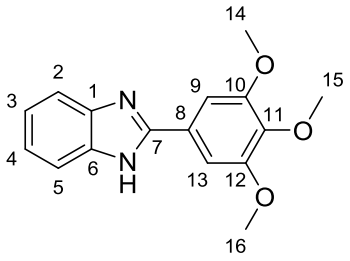

Under a N_2 atmosphere *ortho*-phenylenediamine (**35e**, 7.46 g, 69.02 mmol, 1.00 eq.) and 3,4,5-trimethoxybenzaldehyde (14.90 g, 75.92 mmol, 1.10 eq.) were stirred at 115 °C for 60 minutes without solvent. Acetone (200 mL) then was added which led to the precipitation of the crude product which was filtered off. Subsequently the solid was recrystallized from acetone/ethanol (1:1) to give the pure product **41oa** as colorless needles (3.92 g, 19.62 mmol, 20 %).

Melting point: 263.5 – 263.8 °C.

^{1}H NMR (300 MHz, DMSO-d_6) δ = 12.84 (s, 1H, H-N), 7.64 (d, *J* = 6.7, 1H, H-C2), 7.52 (s, 2H, H-C9 and H-C13), 7.22 – 7.12 (m, 3H, H-C3, H-C4 and H-C5), 3.87 (s, 6H, H_3-C14 and H_3-C16), 3.71 (s, 3H, H_3-C15) ppm.

^{13}C NMR (75 MHz, DMSO-d_6) δ = 153.67 (C10 and C12), 151.68 (C7), 144.20 (C11), 139.37 (C1), 135.41 (C6), 125.92 (C8), 122.85 (C3 or C4), 122.06 (C3 or C4), 119.12 (C2), 111.57 (C5), 104.28 (C9 and C13), 60.56 (C15), 56.45 (C14 and C16) ppm.

IR (ATR) $\tilde{\nu}$ (cm^{-1}): 2959 (w), 2835 (w, br), 1586 (m), 1548 (w), 1536 (w), 1513 (w), 1495 (m), 1480 (m), 1468 (m), 1455 (m), 1443 (m), 1424 (s), 1373 (m), 1334 (w), 1294 (w), 1271 (m), 1231 (s), 1180 (m), 1152 (w), 1124 (vs), 1009 (m), 993 (s), 931 (m), 902 (m), 880 (m), 842 (s), 822 (m), 790 (w), 768 (w), 747 (s), 673 (m).

MS (70 eV, EI) m/z (%): 284 ($[M]^+$, 100), 283 ($[M-H]^+$, 10), 270 ($[M-CH_2]^+$, 11), 269 ($[M-Me]^+$, 59), 241 (15), 226 (13), 211 (20), 155 (16), 142 (14), 127 (10).

HRMS (70 eV, EI): $C_{16}H_{16}N_2O_3$ calc. 284.1161 g/mol $[M]^+$, found 284.1145 g/mol.

Elemental analysis [$C_{16}H_{16}N_2O_3$]

Calc. (%): C 67.59, H 5.67, N 9.85.

Found (%):C 67.38, H 5.69, N 9.77.

1-Methyl-2-(3,4,5-trimethoxyphenyl)-benzimidazole (41ob)

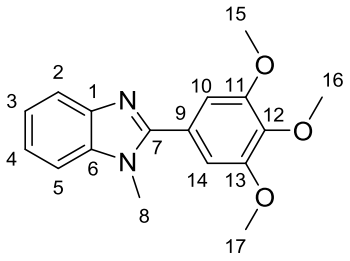

In a Schlenk flask under N_2 atmosphere 2-(3,4,5-trimethoxyphenyl)-benzimidazole (**41oa**, 1.18 g, 4.13 mmol, 1.00 eq.) was dissolved in THF (100 mL). Afterwards *n*-butyllithium (2.5 M solution in hexane, 1.73 mL, 4.33 mmol, 1.05 eq.) was added at room temperature and the solution stirred for 20 minutes. Methyl iodide (1.00 mL, 16.06 mmol, 3.89 eq.) was then added and the solution was stirred for 20 minutes. Afterwards all volatiles were removed under reduced pressure. Distilled water (20 mL) was added, the aqueous phase was extracted three times with DCM, the combined extracts dried over $MgSO_4$ and the solvent was removed under reduced pressure. The crude product was dissolved in DCM (3 mL) and isohexane (50 mL) was added while stirring vigorously for two minutes. The cloudy isohexane layer was filtered off. In this clear solution the product began to grow immediately as white needles. After five minutes the needles were filtered off. Thus, **41ob** was obtained as white, crystalline needles (0.42 g, 1.41 mmol, 34 %).

Melting point: 126.5 – 127.0 °C.

^{1}H NMR (300 MHz, $CDCl_3$) δ = 7.80 (ddd, *J* = 5.0 Hz, 2.9 Hz, 0.7 Hz, 1H, H-C2), 7.38 – 7.26 (m, 3H, H-C3, H-C4 and H-C5), 6.94 (s, 2H, H-C10 and H-C14), 3.91 (s, 9H, H_3-C8, H_3-C15 and H_3-C17), 3.84 (s, 3H, H_3-C16) ppm.

^{13}C NMR (75 MHz, $CDCl_3$) δ = 153.68 (C7), 153.36 (C11 and C13), 142.81 (C12), 139.54 (C1), 136.55 (C6), 125.54 (C9), 122.77 (C3 or C4), 122.44 (C3 or C4), 119.72 (C2), 109.56 (C5), 106.91 (C10 and C14), 60.95 (C16), 56.36 (C15 and C17), 31.70 (C8) ppm.

IR (ATR) $\tilde{\nu}$ (cm^{-1}): 3101 (w), 3008 (vw), 2990 (w), 2969 (w), 2929 (w), 2822 (w), 1942 (w), 1897 (w), 1682 (w), 1603 (w), 1584 (m), 1525 (w), 1484 (m), 1463 (m), 1446 (m), 1436 (m), 1430 (m), 1412 (m), 1384 (m), 1319 (m), 1278 (m), 1244 (s) 1232 (m), 1189 (w), 1168 (m), 1154 (w), 1120 (vs), 1100 (s), 1030 (w), 1010 (s), 1004 (m), 930 (w), 910 (m), 892 (m), 846 (m), 837 (m), 790 (m), 762 (m), 754 (s), 746 (s), 729 (m), 666 (m), 625 (m), 593 (m), 575 (w), 561 (m).

MS (70 eV, EI) m/z (%): 298 ($[M]^+$, 100), 297 ($[M-H]^+$, 34), 283 ($[M-Me]^+$, 44), 253 ($[M-OMe-Me]^+$, 12), 252 ($[M-OMe-Me-H]^+$, 10), 225 (23), 197 (11), 169 (16), 149 (11), 44 (15).

HRMS (70 eV, EI): $C_{17}H_{18}N_2O_3$ calc. 298.1317 g/mol $[M]^+$, found 298.1315 g/mol.

Elemental analysis [$C_{17}H_{18}N_2O_3$]

Calc. (%): C 68.44, H 6.08, N 9.39.

Found (%): C 68.34, H 5.92, N 9.47.

1-Methyl-2-(3,4,5-trimethoxyphenyl)-benzimidazole borane (17o)

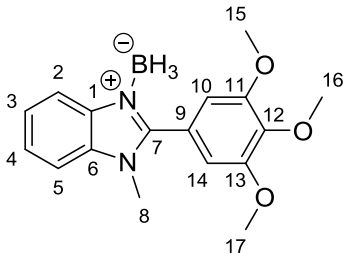

17o was prepared according to general procedure A. 1-Methyl-2-(3,4,5-trimethoxyphenyl)-benzimidazole (**41ob**, 1.00 g, 3.35 mmol, 1.00 eq.) was dissolved in 10 mL THF under N_2 atmosphere. The solution was cooled to 0 °C and a $H_3B{\bullet}SMe_2$ solution (5 M in Et_2O, 0.74 mL, 1.10 eq.) was added. After 10 minutes the external cooling was removed and 100 mL isohexane were added while stirring vigorously. Within 5 minutes a white precititate had formed. The precipitate was filtered off and washed three times with isohexane. After removing all residues of solvent under reduced pressure, **17o** was obtained as a white solid (0.89 g, 2.85 mmol, 85 %).

Decomposition point: 154.8 – 155.4 °C.

^{1}H NMR (300 MHz, $CDCl_3$) δ = 8.15 – 8.04 (m, 2H, H-C2 and H-C5), 7.47 (dd, *J*=6.8 Hz, *J*=3.1 Hz, 2H, H-C3 and H-C4), 6.82 (s, 2H, H-C10 and H-C14), 3.95 (s, 3H, H_3-C8), 3.89 (s, 6H, H_3-C15 and H_3-C17), 3.78 (s, 3H, H_3-C16), 2.97-1.63 (broad, q, 3H, H_3-B) ppm.

^{13}C NMR (75 MHz, $CDCl_3$) δ = 153.23 (C11 and C13), 151.61 (C7), 140.30 (C12), 137.17 (C1), 133.03 (C6), 125.00 (C3 or C4), 124.75 (C3 or C4), 120.15 (C9), 118.05 (C2), 110.04 (C5), 108.31 (C10 and C14), 60.96 (C16), 56.42 (C15 and C17), 31.86 (C8) ppm.

{^{1}H} ^{11}B NMR (270 MHz, $CDCl_3$) δ = −22.07 (s) ppm.

^{11}B NMR (270 MHz, $CDCl_3$) δ = −22.06 (broad, q) ppm.

IR (ATR) $\tilde{\nu}$ (cm^{-1}): 2939 (w), 2361 (m), 2342 (m),2265 (w), 1586 (m), 1492 (m), 1479 (s), 1458 (s), 1430 (m), 1413 (m), 1322 (m), 1244 (s), 1161 (m), 1127 (vs), 998 (m), 958 (w), 891 (w), 847 (m), 791 (w), 742 (s), 668 (w).

MS (70 eV, EI) m/z (%): 312 ($[M]^+$, 6), 309 ($[M\text{-}3H]^+$, 11), 299 ($[M\text{-}BH_2]^+$, 20), 298 ($[M\text{-}BH_3]^+$, 100) 297 ($[M\text{-}Me]^+$, 35), 283 (48), 253 (12), 252 (13), 225 (24), 197 (11), 181 (15), 169 (19), 149 (11), 77 (11).

HRMS (70 eV, EI): $C_{17}H_{21}BN_2O_3$ calc. 312.1645 g/mol $[M]^+$, found 312.1709 g/mol.

Elemental analysis [$C_{17}H_{21}BN_2O_3$]

Calc. (%): C 65.41, H 6.78, N 8.97.

Found (%): C 63.28, H 6.50, N 8.68.

2-(4-Fluorophenyl)-benzimidazole (41pa)

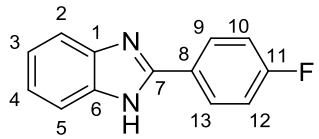

Under a N_2 atmosphere *ortho*-phenylenediamine (**35e**, 8.43 g, 77.97 mmol, 1.00 eq.) and *para*-fluorobenzaldehyde (10.65 g, 85.77 mmol, 1.10 eq.) were stirred at 115 °C for 60 minutes without solvent. Afterwards 200 mL acetone were added which leaded to the precipitation of the crude product which was filtered off. Subsequently the solid was recrystallized from acetone/ethanol (1:1) to give the pure product **41pa** as colorless needles (2.32 g, 16.55 mmol, 14 %).

Melting point: 256.5 – 257.2 °C.

^{1}H NMR (300 MHz, DMSO-d_6) δ = 12.93 (broad, s, 1H, H-N), 8.28 – 8.20 (m, 2H, H-C9 and H-C13), 7.66-7.55 (m, 2H, H-C2 and H-C5), 7.45 – 7.35 (m, 2H, H-C10 and H-C12), 7.25 – 7.16 (m, 2H, H-C3 and H-C4) ppm.

^{13}C NMR (75 MHz, DMSO-d_6) δ = 163.54 (d, ^1J(C,F) = 247.3 Hz, C11), 150.88 (C7), 144.16 (C1), 135.54 (C6), 129.20 (d, ^3J(C,F) = 8.6 Hz, C9 and C13), 127.29 (d, ^4J(C,F) = 3.0 Hz, C8), 122.63 (C3 and C4), 119.25 (C2), 116.46 (d, ^2J(C,F) = 21.9 Hz, C10 and C12), 111.80 (C5) ppm.

^{19}F NMR (376 MHz, DMSO-d_6) δ = −111.12 ppm.

IR (ATR) $\tilde{\nu}$ (cm^{-1}): 2913 (w), 2661 (w, br) 2362 (w), 1623 (w) 1602 (m), 1590 (w), 1496 (m), 1475 (m), 1451 (m), 1430 (s), 1397 (m), 1372 (m), 1320 (m), 1276 (m), 1227 (s), 1155 (m), 1110 (m), 1095 (m), 1011 (m), 966 (m), 925 (w), 903 (w), 879 (w), 836 (vs), 808 (w), 794 (m), 766 (m), 744 (vs), 696 (m).

MS (70 eV, EI) m/z (%): 212 ($[M]^+$, 100), 211 ($[M-H]^+$, 14).

HRMS (70 eV, EI): $C_{13}H_9FN_2$ calc. 212.0750 g/mol $[M]^+$, found 212.0742 g/mol.

Elemental analysis [$C_{13}H_9FN_2$]

Calc. (%): C 73.57, H 4.27, N 13.20.

Found (%): C 73.34, H 4.28, N 13.15.

2-(4-Fluorophenyl)-1-methylbenzimidazole (41pb)

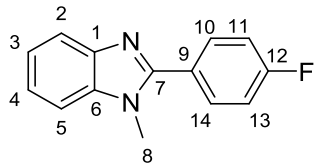

In a Schlenk flask under N_2 atmosphere 2-(4-fluorophenyl)-benzimidazole (**41pa**, 0.55 g, 2.58 mmol, 1.00 eq.) was dissolved in THF (20 mL) and cooled to 0 °C. Afterwards *n*-butyllithium (2.5 M solution in hexane, 1.13 mL, 2.84 mmol, 1.10 eq.) was added, the external cooling removed and the solution stirred for 10 minutes. Methyl iodide (0.18 mL, 2.84 mmol, 1.10 eq.) was then added and the solution was stirred for 20 minutes. Distilled water (10 mL) was added, the aqueous phase was extracted three times with DCM, the combined extracts dried over $MgSO_4$ and the solvent was removed under reduced pressure. The resulting solid was washed two times with isohexane (10 mL). **41pb** was obtained as white solid (0.45 g, 1.97 mmol, 76 %).

Melting point: 95.9 – 96.1 °C.

^{1}H NMR (300 MHz, $CDCl_3$) δ = 7.81 (ddd, *J* = 5.8 Hz, 3.2 Hz, 0.8 Hz, 1H, H-C2), 7.76 – 7.69 (m, 2H, aromatic), 7.37 – 7.27 (m, 3H, aromatic), 7.23 – 7.15 (m, 2H, aromatic), 3.79 (s, 3H, H_3-C8) ppm.

^{13}C NMR (75 MHz, $CDCl_3$) δ = 163.57 (d, ^1J(C,F) = 250.4 Hz, C12), 152.75 (C7), 142.84 (C1), 136.51 (C6), 131.35 (d, ^3J(C,F) = 8.5 Hz, C10 and C14), 126.37 (d, ^4J(C,F) = 3.4 Hz, C9), 122.85 (C3 or C4), 122.50 (C3 or C4), 119.76 (C2), 115.83 (d, ^2J(C,F) = 21.9 Hz, C11 and C13), 109.63 (C5), 31.59 (C8) ppm.

^{19}F NMR (376 MHz, $CDCl_3$) δ = −110.61 ppm.

IR (ATR) $\tilde{\nu}$ (cm^{-1}): 2924 (vw), 1605 (m), 1530 (m), 1462 (s), 1437 (m), 1408 (m), 1376 (m), 1324 (m), 1291 (w), 1277 (w), 1222 (s), 1157 (m), 1127 (w), 1096 (m), 1051 (w), 1007 (m), 925 (w), 900 (w), 844 (s), 795 (s), 765 (m), 752 (s), 742 (vs), 732 (s).

MS (70 eV, EI) m/z (%): 226 ($[M]^+$, 78), 225 ($[M-H]^+$, 100), 224 ($[M-2H]^+$, 10).

HRMS (70 eV, EI): $C_{14}H_{11}FN_2$ calc. 226.0906 g/mol $[M]^+$, found 226.0910 g/mol.

Elemental analysis [$C_{14}H_{11}FN_2$]

Calc. (%): C 74.32, H 4.90, N 12.38.

Found (%): C 74.35, H 4.99, N 12.08.

2-(4-Fluorophenyl)-1-methylbenzimidazole borane (17p)

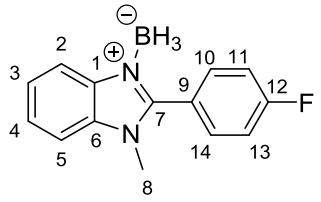

17p was prepared according to general procedure A. 2-(4-Fluorophenyl)-1-methylbenzimidazole (**41pb**, 0.30 g, 1.31 mmol, 1.00 eq.) was dissolved in 5 mL THF under N_2 atmosphere. The solution was cooled to 0 °C and a $H_3B{\bullet}SMe_2$ solution (5 M in Et_2O, 0.29 mL, 1.10 eq.) was added. After 10 minutes the external cooling was removed and 50 mL isohexane were added while stirring vigorously. Within 5 minutes a white precititate had formed. The precipitate was filtered off and washed three times with isohexane. After removing all residues of solvent under reduced pressure, **17p** was obtained as a white solid (0.22 g, 0.92 mmol, 70 %).

Decomposition point: 160.2 – 161.0 °C.

^{1}H NMR (300 MHz, $CDCl_3$) δ = 8.03 (dd, *J* = 6.2 Hz, 1.9 Hz, 1H, H-C2), 7.56 – 7.51 (m, 2H, $H_{aromatic}$), 7.44 – 7.36 (m, 3H, $H_{aromatic}$), 7.22 – 7.16 (m, 2H, $H_{aromatic}$), 3.68 (s, 3H, H_3-C8), 2.68 – 1.68 (broad, q, 3H, H_3-B) ppm.

^{13}C NMR (75 MHz, $CDCl_3$) δ = 164.25 (d, ^1J(C,F) = 252.9 Hz, C12), 150.74 (C7), 137.21 (C1), 133.15 (d, ^3J(C,F) = 8.9 Hz, C10 and C14), 133.07 (C6), 125.17 (C3 or C4), 124.86 (C3 or C4), 121.26 (d, ^4J(C,F) = 3.5 Hz, C9), 118.07 (C2), 115.96 (d, ^2J(C,F) = 22.2 Hz, C11 and C13), 110.22 (C5), 31.85 (C8) ppm.

{^{1}H} ^{11}B NMR (270 MHz, $CDCl_3$) δ = −21.79 (s) ppm.

^{11}B NMR (270 MHz, $CDCl_3$) δ = −21.77 (broad, q) ppm.

^{19}F NMR (376 MHz, $CDCl_3$) δ = −107.57 ppm.

IR (ATR) $\tilde{\nu}$ (cm^{-1}): 2365 (m), 2306 (m), 2261 (m), 1607 (m), 1543 (w), 1478 (s), 1452 (s), 1414 (m), 1398 (m), 1340 (w), 1298 (m), 1249 (w), 1220 (s), 1158 (s), 1126 (s), 1098 (m), 1072 (w), 1013 (m), 986 (w), 939 (m), 845 (s), 793 (s), 780 (w), 759 (s), 734 (w), 708 (w).

MS (70 eV, EI) m/z (%): 240 ($[M]^+$, 1), 237 ($[M\text{-}3H]^+$, 14), 227 ($[M\text{-}BH_2]^+$, 10), 226 ($[M\text{-}BH_3]^+$, 67), 225 ($[M\text{-}Me]^+$, 100), 82 (11).

HRMS (70 eV, EI): $C_{14}H_{14}BFN_2$ calc. 240.1234 g/mol $[M]^+$, found 240.1222 g/mol.

Elemental analysis [$C_{14}H_{14}BFN_2$]

Calc. (%): C 70.04, H 5.88, N 11.67.

Found (%): C 69.75, H 5.87, N 11.54.

4-dimethylaminopyridine borane (DMAP borane, 17q)[85]

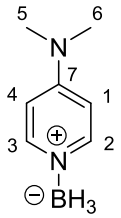

17q was prepared according to general procedure A. 4-Dimethylaminopyridine (**27**, 1.00 g, 8.18 mmol, 1.00 eq.) was dissolved in 10 mL THF under N_2 atmosphere. The solution was cooled to 0 °C and a $H_3B{\bullet}SMe_2$ solution (5 M in Et_2O, 1.80 mL, 1.10 eq.) was added. After 10 minutes the external cooling was removed and 100 mL isohexane were added while stirring vigorously. Within 5 minutes a white precititate had formed. The precipitate was filtered off and washed three times with isohexane. After removing all residues of solvent under reduced pressure, **17q** was obtained as a white solid (0.90 g, 6.63 mmol, 81 %).

Decomposition point: 168.7 – 170.2 °C.

^{1}H NMR (300 MHz, DMSO-d_6) δ = 7.91-7.89 (m, 2H, H-C2 and H-C3), 6.70-6.67 (m, 2H, H-C1, H-C4), 3.02 (s, 6H, H_3-C5 and H_3-C6), 2.44-1.91 (broad, q, 3H, H_3-B) ppm.

^{13}C NMR (75 MHz, DMSO-d_6) δ = 154.84 (C7), 146.46 (C2 and C3), 107.22 (C1 and C4), 39.42 (C5 and C6) ppm.

{^{1}H} ^{11}B NMR (270 MHz, DMSO-d_6) δ = −13.02 ppm.

^{11}B NMR (270 MHz, DMSO-d_6) δ = −13.01 (broad, q) ppm.

IR (ATR) $\tilde{\nu}$ **(cm^{-1})**: 3076 (w), 2922 (w), 2835 (w), 2611 (w), 2358 (m), 2326 (m), 2283 (s), 2245 (s), 1820 (w), 1629 (s), 1531 (vs), 1477 (m), 1459 (m), 1440 (m), 1389 (m), 1341 (m), 1306 (m), 1225 (s), 1172 (s), 1128 (m), 1098 (s), 1067 (s), 1039 (m), 945 (m), 824 (m), 812 (vs), 780 (w), 722 (w).

MS (70 eV, EI) m/z (%): 136 ([M]$^+$, 8), 135 ([M-H]$^+$, 100), 134 ([M-2H]$^+$, 43), 122 ([M-BH3]$^+$, 14), 121 (18), 119 (10), 107 (16).

HRMS (70 eV, EI): $C_7H_{13}BN_2$ calc. 136.1172 g/mol [M]$^+$, found 136.1173 g/mol.

Elemental analysis [$C_7H_{13}BN_2$]

Calc. (%): C 61.82, H 9.63, N 20.60.

Found (%): C 61.78, H 9.48, N 20.55.

4-Pyrrolidinopyridine borane (17r)

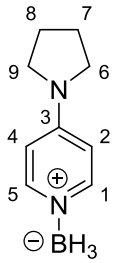

17r was prepared according to general procedure A. 4-Pyrrolidinopyridine (**41r**, 2.53 g, 17.07 mmol, 1.00 eq.) was dissolved in 25 mL THF under N_2 atmosphere. The solution was cooled to 0 °C and a $H_3B{\bullet}SMe_2$ solution (5 M in Et_2O, 3.76 mL, 1.10 eq.) was added. After 10 minutes the external cooling was removed and 200 mL isohexane were added while stirring vigorously. Within 5 minutes a white precititate had formed. The precipitate was filtered off and washed three times with isohexane. After removing all residues of solvent under reduced pressure, **17r** was obtained as a white solid (1.70 g, 10.49 mmol, 61 %).

Decomposition point: 167.0 – 167.7 °C.

^{1}H NMR (300 MHz, $CDCl_3$) δ = 7.95 (d, *J* = 7.3 Hz, 2H, H-C1 and H-C5), 6.33 (d, *J* = 7.3 Hz, 2H, H-C2 and H-C4), 3.38 – 3.27 (m, 4H, H_2-C6 and H_2-C9), 2.09 – 1.97 (m, 4H, H_2-C7 and H_2-C8), 3.02-1.70 (broad, q, 3H, H_3-B) ppm.

^{13}C NMR (75 MHz, $CDCl_3$) δ = 152.01 (C3), 146.56 (C1 and C5), 106.83 (C2 and C4), 47.51 (C6 and C9), 25.22 (C7 and C8) ppm.

{^{1}H} ^{11}B NMR (270 MHz, $CDCl_3$) δ = −14.01 (s) ppm.

^{11}B NMR (270 MHz, $CDCl_3$) δ = −14.00 (broad, q) ppm.

IR (ATR) $\tilde{\nu}$ (cm^{-1}): 2968 (w), 2868 (w) 2575 (vw), 2343 (m), 2298 (m), 2246 (m), 2081 (w) 1741 (w), 1633 (s), 1534 (s), 1483 (m), 1462 (m), 1414 (m), 1350 (m), 1328 (m), 1301 (w), 1288 (m), 1254 (w), 1232 (w), 1212 (w), 1167 (s), 1156 (s), 1117 (m), 1092 (s), 1030 (m), 978 (m), 965 (m), 930 (m), 862 (m), 807 (vs), 718 (m), 662 (w).

MS (70 eV, EI) m/z (%): 162 ($[M]^+$, 11), 161 ($[M-H]^+$, 100), 160 ($[M-2H]^+$, 39), 148 ($[M-BH_3]^+$, 25), 147 (32), 133 (21), 119 (13), 78 (10).

HRMS (70 eV, EI): $C_9H_{15}BN_2$ calc. 162.1328 g/mol $[M]^+$, found 162.1272 g/mol.

Elemental analysis [$C_9H_{15}BN_2$]

Calc. (%): C 66.71, H 9.33, N 17.29.

Found (%): C 66.52, H 9.14, N 17.33.

9-Azajulolidine borane (17s)

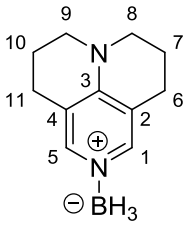

17s was prepared according to general procedure A. 9-Azajulolidine (**41s**, 1.30 g, 7.46 mmol, 1.00 eq.) was dissolved in 15 mL THF under N_2 atmosphere. The solution was cooled to 0 °C and a $H_3B{\bullet}SMe_2$ solution (5 M in Et_2O, 1.64 mL, 1.10 eq.) was added. After 10 minutes the external cooling was removed and 100 mL isohexane were added while stirring vigorously. Within 5 minutes a white precititate had formed. The precipitate was filtered off and washed three times with isohexane. After removing all residues of solvent under reduced pressure, **17s** was obtained as a white solid (0.96 g, 5.10 mmol, 68 %).

Decomposition point: 143.5 – 144.5 °C.

^{1}H NMR (300 MHz, $CDCl_3$) δ = 7.63 (s, 2H, H-C1 and H-C5), 3.30 (t, J = 5.7 Hz, 4H, H_2-C9 and H_2-C8), 2.62 (t, J = 6.2 Hz, 4H, H_2-C6 and H_2-C11), 1.92 (tt, J = 6.1 Hz, J = 5.7 Hz, 4H, H_2-C7 and H_2-C10), 3.06-1.63 (broad, q, 3H, H_3-B) ppm.

^{13}C NMR (75 MHz, $CDCl_3$) δ = 148.53 (C3), 143.35 (C1 and C5), 115.52 (C2 and C4), 49.25 (C8 and C9), 24.12 (C6 and C11), 20.26 (C7 and C10) ppm.

{^{1}H} ^{11}B NMR (270 MHz, $CDCl_3$) δ = −14.15 (s) ppm.

^{11}B NMR (270 MHz, $CDCl_3$) δ = −14.15 (broad, q) ppm.

IR (ATR) $\tilde{\nu}$ (cm^{-1}): 2945 (w), 2848 (w), 2349 (m), 2291 (m), 2249 (m), 1632 (s), 1564 (w), 1539 (s), 1502 (w), 1464 (m), 1444 (m), 1434 (m), 1413 (m), 1358 (w), 1325 (s), 1278 (m), 1206 (w), 1176 (m), 1138 (vs), 1074 (m), 1053 (m), 941 (m), 909 (s), 891 (s), 846 (m), 745 (m).

MS (70 eV, EI) m/z (%): 188 ($[M]^+$, 4), 187 ($[M-H]^+$, 26), 186 ($[M-2H]^+$, 10), 174 ($[M-BH_3]^+$, 67), 173 ($[M-H-BH_3]^+$, 100), 145 (11), 83 (16).

HRMS (70 eV, EI): $C_{11}H_{17}BN_2$ calc. 188.1485 g/mol $[M]^+$, found 188.1386 g/mol.

Elemental analysis [$C_{11}H_{17}BN_2$]

Calc. (%): C 70.25, H 9.11, N 14.89.

Found (%):C 68.73, H 8.97, N 14.30.

Pyridine borane (17t)[86]

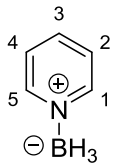

Pyridine (0.95 g, 12.01 mmol, 1.00 eq.) was dissolved in 5 mL THF under N_2 atmosphere. The solution was cooled to 0 °C and a $H_3B{\bullet}SMe_2$ solution (5 M in Et_2O, 2.64 mL, 1.10 eq.) was added. After 10 minutes the external cooling was removed and 50 mL isohexane were added while stirring vigorously. At the bottom of the flask a second layer of the liquid crude product had formed. The upper solvent phase was removed and the crude product was washed twice with isohexane. After removing all residues of solvent under reduced pressure, **17t** was obtained as a colorless oil (0.40 g, 4.30 mmol, 36 %).

^{1}H NMR (300 MHz, $CDCl_3$) δ = 8.47 (d, *J* = 5.5 Hz, 1H, H-C3), 7.90 – 7.85 (m, 2H, H-C1 and H-C5), 7.48 – 7.42 (m, 2H, H-C2 and H-C4) 2.98 – 2.05 (broad, q, 3H, H_3-B) ppm.

^{13}C NMR (75 MHz, $CDCl_3$) δ = 147.30 (C3), 139.40 (C1 and C5), 125.54 (C2 and C4) ppm.

{^{1}H} ^{11}B NMR (270 MHz, $CDCl_3$) δ = −12.22 (s) ppm.

^{11}B NMR (270 MHz, $CDCl_3$) δ = −12.22 (q, *J* = 96.9 Hz) ppm.

IR (ATR) $\tilde{\nu}$ (cm^{-1}): 3068 (vw), 2360 (s), 2310 (s), 2281 (m), 2086 (w), 1855 (w), 1621 (m), 1576 (w), 1486 (m), 1475 (s), 1401 (vw), 1344 (w), 1254 (w), 1167 (s), 1090 (s), 1060 (m), 1023 (m), 967 (w), 925 (m), 751 (s), 705 (w), 684 (s).

MS (70 eV, EI) m/z (%): 93 ($[M]^+$, 6), 92 ($[M\text{-}H]^+$, 100), 91 ($[M\text{-}2H]^+$, 46), 90 ($[M\text{-}3H]^+$, 34), 79 ($[M\text{-}BH_3]^+$, 28), 65 (12), 64 (14), 63 (14), 52 (15).

HRMS (70 eV, EI): C_5H_8BN calc. 93.0750 g/mol $[M]^+$, found 93.0703 g/mol.

Elemental analysis [C_5H_8BN]

Calc. (%): C 64.62, H 8.68, N 15.07.

Found (%): C 64.38, H 8.53, N 16.07.

1-Methylbenzotriazole borane (17u)

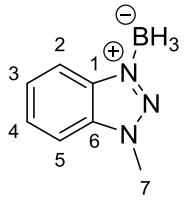

17u was prepared according to general procedure A. 1-Methylbenzotriazole (**41u**, 0.66 g, 5.00 mmol, 1.00 eq.) was dissolved in 15 mL THF under N_2 atmosphere. The solution was cooled to 0 °C and a $H_3B{\bullet}SMe_2$ solution (5 M in Et_2O, 1.10 mL, 1.10 eq.) was added. A white precipitate is forming immediately. After 10 minutes the external cooling was removed and 100 mL isohexane were added while stirring vigorously. The precipitate was filtered off and washed three times with isohexane. After removing all residues of solvent under reduced pressure, **17u** was obtained as a white solid (0.71 g, 4.81 mmol, 97 %).

Decomposition point: 199.3 – 199.8 °C.

^{1}H NMR (300 MHz, $CDCl_3$) δ = 8.15 (m, 1H, H-C2), 7.72 – 7.53 (m, 3H, H-C3, H-C4 and H-C5), 4.37 (s, 3H, H_3-C7), 3.30-1.90 (broad, q, 3H, H_3-B) ppm.

^{13}C NMR (75 MHz, $CDCl_3$) δ = 139.71 (C1), 134.06 (C6), 129.28 (C3), 127.28 (C4), 117.96 (C2), 110.19 (C5), 35.72 (C7) ppm.

{^{1}H} ^{11}B NMR (270 MHz, $CDCl_3$) δ = −20.00 (s) ppm.

^{11}B NMR (270 MHz, $CDCl_3$) δ = −20.01 (broad, q) ppm.

IR (ATR) $\tilde{\nu}$ (cm^{-1}): 3203 (w), 2356 (s), 2263 (m), 1602 (w), 1559 (vw), 1497 (w), 1464 (m), 1431 (w), 1332 (w), 1314 (w), 1285 (w), 1246 (w), 1152 (s), 1125 (m), 1064 (w), 996 (w), 977 (w), 920 (m), 847 (vw), 775 (m), 749 (vs), 668 (w).

MS (70 eV, EI) m/z (%): 147 ($[M]^+$, 7) 146 ($[M-H]^+$, 83), 145 ($[M-2H]^+$, 31), 133 ($[M-BH_3]^+$, 93), 116 (17), 105 (100), 104 (31), 102 (38), 90 (57), 78 (25), 77 (53), 76 (17), 75 (17), 64 (23), 63 (38), 51 (18), 50 (14).

HRMS (70 eV, EI): $C_7H_{10}BN_3$ calc. 147.0968 g/mol $[M]^+$, found 147.0906 g/mol.

Elemental analysis [$C_7H_{10}BN_3$]

Calc. (%): C 57.20, H 6.86, N 28.59.

Found (%): C 55.34, H 6.67, N 27.77.

1-Butyl-3-methylimidazol-2-ylidene borane (17x)[54]

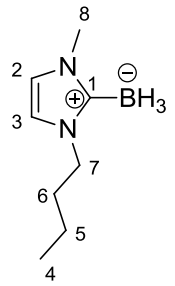

NaHMDS (1 M in THF, 54.96 ml, 54.96 mmol, 1.2 eq.) was added to a suspension of 1-butyl-3-methylimidazolium chloride (8.00 g, 45.80 mmol, 1.0 eq.) in dry THF (120 ml) at −78 °C. The resulting mixture was stirred at −78 °C for 1 h then warmed to room temperature. Trimethylamine-borane (3.27 g, 44.88 mmol, 0.98 eq.) was added and the solution was refluxed for 2 h and concentrated in vacuo. The crude product was purified by column chromatography on silica (0.035-0.070 mm, 60 Å/ DCM; R_f=0.55). We obtained **17x** (5.75g, 37.84 mmol, 84 %) as a colorless liquid.

Melting point: −65 to −63 °C.

^{1}H NMR (300 MHz, $CDCl_3$) δ = 6.80 (s, 2H, H-C2 and H-C3), 4.10 – 4.05 (m, 2H, H_2-C7), 3.70 (s, 3H, H_3-C8), 1.78 – 1.68 (m, 2H, H_2-C6), 1.39 – 1.27 (m, 2H, H_2-C5), 0.92 (t, ^3J = 7.32 Hz, 3H, H_3-C4), 1.42 – 0.56 (broad, q, 3H, H_3-B) ppm.

^{13}C NMR (75 MHz, $CDCl_3$) δ = 13.59 (C4), 19.65 (C5), 32.15 (C8), 35.75 (C6), 48.52 (C7), 118.74 (C2/3), 119.95 (C2/3).

{^{1}H} ^{11}B NMR (270 MHz, $CDCl_3$) δ = −38.34 (s) ppm.

^{11}B NMR (270 MHz, $CDCl_3$) δ = −38.34 (q) ppm.

IR (ATR) $\tilde{\nu}$ (cm^{-1}): 3128 (w), 2958 (m), 2934 (m), 2874 (m), 2335 (s), 2275 (vs), 1572 (w), 1474 (vs), 1411 (m), 1379 (m), 1290 (w), 1238 (s), 1214 (w), 1179 (m), 1125 (vs), 1058 (w), 946 (w), 864 (m), 724 (vs), 680 (w).

MS (70 eV, EI) m/z (%): 152 ($[M]^+$, 4), 151 ($[M-H]^+$, 23), 150 ($[M-2H]^+$, 16), 149 ($[M-3H]^+$, 100), 148 ($[M-4H]^+$, 31), 147 ($[M-5H]^+$, 11), 133 (13), 121 (67), 120 (19), 119 (16), 109 (10), 95 (23), 66 (16), 45 (18), 42 (14), 41 (11).

HRMS (70 eV, EI): $C_8H_{17}BN_2$ calc. 152.1485 g/mol $[M]^+$, found 152.1422 g/mol.

Elemental analysis [$C_8H_{17}BN_2$]

Calc. (%): C 63.20, H 11.27, N 18.42.

Found (%): C 62.66, H 11.48, N 18.42.

1,3-Dimethylimidazol-2-ylidene-borane (17y)[54]

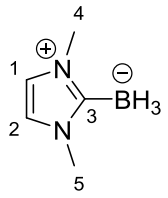

A vacuum dried, N_2 atmosphere Schlenk flask fitted with a reflux condenser was prepared and 1,3- dimethylimidazolium dimethyl phosphate salt (5.40 g, 24.30 mmol, 1.00 eq.) was dissolved in THF. A acetone/dry ice bath was used to cool the flask to -78 °C before the addition of sodium bis(trimethylsilyl)amide (5.32 g, 29.01 mmol, 1.20 eq.). The mixture was then left to stir for 1 hour. After an hour had passed the acetone/dry ice bath was removed and the borane-ammonia complex (0.74 g, 23.81 mmol, 0.98 eq.) added. An oil bath was introduced at this point and the flask heated to 70 °C. The reaction mixture was then left to reflux for two hours. Afterwards the solvent was removed under reduced pressure. This left an orange solid along with some fine crystals. Column chromatography on silica (0.035-0.070 mm, 60 Å/ DCM; R_f=0.7) led to the pure product **17y** as a white solid (1.12 g, 10.21 mmol, 42 %).

Melting point: 133.5 – 134.5 °C.

^{1}H NMR (300 MHz, $CDCl_3$) δ = 6.78 (s, 2H, H-C1, H-C2), 3.70 (s, 6H, H_3-C4, H_3-C5), 1.41-0.55 (broad, q, 3H, H_3-B) ppm.

^{13}C NMR (75 MHz, $CDCl_3$) δ = 119.91 (C1 and C2), 35.88 (C4 and C5) ppm.

{^{1}H} ^{11}B NMR (270 MHz, $CDCl_3$) δ = −37.49 (s) ppm.

^{11}B NMR (270 MHz, $CDCl_3$) δ = −37.49 (q, J = 86.5 Hz) ppm.

IR (ATR) $\tilde{\nu}$ (cm^{-1}): 3167 (w), 3132 (m), 2942 (w), 2270 (s), 2214 (m), 1574 (m), 1477 (s), 1445 (m), 1424 (m), 1412 (m), 1356 (m), 1334 (w), 1238 (s), 1187 (w), 1117 (s), 1096 (s), 1031 (m), 858 (m), 736 (s), 657 (m).

MS (70 eV, EI) m/z (%): 109 ($[M-H]^+$, 84), 108 ($[M-2H]^+$, 50), 107 ($[M-3H]^+$, 23), 97 (11), 96 ($[M-BH_3]^+$, 21), 93 (13), 92 (45), 91 (23), 85 (11), 83 (13), 81 (23), 79 ($[M-2Me-H]^+$, 100), 78 (15), 69 (14), 66 (19), 65 (11), 57 (27), 56 (12), 55 (18), 52 (44), 51 (22), 50 (18), 44 (49), 43 (11), 42 (17), 41 (18).

HRMS (70 eV, EI): $C_5H_{11}BN_2$ calc. 109.0932 g/mol $[M-H]^+$, found 109.0935 g/mol.

Elemental analysis [$C_5H_{11}BN_2$]

Calc. (%): C 54.61, H 10.08, N 25.47.

Found (%):C 54.31, H 9.89, N 24.57.

4-Diethylaminopyridine (DEAP, 24)

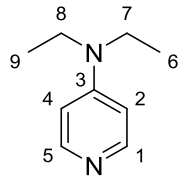

Under a N_2 atmosphere, *para*-aminopyridine (3.00 g, 31.88 mmol, 1.00 eq.) was dissolved in 200 mL THF. Afterwards *n*-butyllithium (1.6 M in hexane, 22.90 mL, 36.66 mmol, 1.15 eq.) was slowly added at room temperature. A chewy precipitate was formed, which was vigorously stirred for 30 minutes until a homogenious suspension had formed. Afterwards ethyl iodide (2.95 mL, 36.66 mmol, 1.15 eq.) was added at room temperature and the mixture was stirred until a clear yellow solution had formed (ca. 20 minutes). Subsequently *n*-butyllithium (1.6 M in hexane, 22.90 mL, 36.66 mmol, 1.15 eq.) was again slowly added at room temperature. The red brown clear solution was stirred for 20 minutes, followed by the addition of ethyl iodide (2.95 mL, 36.66 mmol, 1.15 eq.). After stirring for 15 minutes, distilled water (30 mL) was added, the aqueous phase was three times extracted with chloroform, the organic layer was dried over $MgSO_4$ and the solvent was removed under reduced pressure. To the brown oily crude product isohexane (10 mL) was added and vigorously stirred for one minute. Over an unsoluble oil at the bottom of the flask, a cloudy isohexane phase had formed. The upper hazy isohexane layer was wasted and the procedure repeated. Afterwards the residues of solvent were removed under reduced pressure and ethyl acetate (30 mL) was added to the crude product. After stirring for one minute a brown tar had deposited at the bottom of the flask and the organic layer above had become cloudy due to precipitation of pyridinium salts. This suspension was filtered off and all volatiles of the clear yellow solution were removed under reduced pressure. **24** was obtained as a slightly yellow wax (1.39 g, 9.25 mmol, 29 %).

^{1}H NMR (300 MHz, $CDCl_3$) δ = 8.10 (dd, *J* = 5.0 Hz, 1.6 Hz, 2H, H-C1 and H-C5), 6.39 (dd, *J* = 5.0 Hz, 1.6 Hz, 2H, H-C2 and H-C4), 3.29 (q, *J* = 7.1 Hz, 4H, H_2-C7 and H_2-C8), 1.11 (t, *J* = 7.1 Hz, 6H, H_3-C6 and H_3-C9) ppm.

^{13}C NMR (75 MHz, $CDCl_3$) δ = 152.01 (C3), 149.64 (C1 and C5), 106.18 (C2 and C4), 43.69 (C7 and C8), 12.22 (C6 and C9) ppm.

IR (ATR) $\tilde{\nu}$ (cm^{-1}): 3251 (w), 3092 (w), 2972 (m), 2932 (w), 2873 (w), 2508 (vw), 1643 (w), 1594 (vs), 1536 (m), 1516 (s), 1482 (w), 1469 (m), 1449 (m), 1410 (m), 1377 (m), 1356 (m), 1278 (m), 1256 (w),1229 (m), 1216 (m), 1192 (m), 1164 (w), 1107 (m), 1094 (m), 1077 (m), 1013 (m), 984 (s), 907 (w), 802 (s), 724 (m).

MS (70 eV, EI) m/z (%): 150 ($[M]^+$, 34), 136 ($[M\text{-}CH_2]^+$, 11), 135 ($[M\text{-}Me]^+$, 100), 107 (70), 78 (18), 51 (15).

HRMS (70 eV, EI): $C_9H_{14}N_2$ calc. 150.1157 g/mol $[M]^+$, found 150.1150 g/mol.

Elemental analysis [$C_9H_{14}N_2$]

Calc. (%): C 71.96, H 9.39, N 18.65.

Found (%): C 71.15, H 8.96, N 18.63.

4-Diethylaminopyridine (DEAP borane, 17z)

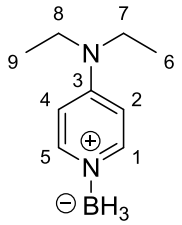

4-Diethylaminopyridine (**24**, 1.50 g, 9.96 mmol, 1.00 eq.) was dissolved in 4 mL THF under N_2 atmosphere. The solution was cooled to 0 °C and a $H_3B{\bullet}SMe_2$ solution (5 M in Et_2O, 2.19 mL, 1.10 eq.) was added. After 10 minutes the external cooling was removed and 20 mL isohexane were added while stirring vigorously. Within 5 minutes a white precititate had formed. The precipitate was filtered off and washed three times with isohexane. The crude product (1.27 g) was dissolved in benzene (10 mL), where an unsoluble precipitate forms. This solid was filtered off and wasted. Benzene was removed under reduced pressure from the crude product. After recrystallisation from benzene (4 mL), **17z** was obtained as a white solid (0.96 g, 5.88 mmol, 59 %).

Melting point: 114.5 – 115.0 °C.

^{1}H NMR (300 MHz, C_6D_6) δ = 7.94 (d, *J* = 7.4 Hz, 2H, H-C1 and H-C5), 5.66 (d, *J* = 7.5 Hz, 2H, H-C2 and H-C4), 2.51 (q, *J* = 7.1 Hz, 4H, H_2-C7 and H_2-C8), 0.55 (t, *J* = 7.1 Hz, 6H, H_3-C6 and H_3-C9), 3.93-2.98 (broad, q, 3H, H_3-B) ppm.

^{13}C NMR (75 MHz, C_6D_6) δ = 152.04 (C3), 146.78 (C1 and C5), 105.81 (C2 and C4), 43.62 (C7 and C8), 11.46 (C6 and C9) ppm.

{^{1}H} ^{11}B NMR (270 MHz, C_6D_6) δ = −12.28 (s) ppm.

^{11}B NMR (270 MHz, C_6D_6) δ = −12.27 (broad, q) ppm.

IR (ATR) $\tilde{\nu}$ (cm^{-1}): 3253 (w), 3135 (w), 2975 (m), 2930 (w), 2359 (m), 2298 (m), 2252 (m), 1631 (vs), 1540 (s), 1530 (s), 1476 (m), 1446 (m), 1416 (m), 1379 (m), 1348 (m), 1328 (m), 1307 (m), 1284 (m), 1217 (w), 1167 (s), 1127 (m), 1093 (s), 1074 (s), 1034 (s), 933 (m), 815 (s), 796 (s), 756 (m), 668 (m).

MS (70 eV, EI) m/z (%): 164 ($[M]^+$, 9), 163 ($[M-H]^+$, 89), 162 ($[M-2H]^+$, 31), 150 ($[M-BH_3]^+$, 33), 136 (10), 135 ($[M-Et]^+$, 100), 119 (14), 107 (62), 78 (17).

HRMS (70 eV, EI): $C_9H_{17}BN_2$ calc. 164.1485 g/mol $[M]^+$, found 164.1420 g/mol.

Elemental analysis [$C_9H_{17}BN_2$]

Calc. (%): C 65.89, H 10.45, N 17.08.

Found (%): C 63.62, H 9.93, N 16.47.

Imidazole borane (17aa)

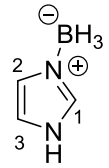

17aa was prepared according to general procedure A. Imidazole (1.00 g, 14.69 mmol, 1.00 eq.) was dissolved in 10 mL THF under N_2 atmosphere. The solution was cooled to 0 °C and a $H_3B{\bullet}SMe_2$ solution (5 M in Et_2O, 3.23 mL, 1.10 eq.) was added. After 10 minutes the external cooling was removed and 100 mL isohexane were added while stirring vigorously. Within 5 minutes a white precititate had formed. The precipitate was filtered off and washed three times with isohexane. After removing all residues of solvent under reduced pressure, **17aa** was obtained as a white solid (1.17 g, 14.25 mmol, 97 %).

Decomposition point: 90.9 – 91.2 °C.

^{1}H-NMR (300 MHz, DMSO-d_6) δ = 13.17-12.78 (broad, 1H, H-N), 8.19 (s, 1H, H-C1), 7.29 (t, *J* = 1.52 Hz, 1H, H-C2), 7.00 (t, *J* = 1.52 Hz, 1H, H-C3), 2.58-1.55 (broad, q, 3H, H_3-B) ppm.

^{13}C-NMR (75 MHz, DMSO-d_6) δ = 136.12 (C1), 126.36 (C2), 118.46 (C3) ppm.

{^{1}H} ^{11}B-NMR (270 MHz, DMSO-d_6) δ = −18.65 ppm.

^{11}B-NMR (270 MHz, DMSO-d_6) δ = −18.66 (broad, q) ppm.

IR (ATR) $\tilde{\nu}$ (cm^{-1}): 3282 (vs), 3136 (s), 3070 (w), 2990 (w), 2867 (w), 2580 (w), 2305 (vs), 2260 (vs), 1713 (w), 1698 (w), 1620 (m), 1559 (s), 1526 (m), 1488 (w), 1439 (m), 1349 (m), 1283 (w), 1195 (s), 1140 (s), 1103 (s), 1076 (s), 992 (m), 957 (m), 915 (w), 847 (vs), 772 (s), 761 (s), 701 (vs).

MS (70 eV, EI) m/z (%): 82 ($[M]^+$, 4), 81 ($[M-H]^+$, 100), 80 ($[M-2H]^+$, 42), 79 ($[M-3H]^+$, 10), 68 ($[M-BH_3]^+$, 16), 53 (21), 52 (24).

HRMS (70 eV, EI): $C_3H_7BN_2$ calc. 82.0702 g/mol $[M]^+$, found 82.0703 g/mol.

Elemental analysis [$C_3H_7BN_2$]

Calc. (%): C 43.99, H 8.61, N 34.20.

Found (%): C 43.36, H 8.07, N 33.78.

1,2-Dimethylbenzimidazole borane (17ab)

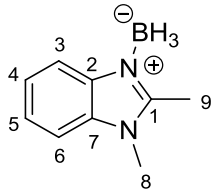

17ab was prepared according to general procedure A. 2-Methylbenzimidazole (1.00 g, 6.84 mmol, 1.00 eq.) was dissolved in 10 mL THF under N_2 atmosphere. The solution was cooled to 0 °C and a $H_3B{\bullet}SMe_2$ solution (5 M in Et_2O, 1.50 mL, 1.10 eq.) was added. After 10 minutes the external cooling was removed and 100 mL isohexane were added while stirring vigorously. Within 5 minutes a white precititate had formed. The precipitate was filtered off and washed three times with isohexane. In this case further impurities had to be removed by again precipitating the solid with isohexane from a saturated DCM solution. As the product still showed small traces of impurity (^{1}H-NMR), a column chromatography on silica (0.035-0.070 mm, 60 Å/ ethyl acetate : DCM : Et_3N = 10 : 1 : 1; R_f=0.57) lead to the pure product **17ab** as a white solid (0.20 g, 1.23 mmol, 18 %).

Decomposition point: 147.5 – 147.8 °C.

^{1}H-NMR (300 MHz, $CDCl_3$) δ = 8.02 – 7.98 (m, 1H, H-C3), 7.44 – 7.33 (m, 3H, H-C4, H-C5 and H-C6), 3.79 (s, 3H, H_3-C8), 2.76 (s, 3H, H_3-C9), 2.94 - 1.69 (broad, q, 3H, H_3-B) ppm.

^{13}C-NMR (75 MHz, $CDCl_3$) δ = 150.89 (C1), 136.79 (C2), 132.65 (C7), 124.30 (C4 or C5), 124.15 (C4 or C5), 117.30 (C3), 109.52 (C6), 30.50 (C8), 11.38 (C9) ppm.

{^{1}H} ^{11}B-NMR (270 MHz, $CDCl_3$) δ = −23.76 (s) ppm.

^{11}B-NMR (270 MHz, $CDCl_3$) δ = −23.85 (broad, q) ppm.

IR (ATR)) $\tilde{\nu}$ (cm^{-1}): 3068 (w), 2952 (w), 2377 (m), 2313 (m), 2270 (m), 2093 (w), 1941 (vw), 1901 (vw), 1782 (vw), 1683 (vw), 1621 (w), 1596 (w), 1521 (m), 1482 (m), 1460 (s), 1419 (m), 1382 (m), 1344 (m), 1304 (m), 1248 (m), 1208 (vw), 1164 (vs), 1124 (m), 1041 (m), 1006 (m), 982 (m), 936 (m), 846 (w), 761 (m), 740 (vs), 686 (m).

MS (70 eV, EI) m/z (%): 160 ($[M]^+$, 8), 159 ($[M-H]^+$, 100), 158 ($[M-2H]^+$, 40), 157 ($[M-3H]^+$, 16), 146 ($[M-BH_3]^+$, 42), 145 ($[M-BH_3-H]^+$, 21), 131 ($[M-BH_3-CH_3]^+$, 18), 116 ($[M-BH_3-CH_3-CH_3]^+$, 11), 77 (14).

HRMS (70 eV, EI): $C_{19}H_{13}BN_2$ calc. 160.1172 g/mol $[M]^+$, found 160.1131 g/mol.

Elemental analysis [$C_{19}H_{13}BN_2$]

Calc. (%): C 67.55, H 8.19, N 17.51.

Found (%): C 67.49, H 8.22, N 17.43.

2-Nonyl-benzimidazole (32ac)

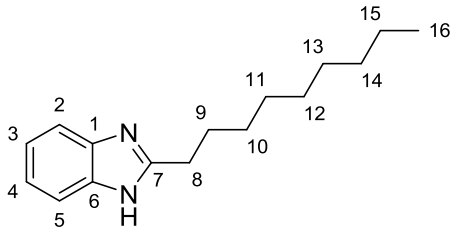

Ortho-phenylenediamine (**35e**, 5.00 g, 46.30 mmol, 1.00 eq.) and decanal (**35f**, 7.24 g, 46.30 mmol, 1.00 eq.) were combined in a 250 mL flask under ambient air and stirred for 10 minutes at 200 °C without solvent. The crude product was cooled to room temperature and washed with 20 mL isohexane to remove remaining aldehyde. The residue was distilled under a nitrogen atmosphere at $5x10^{-2}$ mbar and 200 °C to remove unreacted diamine. Afterwards the distillation temperature was raised to 250 °C (same pressure) which delivers the desired product as a pale yellow wax (when cooled down). The distillation process was three times repeated, which yielded 1.99 g 2-nonyl-benzimidazole (**32ac**, 8.12 mmol, 18 %) as pale yellow wax.

Melting point: 120.7 – 121.4 °C.

^{1}H-NMR (300 MHz, $CDCl_3$) δ = 12.43 – 11.93 (broad, s, 1H, H-N), 7.57 (dd, *J* = 6.0 Hz, 3.2 Hz, 2H, H-C2 and H-C5), 7.22 (dd, *J* = 6.0 Hz, 3.2 Hz, 2H, H-C3 and H-C4), 2.98 (t, *J* = 7.8 Hz, 2H, H_2-C8), 1.94 – 1.83 (m, 2H, H_2-C9), 1.42 – 1.13 (m, 12H, H_2-C10, H_2-C11, H_2-C12, H_2-C13, H_2-C14 and H_2-C15), 0.85 (t, *J* = 6.8 Hz, 3H, H_3-C16) ppm.

^{13}C-NMR (75 MHz, $CDCl_3$) δ = 155.79 (C7), 138.63 (C1 and C6), 121.98 (C3 and C4), 114.57 (C2 and C5), 31.81 (C14), 29.43 ($C_{aliphatic}$), 29.41 ($C_{aliphatic}$), 29.40 ($C_{aliphatic}$), 29.34 ($C_{aliphatic}$), 29.24 ($C_{aliphatic}$), 28.48 (C9), 22.62 (C15), 14.06 (C16) ppm.

IR (ATR) $\tilde{\nu}$ (cm^{-1}): 3087 (w), 3051 (w), 2951 (m), 2922 (s), 2851 (s)2743 (m), 2633 (m), 1621 (w), 1590 (w), 1539 (m), 1482 (w), 1453 (s), 1419 (s), 1377 (w), 1349 (w), 1340 (w), 1321 (w), 1271 (s), 1238 (w), 1217 (m), 1197 (m), 1154 (w), 1110 (w), 1027 (m), 1004 (m), 965 (w), 928 (m), 907 (m), 872 (m), 775 (w), 767 (w), 749 (s), 740 (s), 724 (s).

MS (70 eV, EI) m/z (%): 244 ($[M]^+$, 16), 201 ($[M\text{-}C_3H_7]^+$, 12), 187 ($[M\text{-}C_4H_9]^+$, 19), 146 ($[M\text{-}C_7H_{14}]^+$, 17), 145 ($[M\text{-}C_7H_{15}]^+$, 50), 133 ($[M\text{-}C_8H_{15}]^+$, 10), 132 ($[M\text{-}C_8H_{16}]^+$, 100), 131 ($[M\text{-}C_8H_{17}]^+$, 14).

HRMS (70 eV, EI): $C_{16}H_{24}N_2$ calc. 244.1939 g/mol $[M]^+$, found 244.1941 g/mol.

Elemental analysis [$C_{16}H_{24}N_2$]

Calc. (%): C 78.64, H 9.90, N 11.46.

Found (%): C 78.73, H 9.89, N 11.41.

2-Nonyl-benzimidazole borane (17ac)

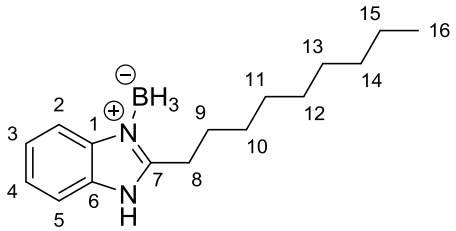

17ac was prepared according to general procedure A. 2-nonyl-benzimidazole (**32ac**, 1.00 g, 4.09 mmol, 1.00 eq.) was dissolved in 5 mL THF under N_2 atmosphere. The solution was cooled to 0 °C and a $H_3B{\bullet}SMe_2$ solution (5 M in Et_2O, 0.90 mL, 1.10 eq.) was added. After 10 minutes the external cooling was removed and 50 mL isohexane were added while stirring vigorously. Within 5 minutes a white precititate had formed. The precipitate was filtered off and washed three times with isohexane. After removing all residues of solvent under reduced pressure, **17ac** was obtained as a white solid (1.01 g, 0.93 mmol, 96 %).

Melting point: 69.8 – 70.2 °C.

^{1}H-NMR (300 MHz, C_6D_6) δ = 9.41 (broad, s, 1H, H-N), 8.18 (d, *J* = 8.2 Hz, 1H, H-C2), 7.19 (d, *J* = 8.2 Hz, 1H, H-C5), 7.10 - 7.00 (m, 2H, H-C3 and H-C4), 3.72 – 2.67 (broad, q, 3H, H_3-B), 2.90 (t, *J* = 7.9, 2H, H_2-C8), 1.66 – 1.51 (m, 2H, H_2-C9), 1.32 – 1.02 (m, 12H, H_2-C10, H_2-C11, H_2-C12, H_2-C13, H_2-C14 and H_2-C15), 0.85 (t, *J* = 7.0 Hz, 3H, H_3-C16) ppm.

^{13}C-NMR (75 MHz, C_6D_6) δ = 153.96 (C7), 137.85 (C1), 130.72 (C6), 124.14 (C3 or C4), 123.75 (C3 or C4), 117.07 (C2), 111.31 (C5), 31.86 (C14), 29.41 ($C_{aliphatic}$), 29.28 ($C_{aliphatic}$), 29.24 ($C_{aliphatic}$), 29.19 ($C_{aliphatic}$), 27.05 ($C_{aliphatic}$), 26.58 ($C_{aliphatic}$), 22.67 (C15), 13.95 (C16) ppm.

{^{1}H} ^{11}B-NMR (270 MHz, C_6D_6) δ = −21.01 (s) ppm.

^{11}B-NMR (270 MHz, C_6D_6) δ = −21.03 (broad, q) ppm.

IR (ATR) $\tilde{\nu}$ (cm^{-1}): 3262 (w), 2953 (m), 1921 (s), 2852 (m), 2434 (m), 2376 (w), 2302 (w), 2261 (w), 1610 (w), 1543 (w), 1454 (s), 1378 (w), 1300 (m), 1242 (w), 1194 (m), 1140 (s), 1123 (s), 1099 (s), 1047 (m), 1014 (m), 961 (m), 933 (m), 859 (w), 738 (s), 723 (s), 667 (m).

MS (70 eV, EI) m/z (%): 258 ($[M]^+$, 5), 257 ($[M-H]^+$, 16), 255 ($[M-3H]^+$, 10), 244 ($[M-BH_3]^+$, 18), 201 ($[M-BH_3-C_3H_7]^+$, 12), 187 ($[M-BH_3-C_4H_9]^+$, 21), 171 (17), 159 (10), 157 (11), 146 (18), 145 (58), 133 (12), 132 ($[M-BH_3-C_8H_{16}]^+$, 100), 131 (19).

HRMS (70 eV, EI): $C_{16}H_{27}BN_2$ calc. 258.2267 g/mol $[M]^+$, found 258.2267 g/mol.

Elemental analysis [$C_{16}H_{27}BN_2$]

Calc. (%):	C 74.42	H 10.54	N 10.84.
Found (%):	C 74.24	H 9.63	N 10.44.

2-Phenylbenzimidazole borane (17ae)

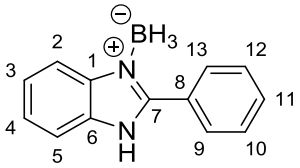

17ae was prepared according to general procedure A. 2-Phenylbenzimidazole (1.00 g, 5.15 mmol, 1.00 eq.) was dissolved in 10 mL THF under N_2 atmosphere. The solution was cooled to 0 °C and a $H_3B{\bullet}SMe_2$ solution (5 M in Et_2O, 1.13 mL, 1.10 eq.) was added. After 10 minutes the external cooling was removed and 100 mL isohexane were added while stirring vigorously. Within 5 minutes a white precititate had formed. The precipitate was filtered off and washed three times with isohexane. After removing all residues of solvent under reduced pressure, **17ae** was obtained as a white solid (1.01 g, 4.84 mmol, 94 %).

Decomposition point: 244.5 – 245.1 °C.

^{1}H NMR (300 MHz, DMSO-*d*$_6$) δ = 13.87 (broad, s, 1H, H-N), 8.03 – 7.96 (m, 2H, H-C9 and H-C13), 7.92 – 7.94 (m, 1H, aromatic), 7.68 – 7.56 (m, 4H, aromatic), 7.46 – 7.38 (m, 2H, H aromatic), 2.74 – 1.85 (broad, q, 3H, H_3-B) ppm.

^{13}C NMR (75 MHz, DMSO-*d*$_6$) δ = 151.02 (C7), 138.40 (C1), 132.14 (C6), 131.55 (C8), 130.78 (C9 and C13), 129.36 (C11), 128.67 (C10 and C12), 125.19 (C3 or C4), 124.31 (C3 or C4), 117.20 (C2), 112.91 (C5) ppm.

{^{1}H} ^{11}B NMR (270 MHz, DMSO-*d*$_6$) δ = −20.11 (s) ppm.

^{11}B NMR (270 MHz, DMSO-*d*$_6$) δ = −20.11 (broad, q) ppm.

IR (ATR) $\tilde{\nu}$ (cm^{-1}): 3288 (m), 3062 (w), 2926 (w), 2863 (w), 2363 (m), 2299 (m), 2251 (m), 1762 (vw), 1624 (w), 1604 (w), 1544 (m), 1498 (m), 1484 (m), 1466 (m), 1453 (s), 1427 (m), 1377 (w), 1323 (m), 1288 (w), 1244 (w), 1186 (s), 1156 (s), 1143 (s), 1077 (w), 1024 (m), 1007 (m), 990 (w), 969 (w), 944 (w), 927 (w), 895 (w), 808 (w), 772 (m), 753 (m), 741 (vs), 697 (s), 690 (s), 670 (m).

MS (70 eV, EI) m/z (%): 207 ($[M-H]^+$, 7), 205 ($[M-3H]^+$, 21), 204 (10), 194 ($[M-BH_3]^+$, 100).

HRMS (70 eV, EI): $C_{13}H_{13}BN_2$ calc. 208.1172 g/mol $[M-H]^+$, found 207.1078 g/mol.

Elemental analysis [$C_{13}H_{13}BN_2$]

Calc. (%): C 75.04, H 6.30, N 13.46.

Found (%): C 74.98, H 6.36, N 13.19.

2-(4-Fluorophenyl)-benzimidazole borane (17af)

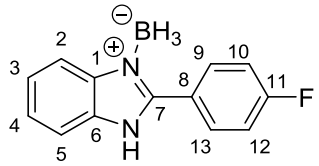

17af was prepared according to general procedure A. 2-(4-Fluorophenyl)-benzimidazole (**41pa**, 1.00 g, 4.71 mmol, 1.00 eq.) was dissolved in 10 mL THF under N_2 atmosphere. The solution was cooled to 0 °C and a $H_3B{\bullet}SMe_2$ solution (5 M in Et_2O, 1.04 mL, 1.10 eq.) was added. After 10 minutes the external cooling was removed and 100 mL isohexane were added while stirring vigorously. Within 5 minutes a white precititate had formed. The precipitate was filtered off and washed three times with isohexane. After removing all residues of solvent under reduced pressure, **17af** was obtained as a white solid (0.93 g, 4.08 mmol, 87 %).

Decomposition point: 203.8 – 204.3 °C.

^{1}H NMR (300 MHz, DMSO-d_6) δ = 13.90 (broad, s, 1H, H-N), 8.23 – 8.16 (m, 1H, aromatic), 8.11 – 8.03 (m, 1H, aromatic), 7.90 – 7.84 (m, 1H, aromatic), 7.68 – 7.61 (m, 1H, aromatic), 7.60 – 7.54 (m, 1H, aromatic), 7.52 – 7.33 (m, 3H, aromatic), 7.22 – 7.14 (m, 1H, aromatic), 2.71 – 1.83 (broad, q, 3H, H_3-B) ppm.

^{13}C NMR (75 MHz, DMSO-d_6) δ = 164.07 (d, ^1J(C,F) = 249.8 Hz, C11), 150.11 (C7), 138.34 (C1), 133.43 (d, ^3J(C,F) = 9.1 Hz, C9 and C13), 132.11 (C6), 125.22 (C3 or C4), 124.33 (C3 or C4), 123.19 (d, ^4J(C,F) = 3.2 Hz, C8), 117.18 (C2), 115.86 (d,^2J(C,F) = 22.1 Hz, C10 and C12), 112.92 (C5) ppm.

{^{1}H} ^{11}B NMR (270 MHz, DMSO-d_6) δ = −21.24 (s) ppm.

^{11}B NMR (270 MHz, DMSO-d_6) δ = −21.24 (broad, q) ppm.

^{19}F NMR (376 MHz, DMSO-d_6) δ = −108.66 ppm.

IR (ATR) $\tilde{\nu}$ (cm^{-1}): 3243 (m), 2941 (w), 2862 (w), 2789 (w), 2334 (m), 2312 (m), 2276 (m), 1769 (w), 1746 (w), 1624 (w), 1606 (m), 1557 (w), 1493 (s), 1456 (s), 1405 (w), 1371 (w), 1325 (w), 1283 (w), 1235 (s), 1202 (s), 1189 (s), 1160 (s), 1116 (w), 1101 (m), 1056 (w), 1013 (m), 1006 (m), 984 (w), 950 (w), 940 (w), 924 (w), 898 (w), 843 (vs), 824 (w), 793 (m), 766 (w), 755 (w), 739 (s), 728 (s), 707 (w).

MS (70 eV, EI) m/z (%): 213 ($[M\text{-}BH_2]^+$, 16), 212 ($[M\text{-}BH_3]^+$, 100), 211 ($[M\text{-}BH_3\text{-}H]^+$, 14).

HRMS (70 eV, EI): $C_{13}H_{12}BFN_2$ calc. 226.1078 g/mol $[M\text{-}BH_3]^+$, found 212.0735 g/mol.

Elemental analysis [$C_{13}H_{12}BFN_2$]

Calc. (%): C 69.07, H 5.35, N 12.39.

Found (%): C 68.92, H 5.24, N 12.48.

2-(3,4,5-Trimethoxyphenyl)-benzimidazole borane (17ag)

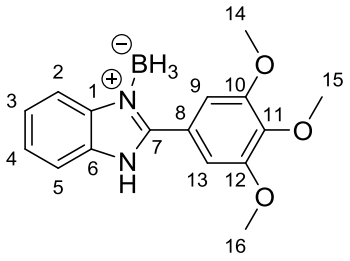

17ag was prepared according to general procedure A. 2-(3,4,5-Trimethoxyphenyl)-benzimidazole (**41oa**, 1.00 g, 3.52 mmol, 1.00 eq.) was dissolved in 10 mL THF under N_2 atmosphere. The solution was cooled to 0 °C and a $H_3B{\bullet}SMe_2$ solution (5 M in Et_2O, 0.77 mL, 1.10 eq.) was added. After 10 minutes the external cooling was removed and 100 mL isohexane were added while stirring vigorously. Within 5 minutes a white precititate had formed. The precipitate was filtered off and washed three times with isohexane. After removing all residues of solvent under reduced pressure, **17ag** was obtained as a white solid (0.94 g, 3.17 mmol, 90 %).

Decomposition point: 155.2 – 155.9 °C.

^{1}H NMR (300 MHz, $CDCl_3$) δ = 11.33 – 10.35 (broad, s, H-N), 8.05 (d, *J* = 8.0 Hz, 1H, H-C2), 7.47 – 7.35 (m, 3H, H-C3, H-C4 and H-C5), 7.13 (s, 2H, H-C9 and H-C13), 3.91 (s, 3H, H_3-C15), 3.75 (s, 6H, H_3-C14 and H_3-C16), 2.55 (broad, s, 3H, H_3-B) ppm.

^{13}C NMR (75 MHz, $CDCl_3$) δ = 152.82 (C10 and C12), 150.40 (C7), 139.74 (C11), 138.54 (C1), 131.15 (C6), 125.18 (C3 or C4), 124.46 (C3 or C4), 121.49 (C8), 117.78 (C2), 111.57 (C5), 107.54 (C9 and C13), 61.00 (C15), 56.16 (C14 and C16) ppm.

{^{1}H} ^{11}B NMR (270 MHz, $CDCl_3$) δ = −23.54 (s) ppm.

^{11}B NMR (270 MHz, $CDCl_3$) δ = −23.53 (broad, q) ppm.

IR (ATR) $\tilde{\nu}$ (cm^{-1}): 3294 (m), 2938 (w), 2855 (w), 2402 (m), 2321 (m), 2239 (m), 1763 (w), 1746 (w), 1587 (m), 1546 (w), 1491 (m), 1468 (m), 1455 (m), 1443 (m), 1429 (m), 1405 (m), 1377 (w), 1365 (w), 1339 (m), 1307 (w), 1288 (w), 1248 (s), 1223 (m), 1182 (m), 1163 (m), 1154 (m), 1124 (vs), 1069 (m), 1030 (m), 997 (s), 965 (m), 918 (w), 894 (w), 885 (m), 843 (m), 833 (m), 789 (w), 760 (s), 753 (m), 735 (w), 724 (w), 695 (w).

MS (70 eV, EI) m/z (%): 298 ($[M]^+$, 100), 297 ($[M-H]^+$, 32), 284 ($[M-BH_3]^+$, 37), 283 ($[M-BH_3-H]^+$, 53), 269 ($[M-BH_3-CH_3]^+$, 18), 225 (22), 197 (10), 146 (22), 145 (23).

HRMS (70 eV, EI): $C_{16}H_{19}BN_2O_3$ calc. 298.1489 g/mol $[M]^+$, found 298.1367 g/mol.

Elemental analysis $[C_{16}H_{19}BN_2O_3]$

Calc. (%): C 64.46, H 6.42, N 9.40.

Found (%): C 64.28, H 6.38, N 9.27.

2-Methylimidazole borane (17ah)

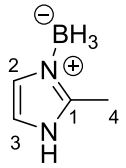

17ah was prepared according to general procedure A. 2-Methylimidazole (1.00 g, 12.19 mmol, 1.00 eq.) was dissolved in 10 mL THF under N_2 atmosphere. The solution was cooled to 0 °C and a $H_3B{\bullet}SMe_2$ solution (5 M in Et_2O, 2.68 mL, 1.10 eq.) was added. After 10 minutes the external cooling was removed and 100 mL isohexane were added while stirring vigorously. Within 5 minutes a white precititate had formed. The precipitate was filtered off and washed three times with isohexane. After removing all residues of solvent under reduced pressure, **17ah** was obtained as a white solid (1.09 g, 11.34 mmol, 93 %).

Decomposition point: 83.2 – 83.7 °C.

^{1}H NMR (300 MHz, $CDCl_3$) δ = 9.62 (broad, s, 1H, H-N), 6.94 (d, *J* = 1.8 Hz, 1H, H-C2), 6.86 (d, *J* = 1.8 Hz, 1H, H-C3), 2.49 (s, 3H, H_3-C4), 2.78 – 1.70 (broad, q, 3H, H_3-B) ppm.

^{13}C NMR (75 MHz, $CDCl_3$) δ = 144.36 (C1), 126.88 (C2), 114.91 (C3), 11.89 (C4) ppm.

{^{1}H} ^{11}B NMR (270 MHz, $CDCl_3$) δ = −20.42 (s) ppm.

^{11}B NMR (270 MHz, $CDCl_3$,) δ = −20.44 (broad, q) ppm.

IR (ATR) $\tilde{\nu}$ (cm^{-1}): 3285 (m), 2944 (w), 2863 (w), 2378 (m), 2283 (m), 2249 (s), 1762 (w), 1746 (w), 1585 (m), 1515 (m), 1436 (w), 1406 (w), 1321 (w), 1294 (m), 1199 (m), 1170 (m), 1153 (vs), 1101 (m), 1058 (m), 1044 (m), 990 (m), 962 (m), 943 (m), 919 (m), 842 (w), 824 (w), 766 (w), 747 (s), 698 (s), 660 (s).

MS (70 eV, EI) m/z (%): 96 ($[M]^+$, 5), 95 ($[M-H]^+$, 81), 94 ($[M-2H]^+$, 24), 93 ($[M-3H]^+$, 11), 82 ($[M-BH_3]^+$, 100), 81 ($[M-BH_3-H]^+$, 49), 54 (35), 53 (11), 52 (15), 42 (15), 41 (12).

HRMS (70 eV, EI): $C_4H_9BN_2$ calc. 96.0859 g/mol $[M]^+$, found 96.0800 g/mol.

Elemental analysis [$C_4H_9BN_2$]

Calc. (%): C 50.08, H 9.46, N 29.20.

Found (%): C 49.17, H 9.17, N 29.38.

4,5-Diphenylimidazole borane (17ai)

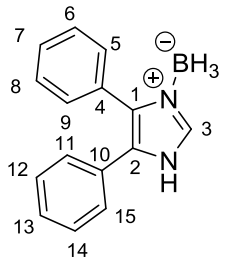

17ai was prepared according to general procedure A. 4,5-Diphenylimidazole (1.00 g, 4.54 mmol, 1.00 eq.) was dissolved in 10 mL THF under N_2 atmosphere. The solution was cooled to 0 °C and a $H_3B{\bullet}SMe_2$ solution (5 M in Et_2O, 1.00 mL, 1.10 eq.) was added. After 10 minutes the external cooling was removed and 100 mL isohexane were added while stirring vigorously. Within 5 minutes a white precititate had formed. The precipitate was filtered off and washed three times with isohexane. After removing all residues of solvent under reduced pressure, **17ai** was obtained as a white solid (0.95 g, 4.04 mmol, 89 %).

Decomposition point: 149.0 – 149.5 °C.

^{1}H NMR (300 MHz, $CDCl_3$) δ = 7.87 (s, 1H, H-C3), 7.39 – 7.36 (m, 2H, aromatic), 7.32 – 7.26 (m, 3H, aromatic), 7.22 – 7.17 (m, 3H, aromatic), 7.13 – 7.08 (m, 2H, aromatic), 2.73 – 1.86 (broad, q, 3H, H_3-B) ppm.

^{13}C NMR (75 MHz, $CDCl_3$) δ = 135.14 (C3), 134.49 (C2), 130.85 (C6 and C8), 129.55 (C4), 128.94 (C12 and C14), 128.80 (C10), 128.58 (C7), 128.51 (C8), 128.32 (C1), 128.28 (C5 and C9), 127.13 (C11 and C15) ppm.

{^{1}H} ^{11}B NMR (270 MHz, $CDCl_3$) δ = −18.96 (s) ppm.

^{11}B NMR (270 MHz, $CDCl_3$) δ = −18.95 (broad, q) ppm.

IR (ATR) $\tilde{\nu}$ (cm^{-1}): 3123 (m), 2936 (m), 2861 (w), 2791 (w), 2304 (m), 2265 (m), 1762 (w), 1746 (w), 1603 (m), 1591 (m), 1522 (m), 1492 (m), 1433 (m), 1406 (m), 1281 (w), 1188 (s), 1163 (m), 1133 (s), 1097 (m), 1073 (m), 1056 (w), 1011 (m), 960 (m), 919 (m), 892 (m), 828 (m), 775 (m), 767 (s), 749 (w), 724 (m), 697 (vs), 670 (m).

MS (70 eV, EI) m/z (%): 232 ($[M-2H]^+$, 8), 231 ($[M-3H]^+$, 19), 230 ($[M-4H]^+$, 42), 229 (39), 221 (12), 220 ($[M-BH_3]^+$, 100), 165 (47), 89 (11).

HRMS (70 eV, EI): $C_{15}H_{15}BN_2$ calc. 234.1328 g/mol $[M-2H]^+$, found 232.1222 g/mol.

Elemental analysis [$C_{15}H_{15}BN_2$]

Calc. (%): C 76.96, H 6.46, N 11.97.

Found (%): C 76.75, H 6.71, N 11.66.

***N*-methylimidazole borane (17aj)**

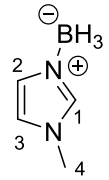

17aj was prepared according to general procedure A. *N*-Methylimidazole (**41aj**, 1.00 g, 12.19 mmol, 1.00 eq.) was dissolved in 10 mL THF under N_2 atmosphere. The solution was cooled to 0 °C and a $H_3B{\bullet}SMe_2$ solution (5 M in Et_2O, 2.68 mL, 1.10 eq.) was added. After 10 minutes the external cooling was removed. The reaction mixture was washed three times with isohexane. After each washing step, the isohexane phase (upper layer) was wasted. Finally all volatiles were removed from the crude oil under reduced pressure and **17aj** was obtained as colorless oil (0.92 g, 11.21 mmol, 92 %).

^{1}H NMR (300 MHz, $CDCl_3$) δ = 7.68 (s, 1H, H-C1), 6.99 (d, *J* = 1.65 Hz, 1H, H-C2), 6.85 (d, *J* = 1.65 Hz, 1H, H-C3), 3.71 (s, 3H, H_3-C4), 2.61 – 1.51 (broad, q, 3H, H_3-B) ppm.

^{13}C NMR (75 MHz, $CDCl_3$) δ = 136.82 (C1), 127.73 (C2), 121.02 (C3), 34.84 (C4) ppm.

{^{1}H} ^{11}B NMR (270 MHz, $CDCl_3$) δ = −20.51 (s) ppm.

^{11}B NMR (270 MHz, $CDCl_3$) δ = −20.51 (broad, q) ppm.

IR (ATR) $\tilde{\nu}$ (cm^{-1}): 3153 (s), 3082 (w), 2953 (m), 2254 (vs), 2101 (w), 1794 (m), 1645 (w), 1589 (m), 1550 (s), 1470 (m), 1425 (m), 1382 (m), 1303 (s), 1252 (m), 1173 (s), 1099 (s), 1129 (s), 1025 (m), 998 (m), 907 (vs), 826 (s).

MS (70 eV, EI) m/z (%): 96 ($[M]^+$, 6), 95 ($[M-H]^+$, 100), 94 ($[M-2H]^+$, 36), 82 ($[M-BH_3]^+$, 32), 67 ($[M-BH_3-CH_3]^+$, 17), 66 ($[M-BH_3-CH_3-H]^+$, 17), 41 (11).

HRMS (70 eV, EI): $C_4H_9BN_2$ calc. 96.0859 g/mol $[M]^+$, 96.0857 found g/mol.

Elemental analysis [$C_4H_9BN_2$]

Calc. (%): C 50.08, H 9.46, N 29.20.

Found (%): C 49.56, H 9.11, N 28.52.

Dihydrobis(4-dimethylaminopyridine)boron(1+) iodide (**29b**)

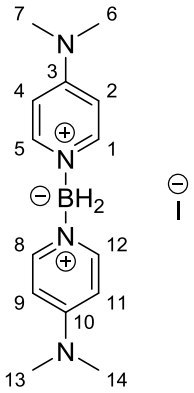

4-Dimethylaminopyridine borane (**17q**) (0.51 g, 3.74 mmol, 1.00 eq.) was dissolved in chloroform (20 mL) under a N_2 atmosphere. Afterwards iodine (0.47 g, 1.87 mmol, 0.5 eq.) was added in small portions. It should be mentioned that the solution should stay colorless and no precipitate should be formed during the addition of iodine. As soon as no elemental iodine was visible, 4-dimethylaminopyridine (**27**) (0.46 mg, 3.74 mmol, 1.00 eq.) was added and stirred for 5 minutes. 10 mL of 2M NaOH were added, the organic phase was removed, dried over $MgSO_4$ and the solvent removed under reduced pressure. The white crude product was washed twice with boiling THF (20 mL). Residues of solvent were removed and **29b** was obtained as a white solid (0.24 g, 0.63 mmol, 17 %).

Melting point: 196.0 – 196.7 °C.

^{1}H NMR (300 MHz, $CDCl_3$) δ = 8.05 (d, *J* = 7.6 Hz, 4H, H-C1, H-C5, H-C8 and H-C12), 6.75 (d, *J* = 7.6 Hz, 4H, H-C2, H-C4, H-C9, H-C11), 3.15 (s, 12H, H_3-C6, H_3-C7, H_3-C13, H_3-C14) ppm.

^{13}C NMR (75 MHz, $CDCl_3$) δ = 155.96 (C3 and C10), 145.76 (C1, C5, C8 and C12), 107.87 (C2, C4, C9 and C11), 40.18 (C6, C7, C13 and C14) ppm.

{^{1}H} ^{11}B NMR (270 MHz, $CDCl_3$) δ = +0.22 ppm.

^{11}B NMR (270 MHz, $CDCl_3$) δ = +0.22 (s) ppm.

IR (ATR) $\tilde{\nu}$ (cm^{-1}): 3468 (w), 3056 (w), 2927 (w), 2630 (w), 2415 (w), 2359 (w), 2293 (w), 1628 (vs), 1556 (s), 1530 (m), 1487 (w), 1443 (w), 1398 (m), 1345 (m), 1317 (w), 1227 (m), 1190 (w), 1154 (s), 1125 (m), 1092 (vs), 1034 (m), 1012 (m), 965 (w), 945 (w), 890 (w), 841 (w), 819 (s), 808 (s), 788 (m), 744 (m), 672 (m), 658 (w).

HRMS (ESI+): $[C_{14}H_{22}BN_4]^+$ calc. 257.1932 g/mol $[M]^+$, found 257.1934 g/mol.

HRMS (ESI-): $[I]^-$ calc. 126.9050 g/mol $[M]^+$, found 126.9050 g/mol.

Elemental analysis $[C_{14}H_{22}BIN_4]$

Calc. (%): C 43.78, H 5.77, N 14.59.

Found (%):C 43.84, H 5.82, N 14.60.

Dihydrobis(4-dimethylaminopyridine)boron(1+) bromide (**29t**)

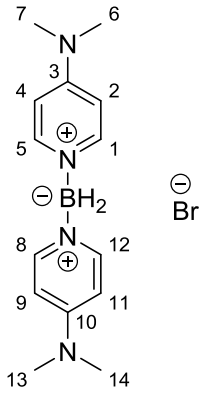

4-Dimethylaminopyridine borane (**17q**) (1.01 g, 7.43 mmol, 1.00 eq.) was dissolved in chloroform (30 mL) under a N_2 atmosphere. Afterwards bromine (0.19 mL, 3.71 mmol, 0.5 eq.) was slowly added (caution: violent reaction). It should be mentioned that no precipitate should be formed during the addition of bromine. Afterwards, 4-dimethylaminopyridine (**27**) (0.91 mg, 7.43 mmol, 1.00 eq.) was added to the slightly yellow solution and stirred for 5 minutes. For purification, 15 mL of 2M NaOH were added, the organic phase was removed, dried over $MgSO_4$ and the solvent removed under reduced pressure. The crude product was washed twice with boiling THF (20 mL). As ^{1}H NMR analysis still showed some impurities (mainly from 4-dimethylaminopyridine-hydrobromide), the purification steps were repeated. Thus, **29t** was obtained as a slightly green solid (0.69 g, 2.03 mmol, 27 %).

Melting point: 139.8 – 140.5 °C.

^{1}H-NMR (300 MHz, $CDCl_3$) δ = 8.03 (d, *J* = 7.6 Hz, 4H, H-C1, H-C5, H-C8 and H-C12), 6.74 (d, *J* = 7.6 Hz, 4H, H-C2, H-C4, H-C9, H-C11), 3.12 (s, 12H, H_3-C6, H_3-C7, H_3-C13, H_3-C14) ppm.

^{13}C-NMR (75 MHz, $CDCl_3$) δ = 155.98 (C3 and C10), 145.71 (C1, C5, C8 and C12), 107.76 (C2, C4, C9 and C11), 39.99 (C6, C7, C13 and C14) ppm.

{^{1}H} ^{11}B-NMR (270 MHz, $CDCl_3$) δ = +0.74 ppm.

^{11}B-NMR (270 MHz, $CDCl_3$) δ = +0.74 (s) ppm.

IR (ATR) υ (cm^{-1}): 3447 (w), 3384 (w), 3050 (vw), 2391 (w), 2352 (w), 2307 (vw), 1633 (vs), 1562 (s), 1530 (m), 1481 (w), 1444 (w), 1403 (m), 1340 (w), 1324 (w), 1307 (w), 1226 (w), 1196 (m), 1161 (s), 1136 (s), 1116 (m), 1089 (vs), 1035 (m), 995 (m), 972 (w), 949 (m), 841 (m), 826 (s), 820 (s), 734 (w), 705 (w), 659 (w).

HRMS (ESI+): $[C_{14}H_{22}BN_4]^+$ calc. 257.1932 g/mol $[M]^+$, found 257.1934 g/mol.

HRMS (ESI-): $[Br]^-$ calc. 80.9168 g/mol $[M]^+$, found 80.9168 g/mol.

Elemental analysis $[C_{14}H_{22}BBrN_4]$

Calc. (%): C 49.89, H 6.58, N 16.62.

Found (%): C 48.19, H 6.85, N 16.09.

4-Dihexylaminopyridine (DHAP, 30a)

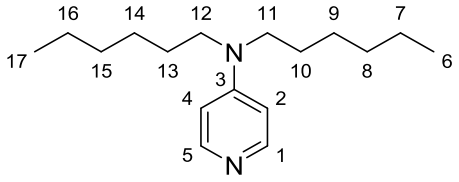

Under a N_2 atmosphere, *para*-aminopyridine (**30b**, 4.00 g, 42.50 mmol, 1.00 eq.) was dissolved in 200 mL THF. Afterwards *n*-butyllithium (2.5 M in hexane, 37.40 mL, 93.50 mmol, 2.20 eq.) was slowly added at room temperature. A chewy precipitate was formed, which was vigorously stirred for 30 minutes. Afterwards *n*-hexyl iodide (13.80 mL, 93.5 mmol, 2.20 eq.) was added and the reaction mixture several times slightly warmed until a clear solution had arised (ca. 30 minutes). Afterwards distilled water (30 mL) was added and the aqueous phase was three times extracted with DCM. The organic layer was dried over $MgSO_4$ and the solvent removed under reduced pressure. ^{1}H NMR and GC/MS analysis of the reaction outcome showed a mixture of the desired product, mono alkylated aminopyridine, aminopyridinum hexyl iodide salts and unreacted hexyl iodide. A column chromatography on silica (0.035-0.070 mm, 60 Å/ DCM : Et_3N = 10 : 1; R_f=0.55) lead to the crude product. ^{1}H NMR analysis revealed this product to be a mixture of 4-dihexylaminopyridine (**30a**) and 4-dihexylaminopyridinium hexyl iodide (**30e**). In order to get rid of the iodide salt, isohexane (50 mL) was added to the mixture, whereas the salt precipitated. The solid was filtered off and the solvent of the liquid phase was removed under reduced pressure. This yielded **30a** as a yellow oil (2.68 g, 10.20 mmol, 24 %).

^{1}H NMR (300 MHz, $CDCl_3$) δ = 8.15 (dd, *J* = 5.0 Hz, *J* = 1.6 Hz, 2H, H-C1 and H-C5), 6.40 (dd, *J* = 5.0 Hz, *J* = 1.6 Hz, 2H, H-C2 and H-C4), 3.25 (t, *J* = 7.6 Hz, 4H, H_2-C11 and H_2-C12), 1.63-1.49 (m, 4H, H_2-C10 and H_2-C13), 1.40-1.24 (m, 12H, H_2-C7, H_2-C8, H_2-C9, H_2-C14, H_2-C15 and H_2-C16), 0.88 (t, *J*=6.6 Hz, 6H, H_3-C6 and H_3-C17) ppm.

^{13}C NMR (75 MHz, $CDCl_3$) δ = 152.36 (C3), 149.88 (C1 and C5), 106.29 (C2 and C4), 50.14 (C11 and C12), 31.60 (C8 and C15), 26.91 (C10 and C13), 26.66 (C9 and C14), 22.60 (C7 and C17), 13.97 (C6 and C17) ppm.

IR (ATR) $\tilde{\nu}$ (cm^{-1}): 3090 (w), 2954 (m), 2926 (m), 2857 (m), 1593 (vs), 1538 (m), 1512 (s), 1466 (m), 1408 (m), 1370 (m), 1298 (w), 1258 (w), 1227 (w), 1205 (m), 1172 (w), 1104 (m), 985 (s), 887 (w), 799 (s), 768 (w), 724 (m).

MS (70 eV, EI) m/z (%): 262 ($[M]^+$, 17), 192 (16), 191 ($[M\text{-}Pent]^+$, 100), 121 (62), 107 (33).

HRMS (70 eV, EI): $C_{17}H_{30}N_2$ calc. 262.2409 g/mol $[M]^+$, found 262.2400 g/mol.

Elemental analysis [$C_{17}H_{30}N_2$]

Calc. (%): C 77.80, H 11.52, N 10.67.

Found (%): C 76.87, H 11.39, N 11.50.

4-dihexylaminopyridine borane (DHAP borane, 30f)

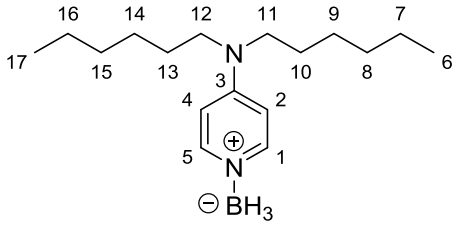

4-Dihexylaminopyridine (**30a**, 1.01 g, 3.83 mmol, 1.00 eq.) was dissolved in 5 mL THF under N_2 atmosphere. The solution was cooled to 0 °C and a $H_3B{\bullet}SMe_2$ solution (5 M in Et_2O, 0.77 mL, 1.01 eq.) was added. After 10 minutes the external cooling was removed. After removing all residues of solvent under reduced pressure, **30f** was obtained as a colorless oil (1.06 g, 3.83 mmol, 100 %).

^{1}H NMR (300 MHz, $CDCl_3$) δ = 7.99 (d, *J* = 7.4 Hz, 2H, H-C1 and H-C5), 6.41 (d, *J* = 7.5 Hz, 2H, H-C2 and H-C4), 3.31 (t, *J* = 7.7 Hz, 4H, H_2-C11 and H_2-C12), 1.70 – 1.45 (m, 4H, H_2-C10 and H_2-C13), 1.44 – 1.11 (m, 12H, H_2-C7, H_2-C8, H_2-C9, H_2-C14, H_2-C15 and H_2-C16), 0.89 (t, *J* = 6.7 Hz, 6H, H_3-C6 and H_3-C17) 3.04-1.85 (broad, q, 3H, H_3-B) ppm.

^{13}C NMR (75 MHz, $CDCl_3$) δ = 153.12 (C3), 146.87 (C1 and C5), 106.24 (C2 and C4), 50.66 (C11 and C12), 31.48 (C8 and C15), 26.74 (C10 and C13), 26.52 (C9 and C14), 22.53 (C7 and C17), 13.93 (C6 and C17) ppm.

{^{1}H} ^{11}B NMR (270 MHz, $CDCl_3$) δ = −13.87 (s) ppm.

^{11}B-NMR (270 MHz, $CDCl_3$) δ = −13.87 (broad, q) ppm.

IR (ATR) $\tilde{\nu}$ (cm^{-1}): 2955 (m), 2928 (m), 2857 (m), 2355 (m), 2294 (m), 2249 (m), 1632 (s), 1534 (vw), 1532 (s), 1502 (vw), 1466 (m), 1416 (m),1371 (m), 1338 (w), 1301 (w), 1262 (w), 1224 (w), 1168 (s), 1098 (s), 1038 (m), 982 (w), 929 (w), 888 (w), 809 (s), 724 (w), 665 (vw).

MS (70 eV, EI) m/z (%): 276 ($[M]^+$, 2), 262 ($[M\text{-}BH_3]^+$, 16), 192 (15), 191 ($[M\text{-}Hex]^+$, 100), 121 (64), 107 (34).

HRMS (70 eV, EI): $C_{17}H_{33}BN_2$ calc. 276.2737 g/mol $[M]^+$, found 276.2736 g/mol.

Elemental analysis [$C_{17}H_{33}BN_2$]

Calc. (%): C 73.91, H 12.04, N 10.14.

Found (%): C 72.49, H 11.66, N 11.06.

5.3.3. Synthesis of substrates

S-dodecyl *O*-ethyl carbonodithioate (18b)

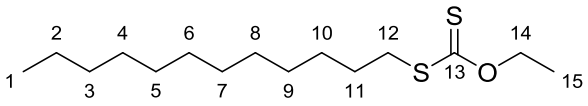

1-Iodododecane (**18d**, 5.00 mL, 20.27 mmol, 1.00 eq.) was dissolved in acetone (50 ml). Afterwards potassium ethyl xantogenate (3.90 g, 24.33 mmol, 1.20 eq.) was slowly added. The suspension was stirred for 15 minutes while a white solid (KI) precipitated. The solvent was removed under reduced pressure. Column chromatography on silica (0.035-0.070 mm, 60 Å/ isohexane; R_f=0.70) led to the pure product **18b** which was isolated as pale yellow oil (5.13 g, 17.67 mmol, 87 %).

^{1}H NMR (300 MHz, $CDCl_3$) δ = 4.57 (q, *J* = 7.1 Hz, 2H, H_2-C14), 3.03 (t, *J* = 7.5 Hz, 2H, H_2-C12), 1.65 – 1.55 (m, 2H, H_2-C11), 1.34 (t, *J* = 7.1 Hz, 3H, H_3-C15), 1.35 – 1.14 (m, 18H, H_2-C2, H_2-C3, H_2-C4, H_2-C5, H_2-C6, H_2-C7, H_2-C8, H_2-C9 and H_2-C10), 0.80 (t, *J* = 6.9 Hz, 3H, H3-C1) ppm.

^{13}C NMR (75 MHz, $CDCl_3$) δ = 215.21 (C13), 69.66 (C14), 35.95 (C12), 31.94 (C11), 29.67 ($C_{aliphatic}$), 29.65 ($C_{aliphatic}$), 29.60 ($C_{aliphatic}$), 29.50 ($C_{aliphatic}$), 29.37 ($C_{aliphatic}$), 29.16 ($C_{aliphatic}$), 28.93 ($C_{aliphatic}$), 28.39 ($C_{aliphatic}$), 22.71 (C2), 14.13 (C1), 13.81 (C15) ppm.

IR (ATR) $\tilde{\nu}$ (cm^{-1}): 2955 (w), 2922 (s), 2853 (m), 1465 (w), 1365 (w), 1292 (w), 1208 (s), 1145 (w), 1111 (s), 1047 (s), 1007 (w), 856 (w), 810 (w), 721 (w). MS (70 eV, EI) m/z (%): 290 ($[M]^+$, 4), 257 (24), 201 (14), 123 (68), 122 ($[M\text{-}C_{12}H_{24}]^+$, 100), 89 (26), 83 (10), 69 (18), 61 (11), 57 (18), 55 (24), 43 (18), 40 (17).

HRMS (70 eV, EI): $C_{15}H_{30}OS_2$ calc. 290.1738 g/mol $[M]^+$, found 290.1737 g/mol.

Elemental analysis [$C_{15}H_{30}OS_2$]

Calc. (%): C 62.01, H 10.41, S 22.07.

Found (%): C 62.25, H 10.36, S 22.62.

O-dodecyl *S*-methyl carbonodithioate (18c)

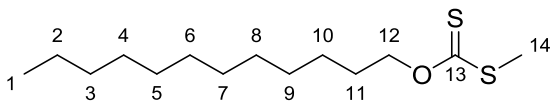

The reaction was carried out under a nitrogen atmosphere. 1-Dodecanol (5.00 mL, 22.35 mmol, 1.00 eq.) was dissolved in 200 mL THF and the solution cooled to 0 °C. Afterwards sodium hydride (60 % suspension in mineral oils, 1.16 g, 29.06 mmol, 1.30 eq.)

was added and stirred at 0 °C for 30 minutes, followed by the addition of CS_2 (2.02 mL, 33.53 mmol, 1.5 eq.). The external cooling was removed and the reaction mixture stirred for one hour. Subsequently methyl iodide (2.38 mL, 38.00 mmol, 1.7 eq.) was added and stirred for 20 minutes. The crude mixture was quenched with distilled water (30 mL) and three times extracted with chloroform. The combined organic phases were dried over $MgSO_4$ and the solvent was removed under reduced pressure. Column chromatography on silica (0.035-0.070 mm, 60 Å/ isohexane; R_f=0.70) led to the pure product **18c** which was isolated as pale yellow oil (5.19 g, 18.74 mmol, 84 %).

^{1}H-NMR (300 MHz, $CDCl_3$) δ = 4.51 (t, *J* = 6.7 Hz, 2H, H_2-C12), 2.48 (s, 3H, H_3-C14), 1.78 – 1.66 (m, 2H, H_2-C11), 1.40 – 1.10 (m, 18H, H_2-C2, H_2-C3, H_2-C4, H_2-C5, H_2-C6, H_2-C7, H_2-C8, H_2-C9 and H_2-C10), 0.81 (t, *J* = 6.9 Hz, 3H, H_3-C1) ppm.

^{13}C-NMR (75 MHz, $CDCl_3$) δ = 215.95 (C13), 74.28 (C12), 31.94 (C3), 29.66 ($C_{aliphatic}$), 29.65 ($C_{aliphatic}$), 29.58 ($C_{aliphatic}$), 29.51 ($C_{aliphatic}$), 29.37 ($C_{aliphatic}$), 29.25 ($C_{aliphatic}$), 28.27 (C11), 25.91 (C10), 22.71 (C2), 18.91 (C14), 14.14 (C1) ppm.

IR (ATR) $\tilde{\nu}$ (cm^{-1}): 2921 (s), 2853 (m), 1456 (w), 1378 (w), 1216 (s), 1127 (w), 1056 (s), 965 (m), 722 (w).

MS (70 eV, EI) m/z (%): 276 ([M]$^+$, 2), 243 (10), 216 (16), 201 (12), 168 ([M-OCS_2CH_3-H]$^+$, 50), 111 (18), 98 (13), 97 (33), 91 (20), 85 (27), 84 (21), 83 (34), 82 (10), 75 (20), 71 (53), 70 (26), 69 (39), 57 ([M-$C_{10}H_{19}OS_2$]$^+$, 100), 56 (25), 55 (52), 43 (83), 42 (11), 41 (47).

HRMS (70 eV, EI): $C_{14}H_{28}OS_2$ calc. 276.1582 g/mol [M]$^+$, found 276.1578 g/mol.

Elemental analysis [$C_{14}H_{28}OS_2$]

Calc. (%): C 60.82, H 10.21, S 23.19.

Found (%):C 60.89, H 10.40, S 22.51.

***O*-decyl *S*-dodecyl carbonodithioate (18e)**

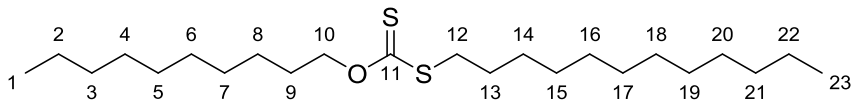

The reaction was carried out under a nitrogen atmosphere. 1-Decanol (1.66 mL, 10.46 mmol, 1.00 eq.) was dissolved in 50 mL THF and the solution cooled to 0 °C. Afterwards *n*-butyllithium (2.5 M solution in hexane, 5.00 mL, 12.56 mmol, 1.20 eq.) was added and stirred at 0 °C for 10 minutes, followed by the addition of CS_2 (0.88 mL, 14.65 mmol, 1.4 eq.). The external cooling was removed and the reaction mixture stirred for one hour. Subsequently 1-iodododecane (**18d**, 4.13 mL, 16.74 mmol, 1.6 eq.) was added and stirred for 30 minutes. The crude mixture was quenched with distilled water (20 mL) and three times extracted with chloroform. The combined organic phases were dried over $MgSO_4$ and the

solvent was removed under reduced pressure. Column chromatography on silica (0.035-0.070 mm, 60 Å/ isohexane; R_f=0.70) led to the pure product **18e** which was isolated as pale yellow oil (2.30 g, 5.71 mmol, 55 %).

^{1}H-NMR (300 MHz, $CDCl_3$) δ = 4.50 (t, *J* = 6.7 Hz, 2H, H_2-C10), 3.02 (t, *J* = 7.5 Hz, 2H, H_2-C12), 1.76 – 1.68 (m, 2H, H_2-C9), 1.65 – 1.57 (m, 2H, H_2-C13), 1.39 – 1.13 (m, 32H, H_2-C2, H_2-C3, H_2-C4, H_2-C5, H_2-C6, H_2-C7, H_2-C8, H_2-C14, H_2-C15, H_2-C16, H_2-C17, H_2-C18, H_2-C19, H_2-C20, H_2-C21 and H_2-C22)), 0.81 (dd, *J*=7.1, 6.5, 6H, H_3-C1 and H_3-C23) ppm.

^{13}C-NMR (75 MHz, $CDCl_3$) δ = 215.29 (C11), 74.00 (C10), 35.86 (C12), 31.94 (C3 or C13), 31.91 (C3 or C13), 29.67 ($C_{aliphatic}$), 29.65 ($C_{aliphatic}$), 29.60 ($C_{aliphatic}$), 29.54 ($C_{aliphatic}$), 29.52 ($C_{aliphatic}$), 29.50 ($C_{aliphatic}$), 29.37 ($C_{aliphatic}$), 29.32 ($C_{aliphatic}$), 29.25 ($C_{aliphatic}$), 29.16 ($C_{aliphatic}$), 28.95 ($C_{aliphatic}$), 28.49 ($C_{aliphatic}$), 28.27 (C9), 25.96 (C8), 22.71 (C2 or C22), 22.70 (C2 or C22), 14.13 (C1 or C23), 14.12 (C1 or C23) ppm.

IR (ATR) $\tilde{\nu}$ (cm^{-1}): 2922 (s), 2853 (m), 1465 (m), 1378 (w), 1212 (s), 1125 (w), 1053 (s), 721 (m).

MS (70 eV, EI) m/z (%): 402 ($[M]^+$, 5), 369 (25), 342 (23), 341 (10), 285 (17), 265 (13), 264 (19), 263 ($[M-C_{10}H_{19}]^+$, 100), 258 (13), 229 (29), 201 (44), 173 (12), 169 (16), 168 (10), 151 (13).

HRMS (70 eV, EI): $C_{23}H_{46}OS_2$ calc. 402.2990 g/mol $[M]^+$, found 402.2987 g/mol.

Elemental analysis [$C_{23}H_{46}OS_2$]

Calc. (%):	C 68.59	H 11.51	S 15.92.
Found (%):	C 68.24	H 11.54	S 16.37.

***O*-(decan-2-yl) *S*-methyl carbonodithioate (18f)**

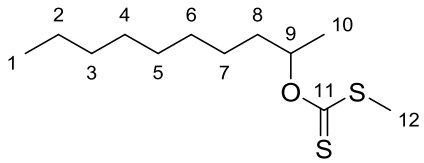

The reaction was carried out under a nitrogen atmosphere. 2-Decanol (**35a**, 2.49 g, 13.38 mmol, 1.00 eq.) was dissolved in 100 mL THF and the solution cooled to 0 °C. Afterwards *n*-butyllithium (2.5 M solution in hexane, 5.90 mL, 14.72 mmol, 1.10 eq.) was added and stirred at 0 °C for 20 minutes, followed by the addition of CS_2 (1.00 mL, 17.39 mmol, 1.3 eq.). The external cooling was removed and the reaction mixture stirred for one hour. Finally methyl iodide (1.30 mL, 20.07 mmol, 1.5 eq.) was added and stirred for 20 minutes. The crude mixture was quenched with distilled water (30 mL) and three times extracted with chloroform. The combined organic phases were dried over $MgSO_4$ and the

solvent was removed under reduced pressure. Column chromatography on silica (0.035-0.070 mm, 60 Å/ isohexane; R_f=0.60) led to the pure product **18f** which was isolated as pale yellow oil (2.59 g, 10.44 mmol, 78 %).

^{1}H-NMR (300 MHz, $CDCl_3$) δ = 5.68 – 5.55 (m, 1H, H-C9), 2.47 (s, 3H, H_3-C12), 1.77 – 1.48 (m, 2H, H_2-C8), 1.28 (d, *J* = 6.2 Hz, 3H, H_3-C10), 1.35 – 1.12 (m, 14H, H_2-C2, H_2-C3, H_2-C4, H_2-C5, H_2-C6 and H_2-C7), 0.80 (t, *J* = 6.9 Hz, 3H, H_3-C1) ppm.

^{13}C-NMR (75 MHz, $CDCl_3$) δ = 215.43 (C11), 81.43 (C9), 35.60 (C8), 31.86 (C3), 29.45 ($C_{aliphatic}$), 29.41 ($C_{aliphatic}$), 29.22 ($C_{aliphatic}$), 25.26 (C7), 22.67 (C2), 19.27 (C10), 18.77 (C12), 14.12 (C1) ppm.

IR (ATR) $\tilde{\nu}$ (cm^{-1}): 2923 (m), 2854 (m), 1464 (w), 1378 (w), 1318 (vw), 1222 (s), 1115 (m), 1043 (s), 963 (m), 905 (w), 823 (w), 722 (w).

MS (70 eV, EI) m/z (%): 248 ([M]$^+$, 1), 140 ([M-OCS_2CH_3-H]$^+$, 60), 91 ([M-$C_{10}H_{21}O$]$^+$, 13), 85 ([M-$C_6H_{11}OS_2$]$^+$, 46), 71 ([M-$C_7H_{13}OS_2$]$^+$, 46), 70 ([M-$C_7H_{13}OS_2$-H]$^+$, 10), 69 ([M-$C_7H_{13}OS_2$-2H]$^+$, 12), 57 ([M-$C_8H_{15}OS_2$]$^+$, 100), 56 ([M-$C_8H_{15}OS_2$-H]$^+$, 14), 55 ([M-$C_8H_{15}OS_2$-2H]$^+$, 30), 43 (90), 42 (10), 40 (39).

HRMS (70 eV, EI): $C_{12}H_{24}OS_2$ calc. 248.1269 g/mol [M]$^+$, found 248.1237 g/mol.

Elemental analysis [$C_{12}H_{24}OS_2$]

Calc. (%):	C 58.01	H 9.74	S 25.81.
Found (%):	C 58.03	H 9.82	S 25.64.

***O*-((3s,5s,7s)-adamantan-1-yl) *S*-methyl carbonodithioate (18g)**

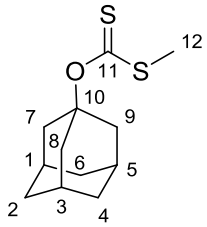

The reaction was carried out under a nitrogen atmosphere. 1-Adamantanol (**35b**, 3.00 g, 19.71 mmol, 1.00 eq.) was dissolved in 200 mL THF and the solution cooled to 0 °C. Afterwards sodium hydride (60 % suspension in mineral oils, 1.02 g, 25.62 mmol, 1.30 eq.) was added, the external cooling was removed and the mixture stirred for 30 minutes, followed by the addition of CS_2 (1.78 mL, 29.56 mmol, 1.5 eq.). The suspension was warmed up to 40 °C and stirred for 3.5 hours. Subsequently methyl iodide (2.09 mL, 33.50 mmol, 1.7 eq.) was added and stirred for 30 minutes at room temperature. All solids were filtered off and the solvent was removed from the crude product under reduced pressure. The residue was mixed with warm isohexane, whereas the xanthate dissolves, but not the remaining

alcohol. The solid is filtered off and the pure xanthate begins to grow as yellow needles from the clear isohexane solution by cooling down. The pure product was filtered off, remaining solvent was removed *in vacuo* and xanthate **18g** was obtained as yellow needles (2.06 g, 8.51 mmol, 43 %).

Melting point: 107.5 – 107.8 °C.

^{1}H-NMR (300 MHz, $CDCl_3$) δ = 2.44 (s, 3H, H_3-C12), 2.43 – 2.41 (m, 6H, H_2-C7, H_2-C8 and H_2-C9), 2.26 – 2.20 (m, 6H, H_2-C2, H_2-C4 and H_2-C6), 1.70 – 1.65 (m, 3H, H-C1, H-3 and H-C5) ppm.

^{13}C-NMR (75 MHz, $CDCl_3$) δ = 212.58 (C11), 91.24 (C10), 41.11 (C7, C8 and C9), 36.06 (C2, C4 and C6), 31.42 (C1, C3 and C5), 19.08 (C12) ppm.

IR (ATR) $\tilde{\nu}$ (cm^{-1}): 2910 (m), 2848 (m), 1456 (w), 1409 (w), 1368 (w), 1354 (w), 1316 (w), 1304 (w), 1291 (w), 1275 (w), 1220 (s), 1185 (m), 1146 (w), 1105 (m), 1046 (m), 1021 (s), 984 (m), 954 (s), 858 (m), 814 (m), 714 (m), 665 (w).

MS (70 eV, EI) m/z (%): 242 ($[M]^+$, 1), 136 ($[M\text{-}OCS_2CH_2]^+$, 11), 135 ($[M\text{-}OCS_2CH_3]^+$, 100), 93 (17), 79 (16).

HRMS (70 eV, EI): $C_{12}H_{18}OS_2$ calc. 242.0799 g/mol $[M]^+$, found 242.0797 g/mol.

Elemental analysis [$C_{12}H_{18}OS_2$]

Calc. (%):	C 59.46	H 7.49	S 26.45.
Found (%):	C 59.72	H 7.51	S 26.42.

***S*-methyl *O*-(naphthalen-1-ylmethyl) carbonodithioate (18h)**

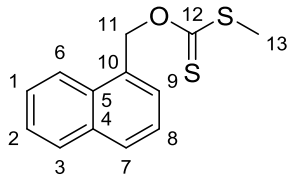

The reaction was carried out under a nitrogen atmosphere. 1-Naphthylmethanol (**35c**, 1.65 g, 10.41 mmol, 1.00 eq.) was dissolved in 50 mL THF and the solution cooled to 0 °C. Then, *n*-butyllithium (2.5 M solution in hexane, 5.00 mL, 12.49 mmol, 1.20 eq.) was added and stirred at 0 °C for 10 minutes, followed by the addition of CS_2 (0.94 mL, 15.62 mmol, 1.5 eq.). The external cooling was removed and the solution stirred for one hour. Afterwards, methyl iodide (1.11 mL, 17.70 mmol, 1.7 eq.) was added and stirred for 15 minutes. The crude reaction mixture was quenched with distilled water (15 mL) and three times extracted with chloroform. The combined organic phases were dried over $MgSO_4$ and the solvent was removed under reduced pressure. Column chromatography on silica (0.035-0.070 mm,

60 Å/ isohexane; R_f=0.75) led to the pure product **18h** which was isolated as viscous yellow oil (0.66 g, 2.66 mmol, 26 %).

^{1}H-NMR (300 MHz, $CDCl_3$) δ = 7.93 (d, *J* = 8.2 Hz, 1H, H-C6), 7.87 – 7.81 (m, 2H, H-C3 and H-C7), 7.57 – 7.46 (m, 3H, H-C1, H-C2, H-C8), 7.42 (dd, *J* = 8.2 Hz, 7.1 Hz, 1H, H-C9), 6.02 (s, 2H, H_2-C11), 2.50 (s, 3H, H_3-C13). ppm.

^{13}C-NMR (75 MHz, $CDCl_3$) δ = 215.65 (C12), 133.79 (C10), 131.84 (C4), 130.38 (C5), 129.92 (C3), 128.82 (C9), 128.39 (C7), 126.88 (C1), 126.17 (C2), 125.27 (C8), 123.62 (C6), 73.80 (C11), 19.16 (C13) ppm.

IR (ATR) $\tilde{\nu}$ (cm^{-1}): 3046 (w), 2918 (w), 1643 (w), 1598 (w), 1511 (m), 1459 (w), 1422 (w), 1368 (vw), 1349 (vw), 1317 (w), 1195 (s), 1160 (m), 1082 (m), 1063 (s), 1047 (s), 963 (m), 920 (m), 899 (m), 881 (m), 856 (m), 800 (m), 791 (s), 773 (s), 727 (m), 677 (m).

MS (70 eV, EI) m/z (%): 248 ($[M]^+$, 4), 142 ($[M\text{-}OCS_2CH_2]^+$, 13), 141 ($[M\text{-}OCS_2CH_3]^+$, 100), 115 (13).

HRMS (70 eV, EI): $C_{13}H_{12}OS_2$ calc. 248.0330 g/mol $[M]^+$, found 248.0327 g/mol.

Elemental analysis [$C_{13}H_{12}OS_2$]

Calc. (%):	C 62.87	H 4.87	S 25.82.
Found (%):	C 63.16	H 4.98	S 25.99.

4-(Dimethylamino)pyridin-1-ium iodide (29f)

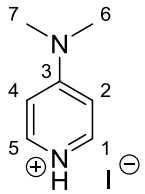

A solution of 4-Dimethylaminopyridine (**27**, 1.50 g, 12.28 mmol, 1.00 eq.) in chloroform (10 mL) was prepared. Afterwards HI (57 % in water, 3.00 mL) was added in excess and the resulting reaction mixture was stirred for five minutes. The solution was poured into THF (250 mL), whereas a white precipitate appeared. The crude product was filtered off and washed twice with THF (100 mL). After removal of residues of solvent, **29f** was obtained as white solid (2.05 g, 8.21 mmol, 67 %).

Melting point: 202.5 – 203.0 °C.

^{1}H NMR (300 MHz, $CDCl_3$) δ = 8.13 (d, *J* = 7.4 Hz, 2H, H-C1 and H-C5), 6.88 (d, *J* = 7.4 Hz, 2H, H-C2 and H-C4), 3.28 (s, 6H, H_3-C6 and H_3-C7) ppm.

^{13}C NMR (75 MHz, $CDCl_3$) δ = 157.55 (C3), 138.23 (C1 and C5), 107.07 (C2 and C4), 40.71 (C6 and C7) ppm.

IR (ATR) $\tilde{\nu}$ (cm^{-1}): 3167 (w), 3020 (w), 2929 (m), 2825 (w), 2807 (w), 1644 (m), 1579 (m), 1563 (s), 1522 (m), 1460 (w), 1436 (m), 1401 (m), 1236 (vw), 1210 (s), 1131 (w), 1104 (w), 1072 (m), 1054 (vw), 994 (s), 941 (w), 839 (w), 788 (s), 746 (m), 708 (w).

Elemental analysis [$C_7H_{11}IN_2$]

Calc. (%): C 33.62, H 4.43, N 11.20.

Found (%): C 33.53, H 4.45, N 11.16.

5.3.4. Radical experiments

General procedure B: Setup for radical experiments:

Stock solutions for radical starters were prepared under a nitrogen atmosphere. A typical setup is explained for TBHN (**2d**) as initiator, but was conducted similarly with other starters like AIBN (**2a**). A 0.20 M solution of TBHN (**2d**) in toluene-d_8 was prepared. This solution was stored under nitrogen at –18 °C. For quality control, ^{1}H NMR measurements of this solution were done regularly. At that temperature, the solution can be kept for several weeks. Nevertheless it seemed advisable not keep larger amounts than 1 mL. A second stock solution for the thiol (TDT (**15b**), 0.1 M in toluene-d_8) was prepared similarly and stored at room temperature.

Under an inert gas atmosphere 0.10 mmol of the substrate (eg. 1-iododododecane (**18d**) or a xanthate) was put into a flask (or microwave vessel). Afterwards, the desired equivalents of a borane complex and a defined amount of internal standard (TMB (**22**), usually 0.1 to 0.15 mmol) were added. If desired, the thiol was added by a Hamilton syringe from the stock solution. The same was done for the radical starter. Finally, the flask was filled with toluene-d_8 to a total volume of 0.60 mL and the solution was stirred until all solids had dissolved. This solution was subsequently reacted (in an oil bath or in the microwave as closed vessel) or transferred to an NMR tube, to do the reaction directly in the NMR machine.

For NMR experiments with DMAP borane (which is not soluble at room temperature), the entire preparation was done directly in a NMR tube, as the crude reaction suspension could not be transferred without loss of solid.

Furthermore it should be mentioned, that all NMR experiments were conducted in NMR tubes, which were only closed with a standard plastic cap, as gas evolution during the reactions is present.

The reaction outcome was determined by integrating the decay of starting materials (or evolution of products) against the internal standard and by GC/MS analysis.

5.3.5. Reductions of carbonyl compounds

5.3.5.1. General procedures

General procedure C: Reductions with borane-complexes; column workup:

All reactions can be performed at room temperature and without inert gas atmosphere. The obtained results are similar compared to reactions carried out under N_2 atmosphere.

1.5 mmol of a substrate (ketone or aldehyde) was dissolved in 3 ml THF. Afterwards a borane-complex (1.0 eq.) was added to this solution and stirred for 5 minutes. Subsequently the solvent was removed under reduced pressure. 2 mL methanol and 200 mg silica were added and again stirred for 2 minutes. After evaporation of methanol the crude product on silica was put to a column chromatography (silica 0.035-0.070 mm, 60 Å/ EtOAc:Isohexane = 5:1, R_f = 0.7-0.8). To obtain the pure alcohols in high yields, the solvents were removed under reduced pressure. The final products were analyzed by ^{1}H NMR spectroscopy and GC/MS. ^{1}H NMR measurements were compared with the literature.

General procedure D: Reductions with borane-complexes; extraction workup:

All reactions can be performed at room temperature and without inert gas atmosphere. The obtained results are similar compared to reactions carried out under N_2 atmosphere.

1.5 mmol of a substrate (ketone or aldehyde) was dissolved in 3 ml THF or MeOH. Afterwards a borane-complex (1.0 eq.) was added to this solution and stirred for 5 minutes. Subsequently the solvent was removed under reduced pressure. 3 mL chloroform and 3 mL 2 M aqueous HCl (2.0 eq.) were added and again stirred for 5 minutes. The phases were separated and the aqueous layer washed once with 5 mL chloroform. Subsequently, the organic phase was dried over anhydrous $MgSO_4$. To obtain the pure alcohols in high yields, the solvents were removed under reduced pressure. The final products were analyzed by ^{1}H NMR spectroscopy and GC/MS. ^{1}H NMR measurements were compared with the literature.

5.3.5.2. Analytical data of products

1,3-diphenylpropan-2-ol (38a)[87]

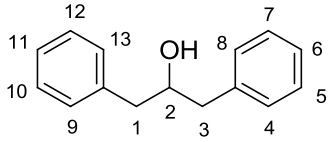

^{1}H-NMR (300 MHz, $CDCl_3$) δ = 7.39-7.24 (m, 10H, H-C4, H-C5, H-C6, H-C7, H-C8, H-C9, H-C10, H-C11, H-C12 and H-C13), 4.09 (tt, *J* = 8.04 Hz, *J* = 4.78, Hz, 1H, H-C2), 2.84 (ddd, *J* = 21.69 Hz, *J* = 13.65 Hz, *J* = 6.40, 4H, H_2-C1, H_2-C3), 1.81 (s, 1H, H-O) Hz ppm.

1-(4-Chlorophenyl)ethanol (38b)[88]

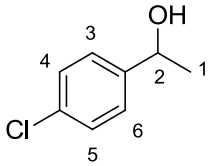

^{1}H-NMR (300 MHz, $CDCl_3$) δ = 7.37-7.22 (m, 4H, H-C3, H-C4, H-C5 and H-C6), 4.85 (q, *J* = 6.45 Hz, 1H, H-C2), 2.43-2.17 (broad, s, 1H, H-O), 1.45 (d, *J* = 6.29 Hz, 3H, H_3-C1) ppm.

1-(*p*-tolyl)ethanol (38c)[89]

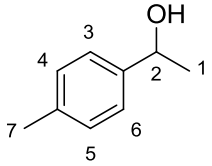

^{1}H-NMR (300 MHz, $CDCl_3$) δ = 7.29-7.15 (m, 4H, H-C3, H-C4, H-C5 and H-C6), 4.85 (q, *J* = 6.45 Hz, 1H, H-C2), 2.36 (s, 3H, H_3-C7), 2.10 (s, 1H, H-O), 1.48 (dd, *J* = 6.45 Hz, *J* = 0.43 Hz, 3H, H_3-C1) ppm.

1-Phenylethanol (26c)[90]

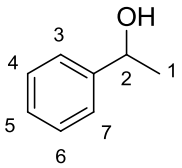

^{1}H-NMR (300 MHz, $CDCl_3$) δ = 7.39-7.23 (m, 5H, H-C3, H-C4, H-C5, H-C6 and H-C7), 4.86 (q, *J* = 6.45 Hz, 1H, H-C2), 2.36 (s, 1H, H-O), 1.48 (d, *J* = 6.46 Hz, 3H, H_3-C1) ppm.

(4-chlorophenyl)methanol (38f)[91]

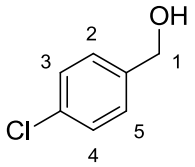

^{1}H-NMR (300 MHz, $CDCl_3$) δ = 7.37-7.24 (m, 4H, H-C2, H-C3, H-C4 and H-C5), 4.63 (s, 2H, H_2-C1), 2.09 (broad, s, 1H, H-O) ppm.

***p*-tolylmethanol (38g)**[92]

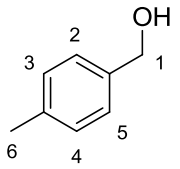

^{1}H-NMR (300 MHz, $CDCl_3$) δ = 7.26-7.16 (m, 4H, H-C2, H-C3, H-C4 and H-C5), 4.63 (s, 2H, H_2-C1), 2.74 (broad, s, 1H, H-O), 2.36 (s, 3H, H_3-C6) ppm.

Phenylmethanol (38h)[93]

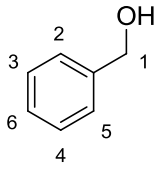

^{1}H-NMR (300 MHz, $CDCl_3$) δ = 7.38-7.26 (m, 5H, H-C2, H-C3, H-C4, H-C5 and H-C6), 4.67 (d, *J* = 1.36 Hz, 2H, H_2-C1), 2.29-2.01 (broad, s, 1H, H-O) ppm.

2,2,4,4-Tetramethylpentan-3-ol (38e)[94]

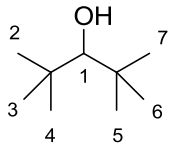

^{1}H-NMR (300 MHz, $CDCl_3$) δ = 2.92 (d, *J* = 6.0 Hz, 1H, H-C1), 1.47 (d, *J*=6.0, 1H, H-O), 0.95 (s, 18H, H_3-C2, H_3-C3, H_3-C4, H_3-C5, H_3-C6 and H_3-C7) ppm.

N-benzylaniline (38s)[95]

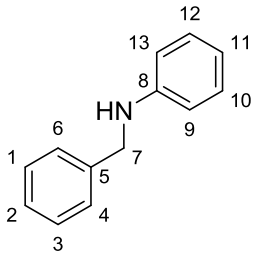

^{1}H-NMR (300 MHz, $CDCl_3$) δ = 7.43 – 7.28 (m, 5H, H-C1, H-C2, H-C3, H-C4 and H-C6), 7.25 – 7.19 (m, 2H, H-C10 and H-C12), 6.80 – 6.73 (m, 1H, H-C11), 6.70 – 6.65 (m, 2H, H-C9 and H-C13), 4.36 (s, 2H, H_2-C7), 4.05 (broad, s, 1H, H-N).

5.3.5.3. ESI-MS spectrometry experiments

5.3.5.3.1. Imidazole borane (17aa)

All preparation steps were carried out under a nitrogen atmosphere. A suspension of imidazole-borane (**17aa**, 0.200 g, 2.442 mmol) in destilled $CDCl_3$ (1 ml) was prepared. Afterwards acetone (0.180 ml, 2.442 mmol, 1 eq.) was added and stirred for 15 minutes at room temperature. All volatiles were then removed under reduced pressure. The colorless viscous substance was taken up in dry THF (1 ml) and a diluted solution (10 drops in 2 ml dry THF) was immediately used for ESI-MS spectrometry.

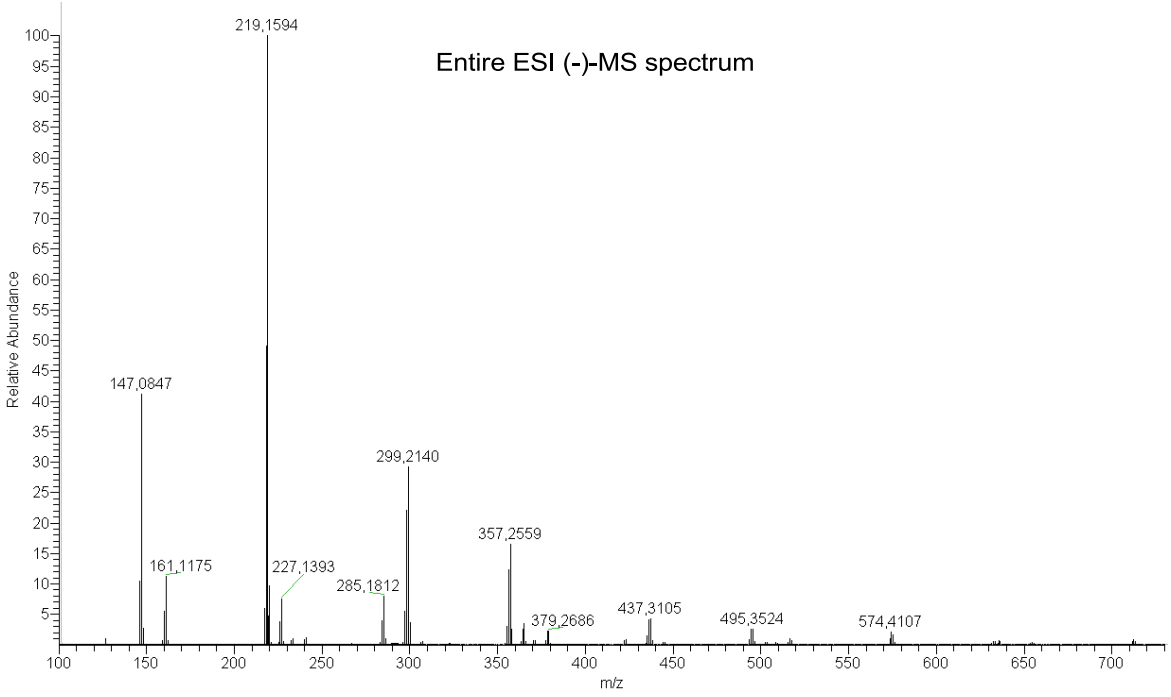

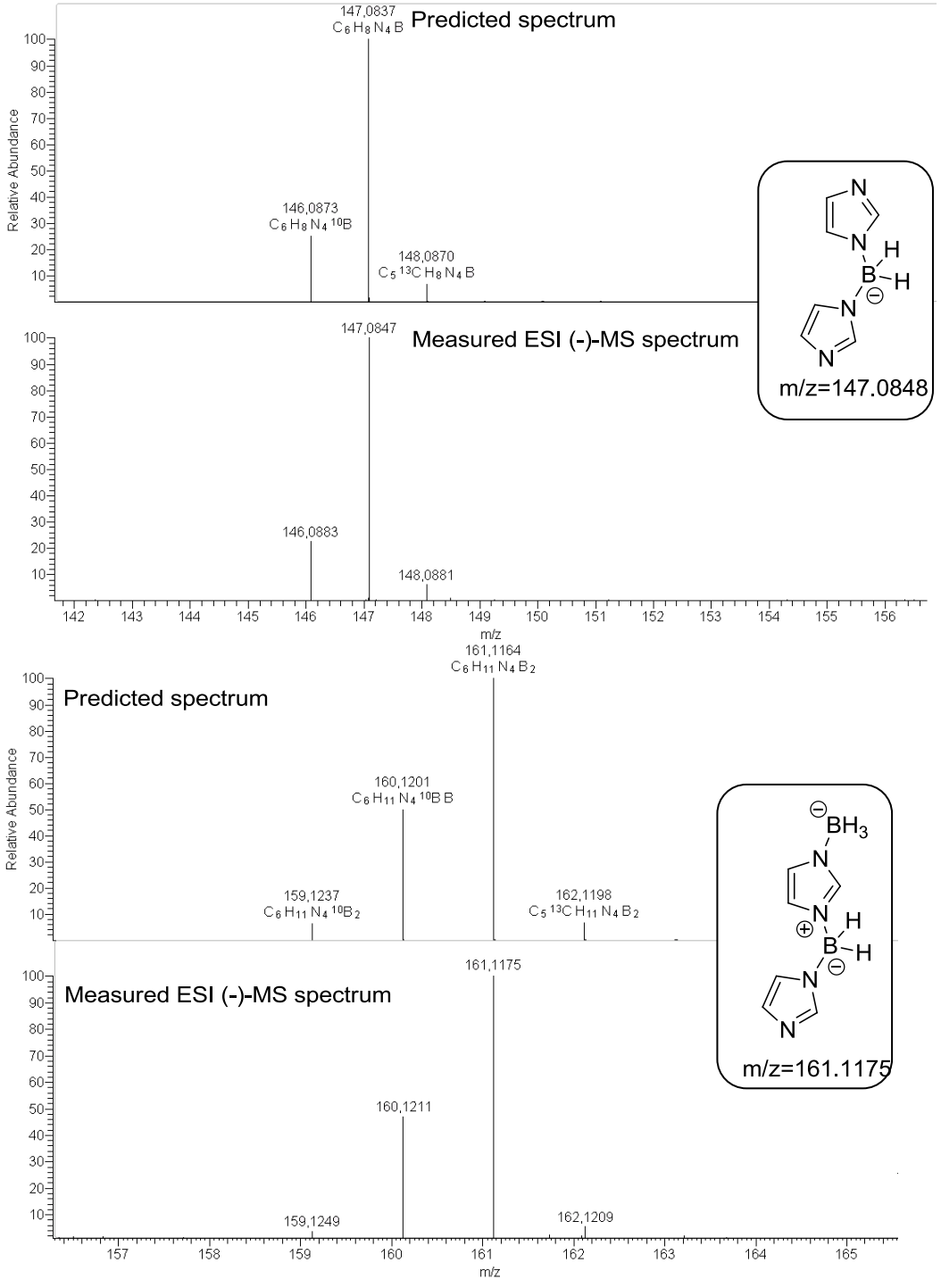
147,0837
C6H8N4B
Predicted spectrum
Relative Abundance
146,0873
C6H8N4 10B
148,0870
C5 13C H8N4B
147,0847
Measured ESI (-)-MS spectrum
146,0883
148,0881
m/z
m/z=147.0848
161,1164
C6H11N4B2
Predicted spectrum
160,1201
C6H11N4 10B B
159,1237
C6H11N4 10B2
162,1198
C5 13C H11N4B2
161,1175
Measured ESI (-)-MS spectrum
160,1211
159,1249
162,1209
m/z
m/z=161.1175

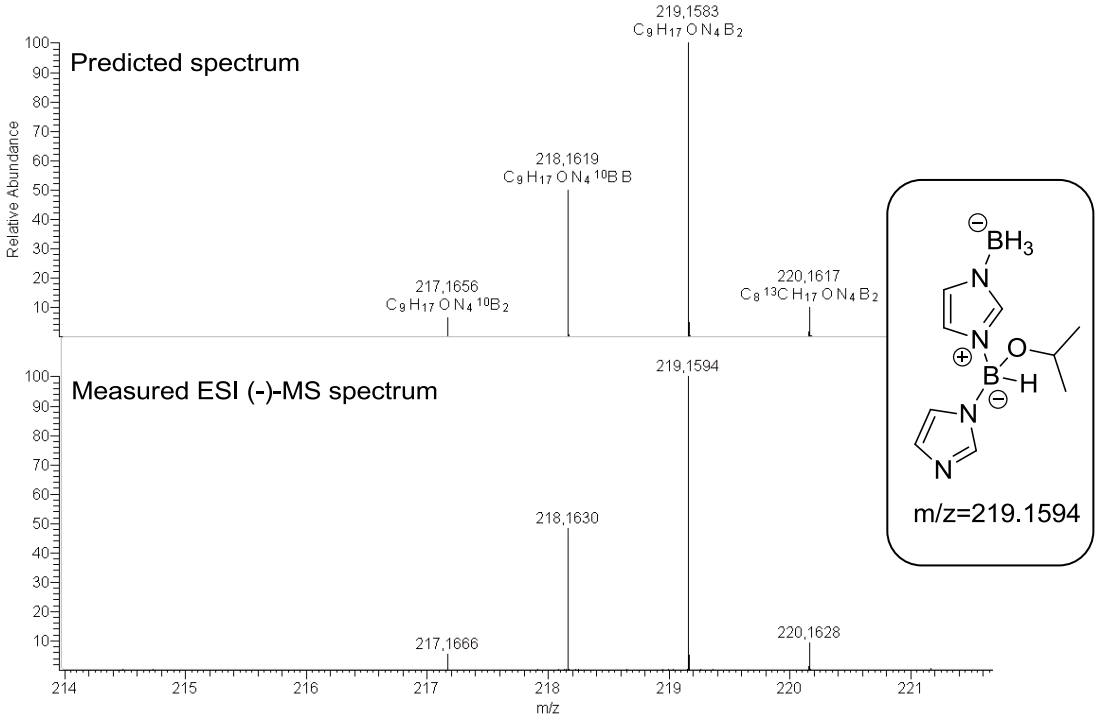
Predicted spectrum
219,1583
C9H17ON4B2
218,1619
C9H17ON4 10BB
217,1656
C9H17ON4 10B2
220,1617
C8 13CH17ON4B2
Measured ESI (-)-MS spectrum
219,1594
218,1630
217,1666
220,1628
Relative Abundance
m/z
m/z=219.1594

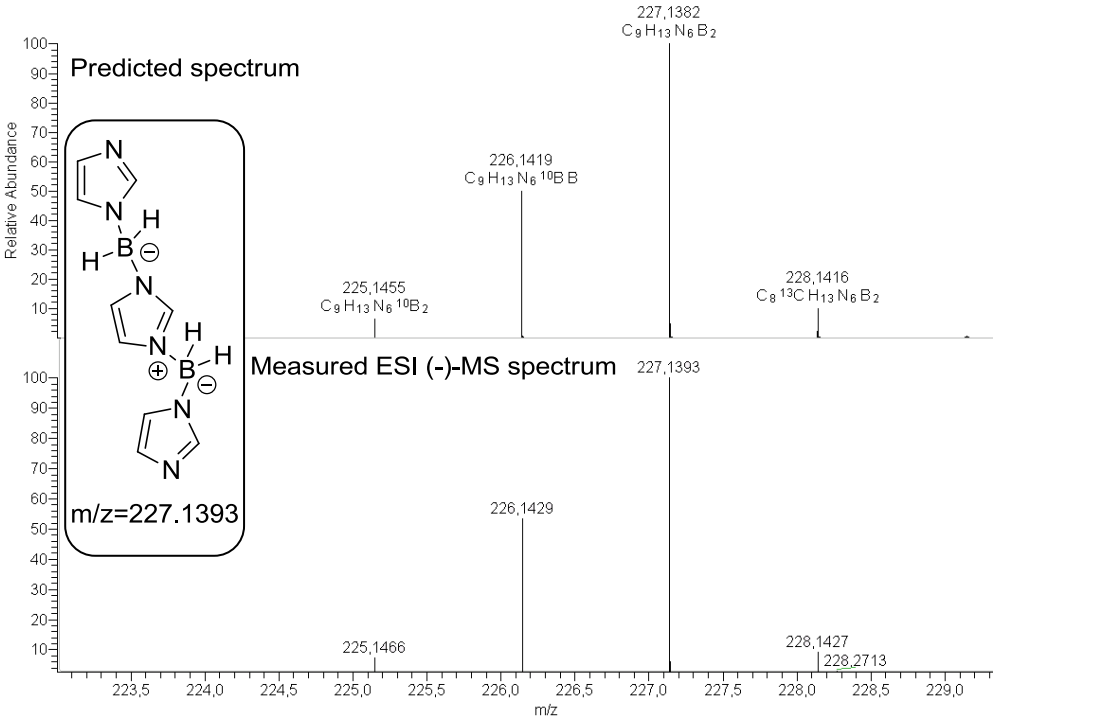
Predicted spectrum
227,1382
C9H13N6B2
226,1419
C9H13N6 10BB
225,1455
C9H13N6 10B2
228,1416
C8 13CH13N6B2
Measured ESI (-)-MS spectrum
227,1393
226,1429
225,1466
228,1427
228,2713
Relative Abundance
m/z
m/z=227.1393

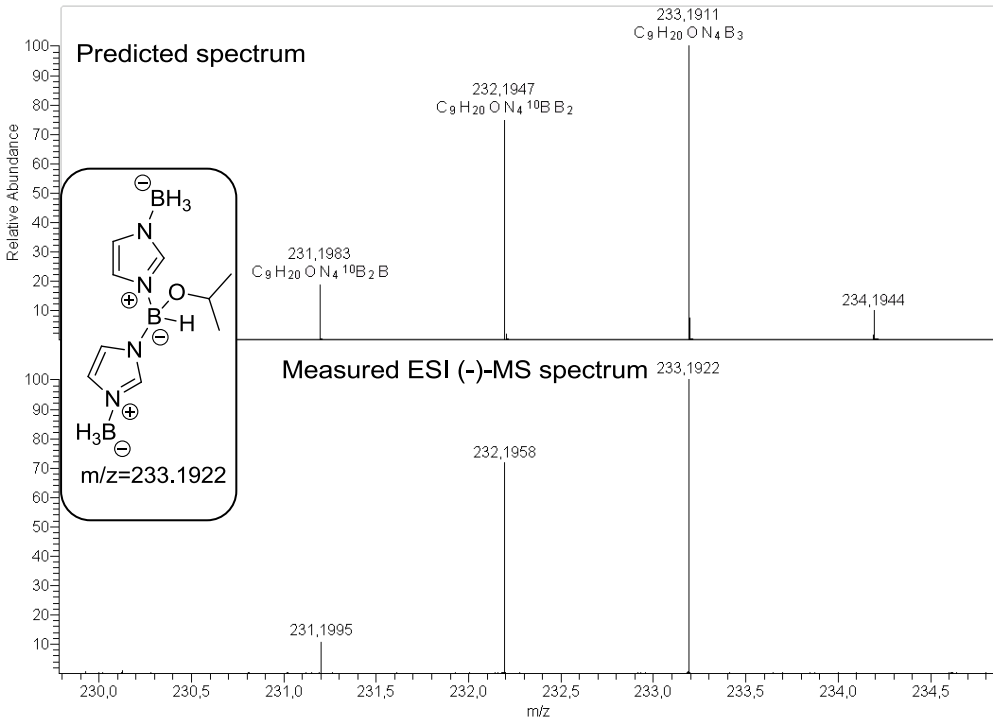
Predicted spectrum
233,1911
C9H20ON4B3
232,1947
C9H20ON4 10B B2
231,1983
C9H20ON4 10B2 B
234,1944
Measured ESI (-)-MS spectrum
233,1922
232,1958
231,1995
m/z=233.1922
Relative Abundance
m/z

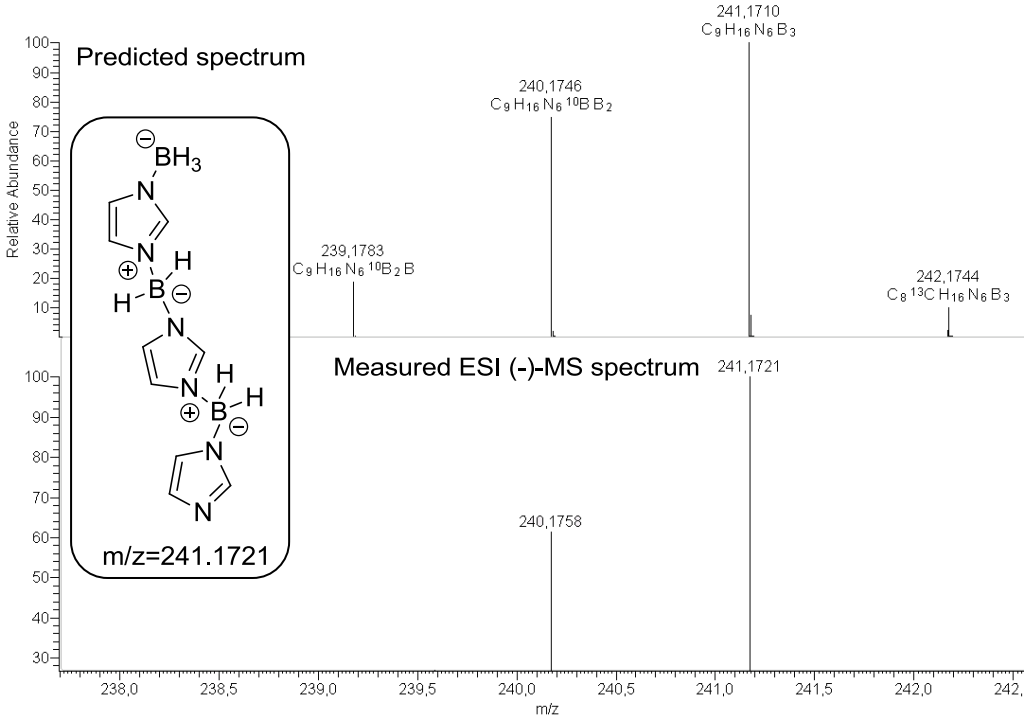
Predicted spectrum
241,1710
C9H16N6B3
240,1746
C9H16N6 10B B2
239,1783
C9H16N6 10B2 B
242,1744
C8 13C H16N6B3
Measured ESI (-)-MS spectrum
241,1721
240,1758
m/z=241.1721
Relative Abundance
m/z

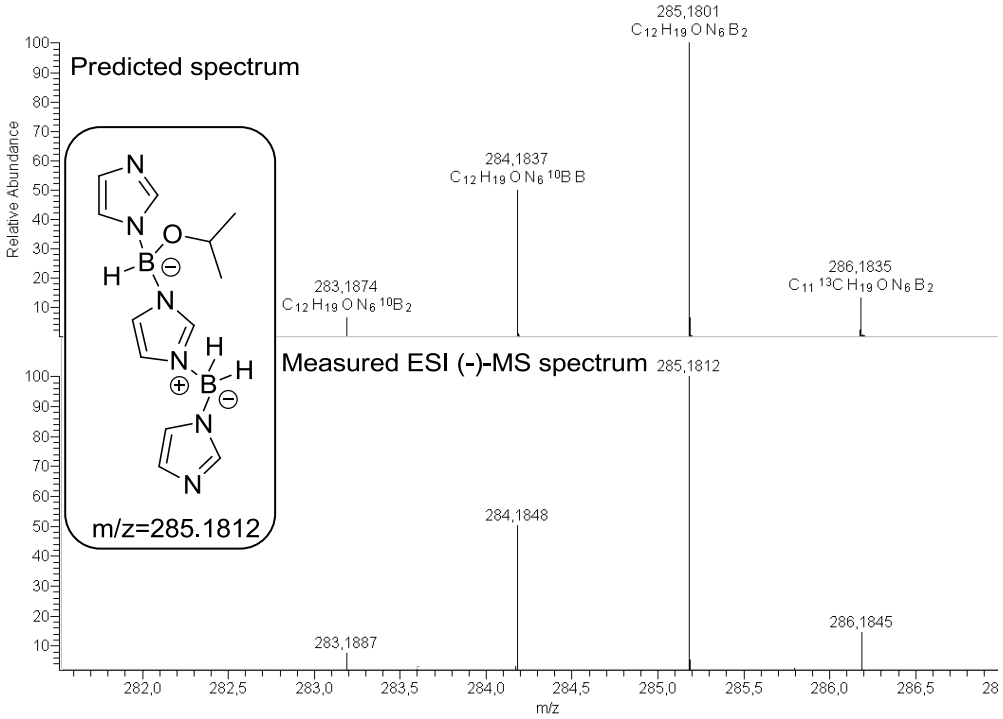
Predicted spectrum
285,1801
C12H19ON6B2
284,1837
C12H19ON6 10BB
283,1874
C12H19ON6 10B2
286,1835
C11 13CH19ON6B2
Measured ESI (-)-MS spectrum
285,1812
284,1848
283,1887
286,1845
m/z=285.1812
Relative Abundance
m/z

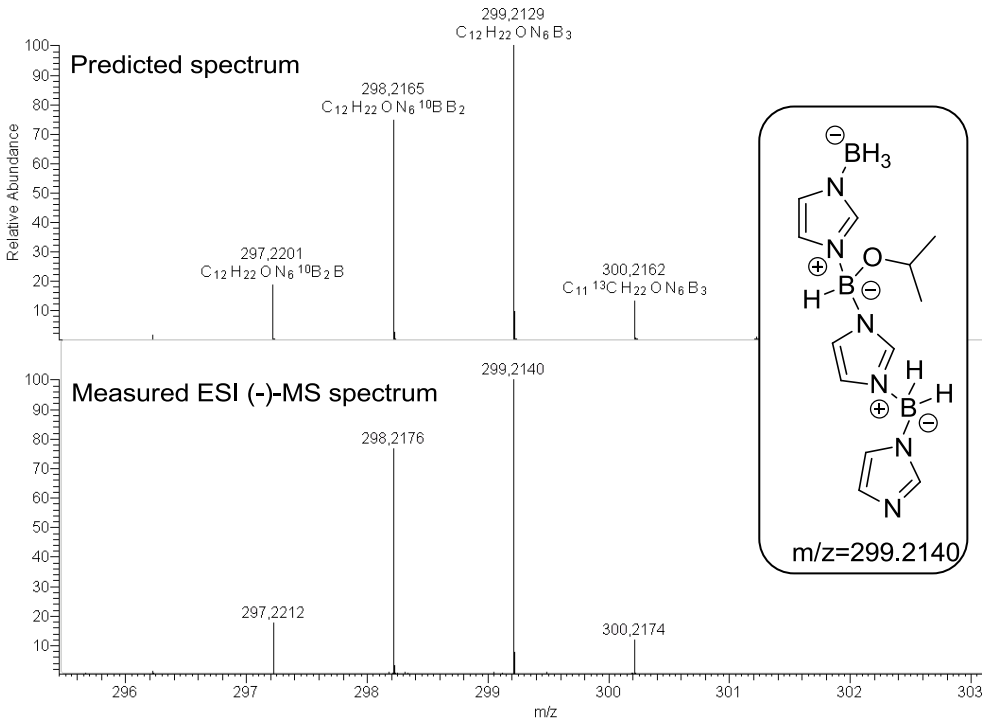
Predicted spectrum
299,2129
C12H22ON6B3
298,2165
C12H22ON6 10BB2
297,2201
C12H22ON6 10B2B
300,2162
C11 13CH22ON6B3
Measured ESI (-)-MS spectrum
299,2140
298,2176
297,2212
300,2174
m/z=299.2140
Relative Abundance
m/z

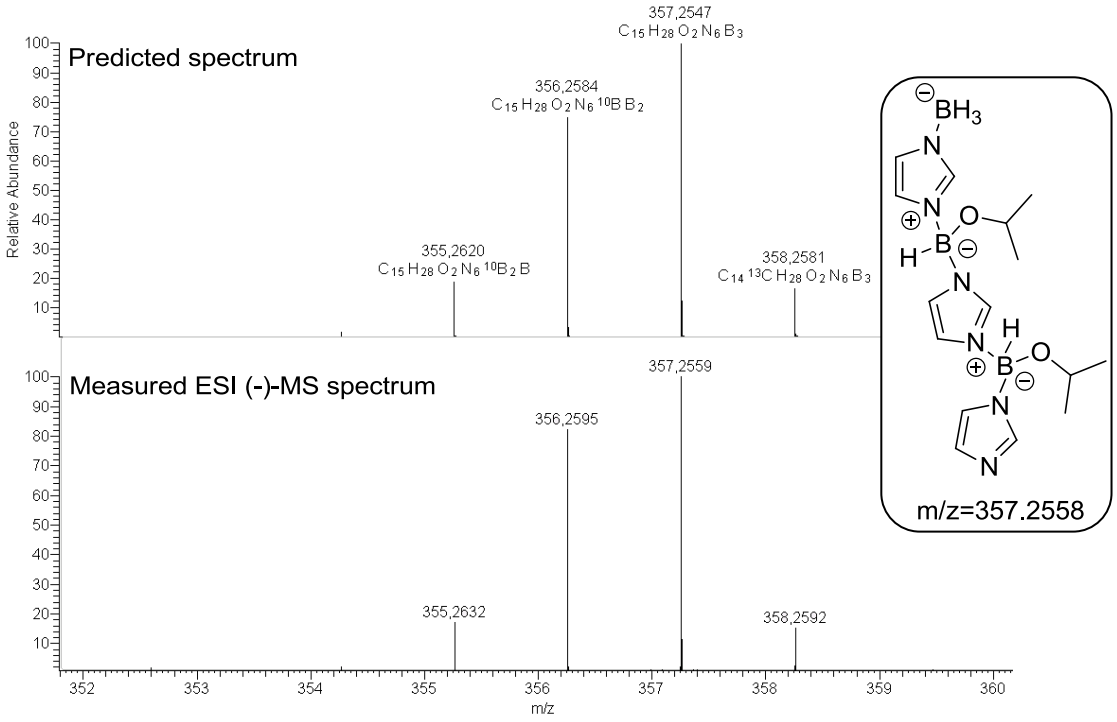
Predicted spectrum
357,2547
C15 H28 O2 N6 B3
356,2584
C15 H28 O2 N6 10B B2
355,2620
C15 H28 O2 N6 10B2 B
358,2581
C14 13C H28 O2 N6 B3
Relative Abundance
Measured ESI (-)-MS spectrum
357,2559
356,2595
355,2632
358,2592
m/z
m/z=357.2558

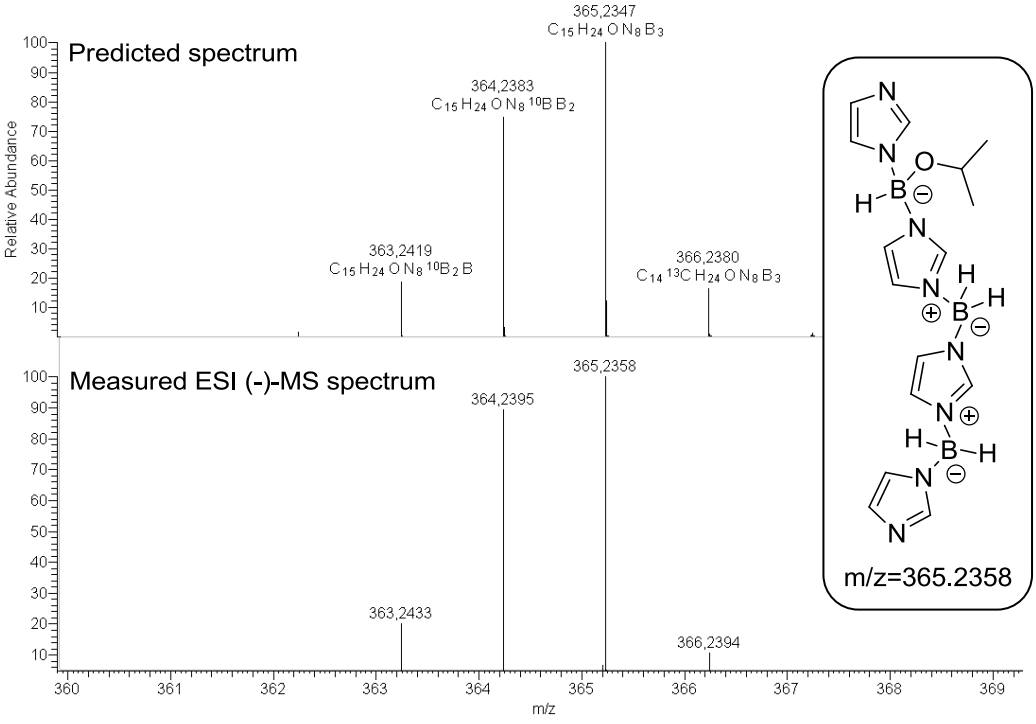
Predicted spectrum
365,2347
C15 H24 O N8 B3
364,2383
C15 H24 O N8 10B B2
363,2419
C15 H24 O N8 10B2 B
366,2380
C14 13C H24 O N8 B3
Relative Abundance
Measured ESI (-)-MS spectrum
365,2358
364,2395
363,2433
366,2394
m/z
m/z=365.2358

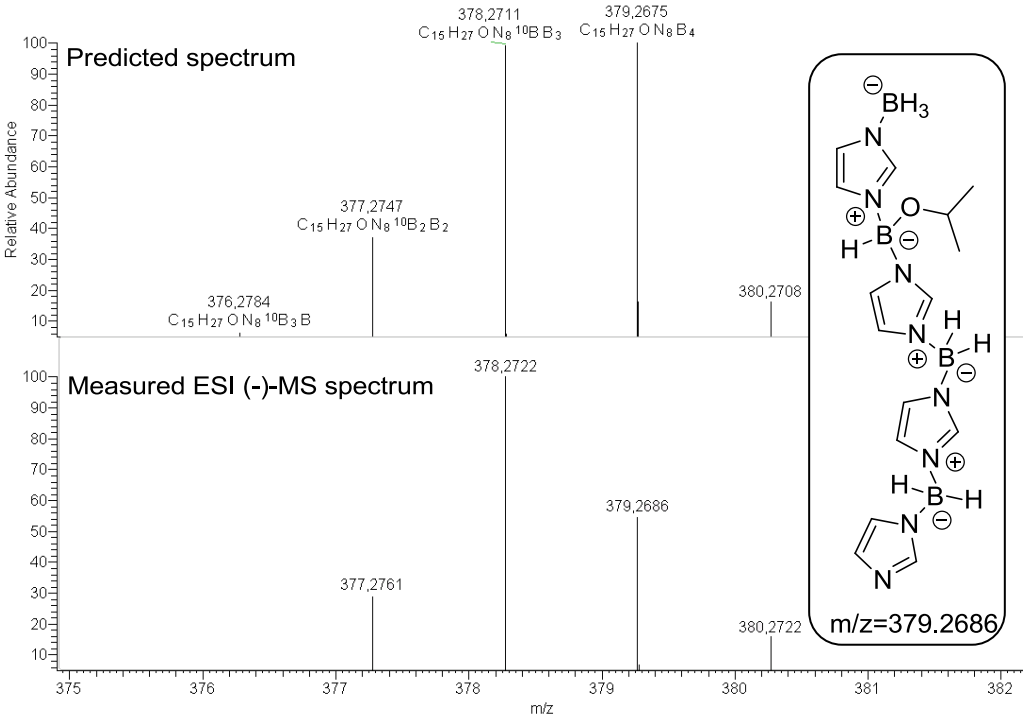
Predicted spectrum
Measured ESI (-)-MS spectrum
Relative Abundance
m/z
378,2711
C15H27ON8 10B B3
379,2675
C15H27ON8B4
377,2747
C15H27ON8 10B2 B2
376,2784
C15H27ON8 10B3 B
380,2708
378,2722
379,2686
377,2761
380,2722
m/z=379.2686

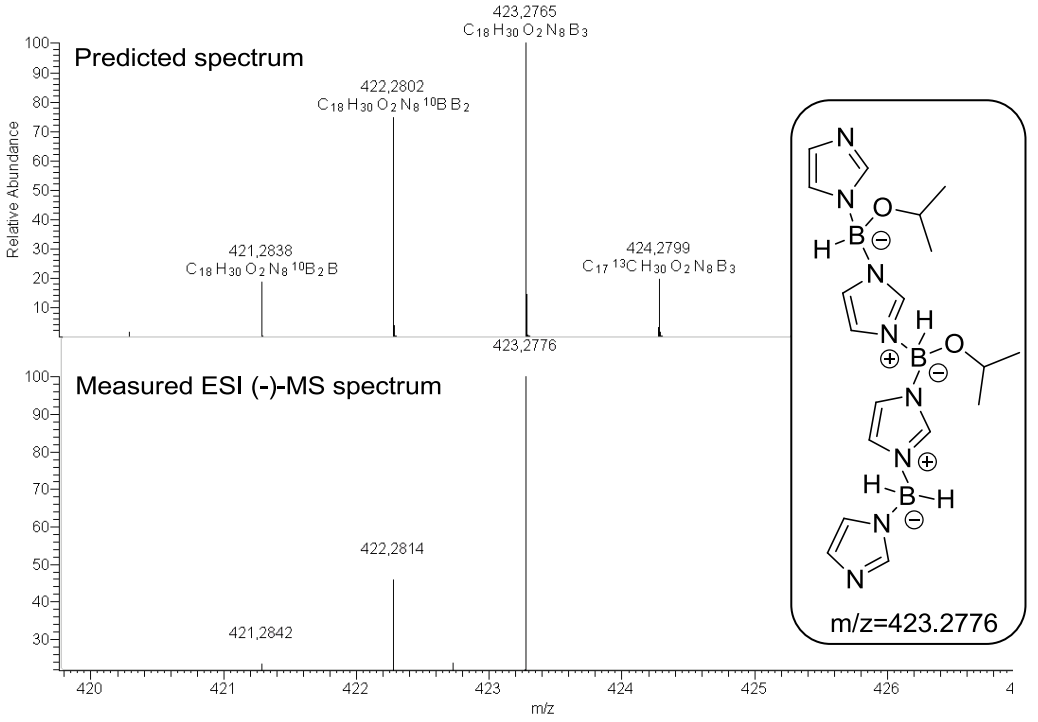
Predicted spectrum
423,2765
C18 H30 O2 N8 B3
422,2802
C18 H30 O2 N8 10B B2
421,2838
C18 H30 O2 N8 10B2 B
424,2799
C17 13C H30 O2 N8 B3
Relative Abundance
Measured ESI (-)-MS spectrum
423,2776
422,2814
421,2842
m/z
m/z=423.2776

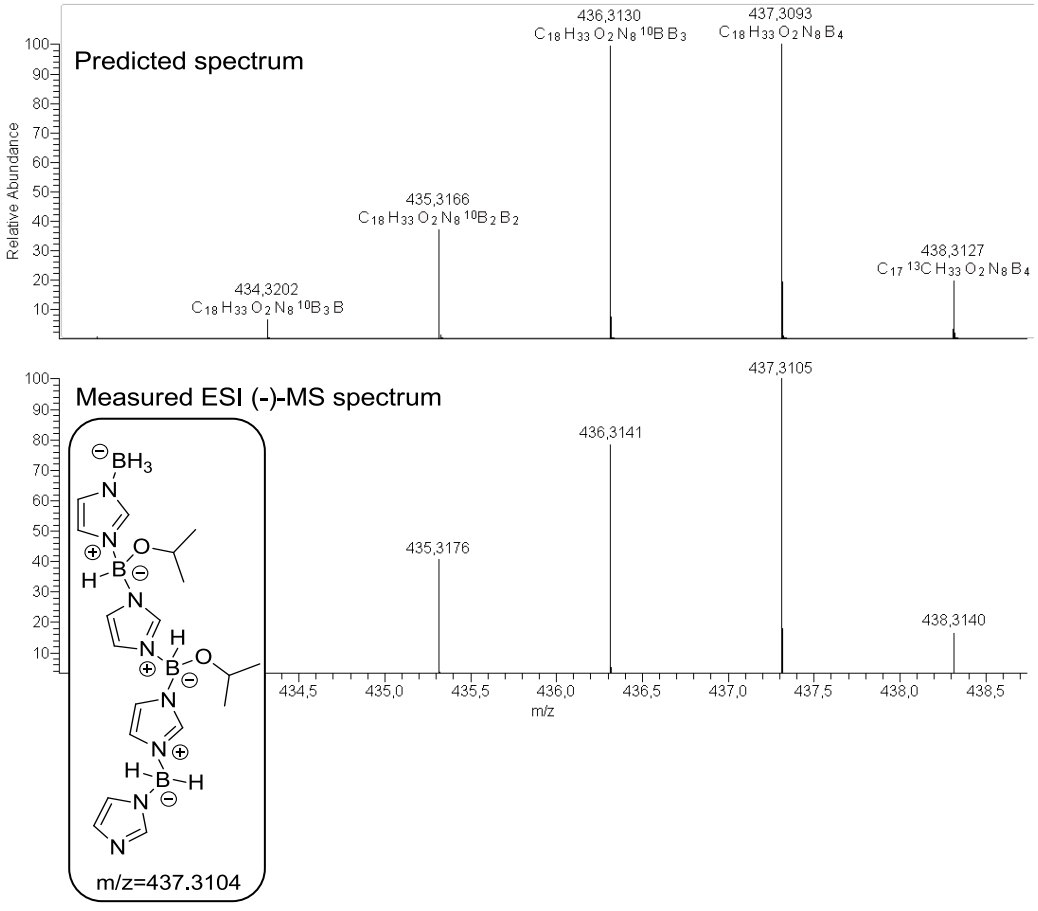
Predicted spectrum
436,3130
C18 H33 O2 N8 10B B3
437,3093
C18 H33 O2 N8 B4
435,3166
C18 H33 O2 N8 10B2 B2
438,3127
C17 13C H33 O2 N8 B4
434,3202
C18 H33 O2 N8 10B3 B
Relative Abundance
Measured ESI (-)-MS spectrum
437,3105
436,3141
435,3176
438,3140
m/z
m/z=437.3104

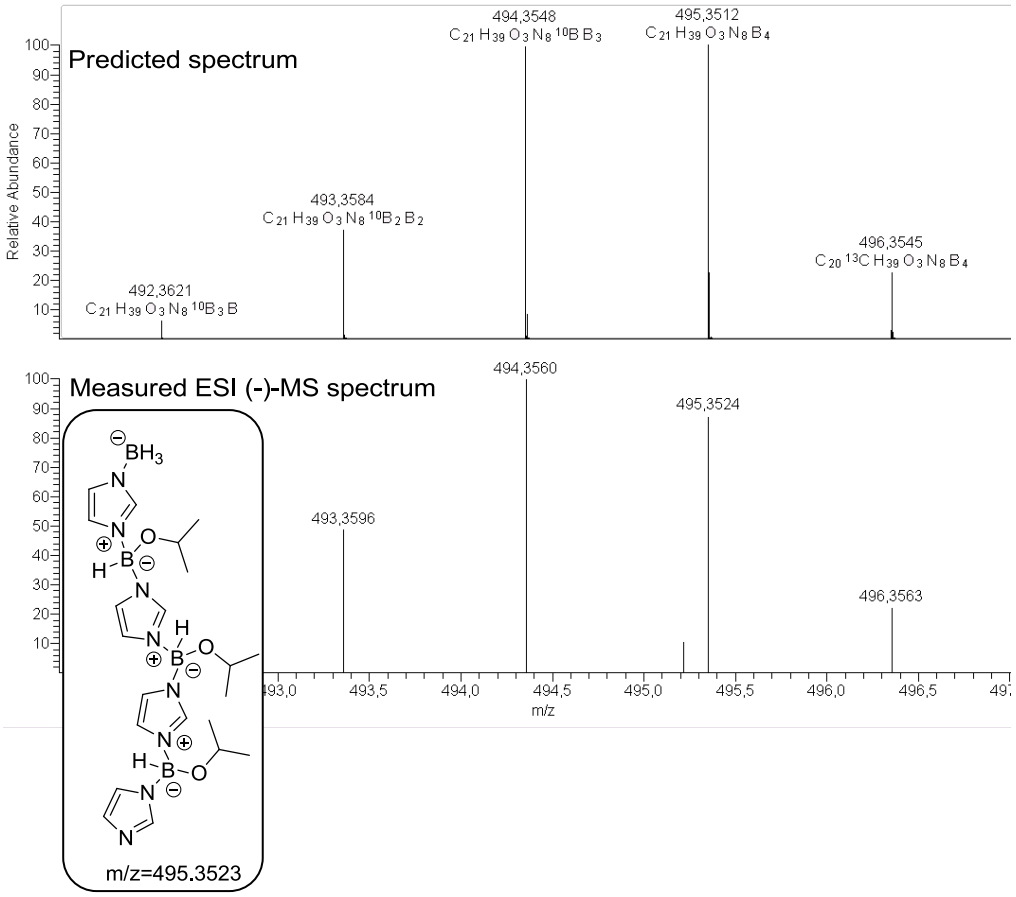
Predicted spectrum
494,3548
C21 H39 O3 N8 10B B3
495,3512
C21 H39 O3 N8 B4
493,3584
C21 H39 O3 N8 10B2 B2
496,3545
C20 13C H39 O3 N8 B4
492,3621
C21 H39 O3 N8 10B3 B
Relative Abundance
Measured ESI (-)-MS spectrum
494,3560
495,3524
493,3596
496,3563
m/z
m/z=495.3523

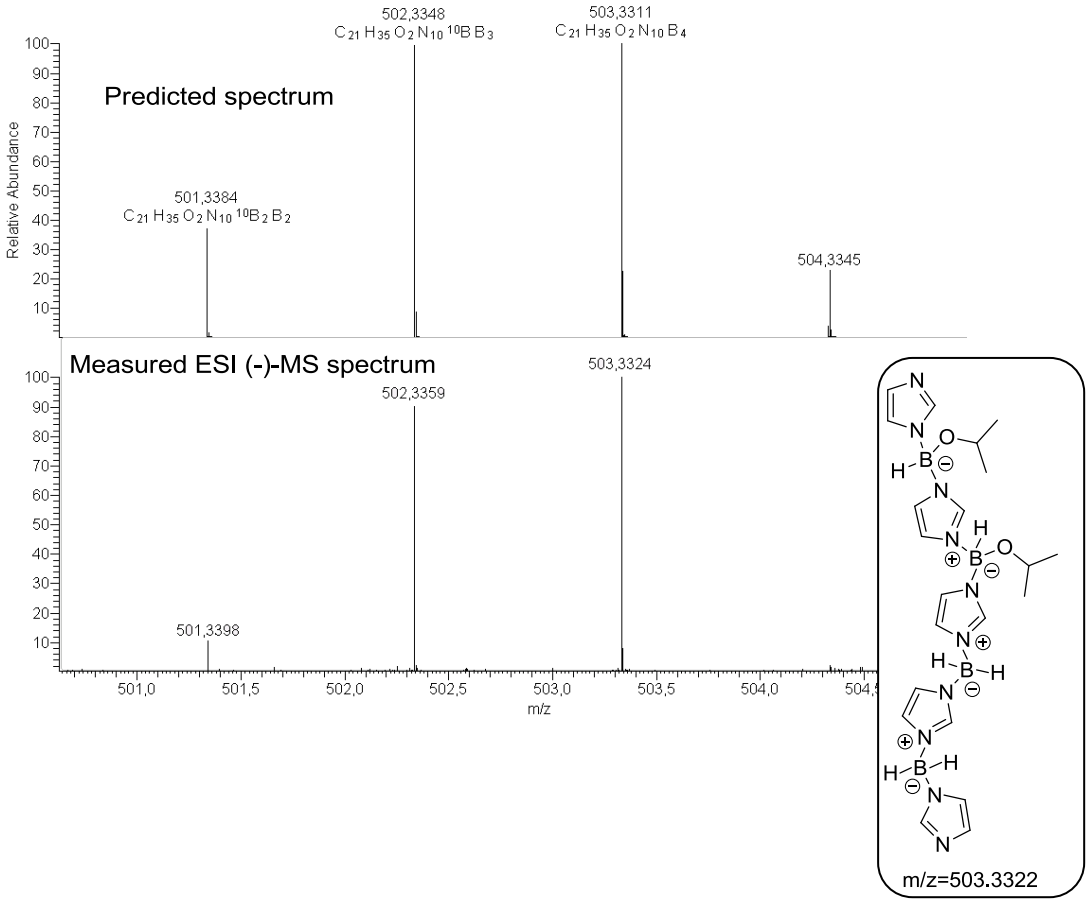
Predicted spectrum
502,3348
C21 H35 O2 N10 10B B3
503,3311
C21 H35 O2 N10 B4
501,3384
C21 H35 O2 N10 10B2 B2
504,3345
Relative Abundance
Measured ESI (-)-MS spectrum
503,3324
502,3359
501,3398
m/z
m/z=503.3322

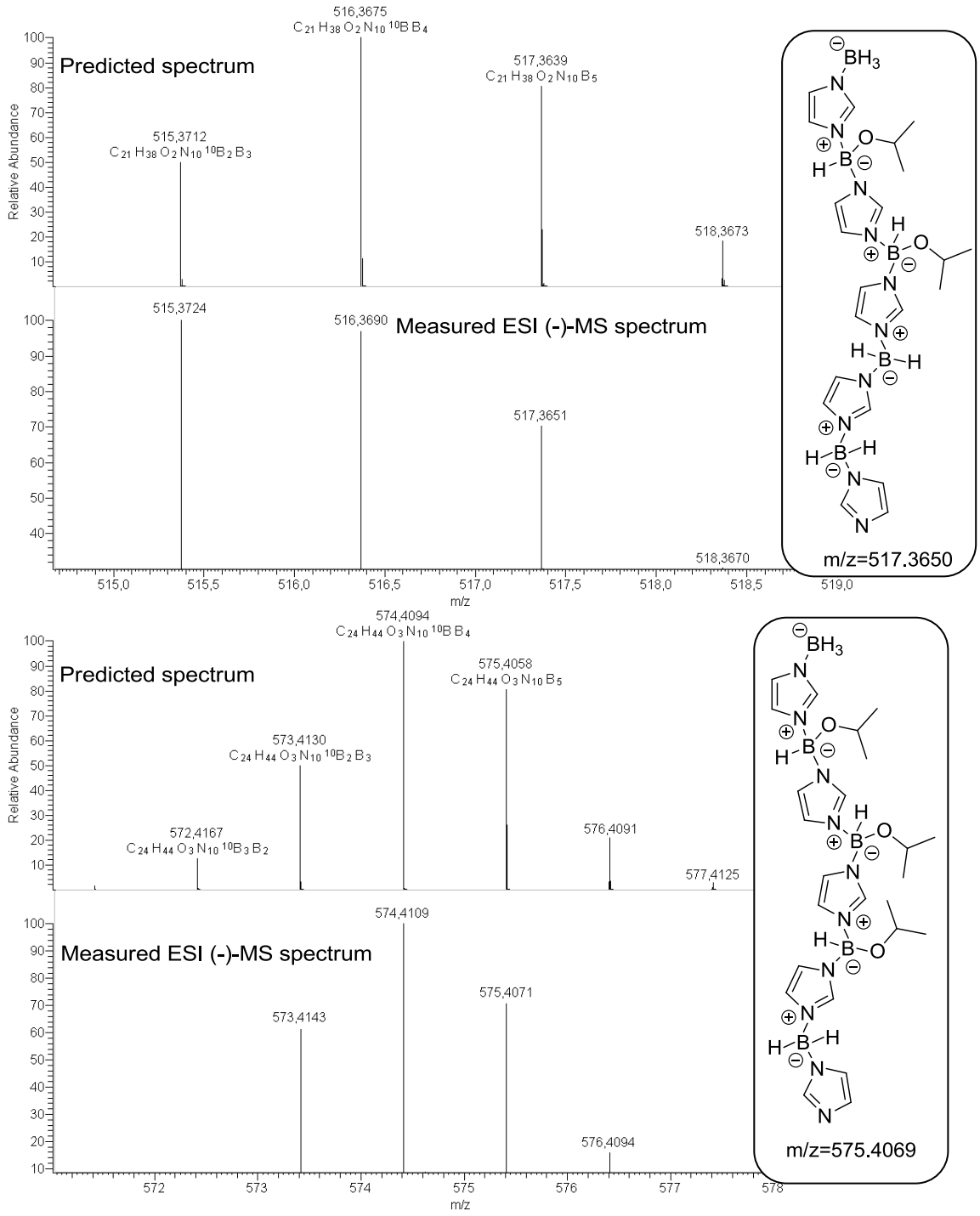
Predicted spectrum
516,3675
C21 H38 O2 N10 10B B4
517,3639
C21 H38 O2 N10 B5
515,3712
C21 H38 O2 N10 10B2 B3
518,3673
Measured ESI (-)-MS spectrum
515,3724
516,3690
517,3651
518,3670
Relative Abundance
m/z
m/z=517.3650
Predicted spectrum
574,4094
C24 H44 O3 N10 10B B4
575,4058
C24 H44 O3 N10 B5
573,4130
C24 H44 O3 N10 10B2 B3
572,4167
C24 H44 O3 N10 10B3 B2
576,4091
577,4125
Measured ESI (-)-MS spectrum
574,4109
575,4071
573,4143
576,4094
Relative Abundance
m/z
m/z=575.4069

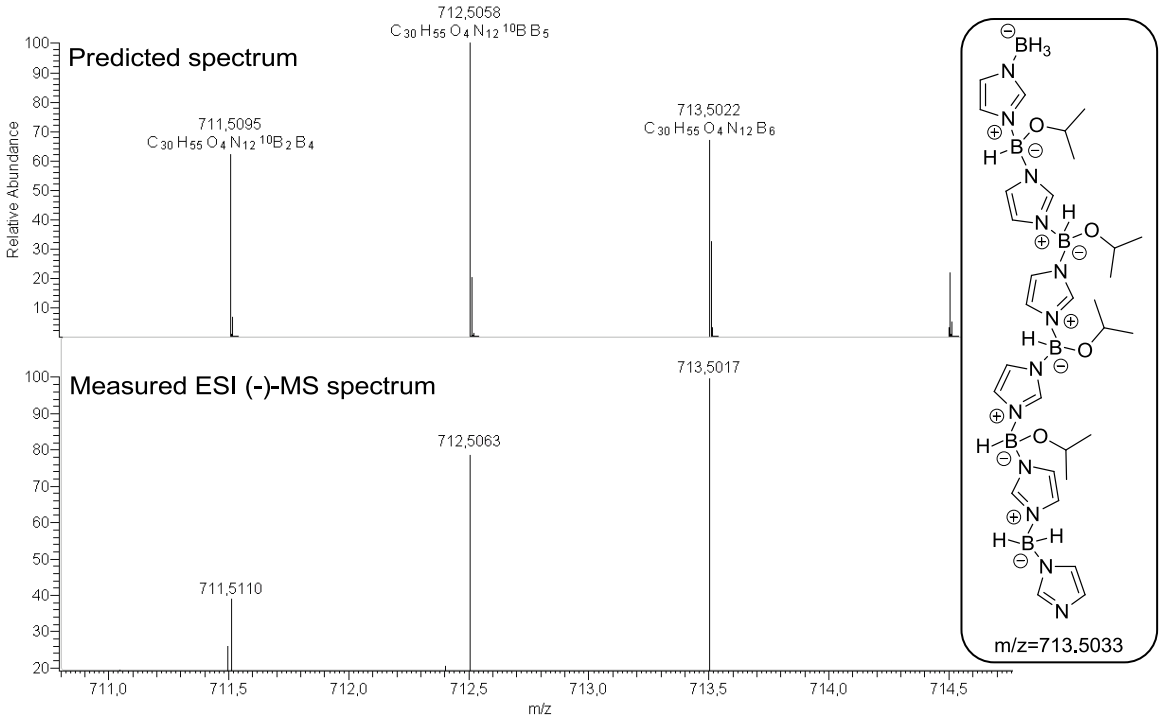
Predicted spectrum
712,5058
C30 H55 O4 N12 10B B5
711,5095
C30 H55 O4 N12 10B2 B4
713,5022
C30 H55 O4 N12 B6
Measured ESI (-)-MS spectrum
713,5017
712,5063
711,5110
Relative Abundance
m/z
m/z=713.5033

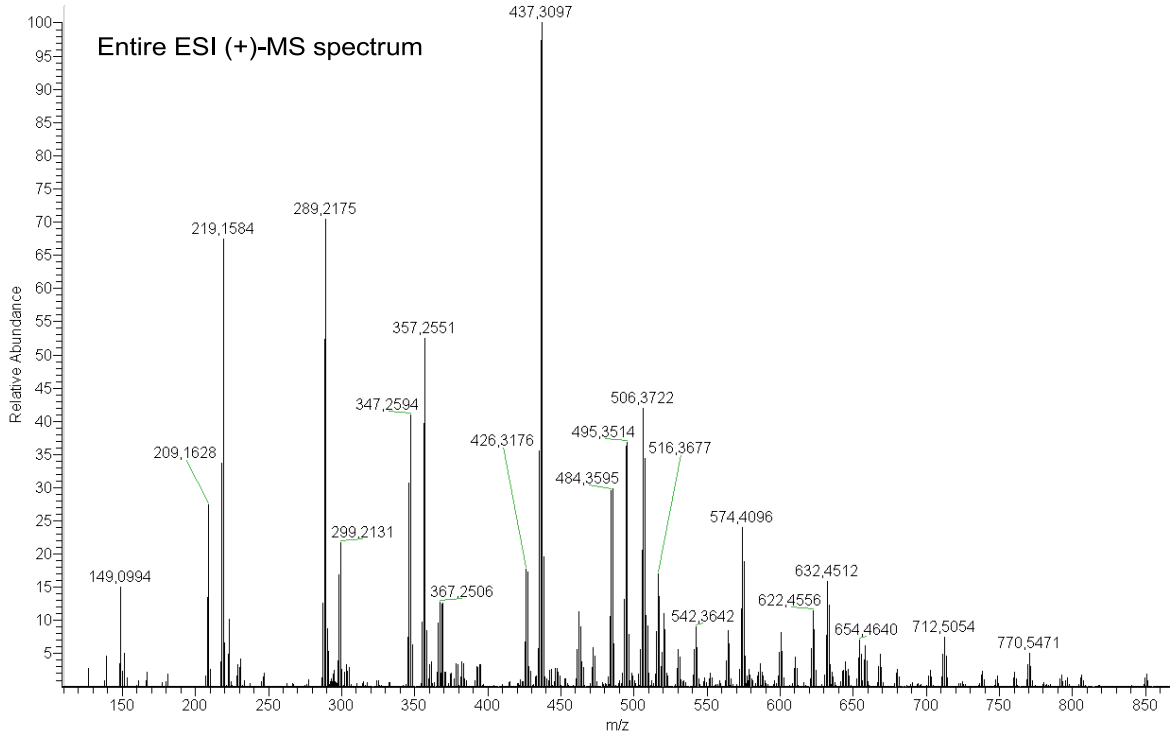
Entire ESI (+)-MS spectrum
437,3097
289,2175
219,1584
357,2551
347,2594
506,3722
495,3514
426,3176
516,3677
209,1628
484,3595
574,4096
299,2131
632,4512
149,0994
367,2506
622,4556
542,3642
654,4640
712,5054
770,5471
Relative Abundance
m/z

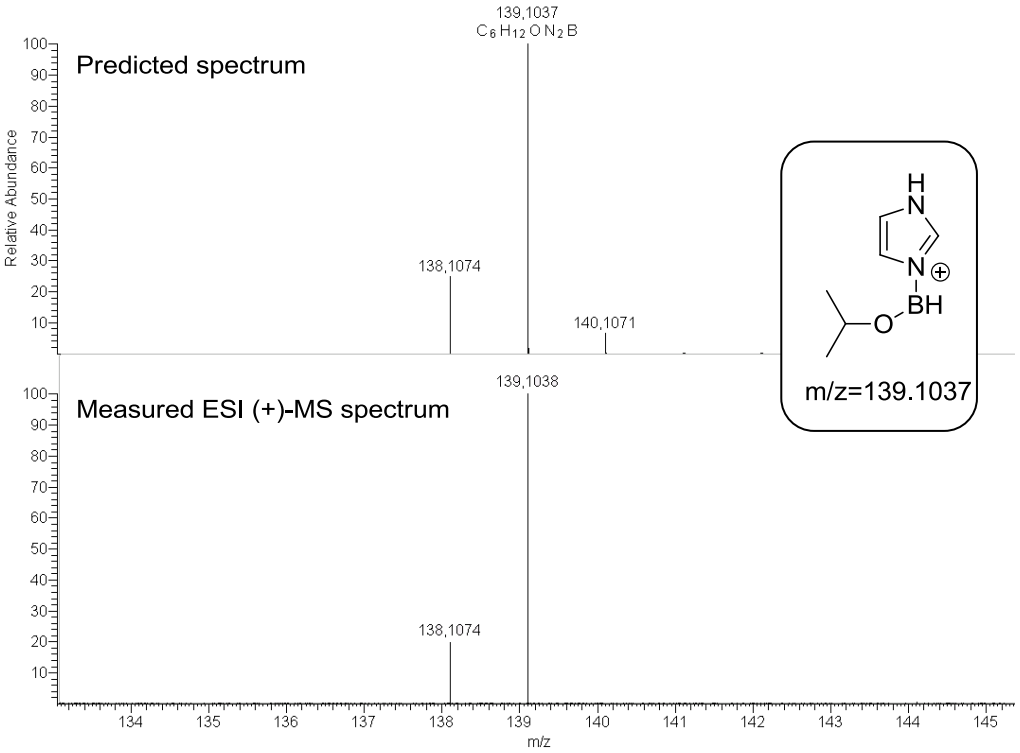
139,1037
C6H12ON2B
Predicted spectrum
Relative Abundance
138,1074
140,1071
m/z=139.1037
Measured ESI (+)-MS spectrum
139,1038
138,1074
m/z

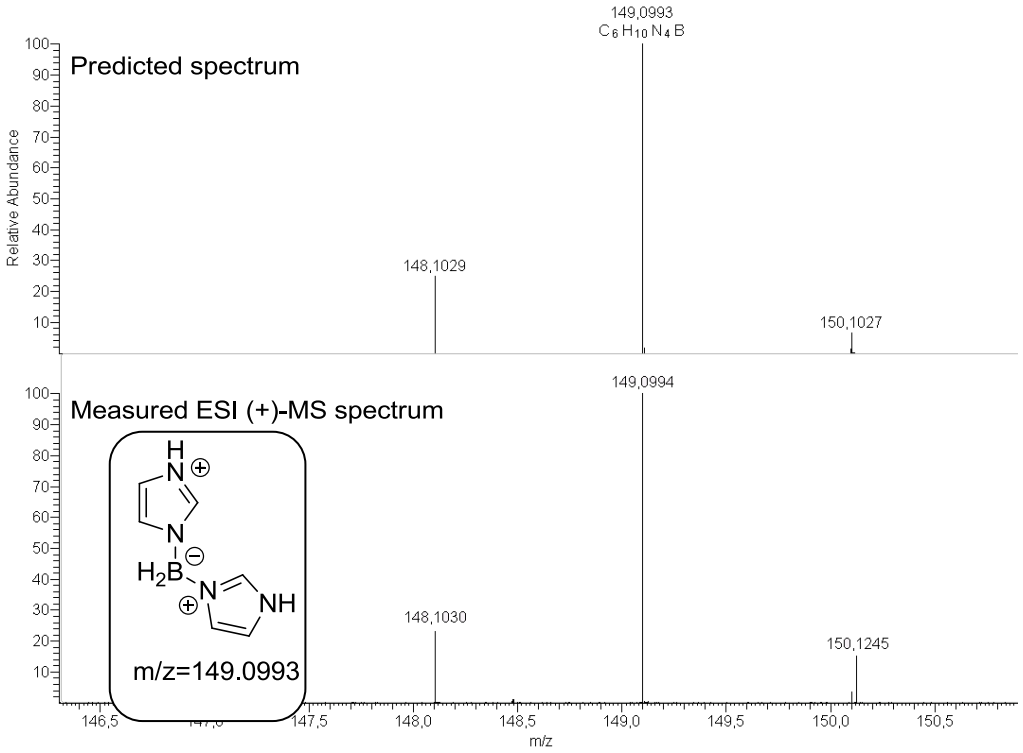
149,0993
C6H10N4B
Predicted spectrum
Relative Abundance
148,1029
150,1027
Measured ESI (+)-MS spectrum
149,0994
148,1030
150,1245
m/z=149.0993
m/z

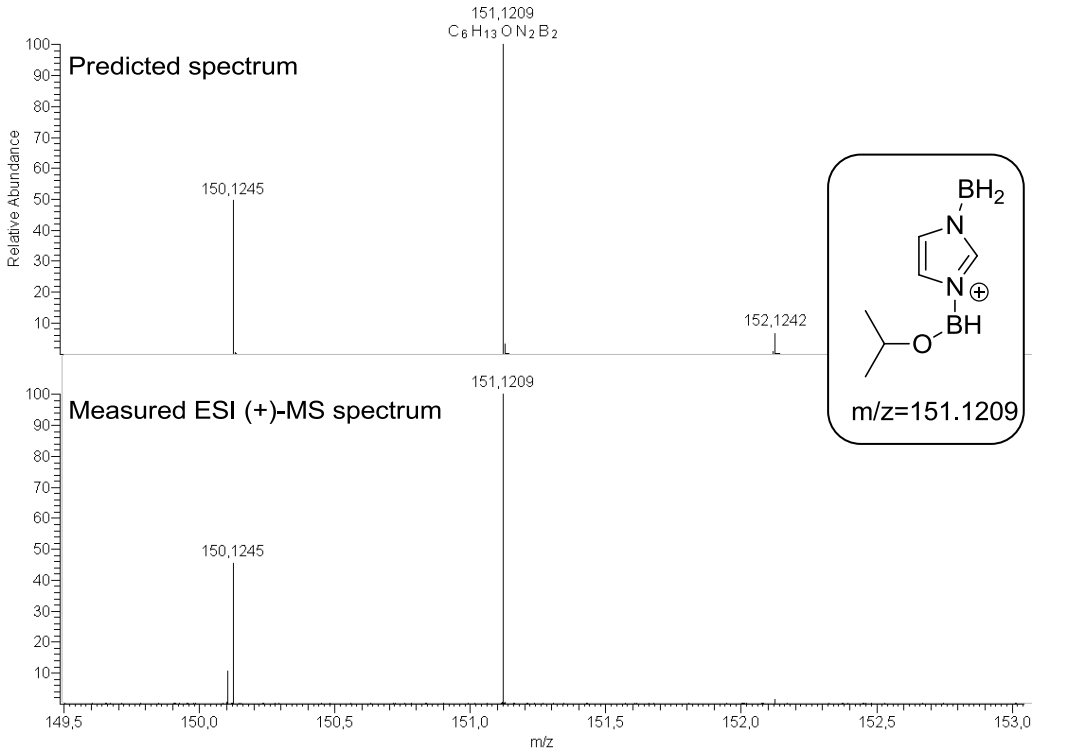
151,1209
C6H13ON2B2
Predicted spectrum
150,1245
152,1242
Measured ESI (+)-MS spectrum
151,1209
150,1245
Relative Abundance
m/z
m/z=151.1209

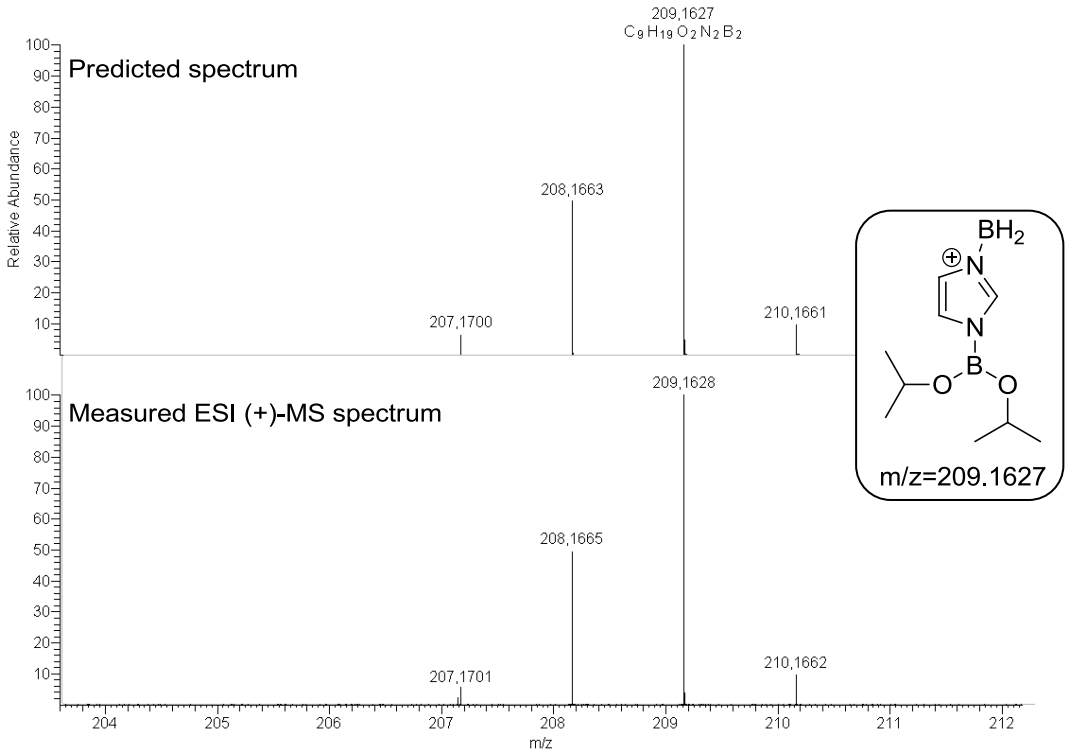
209,1627
C9H19O2N2B2
Predicted spectrum
208,1663
207,1700
210,1661
Measured ESI (+)-MS spectrum
209,1628
208,1665
207,1701
210,1662
Relative Abundance
m/z
m/z=209.1627

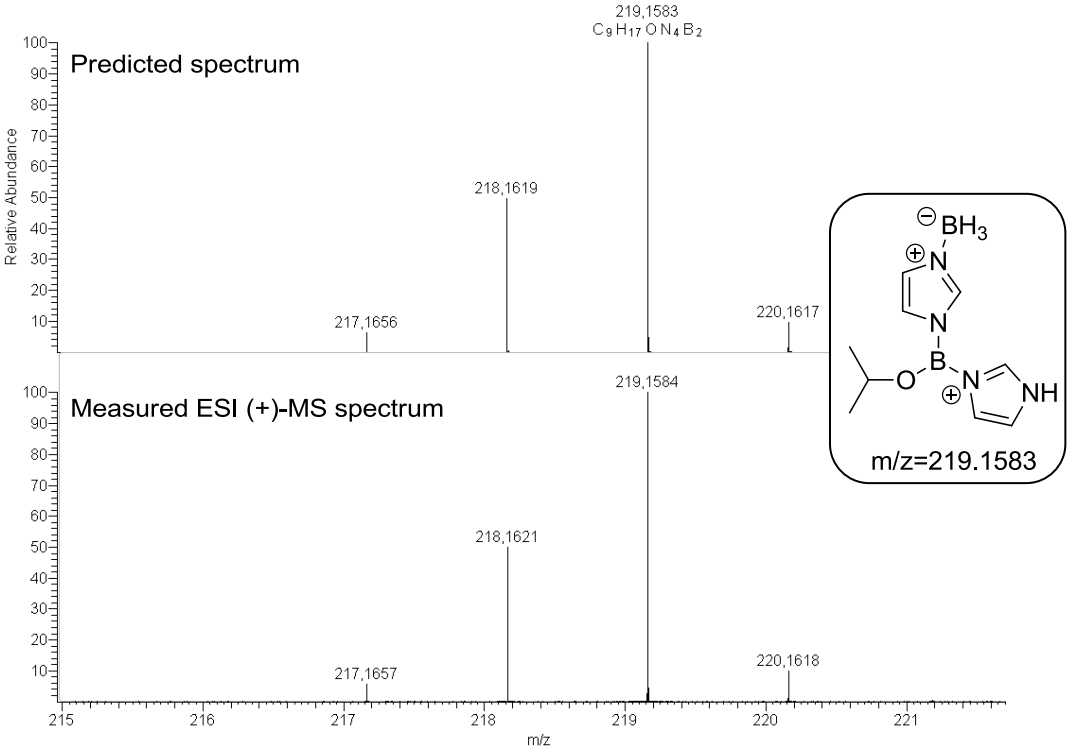
Predicted spectrum
219,1583
C9H17ON4B2
218,1619
217,1656
220,1617
Measured ESI (+)-MS spectrum
219,1584
218,1621
217,1657
220,1618
Relative Abundance
m/z
m/z=219.1583

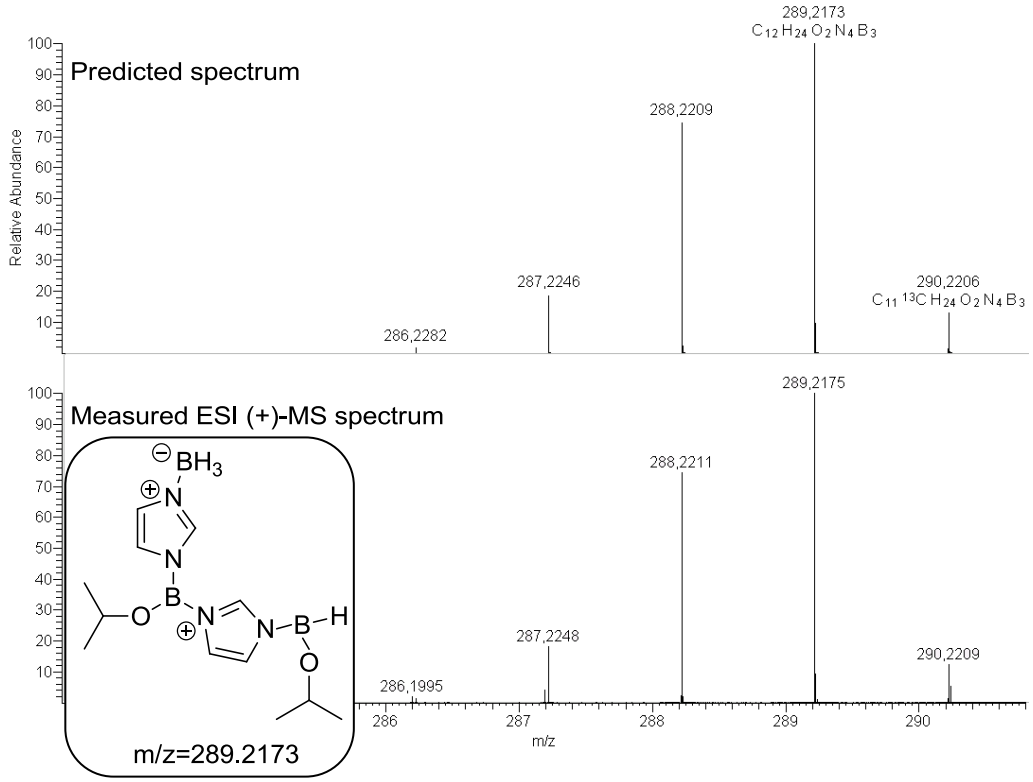
Predicted spectrum
289,2173
C12H24O2N4B3
288,2209
287,2246
286,2282
290,2206
C11 13CH24O2N4B3
Measured ESI (+)-MS spectrum
289,2175
288,2211
287,2248
286,1995
290,2209
Relative Abundance
m/z
m/z=289.2173

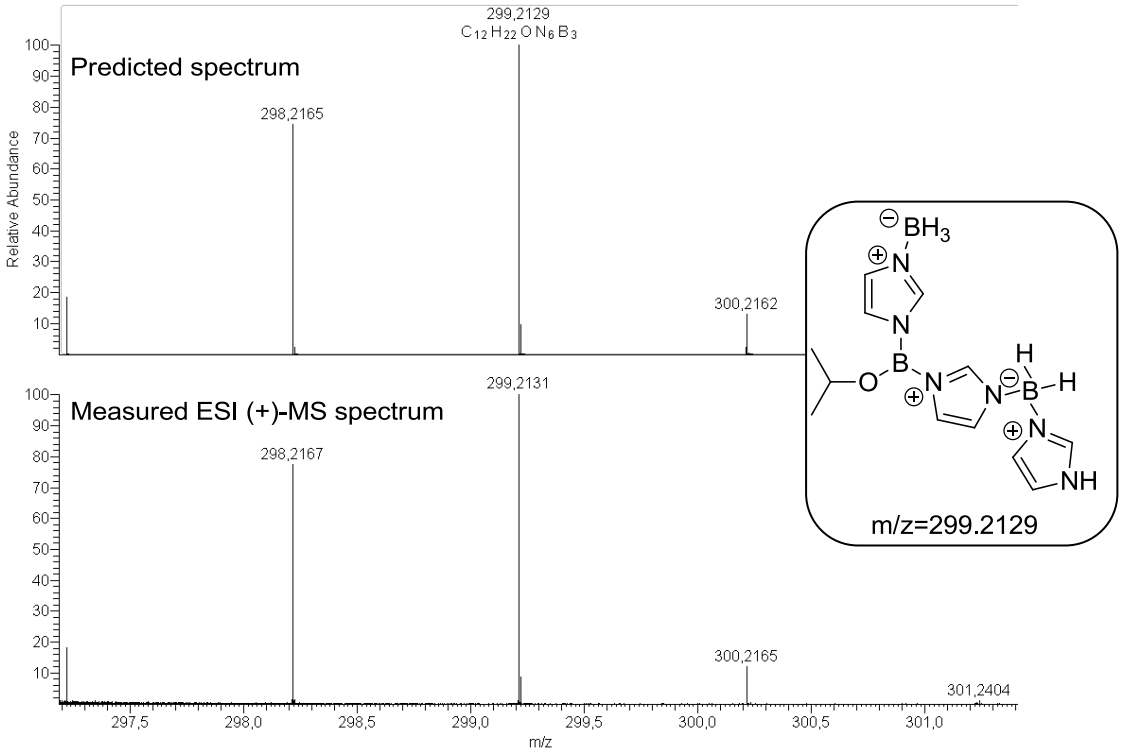
Predicted spectrum
299,2129
C12 H22 O N6 B3
298,2165
300,2162
Measured ESI (+)-MS spectrum
299,2131
298,2167
300,2165
301,2404
Relative Abundance
m/z
m/z=299.2129

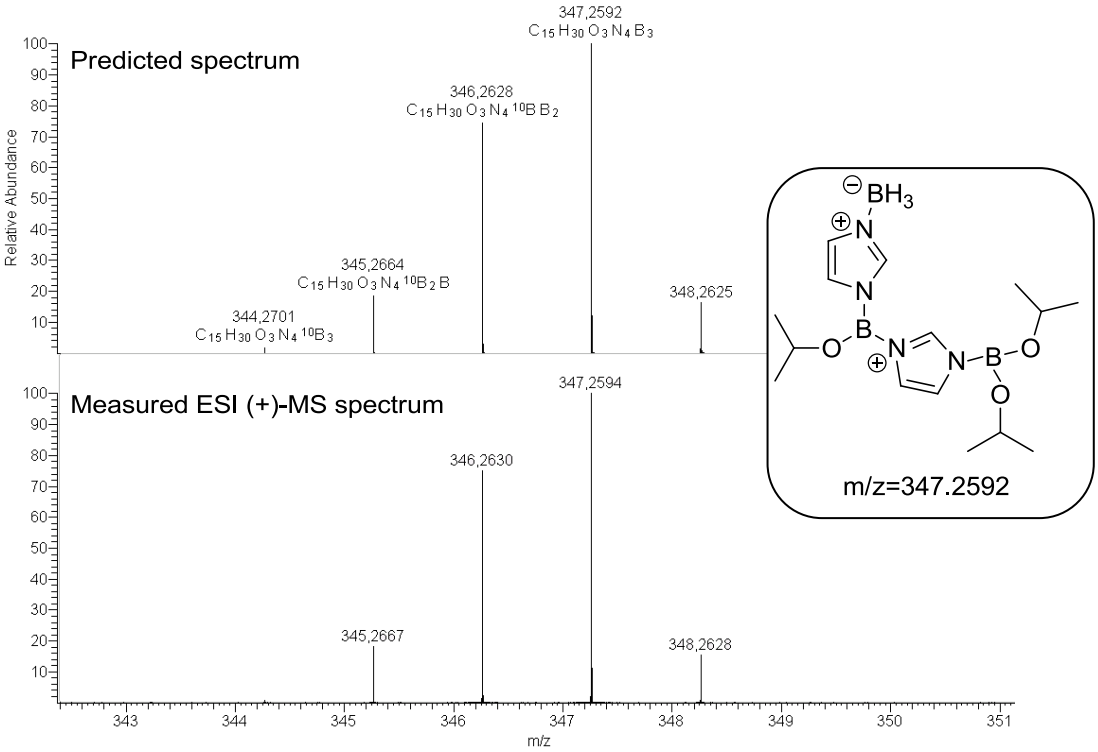
Predicted spectrum
347,2592
C15 H30 O3 N4 B3
346,2628
C15 H30 O3 N4 10B B2
345,2664
C15 H30 O3 N4 10B2 B
344,2701
C15 H30 O3 N4 10B3
348,2625
Measured ESI (+)-MS spectrum
347,2594
346,2630
345,2667
348,2628
Relative Abundance
m/z
m/z=347.2592

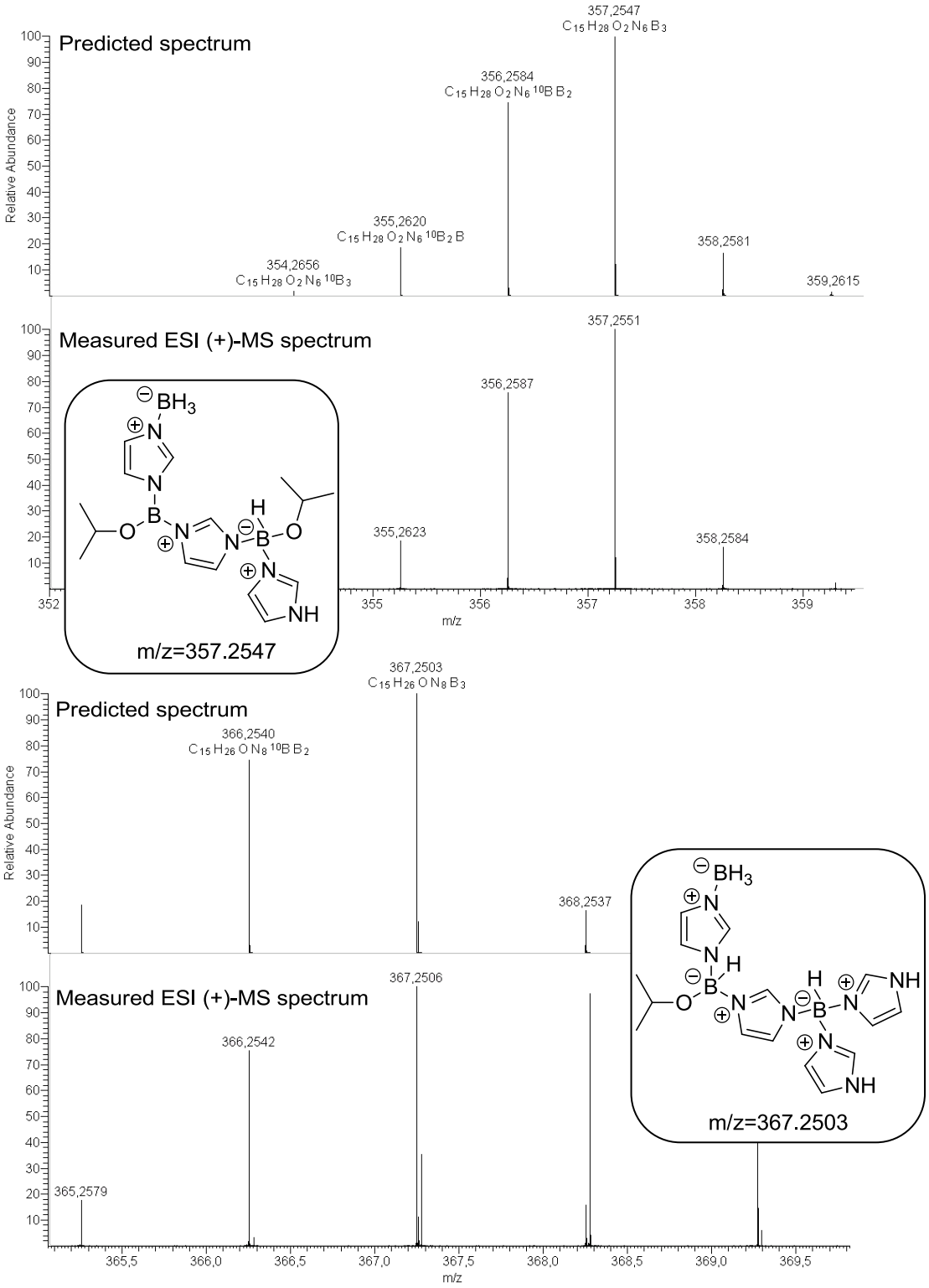
Predicted spectrum
357,2547
C15 H28 O2 N6 B3
356,2584
C15 H28 O2 N6 10B B2
355,2620
C15 H28 O2 N6 10B2 B
354,2656
C15 H28 O2 N6 10B3
358,2581
359,2615
Relative Abundance
Measured ESI (+)-MS spectrum
357,2551
356,2587
355,2623
358,2584
m/z
m/z=357.2547
Predicted spectrum
367,2503
C15 H26 O N8 B3
366,2540
C15 H26 O N8 10B B2
368,2537
Measured ESI (+)-MS spectrum
367,2506
366,2542
365,2579
m/z
m/z=367.2503

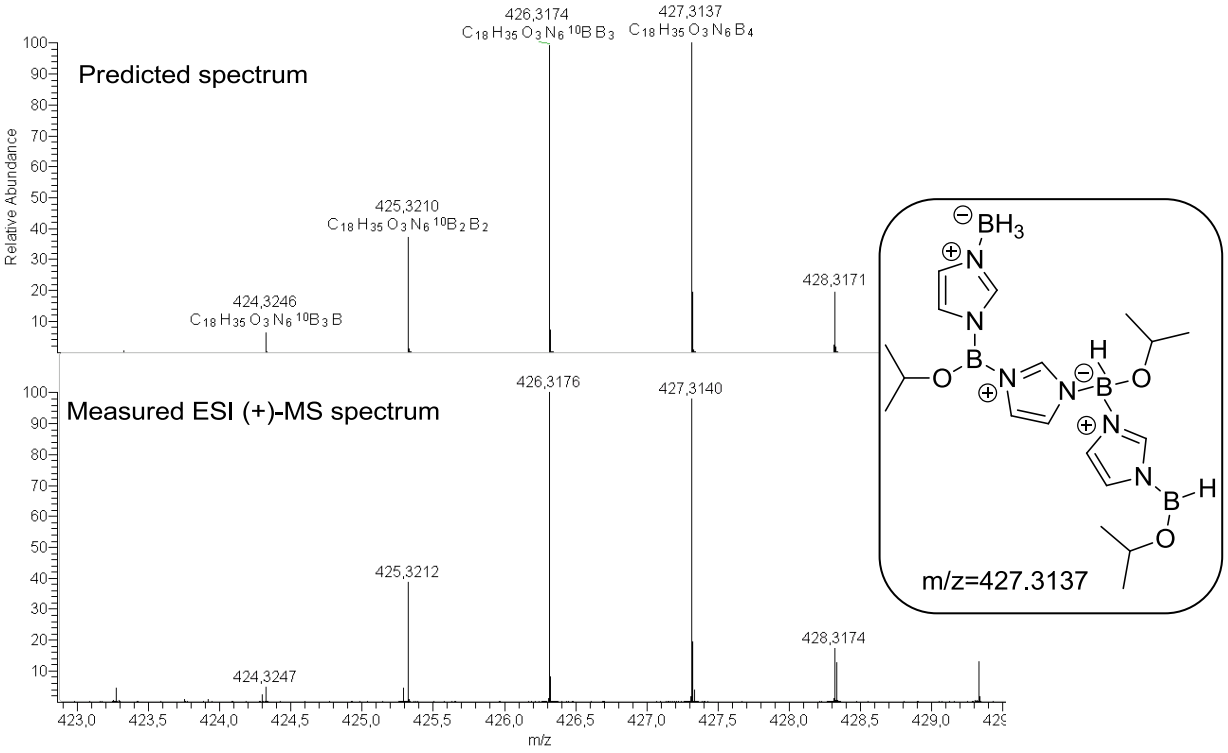
Predicted spectrum
426,3174
C18 H35 O3 N6 10B B3
427,3137
C18 H35 O3 N6 B4
425,3210
C18 H35 O3 N6 10B2 B2
424,3246
C18 H35 O3 N6 10B3 B
428,3171
Measured ESI (+)-MS spectrum
426,3176
427,3140
425,3212
424,3247
428,3174
Relative Abundance
m/z
m/z=427.3137

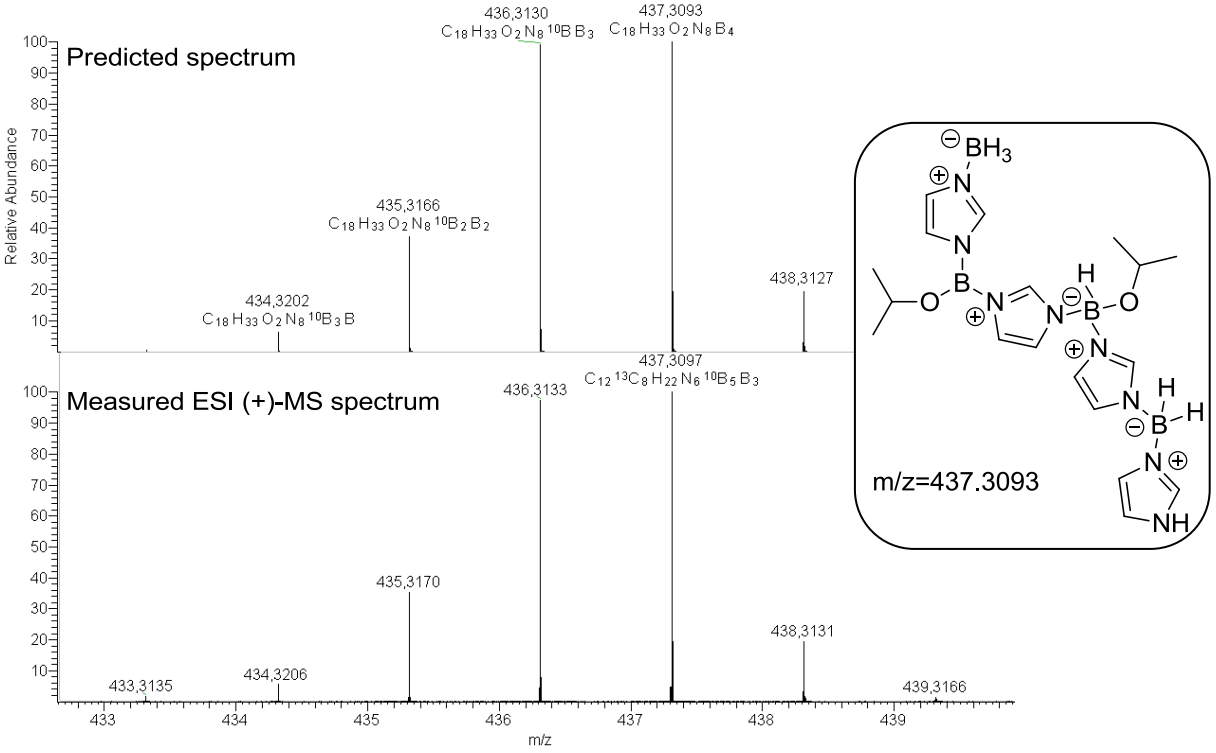
Predicted spectrum
436,3130
C18 H33 O2 N8 10B B3
437,3093
C18 H33 O2 N8 B4
435,3166
C18 H33 O2 N8 10B2 B2
434,3202
C18 H33 O2 N8 10B3 B
438,3127
Measured ESI (+)-MS spectrum
437,3097
C12 13C8 H22 N6 10B5 B3
436,3133
435,3170
438,3131
433,3135
434,3206
439,3166
Relative Abundance
m/z
m/z=437.3093

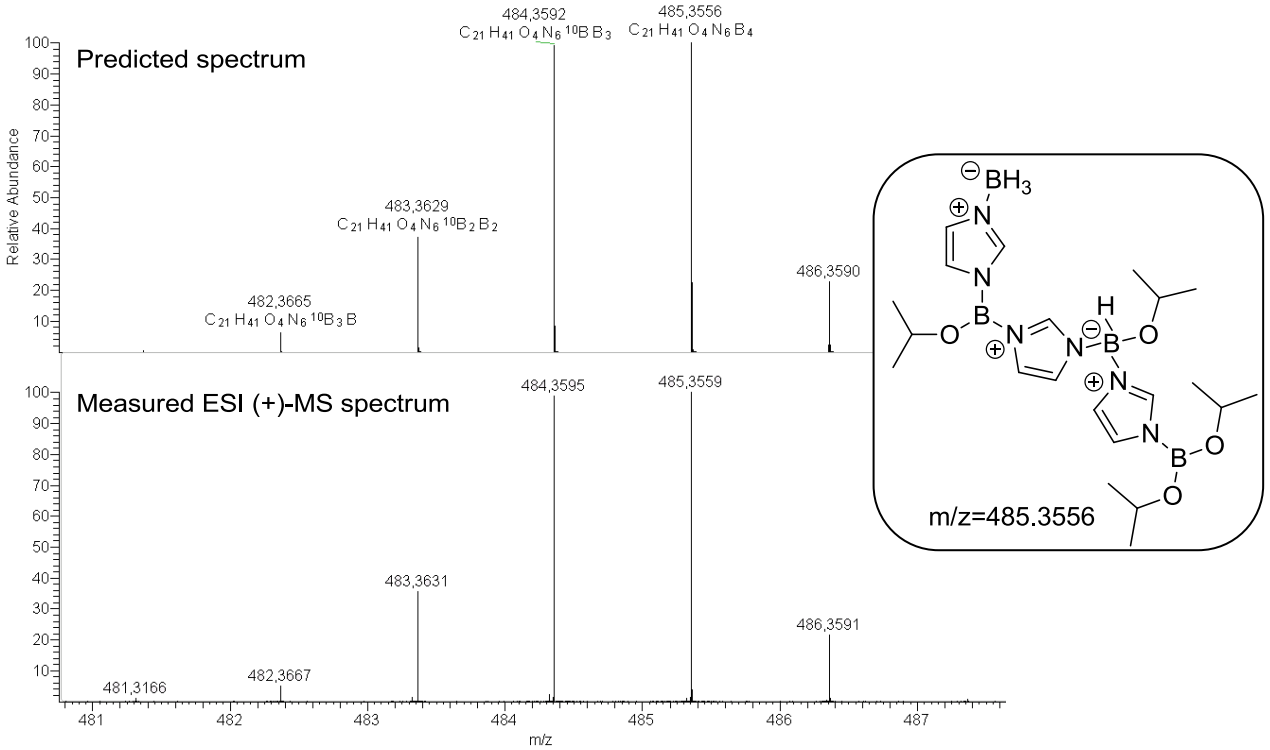
Predicted spectrum
484,3592
C21 H41 O4 N6 10B B3
485,3556
C21 H41 O4 N6 B4
483,3629
C21 H41 O4 N6 10B2 B2
482,3665
C21 H41 O4 N6 10B3 B
486,3590
Measured ESI (+)-MS spectrum
484,3595
485,3559
483,3631
486,3591
481,3166
482,3667
Relative Abundance
m/z
m/z=485.3556

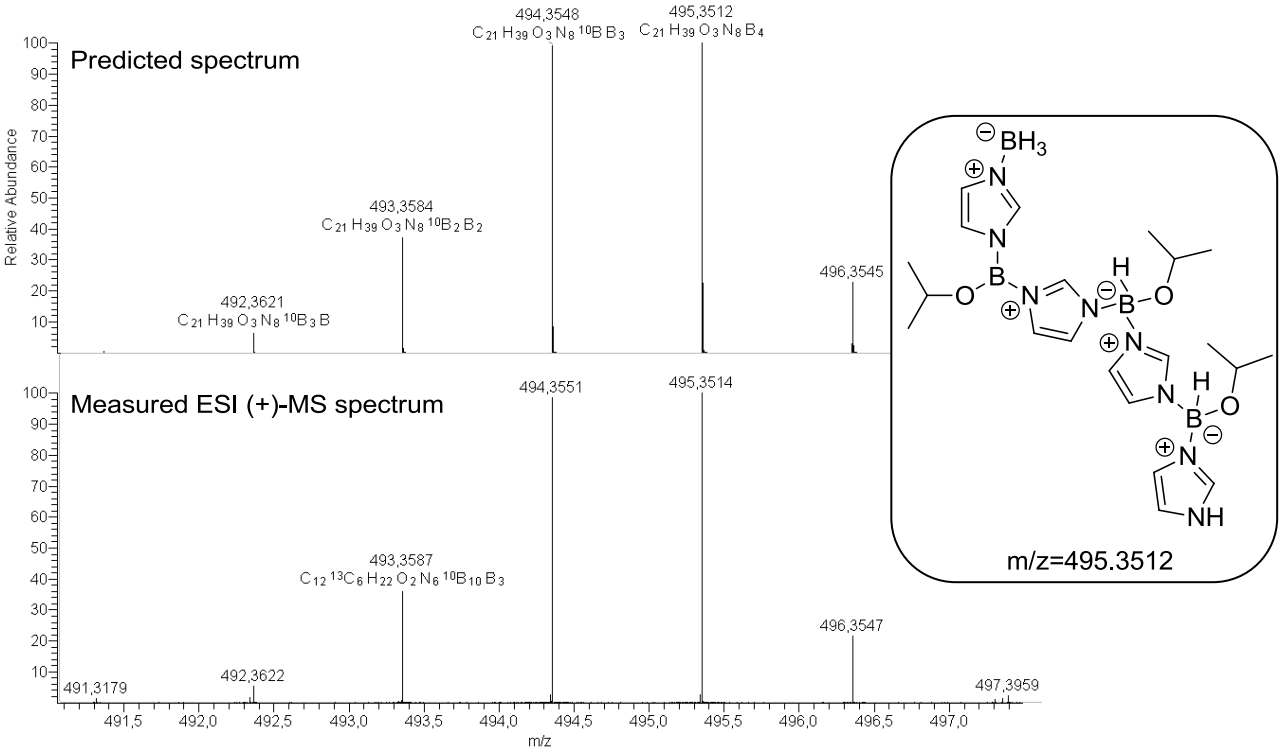
Predicted spectrum
494,3548
C21 H39 O3 N8 10B B3
495,3512
C21 H39 O3 N8 B4
493,3584
C21 H39 O3 N8 10B2 B2
492,3621
C21 H39 O3 N8 10B3 B
496,3545
Measured ESI (+)-MS spectrum
494,3551
495,3514
493,3587
C12 13C6 H22 O2 N6 10B10 B3
496,3547
491,3179
492,3622
497,3959
Relative Abundance
m/z
m/z=495.3512

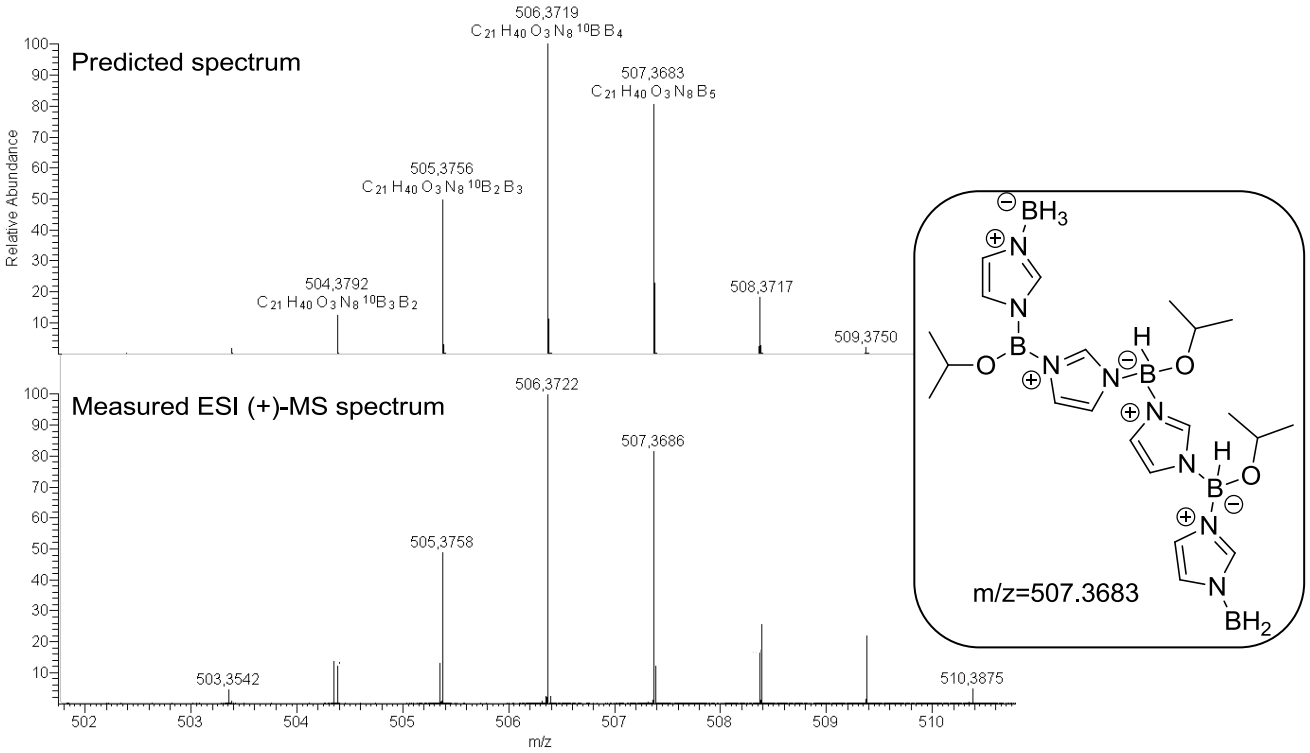
Predicted spectrum
506,3719
C21 H40 O3 N8 10B B4
507,3683
C21 H40 O3 N8 B5
505,3756
C21 H40 O3 N8 10B2 B3
504,3792
C21 H40 O3 N8 10B3 B2
508,3717
509,3750
Measured ESI (+)-MS spectrum
506,3722
507,3686
505,3758
503,3542
510,3875
Relative Abundance
m/z
m/z=507.3683

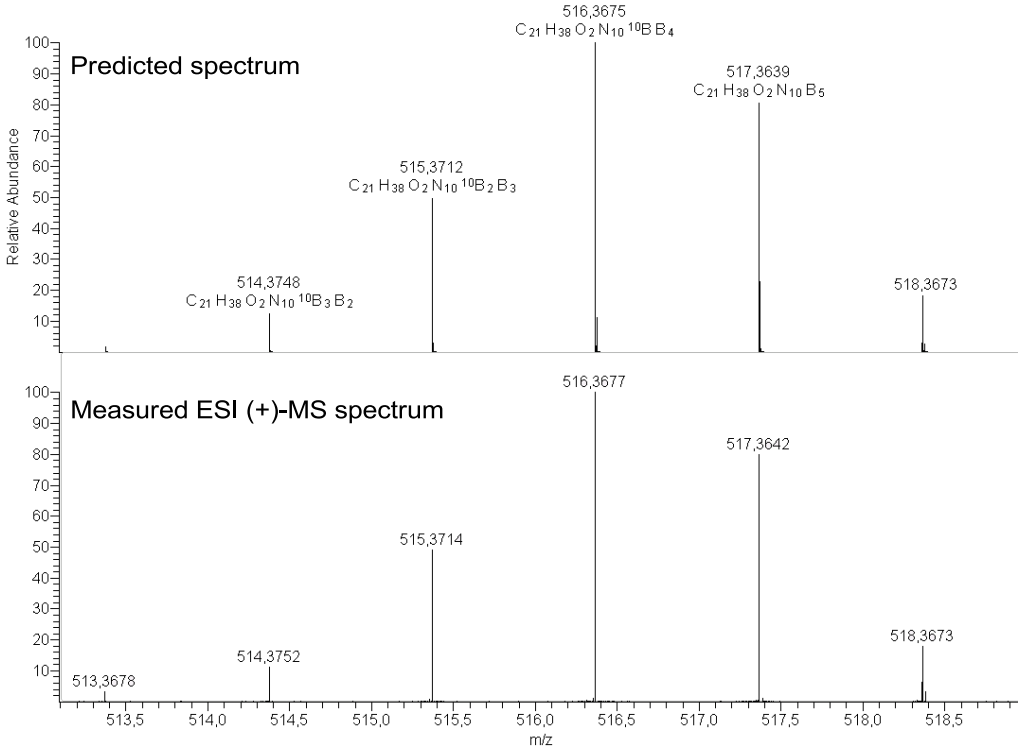
Predicted spectrum
516,3675
C21 H38 O2 N10 10B B4
517,3639
C21 H38 O2 N10 B5
515,3712
C21 H38 O2 N10 10B2 B3
514,3748
C21 H38 O2 N10 10B3 B2
518,3673
Relative Abundance
Measured ESI (+)-MS spectrum
516,3677
517,3642
515,3714
518,3673
514,3752
513,3678
m/z

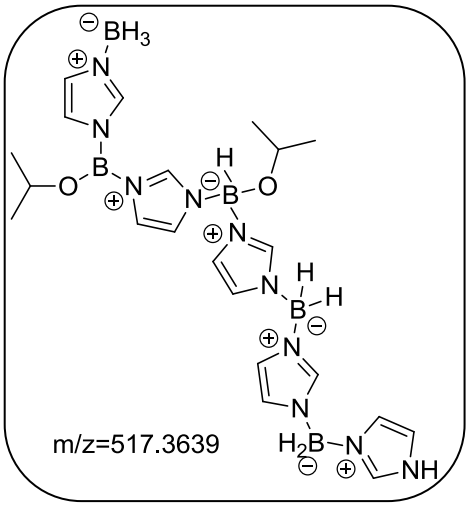
m/z=517.3639

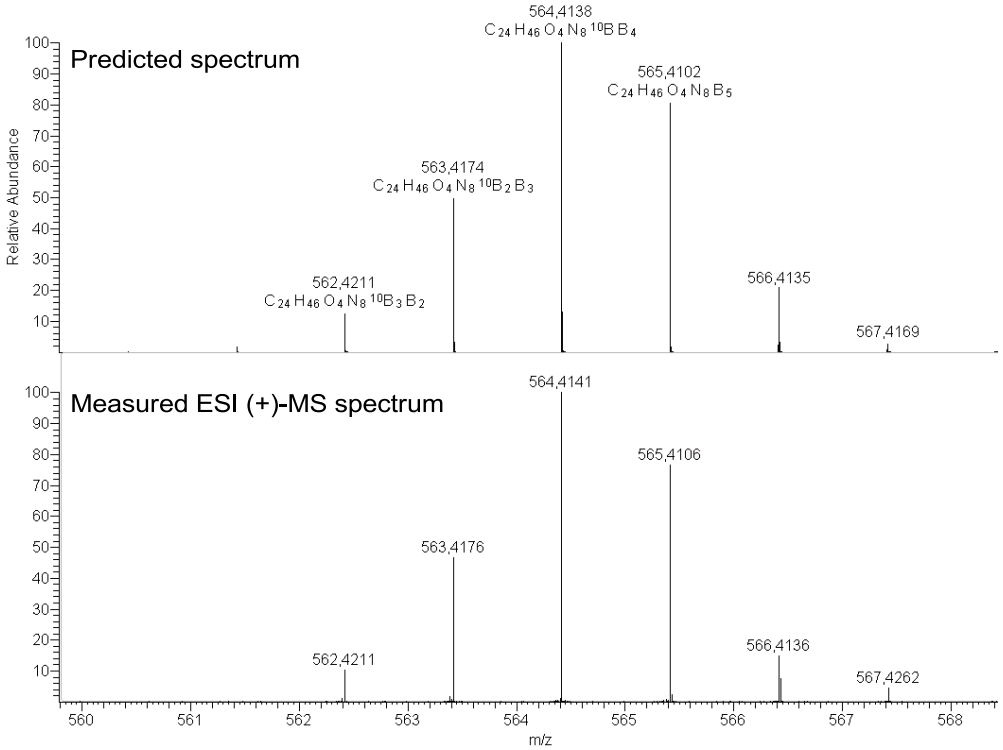
Predicted spectrum
564,4138
C24 H46 O4 N8 10B B4
565,4102
C24 H46 O4 N8 B5
563,4174
C24 H46 O4 N8 10B2 B3
562,4211
C24 H46 O4 N8 10B3 B2
566,4135
567,4169
Relative Abundance
Measured ESI (+)-MS spectrum
564,4141
565,4106
563,4176
562,4211
566,4136
567,4262
m/z

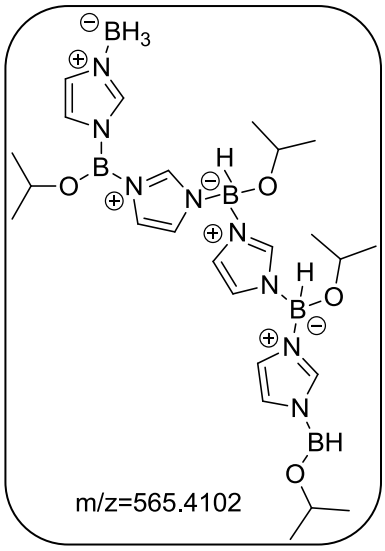
m/z=565.4102

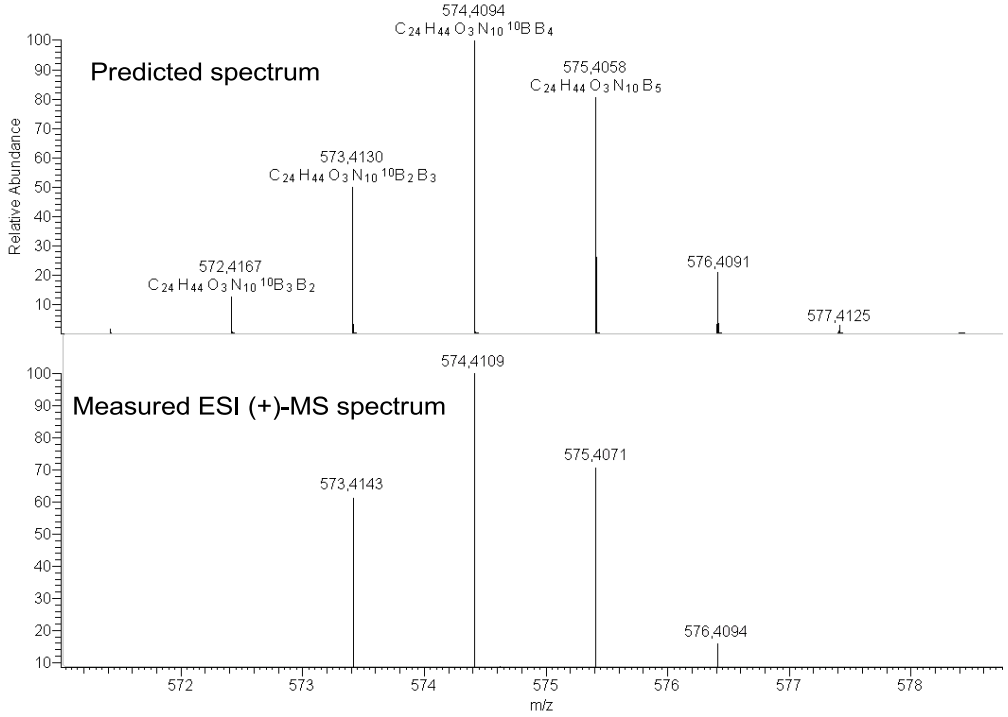
Predicted spectrum
574,4094
C24 H44 O3 N10 10B B4
575,4058
C24 H44 O3 N10 B5
573,4130
C24 H44 O3 N10 10B2 B3
572,4167
C24 H44 O3 N10 10B3 B2
576,4091
577,4125
Measured ESI (+)-MS spectrum
574,4109
575,4071
573,4143
576,4094
Relative Abundance
m/z

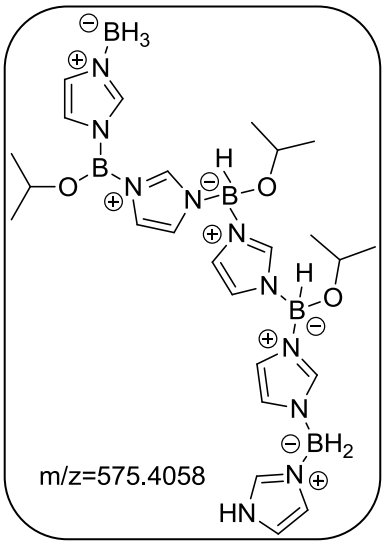
m/z=575.4058

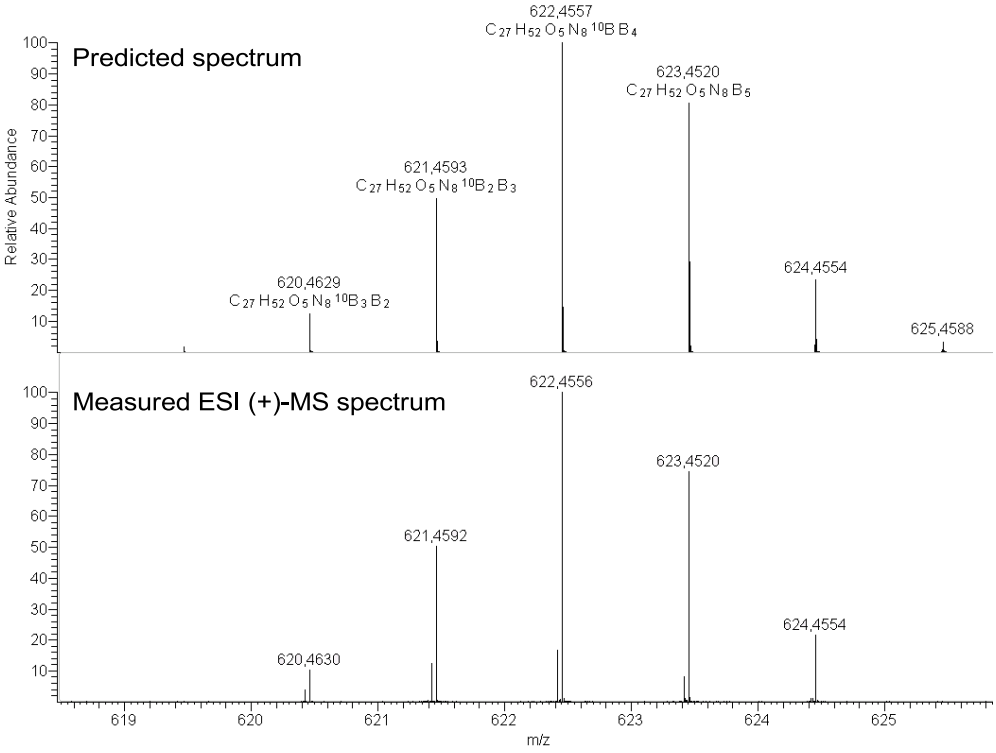
Predicted spectrum
622,4557
C27 H52 O5 N8 10B B4
623,4520
C27 H52 O5 N8 B5
621,4593
C27 H52 O5 N8 10B2 B3
620,4629
C27 H52 O5 N8 10B3 B2
624,4554
625,4588
Measured ESI (+)-MS spectrum
622,4556
623,4520
621,4592
624,4554
620,4630
Relative Abundance
m/z

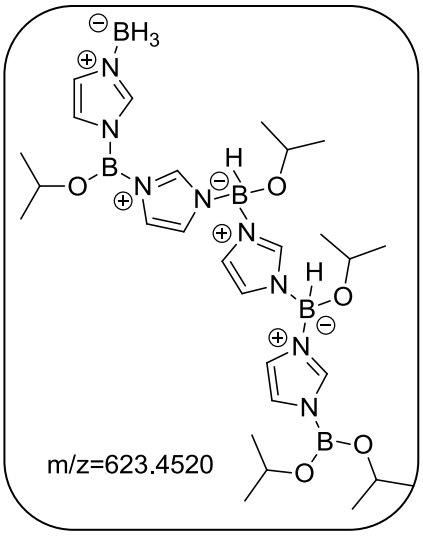
m/z=623.4520

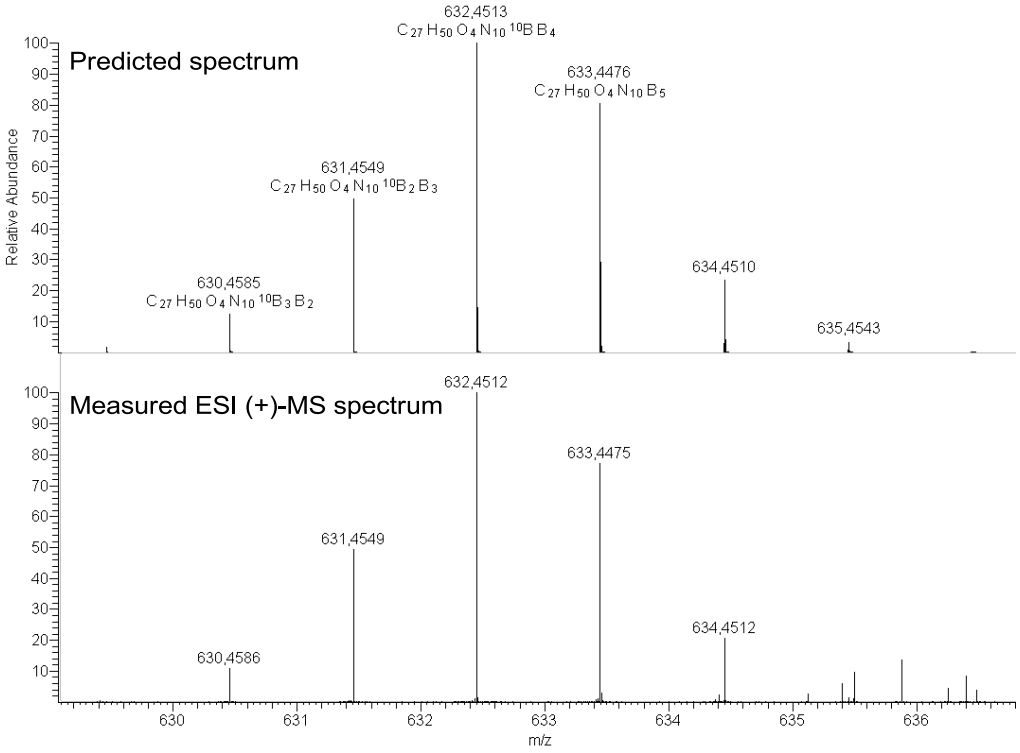
Predicted spectrum
632,4513
C27 H50 O4 N10 10B B4
633,4476
C27 H50 O4 N10 B5
631,4549
C27 H50 O4 N10 10B2 B3
630,4585
C27 H50 O4 N10 10B3 B2
634,4510
635,4543
Measured ESI (+)-MS spectrum
632,4512
633,4475
631,4549
634,4512
630,4586
Relative Abundance
m/z

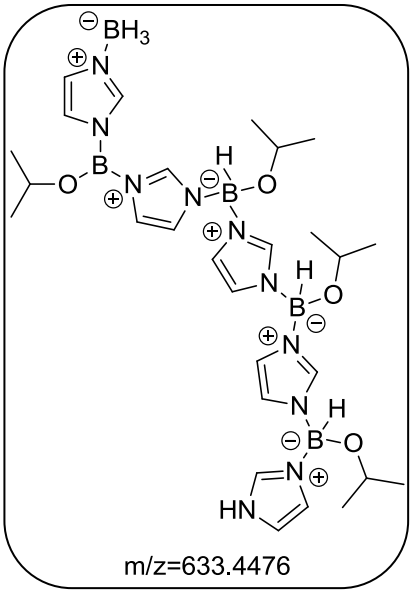
m/z=633.4476

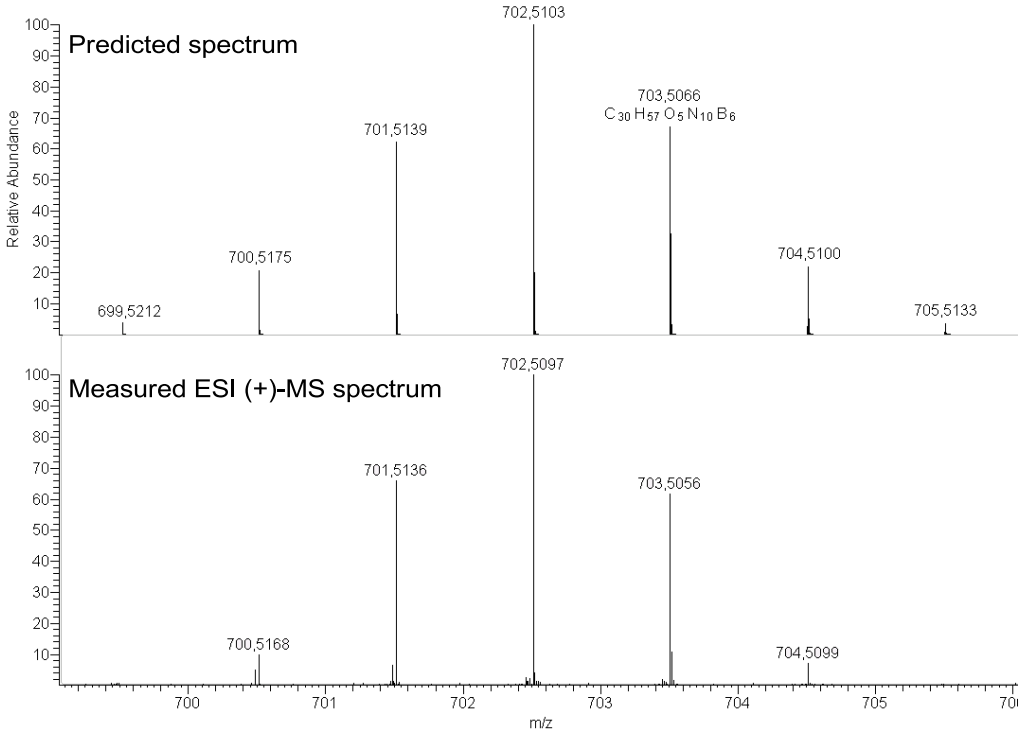
Predicted spectrum
Relative Abundance
702,5103
703,5066
C30 H57 O5 N10 B6
701,5139
700,5175
704,5100
699,5212
705,5133
Measured ESI (+)-MS spectrum
702,5097
701,5136
703,5056
700,5168
704,5099
m/z

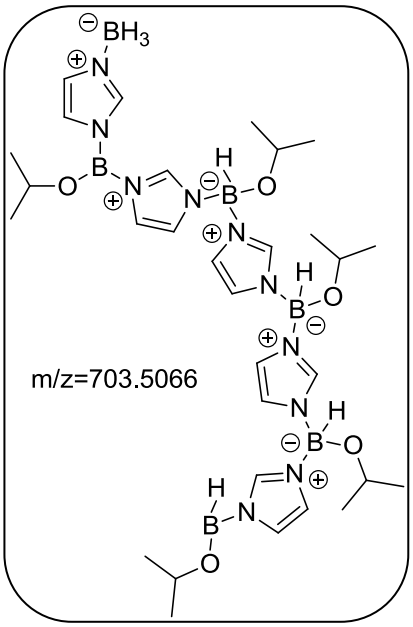
m/z=703.5066

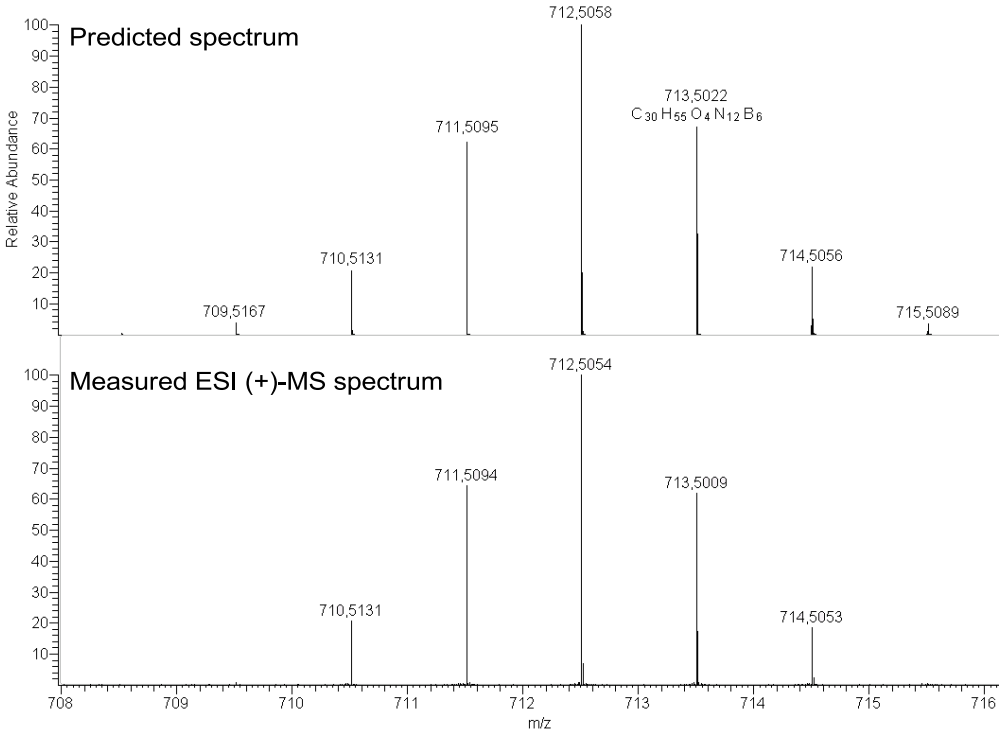
Predicted spectrum
712,5058
713,5022
C30 H55 O4 N12 B6
711,5095
710,5131
714,5056
709,5167
715,5089
Measured ESI (+)-MS spectrum
712,5054
711,5094
713,5009
710,5131
714,5053
Relative Abundance
m/z

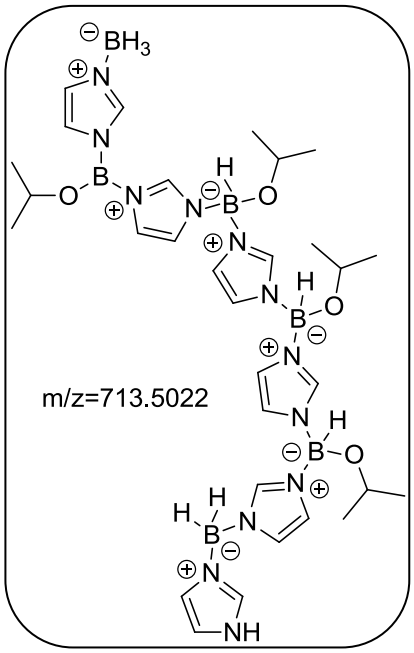
m/z=713.5022

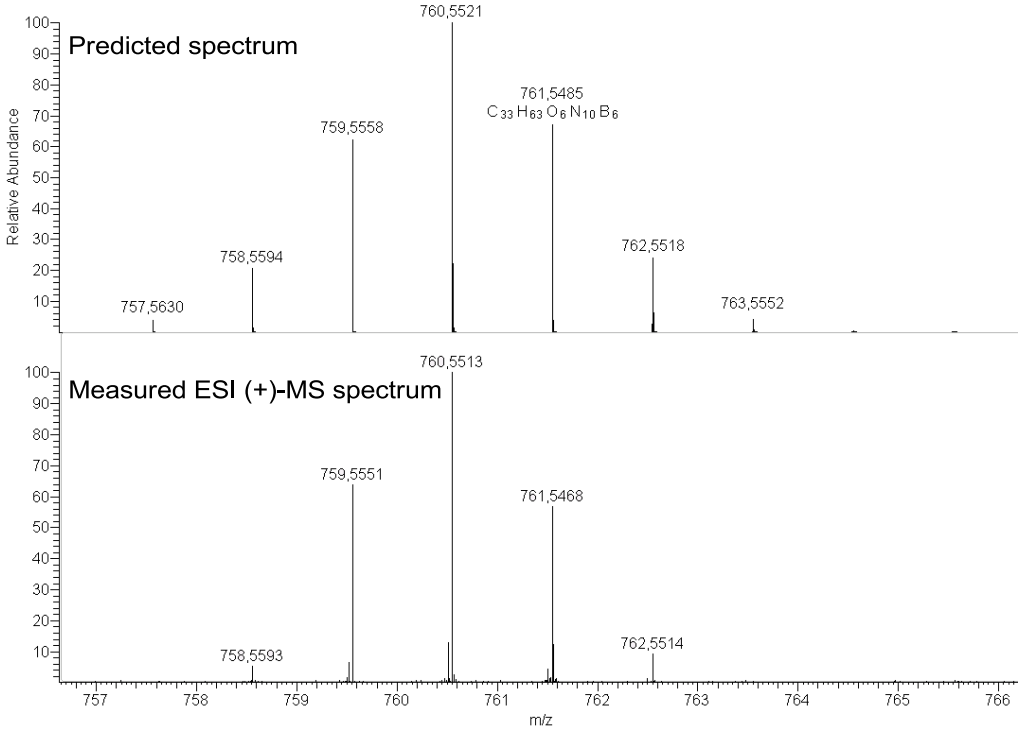
Predicted spectrum
760,5521
761,5485
C33 H63 O6 N10 B6
759,5558
758,5594
762,5518
757,5630
763,5552
Measured ESI (+)-MS spectrum
760,5513
759,5551
761,5468
758,5593
762,5514
Relative Abundance
m/z

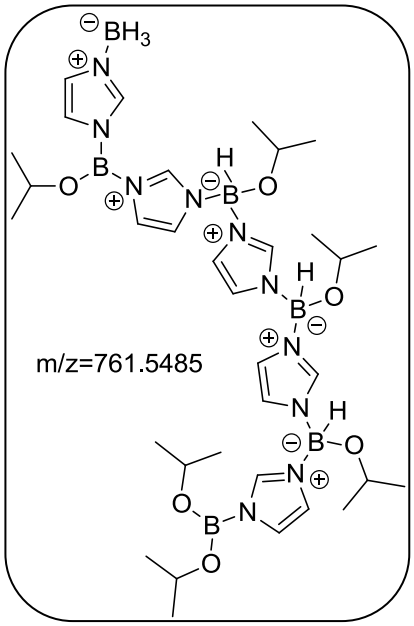
m/z=761.5485

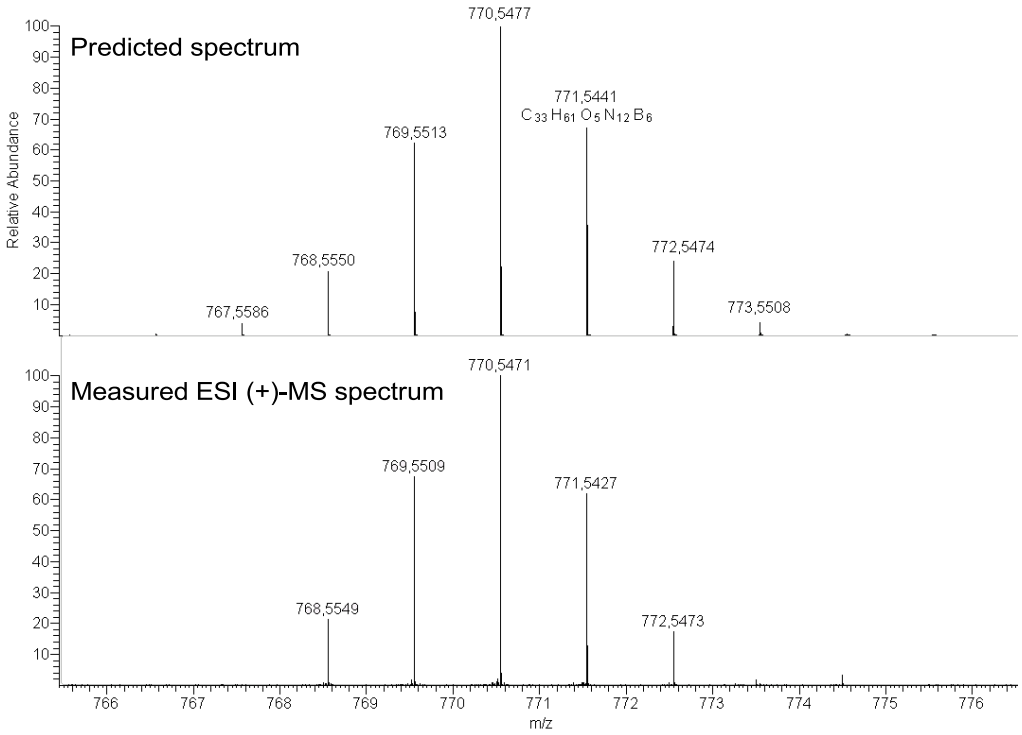
Predicted spectrum
770,5477
771,5441
C33 H61 O5 N12 B6
769,5513
768,5550
772,5474
767,5586
773,5508
Measured ESI (+)-MS spectrum
770,5471
769,5509
771,5427
768,5549
772,5473
Relative Abundance
m/z

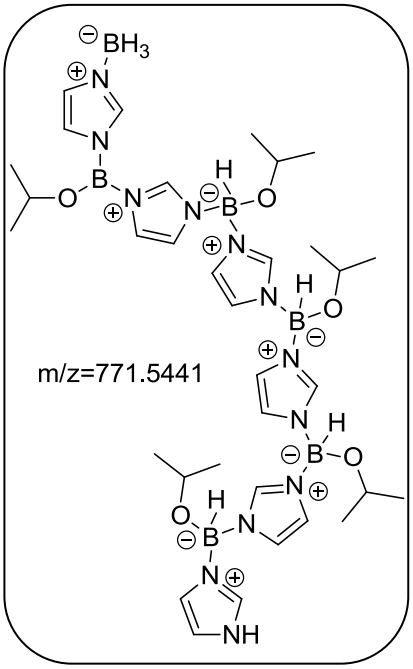
m/z=771.5441

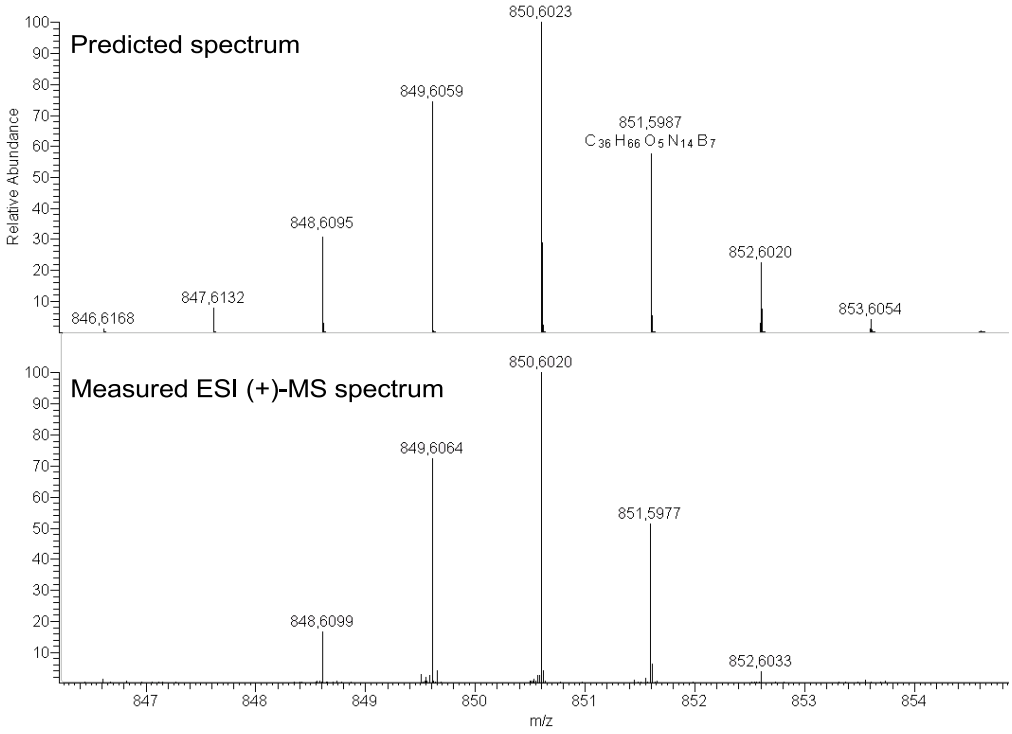
Predicted spectrum
Relative Abundance
850,6023
849,6059
851,5987
C36 H66 O5 N14 B7
848,6095
852,6020
847,6132
853,6054
846,6168
Measured ESI (+)-MS spectrum
850,6020
849,6064
851,5977
848,6099
852,6033
847
848
849
850
851
852
853
854
m/z

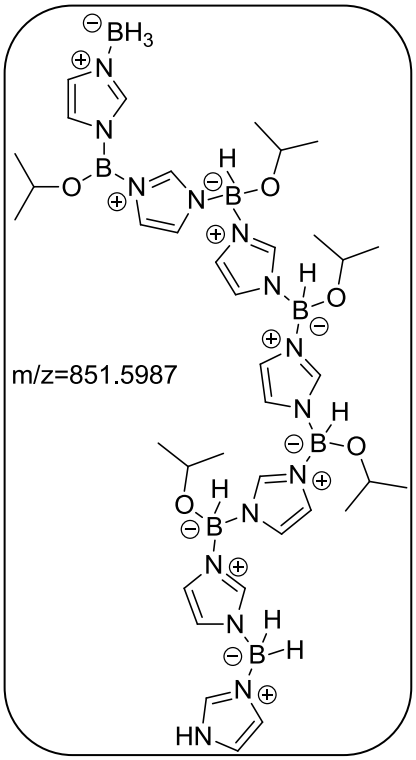
m/z=851.5987

Cyclic structures:

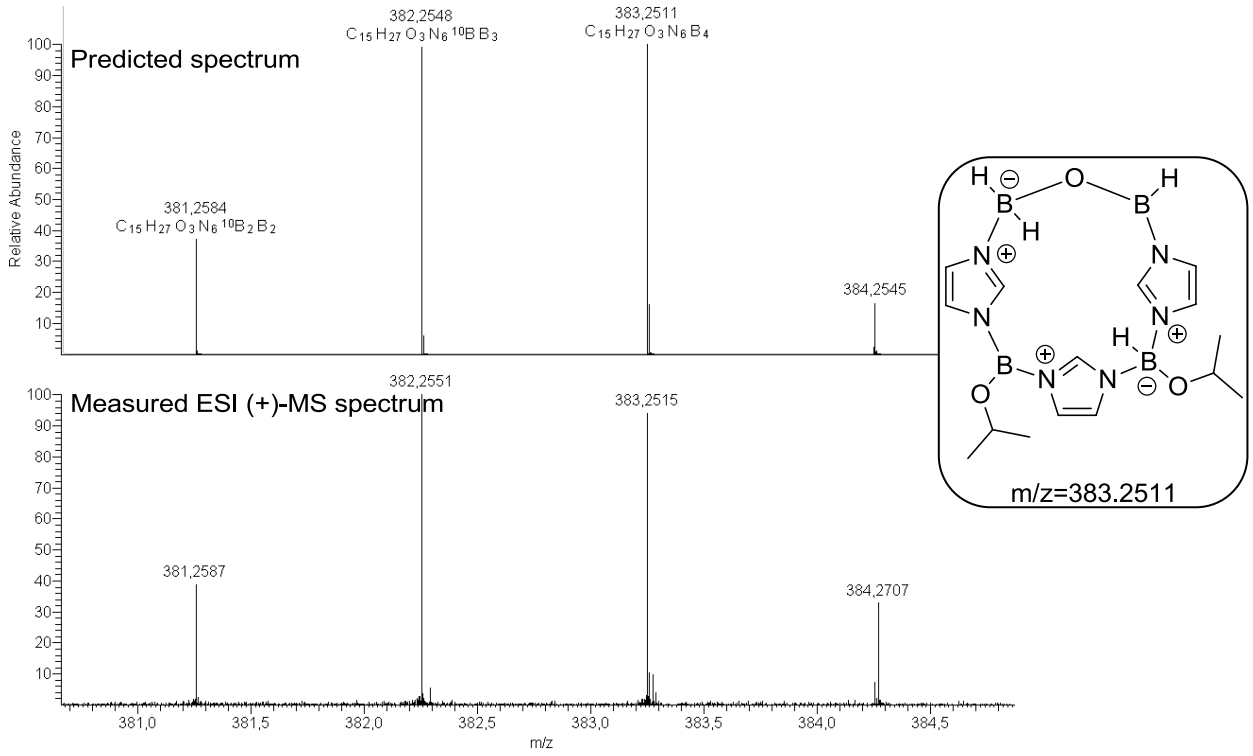

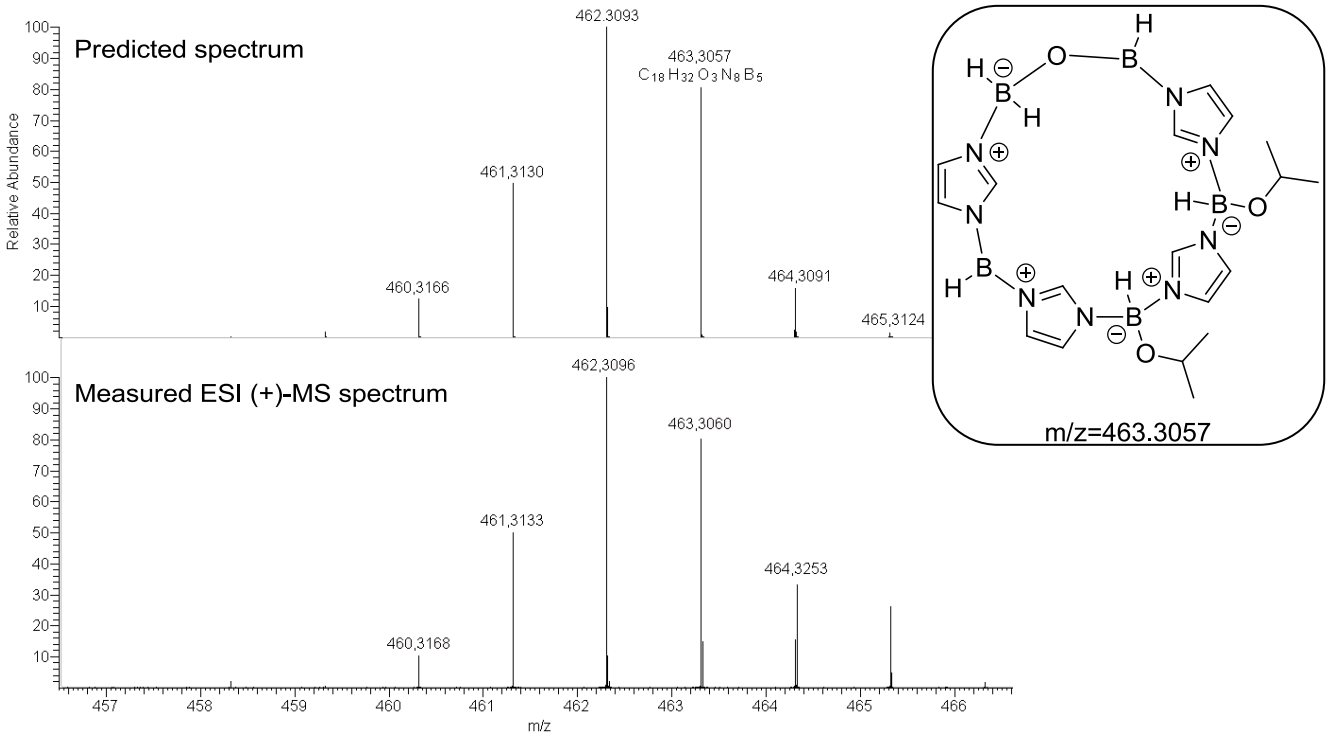

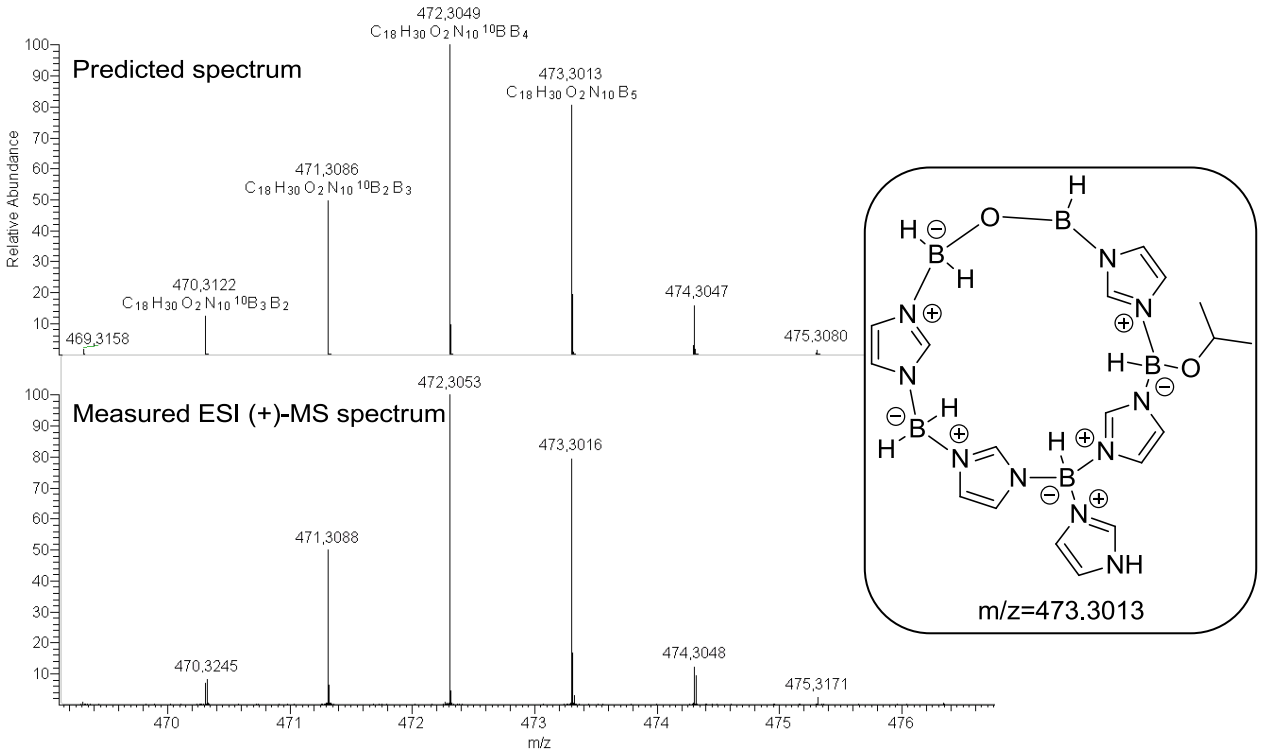
Predicted spectrum
472,3049
C18 H30 O2 N10 10B B4
473,3013
C18 H30 O2 N10 B5
471,3086
C18 H30 O2 N10 10B2 B3
470,3122
C18 H30 O2 N10 10B3 B2
469,3158
474,3047
475,3080
Measured ESI (+)-MS spectrum
472,3053
473,3016
471,3088
470,3245
474,3048
475,3171
Relative Abundance
m/z
m/z=473.3013

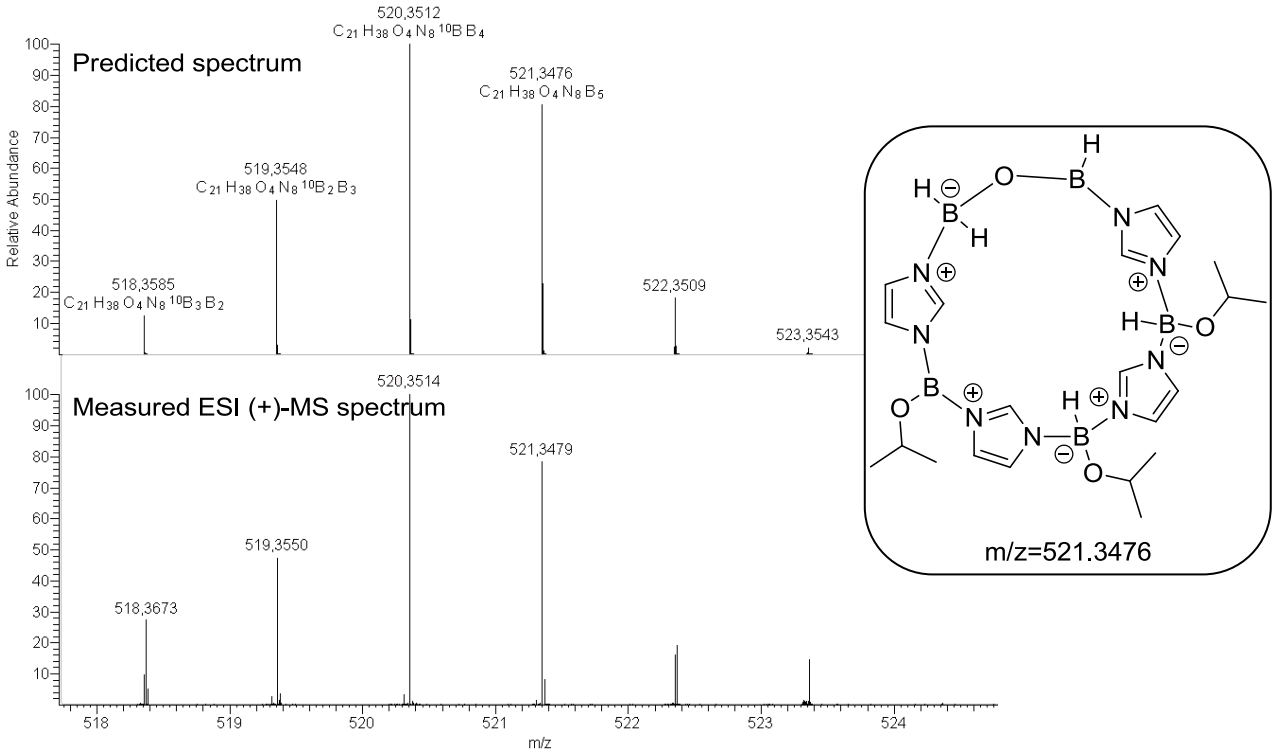
Predicted spectrum
520,3512
C21 H38 O4 N8 10B B4
521,3476
C21 H38 O4 N8 B5
519,3548
C21 H38 O4 N8 10B2 B3
518,3585
C21 H38 O4 N8 10B3 B2
522,3509
523,3543
Measured ESI (+)-MS spectrum
520,3514
521,3479
519,3550
518,3673
Relative Abundance
m/z
m/z=521.3476

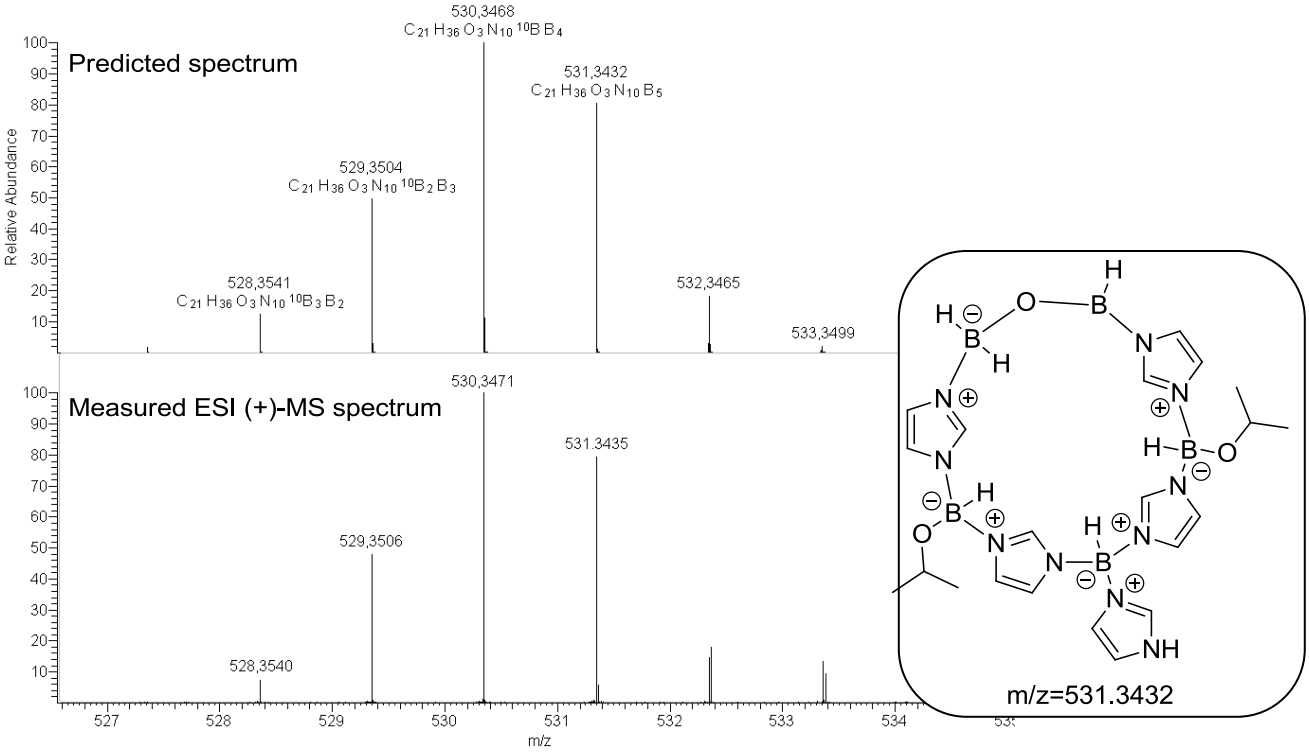
Predicted spectrum
530,3468
C21 H36 O3 N10 10B B4
531,3432
C21 H36 O3 N10 B5
529,3504
C21 H36 O3 N10 10B2 B3
528,3541
C21 H36 O3 N10 10B3 B2
532,3465
533,3499
Measured ESI (+)-MS spectrum
530,3471
531.3435
529,3506
528,3540
Relative Abundance
m/z
m/z=531.3432

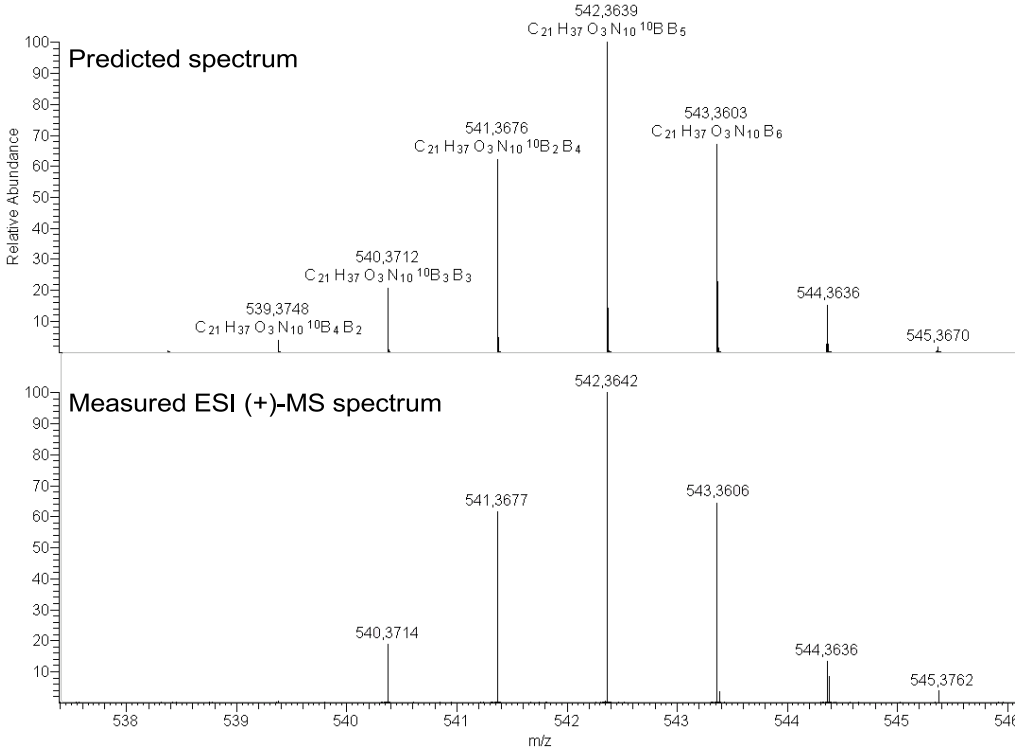
Predicted spectrum
542,3639
C21 H37 O3 N10 10B B5
541,3676
C21 H37 O3 N10 10B2 B4
543,3603
C21 H37 O3 N10 B6
540,3712
C21 H37 O3 N10 10B3 B3
539,3748
C21 H37 O3 N10 10B4 B2
544,3636
545,3670
Measured ESI (+)-MS spectrum
542,3642
541,3677
543,3606
540,3714
544,3636
545,3762
Relative Abundance
m/z
538
539
540
541
542
543
544
545

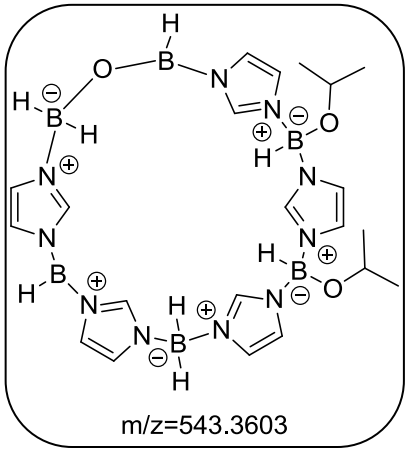
m/z=543.3603

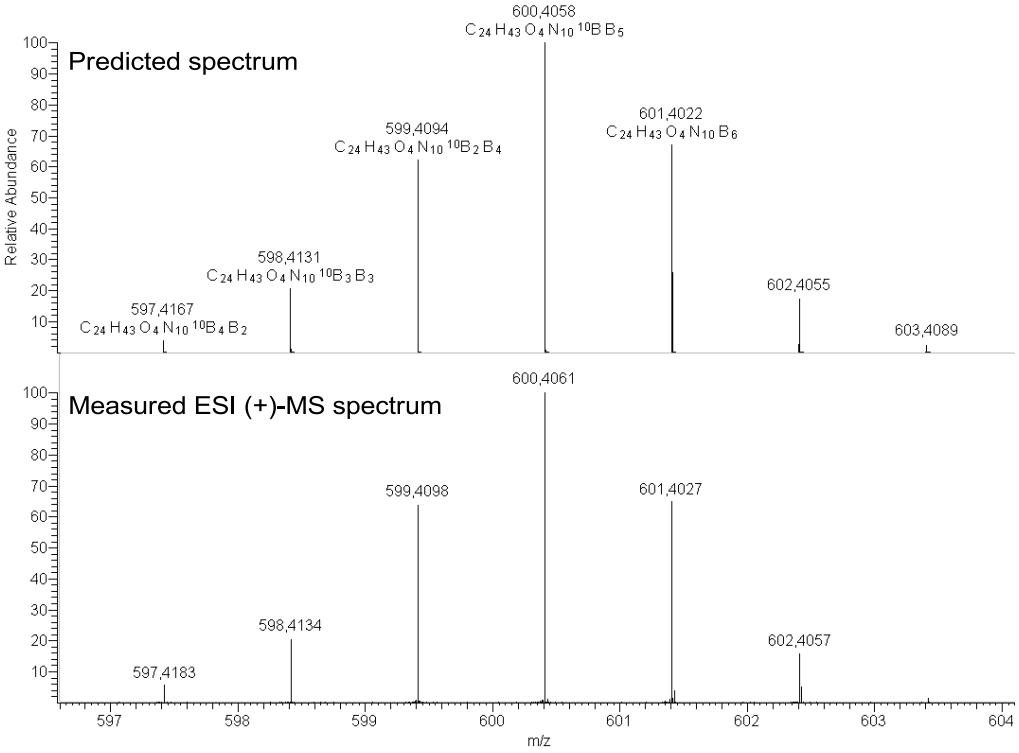
Predicted spectrum
600,4058
C24 H43 O4 N10 10B B5
599,4094
C24 H43 O4 N10 10B2 B4
601,4022
C24 H43 O4 N10 B6
598,4131
C24 H43 O4 N10 10B3 B3
602,4055
597,4167
C24 H43 O4 N10 10B4 B2
603,4089
Measured ESI (+)-MS spectrum
600,4061
599,4098
601,4027
598,4134
602,4057
597,4183
Relative Abundance
m/z

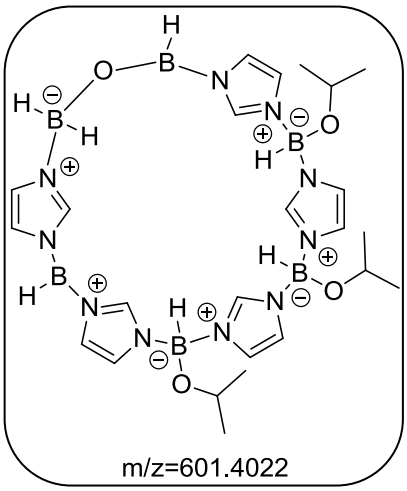
m/z=601.4022

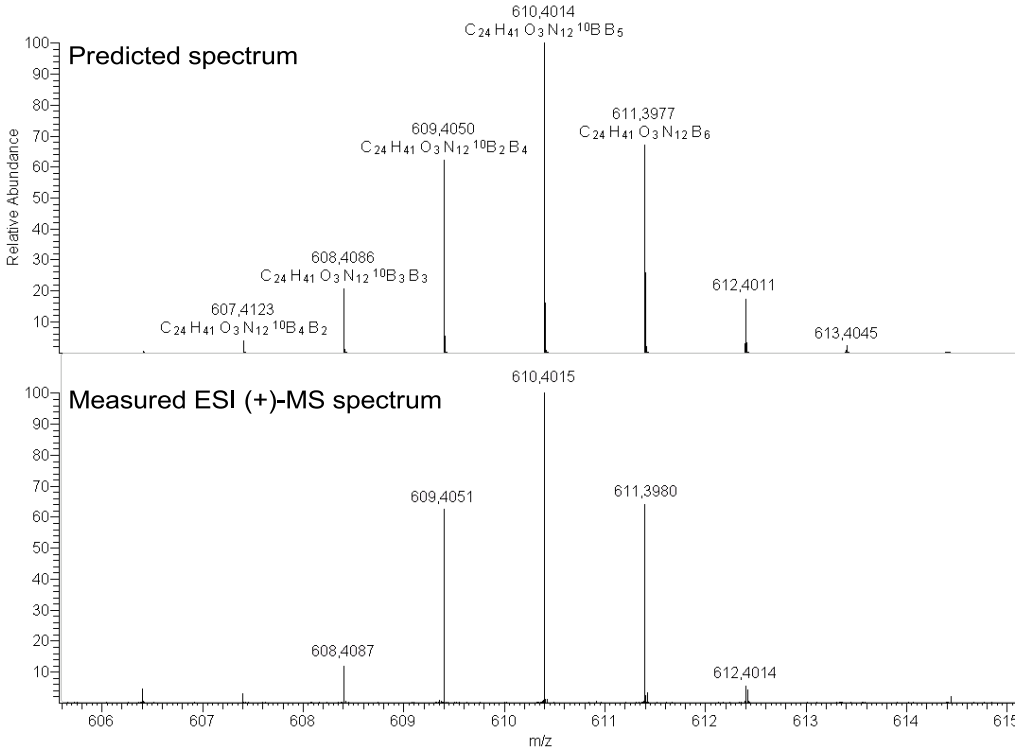
Predicted spectrum
610,4014
C24 H41 O3 N12 10B B5
609,4050
C24 H41 O3 N12 10B2 B4
611,3977
C24 H41 O3 N12 B6
608,4086
C24 H41 O3 N12 10B3 B3
607,4123
C24 H41 O3 N12 10B4 B2
612,4011
613,4045
Relative Abundance
Measured ESI (+)-MS spectrum
610,4015
609,4051
611,3980
608,4087
612,4014
m/z

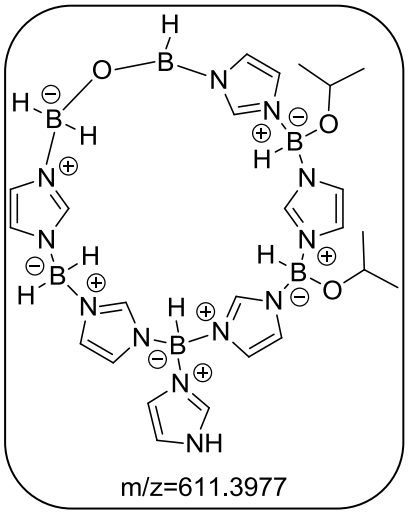
m/z=611.3977

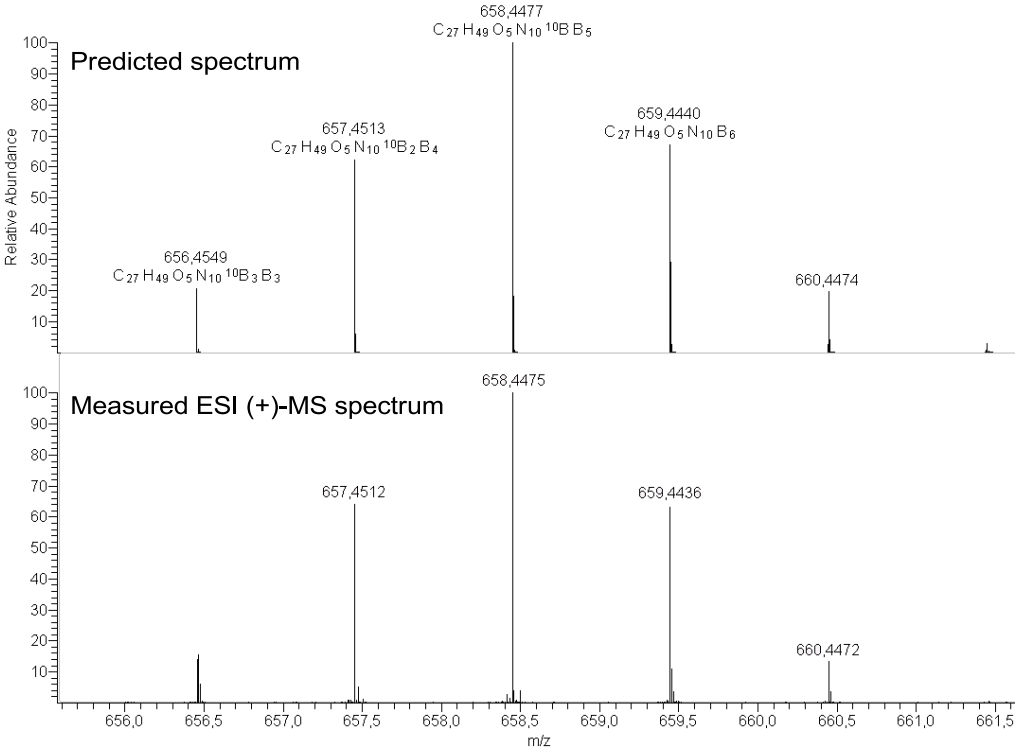
Predicted spectrum
658,4477
C27 H49 O5 N10 10B B5
657,4513
C27 H49 O5 N10 10B2 B4
659,4440
C27 H49 O5 N10 B6
656,4549
C27 H49 O5 N10 10B3 B3
660,4474
Measured ESI (+)-MS spectrum
658,4475
657,4512
659,4436
660,4472
Relative Abundance
m/z

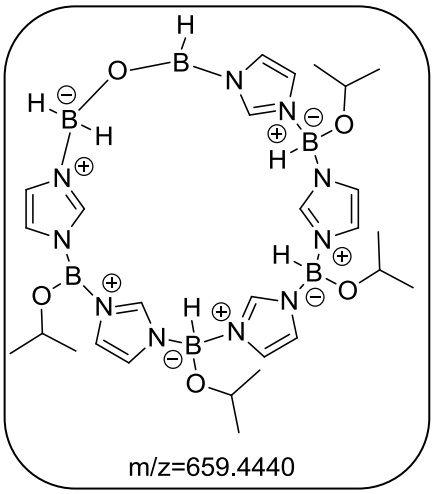
m/z=659.4440

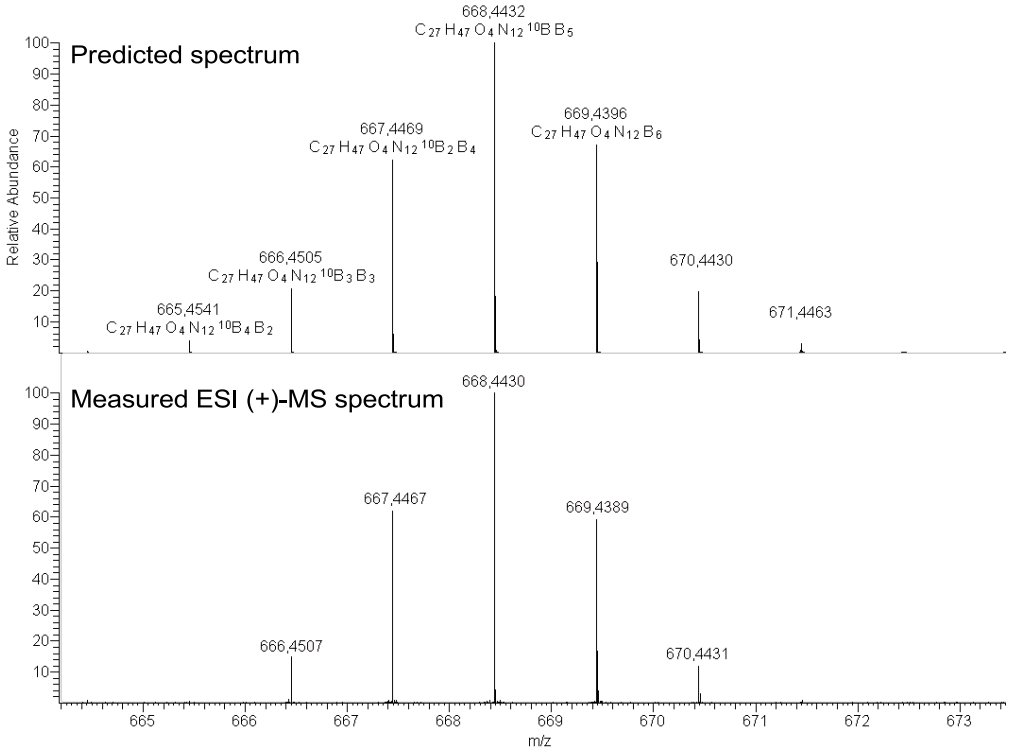
Predicted spectrum
668,4432
C27 H47 O4 N12 10B B5
669,4396
C27 H47 O4 N12 B6
667,4469
C27 H47 O4 N12 10B2 B4
666,4505
C27 H47 O4 N12 10B3 B3
670,4430
665,4541
C27 H47 O4 N12 10B4 B2
671,4463
Measured ESI (+)-MS spectrum
668,4430
667,4467
669,4389
666,4507
670,4431
Relative Abundance
m/z

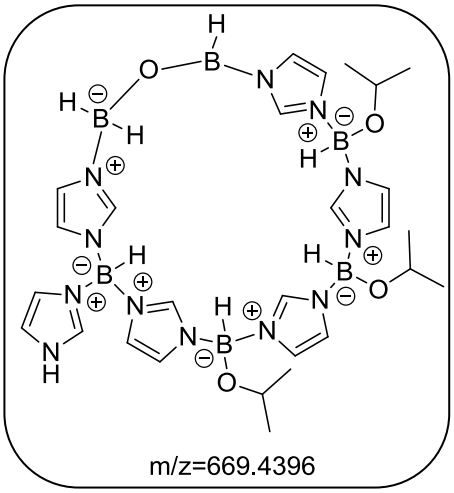
m/z=669.4396

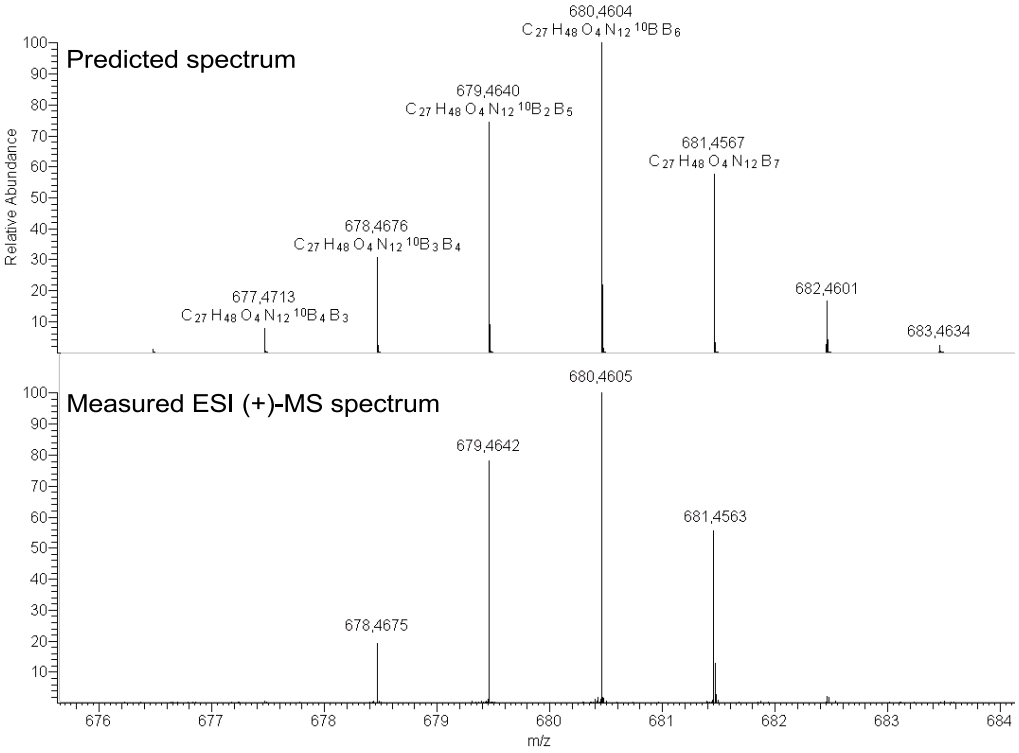
Predicted spectrum
680,4604
C27 H48 O4 N12 10B B6
679,4640
C27 H48 O4 N12 10B2 B5
681,4567
C27 H48 O4 N12 B7
678,4676
C27 H48 O4 N12 10B3 B4
677,4713
C27 H48 O4 N12 10B4 B3
682,4601
683,4634
Measured ESI (+)-MS spectrum
680,4605
679,4642
681,4563
678,4675
Relative Abundance
m/z

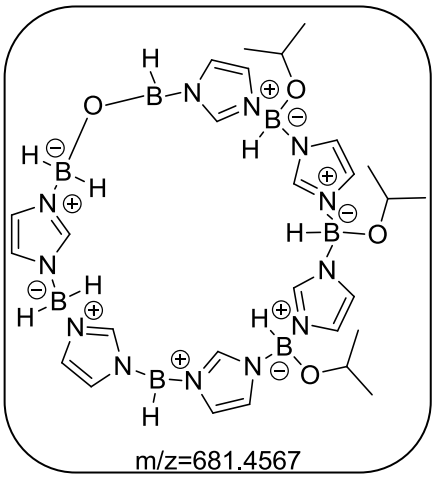
m/z=681.4567

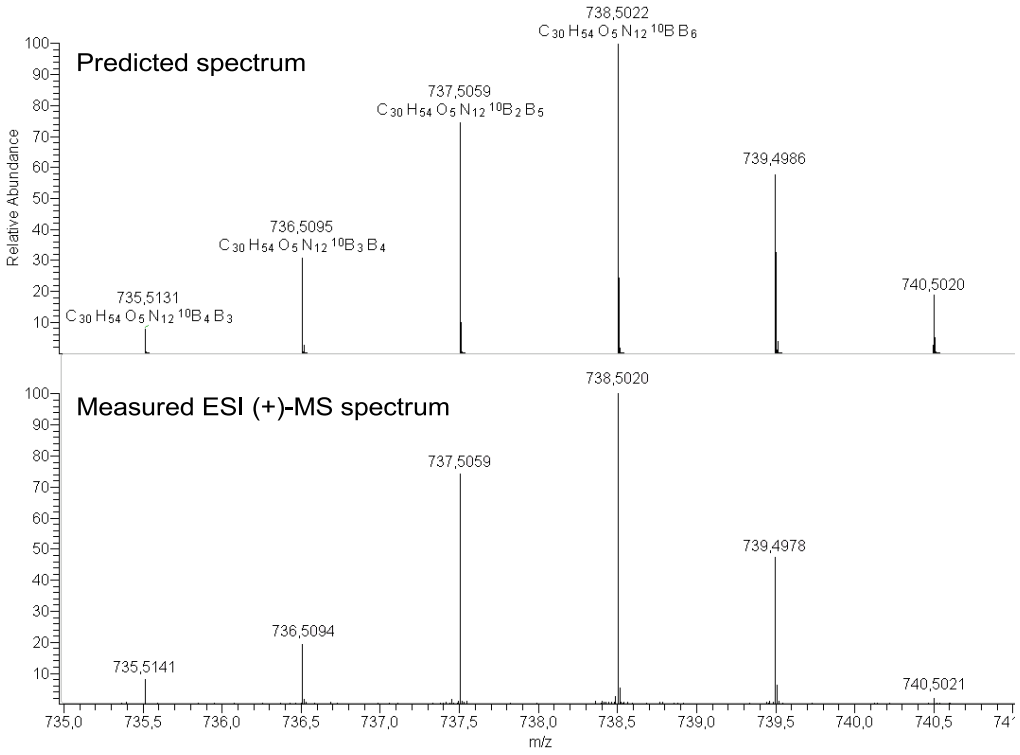
Predicted spectrum
738,5022
C30 H54 O5 N12 10B B6
737,5059
C30 H54 O5 N12 10B2 B5
739,4986
736,5095
C30 H54 O5 N12 10B3 B4
740,5020
735,5131
C30 H54 O5 N12 10B4 B3
Relative Abundance
Measured ESI (+)-MS spectrum
738,5020
737,5059
739,4978
736,5094
735,5141
740,5021
m/z

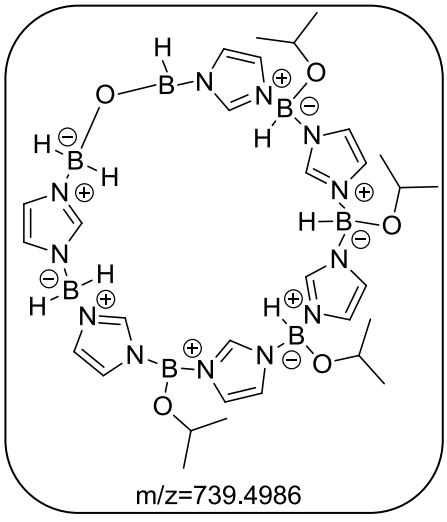
m/z=739.4986

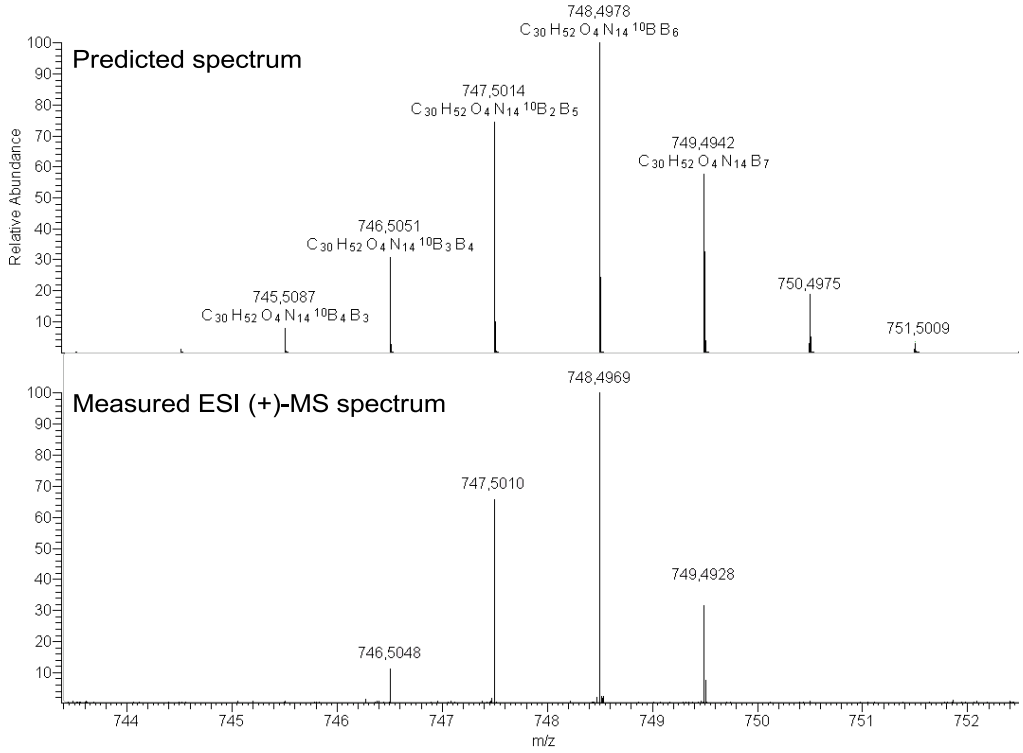
Predicted spectrum
748,4978
C30 H52 O4 N14 10B B6
747,5014
C30 H52 O4 N14 10B2 B5
749,4942
C30 H52 O4 N14 B7
746,5051
C30 H52 O4 N14 10B3 B4
745,5087
C30 H52 O4 N14 10B4 B3
750,4975
751,5009
Relative Abundance
Measured ESI (+)-MS spectrum
748,4969
747,5010
749,4928
746,5048
744
745
746
747
748
749
750
751
752
m/z

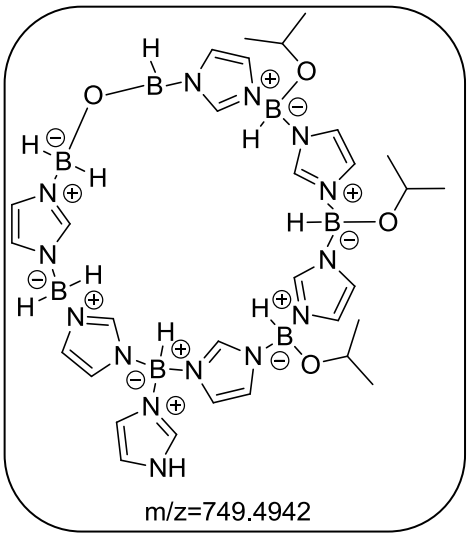
m/z=749.4942

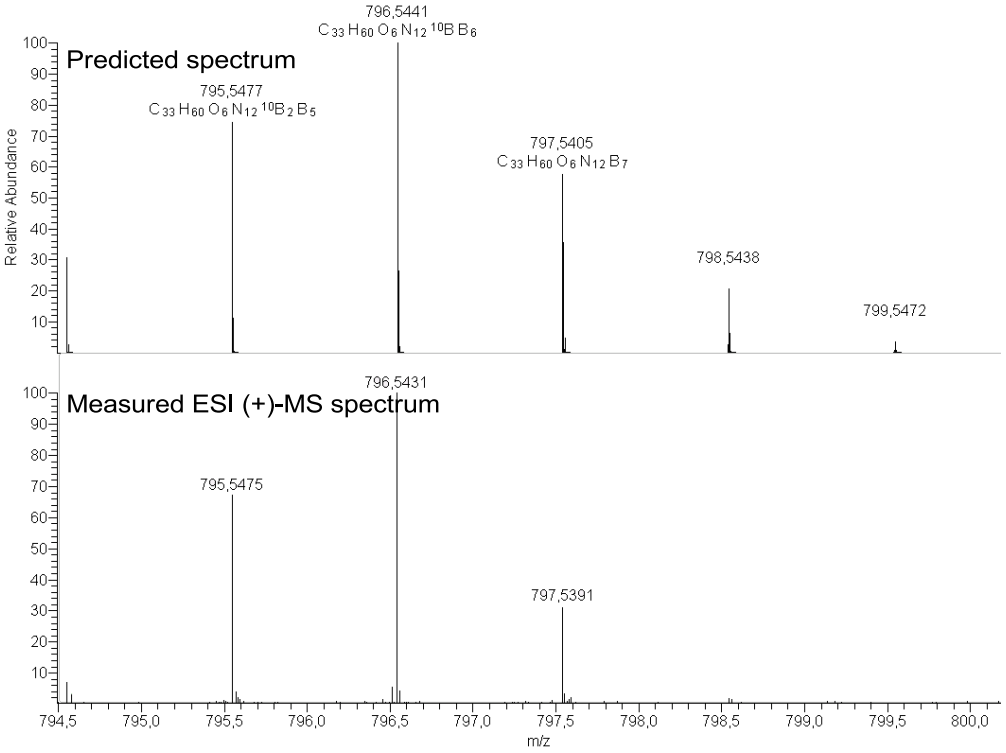
Predicted spectrum
796,5441
C33 H60 O6 N12 10B B6
795,5477
C33 H60 O6 N12 10B2 B5
797,5405
C33 H60 O6 N12 B7
798,5438
799,5472
Measured ESI (+)-MS spectrum
796,5431
795,5475
797,5391
Relative Abundance
m/z

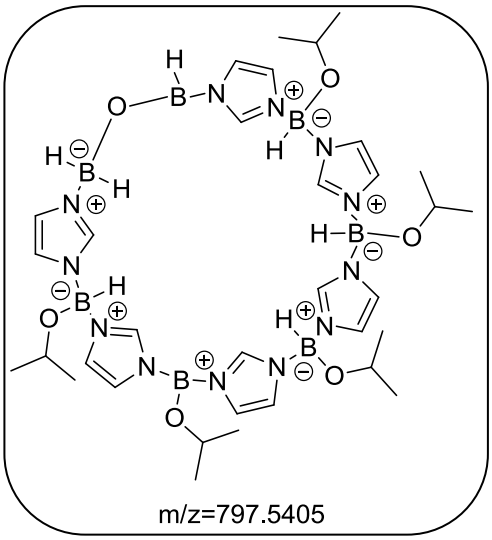
m/z=797.5405

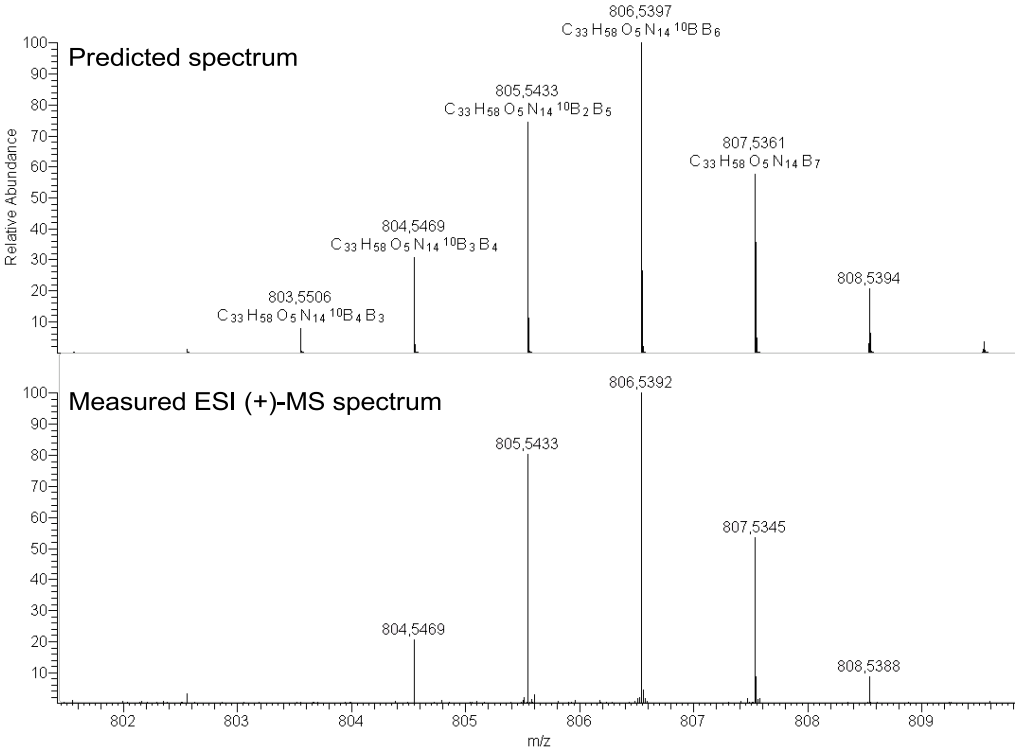
Predicted spectrum
806,5397
C33 H58 O5 N14 10B B6
805,5433
C33 H58 O5 N14 10B2 B5
807,5361
C33 H58 O5 N14 B7
804,5469
C33 H58 O5 N14 10B3 B4
808,5394
803,5506
C33 H58 O5 N14 10B4 B3
Measured ESI (+)-MS spectrum
806,5392
805,5433
807,5345
804,5469
808,5388
Relative Abundance
m/z

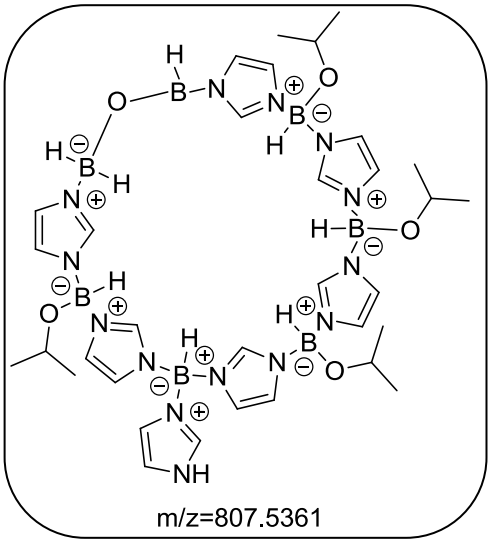
m/z=807.5361

5.3.5.3.2. Benzimidazole borane (17e)

All preparation steps were carried out under a nitrogen atmosphere. A suspension of benzimidazole borane (**17e**, 0.200 g, 1.515 mmol) in destilled $CDCl_3$ (1 ml) was prepared. Afterwards acetone (0.111 ml, 1.515 mmol, 1 eq.) was added and stirred for 15 minutes at room temperature. All volatiles were then removed under reduced pressure. The colorless solid was taken up in dry THF (1 ml) and a diluted solution (10 drops in 2 ml dry THF) was immediately used for ESI-MS spectrometry.

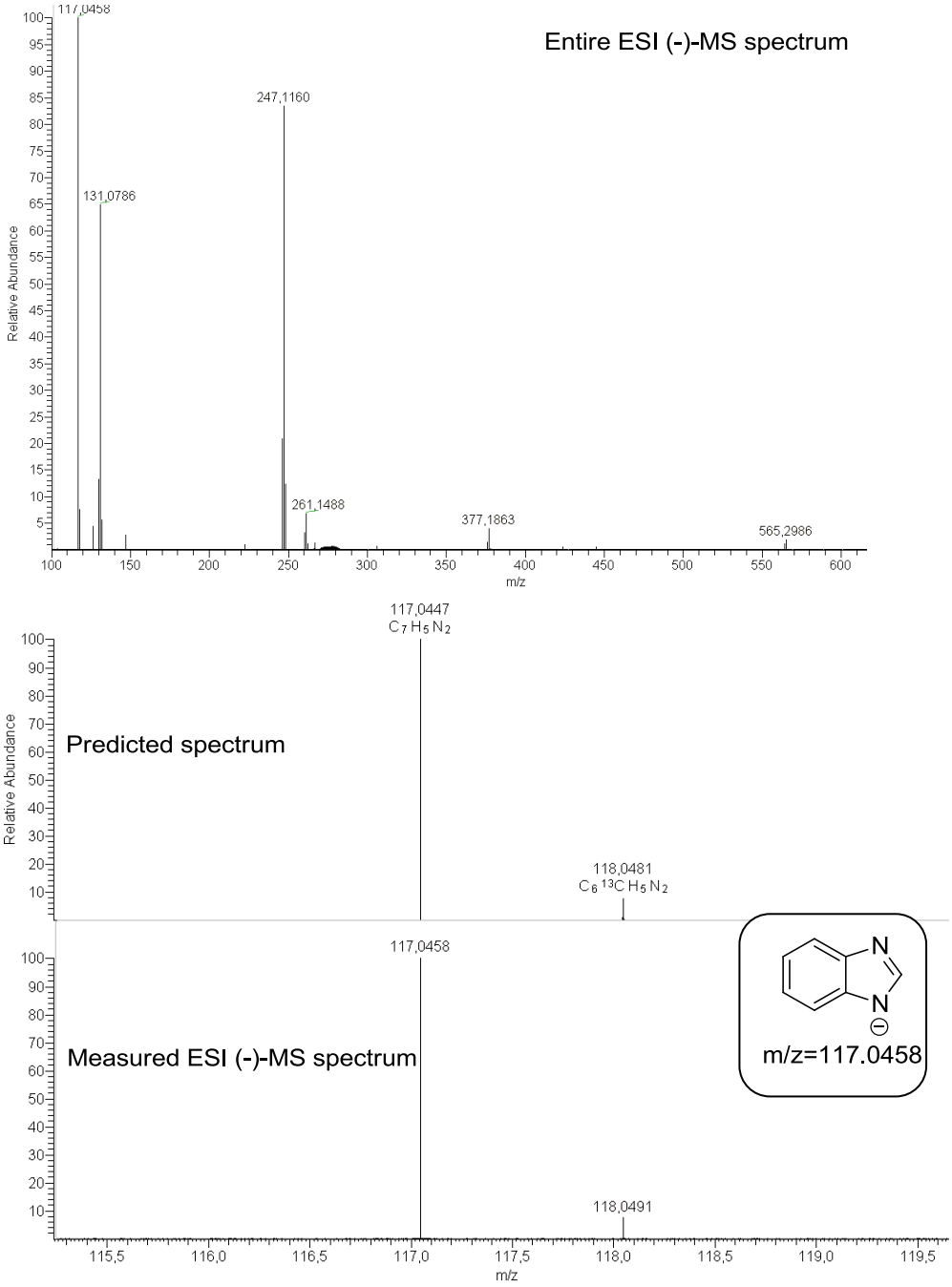

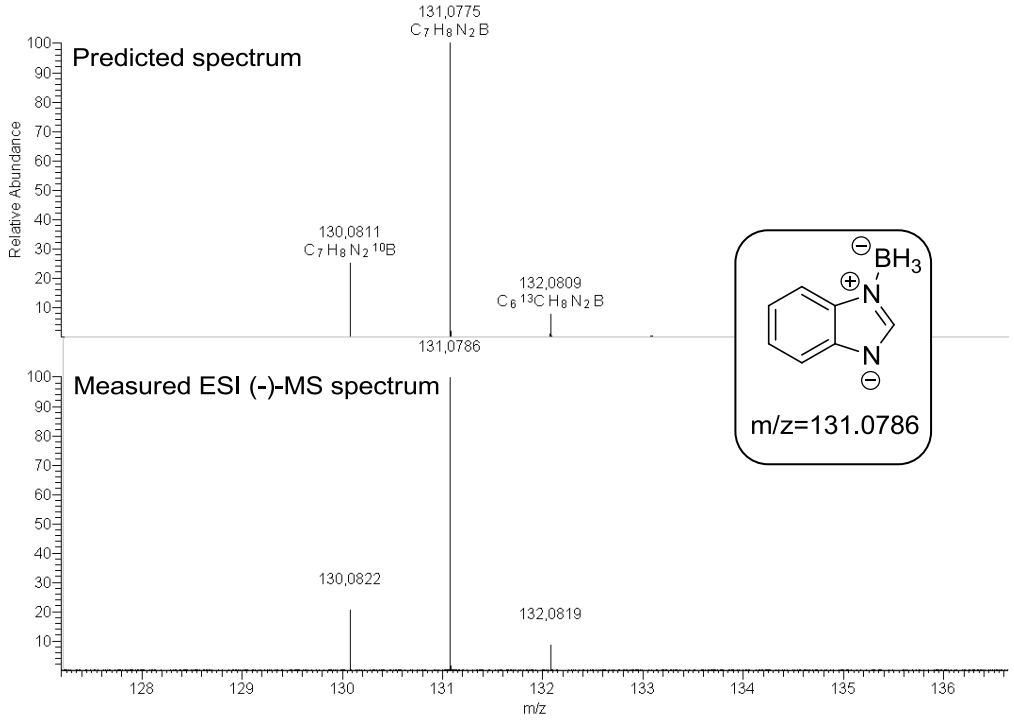
Predicted spectrum
131,0775
C7 H8 N2 B
130,0811
C7 H8 N2 10B
132,0809
C6 13C H8 N2 B
131,0786
Measured ESI (-)-MS spectrum
130,0822
132,0819
Relative Abundance
m/z
m/z=131.0786

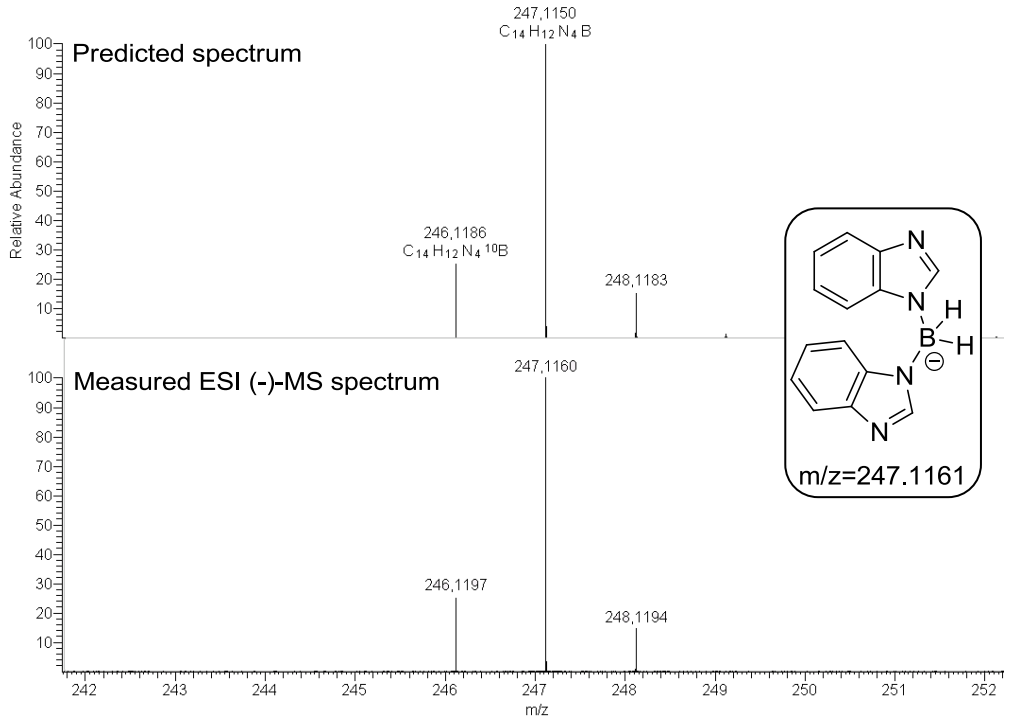
Predicted spectrum
247,1150
C14 H12 N4 B
246,1186
C14 H12 N4 10B
248,1183
Measured ESI (-)-MS spectrum
247,1160
246,1197
248,1194
Relative Abundance
m/z
m/z=247.1161

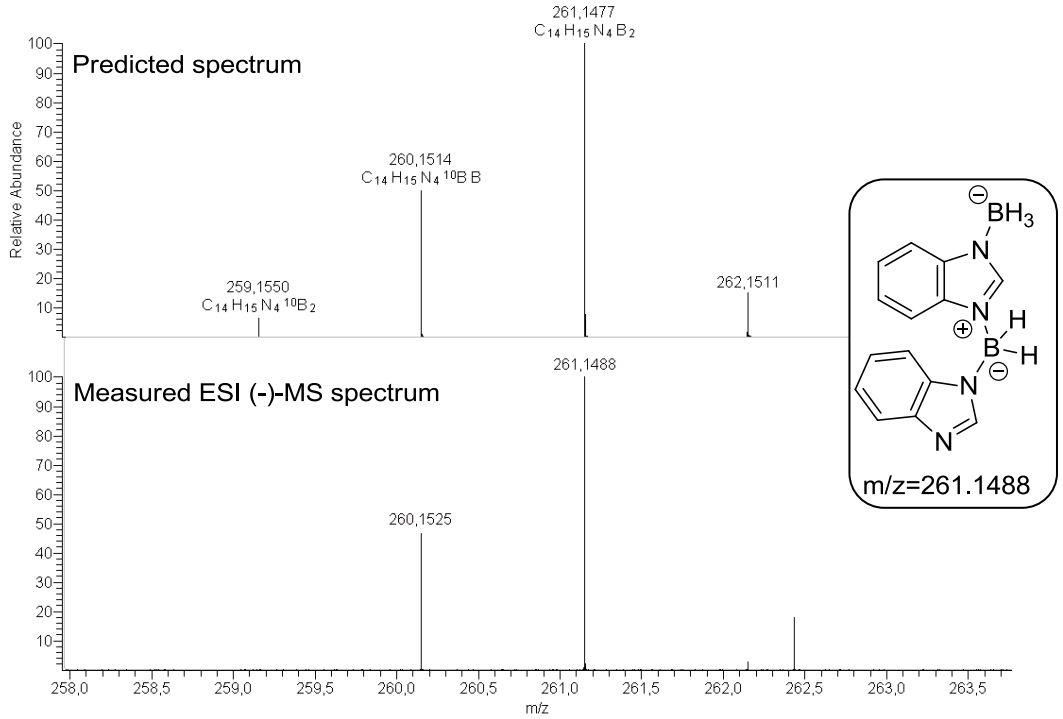
Predicted spectrum
261,1477
C14H15N4B2
260,1514
C14H15N4 10B B
259,1550
C14H15N4 10B2
262,1511
Measured ESI (-)-MS spectrum
261,1488
260,1525
Relative Abundance
m/z
m/z=261.1488

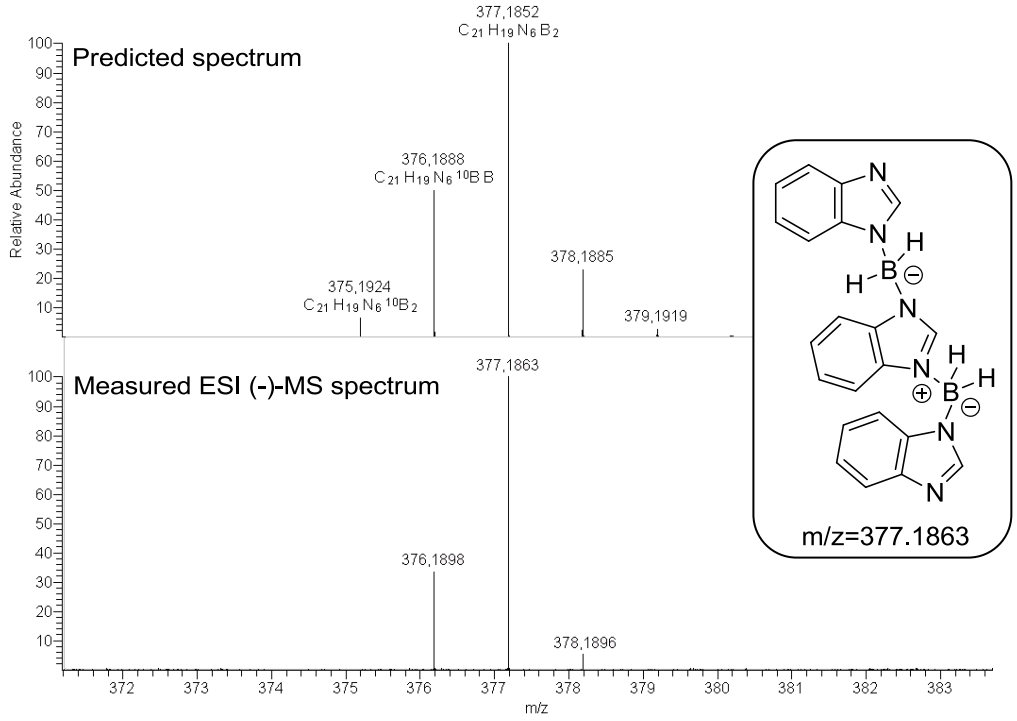
Predicted spectrum
377,1852
C21H19N6B2
376,1888
C21H19N6 10B B
375,1924
C21H19N6 10B2
378,1885
379,1919
Measured ESI (-)-MS spectrum
377,1863
376,1898
378,1896
Relative Abundance
m/z
m/z=377.1863

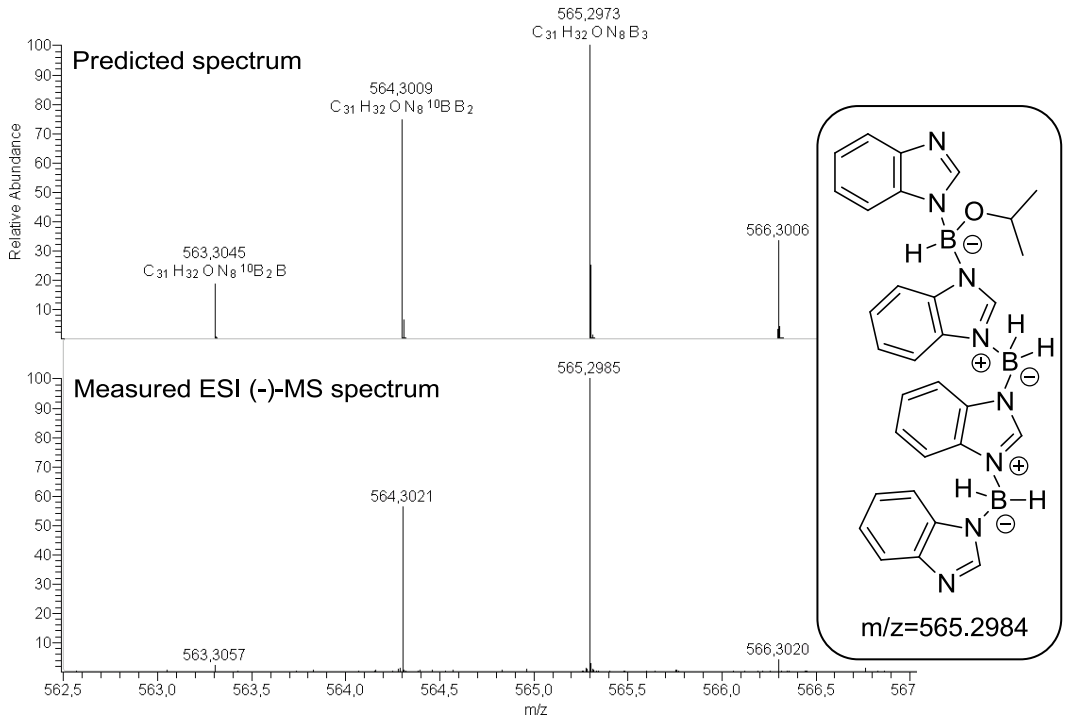
Predicted spectrum
565,2973
C31 H32 O N8 B3
564,3009
C31 H32 O N8 10B B2
563,3045
C31 H32 O N8 10B2 B
566,3006
Measured ESI (-)-MS spectrum
565,2985
564,3021
563,3057
566,3020
Relative Abundance
m/z
m/z=565.2984

5.3.5.3.3. N-methylimidazole (17aj)

All preparation steps were carried out under a nitrogen atmosphere. *N*-methylimidazole-borane (**17aj**, 79 mg) was stirred in acetone-d_6 (1 ml) for 5 days. Afterwards 0.1 ml of the solution was diluted with acetone-d_6 (2 ml) and used for ESI-MS spectrometry.

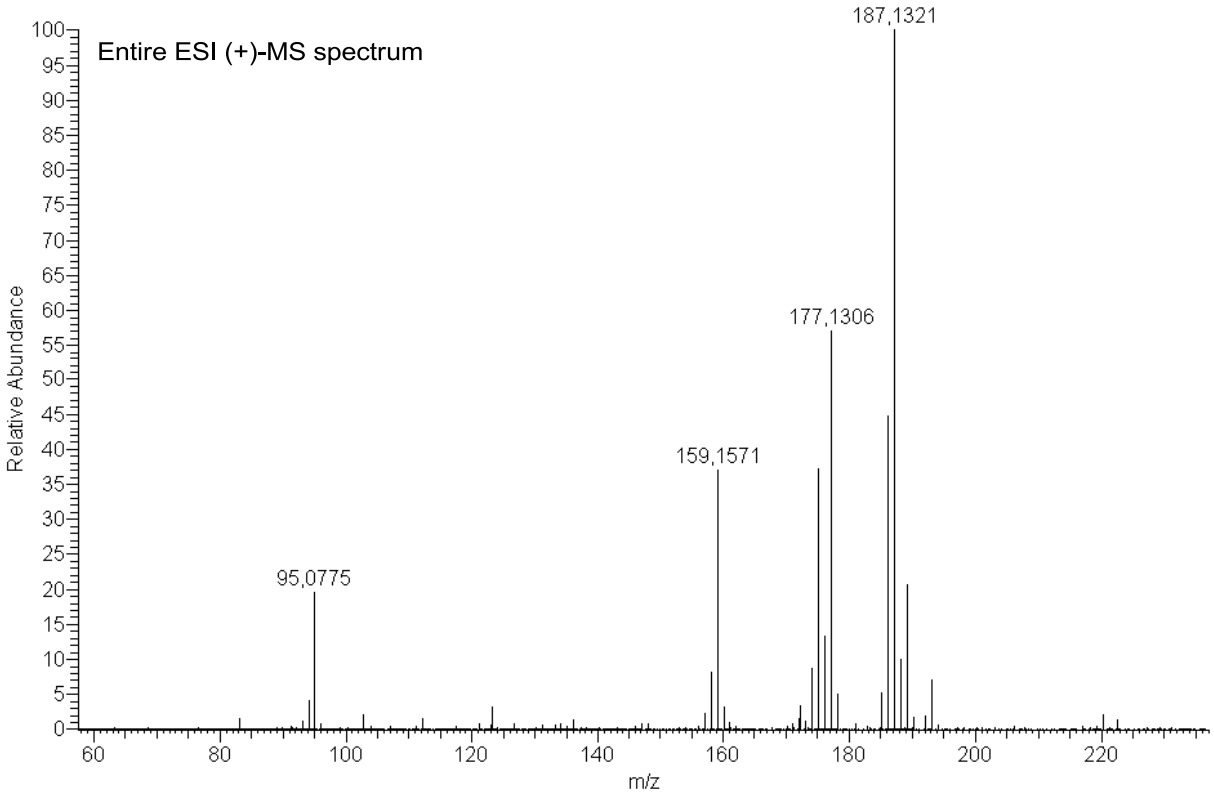

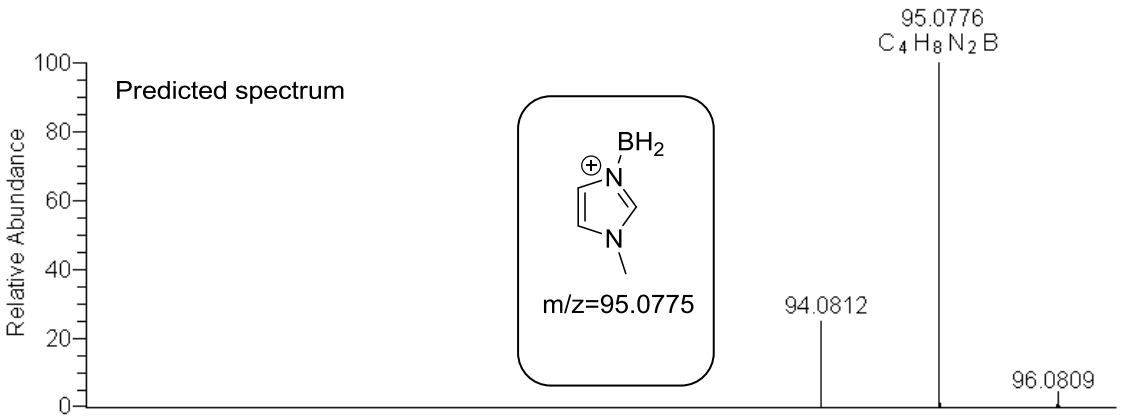
Predicted spectrum
95.0776
C4 H8 N2 B
BH2
N
N
m/z=95.0775
94.0812
96.0809
Relative Abundance
100
80
60
40
20
0

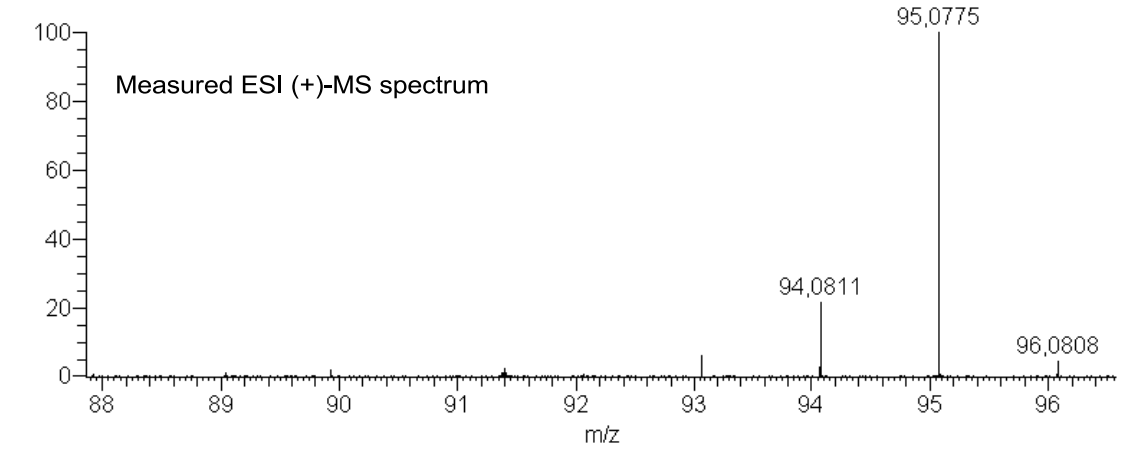
Measured ESI (+)-MS spectrum
95,0775
94,0811
96,0808
Relative Abundance
100
80
60
40
20
0
88
89
90
91
92
93
94
95
96
m/z

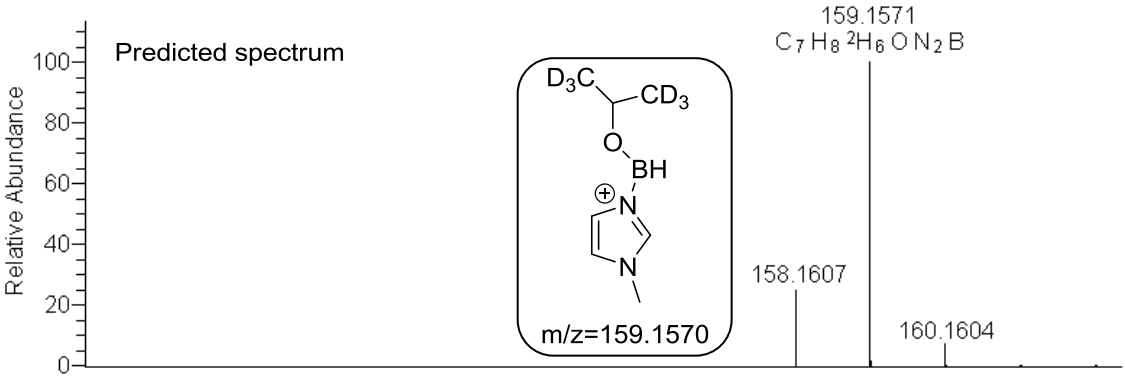
Predicted spectrum
159.1571
C7 H8 2H6 O N2 B
D3C
CD3
O
BH
N
N
m/z=159.1570
158.1607
160.1604
Relative Abundance
100
80
60
40
20
0

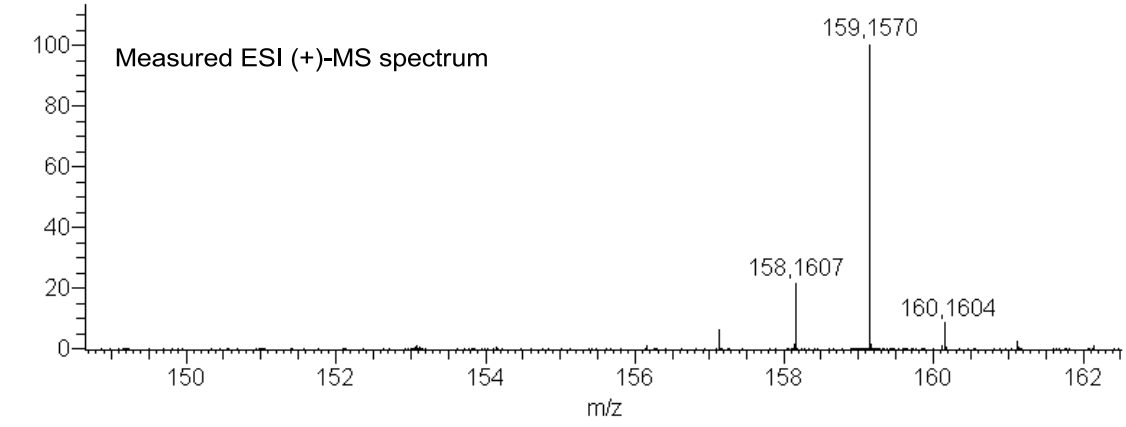
Measured ESI (+)-MS spectrum
159,1570
158,1607
160,1604
Relative Abundance
100
80
60
40
20
0
150
152
154
156
158
160
162
m/z

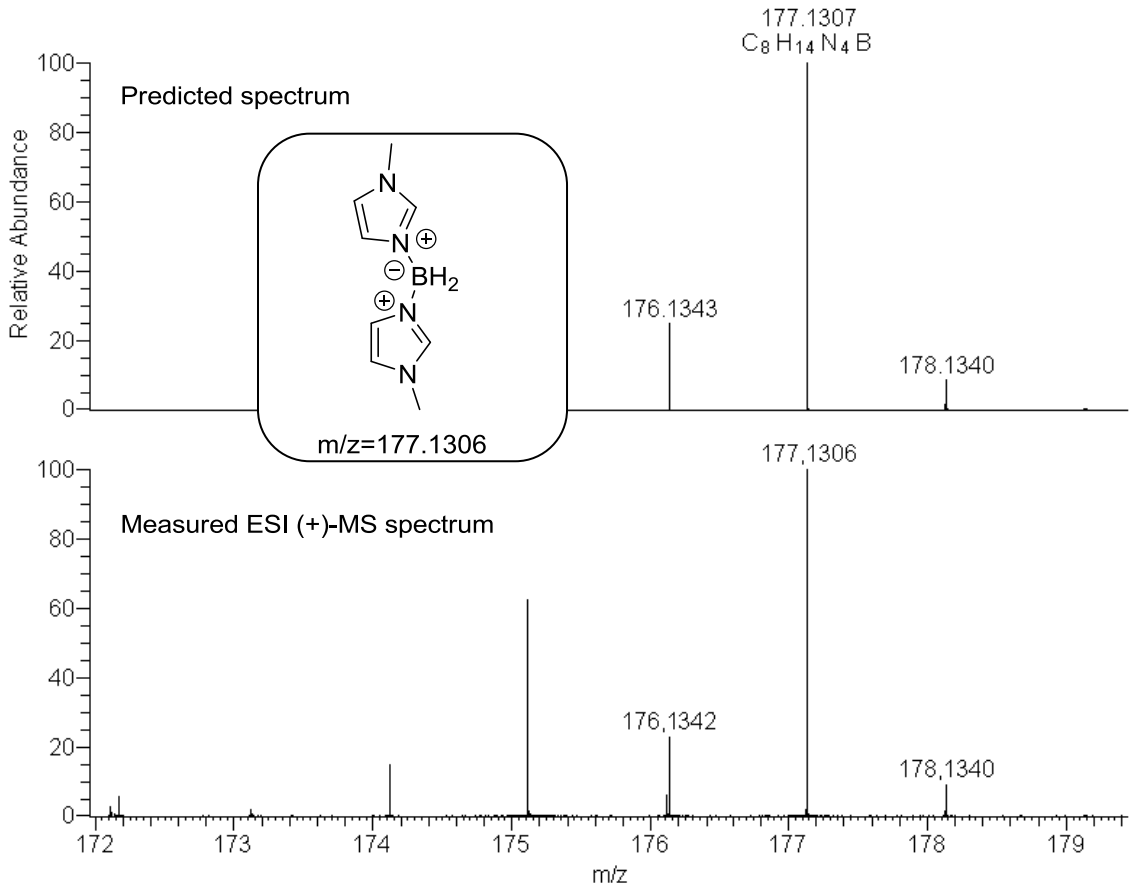
177.1307
C8H14N4B
Predicted spectrum
Relative Abundance
176.1343
178.1340
m/z=177.1306
177,1306
Measured ESI (+)-MS spectrum
176,1342
178,1340
m/z

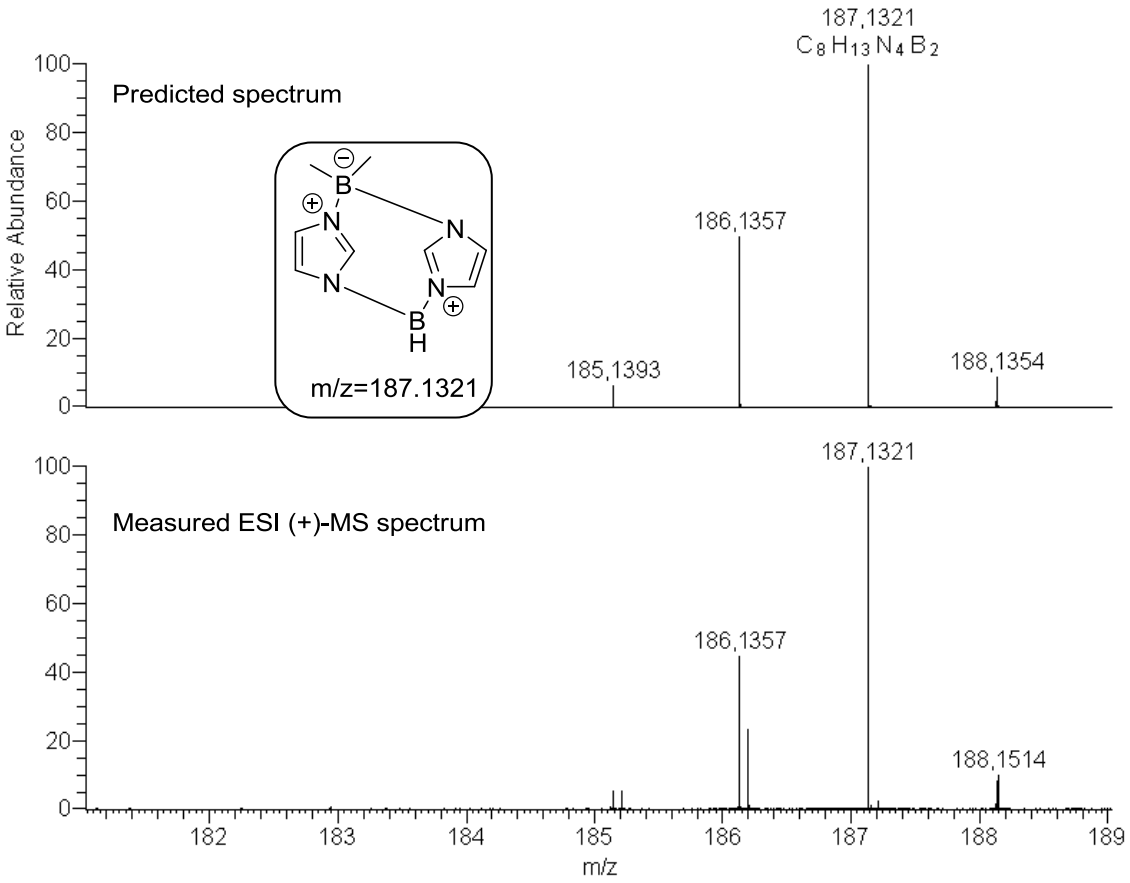
187,1321
C8H13N4B2
Predicted spectrum
Relative Abundance
186,1357
185,1393
188,1354
m/z=187.1321
187,1321
Measured ESI (+)-MS spectrum
186,1357
188,1514
m/z

The following scheme shows the fragments found in the ESI (-)-MS spectra. Despite some minor signals, all signals could be assigned.

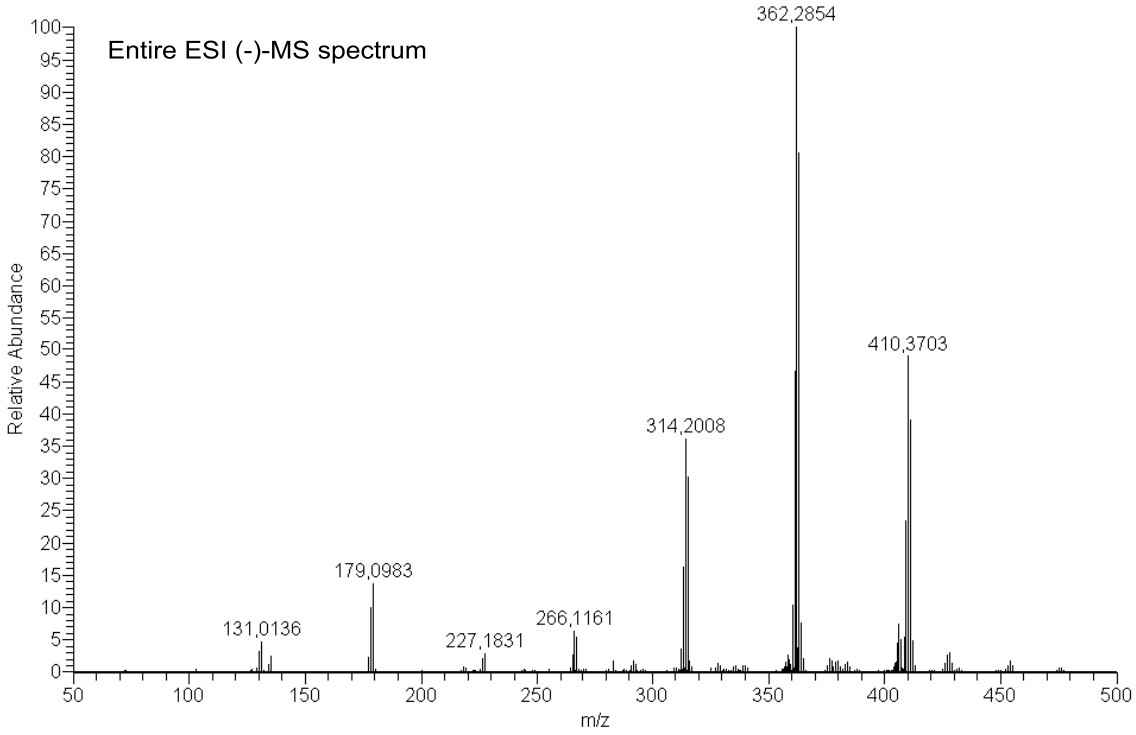

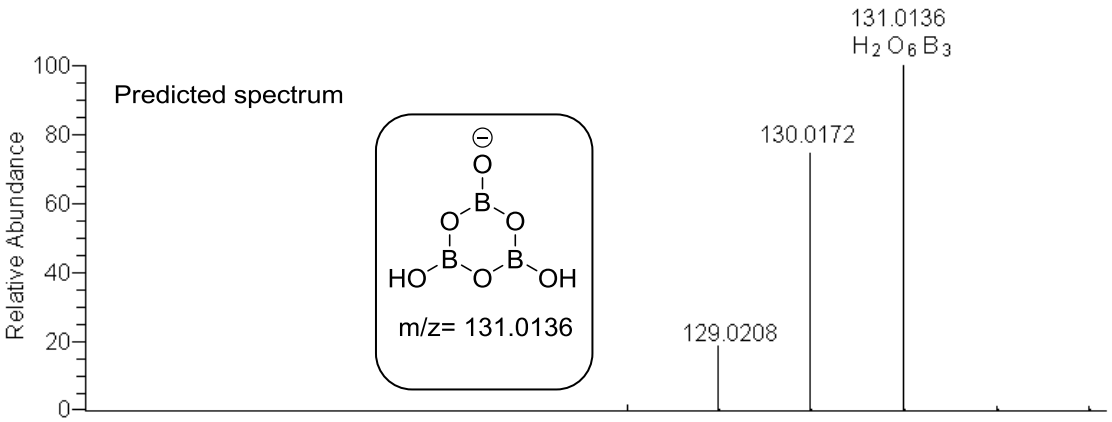

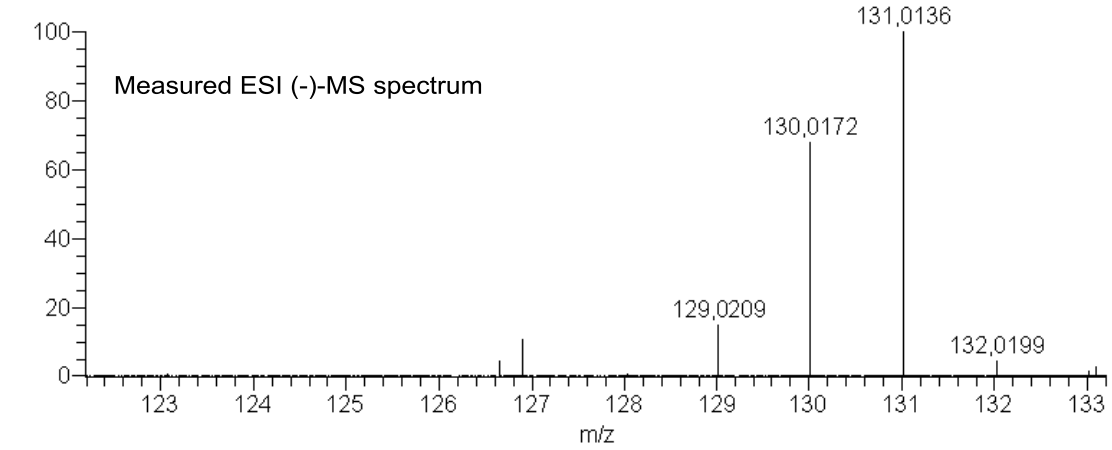

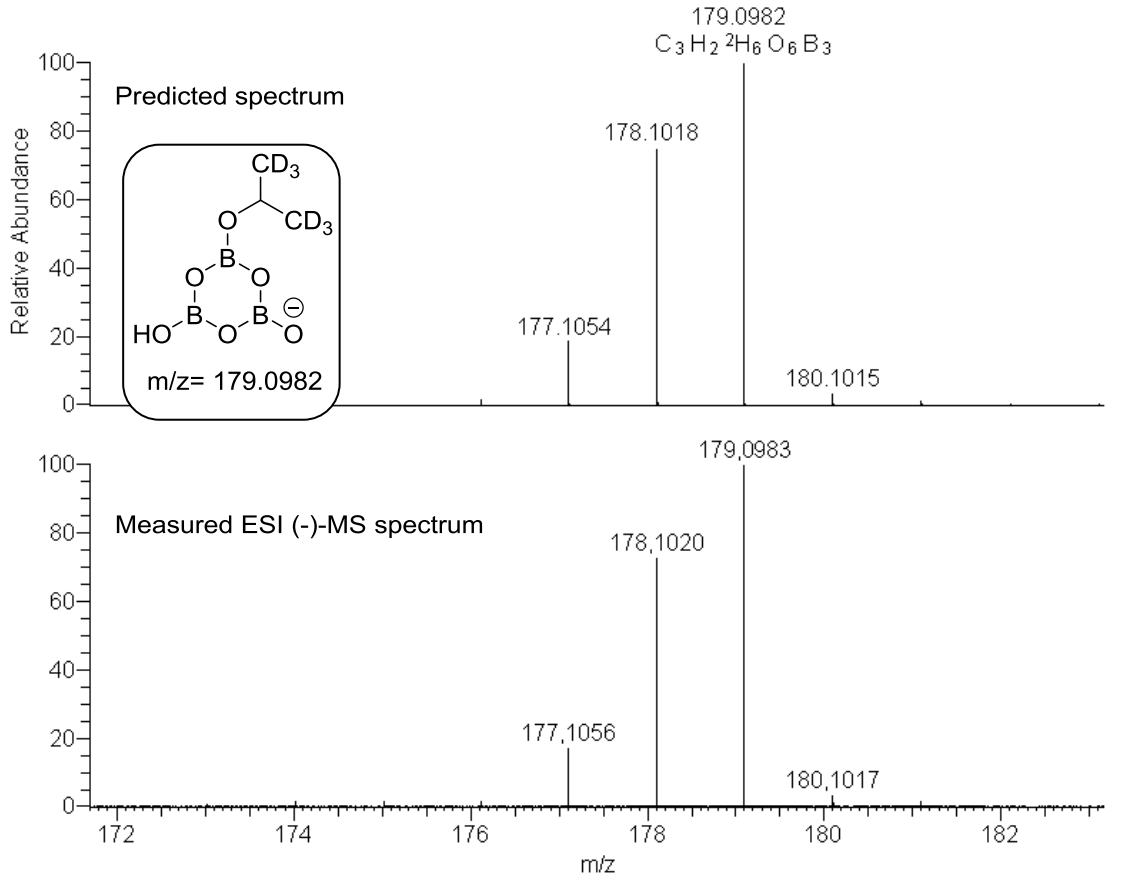
179.0982
C3 H2 2H6 O6 B3
Predicted spectrum
178.1018
177.1054
180.1015
m/z= 179.0982
Relative Abundance
179,0983
Measured ESI (-)-MS spectrum
178,1020
177,1056
180,1017
m/z

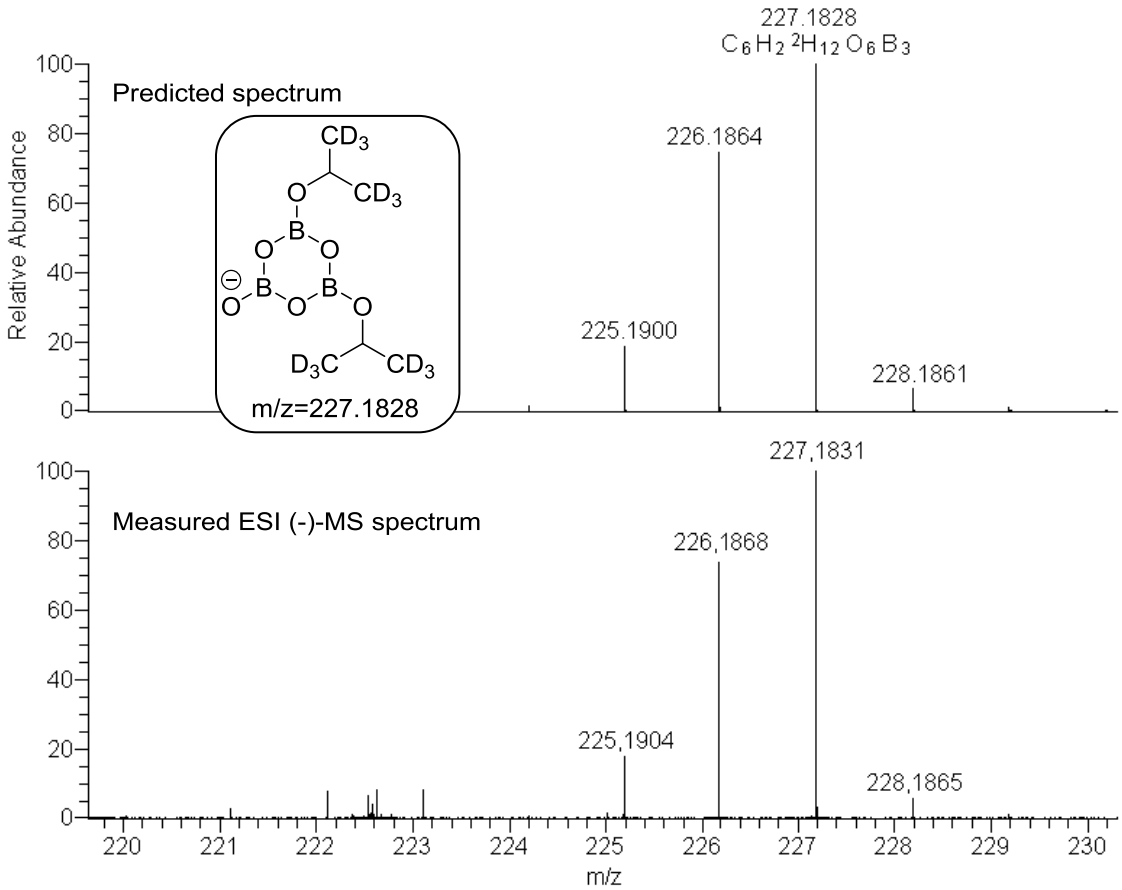
227.1828
C6 H2 2H12 O6 B3
Predicted spectrum
226.1864
225.1900
228.1861
m/z=227.1828
Relative Abundance
227,1831
Measured ESI (-)-MS spectrum
226,1868
225,1904
228,1865
m/z

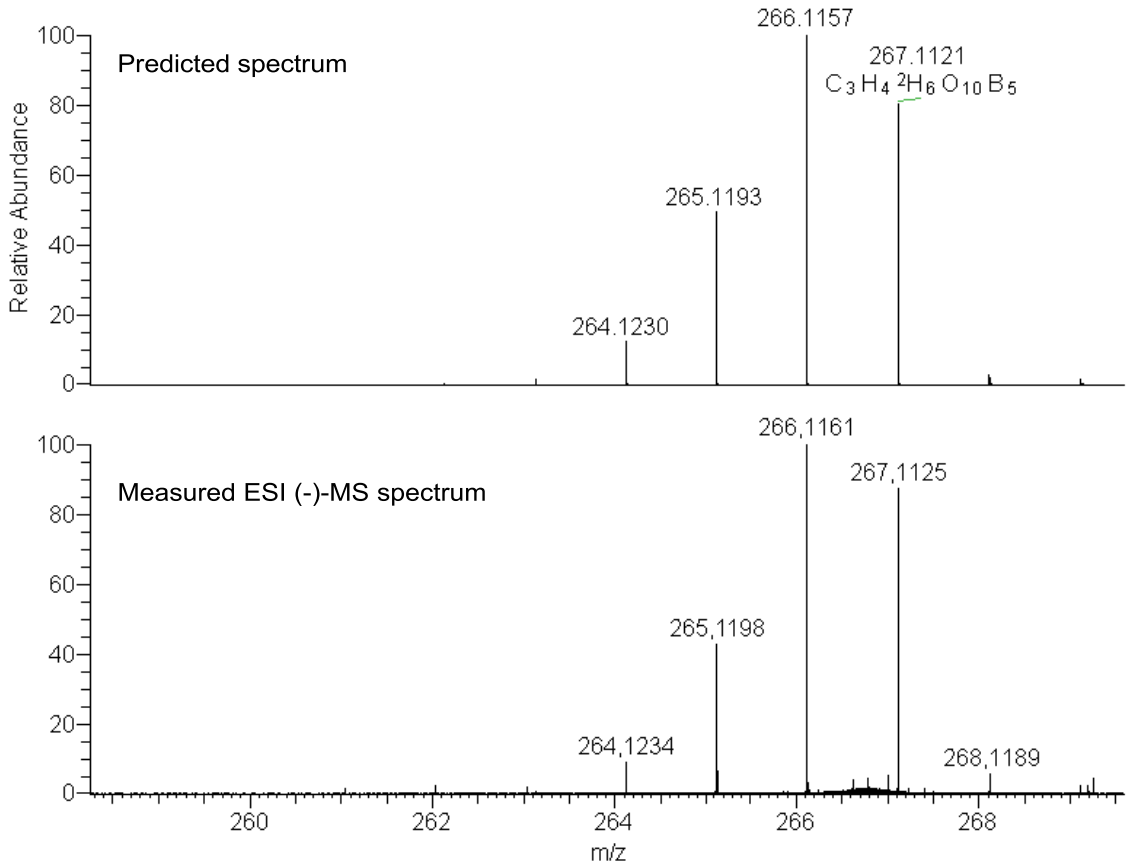
Predicted spectrum
266.1157
267.1121
C3 H4 2H6 O10 B5
265.1193
264.1230
Relative Abundance
Measured ESI (-)-MS spectrum
266,1161
267,1125
265,1198
264,1234
268,1189
m/z

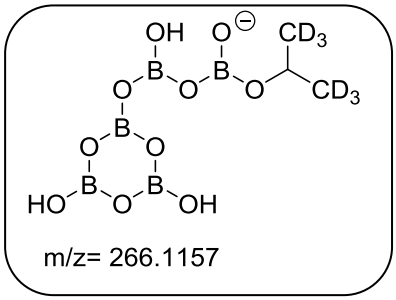
OH
O
CD3
B
O
B
O
CD3
B
O
O
HO
B
B
OH
m/z= 266.1157

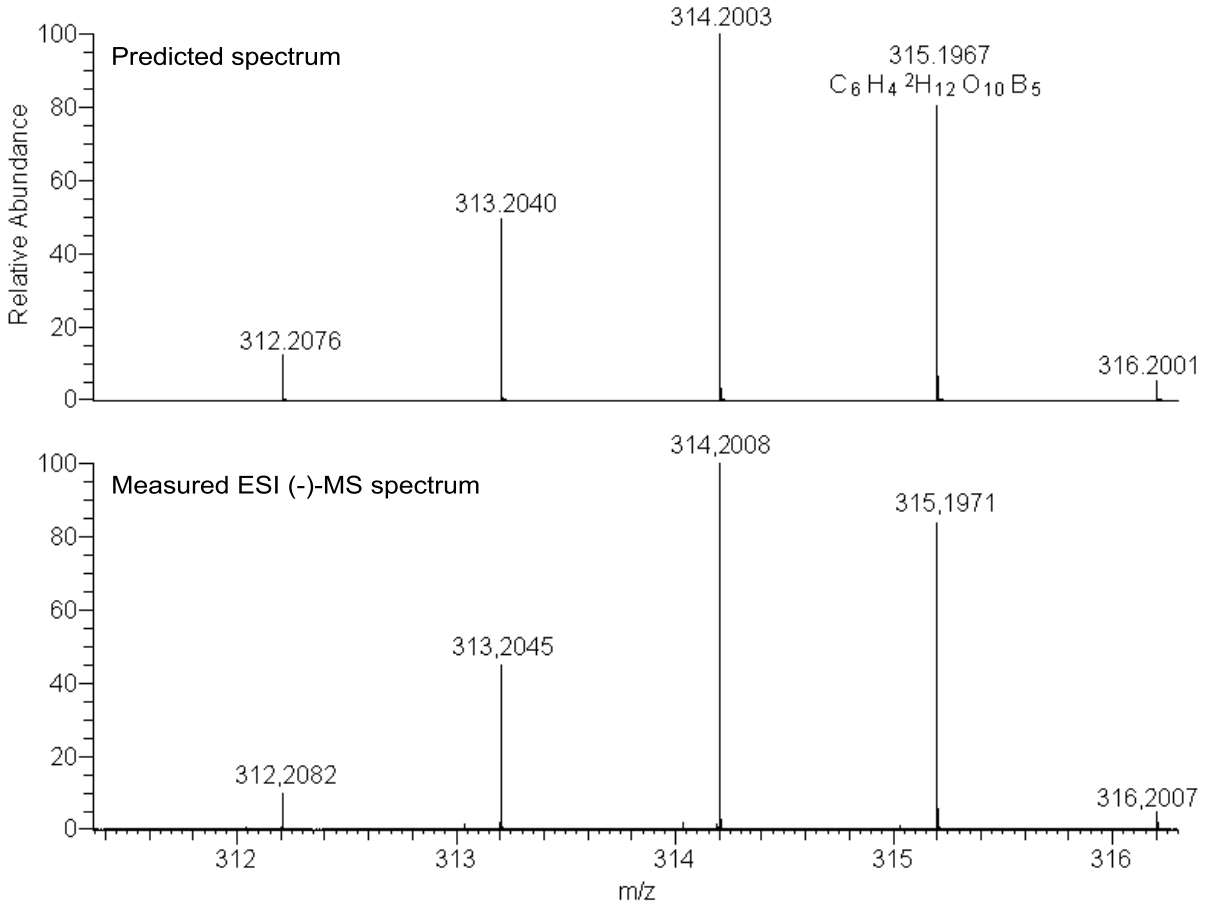
Predicted spectrum
314.2003
315.1967
C6 H4 2H12 O10 B5
313.2040
312.2076
316.2001
Measured ESI (-)-MS spectrum
314,2008
315,1971
313,2045
312,2082
316,2007
Relative Abundance
m/z
100
80
60
40
20
0
312
313
314
315
316

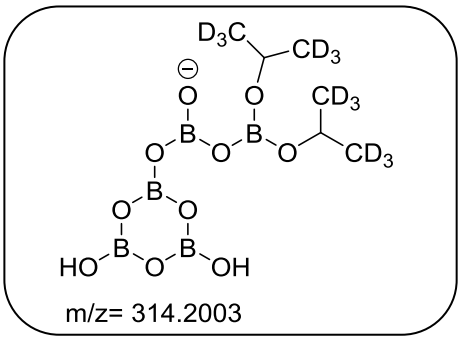
D3C
CD3
CD3
CD3
HO
OH
m/z= 314.2003

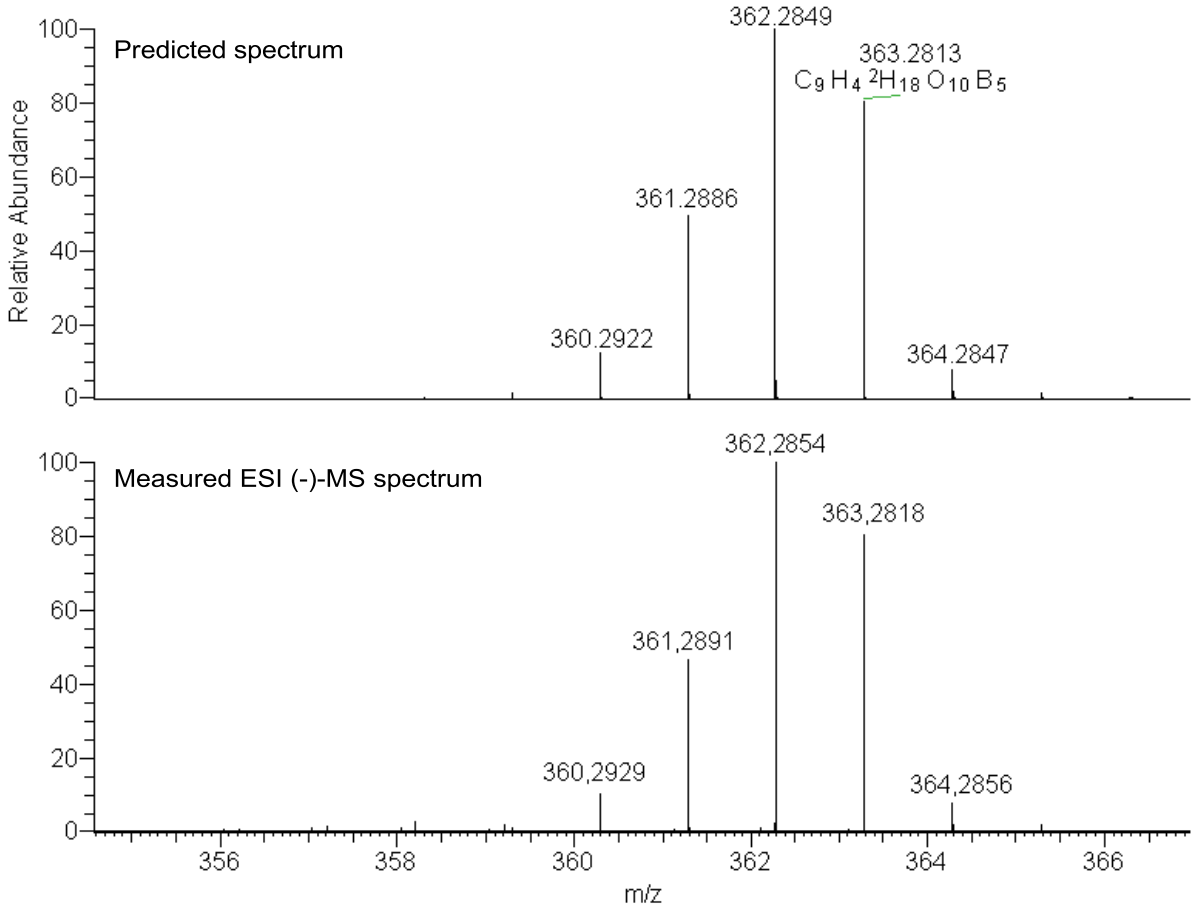
Predicted spectrum
362.2849
363.2813
C9 H4 2H18 O10 B5
361.2886
360.2922
364.2847
Measured ESI (-)-MS spectrum
362,2854
363,2818
361,2891
360,2929
364,2856
Relative Abundance
m/z
100
80
60
40
20
0
356
358
360
362
364
366

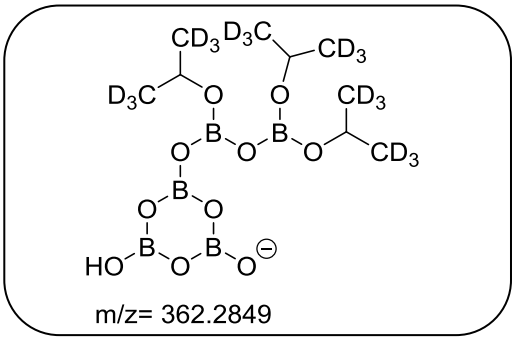
m/z= 362.2849

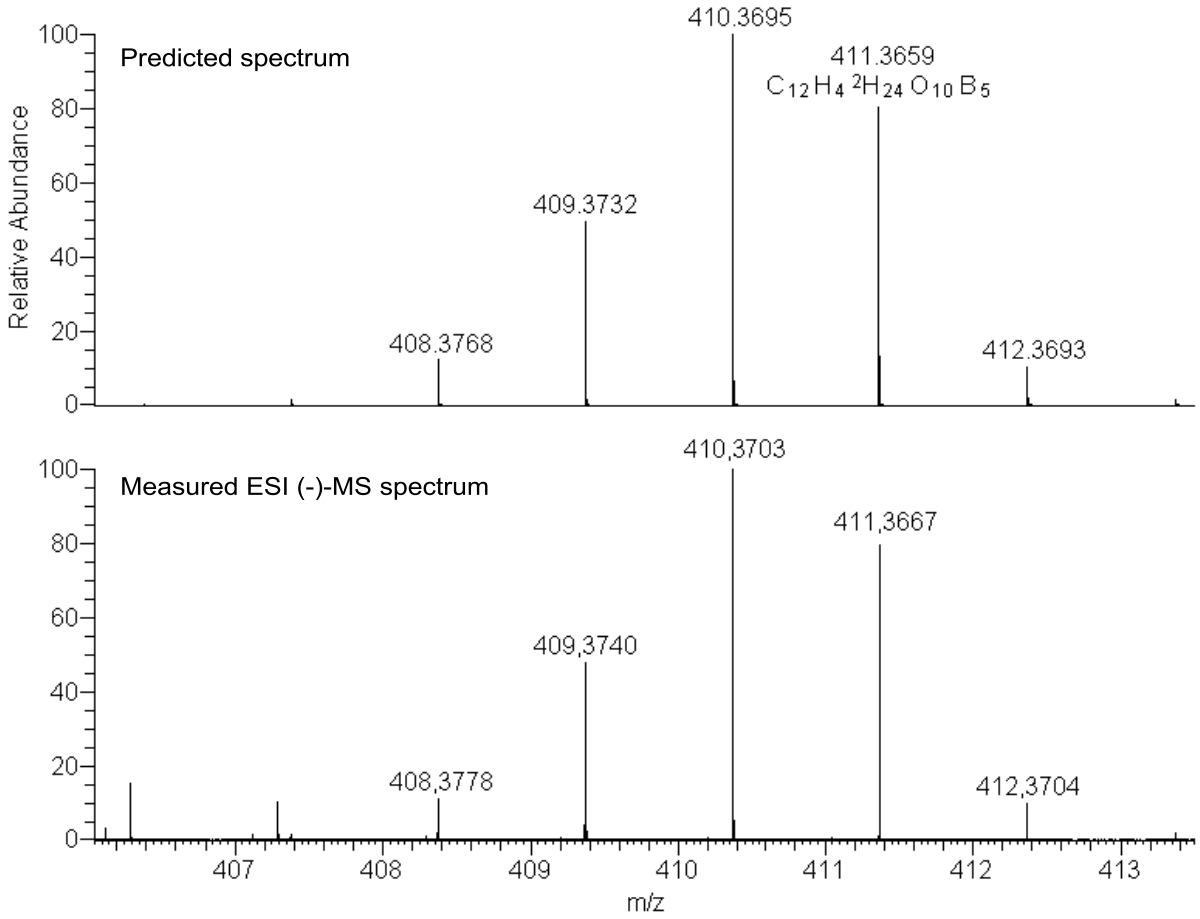
Predicted spectrum
410.3695
411.3659
C12H4 2H24 O10 B5
409.3732
408.3768
412.3693
Measured ESI (-)-MS spectrum
410,3703
411,3667
409,3740
408,3778
412,3704
Relative Abundance
m/z
100
80
60
40
20
0
407
408
409
410
411
412
413

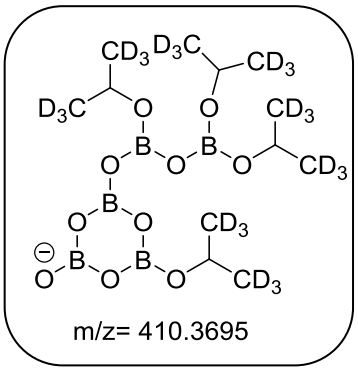
m/z= 410.3695

5.3.6. Reductions of alkyl halides

General procedure E: Setup for reductions of alkyl halides with dialkylaminopyridine boranes.

An alkyl halide (**18a**, **18d** or **18i**, 0.10 mmol) was transferred into a microwave vessel under ambient air by a Hamilton syringe. Afterwards, TMB (**22**, 0.10 to 0.15 mmol) was added as internal NMR standard as well as a dialkylaminopyridine borane complex (0.10 to 0.30 mmol; 1.00 to 3.00 eq.). Finally, 0.60 mL toluene-d_8 were added, the vessel was closed and reacted in the microwave at the desired temperature and time, depending on the experiment. Afterwards the vial was allowed to cool down to room temperature, followed by a ^{1}H NMR analysis. For quantification of the product formation, the decay of the starting alkyl halide was considered, as the corresponding alkane (here dodecane (**16a**)) is formed exclusively. Therefore, a ^{1}H NMR signal from the substrate was integrated against the internal standard. For GC/MS analysis, a small sample of the reaction mixture (usually 0.10 mL) was diluted with benzene (1.00 mL), solids were filtered off and the clear solution was analyzed.

5.4. Crystallographic data

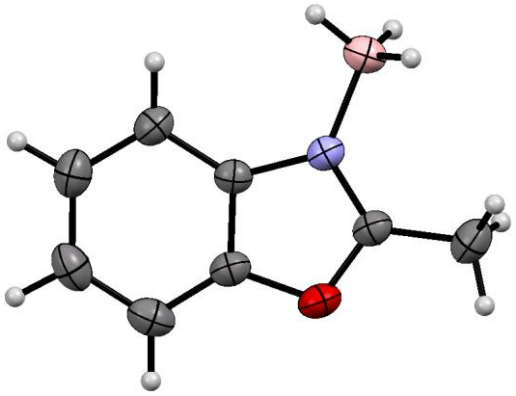

Table 18: X-ray structure of **17a**.

net formula	$C_8H_{10}BNO$	absorption correction	'multi-scan'
M_r/g mol^{-1}	146.982	transmission factor range	0.95714–1.00000
crystal size/mm	0.31 × 0.21 × 0.08	refls. measured	5772
T/K	173(2)	R_{int}	0.0254
radiation	MoKα	mean σ(*I*)/*I*	0.0307
diffractometer	'Oxford XCalibur'	θ range	4.19–26.35
crystal system	monoclinic	observed refls.	1143
space group	$P2_1/c$	*x, y* (weighting scheme)	0.0701, 0
a/Å	8.2509(6)	hydrogen refinement	constr
b/Å	12.3121(7)	refls in refinement	1629
c/Å	7.9124(5)	parameters	102
α/°	90	restraints	0
β/°	90.849(6)	$R(F_{obs})$	0.0390
γ/°	90	$R_w(F^2)$	0.1135
V/Å^3	803.70(9)	*S*	0.990
Z	4	shift/error$_{max}$	0.001
calc. density/g cm^{-3}	1.21475(14)	max electron density/e Å^{-3}	0.155
μ/mm^{-1}	0.078	min electron density/e Å^{-3}	−0.211

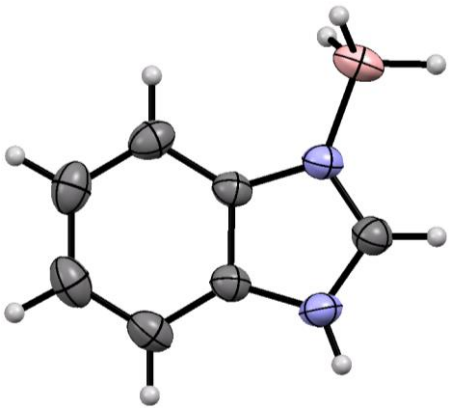

Table 19: X-ray structure of **17e**.

net formula	$C_7H_9BN_2$	absorption correction	'multi-scan'
M_r/g mol^{-1}	131.971	transmission factor range	0.63119–1.00000
crystal size/mm	0.37 × 0.25 × 0.03	refls. measured	2487
T/K	173(2)	R_{int}	0.0236
radiation	MoKα	mean σ(*I*)/*I*	0.0448
diffractometer	'Oxford XCalibur'	θ range	4.45–26.37
crystal system	monoclinic	observed refls.	1135
space group	$P2_1/n$	*x, y* (weighting scheme)	0.0470, 0.0877
a/Å	8.6874(15)	hydrogen refinement	mixed
b/Å	6.6993(13)	refls in refinement	1482
c/Å	13.119(3)	parameters	96
α/°	90	restraints	0
β/°	106.851(19)	$R(F_{obs})$	0.0473
γ/°	90	$R_w(F^2)$	0.1222
V/Å^3	730.7(3)	*S*	1.065
Z	4	shift/error$_{max}$	0.001
calc. density/g cm^{-3}	1.1996(5)	max electron density/e Å^{-3}	0.129
μ/mm^{-1}	0.072	min electron density/e Å^{-3}	−0.148

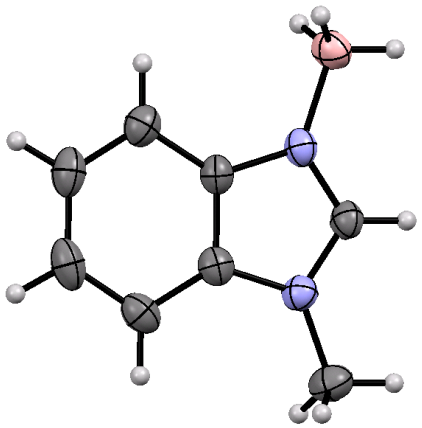

Table 20: X-ray structure of **17f**.

net formula	$C_8H_{11}BN_2$	absorption correction	'multi-scan'
M_r/g mol^{-1}	145.997	transmission factor range	0.82398–1.00000
crystal size/mm	0.28 × 0.16 × 0.04	refls. measured	6463
T/K	173(2)	R_{int}	0.0525
radiation	MoKα	mean σ(*I*)/*I*	0.0705
diffractometer	'Oxford XCalibur'	θ range	4.17–26.33
crystal system	monoclinic	observed refls.	1127
space group	$P2_1/c$	*x, y* (weighting scheme)	0.0443, 0
a/Å	7.1199(6)	hydrogen refinement	constr
b/Å	14.9271(10)	refls in refinement	1719
c/Å	8.5528(8)	parameters	103
α/°	90	restraints	0
β/°	114.535(10)	$R(F_{obs})$	0.0399
γ/°	90	$R_w(F^2)$	0.0943
V/Å^3	826.91(14)	*S*	0.887
Z	4	shift/error$_{max}$	0.001
calc. density/g cm^{-3}	1.17274(17)	max electron density/e Å^{-3}	0.171
μ/mm^{-1}	0.070	min electron density/e Å^{-3}	−0.154

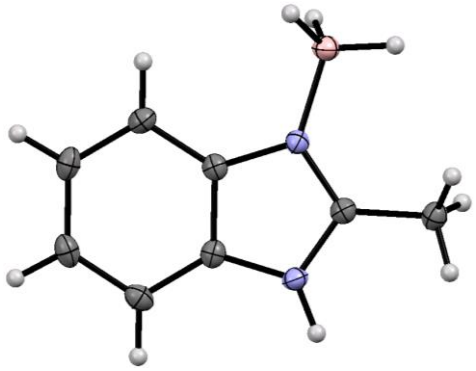

Table 21: X-ray structure of **17g**.

net formula	$C_8H_{11}BN_2$	absorption correction	'multi-scan'
M_r/g mol^{-1}	145.997	transmission factor range	0.83612–1.00000
crystal size/mm	0.337 × 0.172 × 0.096	refls. measured	2438
T/K	100(2)	R_{int}	0.0172
radiation	MoKα	mean σ(I)/I	0.0337
diffractometer	'Oxford XCalibur'	θ range	4.31–25.34
crystal system	monoclinic	observed refls.	1163
space group	$P2_1/c$	x, y (weighting scheme)	0.0494, 0.2251
a/Å	7.2225(5)	hydrogen refinement	mixed
b/Å	6.6630(6)	refls in refinement	1407
c/Å	17.4495(13)	parameters	107
α/°	90	restraints	0
β/°	111.762(5)	$R(F_{obs})$	0.0394
γ/°	90	$R_w(F^2)$	0.1038
V/Å^3	779.89(11)	S	1.026
Z	4	shift/error$_{max}$	0.001
calc. density/g cm^{-3}	1.24345(18)	max electron density/e Å^{-3}	0.198
μ/mm^{-1}	0.074	min electron density/e Å^{-3}	−0.245

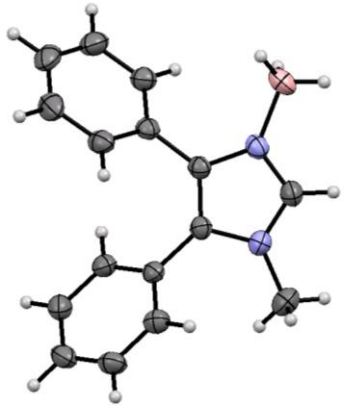

Table 22: X-ray structure of **17m**.

net formula	$C_{16}H_{17}BN_2$	absorption correction	'multi-scan'
M_r/g mol^{-1}	248.131	transmission factor range	0.40858–1.00000
crystal size/mm	0.42 × 0.27 × 0.12	refls. measured	7231
T/K	173(2)	R_{int}	0.0424
radiation	MoKα	mean σ(*I*)/*I*	0.0469
diffractometer	'Oxford XCalibur'	θ range	4.22–26.37
crystal system	monoclinic	observed refls.	2155
space group	$P2_1/c$	*x, y* (weighting scheme)	0.0679, 0.1673
a/Å	13.2179(18)	hydrogen refinement	constr
b/Å	8.5461(10)	refls in refinement	2811
c/Å	12.2286(15)	parameters	174
α/°	90	restraints	0
β/°	91.051(11)	$R(F_{obs})$	0.0477
γ/°	90	$R_w(F^2)$	0.1424
V/Å^3	1381.1(3)	*S*	1.047
Z	4	shift/error$_{max}$	0.001
calc. density/g cm^{-3}	1.1934(3)	max electron density/e Å^{-3}	0.220
μ/mm^{-1}	0.070	min electron density/e Å^{-3}	−0.208

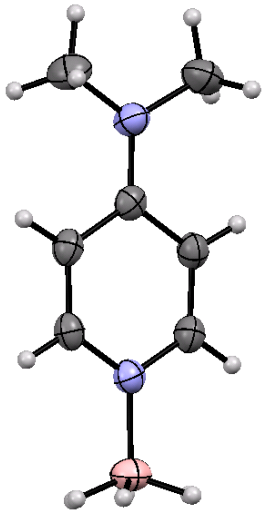

Table 23: X-ray structure of **17q**.

net formula	$C_7H_{13}BN_2$	absorption correction	'multi-scan'
M_r/g mol^{-1}	136.003	transmission factor range	0.91755–1.00000
crystal size/mm	0.49 × 0.41 × 0.11	refls. measured	3826
T/K	173(2)	R_{int}	0.0189
radiation	MoKα	mean σ(*I*)/*I*	0.0394
diffractometer	'Oxford XCalibur'	θ range	4.41–26.33
crystal system	orthorhombic	observed refls.	992
space group	*Pbca*	*x, y* (weighting scheme)	0.0483, 0
a/Å	10.3969(5)	hydrogen refinement	mixed
b/Å	7.7088(5)	refls in refinement	1629
c/Å	20.1359(11)	parameters	112
α/°	90	restraints	0
β/°	90	$R(F_{obs})$	0.0372
γ/°	90	$R_w(F^2)$	0.0881
V/Å^3	1613.84(16)	*S*	0.859
Z	8	shift/error$_{max}$	0.001
calc. density/g cm^{-3}	1.11952(11)	max electron density/e Å^{-3}	0.124
μ/mm^{-1}	0.067	min electron density/e Å^{-3}	−0.190

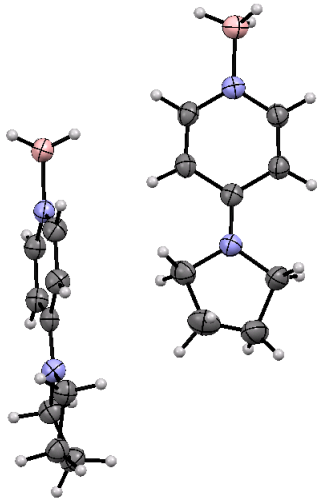

Table 24: X-ray structure of **17r**.

net formula	$C_9H_{15}BN_2$	μ/mm^{-1}	0.067
M_r/g mol^{-1}	162.040	absorption correction	none
crystal size/mm	0.24 × 0.16 × 0.12	refls. measured	15208
T/K	200(2)	R_{int}	0.0227
radiation	MoKα	mean σ(I)/I	0.0215
diffractometer	'KappaCCD'	θ range	3.60–27.48
crystal system	monoclinic	observed refls.	3526
space group	$P2_1/c$	x, y (weighting scheme)	0.0639, 0.5499
a/Å	10.2505(2)	hydrogen refinement	constr
b/Å	18.5747(4)	refls in refinement	4315
c/Å	9.9369(2)	parameters	219
α/°	90	restraints	0
β/°	90.0450(13)	$R(F_{obs})$	0.0465
γ/°	90	$R_w(F^2)$	0.1342
V/Å^3	1891.98(7)	S	1.039
Z	8	shift/error$_{max}$	0.001
calc. density/g cm^{-3}	1.13776(4)	max electron density/e Å^{-3}	0.242
		min electron density/e Å^{-3}	−0.198

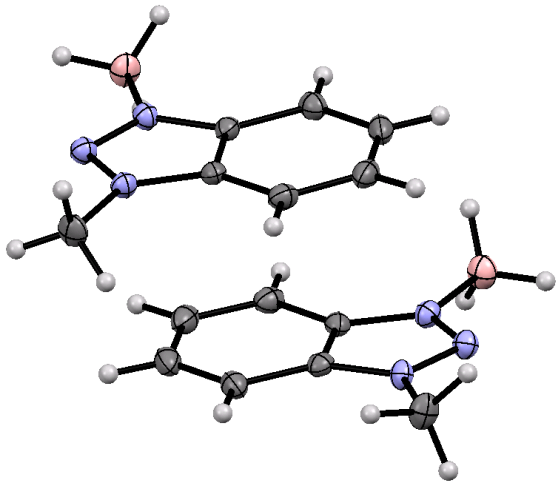

Table 25: X-ray structure of **17u**.

net formula	$C_7H_{10}BN_3$	absorption correction	'multi-scan'
M_r/g mol^{-1}	146.986	transmission factor range	0.97578–1.00000
crystal size/mm	0.36 × 0.19 × 0.10	refls. measured	5531
T/K	103(2)	R_{int}	0.0146
radiation	MoKα	mean σ(*I*)/*I*	0.0383
diffractometer	'Oxford XCalibur'	θ range	4.48–26.31
crystal system	triclinic	observed refls.	2168
space group	*P*1bar	*x, y* (weighting scheme)	0.0673, 0
a/Å	8.1249(6)	hydrogen refinement	constr
b/Å	8.2968(6)	refls in refinement	3124
c/Å	11.9199(7)	parameters	203
α/°	93.776(5)	restraints	0
β/°	103.426(5)	$R(F_{obs})$	0.0401
γ/°	94.779(6)	$R_w(F^2)$	0.1152
V/Å^3	775.84(9)	*S*	0.994
Z	4	shift/error$_{max}$	0.001
calc. density/g cm^{-3}	1.25840(15)	max electron density/e Å^{-3}	0.233
μ/mm^{-1}	0.078	min electron density/e Å^{-3}	−0.218

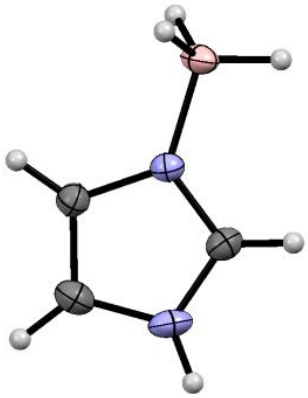

Table 26: X-ray structure of **17aa**.

net formula	$C_3H_7BN_2$	absorption correction	multi-scan
M_r/g mol^{-1}	81.912	transmission factor range	0.9247–0.9585
crystal size/mm	0.153 × 0.061 × 0.047	refls. measured	16412
T/K	123(2)	R_{int}	0.0526
radiation	'Mo Kα	mean σ(I)/I	0.0185
diffractometer	'Bruker D8Venture'	θ range	3.26–26.46
crystal system	orthorhombic	observed refls.	795
space group	*Pbca*	x, y (weighting scheme)	0.0459, 0.3075
a/Å	5.3376(2)	hydrogen refinement	mixed
b/Å	12.4830(5)	refls in refinement	973
c/Å	14.3227(6)	parameters	71
α/°	90	restraints	0
β/°	90	$R(F_{obs})$	0.0372
γ/°	90	$R_w(F^2)$	0.0973
V/Å^3	954.31(7)	S	1.060
Z	8	shift/error$_{max}$	0.001
calc. density/g cm^{-3}	1.14026(8)	max electron density/e Å^{-3}	0.210
μ/mm^{-1}	0.071	min electron density/e Å^{-3}	−0.169

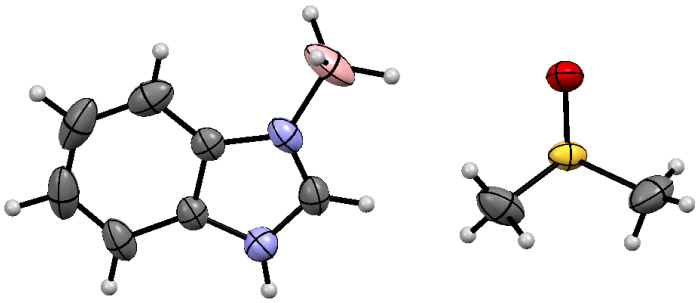

Table 27: X-ray structure of **17ad**.

net formula	$C_{16}H_{24}B_2N_4OS$	absorption correction	multi-scan
M_r/g mol^{-1}	342.076	transmission factor range	0.8355–0.8621
crystal size/mm	0.178 × 0.115 × 0.088	refls. measured	18674
T/K	173(2)	R_{int}	0.0371
radiation	'Mo Kα	mean σ(I)/I	0.0239
diffractometer	'Bruker D8Venture'	θ range	2.87–27.59
crystal system	monoclinic	observed refls.	1778
space group	$C2/c$	x, y (weighting scheme)	0.0715, 1.2191
a/Å	15.2805(8)	hydrogen refinement	mixed
b/Å	8.3809(5)	refls in refinement	2206
c/Å	16.0399(9)	parameters	133
α/°	90	restraints	0
β/°	111.546(3)	$R(F_{obs})$	0.0466
γ/°	90	$R_w(F^2)$	0.1392
V/Å^3	1910.60(19)	S	1.055
Z	4	shift/error$_{max}$	0.001
calc. density/g cm^{-3}	1.18924(12)	max electron density/e Å^{-3}	0.249
μ/mm^{-1}	0.179	min electron density/e Å^{-3}	−0.234

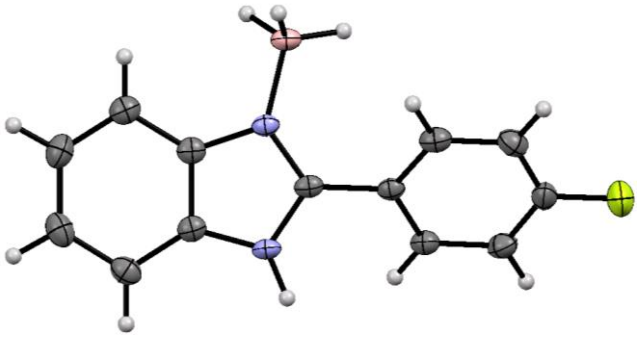

Table 28: X-ray structure of **17af**.

net formula	$C_{13}H_{12}BFN_2$	absorption correction	multi-scan
M_r/g mol^{-1}	226.057	transmission factor range	0.8956–0.9579
crystal size/mm	0.118 × 0.063 × 0.049	refls. measured	6511
T/K	123(2)	R_{int}	0.0412
radiation	'Mo Kα	mean σ(I)/I	0.0409
diffractometer	'Bruker D8Venture'	θ range	3.02–25.01
crystal system	monoclinic	observed refls.	1607
space group	$C2/c$	x, y (weighting scheme)	0.0447, 3.4775
a/Å	24.099(3)	hydrogen refinement	mixed
b/Å	13.4697(13)	refls in refinement	1991
c/Å	7.2558(8)	parameters	170
α/°	90	restraints	0
β/°	105.675(4)	$R(F_{obs})$	0.0461
γ/°	90	$R_w(F^2)$	0.1221
V/Å^3	2267.7(4)	S	1.083
Z	8	shift/error$_{max}$	0.001
calc. density/g cm^{-3}	1.3243(2)	max electron density/e Å^{-3}	0.197
μ/mm^{-1}	0.090	min electron density/e Å^{-3}	−0.202

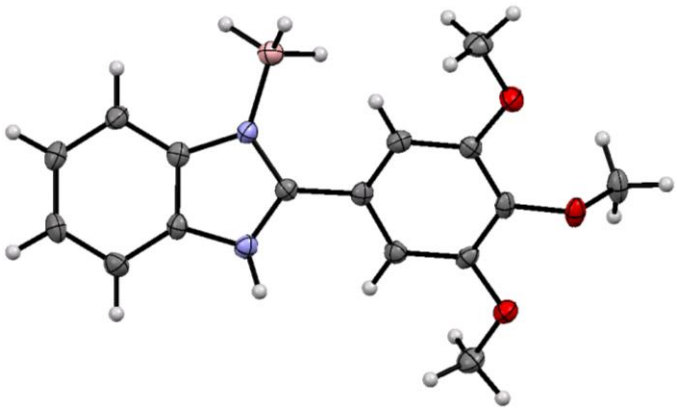

Table 29: X-ray structure of **17ag**.

net formula	$C_{16}H_{19}BN_2O_3$	absorption correction	multi-scan
M_r/g mol^{-1}	298.145	transmission factor range	0.9032–0.9580
crystal size/mm	0.242 × 0.027 × 0.021	refls. measured	22020
T/K	123(2)	R_{int}	0.0788
radiation	'Mo Kα	mean σ(I)/I	0.0554
diffractometer	'Bruker D8Venture'	θ range	3.04–25.36
crystal system	monoclinic	observed refls.	1980
space group	$P2_1/c$	x, y (weighting scheme)	0.0283, 1.3854
a/Å	6.9403(6)	hydrogen refinement	mixed
b/Å	28.139(3)	refls in refinement	2707
c/Å	7.6612(8)	parameters	218
α/°	90	restraints	0
β/°	96.032(3)	$R(F_{obs})$	0.0553
γ/°	90	$R_w(F^2)$	0.1167
V/Å^3	1487.9(2)	S	1.116
Z	4	shift/error$_{max}$	0.001
calc. density/g cm^{-3}	1.33097(18)	max electron density/e Å^{-3}	0.230
μ/mm^{-1}	0.091	min electron density/e Å^{-3}	−0.199

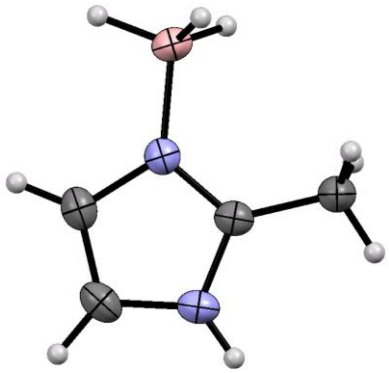

Table 30: X-ray structure of **17ah**.

net formula	$C_4H_9BN_2$	absorption correction	'multi-scan'
M_r/g mol^{-1}	95.939	transmission factor range	0.89865–1.00000
crystal size/mm	0.219 × 0.184 × 0.117	refls. measured	2147
T/K	100(2)	R_{int}	0.0307
radiation	MoKα	mean σ(I)/I	0.0348
diffractometer	'Oxford XCalibur'	θ range	4.40–28.43
crystal system	orthorhombic	observed refls.	570
space group	*Pnma*	x, y (weighting scheme)	0.0438, 0.0750
a/Å	11.7314(10)	hydrogen refinement	mixed
b/Å	6.6939(5)	refls in refinement	743
c/Å	7.5679(6)	parameters	58
α/°	90	restraints	0
β/°	90	$R(F_{obs})$	0.0430
γ/°	90	$R_w(F^2)$	0.1060
V/Å^3	594.30(8)	S	1.054
Z	4	shift/error$_{max}$	0.001
calc. density/g cm^{-3}	1.07227(14)	max electron density/e Å^{-3}	0.168
μ/mm^{-1}	0.066	min electron density/e Å^{-3}	−0.188

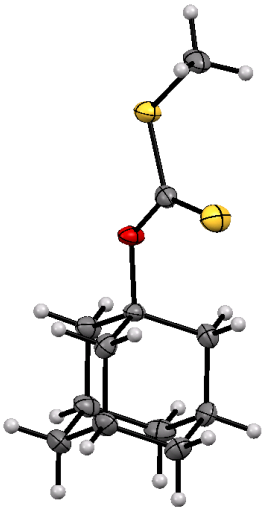

Table 31: X-ray structure of **18g**.

net formula	$C_{12}H_{18}OS_2$	absorption correction	multi-scan
M_r/g mol^{-1}	242.403	transmission factor range	0.8757–0.9585
crystal size/mm	0.194 × 0.123 × 0.119	refls. measured	20348
T/K	173(2)	R_{int}	0.0595
radiation	'Mo Kα	mean σ(I)/I	0.0375
diffractometer	'Bruker D8Quest'	θ range	2.42–26.38
crystal system	monoclinic	observed refls.	1904
space group	$P2_1/c$	x, y (weighting scheme)	0.0380, 0.3479
a/Å	6.7781(4)	hydrogen refinement	constr
b/Å	18.7053(10)	refls in refinement	2452
c/Å	9.4522(6)	parameters	137
α/°	90	restraints	0
β/°	93.3091(19)	$R(F_{obs})$	0.0375
γ/°	90	$R_w(F^2)$	0.0823
V/Å^3	1196.41(12)	S	1.058
Z	4	shift/error$_{max}$	0.001
calc. density/g cm^{-3}	1.34578(13)	max electron density/e Å^{-3}	0.301
μ/mm^{-1}	0.416	min electron density/e Å^{-3}	−0.280

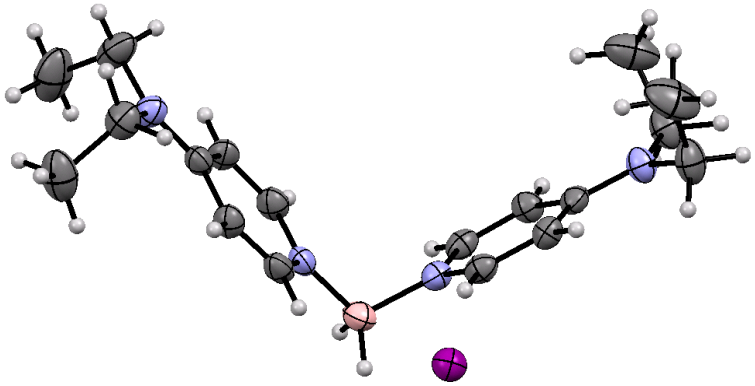

Table 32: X-ray structure of **25i**.

net formula	$C_{18}H_{30}BIN_4$	absorption correction	'multi-scan'
M_r/g mol^{-1}	440.173	transmission factor range	0.92190–1.00000
crystal size/mm	0.25 × 0.12 × 0.10	refls. measured	11966
T/K	173(2)	R_{int}	0.0382
radiation	MoKα	mean σ(I)/I	0.0519
diffractometer	'Oxford XCalibur'	θ range	4.20–27.94
crystal system	monoclinic	observed refls.	3276
space group	$P2_1/c$	x, y (weighting scheme)	0.0237, 0
a/Å	11.2557(6)	hydrogen refinement	mixed
b/Å	10.7537(4)	refls in refinement	4450
c/Å	17.3884(7)	parameters	222
α/°	90	restraints	0
β/°	90.071(4)	$R(F_{obs})$	0.0362
γ/°	90	$R_w(F^2)$	0.0751
V/Å^3	2104.68(15)	S	1.048
Z	4	shift/error$_{max}$	0.001
calc. density/g cm^{-3}	1.38916(10)	max electron density/e Å^{-3}	0.900
μ/mm^{-1}	1.528	min electron density/e Å^{-3}	−0.496

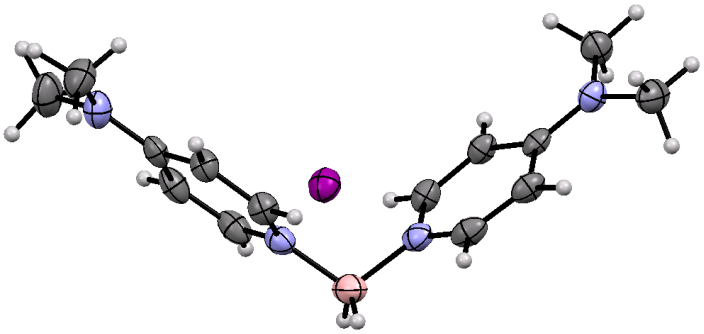

Table 33: X-ray structure of **29b**.

net formula	$C_{14}H_{22}BIN_4$	absorption correction	multi-scan
M_r/g mol^{-1}	384.067	transmission factor range	0.6976–0.7454
crystal size/mm	0.090 × 0.060 × 0.040	refls. measured	40152
T/K	173(2)	R_{int}	0.0378
radiation	'Mo Kα	mean σ(I)/I	0.0177
diffractometer	'Bruker D8Venture'	θ range	2.99–26.43
crystal system	monoclinic	observed refls.	2903
space group	$P2_1/c$	x, y (weighting scheme)	0.0233, 0.8178
a/Å	14.7515(6)	hydrogen refinement	mixed
b/Å	14.9918(6)	refls in refinement	3464
c/Å	7.8341(3)	parameters	193
α/°	90	restraints	0
β/°	102.6340(10)	$R(F_{obs})$	0.0221
γ/°	90	$R_w(F^2)$	0.0503
V/Å^3	1690.57(12)	S	1.037
Z	4	shift/error$_{max}$	0.002
calc. density/g cm^{-3}	1.50900(11)	max electron density/e Å^{-3}	0.467
μ/mm^{-1}	1.890	min electron density/e Å^{-3}	−0.271

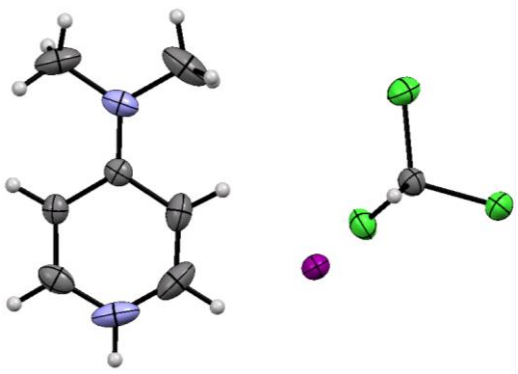

Table 34: X-ray structure of **29f**.

net formula	$C_8H_{12}Cl_3IN_2$	absorption correction	multi-scan
M_r/g mol^{-1}	369.457	transmission factor range	0.7784–0.8621
crystal size/mm	0.080 × 0.050 × 0.030	refls. measured	21644
T/K	173(2)	R_{int}	0.0296
radiation	'Mo Kα	mean σ(I)/I	0.0179
diffractometer	'Bruker D8Venture'	θ range	2.96–27.48
crystal system	triclinic	observed refls.	2735
space group	P1bar	x, y (weighting scheme)	0.0169, 0.4110
a/Å	6.9788(3)	hydrogen refinement	constr
b/Å	8.6745(4)	refls in refinement	3049
c/Å	11.4980(5)	parameters	129
α/°	104.7330(12)	restraints	0
β/°	99.4295(13)	$R(F_{obs})$	0.0191
γ/°	91.1512(13)	$R_w(F^2)$	0.0431
V/Å^3	662.69(5)	S	1.088
Z	2	shift/error$_{max}$	0.001
calc. density/g cm^{-3}	1.85156(14)	max electron density/e Å^{-3}	0.476
μ/mm^{-1}	2.989	min electron density/e Å^{-3}	−0.269

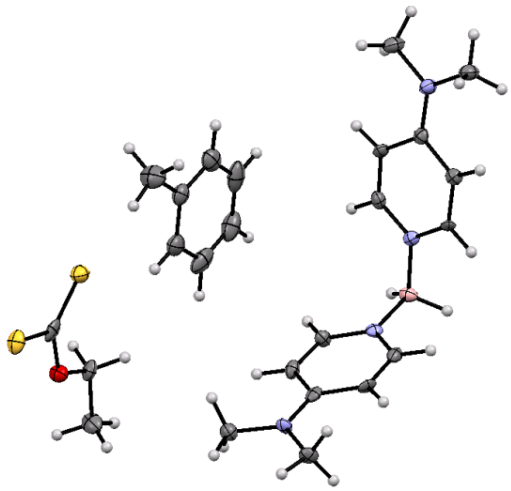

Table 35: X-ray structure of **29n**.

net formula	$C_{41}H_{62}B_2N_8O_2S_4$	μ/mm^{-1}	0.259
M_r/g mol^{-1}	848.84	absorption correction	multi-scan
crystal size/mm	0.120 × 0.070 × 0.020	transmission factor range	0.8020–0.9281
T/K	100(2)	refls. measured	1019
radiation	MoKα	mean σ(*I*)/*I*	0.0328
diffractometer	'Bruker D8Venture'	θ range	2.839–25.40
crystal system	monoclinic	observed refls.	2904
space group	'C 2/c'	*x*, *y* (weighting scheme)	0.0796, 25.0388
a/Å	18.0525(10)	hydrogen refinement	mixed
b/Å	8.4999(4)	refls in refinement	3264
c/Å	30.0560(17)	parameters	266
α/°	90	restraints	0
β/°	105.7399(16)	$R(F_{obs})$	0.0562
γ/°	90	$R_w(F^2)$	0.1699
V/Å^3	4439.0(4)	*S*	1.085
Z	4	shift/error$_{max}$	0.001
calc. density/g cm^{-3}	1.270	max electron density/e Å^{-3}	0.405
		min electron density/e Å^{-3}	−0.383

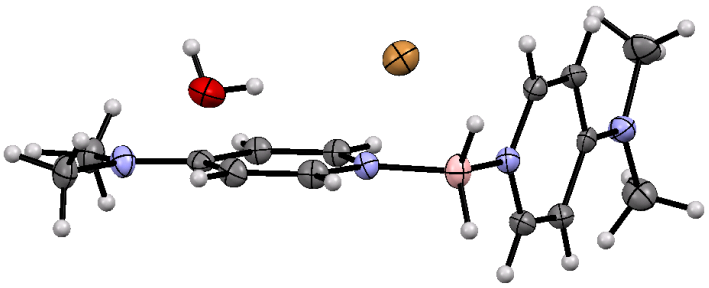

Table 36: X-ray structure of **29t**.

net formula	$C_{14}H_{24}BBrN_4O$	absorption correction	multi-scan
M_r/g mol^{-1}	355.082	transmission factor range	0.6028–0.6468
crystal size/mm	0.100 × 0.080 × 0.060	refls. measured	24338
T/K	173(2)	R_{int}	0.0273
radiation	'Mo Kα	mean σ(I)/I	0.0206
diffractometer	'Bruker D8Venture'	θ range	2.92–27.50
crystal system	triclinic	observed refls.	3306
space group	P1bar	x, y (weighting scheme)	0.0545, 0.8466
a/Å	8.4039(4)	hydrogen refinement	mixed
b/Å	9.7687(4)	refls in refinement	3799
c/Å	11.5059(5)	parameters	210
α/°	83.4698(12)	restraints	2
β/°	75.7506(13)	$R(F_{obs})$	0.0354
γ/°	64.8600(11)	$R_w(F^2)$	0.1013
V/Å^3	828.75(6)	S	1.073
Z	2	shift/error$_{max}$	0.001
calc. density/g cm^{-3}	1.42295(10)	max electron density/e Å^{-3}	0.515
μ/mm^{-1}	2.484	min electron density/e Å^{-3}	−0.337

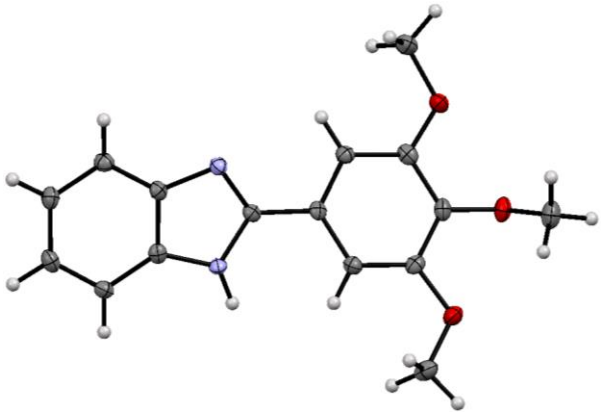

Table 37: X-ray structure of **41oa**.

net formula	$C_{16}H_{16}N_2O_3$	absorption correction	'multi-scan'
M_r/g mol^{-1}	284.310	transmission factor range	0.97550–1.00000
crystal size/mm	0.342 × 0.135 × 0.120	refls. measured	14980
T/K	100(2)	R_{int}	0.0638
radiation	MoKα	mean σ(I)/I	0.0549
diffractometer	'Oxford XCalibur'	θ range	4.16–26.37
crystal system	orthorhombic	observed refls.	2147
space group	*Pbca*	x, y (weighting scheme)	0.0253, 1.2524
a/Å	8.1452(5)	hydrogen refinement	mixed
b/Å	9.3977(6)	refls in refinement	2879
c/Å	36.820(3)	parameters	197
α/°	90	restraints	0
β/°	90	$R(F_{obs})$	0.0451
γ/°	90	$R_w(F^2)$	0.0984
V/Å^3	2818.4(3)	S	1.060
Z	8	shift/error$_{max}$	0.001
calc. density/g cm^{-3}	1.34009(14)	max electron density/e Å^{-3}	0.253
μ/mm^{-1}	0.094	min electron density/e Å^{-3}	−0.220

6. Literature

[1] M. Gomberg, *J. Am. Chem. Soc.* **1900**, *22*, 757.
[2] B. Giese, *Radicals in Organic Synthesis: Formation of Carbon-Carbon Bonds*, Pergamon, Oxford, **1986**.
[3] W. B. Motherwell, D. Crich, *Free Radical Chain Reactions in Organic Synthesis*, Academic Press, London, **1992**; J. E. Leffler, *An Introduction to Free Radicals*, Wiley-Interscience, New York, **1993**; D. P. Curran, N. A. Porter, B. Giese, *Stereochemistry of Radical Reactions*, VCH, Weinheim, **1995**; T. Linker, M. Schmittel, *Radikale und Radikalreaktionen in der Organischen Synthese*, Wiley-VCH, Weinheim, **2001**.
[4] J. Fossey, D. Lefort, J. Sorba, *Free Radicals in Organic Chemistry*, John Wiley & Sons, Chichester, New York, Brisbane, Toronto, Singapore, **1995**.
[5] H. G. Kuivila, *Acc. Chem. Res.* **1968**, *1*, 299; W. P. Neumann, *Synthesis* **1987**, 665; M. Pereyre, J.-P. Quintard, A. Rahm, *Tin in Organic Synthesis*, Butterworths, Toronto, **1987**; T. V. RajanBabu, *Encyclopedia of Reagents for Organic Synthesis*, *Vol. 7* (Ed.: L. Paquette), Wiley, New York, **1995**, p. 5016; A. G. Davies, *Organotin Chemistry*, Wiley-VCH, Weinheim, **1997**.
[6] G. J. M. van der Kerk, J. G. Noltes, J. G. A. Luijten, *J. Appl. Chem.* **1957**, *7*, 356.
[7] C. P. Jasperse, D. P. Curran, T. L. Fevig, *Chem. Rev.* **1991**, *91*, 1237; U. Koert*, Angew. Chem.* **1996**, *108*, 441; F. Aldabbagh, W. R. Browman, *Contemp. Org. Synth.* **1997**, 261.
[8] R. K. Ingham, S. D. Rosenberg, H. Gilman, *Chem. Rev.* **1960**, *60*, 459; I. J. Boyer, *Toxicology* **1989**, *55*, 253.
[9] P. A. Baguley, J. C. Walton, *Angew. Chem.* **1998**, *110*, 3273; A. F. Parsons, *Chem. Brit.* **2002**, *42*; A. Studer, S. Amrein, *Synthesis* **2002**, 835.
[10] C. Chatgilialoglu, *Acc. Chem. Res.* **1992**, *25*, 188.
[11] M. Newcomb, S. U. Park, *J. Am. Chem. Soc.* **1986**, *108*, 4132.
[12] L. J. J. Laarhoven, P. Mulder, D. D. M. Wayner, *Acc. Chem. Res.* **1999**, *32*, 342.
[13] C. Chatgilialoglu, *Organosilanes in Radical Chemistry*, John Wiley & Sons, Inc., **2004**.
[14] C. Chatgilialoglu, *Adv. Organometal. Chem.* **1999**, *44*, 67- 112.
[15] R. Walsh, *Acc. Chem. Res.* **1981**, *14*, 246.
[16] M. Ballestri, C. Chatgilialoglu, M. Guerra, A. Guerrini, M. Lucarini, G. Seconi*, J. Chem. Soc., Perkin Trans. 2* **1993**, 421.
[17] C. Chatgilialoglu, M. Newcomb*, Adv. Organomet. Chem.* **1999**, *44*, 67.
[18] D. H. R. Barton, D. O. Jang, J. C. Jaszberenyi, *Tetrahedron Lett.* **1991**, *32*, 7187; D. H. R. Barton, D. O. Jang, J. C. Jaszberenyi, *Tetrahedron* **1993**, *49*, 2793; D. H. R. Barton, D. O. Jang, J. C. Jaszberenyi, *Tetrahedron* **1993**, *49*, 7193; D. O. Jang, J. Kim, D. H. Cho, C.-M. Chung, *Tetrahedron Lett.* **2001**, *42*, 1073; P. Meffre, R. H. Dave, J. Leroy, B. Badet, *Tetrahedron Lett.* **2001**, *42*, 8625; S. Takamatsu, T. Maruyama, S. Katayama, N. Hirose, K. Izawa, *Tetrahedron Lett.* **2001**, *42*, 2321.
[19] J. M. Kanabus-Kaminska, J. A. Hawari, D. Griller, C. Chatgilialoglu, *J. Am. Chem. Soc.* **1987**, *109*, 5267.
[20] H. Gilman, W. H. Atwell, P. K. Sen, C. L. Smith*, J. Organomet. Chem.* **1965**, *4*, 163.
[21] C. Chatgilialoglu, C. H. Schiesser, *The Chemistry of Organic Silicon Compounds, Vol. 3* (Eds.: Z. Rappoport, Y. Apeloig), Wiley, London, **2001**, 341.
[22] C. Chatgilialoglu, C. Ferreri, T. Gimisis*, The Chemistry of Organic Silicon Compounds, Vol. 2* (Eds.: Z. Rappoport, Y. Apeloig), Wiley, London, **1998**, 1539.
[23] M. Ballestri, C. Chatgilialoglu, N. Cardi, A. Sommazzi, *Tetrahedron Lett.* **1992**, *33*, 1787.

[24] M. Ballestri, C. Chatgilialoglu, K. B. Clark, D. Griller, B. Giese, B. Kopping, *J. Org. Chem.* **1991**, *56*, 678.
[25] D. H. R. Barton, D. O. Jang, J. C. Jaszberenyi, *Tetrahedron Lett.* **1990**, *31*, 4681.
[26] M.-L. Bennasar, C. Juan, J. Bosch, *Chem. Comm.* **2000**, 2459.
[27] B. Giese, B. Kopping, C. Chatgilialoglu, *Tetrahedron Lett.* **1989**, *30*, 681.
[28] R. Romeo, L. A. Wozniak, C. Chatgilialoglu, *Tetrahedron Lett.* **2000**, *41*, 9899.
[29] C. Chatgilialoglu, M. Ballestri, *Organometallics* **1995**, *14*, 5017.
[30] H. N. C. Wong, F. Sondheimer, *Tetrahedron Lett.* **1980**, *21*, 217; T. P. Lockhart, C. B. Mallon, R. G. Bergman, *J. Am. Chem. Soc.* **1980**, *102*, 5967; K. C. Nicolaou, W.-M. Dai, *Angew. Chem.* **1991**, *103*, 1453.
[31] Nicolaou et al., *J. Med. Chem.* **1996**, 2103.
[32] B. P. Roberts, *Chem. Soc. Rev.* **1999**, *28*, 25.
[33] D. H. R. Barton, D. O. Jang, J. C. Jaszberenyi, *Tetrahedron Lett.* **1992**, *33*, 2311.
[34] D. H. R. Barton, D. O. Jang, J. C. Jaszberenyi, *Tetrahedron Lett.* **1992**, *33*, 5709.
[35] D. F. Taber, Y. Wang, T. F. Pahutski Jr., *J. Org. Chem.* **2000**, *65*, 3861; D. F. Taber, P. V. Joshi, *C. R. Acad. Sci. Paris Chimie* **2001**,*4*, 557.
[36] J. A. Baban, B. P. Roberts, *J. Chem. Soc., Perkin Trans. 2* **1988**, 1195.
[37] V. P. J. Marti, B. P. Roberts, *J. Chem. Soc., Perkin Trans. 2* **1986**, 1613; J. A. Baban, B. P. Roberts, *J. Chem. Soc., Perkin Trans. 2* **1986**, 1607; V. Paul, B. P. Roberts, *J. Chem. Soc., Perkin Trans. 2* **1988**, 1895; J. A. Baban, B. P. Roberts, *J. Chem. Soc., Perkin Trans. 2* **1984**, 1717.
[38] B. Sheeller, K. U. Ingold, *J. Chem. Soc., Perkin Trans. 2* **2001**, 480.
[39] M. Lucarini, G. F. Pedulli, L. Valgimigli, *J. Org. Chem.* **1996**, *61*, 1161.
[40] D. H. R. Barton, M. Jacob, *Tetrahedron Lett.* **1998**, *39*, 1331.
[41] S.-H. Ueng, M. Makhlouf Brahmi, É. Derat, L. Fensterbank, E. Lacôte,M. Malacria, D. P. Curran, *J. Am. Chem. Soc.* **2008**, *130*, 10082 – 10083.
[42] J. Hioe, A. Karton, J. M. L. Martin, H. Zipse, *Chem. Eur. J.* **2010**, *16*, 6861 – 6865.
[43] D. P. Curran, A. Solovyev, M. Makhlouf Brahmi, L. Fensterbank, M. Malacria, E. Lacôte, *Angew. Chem. Int. Ed.* **2011**, *50*, 10294 – 10317.
[44] A. Solovyev, S.-H. Ueng, J. Monot, L. Fensterbank, M. Malacria, E. Lacôte, D. P. Curran, *Org. Lett.* **2010**, *12*, 2998 – 3001.
[45] J. C. Walton, M. Makhlouf Brahmi, L. Fensterbank, E. Lacôte, M. Malacria, Q. Chu, S.-H. Ueng, A. Solovyev, D. P. Curran, *J. Am. Chem. Soc.* **2010**, *132*, 2350 – 2358.
[46] S.-H. Ueng, L. Fensterbank, E. Lacôte, M. Malacria, D. P. Curran, *Org. Lett.* **2010**, *12*, 3002 – 3005.
[47] S.-H. Ueng, L. Fensterbank, E. Lacôte, M. Malacria, D. P. Curran, *Org. Biomol. Chem.* **2011**, *9*, 3415 – 3420.
[48] S.-H. Ueng, L. Fensterbank, E. Lacôte, M. Malacria, D. P. Curran, *Org. Lett.* **2010**, *12*, 3002 – 3005.
[49] S.-H. Ueng, L. Fensterbank, E. Lacôte, M. Malacria, D. P. Curran, *Org. Biomol. Chem.* **2011**, *9*, 3415 – 3420.
[50] K. E. J. Barrett, W. A. Waters, *Discuss. Faraday Soc.* **1953**,*14*, 211 – 277; C. Chatgilialoglu, C. Ferreri, T. Gimisis, In *Chemistry of Organic Silicon Compounds*; Z. Rappoport, Y. Apeloig, Eds.; Wiley: Chichester, U.K., **1998**; *Vol. 2*, pp 1539 – 1579; B. P. Roberts, *Chem. Soc. Rev.* **1999**, *28*, 25 – 35; D. Crich, D. Grant, V. Krishnamurthy, M. Patel, *Acc. Chem. Res.* **2007**, *40*, 453 – 463.
[51] X. Pan, E. Lacôte, J. Lalevée, D. P. Curran, *J. Am. Chem. Soc.* **2012**, *134*, 5669 – 5674.

[52]
https://www.akzonobel.com/polymer/system/images/AkzoNobel_Initiators_and_Reactor_Additives_for_Thermoplastics_Low-res_protected_July%202010_tcm96-39468.pdf
[53] Neufingerl: *Chemie 1 - Allgemeine und anorganische Chemie*, Jugend & Volk, Wien **2006**; ISBN 978-3-7100-1184-9, 47.
[54] M. M. Brahmi, J. Monot, M. Desage-El Murr, D. P. Curran, L. Fensterbank, E. Lacôte, M. Malacria, *J. Org. Chem.* **2010**, *75*, 6983-6985.
[55] J. P. Barnier, J. Champion, J. M. Conia, *Organic Syntheses* **1981**, *60*, 25.
[56] B. Koppenhöfer, V. Schurig, *Organic Syntheses* **1988**, *66*,160.
[57] M. T. Reetz, M. W. Drewes, R. Schwickardi, *Organic Syntheses* **1999**, *76*, 110.
[58] R. Oi, K. B. Sharpless, *Organic Syntheses* **1996**, *73*, 1.
[59] D. Seebach, H.-O. Kalinowski, W. Langer, G. Crass, E.-M. Wilka, *Organic Syntheses* **1983**, *61*, 24.
[60] C. H. Park, H. E. Simmons, *Organic Syntheses* **1974**, *54*, 88.
[61] Y. K. Chen, S.-J. Jeon, P. J. Walsh, W. A., *Organic Syntheses* **2005**, *82*, 87.
[62] K. Schwetlick, *Organikum* **2009**.
[63] R. Brückner*, Reaktionsmechanismen - Organische Reaktionen, Stereochemie, moderne Synthesemethoden* **1996**, Spektrum - Akademischer Verlag.
[64] F. Carey, R. Sundberg, *Organische Chemie* **1995**, Wiley-VCH.
[65] A. L. Gemal, J.-L. Luche, *J. Am. Chem. Soc.* **1981**, *103*, 5454 – 5459.
[66] C. R. Johnson, B. D. Tait, *J. Org. Chem.* **1987**, *52*, 281 – 283.
[67] A. R. Jagdale, A. S. Paraskar, A. Sudalai, *Synthesis*, **2009**, 660 – 664.
[68] L. Blackburn, R. J. K. Taylor, *Org. Lett.*, **2001**, *3*, 1637 – 1639.
[69] A. F. Abdel-Magid, K. G. Carson, B. D. Harris, C. A. Maryanoff, R. D. Shah, *J. Org. Chem.,* **1996**, *61*, 3849 – 3862.
[70] M. Taibakhsh, R. Hosseinzadeh, H. Alinezhad, S. Ghahari, A. Heydari, S. Khaksar, *Synthesis*, **2011**, 490 – 496.
[71] E. J. Corey, S. Shibata, R. K. Bakshi, *J. Org, Chem.*, **1988**, *53*, 2861 – 2863.
[72] H. C. Brown, B. C. S. Rao, *J. Am. Chem. Soc.* **1956**, *78*, 5694 – 5695.
[73] A. Prokofjevs, A. Boussonnière, L. Li, H. Bonin, E. Lacôte, D. P. Curran, E. Vedejs, *J. Am. Chem. Soc.* **2012**, *134*, 12281 – 12288.
[74] X. Pan, A. Boussonnière, D. P. Curran, *J. Am. Chem. Soc.* **2013**, *135*, 14433 – 14437.
[75] A. Boussonnière, X. Pan, S. J. Geib, D. P. Curran, *Organometallics* **2013**, *32*, 7445 – 7450.
[76] T. Taniguchi, D. P. Curran, *Angew. Chem. Int. Ed.* **2014**, *53*, 13150 – 13154.
[77] Q. Chu, M. M. Brahmi, A. Solovyev, S.-H. Ueng, D. P. Curran, M. Malacria, L. Fensterbank, E. Lacôte, *Chem. Eur. J.* **2009**, *15*, 12937 – 12940.
[78] M. Horn, H. Mayr, E. Lacôte, E. Merling, J. Deaner, S. Wells, T. McFadden, D. P. Curran, *Org. Lett.* **2012**, *Vol. 14, No. 1*, 82 – 85.
[79] T. Taniguchi, D. P. Curran, *Org. Lett.* **2012**, *Vol. 14, No. 17*, 4540 – 4543.
[80] H. Gottlieb, V. Kotlyar, A. Nudelman, *J. Org. Chem.* **1997**, *62*, 7512 – 7515.
[81] G. D. Mendenhall, *Tetrahedron Letters* **1983**, *Vol. 24, No.5*, 451 – 45.
[82] H. Kiefer and T.G. Traylor, *Tetrahedron Letters* **1966**, 6163.
[83] J. T. Banks, J. C. Scaiano, W. Adam, R. Schulte Oestrich, *J. Am. Chem. Soc.* **1993**, *115*, 2413 – 2411.
[84] N. Arulsamy , D. S. Bohle , J. A. Imonigie , E. S. Sagan, *J. Am. Chem. Soc.*, **2000**, *122 (23)*, 5539 – 5549.

[85] J. Lalevée, N. Blanchard, A.-C. Chany, M.-A. Tehfe, X. Allonas, J.-P. Fouassier, *J. Phys. Org. Chem.* **2009**, *22*, 986 – 993.
[86] http://sdbs.db.aist.go.jp/sdbs/cgi-bin/direct_frame_disp.cgi?sdbsno=12578
[87] L. C. Misal Castro, D. Bézier, J.-B. Sortais, C. Darcel, *Adv. Synth. Catal.* **2011**, *353*, 1279 – 1284.
[88] http://sdbs.db.aist.go.jp/sdbs/cgi-bin/direct_frame_disp.cgi?sdbsno=6159
[89] http://sdbs.db.aist.go.jp/sdbs/cgi-bin/direct_frame_disp.cgi?sdbsno=6389
[90] http://sdbs.db.aist.go.jp/sdbs/cgi-bin/direct_frame_disp.cgi?sdbsno=2365
[91] http://sdbs.db.aist.go.jp/sdbs/cgi-bin/direct_frame_disp.cgi?sdbsno=5668
[92] http://sdbs.db.aist.go.jp/sdbs/cgi-bin/direct_frame_disp.cgi?sdbsno=6196
[93] http://sdbs.db.aist.go.jp/sdbs/cgi-bin/direct_frame_disp.cgi?sdbsno=685
[94] J. S. Lomas, *J. Phys. Org. Chem.* **2005**, *18*, 1001 – 1012.
[95] http://sdbs.db.aist.go.jp/sdbs/cgi-bin/direct_frame_disp.cgi?sdbsno=8016